EVALUATION OF ANTICARCINOGENIC AND CHEMOPROTECTIVE EFFECT OF SIMAROUBA GLAUCA DC

Thesis submitted to

UNIVERSITY OF CALICUT
Malappuram, Kerala, India

For the Degree of

Doctor of Philosophy in Zoology
(Faculty of Science)

By

SHAJI E. M., M.Sc., B.Ed., M.Phil.

Under the guidance of

Dr. ACHUTHAN C. R., Ph.D.,
Associate Professor, Department of Biochemistry,
Amala Cancer Research Centre, Thrissur

&

Co-guidance of

Dr. BALU T. KUZHIVELIL, Ph.D.,
Associate Professor, Department of Zoology,
Christ College, Irinjalakuda

at

AMALA CANCER RESEARCH CENTRE
Thrissur, Kerala, India
September 2019

DECLARATION

I hereby declare that the thesis entitled **"EVALUATION OF ANTICARCINOGENIC AND CHEMOPROTECTIVE EFFECT OF SIMAROUBA GLAUCA DC"** is based on the original work carried out by me at Department of Biochemistry, Amala Cancer Research Centre, Thrissur, Kerala, under the guidance and supervision of Dr. Achuthan C. R., Associate Professor, Department of Biochemistry, Amala Cancer Research Centre, Thrissur, Kerala and Co-guidance of Dr. Balu T. Kuzhivelil, Associate Professor (Retd.), Department of Zoology, Christ College, Irinjalakuda, Kerala. The thesis has been subjected to plagiarism check and no part thereof has been presented for the award of any degree, diploma, fellowship or other similar title.

Place: Thrissur,
Date: 25.09.2019.

SHAJI E. M.
Assistant Professor, (on FDP),
Department of Zoology,
KKTM Govt. College, Pullut,
Kodungallur, Thrissur 680663.

E-mail : amalacancerresearch@gmail.com

Phone: 0487 2307968
FAX : 91 487 2307968

Amala Cancer Research Centre Society

(A Society Registered T. C Act, XII of 1955 sl. No. 56 of 1984)

MANAGING DIRECTOR : FR. FRANCIS KURISSERY, C M I
RESEARCH DIRECTOR : DR. RAMADASAN KUTTAN, Ph.D

AMALANAGAR - 680 555, THRISSUR
KERALA, INDIA

Ref :

Date:

CERTIFICATE

This is to certify that the thesis entitled **"EVALUATION OF ANTICARCINOGENIC AND CHEMOPROTECTIVE EFFECT OF SIMAROUBA GLAUCA DC"** is a bonafide record of research work carried out by **Mr. SHAJI E. M.**, (Reg No: 28432/RESEARCH-B-ASST-2/2014/CU, Dated: 20.01.2015) under my guidance and supervision at **Department of Biochemistry, Amala Cancer Research Centre, Thrissur, Kerala** and no part thereof has been presented for the award of any other degree, diploma or other similar titles. The contents of the thesis have been subjected to plagiarism check and the percentage of similar content was found to be within the acceptable maximum limit.

Place: Thrissur,
Date: 24.09.2019.

Dr. ACHUTHAN C. R.
(Associate Professor & Supervising Guide)

Dr. Achuthan C. Raghavamenon, Ph.D.
Associate Professor
Dept. of Biochemistry
Amala Cancer Research Centre
Amala Nagar, Thrissur- 680 555, Kerala

DEPARTMENT OF ZOOLOGY
CHRIST COLLEGE,
IRINJALAKUDA, KERALA-680 125, INDIA
PHONE: 0480 – 2825258; Fax 0480-2831552

Dr. Balu T. Kuzhivelil M.Sc., Ph.D.
Associate Professor (Retired).

Date: 24.09.2019

CERTIFICATE

This is to certify that the thesis entitled "**EVALUATION OF ANTICARCINOGENIC AND CHEMOPROTECTIVE EFFECT OF SIMAROUBA GLAUCA DC**" is a bonafide record of research work carried out by **Mr. SHAJI E. M.** (Reg. No: 28432/RESEARCH-B-ASST-2/2014/CU, Dated: 20.01.2015) under my co-guidance and supervision at **Department of Biochemistry, Amala Cancer Research Centre, Thrissur, Kerala** and no part thereof has been presented for the award of any other degree, diploma or other similar titles. The contents of the thesis have been subjected to plagiarism check and the percentage of similar content was found to be within the acceptable maximum limit.

Place: Irinjalakuda,
Date: 24.09.2019.

Dr. BALU T. KUZHIVELIL,
(Co-guide)

Telephone: Residence: 0480 – 2829113, Mobile: 9447528917
Email: balukuzhivel@gmail.com; balu99@rediff.com

Format for plagiarism check certificate

UNIVERSITY OF CALICUT
CERTIFICATE ON PLAGIARISM CHECK

1.	Name of the research scholar	SHAJI E.M.		
2.	Title of thesis/dissertation	EVALUATION OF ANTICARCINOGENIC AND CHEMOPROTECTIVE EFFECT OF SIMAROUBA GLAUCA DC.		
3.	Name of the supervisor	Dr. Achuthan C.R. (Guide) Dr. Balu T. Kuzhivelil (Co-guide)		
4.	Department/Institution	Amala Cancer Research Centre, Thrissur.		
5.		**Introduction/ Review of literature**	**Materials and Methods**	**Result/ Discussion/Summary/ Conclusion**
	Similar content (%) identified	1%	0%	0%
	Acceptable maximum limit (%)	25 /35	25	10
6.	Software used	Urkund		
7.	Date of verification	26/9/2019		

**Report on plagiarism check, specifying included/excluded items with % of similarity to be attached.*

Checked by (with name, designation & signature) Dr. VINOD. V. M, Assistant Librarian(Sr.Scale), University of Calicut

Name & Signature of the Researcher SHAJI E.M.

Name & Signature of the Supervisor Dr. Achuthan C. Raghavamenon, Ph.D., Associate Professor, Dept. of Biochemistry, Amala Cancer Research Centre, Amala Nagar, Thrissur- 680 555, Kerala

Dr. Balu T. Kuzhivelil, Co-Guide

The Doctoral Committee* has verified the report on plagiarism check with the contents of the thesis, as summarized above and appropriate measures have been taken to ensure originality of the Research accomplished herein.

Dr. RAMADASAN KUTTAN Ph.D, Research Director, Amala Cancer Research Centre, Thrissur - 680 555, Kerala

Name & Signature of the HoD/HoI (Chairperson of the Doctoral Committee)

** In case of languages like Malayalam, Tamil, etc. on which no software is available for plagiarism check, a manual check shall be made by the Doctoral Committee, for which an additional certificate has to be attached*

Acknowledgement……

At the outset, I thank the omnipresent and omnipotent Almighty for all the blessings that He has showered on me.

Foremost, I express my deep-hearted and sincere gratitude to the supervising guide of my research work, ***Dr. Achuthan C. R.,*** *Associate Professor, Department of Biochemistry, Amala Cancer Research Centre, Thrissur, for suggesting this problem for the study. He taught me how to handle situations with new perspectives. His selfless interest, patient listening, constant help and guidance during the period of work are thankfully acknowledged.*

I extremely indebted to ***Dr. Balu T. Kuzhivelil****, Associate Professor, Department of Zoology, Christ College, Irinjalakuda who agreed to guide me as co-guide in this study and he has wholeheartedly supported me in all the stages of work.*

With all gratitude in heart, I would recollect the benevolence of the Research Director of Amala Cancer Research Centre, ***Dr. Ramadasan Kuttan,*** *in accommodating me as a part-time research scholar in the prestigious institution. He has supported me in all the stages of work and provided all the necessary facilities to carry out the work.*

The Management of Amala Cancer Research Centre has offered me the opportunity to work here as a Ph.D. student, with the most ambient facility required for the progress of the work. I express my heartful thanks to the former Director, ***Rev. Fr. Walter Thelappilly****, CMI and the present Director* ***Rev. Fr. Francis Kurissery,*** *CMI of Amala Cancer Hospital and Research Centre for permitting me to carry out the work in this centre and also providing the necessary facilities.*

I am greatly indebted to the ***University Grants Commission (UGC)*** *for permitting me to do research under Faculty Development Programme. I also extend sincere thanks to* ***Director****,* ***Higher Education Department of Kerala*** *and* ***Director****,* ***Collegiate Education Department, Kerala*** *for their valuable help to avail FDP fellowship.*

I am extremely thankful to ***Dr. Babu T. D.****, Associate Professor, Department of Biochemistry, Amala Cancer Research Centre for the timely advice, academic support and valuable suggestions I received during the study. The rectifications he suggested*

in my research papers published in the Amala research bulletin were very relevant and helpful.

I owe to ***Dr. Jose Padikkala****,* ***Dr. Girija Kuttan****,* ***Dr. K. K. Janardhanan*** *and* ***Dr. Suraj K.,*** *the teaching staff of Amala Cancer Research Centre, for the help they have extended to me during the study.*

It is a great pleasure to thank ***Mrs. Preetha C. G., Mrs. Sunitha, Ms. Liji*** *and* ***Mrs. Hemalatha,*** *the office staff of Amala Cancer Research Centre, for their warm and unlimited support. My extreme thanks are addressed to* ***Ms. Thankammani, Mrs. Sumathy****,* ***Mrs. Santha*** *and* ***Mrs. Shiju,*** *the staff of Amala Cancer Research Centre for accompanying my work in the animal house.*

I am thankful to ***Dr. Vineetha Achuthan****, who showed the plant (S. glauca) to me in the Amala Ayurvedic garden and arranged necessary help to collect leaves from the plant.*

I am grateful to ***Dr. C. N. Sunil****, Associate Professor, Department of Botany, SNM College, Maliankara who identified and authenticated the plant for the work.*

I am most delighted to express my gratitude and love to ***Dr. Smitha K. R.****, my fellow researcher who taught me how to perform different experiments at the beginning of my work. I express special thanks to* ***Ms. Silpa Prabha****, who supported me very much for doing different experiments, especially in vivo experiments. I would like to acknowledge the support provided by* ***Mrs. Indu M. S.*** *during the study. I am privileged to thank* ***Mr. Arunaksharan Narayanankutty****, my fellow researcher, from whom I have learned many techniques related to research. I acknowledge my profound gratitude and thanks to* ***Dr. Liju V. B., Dr. Seema Menon Dr. Jeksy Jos Manalil, Dr. Lincy Lawrence*** *and* ***Dr. Vipin Sivaram*** *for providing help whenever I needed in different ways. I also express my sincere gratitude to* ***Mrs. Meera Nair, Ms. Surya P. I., Mr. Pareeth C.M., Ms. Sruthy P. K., Mrs. Sowmya V. V., Mrs. Veena Gopinath*** *and* ***Mrs. Aswathi C.V.*** *for their help in the research work.*

The immense love and support I enjoyed from the contemporary researchers and technicians of other labs in Amala Cancer Research Centre are worth-mentioning. It is a great pleasure to offer my love and gratitude to ***Mrs. Ramya M. K., Dr. Binitha P. P.****,* ***Mrs. Sheema Dharmapal****,* ***Dr. Salini Sasidharan****,* ***Dr. Sindhu E R****,* ***Dr. Jeena K****,* ***Dr. Veena Ravindran****,* ***Dr. Greeshma P. V., Mr. Ravikumar K. S., Dr. Ramya,***

Dr. Chubika Thomas *and* ***Dr. Vishnupriya Murali****, individually for their support and help. I express my sincere gratitude to* ***Mrs. Neethu Soman****,* ***Mr. Midhun Gopinath, Mrs. Rosemol M. J. Mr. Asif*** *and* ***Mr. Shehasad*** *project students for their help.*

I acknowledge my profound gratitude and thanks to ***Dr. K. K. Subhash Babu,*** *Assistant Professor, Department of Marine Biology and Fisheries, College of Science and Technology, Asmara, Eritrea for directing and acquainting me to Dr. Achuthan C.R. Throughout the period of work, his constant motivation and moral support has helped me a lot.*

I take this opportunity to thank ***Dr. Dhanush Krishna B.,*** *Assistant Professor, Department of Veterinary Pathology, College of Veterinary and Animal Sciences, Mannuthy for helping me to do necropsy and the histological analysis related with this study.*

I express my sincere thanks to Principal, teaching staff especially ***Mr. Shihabudeen A. S., Mr. Prasad N. K., Mrs. Soumya K. C.*** *and* ***office staff****, KKTM Govt. College, Pullut, Kodungallur for their support and encouragement.*

With great reverence, I thank all my ***teachers*** *who taught me in various stages of academic life.*

I express my sincere thanks to ***library staff****, Amala Cancer Research Centre for their valuable help.*

I am grateful to ***Dr. Vinod V.M.****, Assistant Librarian, University of Calicut who did the plagiarism checks of the thesis.*

My love and gratitude are expressed to my wife ***Saritha P. I.*** *for her endurance, valuable prayers, love and support. I express my profound gratitude to my little princesses* ***Agnes E. S.*** *and* ***Therese E. S.*** *who suffered a lot in this journey. My appreciation is also expressed to my parents, in-laws, sisters and other family members for their constant prayers, moral support and encouragement throughout my study and career.*

SHAJI E. M.

Abstract

Abstract

Simarouba glauca DC (Paradise tree or Laxmitaru) is an exotic plant, belongs to the family Simaroubaceae. Several phytochemicals have been isolated from this plant mainly, alkaloids with high cytotoxicity, quassinoids with antifungal and anticancer activity and triterpenes with anti protozoan activity. However, no scientific study has been conducted regarding the anticarcinogenic and chemoprotective effect of crude extract of *S. glauca* DC.

In the beginning, twigs of *S. glauca* were collected from herbal medicine garden of Amala Ayurvedic Hospital, Thrissur and identified by a plant taxonomist. Hot water extract (HE) and methanolic extract (ME) was prepared by using mature leaves. HE was produced from the decoction which was prepared as per the existing protocol followed by people for treatment purpose and ME was prepared by using 99.9% methanol. Preliminary phytochemical screening and TLC analysis revealed the presence of similar phytochemicals like flavonoids, triterpenoids, terpenoids, alkaloids and phenolics in both the extracts. The cytotoxic potential was evaluated by *in vitro* short term cytotoxicity assay (Trypan blue exclusion) using DLA and EAC cells and rat spleen cells and long term antiproliferative assay was performed using HCT -15, RAW 264.7, HeLa, HepG2, MDA-MB-231, MCF-7 and Vero-E6. In general, the toxicity of HE and ME was found low to the murine cancer cells and normal cells studied and IC_{50} was found >100 μg/mL. But, in the antiproliferative study, HE showed a lower IC_{50} with HCT-15 (71.53 ± 0.72), RAW 264.7 (85.32 ± 3.17) and HeLa (98.33 ± 7.35) μg/mL.

In vitro antioxidant efficacy of HE and ME were assessed based on the hydroxyl radical scavenging activity, DPPH radical scavenging activity, nitric oxide radical inhibition, ferric reducing/antioxidant power, inhibition of lipid peroxidation, total antioxidant capacity and lipoxygenase inhibition. It was revealed from the study that both HE and ME possess a significant antioxidant capacity. In comparison, HE documented the highest antioxidant potential with depicted IC_{50} values 77.88 ± 2.75, 7.47 ± 0.48 and 63.13 ± 2.34 μg/mL respectively in hydroxyl, DPPH and nitric oxide scavenging activity. The half-maximal effective concentration (EC_{50}) was found to be 3.66 ± 0.29 and 77.85 ± 3.45 μg/mL respectively in FRAP and total antioxidant capacity assays for HE. In corroboration, HE was found to have a high amount of

total flavonoid (27.13 ± 2.65 mg QTE/gm extract) and an equal amount of polyphenolics (77.58 ± 0.65 mg GAE/gm extract) with respect to ME. Based on these results, HE was found biologically most active and selected for further detailed study. The UPLC-Q-TOF-MS analysis of HE revealed as many as 93 constituents and 79 compounds were pharmacologically known compounds. Out of this, 9 active components with antioxidant, anti-inflammatory and anticancer properties were identified.

Safety evaluation using acute and sub-acute toxicity models were carried out for the selection of pharmacological doses of the HE as per OECD guidelines before conducting *in vivo* studies. The different parameters like change in body weight, change in feed consumption rate and change in water consumption were analysed. General appearance and behaviour parameters like change in the skin, eye colour, drowsiness, sedation, diarrhoea, etc, were noted. Necropsy studies were also conducted at the end of the experiment. In the acute toxicity study single administration of HE was found safe up to 2000 mg/kg b. wt for Swiss albino mice of both sexes and no mortality was observed. Moreover, the necropsy analysis revealed no abnormal changes in size, colour and texture of visceral organs with respect to untreated animals. This suggested that the LD_{50} value may be above to 2000 mg/kg b. wt.

The sub-acute toxicity study revealed that, the administration of HE for 28 consecutive days at various doses like 200, 300 and 400 mg/kg b. wt is non-toxic to Swiss albino mice of both sexes. No mortality was reported from any of the treated groups and the food and water consumption rates were found unaffected in the animals during the study period. The general appearance and behaviour pattern were equal to that of normal group animals in all the treated animals during the entire period of study. Moreover, body weight was found increased in all animals. Necropsy analysis of treated animals did not show any pathological abnormalities. No significant variation was noted in the organosomatic index of various organs of HE administered animals with respect to normal animals in this study. The haematological parameters like Hb level and total leucocyte count were found close to that of untreated animals in the study. Liver and renal function parameters did not show any variation compared to the untreated animals in the HE administered groups

of animals. Serum electrolytes and lipid profile parameters showed no abnormal variations with respect to untreated group animals. Histological examination of the organs of animals treated with various doses of HE did not show any adverse toxicological effects when compared with the untreated group of animals. If the finding of this study extrapolates to humans, the regular consumption of hot water extract of leaves *S. glauca* can be considered comparatively safe. This study also provides a positive nod to the use of HE for conducting *in vivo* experiments.

Antitumour effect of HE of *S. glauca* was conducted in both ascites and solid tumour bearing mice. EAC and DLA cells were used respectively for inoculating ascites and solid tumour in Swiss albino mice. The experiment was designed four different ways for each model as follows: 1) simultaneous administration of HE with ascites/solid tumour inoculated mice 2) pre and simultaneous administration of HE with ascites/solid tumour inoculated mice 3) administration of HE to the ascites/solid tumour bearing mice and 4) administration of HE (lower dose) in combination with cyclophosphamide (CTX) with ascites/solid tumour inoculated mice. Lower (LDHE: 160 mg/kg b. wt; equal to human consumption rate) and higher (HDHE: 260 mg/kg b. wt) doses of HE were orally administered by dissolving in 1% propylene glycol.

In ascites tumour model, mean survival days and percentage increase in the life span of animals were calculated. The % increase in the life span of LDHE (19.80) and HDHE (21.78) simultaneously administered in ascites tumour inoculated mice was found increased. The pre and simultaneous administration of LDHE and HDHE in ascites inoculated mice made 21.53 and 23.53% increase in their life span. The administration of HE in ascites tumour bearing mice made 16.50 and 17.48% increase in the life span respectively in LDHE and HDHE group. The administration of HE, with a combination of different concentrations of CTX in ascites tumour inoculated mice, produced a promising result. Out of 6 animals in each group 2, 3 and 2 animals were survived even after 50 days respectively from LDHE + CTX (15 mg/kg b. wt), LDHE + CTX (10 mg/kg b. wt) and LDHE (5 mg/kg b. wt) administered groups.

In solid tumour model, tumour volume and change in body weight were measured in every three days up to 28 days. Haematological parameters were analysed on 0, 14 and 28^{th} day. At the end of the experiment, the tumour was isolated and weighed. Histological analysis of the hind limb of mice was done. A reduction in the tumour

volume and tumour weight was noted in LDHE and HDHE treated groups of all different models of solid tumour experiments conducted. The administration of HE in different doses showed a tendency to prevent myelosuppression with respect to the control group. Histological examinations revealed the antitumour efficacy of different doses of HE.

The antioxidant efficacy of HE was administered in three different ways. In the first method, the HE in different doses was administered for 30 days to Swiss albino mice and their antioxidant status of haemolysate, liver and kidney was analysed. In the second method, the protective effect of HE was determined against sodium fluoride (NaF)-induced oxidative stress in mice. In the third method, the protective effect of HE on PMA induced superoxide radical scavenging activity was analysed.

In the first experiment, the enzymatic and non-enzymatic antioxidant status of blood, liver and kidney tissue of HE administered groups of animals were found improved significantly with respect to the normal group of animals. The detailed investigations of HE for its antioxidant effect using NaF-induced oxidative stress in mice revealed that the extract at 160 and 260 mg/kg b. wt reversed the NaF induced drop in the enzymatic and non-enzymatic status of blood and liver in Swiss albino mice. The histological examinations of the liver tissue of HE administered animals well corroborated with the results obtained in the biochemical studies. In the third experiment, LDHE (160 mg/kg b. wt) and HDHE (260 mg/kg b. wt) were shown 74.18 and 73.57% efficacy in the inhibition of superoxide radical generation in the macrophages in mice peritoneum with respect to control group of animals.

Acute anti-inflammatory *in vivo* models like carrageenan and dextran and formalin-induced chronic anti-inflammatory models were used to evaluate the anti-inflammatory status of HE. The Evans blue dye extravasation method was also performed in the carrageenan model. Oral administration of LDHE and HDHE was found to reduce the carrageenan-induced paw oedema by 43.70 and 39.51% at the third hour in mice. Similar to this, 29.35 and 28.67% reduction in the paw thickness was noted in the dextran-induced paw oedema model at third our in LDHE and HDHE treated mice. In the formalin model, 44.39 and 39.39% decrease in the paw thickness in animals treated with LDHE and HDHE were noted on the sixth day. The histological analysis of paw tissue from HE treated animals of each model study

affirmed the earlier observations. In the Evans blue dye extravasation study, the percentage inhibition of the retention of Evans blue dye in the paw tissue of LDHE and HDHE treated mice were found to be 80.78 and 82.04% respectively.

Chemoprotective effect of HE was assessed by using cisplatin-induced renal toxicity, cyclophosphamide-induced systemic toxicity in normal and tumour bearing mice. In the cisplatin-induced renal toxicity model, the bone marrow cellularity and alpha esterase activity, serum urea and creatinine, oxidative stress status of renal tissue were evaluated along with histological analysis. In this study, HE administered animals maintained Hb and leucocyte count which, was found close to the normal group of animals. The bone marrow cellularity of HE treated animals were found elevated in comparison with the normal group. Renal function markers were found improved in HE treated groups. Antioxidant status in renal tissue found supported by HE administered animals with respect to the control group. The histological analysis of renal tissue of HE administered animals showed less damage into the tissue architecture.

The chemoprotective effect of HE in cyclophosphamide-induced toxicity among tumour bearing and non-bearing animals showed a beneficial action. In this study also the haematological, antioxidant status of liver and kidney, liver function parameters and renal function parameters were found supported by HE administration. In conclusion, the study revealed the efficient chemoprotective nature of HE and it may be attributed to the potential phytochemicals present in it.

The anticarcinogenic effect of HE was analyzed by using the DMBA-induced mammary tumour model in mice. The survival capacity of animals treated with HE was found increased. The mammary pad analysis and histological examinations revealed the chemopreventive nature of HE. The haematological parameters and liver function parameters of HE administered group were found close to the normal group of animals with respect to the control group animals. The necropsy showed less tumour progression in the ovary of HE administered animals. Histological analysis of ovaries and liver showed the beneficial action of HE at the tissue level.

From the overall study, the HE extract of *Simarouba glauca* DC has been showed anticarcinogenic efficacy in cell-induced and chemical-induced cancer model studies.

It is found that the action HE is more beneficial in the earlier stages of tumour formation rather than in well-developed tumours indicating the preventive nature of the drug rather than curative nature. Moreover, HE is found to be a good chemoprotective agent. The HE has immense antioxidant potential and it may be due to the presence of potential phytochemicals present in it. Both lower and higher doses of HE showed somewhat similar beneficial role. Furthermore, HE is safe for consumption.

Keywords: *Simarouba glauca* DC**,** phytochemical, safety evaluation, antioxidant, anti-inflammatory, anticarcinogenic, chemoprotective, antitumour

Preface

Preface

With the advent of newer detection methods, treatment options, and better management strategies cancer has now been accepted as largely curable. However due to wide spectrum of side effects under treatment regimen, socio-economic unbalance, and anxiety, patients and their families increasingly adopt the area-specific unscientific mode of natural healing publicized widely around the globe. In most cases, terminally ill patients are most lean to these as the final hope however it is not uncommon that patients detected with cancer undergo such treatments.

Nowadays, the internet and social media are over-full of “miracle cures” of cancer and alleged sure-fire ways to prevent and cure this dreadful disease. Many cancer patients think that the mainstream treatment modalities are not sufficient to heal their disease and cause adverse side effects, search for treatments whose efficacy are not really supported by scientific confirmation or may even prove unsafe. During an occasion of uncertainty and worry, it is understandable that every hope for a cure, even if it is not medically confirmed is attractive.

Many natural products are listed as “cure-all” solutions that claim to eliminate cancer. Cannabis oil, laetrile (a purified form of amygdalin), aloe, capsicum, cassava, castor oil, different mushrooms, etc, are promoted to treat or prevent cancer in humans but lack scientific and medical evidence of effectiveness. In recent years Shimoga district of Karnataka has gained wide attention for beneficial herbal treatment for cancer and other incurable medical conditions.

A similar situation has been originated in case of an exotic plant *Simarouba glauca* DC, commonly called Laxmitaru or paradise tree in southern states of India, recently. Many cancer patients from Karnataka, Kerala, and Tamil Nadu claim that the decoction prepared by the leaves of this plant in a specific way is very effective in the treatment of cancer of first and second stages, whereas in advanced stages improves the quality of life. Several patients underwent conventional treatments against cancer believe in their heart that it is the decoction of Laxmitaru brought down the side effects of chemotherapy, minimized appetite loss and ensured a fast recovery. Like any other complementary and alternative medicine therapies, the consumption of this decoction is also criticized by modern medical practitioners by pointing the fact that

the efficacy of this in treatment of cancer has not been proved by any scientific studies. They believe that the effectiveness of this treatment is unrelated to the real cause of the disease.

In the current scenario, the wide popularity the plant attained as a “solace for cancer patients” through different media and the criticism arose from the conventional medical therapists against this has created a great deal of confusion among the public. As stated above, the lack of scientific validation is the primary cause of this social concern; the current research is an even-handed attempt to understand the anticarcinogenic and chemoprotective evaluation of *Simarouba glauca* DC.

Table of contents

Chapter	Title	Pages
1	Introduction and Review	1 - 54
2	Materials and Methods	55 - 123
3	Phytochemical and pharmacological screening of *Simarouba glauca* DC	124 - 155
4	Safety evaluation of hot water extract of *Simarouba glauca* DC	156 - 181
5	Evaluation of antitumour efficacy of *Simarouba glauca* DC	182 – 221
6	Antioxidant and anti-inflammatory aspects of *Simarouba glauca* DC	222 – 252
7	Chemoprotective effects of *Simarouba glauca* DC	253 – 302
8	Anticarcinogenic effect of *Simarouba glauca* DC	303 - 325
	Summary	326 - 327
	Bibliography	328 - 368
	List of publications	369

List of tables

Table 1.1. Incidence, mortality and prevalence of cancer among Indian population in 2018 (source, GLOBOCAN 2018)

Table 1.2. Major risk factors associated with cancer (source: Wu et al., 2018)

Table 1.3. List of oncogenes and their action

Table 1.4. List of tumor suppressor genes and their action

Table 1.5. List of some ROS inducers/mediators involved in cancer types

Table 1.6. Chronic conditions and biological agents associated with the induction of cancer

Table 1.7. List of some chemotherapeutic drugs

Table1.8. Ayurvedic herbs used in the management of cancer

Table 1.9. List of phytochemicals used in cancer therapy

Table1.10. Biologically significant plants belong to Simaroubaceae family

Table 1.11. Potential compounds isolated from Simaroubaceae family plants

Table 1.12. The major chemicals isolated from different *Simarouba sps.* with biological action

Table 2.1. List of chemicals used

Table 2.2. List of diagnostic kits used

Table 2.3. List of instruments used

Table 3.1. Phytochemical screening of different extracts of *S. glauca* leaves

Table 3.2. Rf values of fractions obtained in TLC of HE of *S. glauca* viewed under visible light, visible light after exposure to iodine vapour and UV (254 nm)

Table 3.3. Rf values of fractions obtained in TLC of ME of *S. glauca* viewed under visible light, visible light after exposure to iodine vapour and UV (254 nm)

Table 3.4. Antiproliferative effect of extracts of *S. glauca* on various cell lines

Table 3.5. Total phenol and flavonoid content of different extracts of *S. glauca*

Table 3.6. Different constituents of HE of *S. glauca* identified by UPLC-Q-TOF-MS

Table 3.7. The important chemical constituents of HE of *S. glauca* detected by UPLC-Q-TOF-MS and their properties

Table 4.1. Effect of acute administration of HE on body weight (gm) of mice

Table 4.2. Effect of acute administration of HE on general appearance and behaviour of mice

Table 4.3a. Effect of sub-acute administration of HE on relative organ weight of male and female Swiss albino mice

Table 4.3b. Effect of sub-acute administration of HE on relative organ weight of male and female Swiss albino mice

Table 4.4. Effect of sub-acute administration of HE on hematological parameters of Swiss albino mice

Table 4.5. Effect of sub-acute administration of HE on liver function parameters of Swiss albino mice

Table 4.6. Effect of sub-acute administration of HE on renal function parameters

Table 4.7. Effect of sub-acute administration of HE on serum electrolytes of Swiss albino mice

Table 4.8. Effect of sub-acute administration of HE on lipid profile of Swiss albino mice

Table 5.1. Effect of HE on the mean survival days and percentage increase in the life span of Swiss albino mice along with the inoculation of ascites tumour

Table 5.2. Effect of HE on the mean survival days and percentage increase in the life span of Swiss albino mice before and after the inoculation of ascites tumour

Table 5.3. Effect of HE on the mean survival days and percentage increase in the life span of Swiss albino mice ten days after the inoculation of ascites tumour

Table 5.4. Mean survival days of mice administered with HE in a combination of cyclophosphamide, one day after the inoculation of ascites tumour

Table 5.5. Characteristics of mice administered with HE along with the inoculation of solid tumour

Table 5.6. Effect of HE on total leucocyte count of mice administered with HE along with the inoculation of solid tumour

Table 5.7. Characteristics of mice administered with HE before and after the inoculation of solid tumour

Table 5.8. Effect of HE on total leucocyte count of mice administered with HE before and after the inoculation of solid tumour

Table 5.9. Characteristics of mice administered with HE, ten days after the inoculation of solid tumour

Table 5.10. Effect of HE on total leucocyte count of mice administered with HE, ten days after the inoculation of solid tumour

Table 5.11. Characteristics of mice administered with HE in combination with cyclophosphamide after the inoculation of solid tumour

Table 5.12. Effect of HE on total leucocyte count of mice administered with HE in combination with cyclophosphamide after the inoculation of solid tumour

Table 6.1. Percentage inhibition by HE on PMA induced superoxide radical generation in mice peritoneal macrophages

Table 6.2. Anti-inflammatory effect (% inhibition) of HE of *S. glauca* in comparison with other treatments on carrageenan-induced acute paw oedema in mice

Table 6.3. Anti-inflammatory effect (% inhibition) of HE of *S. glauca* in comparison with other treatments on dextran-induced acute paw oedema in mice

Table 6.4. Anti-inflammatory effect (% inhibition) of HE of *S. glauca* in comparison with other treatments on formalin-induced chronic paw oedema in mice

Table 7.1. Protective effect of HE on the organosomatic index of liver, kidney and spleen of cyclophosphamide-induced mice

Table 7.2. Protective effect of HE treatment on liver function parameters in cyclophosphamide-induced mice

Table 7.3. Protective effect of HE treatment on renal function parameters in cyclophosphamide-induced mice

Table 7.4. Protective effect of HE on the organosomatic index of liver, kidney and spleen of cyclophosphamide-induced toxicity in tumour bearing mice

Table 7.5. Protective effect of HE treatment on liver function parameters in

cyclophosphamide-induced toxicity in tumour-bearing mice

Table 7.6. Protective effect of HE treatment on renal function parameters in cyclophosphamide-induced toxicity in tumour-bearing mice.

Table 8.1. Anticarcinogenic effect of HE on the organ weight of DMBA-induced cancer development in Swiss albino mouse

Table 8.2. Anticarcinogenic effect of HE on the liver function parameters of DMBA-induced cancer development in Swiss albino mouse

List of figures

Figure 1.1. Global cancer incidence and cancer mortality in 2018 (based on GLOBOCAN 2018)

Figure 1.2. Number of new cancer incidences and deaths reported in populations of both sexes of all ages in the world during 2018 (based on GLOBOCAN 2018)

Figure 1.3. Acquired characteristics of cancer (Hanahan and Weinberg, 2000)

Figure 1.4. Emerging hallmarks and enabling characteristics of cancer (Hanahan and Weinberg, 2011)

Figure 1.5. Classification of Complementary and Alternative Medicine (Subramani and Lakshmanaswamy, 2017)

Figure 1.6. *Simarouba glauca* DC

Figure 1.7. Inflorescence of *Simarouba glauca* DC

Figure 3.1. TLC of HE

Figure 3.2. Phytochemical profile of HE

Figure 3.3. TLC of ME

Figure 3.4. Phytochemical profile of ME

Figure 3.5. Toxicity of HE towards DLA, EAC and spleenocytes

Figure 3.6. Toxicity of ME towards DLA, EAC and spleenocytes

Figure 3.7. Antiproliferative activity of leaf extracts (ME and HE) of *S. glauca* against A) HCT-15, B) RAW 264.7 and HeLa cells

Figure 3.8. Morphological changes observed under a phase-contrast microscope (200X) in A) HCT 15, B) RAW 264 and C) HeLa cells

Figure 3.9. Antiproliferative activity of leaf extracts (ME and HE) of *S. glauca* against D) HepG2 E) MDA-MB-231 F) MCF-7, and G) Vero-E6 cells

Figure 3.10. Morphological changes observed under an inverted microscope using phase-contrast microscope (200X) in D) HepG2 E) MDA-MB-231 F) MCF-7, and G) Vero-E6 cells

Figure 3.11. The *in vitro* free radical scavenging activities of HE and ME of *S. glauca* leaves

Figure 3.12. The *in vitro* free radical scavenging activities of HE and ME of *S. glauca* leaves.

Figure 3.13. Total ion chromatogram of the HE of *S. glauca* when subjected to UPLC-Q-TOF-MS analysis

Figure 3.14. The compounds identified from HE of *S. glauca* by UPLC-Q-TOF-MS analysis: (A) Chlorogenic acid, (B) Loganin, (C) Acetylsalicylic acid, (D) Irigenin, and (E) Dihydrorobinetin

Figure 3.15. The compounds tentatively identified from HE of *S. glauca* by UPLC-Q-TOF-MS analysis: (F) Gitoxin, (G) Oleandrin, (H) Cucurbitacin B, and (I) Cucurbitacin L

Figure 4.1a. Effect of sub-acute administration of 200, 300 and 400 mg/kg b. wt. of HE on body weight (gm) of male mice

Figure 4.1b. Effect of sub-acute administration of 200, 300 and 400 mg/kg b. wt. of HE on body weight (gm) of female mice

Figure 4.2a. Effect of sub-acute administration of 200, 300 and 400 mg/kg b. wt. of HE on feed consumption (gm/day/group) of male mice

Figure 4.2b**.** Effect of sub-acute administration of 200, 300 and 400 mg/kg b. wt. of HE on feed consumption (gm/day/group) of female mice

Figure 4.3a. Effect of sub-acute administration of 200, 300 and 400 mg/kg b. wt. of HE on water consumption (mL/day/group) of male mice

Figure 4.3b**.** Effect of sub-acute administration of 200, 300 and 400 mg/kg b. wt. of HE on water consumption (mL/day/group) of female mice

Figure 4.4. Effect of sub-acute administration of HE on the viscera of male (A) and female (B) Swiss albino mice

Figure 4.5a. Histological analysis of different organs of female Swiss albino mice received orally HE (400 mg/kg b. wt.) of *S. glauca*

Figure 4.5b. Histological analysis of different organs of female Swiss albino mice received HE (400 mg/kg. b. wt.) of *S. glauca*

Figure 5.1. Percent survival of mice administered with HE along with the inoculation of ascites tumour

Figure 5.2. Percent survival of mice administered with HE before and after the inoculation of ascites tumour

Figure 5.3. Percent survival of mice administered with HE ten days after the inoculation of ascites tumour

Figure 5.4. Percent survival of mice administered with HE in a combination of cyclophosphamide, one day after the inoculation of ascites tumour

Figure 5.5. Tumour volume of mice administered with HE along with the inoculation of solid tumour

Figure 5.6. Morphology of mice administered with HE along with the inoculation of solid tumour

Figure 5.7. Tumour isolated from the mice administered with HE along with the inoculation of solid tumour

Figure 5.8. Histology of H & E stained section of solid tumour from the mice administered with HE along with the inoculation of solid tumour

Figure 5.9. Effect of HE on Hb in mice administered with HE along with the inoculation of solid tumour

Figure 5.10. Tumour volume of mice administered with HE before and after the inoculation of solid tumour

Figure 5.11. Morphology of mice administered with HE before and after the inoculation of solid tumour

Figure 5.12. Tumour isolated from the mice administered with HE before and after the inoculation of solid tumour

Figure 5.13. Histology of H & E stained section of solid tumour from the mice administered with HE before and after the inoculation of solid tumour

Figure 5.14. Effect of HE on Hb in mice administered with HE before and after the inoculation of solid tumour

Figure 5.15. Tumour volume of mice administered with HE, ten days after the inoculation of solid tumour

Figure 5.16. Morphology of mice administered with HE, ten days after the inoculation of solid tumour

Figure 5.17. Tumour isolated from the mice administered with HE, ten days after the inoculation of solid tumour

Figure 5.18. Histology of H & E stained section of solid tumour from the mice administered with HE, ten days after the inoculation of solid tumour

Figure 5.19. Effect of HE on Hb in mice administered with HE, ten days after the inoculation of solid tumour

Figure 5.20. Tumour volume of mice administered with HE in combination with cyclophosphamide one day after the inoculation of solid tumour

Figure 5.21. Morphology of mice administered with HE in combination with cyclophosphamide after the inoculation of solid tumour

Figure 5.22. Tumour isolated from the mice administered with HE in combination with cyclophosphamide after the inoculation of solid tumour

Figure 5.23. Histology of H & E stained section of solid tumour from the mice administered with HE in combination with cyclophosphamide after the inoculation of solid tumour

Figure 5.24. Effect of HE on Hb in mice administered with HE in combination with cyclophosphamide after the inoculation of solid tumour

Figure 6.1. Effect of HE on the antioxidant status of blood

Figure 6.2. Effect of HE on the antioxidant status of liver

Figure 6.3. Effect of HE on the antioxidant status of liver

Figure 6.4. Effect of HE on the antioxidant status of kidney

Figure 6.5. Effect of HE on the antioxidant status of kidney

Figure 6.6. Protective effect of HE on the antioxidant status of blood following NaF induced oxidative damage

Figure 6.7. Protective effect of HE on the antioxidant status of the liver following NaF-induced oxidative damage

Figure 6.8. Protective effect of HE on the antioxidant status of the liver following NaF-induced oxidative damage

Figure 6.9. Protective effect of HE on the histology of the liver following NaF-induced oxidative damage

Figure 6.10. Effect of HE on PMA-induced superoxide radical generation in mice peritoneal macrophages

Figure 6.11. *In vivo* anti-inflammatory effect of HE on carrageenan-induced acute paw oedema in mice

Figure 6.12. Morphological changes occurred at the third hour on the hind paw of mice belongs to various experimental groups in acute oedema induced by carrageenan

Figure 6.13. Anti-inflammatory effect of HE on histological changes in skin tissue of the plantar region of mouse paw

Figure 6.14. Morphological changes occurred on the hind paw of mice belongs to various experimental groups in the Evans blue extravasation assay

Figure 6.15a. Quantification of Evans blue dye extracted from carrageenan-induced paw oedema in mice from various groups

Figure 6.15b. Quantification of Evans blue dye extracted from carrageenan-induced paw oedema in mice from various groups

Figure 6.16. *In vivo* anti-inflammatory effect of HE on dextran induced acute paw oedema in mice

Figure 6.17. *In vivo* anti-inflammatory effect of HE on formalin-induced chronic paw oedema in mice

Figure 6.18. Morphological changes occurred on the hind paw of mice belongs to various experimental groups in chronic oedema induced by formalin

Figure 6.19. Anti-inflammatory effect of HE on histological changes in skin tissue of the plantar region of mouse paw

Figure 7.1. Effect of HE on haematological parameters in cisplatin-induced renal toxicity in mice

Figure 7.2. Effect of HE on A) bone marrow cellularity and B) alpha esterase positive cells in cisplatin-induced renal toxicity in mice

Figure 7.3. Effect of HE on renal function markers in cisplatin-induced renal toxicity in mice

Figure 7.4. Effect of HE on renal antioxidant enzymes in cisplatin-induced renal toxicity in mice

Figure 7.5. Effect of HE on biomarkers in cisplatin-induced renal toxicity in mice

Figure 7.6. Effect of HE on the histology of kidney tissue in cisplatin-induced mice.

Figure 7.7. Protective effect of HE treatment on the average body weight of cyclophosphamide-induced mice

Figure 7.8. Protective effect of HE treatment on (A) the bone marrow cellularity and (B) Number of alpha esterase positive cells in cyclophosphamide-induced mice

Figure 7.9. Protective effect of HE treatment on the haematological parameters in cyclophosphamide-induced mice

Figure 7.10. Protective effect of HE treatment on the liver antioxidant status in cyclophosphamide-induced mice

Figure 7.11. Protective effect of HE treatment on the liver antioxidant status in cyclophosphamide-induced mice

Figure 7.12. Protective effect of HE treatment on the kidney antioxidant status in cyclophosphamide-induced mice

Figure 7.13. Protective effect of HE treatment on the kidney antioxidant status in cyclophosphamide-induced mice

Figure 7.14. Histological evaluation of the protective effect of HE treatment on the liver in cyclophosphamide administered mice

Figure 7.15. Histological evaluation of the protective effect of HE treatment on the kidney in cyclophosphamide administered mice

Figure 7.16. Histological evaluation of the protective effect of HE treatment on the spleen in cyclophosphamide administered mice

Figure 7.17. Histological evaluation of the protective effect of HE treatment on the small intestine in cyclophosphamide administered mice

Figure 7.18. Protective effect of HE treatment on the average body weight of cyclophosphamide-induced toxicity in tumour-bearing mice

Figure 7.19. Protective effect of HE treatment on the average tumour volume (cm^3) of cyclophosphamide-induced toxicity in tumour-bearing mice

Figure 7.20. Protective effect of HE treatment on the average tumour weight of cyclophosphamide-induced toxicity in tumour-bearing mice

Figure 7.21. Protective effect of HE treatment on the haematological parameters of cyclophosphamide-induced toxicity in tumour-bearing mice

Figure 7.22. Protective effect of HE treatment on the liver antioxidant status of cyclophosphamide-induced toxicity in tumour-bearing mice

Figure 7.23. Protective effect of HE treatment on the liver antioxidant status of cyclophosphamide-induced toxicity in tumour-bearing mice

Figure 7.24. Protective effect of HE treatment on the kidney antioxidant status of cyclophosphamide-induced toxicity in tumour-bearing mice

Figure 7. 25. Protective effect of HE treatment on the kidney antioxidant status of cyclophosphamide-induced toxicity in tumour-bearing mice

Figure 8.1. Kaplan Meir survival curve shows the anticarcinogenic effect of HE on the survival rate of experimental animals

Figure 8.2. Effect of HE on the size of mammary gland tumors and its vascularisation

Figure 8.3. Effect of HE on the fat pad of mammary gland

Figure 8.4. Effect of HE on ovarian tumour

Figure 8.5. Effect of HE on haematological parameters of DMBA-induced breast cancer in mice

Figure 8.6. Effect of HE on the activity of (A) catalase and (B) SOD in the liver tissue of DMBA-induced breast cancer in mice

Figure 8.6. Effect of HE on the activity of (C) GPx, (D) the concentration of GSH and (E) MDA in the liver tissue of DMBA-induced breast cancer in mice

Figure 8.7. Anticarcinogenic effect of HE on the histology of DMBA-induced cancer in the mammary gland of Swiss albino mice

Figure 8.8. Anticarcinogenic effect of HE on the histology of DMBA-induced cancer in the ovary of Swiss albino mice

Figure 8.9. Anticarcinogenic effect of HE on the histology of DMBA-induced cancer in the liver of Swiss albino mice

Abbreviations

ALP	Alkaline phosphatase
ALT	Alanine Aminotransferase
ANOVA	Analysis of variance
AST	Aspartate Aminotransferase
b wt.	Body weight
CAM	Complementary and alternative medicine
CAT	Catalase
CMC	Carboxy methyl cellulose
CTX	Cyclophosphamide
DC	de Candolle
dL	Deciliter
DLA	Dalton's Lymphoma Ascites
DMBA	7,12-Dimethylbenz(a)anthracene
DMEM	Dulbecco's modified eagle medium
DMSO	Dimethyl sulphoxide
DPPH	1, 2-diphynyl-2-picrylhydrazyl
DTNB	5, 5'-dithiobis-(2-nitrobenzoic acid)
EAC	Ehrlich Ascites Carcinoma
e.g.	Example
EDTA	Ethylene diamine tetra acetic acid
EMT	Epithelial Mesenchymal Transition
FBS	Fetal bovine serum
FDA	Food and drug administration
FRAP	Ferric reducing antioxidant power assay
gm	Gram
GAE	Gallic acid equivalents
GPx	Glutathione peroxidase
GR	Glutathione reductase

GSH	Glutathione
GST	Glutathione S-reducatase
Hb	Hemoglobin
HDHE	High dose of hot water extract of leaves of *Simarouba glauca* DC
HDL	High-density lipoprotein
HDLc	High-density lipoprotein cholesterol
HE	Hot water extract of leaves of *Simarouba glauca* DC
IACR	Indian Council of Agricultural Research
kg	Kilogram
LDHE	Low dose of hot water extract of leaves of *Simarouba glauca* DC
LDL	Low density lipoprotein
LPO	Lipid peroxidation
MDA	Malondialdehyde
ME	Aqueous methanolic extract of leaves of *Simarouba glauca* DC
mEq/L	Milliequivalents per litre
mg	Milligram
mL	Millilitre
mM	Millimolar
MTT	3-(4,5-dimethylthiazol-2-yl)-2,5-diphenyltetrazolium bromide
NAA	Naphthalene acetic acid
Na_2HPO_4	Sodium hydrogen phosphate
NaCl	Sodium chloride
NaF	Sodium fluoride
$NaHCO_3$	Sodium hydrogen carbonate
NBT	Nitroblue-tetrazolium
NCCAM	National centre for complementary and alternative medicine
NCCS	National centre for cell science
NCDs	Non communicable diseases
OECD	Organization for economic co-operation and development

PBS	Phosphate buffered saline
PCV	Packed cell volume
pH	Potential of hydrogen
PLT	Platelet count
PMA	Phorbol 12-myristate 13-acetate
QE	Quercetin equivalents
Rf	Retardation factor
ROS	Reactive oxygen species
RNS	Reactive nitrogen species
rpm	Revolutions per minute
RPMI	Rosewell Park Memorial Institute medium
SD	Standard deviation
SDS	Sodium dodecyl sulfate
SGOT	Serum Glutamate Oxaloacetate Transaminase
SGPT	SERUM Glutamate Pyruvate Transaminase
SOD	Superoxide dismutase
TBA	Thiobarbituric acid
TBARS	Thiobarbituric acid reacting substance
TC	Total leucocyte count
TCA	Trichloroacetic acid
TCM	Traditional Chinese Medicine
TLC	Thin Layer Chromatography
U	Unit of enzyme’s catalytic activity
UHPLC	Ultra high performance liquid chromatography
UV	Ultra Violet
VLDL	Very low-density lipoprotein
v/v	Volume/volume
WBC	White blood cells
WHO	World Health Organization

w/v	Weight/volume
%	Percentage
ºC	Degree Celsius
μg	Microgram
μL	Microlitre
μM	Micromolar

Chapter 1

Introduction and Review

Contents

1.1. Introduction

1.2. Cancer

1.2.1. Global cancer statistics

1.2.2. Cancer in Indian scenario

1.3. Causes and types of cancer

1.3.1. Causes

1.3.2. Types of cancer

1.4. Cancer biology

1.4.1. Morphological changes

1.4.2. Sovereignty in growth signals

1.4.3. High replicative potential

1.4.4. Resisting apoptosis

1.4.5. Metastasis

1.4.6. Inducing angiogenesis

1.4.7. Insensitivity to anti-growth signals

1.4.8. Metabolism

1.4.9. Genetics

1.4.9.1. Oncogenes

1.4.9.2. Tumor-suppressor genes

1.4.9.3. Micro RNA genes

1.5. Role of chronic oxidative stress and inflammation in cancer

1.5.1. Role of chronic oxidative stress in cancer development

1.5.2. Inflammation and cancer

1.6. Cancer management

1.6.1. Preventive management strategies

1.6.2. Curative treatment strategies

1.6.2.1. Surgery

1.6.2.2. Chemotherapy

1.6.2.2.1. Limitations/challenges of chemotherapy

1.6.2.3. Radiation therapy

1.6.2.4. Hormone therapy

1.6.2.5. Immunotherapy

1.6.2.6. Gene therapy

1.6.2.7. Other novel treatment types

1.6.2.8. Complementary and Alternative Medicine

1.7. Herbal medicine in cancer treatment

1.7.1. Ayurveda (Ayurvedic Medicine)

1.7.2. Traditional Chinese Medicine

1.7.3. Herbal products

1.8. Family Simaroubaceae: an analysis of its medicinal potentialities

1.8.1. Biologically potent plants belong to genus Simarouba

1.9. *Simarouba glauca* DC.

1.9.1. Description

1.9.1.1. Taxonomic classification

1.9.1.2. Common name

1.9.1.3. General characters/botanical description

1.9.1.4. Habitat

1.9.1.4.1. Geographical distribution

1.9.1.4.2. In India

1.9.2. Uses of *S. glauca* DC.

1.9.2.1. General use

1.9.2.2. Ethnobotanical uses

1.9.2.3. Pharmacological properties

1.1. Introduction

Cancer; a group of diseases, is increasingly growing as a serious health issue in both developed and developing countries along with the other chronic diseases. The disease imposes a serious economic, health and social burden to several nations. Cancer toll is rapidly increasing in low and middle-income countries, where resources for prevention, diagnosis, and treatment for this disease are limited (2018b). It is calculated that by 2025, there will be an increased rate of 19.3 million new cases per year (2019a). Surgery, radiotherapy and systemic treatments including cytotoxic chemotherapy, immunotherapy, hormonal therapy and targeted therapies are the current treatments for cancer (Palumbo et al., 2013). However, the restricted effectiveness of these therapies and their severe side effects have encouraged the search for novel anticancer agents based on natural products and plant extracts as single therapies or in combination with other medications (Talib, 2017). Preventive, as well as curative approaches, are equally important in the management of onset of cancer and its recurrence.

From time immemorial, plants are used by almost all human societies not only as a source of nutrition but also as a medicine against various diseases. They are also used by people for improving general health and wellbeing. More than 50% of all drugs used today are natural products or their derivatives. Still, all over the world, people are searching for solutions to a wide range of ailments from the common diseases to dreadful diseases including cancer.

Many modern pharmaceutical medicines are rooted in only one active ingredient, which derived from plant sources. But practitioners of herbal medicine trust that an active component can lose its impact or not become secure if used in a purified form from the rest of the plant. They believe that the effect of using crude extract is better than its purified component. Many people mistakenly believe that herbal formulations are completely safe because they are natural products. The excess or imprudent use of herbal medicines is dangerous. Herbal medicines and supplements can interact in harmful ways with pharmaceutical drugs. Taking herbal supplements may decrease the effectiveness of other drugs and may increase the negative side effects. Further, some herbal components can cause toxicity to internal organs. (Asif, 2012)

The present study is concentrated on the analysis of anti-cancer and chemoprotective activities of hot water extract of leaves of *Simarouba glauca DC*, a plant which has gained wide popularity among cancer patients in south India, especially in Kerala recently over media. Many cancer patients in the states of Goa, Karnataka and Kerala consider this tree as solace for cancer. In several parts of these states, people started growing this plant in their backyard for collecting fresh leaves for preparing a decoction. Due to the lack of scientific validation, consumption of hot water decoction prepared by *S. glauca* leaves are started a heated debate among the scientific community. The study also attempts to check the detailed phytochemical analysis and toxicity study of hot water extract of leaves of this plant by using the murine model.

1.2. Cancer

Nowadays, noncommunicable diseases (NCDs) are mainly culpable for the majority of global death, and among the NCDs, cancer is expected to rank as the principal cause and the single most important barrier to increasing life expectancy in every country of the world in the 21st century. According to the estimates of the World Health Organization (WHO) in 2015, cancer is the first or second leading cause of death before age 70 years in 91 of 172 countries, and it stands third or fourth in an additional 22 countries (Bray et al., 2018). Cancer incidence and related mortality are growing worldwide. The reasons are complex but reflect both aging and growth of the population, as well as changes in the prevalence and distribution of the main risk factors for cancer, several of which are associated with socioeconomic development (Omran, 2005, Gersten and Wilmoth, 2002). With rapid population growth and aging worldwide, the rising prominence of cancer as a leading cause of death partially reflects marked declines in death rates of stroke and coronary heart disease, relative to cancer, in many countries (Bray et al., 2018).

1.2.1. Global Cancer statistics

The latest global cancer data GLOBOCAN 2018, (GLOBOCAN 2018, an online database providing estimates of occurrence and mortality in 185 countries for 36 kinds of cancer, and for all cancer, sites combined) published in Switzerland on September 2018 estimated 18.1 million new cancer cases and 9.6 million deaths due to cancer in the year 2018. According to this report, about 48.4% of new cancer

incidence (all cancer types, in both sexes of all ages) occurred in Asian countries in 2018. Among this, 23.0 % of cancer incidence was reported in China followed by India (9.8%). The second position was occupied by European countries (23.4%), followed by North America (13.2%), Latin American and Caribbean countries (7.8%), Africa (5.8%) and Oceania (1.4%). A comparative study report published by the same agency regarding the total cancer mortality occurred among the different populations of the world in the year 2018 (9.56 million) revealed similar data to the previous statistics. Estimated number of death caused by all cancers among the population of both sexes of all ages was high in Asia (57.3%). Europe (20.3%), North America (7.3%), Africa (7.3%), Latin America (7.0%) and Oceania (0.2%) were the ordinal status of other different populations in this list (Bray et al., 2018) (Figure 1.1).

Among the different cancer types in males and females, lung cancer was the most commonly detected cancer (11.6% of the total cases) and the principal cause of cancer death (18.4% of the total cancer deaths) in the world. Female breast cancer (2.089 million), colorectal cancer (1.8 million), prostate cancer (1.3 million) and stomach cancer (1.0 million) were the other cancer types placed behind to lung cancer in the list of types of cancer with the highest rate of incidence. Colorectal cancer (9.2%), stomach cancer (8.2%), liver cancer (8.2%) and breast cancer (6.6%) were the other cancer types caused highest mortality rate around the globe during the year 2018. Among males apart from lung cancer, the most frequent type of cancer and cancer that cause a high percentage of death were prostate and colorectal cancer (for occurrence) and liver and stomach cancer (in mortality rate). As mentioned before among females, breast cancer is the prominently diagnosed cancer and the leading cause of cancer death, followed by colorectal and lung cancer and cervical cancer placed fourth for incidence. The type of frequently diagnosed cancer and cancer which causes high mortality rate, however, vary among the countries and within each country depending on the economic development and related social and lifestyle factors (Bray et al., 2018) (Figure 1.2).

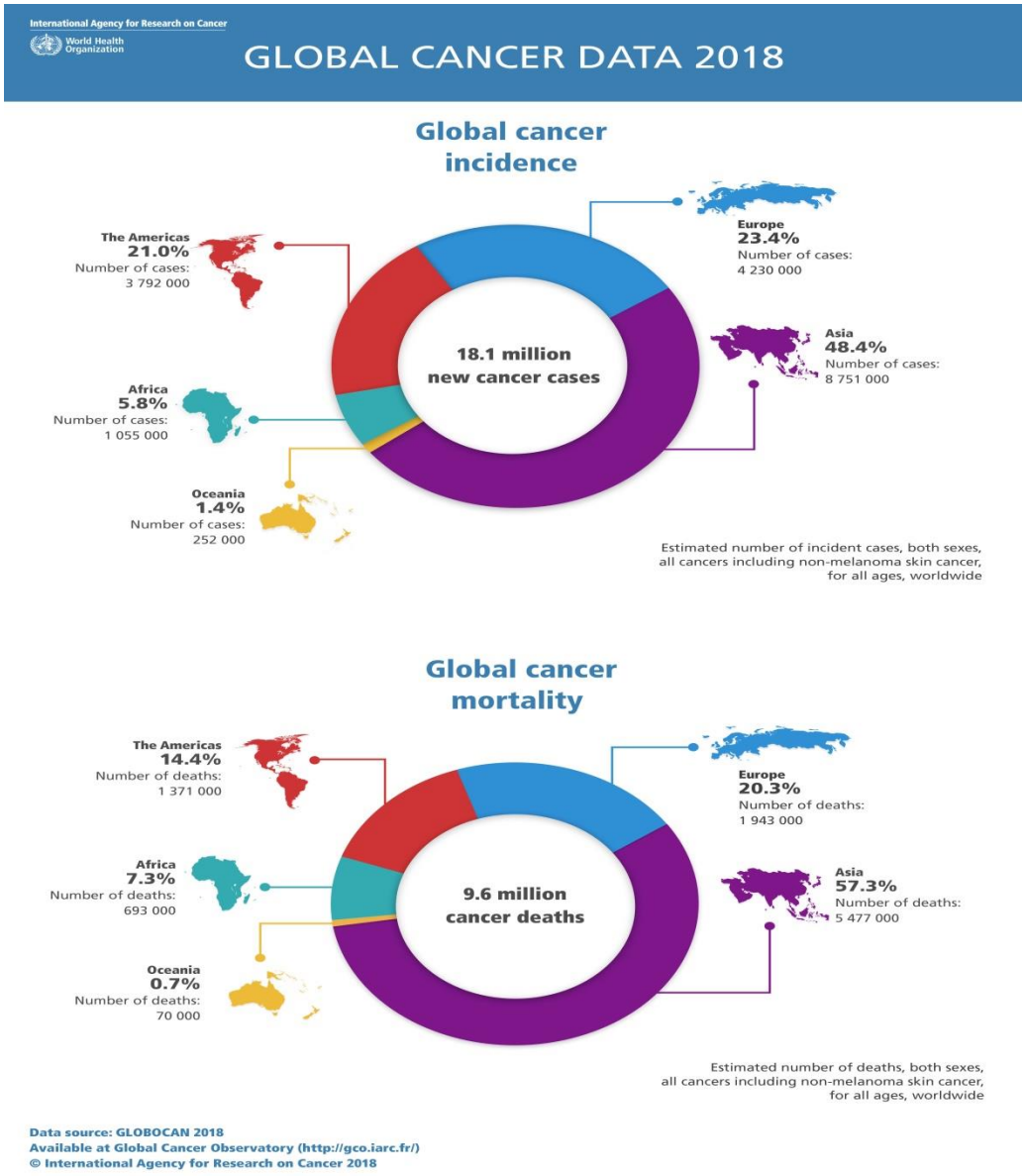

Figure 1.1. Global cancer incidence and cancer mortality in 2018 (based on GLOBOCAN 2018)

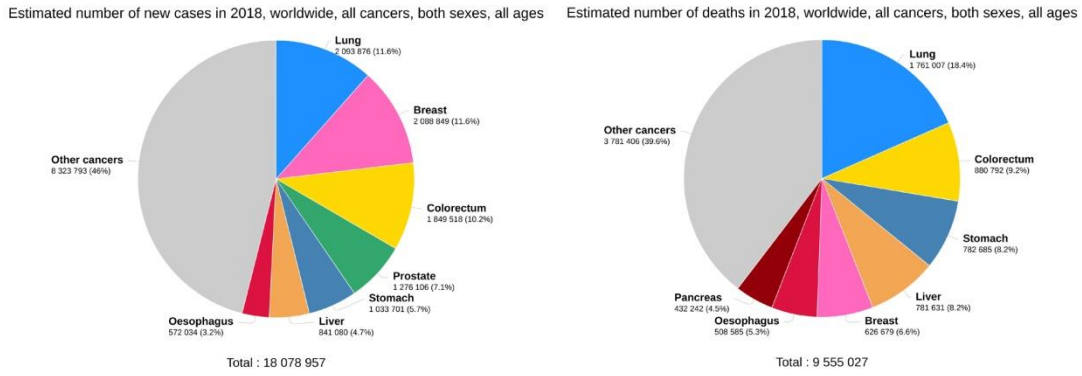

Figure 1.2. Number of new cancer incidences and deaths reported in populations of both sexes of all ages in the world during 2018 (based on GLOBOCAN 2018)

1.2.2. Cancer in Indian scenario

As per the GLOBOCAN 2018, 1.16 million number of new cancer cases (including men and women of all ages) were reported from India. Among this list, the topmost one was breast cancer (14%). It was followed by cancers related to mouth (lip or oral cavity) (10.4%), cervical cancer (8.4%), lung cancer (5.9%) and stomach cancer (5.0%). The cancer incidence related to other types of cancer was estimated at 56.4%. A total number of 7.85 lakh cancer deaths were reported in 2018 from this country. The number of deaths was more among males than females. A summary regarding the cancer statics of India during the year 2018 is given below (Table 1.1.).

Table 1.1. Incidence, mortality and prevalence of cancer among the Indian population in 2018 (source, GLOBOCAN 2018)

Summary statistic 2018			
	Males	**Females**	**Both sexes**
Population	701 546 980	652 504 878	1 354 051 855
Number of new cancer cases	570 045	587 249	1 157 294
Age-standardized incidence rate (World)	89.8	90.0	89.4
Risk of developing cancer before the age of 75 years (%)	9.8	9.4	9.6
Number of cancer deaths	413 519	371 302	784 821
Age-standardized mortality rate (World)	65.8	57.5	61.4
Risk of dying from cancer before the age of 75 years (%)	7.3	6.3	6.8
5-year prevalent cases	1 000 485	1 257 723	2 258 208
Top 5 most frequent cancers excluding non-melanoma skin cancer (ranked by cases)	Lip, oral cavity Lung Stomach Colorectum Oesophagus	Breast Cervix uteri Ovary Lip, oral cavity Colorectum	Breast Lip, oral cavity Cervix uteri Lung Stomach

The maximum number of cancer cases in India is reported from Kerala, followed by Mizoram, Haryana, Delhi and Karnataka, while it is the lowest in Bihar. In 2016, cancer occurrence rate in Kerala was 135.3 per one lakh people, while in the country it was 106.6 per one lakh people. The mortality and disability rates due to cancer are also high in Kerala. The highest death rate for both sexes related to cancer was highest in Mizoram, followed by Kerala and Haryana. Kerala had witnessed 73.5 deaths per one lakh females and 103.4 per one lakh males in 2016. It is believed that the presence of a high number of aged people when compared to the rest of the country, maybe the main reason for this high incidence of cancer occurrence in Kerala (2018a). It is very clear that cancer is an urgent challenge and governments and people working in health sector must take measures to scale up prevention, early detection and diagnosis, treatment and care services.

1.3. Causes and types of cancer

1.3.1. Causes

Usually, the development of cancer occurs due to the end result of multiple mutations in many genes concerned in controlling the growth of cells and malformed metabolic changes in tumor cells and the tumor microenvironment that make possible or hurry the ultimate growth of cancer (Pickup et al., 2014). Cancer risk factors are generally divided into two mutually exclusive components like intrinsic risk factors and non-intrinsic risk factors. Intrinsic risk factors are unmodifiable but the non-intrinsic risk factors are modifiable or partially modifiable. The intrinsic risk factors of cancer denote to random errors resulting from DNA replication. The non-intrinsic factors are further classified into exogenous and endogenous risk factors depending on whether such factors are more external or internal to a person (Table 1.2) (Wu et al., 2018).

Table1.2. Major risk factors associated with cancer (source: Wu et al., 2018)

Intrinsic risk factors	**Non-intrinsic risk factors**	
	Endogenous risk factors	**Exogenous risk factors**
• Random errors in DNA replication (Unmodifiable)	• Biologic aging • Genetic susceptibility • DNA repair machinery • Hormones • Growth factors • Inflammation (Partially modifiable)	• Radiation • Chemical carcinogens • Tumour causing viruses • Bad lifestyles such as smoking, lack of exercise, nutrient imbalance (Unmodifiable)

1.3.2. Types of cancer

Cancer is not a single disease. Over a hundred different types of cancers affect human beings (2015b). There are a number of ways in which cancers are named and grouped, including based on their point of beginning (cell, tissue, area), DNA profile, tumor

grade, stage, etc. Cancers are primarily named for the part of the body in which they originate and the form of cell they are made of, even if they metastasize. Primarily cancers may be referred to as solid type or blood-related cancer types. Blood-related cancers consist of lymphomas, leukemias, myelomas, etc. While solid cancers include all the other types.

Based on cell or tissue type cancers are differentiated into Carcinomas (most common type of cancer, cancer arise in epithelial cells), Sarcomas (cancer originates in mesenchymal cells), Myelomas (cancer of cells in the immune system; plasma cells), Leukaemias (cancer of blood cells), Lymphomas (cancer in the immune system cells and may arise in lymph nodes and spleen) and mixed types (including blastomas). Each one of these said categories of cancer is further divided into many subcategories. For example, there are different subtypes under carcinoma includes adenocarcinomas, squamous cell carcinomas, basal cell carcinomas, transitional cell carcinomas, etc. (2018c).

Cancers are also classified by the organ systems or organs in which they originate. For example a) Central Nervous System Cancers (cancer in brain or in spinal cord) b) Head and Neck Cancers (oral cancer, throat cancer, laryngeal cancer, cancer in tongue, tonsils, nasal passage and pharynx) c) Breast cancers d) Respiratory cancers e) Digestive System Cancers (Oesophageal cancer, Stomach cancer, Pancreatic cancer, Liver cancer, Colon cancer, Anal cancer) f) Urinary System Cancers (Kidney cancer, Bladder cancer, Prostate cancer) g) Reproductive System Cancers (Testicular cancer, Ovarian cancer, Fallopian tube cancer, Uterine cancer, and Cervical cancer) h) Endocrine System Cancers (Thyroid cancer, Multiple Endocrine Neoplasia) i) Bone and Soft Tissue Cancer (Osteosarcoma, Kaposi's Sarcoma, Ewing's Sarcoma) j) Blood-related cancers (Myeloma, Leukaemia, Lymphoma) k) Skin Cancers (Melanoma, Non-melanoma) (2019b)

1.4. Cancer biology

In simple words, cancer biology includes the detailed understanding of unique characteristics of cancer cells, which facilitates the tumour growth and metastasis and also comprehends the role of tumour microenvironment in the development of tumour (Bertram, 2000). Hanahan and Weinberg (2000) published a detailed review of the

intricacies of cancer biology. They categorized the complex biology of cancer into six major hallmarks. According to them, the major characters of cancer include, self-sufficiency in growth signals, evading growth suppressors, avoiding apoptosis, high replicative potential, promoting angiogenesis and active tissue invasion and metastasis (Figure1.3).

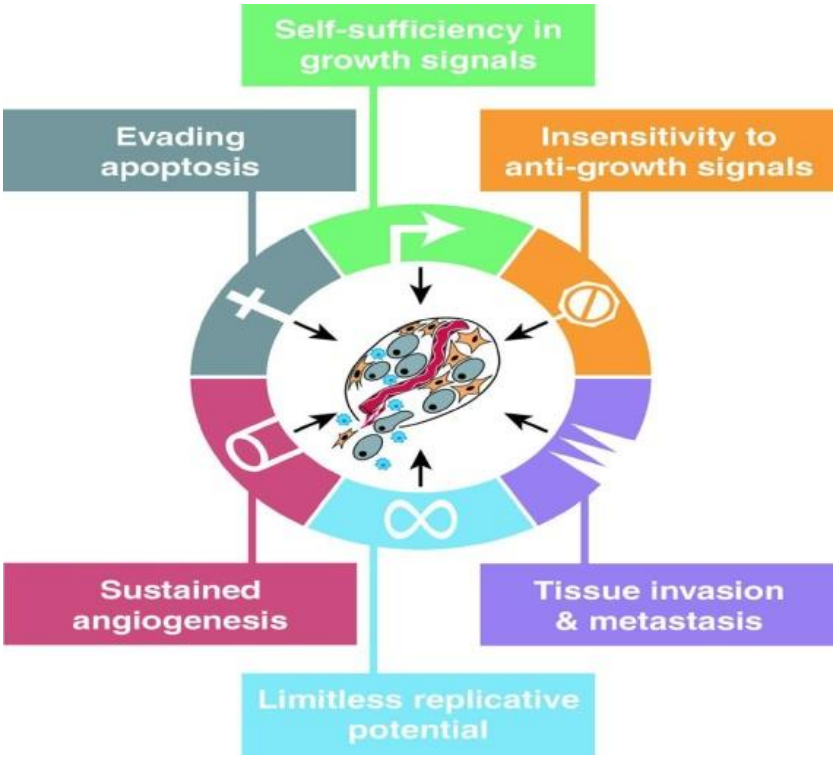

Figure 1.3. Acquired characteristics of cancer (Hanahan and Weinberg, 2000)

In 2011, they added two more hallmarks of cancer cells to the existing list: reprogramming of energy metabolism and avoiding immune response. The factors which foster the hallmarks of cancer cells are genomic instability, which causes genetic diversity and inflammation. Generation of tumour microenvironment by a stock of recruited, ostensibly normal cells increases the dimension of complexity of tumours (Hanahan and Weinberg, 2011) (Figure 1.4).

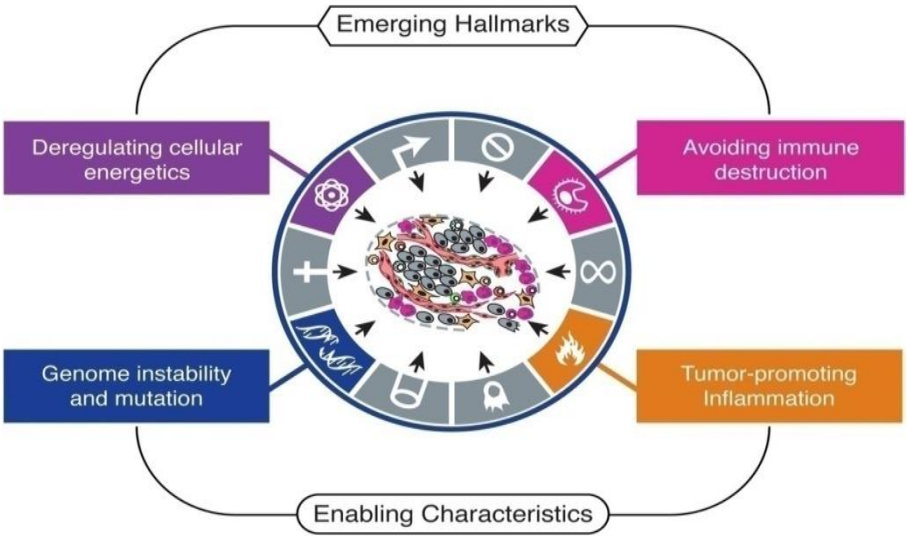

Figure 1.4. Emerging hallmarks and enabling characteristics of cancer (Hanahan and Weinberg, 2011)

1.4.1. Morphological changes

Cancer cells show altered and abnormal morphology when compared with normal cells from the same tissue. In general, a cancerous cell is morphologically characterized by a large nucleus. The nuclei may be irregular in size and shape (pleomorphic). The nucleus is very large and the cytoplasm of the cancer cells is scarce so cancer cells show high nucleo-cytoplasmic index. The nucleoli of cancer cells are very prominent. The cell adhesion capacity of cancer cells is very less. The reason behind the distorted morphological characteristics directly connected with the alternations which occurred in their genetic level. A lot of surface molecular changes occur in the plasma membrane, which plays a very important role in cancer cell formation. Increase or decrease in the number of surface receptors, structural changes occur to the surface receptors and presence of new surface molecules, etc. are the major changes occur in the plasma membrane during the transformation of a normal cell to a cancer cell (Baba A. I., 2007).

1.4.2. Sovereignty in growth signals

Normal cells can do cell division only in the presence of growth signalling molecules. Many of these signalling molecules are originated exogenously. The growth signals are transmitted into the particular cells by transmembrane receptors which bind distinctive classes of signalling molecules like (a) diffusible growth factors, (b) extracellular matrix components and (c) cell to cell adhesion or interaction molecules.

Cancer cells are able to sustain the proliferative signalling in many alternative ways. Tumour cells generate growth factor ligands by themselves and thereby reduce their dependence on stimulation from normal tissue environment (autocrine proliferative stimulation) (Hanahan and Weinberg, 2011). Cancer cells may motivate normal cells within the tumor-associated stroma to produce various growth factors for them (Cheng et al., 2008). Deregulation of receptor signalling by increasing levels of receptor proteins on the cell surface, making such cells over-responsive to the negligible quantity of growth factor ligand is another way of attaining self-sufficiency in growth signals by cancer cells. Making structural alternation in the receptor for growth signalling molecules may also support ligand-independent stimulation of cell proliferation. Another unique mechanism which helps the cancer cells to skip the requirement of specific growth factors for proliferation is the activation of post-receptor pathways, which circumvent the growth factor receptor requirement for cell division. The acquired capability of cancer cells in the self-sufficiency in growth signals disrupts the homeostatic mechanisms of the body that regulates to ensure normal behaviour of the cells within the tissue.

1.4.3. High replication potential

Cancer cells exhibit unlimited replicative potential (immortalization). The foremost reason regarding the high replicative potential of cancer cells is the significant levels of the enzyme telomerase, which protect the terminals of chromosomes. Tumour cells can prevent telomere loss by aberrantly doing the upregulation of telomerase (Blasco, 2005). The presence of high telomerase and their related action is very much correlated with the resistance of both senescence and apoptosis (Hanahan and Weinberg, 2011). Another reason which permits limitless replication potential of cancer cells is the presence of faulty proteins which controls different events of the cell cycle. The different steps of the cell cycle are strictly regulated by a large number of factors in the normal cells. A cell begins to do nuclear division (first part of cell division) only when exposed to a variety of growth-promoting factors and growth-inhibiting factors in required levels. Different checkpoints exist at different levels of the cell cycle if a previous step has occurred without error the only the cell determines to proceed the next stage of cell division (Pelengaris, 2006).

1.4.4. Resisting apoptosis

The cell death programme, apoptosis is a natural cellular mechanism, which helps the multicellular organisms to destroy the worn out or aged cells. It helps in organ sculpting during embryonic development and also facilitates the adult tissue homeostasis (Gregory and Paterson, 2018). Macrophages phagocytise the apoptotic cells including their membrane-bounded apoptotic fractions (Pelengaris, 2006). The machinery of apoptosis composed of upstream regulators and downstream effectors (Adams and Cory, 2007). The regulators involved in apoptotic machinery are categorised into two major circuits like extrinsic and intrinsic pathways. Extrinsic pathway receives and processes the extracellular death-inducing signals and intrinsic pathway detects the variety of death promoting signals which evolve in the cell itself (intracellular origin). Each of these pathways can activate the dormant protease (caspases 8 and 9, respectively), which further proceeds to a series of proteolytic actions by involving effector caspases (Hanahan and Weinberg, 2011). The counterbalanced action between pro and anti-apoptotic members of the Bcl-2 family proteins conveys the apoptotic trigger signals between the regulators and effectors involved in apoptosis (Adams and Cory, 2007).

Cancer cells have evolved a variety of mechanisms to limit or to avoid apoptosis. The loss of tumour protein 53 (TP53) suppressor function is the prime important one. Increasing expression of anti-apoptotic regulators like Bcl-2, Bcl-x_L and survival signals (eg., lgf 1/2), are other mechanisms cancer cells use to avoid apoptosis. The down regulations of proapoptotic factors like Bax, Bim, Puma, etc. are occurring in tumour cells simultaneously (Hanahan and Weinberg, 2011).

1.4.5. Metastasis

It is the spreading of cancer cells from their original site to adjacent tissues and founding new tumour growth. 90% of human cancer deaths are directly linked with metastases (Sporn, 1996). Metastasis is a multistep process which includes invasion, intravasation, dissemination, extravasation and colonization and known as the invasion-metastasis cascade (Talmadge and Fidler, 2010). Development of alterations in the shape and cell to cell attachment due to the less expression of E-cadherin molecules in cancer cells helps them to perform invasion and metastasis (Berx and

van Roy, 2009). The invasion and metastasis of cancer cells are broadly supported by Epithelial-Mesenchymal-Transition (EMT) programme (Klymkowsky and Savagner, 2009). It has been proven that some superfluous communication between cancer cells and neoplastic stroma cells is directly linked to invasiveness and metastasis (Egeblad et al., 2010). Metalloproteinases and Cysteine cathepsin proteases (matrix-degrading enzymes) released by macrophages on the tumour periphery can stimulate invasion of cancer cells (Kessenbrock et al., 2010). Interleukins (IL-4) released by the cancer cells stimulate the said action of invasion promoting macrophages (Gocheva et al., 2010). Extracellular matrix digesting enzymes and other factors produced by inflammatory cells, which assembles in the tumour boundaries facilitates the cancer cell invasion (Kessenbrock et al., 2010).

Invasion of cancer cells may be “collective invasion” and “amoeboid invasion”. In collective invasion cancer cells move as a group into adjacent tissues but in amoeboid form of invasion individual cancer cells show morphological efficacy, which enables them to pass through the extracellular matrix to vascular structure and finally to reach in new localities (Madsen and Sahai, 2010).

1.4.6. Inducing Angiogenesis

Tumour requires a steady supply of nutrients and oxygen for their proliferation and an efficient evacuation system for the removal of metabolic wastes and carbon dioxide. Normal vasculature of tissue wherein tumor grows is inefficient to satisfy this. During tumour progression, the sprouting of new blood vessels (angiogenesis) can be noted that help the expansion of neoplastic growths (Hanahan and Folkman, 1996). The angiogenesis which occurs during tumour progression occurs when the balance between pro and anti-angiogenic factors lean towards a pro-angiogenic state to the vascularized tumour and finally to a malignant tumour (Baeriswyl and Christofori, 2009). Vascular Endothelial Growth Factor-A (VEGF-A) and Fibroblast Growth Factor (FGF) are identified as angiogenesis inducers though their expression is chronically upregulated during tumour progression (Baeriswyl and Christofori, 2009). Thrombospondin-1 (TSP-1), which has transmembrane receptors on endothelial cells is considered a counterbalancing molecule in angiogenesis (Kazerounian et al., 2008).

1.4.7. Insensitivity to anti-growth signals

In normal tissue, the tissue homeostasis is maintained by multiple anti-growth signals. These factors or signals include soluble growth suppressors and inhibitors fixed in the extracellular matrix and on the plasma membrane of nearby cells. These anti-growth signals are received by particular transmembrane cell surface receptors, which coupled to intracellular signalling pathways.

Cancer cells possess an unlimited capability to evade from the action of these anti-growth signals. For example disruption of retinoblastoma protein (pRb) pathway liberates E2Fs transcription factors, which regulate the expression of many genes essential for the progression of the cell cycle from the G1 phase into S phase, facilitates cell proliferation. Transforming or Tumour Growth Factors (TGF) especially TGFβ is a soluble signalling molecule which plays crucial roles in tissue regeneration, cell differentiation, and embryonic development is upregulated in many human cancers (Hanahan and Weinberg, 2000).

1.4.8. Metabolism

Cancer metabolism denotes the alternations in cellular metabolism pathways that are obvious in cancer cells compared with the majority of normal tissue cells. It is often considered as an adaptation to sustain cancer proliferation. Change in metabolic pathways in cancer cells is not only required for energy production but also essential for the synthesis of substances like nucleotides, proteins, and lipids. They act as the building blocks to support uncontrolled tumor proliferation and growth. Acquisition of necessary nutrients from a normally nutrient-deprived environment and use these nutrients for existence and proliferation is a common feature of cancer cell metabolism (DeBerardinis and Chandel, 2016). The variations in intracellular and extracellular metabolites that can go together with cancer connected metabolic reprogramming have intense effects on cellular differentiation, gene expression, and the tumor microenvironment. According to Pavlova and Thompson (2016), six major changes occur in the metabolism of cancer cells. They are (a) deregulated intake of glucose and amino acids, (b) utilization of opportunistic modes of nutrient gaining, (c) use of glycolysis/TCA cycle intermediates for the biosynthesis and NADPH production, (d) an increased demand for nitrogen, (e) change in metabolite driven

gene regulation, and (g) metabolic interactions with the microenvironment (Pavlova and Thompson, 2016). It is not apparent to see all above-mentioned hallmarks in all tumors, but most of them show several.

Many factors especially physiological stresses are one of the main drivers that make a change in the metabolic switch in tumor cells. Hypoxia (lack of oxygen), increased levels of reactive oxygen species (ROS), are important among them (Gentric et al., 2017). Under hypoxia, the hypoxia-inducible factor-1 transcription factor accumulates and provides oxygen to tumor cells by increasing angiogenesis, erythropoiesis, and glycolysis (Casazza et al., 2014).

Glucose utilization and carbon sources in tumors are much more heterogeneous than initially thought. New studies have revealed a dual capacity of tumor cells for glycolytic and oxidative phosphorylation metabolism (Gentric et al., 2017).

1.4. 9. Genetics

Basically, cancer is a genetic disease and is caused by some alterations to genes that control the way the cells function, particularly how do they grow and multiply. Cancer-causing genetic alterations can be inherited from parents or acquired during a lifetime. It is significant that each person's cancer has a unique combination of genetic changes. Inherited genetic mutations play a major role in about 5 to 10% of all cancers (2017c). Cancer is caused by changes which occur in oncogenes, tumor suppressor genes and microRNA genes. A single genetic alteration is insufficient for the development of a malignant tumour. Most of the experimental evidence point to a multistep process of sequential changes in numerous, often many, oncogenes, tumor-suppressor genes, and micro RNA genes in cancer cells (Croce, 2008).

1.4.9.1. Oncogenes

Oncogenes support the initiation of tumor in different organs of the body. They mainly encode proteins that control cell proliferation, apoptosis, or both. They are activated by structural alterations due to mutation or gene fusion, by juxtaposition to enhancer elements, or by amplification. The products of oncogenes are classified into six broad categories: transcription factors, growth factors, growth factor receptors,

chromatin remodelers, signal transducers, and apoptosis regulators (Croce, 2008). Examples and action of some oncogenes are given in a table (Table 1.3).

Table 1.3. List of oncogenes and their action

Name of the oncogene	Proto-oncogene action	Method of activation of the gene	Cancer
Myc	Transcription factor	Amplification, Translocation, and deregulation	Neuroblastoma, glioblastoma and cancer in breast, stomach, colon, lung, and cervix.
Jun	Transcription factor	Deregulation	Sarcoma
Fos	Transcription factor	Deregulation	Osteosarcoma
Ras (K-ras)	GTP-binding protein	Mutation	Pancreatic cancer, colorectal carcinoma, and non-small cell lung carcinoma
Src	Tyrosine-specific protein kinase	Mutation	Colon, breast, and prostate
ErbB	Epidermal growth factor receptor	Deregulation	Breast, ovarian, bladder, non-small cell lung carcinoma
Sis	Platelet-derived growth factor		Glioma/fibrosarcoma

1.4.9.2. Tumor-suppressor genes

Tumor suppressor genes play a pivotal role in preventing the development of tumor cells. These genes code for proteins, which regulate the growth and proliferation of the cells. When these genes are altered or inactivated by mutation, they make less effective protein molecules. Some tumor suppressor genes and their action and cancer associated with their malfunction are given below (Table 1.4).

Table 1.4. List of tumor suppressor genes and their action

Name of the Tumor suppressor gene	Action	Cancer-associated with its dysfunction
BRCA1 & BRACA2	DNA repair	Breast cancer, ovarian cancer
MSH2		Colon cancer
pRb/P53/TP53	Cell cycle regulation	Retinoblastoma, sarcoma, lymphoma, breast cancer and brain tumor
CDKN2A		Sarcoma, lymphoma and Melanoma
CDKN2C/INK4C		Testicular cancer
WT1	Transcription regulation	Kidney cancer in children
VHL		Hemangioblastoma, pheochromocytoma, renal cancer
PTEN	Cell signalling	Breast cancer, prostate cancer, and tumor growth in the brain

1.4.9.3. Micro RNA genes

Unlike other genes, micro RNA genes, are involved in cancer do not encode any proteins. The product of these genes is a single RNA strand (21 to 23 nucleotides). The main function of this RNA strand is regulation of gene expression. The micro RNA molecule is capable of annealing with a messenger RNA containing a nucleotide sequence which complements the sequence of the micro RNA. By this way, the micro RNA can block protein synthesis and also makes the degradation of the messenger RNA. For example, miR-15 and miR16-1, are deleted or down-regulated in chronic

lymphocytic leukaemia, suggesting an early event in the pathogenesis of this disease (Calin et al., 2002).

1.5. Role of chronic oxidative stress and inflammation in cancer

Many risk factors associated with cancer (a western-style diet, obesity, consumption of variety of soft drinks, alcohol consumption and smoking) and pathophysiological conditions (chronic infections) are responsible for genetic instability mediated by oxidative stress in the body. Chronic oxidative stress either endogenous or exogenous factors or together connected with inflammation may contribute to different steps of cancer formation.

1.5.1. Role of chronic oxidative stress in cancer development

Two important oxidative molecules, Reactive oxygen species (ROS) and reactive nitrogen species (RNS) are constantly formed inside the cell in minuscule during the normal cell metabolism. Oxidative molecules produced by cells, especially neutrophils have a dual role. On one way they act as potent antimicrobial agents to kill invaded microbial pathogens directly. On the other hand, they act as signalling molecules that control diverse physiological signalling pathways in the cells. They also function as modulators of protein and lipid kinases and phosphatases, ion channels, membrane receptors, and many transcription factors including NF-kB. This is the way by which they are connected with the inflammatory response of the body and can modulate phagocytosis, gene expression, apoptosis and further secretion of chemical molecules (Fialkow et al., 2007). Mild oxidative stress occurs on a daily basis is considered as a key factor in maintaining homeostasis (Prasad et al., 2017).

But, this excess amount of these ubiquitous, short-lived, highly reactive chemical molecules contain oxygen can react with neighbouring molecules at the time of formation. Everyday exposure to strenuous physical exercise and psychological or environmental stress provoke changes on the cellular level resulting in excessive production of reactive oxygen species (ROS) and reactive nitrogen species (RNS). Therefore, cells are evolved very efficient enzymatic and non-enzymatic antioxidant mechanisms to handle the ROS and other oxidative molecules. If the antioxidant mechanisms are overwhelmed by ROS and other oxidative molecules it creates oxidative stress which can cause cancer by inducing DNA damage to cells. The

modulatory action of ROS on cell signalling pathways, via biomolecules like NF-kB and STAT3, hypoxia-inducible factor-1α, growth factors, cytokines, kinases and other enzymes and proteins, supports cellular transformation, chronic inflammation, tumour survival, proliferation, angiogenesis, invasion and metastasis (Fu and Xie, 2019, Prasad et al., 2017).

The antioxidant defence system in the human body includes enzymes like catalase (CAT), superoxide dismutase (SOD), glutathione reductase (GR), glutathione peroxidase (GPx), glutathione S-transferase (GST) and non-enzyme molecule glutathione (GSH) (Paulsen and Carroll, 2013). ROS form in our body include oxygen radicals [superoxide ($O_2^{\bullet -}$), peroxyl ($RO_2\bullet$), hydroxyl ($\bullet OH$) and alkoxyl ($RO\bullet$)] and some nonradicals that are either oxidising agents or easily converted into radicals, like hypochlorous acid (HOCL), singlet oxygen ($^1O_2$), ozone (O_3) and hydrogen peroxide (H_2O_2). As already stated many endogenous and exogenous sources can produce ROS in the body. ROS of endogenous origin is chiefly originated as by-products in intracellular organelles such as mitochondria, peroxisomes, etc. Exogenous sources of ROS include tobacco, smoke, different drugs, pollutants, xenobiotics, and radiation (Prasad et al., 2017). Ionising radiations generate ROS through their interaction with water (Poljsak and Dahmane, 2012). Many intracellular mechanisms are involved in the production of intracellular ROS, which varies based on the cell and tissue types. NADPH oxidase (NOX) complexes found in cell membrane, mitochondria, peroxisomes and endoplasmic reticulum are primarily responsible to generate ROS instead of producing ROS as a by-product (Hernandes and Britto, 2012). A detailed account on the involvement of ROS and ROS inducer at various stages of tumourigenesis is given in table (Table 1.5).

Table 1.5. List of some ROS inducers/mediators involved in cancer types

ROS inducer/ mediator	Cancer type
In Transformation of cells	
Chromium (VI)	Lung cancer (Kryston et al., 2011)
Cigarette smoke	Breast cancer (Li et al., 2011)
Benzo[a]pyrene	Lung cancer (Wang et al., 2011)
Arsenic	Lung cancer (Huang and Zheng, 2006), (Azad et al., 2010)

In Cancer cell survival	
Lithium chloride	Colorectal cancer cells (Edderkaoui et al., 2005)
In Cancer cell proliferation	
Cancer-derived IgG	Breast cancer (Venkataraman et al., 2004)
peroxiredoxin	Breast cancer (Qin, 2010)
Sodium arsenite	Breast cancer (Muniyan et al., 2015)
In Cancer cell invasion	
Adrenaline/noradrenaline	Breast cancer (Liu et al., 2014)
Epidermal growth factor	Prostate cancer (Ruiz-Ramos et al., 2009)
Mitochondrial dysfunction	Breast cancer (Ma et al., 2013)
Ionising radiation	Breast cancer (Yamazaki et al., 2014)
Ethanol	Breast cancer (Ma et al., 2013)
In angiogenesis	
Cyclosporine A	Endothelial cells (Luanpitpong et al., 2010)
Ethanol	Colon cancer (Maulik and Das, 2002)
NADPH oxidases	Several cancer (Li et al., 2013)

1.5.2. Inflammation and cancer

Numerous studies have shown a strong relationship between cancer and chronic inflammation and it is one of the most important fields for both clinical and translational research (Allavena et al., 2011). Inflammatory infiltrates are observed both in benign and in malignant lesions. Inflammatory cells can express and release several cytokines, which are capable to activate signal cascades involved in the cell growth, proliferation (Schillaci et al., 2019) and distant spread (Mantovani et al., 2010).

Tumor Necrosis Factor (TNF), Nuclear Factor Kappa B (NF-kB), interleukin (IL), 1β, IL6, IL 18, CCR7, CCL21 and PTX 3 are important molecules related with inflammation. TNF is involved in the stimulation of tumour angiogenesis in the development of prostate cancer and also play a significant role in both epithelial to mesenchymal transition and the aberrant regulation of eicosanoid pathways (Tse et al., 2012). NK-kB is critical in human health, and unusual activation of this molecule

contributes to the development of different diseases and malignant tumors (Park and Hong, 2016). Chemokines and their receptors are very important molecules in cancer-related inflammation (Mantovani et al., 2010). Moreover, the inflammatory infiltrate accelerates the tumor neoangiogenesis, DNA damage, remodelling of cytoskeletal structures and extracellular matrix degradation which facilitates the growth of nearby cells (Coussens and Werb, 2002). Many chronic conditions, (both abiotic and biotic) are associated with neoplasms and they are given in the table (Table 1.6) below (Coussens and Werb, 2002)

Table 1.6. Chronic conditions and biological agents associated with the induction of cancer

Pathogenic condition	**Neoplasm associated with**	**Aetiological agent**
Asbestosis, silicosis	Mesothelioma, lung carcinoma	Asbestos fibres, silica particles
Bronchitis	Lung carcinoma	Silica, asbestos, smoking (nitrosamines, peroxides)
Cystitis, bladder inflammation	Bladder carcinoma	Chronic indwelling, urinary catheters
Gingivitis, lichen planus	Oral squamous cell carcinoma	
Inflammatory bowel disease, Crohn's disease, chronic ulcerative colitis	Colorectal carcinoma	
Lichen scleroses	Vulvar squamous cell carcinoma	
Chronic pancreatitis, hereditary pancreatitis	Pancreatic carcinoma	Alcoholism, a mutation in the trypsinogen gene on chromosome no. 7
Reflux oesophagitis, Barrett's oesophagus	Oesophageal carcinoma	Gastric acids
Sialadenitis	Salivary gland carcinoma	
Sjoren syndrome, Hashimoto's thyroiditis	MALT lymphoma	
Skin inflammation	Melanoma	Ultraviolet light

Cancers associated with infection agents		
Opisthorchis, Cholangitis	Cholangiosarcoma, colon carcinoma	Liver flukes (*Opisthorchis viverrini*), bile acids.
Chronic cholecystitis	Gall bladder cancer	Bacteria, gall bladder stones
Gastritis/ulcers	Gastric adenocarcinoma, MALT	*Helicobacter pylori*
Hepatitis	Hepatocellular carcinoma	Hepatitis B and/or C virus
Mononucleosis	Non-Hodgkin's lymphoma, squamous cell carcinomas, Kaposi's sarcoma	Human immunodeficiency virus, human herpesvirus type 8
osteomyelitis	Skin carcinoma in draining sinuses	Bacterial infection
Pelvic inflammatory disease' chronic cervicitis	Ovarian carcinoma, cervical/anal carcinoma	Gonorrhoea, Chlamydia, human papilloma virus
Chronic cystitis	Bladder, liver, rectal carcinoma, follicular lymphoma of the spleen	Schistosomiasis

1.6. Cancer management

It is noted that about 90-95% of cancer can be preventable. This is possible only by avoiding the risk factors associated with its origin. Genetic predisposition factors account for 5-10% of cancer development and cancers originate due these factors are difficult to prevent. It has been noted that all most all risk factors connected with the formation of cancer are chronic oxidative stress and associated inflammatory conditions. Managing chronic oxidative stress and associated inflammatory responses require prime importance in cancer management. Two management strategies either alone or together practice by people for defeating cancer. They are preventive management strategies and curative management strategies.

1.6.1. Preventive management strategies

The primary aim of preventive management strategies of cancer prevention is to totally prevent or make delay the beginning of cancer by adopting an appropriate

method or combination of methods. The different primary cancer-preventive management strategies include maintenance of healthy lifestyle, evading of exposure to carcinogens or toxicants and consumption of dietary agents and drugs which have chemopreventive potential. The secondary aim of preventive management strategies of cancer depends on the earlier detection of cancer which may help the better management and treatment of the disease. The tertiary aim of cancer prevention engages the reduction of risk of spreading of cancer cells (metastases), secondary tumour formation and recurrence, by using preventive agents (Zubair et al., 2017) Vitamins, minerals and many natural products from various botanicals and herbs have been confirmed all the three aims of cancer prevention (Janakiram et al., 2016, Chih et al., 2013) Among the diverse types of natural products, phytochemicals plays a pivotal role. Dietary intake of fruits and herbal medicines is considered as an effective and convenient method of administering these phytochemicals in an effective way (Terry and Wolk, 2001, Van Duyn and Pivonka, 2000). According to Tseng M., (2009) 20% of all types of cancers can be avoided by the consumption of a diet with rich in fruits and vegetables (>400 gm/ day) as source of phytochemicals. But, unfortunately the efficacy showed by various phytochemicals in the laboratory has not been able to reproduce in the clinic. There are several reasons for this like the inherent differences between human physiological conditions and *in vitro* laboratory conditions. The reduction in bioavailability of phytochemicals in the body tissue may be another possible reason for its lesser performance. Majority of the phytochemicals present in human diet are metabolized and cleared by the body so, their availability to systems and the therapeutic effects may be minuscule (Stylos et al., 2017). Because of their dietary origin, phytochemical are generally considered as lesser toxic and better tolerated in the body. Curcumin, resveratrol, honokiol, plumbagin and epigallocatechin-3-gallate are important phytochemicals present in various dietary substances with proven anticancer potentials.

1.6.2. Curative treatment strategies

Curative treatment strategies focus on the elimination of cancer cells in the body. Though cancer has many different origins it must be treated by adopting different treatment methods. The type of treatment that a patient must receive depend on the type of cancer he has and how advanced it is. The doctors also consider the possible

side effects and the patient's overall health and preferences, etc. for deciding the treatment modality for cancer. Some patient with cancer will have only one treatment but, most people have a combination of treatments. Complete cure from cancer without getting any damage to the rest of the body organs is the ultimate goal of curative strategies of cancer treatment.

Even if a lot of curative treatment modalities are available to combat cancer the success stories are few in case of cancer diagnosed in later stages. There are several difficulties exists in cancer treatment. Targeting cancer stem cells (CSCs) is considered as a prime difficulty in cancer treatment. The study on CSCs is still in its early days, so several barriers have to be overcome for the identification and targeting cancer cells. The self-renewal process of several cancer cells is still unidentified. Development of drug resistance capacities of cancer stem cells is another obstacle to modern cancer treatment strategies. The drug resistance characters of CSCs make them invulnerable to many anticancer drugs. The third impediment modern cancer treatment modalities face is the deficiency of cancer epigenetic profiling techniques and specificity of currently using epi-drugs. Apart from these, the non-specific nature of cancer symptoms makes diagnosis difficult and is considered as another impediment in modern cancer treatment strategies (Chakraborty and Rahman, 2012).

Cancer can be treated by chemotherapy, surgery, targeted therapy, radiation therapy, hormone therapy, immunotherapy, etc.

1.6.2.1. Surgery

It is a medical procedure to examine, remove or repair non-haematological body tissues. The main goal of surgery to treat cancer may be curative (to remove the tumor or cancerous tissue from a specific part in the body). Since the tumour is in a specific location, surgery is most effective at an early stage of the disease. Surgery is also effective to treat cancer that has spread from where it originated to other parts of the body. During surgery, the surgeon removes a small amount of normal tissue all around and few lymph nodes close to cancer to make sure that there are no cancer cells left behind. The quantity of normal tissue will be excised strictly depends on the type and location of the tumour. The lymph node dissection will help the grading of cancer. Surgery can be done for preventing cancer, for diagnosis and to identify the

stage or grade of cancer, for relieving symptoms of cancer for lowering the chance of recurrence of cancer, for repairing damaged tissues (reconstructive surgery), for supporting other treatment modalities, for supporting body functions (like breathing and getting enough nutrition) etc. Surgery is also done along with other treatment modalities (chemotherapy and radiation therapy). Conducting surgery may not be possible in all the situations like the position of cancer makes it complicated to remove without damaging nearby organs, big cancer tumour, cancer is too tiny to be seen by the surgeon or to detect by tests, general health of patient makes the surgery too risky. If the entire tumor cannot be removed (curative surgery), the surgeon removes the cancerous tissue as possible. This will help the reduction of a number of cancer cells present in the organ and is called cytoreductive surgery. This method of surgery may make other treatment modalities like chemotherapy and radiation therapy more effective. Neo-adjuvant therapy is the treatment method to give to reduce the size of a tumour before surgery. Chemotherapy, radiation therapy or both may be given as neoadjuvant therapy. The further treatment given to the patient for complete cure from the disease is called adjuvant therapy. Chemotherapy, radiation therapy or both can be used as adjuvant therapy. This will not be started too soon after surgery because they can affect the wound healing ability in a negative way (2011).

1.6.2.2. Chemotherapy

In this treatment modality, one or more anticancer drugs or chemotherapeutic agents are used to manage the disease. The main intention of chemotherapy may be curative, or it targets to prolong life or to lessen the symptoms of cancer (palliative chemotherapy). In a combined chemotherapy method, anticancer drugs are used along with some other traditional chemotherapeutic agents. In general chemotherapeutic drugs are cytotoxic and they impede the cell division, which leads to apoptosis and finally cells death. Salvage chemotherapy or palliative chemotherapy is given without the intention of healing the disease, but reduce tumor burden and increase life expectancy. Because only a small portion of the cells in a tumor die with each treatment, frequent doses must be administered to continue to decrease the size of the tumor. The frequency and duration of chemotherapeutic drug administration are limited by toxicity (2016).

There are many categories of drugs available for chemotherapy. According to the different cell cycle phases targeted by these agents, they're grouped into a) alkylating agents, b) anti-microtubule agents, c) anti-metabolites and d) topoisomerases inhibitors. Other than these, many cytotoxic antibiotics, enzymes, and biological agents targeting gene expression and signal transduction are used in chemotherapy (Table 1.7).

Most chemotherapeutic agents are delivered intravenously, although some can be administered orally. Depending on the health of the person, type and the stage of cancer, the kind of chemotherapy and the dose, intravenous chemotherapy may be administered on either an inpatient or an outpatient basis.

It has been noted that some chemotherapeutic drugs have immunomodulatory actions. For example, famous chemotherapeutic drug cisplatin has already proven its immunomodulatory effects. four different mechanisms are involved in the immunomodulation cisplatin like a) the up-regulation of MHC class I expression; b) increase the proliferation and recruitment of effector cells; c) acceleration of the lytic activity of cytotoxic effectors and d) downregulation of the immunosuppressive microenvironment (de Biasi et al., 2014). Moreover, in recent years a combination of standard chemotherapy synergize with active immunization is practicing for defeating cancer. The treatment involves a vaccination towards tumour connected antigens which can sensitize the tumour against successive treatment with cytotoxic drugs. This combined approach of traditional chemotherapy and immunotherapy in cancer treatment is known as combinatorial chemotherapy. The combinatorial treatments are advised for the treatment of tumours in earlier stages. (Baxevanis et al., 2009).

Most chemotherapeutic agents are delivered intravenously, although some can be administered orally. Depending on the health of the person, type and the stage of cancer, the kind of chemotherapy and the dose, intravenous chemotherapy may be administered on either an inpatient or an outpatient basis.

Table 1.7. List of some chemotherapeutic drugs

Alkylating agents	
Category	**Examples**
Nitrogen mustards	Cyclophosphamide, Chlorambucil, Mechlorethamine, Melphalan
Alkyl sulfonates	Busulfan
Aziridines	Thiotepa
Nitrosoureas	Carmustine, Lomustine, Streptozocin
Platinum complexes	Cisplatin, Carboplatin, Oxaliplatin
Anti-microtubule agents	
Vinca alkaloids	Vincristine, vinblastin, Vinorelbine
Taxanes	Paclitaxel
Anti-metabolites	
Folate antagonists	Methotrexate
Arabinosides	Fludarabine
Anti-pyrimidines	5 fluorouracil, Gemcitabine, Floxuridine, Cytarabine
Anti-purines	6 mercapto purine, Fludarabine, Thioguanine
Topoisomerase inhibitors	
Topoisomerase I inhibitor	Camptothecin, Irinotecan, Topotecan
Topoisomerase II inhibitor	Epipodophyllotoxins, Etoposide, teniposide
Antitumour antibiotics	
Antrhacyclines	Doxorubicine, Daunorubicin, Epirubicin, Idarubicin
Non-anthracyclines	Bleomycin, Actinomycin D
Cytotoxic enzymes	
Asparaginase	
Chemotherapeutic agents	
Transtuzumab, Cetuximab, Pertuzumab, Bevacizumab	

It has been noted that some chemotherapeutic drugs have immunomodulatory actions. For example, famous chemotherapeutic drug cisplatin has already proven its immunomodulatory effects. four different mechanisms are involved in the immunomodulation cisplatin like a) the up-regulation of MHC class I expression; b) increase the proliferation and recruitment of effector cells; c) acceleration of the lytic activity of cytotoxic effectors and d) downregulation of the immunosuppressive microenvironment (de Biasi et al., 2014). Moreover, in recent years a combination of standard chemotherapy synergize with active immunization is practicing for defeating cancer. The treatment involves a vaccination towards tumour connected antigens which can sensitize the tumour against successive treatment with cytotoxic drugs. This combined approach of traditional chemotherapy and immunotherapy in cancer treatment is known as combinatorial chemotherapy. The combinatorial treatments are advised for the treatment of tumours in earlier stages. (Baxevanis et al., 2009).

In recent times, the use of phytochemicals has fascinated the researchers' attention based on their enormous affinity in sensitizing tumour cells and bestowing synergistic action to chemotherapeutic agents (Sabra et al., 2018, Kabary et al., 2018). Resveratrol, a polyphenolic phytoalexin produced in various plants during stress has already proved its combinatorial effects in cancer treatment (Elzoghby et al., 2017). An amalgamation of resveratrol and pemetrexed has been proved as a hopeful synergistic combination in cancer treatment (Chen et al., 2013).

1.6.2.2.1. Limitations/challenges of chemotherapy

Chemotherapeutic techniques have a wide range of side-effects that depend on the category of medications used. Majority of the medications affect chiefly the fast-dividing cells of the body, like hair follicles, blood cells and the cells which cover the cavity of the mouth, stomach, and intestines. The side effects of chemotherapy may occur acutely or chronically. Myelosuppression which leads to immunosuppression, hair fall (alopecia) and mucositis (painful ulceration and inflammation on gastric mucosa), etc are the common side effects of chemotherapy. Gastrointestinal problems like nausea, vomiting, diarrhoea, abdominal cramps, anorexia and constipation are some common side-effects of chemotherapeutic medications. Typhlitis is a life-threatening gastrointestinal problem of chemotherapy. Malnutrition and dehydration are also reported which may finally result in anemia, fatigue, weight loss, etc.

Because of negative effects on immune cells, chemotherapy drugs often make the body susceptible to many diseases including autoimmune diseases. Apart from this, some sorts of chemotherapy are gonadotoxic and may cause infertility. Many chemotherapeutic drugs are teratogenic, especially during the first trimester of pregnancy. Exposure to chemotherapy during second and third-trimester cause adverse effects on cognitive development and may increase the complications of pregnancy and foetal myelosuppression. Prolonged exposure to chemotherapeutic drugs makes cardiac toxicity, hepatotoxicity, nephrotoxicity and ototoxicity (Liu et al., 2015).

1.6.2.3. Radiotherapy

Radiation therapy is a local cancer treatment method which cures many types of cancer effectively. High doses of radiation therapy are used to kill cancer cells or slow their growth by damaging their nuclear content. Cells whose DNA content is damaged beyond repair stop dividing or die. Radiotherapy is prescribed in units of Grays (GY); one Gray is equal to one joule of energy absorbed per kilogram of mass. External radiotherapy is carried out by machines such as X-ray, cobalt gamma-ray machines and linear accelerators, which bombard a tungsten target resulting in the production of X-rays. Radiation therapy is classified into two types; external radiation or external beam radiation and internal radiation based on the place where which the source of radiation is positioned. External beam radiation therapy is used to treat many types of cancer but, internal radiation therapy (brachytherapy) is used to treat cancers of the head and neck, breast, cervix, prostate, eye and certain types of thyroid cancer. Brachytherapy involves the placing of radioactive source like iodine-125, caesium-137 or iridium-192 close to the cancer tissue. In systemic radiation therapy, internal radiation is administered with a liquid source. In this method, radioactive drugs give by mouth or put into a vein and the drugs are capable to travel throughout the body (2018e). Radiation therapy may be the only treatment some patients need but, most often, patients need radiation therapy with other cancer treatment modalities. There is a lifetime dose limit to the amount of radiation an area of a patient’s body can safely receive over the course of his or her lifetime. But like other cancer treatment methods, radiotherapy often causes side effects, which will be different for each person. They also depend on the sort of cancer, its location, the radiation therapy dose, and the

general health status of the patient. Skin problems like dryness, itching, blistering, or peeling, fatigue are the short term side effects of radiation therapy. If the radiation therapy is aimed at a person's head and/or neck, he or she may experience the side effects like dry mouth, mouth and gum sores, difficulty in swallowing, stiffness in the jaw, nausea lymphedema and tooth decay. Shortness of breath, breast or nipple soreness, shoulder stiffness, cough, fever, the fullness of the chest and radiation fibrosis, etc are related to radiation therapy aimed at the chest. Radiation therapy aimed at the stomach and pelvis cause side effects like nausea, vomiting, diarrhoea, rectal bleeding, incontinence and bladder irritation. In addition, radiation therapy to the pelvic region causes different symptoms for men and women. In men, sexual problems such as erectile dysfunction, lowered sperm counts, reduced sperm activity, etc is noted. In women, changes in menstruation, vaginal itching, burning and dryness, infertility are the common side effects of radiation therapy to the pelvic region. Chronic side effects of radiation therapy may comprise the probability to develop second cancer. Nowadays, major advances occurred in radiation technology have made it more precise with lesser side effects (2017e).

1.6.2.4. Hormone therapy

Hormone therapy or endocrine therapy slows or stops the growth of cancer cells that uses the hormone to grow and divide (hormone-sensitive or hormone-dependent). This therapy implies the manipulation of the endocrine system and related organs through exogenous administration of specific hormones, particularly by using steroid hormones, or drugs which inhibit the production or action of such hormones. Hormone therapy may be given usually through oral route or in the form of injections. Surgical removal of some endocrine organs, like orchiectomy and oophorectomy can also be considered as a form of hormonal therapy. Hormone therapy is primarily used to treat prostate, breast, ovarian and womb cancers (2017b).

Like other cancer treatment modalities, hormone therapy can cause side effects because this therapy prevents the ability of a person's body to produce hormones. It also impedes the action of produced hormones in the body. Side effects depend on the type of hormone therapy a person receives and how his or her body responds to it. Some common side effects for men who receive hormone therapy for prostate cancer include hot flashes, weakened bones, diarrhoea, nausea, fatigue, lack of sexual desire

and enlarged breasts. Hot flashes, vaginal dryness, nausea, fatigue, mood changes and changes in the menstrual period, etc. are some common side effects reported in women who receive hormone therapy for breast cancer (2015a).

1.6.2.5. Immunotherapy

Immunotherapy is also called biologic therapy is a type of cancer treatment that facilitates the immune system to fight against cancer directly or indirectly. Checkpoint inhibitors, adoptive cell transfer, monoclonal antibodies, treatment vaccines are the different immunotherapy ways that help the immune system act directly against cancer. Administration of cytokines like interferons and interleukins enhance the body's immune response to fight against cancer. The common side effects of immunotherapy include fever, chills, dizziness, nausea, weakness, fatigue, variation in blood pressure, headache, etc. Apart from this immunotherapy may cause severe or fatal allergic reactions. Immunotherapy may be given oral, intravenous, topical (apply on the skin) and intravesical (directly into the bladder) (2018d).

1.6.2.6. Gene therapy

Gene therapy is a type of cancer treatment which uses genes to treat cancer and that is still in the early stage of research. Gene therapy works in different ways. In some types of gene therapy, the natural immune response of the body to cancer cells is boosted. In some gene therapies, new genes are inserted into cancer cells to make these cells more prone to another type of treatments. In another method of gene therapy (pro-drug-gene therapy), the inserted genes in the cancer cells allow the cells to change drugs from an inactive form to an active form which finally destroys the cell. Some gene therapies are intended to block the processes that cancer cells use to survive (2017a).

1.6.2.7. Other novel treatment types

There are many other cancer treatment modalities which are in developing stages. Radiofrequency ablation (RFA), laser treatment, High intensity focused ultrasound (HIFU), photodynamic therapy, cryotherapy, ultraviolet light treatment, and electro-chemotherapy are the different treatment techniques belong to this category (2017d).

1.6.2.8. Complementary and Alternative Medicine

Complementary and Alternative Medicine (CAM) is the term used to describe the additional methods of treatment that may be given to the patient alongside with standard care, but are not the part of conventional treatments (Subramani and Lakshmanaswamy, 2017). They may help people with cancer to cope better with symptoms to feel healthier and can improve the quality of their life by reducing the side effects caused by modern cancer treatment methods. CAM therapies have been used widely throughout the globe for centuries. A survey conducted among the cancer patients in United States, Australia, Canada, New Zealand and Europe revealed that the United States has the highest number of patients using complementary and alternative medicine and the number has been increasing over the past three decades (Horneber et al., 2012).

Several health professionals are supportive of cancer patients using complementary therapies, but many are reluctant for their patients to use this since these therapies have not been subjected to rigorous investigations. Conventional cancer treatments, like chemotherapy, radiotherapy, etc have to go through precise testing by law in order to prove their efficacy. Majority of CAM therapies have not been undergoing such testing. Many CAM therapists and related companies often rely on the reports of individual experiences from people who say therapy has cured their diseases but is not enough scientist and conventional practitioners to prove anything. Even if the study on CAM is growing, there remain lacunae regarding its risks, benefits, side effects and how it interacts with standard therapies, etc. In integrative medicine, a modern and multidimensional approach originated where a combination of conventional and CAM treatments are provided to cancer patients (Subramani and Lakshmanaswamy, 2017).

There are many different types of complementary and alternative therapy techniques, like aromatherapy, acupuncture, herbal medicine, consumption of dietary supplements, art therapy, massage therapy, visualization, hypnosis and yoga are prevail on the world (Luo and Asher, 2017). The National Centre for Complementary and Alternative Medicine (NCCAM) has classified CAM treatments into five major classes: a) whole medical systems, b) mind and body interventions, c) biological

substance-based practices, d) manipulative and body-based practices and e) energy medicine (Kim et al., 2015) (Figure 1.5).

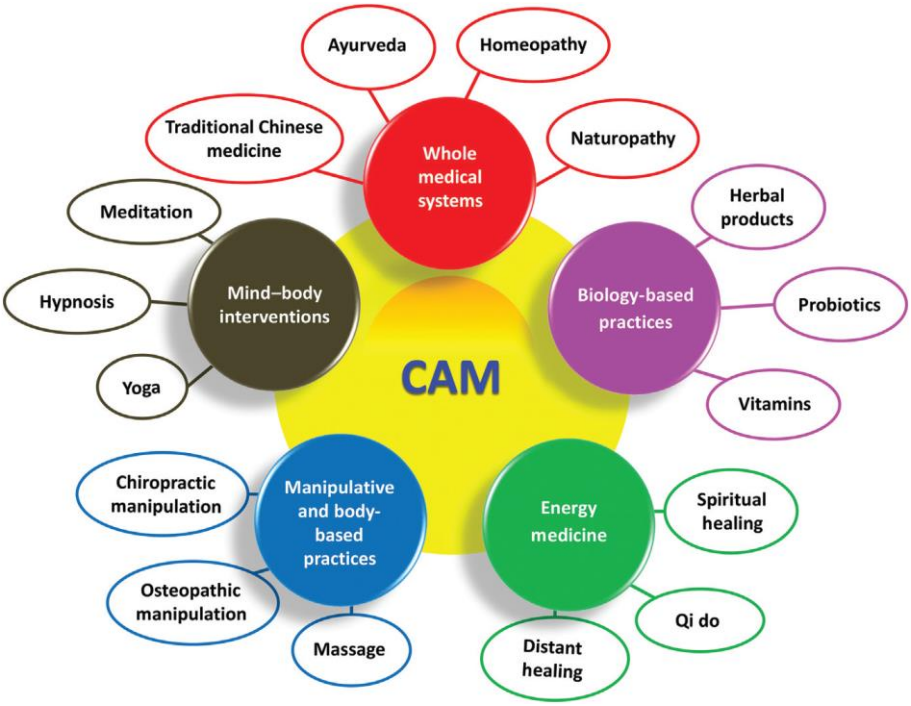

Figure 1.5. Classification of Complementary and Alternative Medicine (Subramani and Lakshmanaswamy, 2017)

1.7. Herbal medicine in cancer treatment

Herbal medicine is also called as Phytomedicine, Phytotherapy or botanical medicine. Indian Ayurvedic Medicine, Traditional Chinese Medicine, usage of herbal products, etc. are included in this category. Plants consist of numerous bioactive compounds. The quality and quantity of these bioactive substances may differ according to the locality the herbs grow, their harvest season, their postharvest processing and storage (Subramani and Lakshmanaswamy, 2017).

1.7.1. Ayurveda (Ayurvedic Medicine)

Ayurveda is one among the world's oldest holistic natural healing systems and was developed in India over 3000 years ago. The term 'Ayurveda' literally means "the science of life". It is a comprehensive system of medicine, which recognizes the body, the mind and the spirit to be equally significant in the restoration of the innate harmony of the person. The key intention of Ayurveda is to promote health, rather

than fight against diseases. According to this system, the normal body functioning is governed by the mutually coordinated action between the major system of the body like nervous system (Vata or air), venous system (Pitta or fire) and arterial system (Kapha or water). Any imbalance occurs in any of the three systems cause diseases. According to Ayurveda, the origin of benign tumour is due to the imbalance in one or two of the three bodily systems, while the malignant tumours arouse in the body due to the lost of mutual coordination of all the three system of the body (Balachandran and Govindarajan, 2005). The major components of Ayurveda include proper diet, meditation, herbs, regular exercise, body massage, exposure to sunlight and controlled breathing.

Many herbs used in Ayurvedic treatment posses anticancer properties (Desai et al., 2008) (Table 1.8). They are generally consumed in the form of decoctions of multiple herbs. These anticancer Ayurvedic herbal formulations are reported to work on numerous biochemical pathways and are capable of making a positive influence on several organ systems of the body simultaneously (Balachandran and Govindarajan, 2005). The most important quality of an herbal decoction is that it can nurture the entire body by supporting its organ systems (Treadway, 1998).

Table1.8. Ayurvedic herbs used in the management of cancer

Plant	Compounds isolated	Action
Andrographis paniculata	Andrographiside Neoandrographolide	Anti-lipoperoxidative (Trivedi, 1998), Cytotoxic against cancer cell lines (Kumar et al., 2004)
Annona atemoya	Bullatacin	Induce apoptosis in tumour cells (Chih et al., 2001)
Annona muricata	Muricins A–G, Muricatetrocin A and B, Longifolicin, Corossolin, Corossolone	*In vitro* cyctotoxicity to tumour cells (Chang and Wu, 2001)
Phyllanthus niruri	Gallic acid	*In vitro* cytotoxicity to tumour cells

Ziziphus nummularia	Betulin	Antitumour activity (Sarek et al., 2005)
	Betulinic acid	Promote apoptosis in cancer cells (Eiznhamer and Xu, 2004)
Centella asiatica	Asiaticoside, hydrocotyline, valllerine, stigmasterol, pectic acid	*In vitro* cytotoxicity to tumour cells (Babu et al., 1995)
Curcuma longa	Curcumin	*In vitro* anti proliferative and induces apoptosis (Shao et al., 2002), Inhibits metastasis (*in vitro*) (Mitra et al., 2006) Reduces angiogenesis (*in vivo*) (Kerbel and Folkman, 2002), Prevents cancer development in rodents (Ikezaki et al., 2001). Antioxidant, anti-inflammatory and anticancer effects (Kocaadam and Sanlier, 2017)
Withania somnifera	Withanolide A, Withanolide D	Interrupt carcinogenesis (Palliyaguru et al., 2016)
	Withaferin A	Induce apoptosis in cancer cells (Malik et al., 2007)
Tinospora cordifolia	20 β-hydroxyecdysterone, Cordioside, Columbin	Cytotoxic against cancer cells (HeLa) (Jagetia et al., 1998)
Piper longum	Piperine	Anti-oxidative potency *(in vitro* and *in vivo* conditions) (Koul and Kapil, 1993), Immunomodulatory and antitumour activity (Sunila and Kuttan, 2004)
Podophyllum hexandrum	Podophyllin	Anticancer (against sarcoma, adenocarcinomas and melanoma) (Balachandran and Govindarajan, 2005)

Allium sativum	Allicin	Induce programmed cell death in cancer cells (Thatte et al., 2000)
	Ajoene	Induce apoptosis and arrests the growth of cancer cells (Kaschula et al., 2016).
Zingiber officinale	6-Gingerol	Chemopreventive and anticancer (Wang et al., 2014)
	10-Gingerol	Induce apoptosis (Martin et al., 2017)

1.7.2. Traditional Chinese Medicine

Traditional Chinese Medicine (TCM) is aroused in ancient China and evolved over thousands of years. Related systems also exist in Korea, Japan and Vietnam. Several treatment practices like Chinese herbal medicine, acupuncture, massages, dietary therapy, etc. are included in TCM. The primary motive to use herbal plants in Chinese medicine is to restore the qi (vital energy) and to balance the yin (passive energy) and yang (active energy) forces. In this system of medicine, herbs are usually used to treat the root cause of the disease and also used to improve the immunity of a person to prevent the origin of any diseases (Subramani and Lakshmanaswamy, 2017).

Many anticancer compounds are isolated from different plants used in TCM. Homoisofavanone-1 is a phenolic compound isolated from *Polygonatum odoratum*, significantly apoptosis in A549 non-small cell lung cancer cells (Ning et al., 2018). Myricetin is another compound present in multiple Chinese herbs shows excellent anticancer potential (Li et al., 2019a). Esculetin, a natural coumarins compound extracted from TCM herbs has been reported to alleviate cancer progression by inducing apoptosis in cancer cells (Li et al., 2017). Like Ayurvedic medicine rhizome of turmeric and ginger is widely used in TCM for cancer treatment. *Tripterygium wilfordii* is another plant used in TCM is proved as a good source of a terpenoid compound Triptolide, which exerts broad-spectrum anticancer activities (Zhou et al., 2018). Thymoquinone, an active constituent extracted from the seeds of *Nigella sativa* is reported to show antitumour and anti-inflammatory activities (Zhang et al., 2018). Ginseng, a herbal drug of TCM, is used extensively in China to support human vitality. Ginsenosides, the pharmacologically active ingredient of ginseng, is reported to have anticarcinogenic activities (Mohanan et al., 2018).

Xihuang pill, popular traditional Chinese pill consists of four rare Chinese herbs (bezoar, musk, frankincense and myrrh) is found very effective in the treatment of the different type of cancer treatments (Yu and An, 2017, Guo et al., 2015). *Lithospermum*, a traditional Chinese herb is an excellent source of Shikonin, which can inhibit the proliferation of breast cancer cells by decreasing the release of tumor-derived exosomes. The anticancer property of Bakuchiol, found in the Chinese herb *Fructus psoraleae*, is established by many *in vitro* and *in vivo* experimental conditions (Subramani and Lakshmanaswamy, 2017).

1.7.3. Herbal products

Using herbs and their products is an ancient practice in many civilizations to strengthen, cure and balance human health. The ease of availability, safety, fewer side effects and cost-effectiveness are the factors made wide acceptability of herbal products among the public (Elkady et al., 2014, Ahmed et al., 2016). Food and Drug Administration (FDA) consent is not necessary for natural remedies except in the case of a novel food ingredient. Herbal supplements are the most widely used CAMs by cancer patients (Novak and Chapman, 2001). In traditional treatment, the whole plant or the crude extract or mixtures of herbs were used in order to maintain the delicate chemical balance between the compounds for the effective remedy. Since, the past few decades, research works have been concentrated to isolate the active compounds and understand their anticancer effects. These isolated phytochemicals exert antioxidative, anti-inflammatory, anti-angiogenic, antiproliferative and pro-apoptotic effects by affecting various signalling pathways of cancer cells.

Many modern drugs use in conventional cancer therapy today are evolved from plants. Paclitaxel, silymarin, vincristine, vinblastin, irinotecan, genipin, quercetin, etc. are classic examples of herbal originated drugs approved by the FDA for cancer treatment. It is reported that amygdalin, from apricot kernels, induces apoptosis and causes cell cycle arrest in cancer cells (Saleem et al., 2018). According to Yamshanov et al., (2016), amygdaline from apricot kernel produced a pronounced antitumor effect on the transplanted tumor in mice. The details of phytochemicals isolated from various plants for cancer treatment are given in Table 1.9.

Table 1.9. List of phytochemicals used in cancer therapy

Plant/s	Phytochemical/s	Action
Taxus brevifolia	Paclitaxel	Cytotoxic (Barbuti and Chen, 2015)
Silybum marianum	Silymarin	Induce apoptosis, anti-inflammatory and anti-metastatic activity (Ramasamy and Agarwal, 2008)
Catharanthus roseus	Vincristine, Vinblastin, vinorelbin	Cytotoxic and antitumour (Moudi et al., 2013)
Camptotheca acuminata	Irinotecan	Anticancer (Gao et al., 2014)
Gardenia jasminoides	Genipin	Antioxidant, anti-inflammatory and anticancer (Shanmugam et al., 2018)
Allium cepa, Solanum lycopersicum, Prunus nigra	Quercetin	Antimetastatic (Lin et al., 2017)
Reseda luteola, Punica granatum	Luteolin	Antimetastatic (Lin et al., 2017, Liu et al., 2017))
Morus alba	Cyanidin-3-glucoside	Anticancer (Cho et al., 2017)
Brassica oleracea, *Malus domestica*, *Camellia sinensis*, *Fragaria ananassa*, etc.	Kaempferol	Antioxidant, anti-inflammatory and antitumour (Devi et al., 2015, Wang et al., 2018)
Camptotheca acuminata	Camptothecin	Inducing apoptosis in cancer cells (Lu et al., 2012), (Tai et al., 2019).
Coptis sp., Berberis sp.	Berberine	Antioxidant, anti-inflammatory and antitumour (Wang et al., 2017)
Green tea (*Camellia sinensis*)	Epigallocatechin gallate	Prevents Epithelial-Mesenchymal transition (Li et al., 2019b)
Genista tinctoria	Genistein	Inducing apoptosis, anti-angiogenesis and inhibiting metastasis (Mukund et al., 2017)

Many natural products are listed as “cure-all” solutions that claim to eliminate cancer. Cannabis oil, laetrile (a purified form of amygdalin), aloe, capsicum, cassava, castor oil, different mushrooms, etc, are promoted to treat or prevent cancer in humans but which lack scientific and medical evidence of effectiveness. In recent years an Ayurveda practitioner named Vaidya Narayana Murthy hails from Narasipura in Shimoga district of Karnataka has been gained wide attention for performing beneficial treatment for cancer and other incurable medical conditions. Thousands of people from various parts of the country consult him as a very last resort when contemporary medication has no other treatment to suggest for cancer and claim that the treatment is highly helpful. Mr. Murthy’s medicines are primarily from herbal/plant sources. He uses barks, stems and leaves of certain plants and trees of his backyard for the preparation of medicine and people still have a positive attitude about his treatments.

A similar situation has been originated in case of an exotic plant *Simarouba glauca* DC (family Simaroubaceae), commonly called Laxmitaru or paradise tree in southern states of India, recently. Many cancer patients from Karnataka, Kerala, and Tamil Nadu claim that the decoction prepared by the leaves of this plant in a specific way is very effective in the treatment of cancer of first and second stages, whereas in advanced stages improves the quality of life. Several patients underwent conventional treatments against cancer believe in their heart that it is the decoction of Laxmitaru brought down the side effects of chemotherapy, minimized appetite loss and ensured a fast recovery. Like any other complementary and alternative medicine therapies, the consumption of this decoction is also criticized by modern medical practitioners by pointing the fact that the efficacy of this in treatment of cancer has been not proved by any scientific studies. They believe that the effectiveness of this treatment is unrelated to the real cause of the disease.

1. 8. Family Simaroubaceae: an analysis of its medicinal potentialities

The plant family Simaroubaceae consists of 32 genera and nearly 200 species of trees and bushes of tropical distribution. This family is characterised by its contents of bitter principles quassinoids, which are mainly responsible for its pharmaceutical properties (Muhammad et al., 2004). The members of this family are distributed to tropical areas of America, extending to Africa, Madagascar and Australia (Vikas et

al., 2017). *Ailanthus excelsa* belongs to family Simaroubaceae is indigenous to central and southern India, and is widely used in Ayurveda. *A. excelsa* is an important content in most of the Ayurvedic preparations like Pusyanuga churna, Aralu putpaka and Brahat Gangadhara churna used in the treatment of dysentery, diarrhoea, worm infection, intestinal disorders. The roots of *A. excelsa* is used as a substitute for *Oroxylum indicum*, one of the ten medicinal plants which are used in the preparations Ayurvedic formulations called Dasamoola (Lavhale and Mishra, 2007). The tribal populations of these regions use this plant for anthelminthic, antifertility and rejuvenating purpose. Different parts of Simaroubaceae species are used in traditional medicine as antiviral, anti-amoebae, antimalarial, antihelminthic, antifungal, antituberculosis agents and for treatment of cancer. The important plants of the Simaroubaceae family with biological activity detected already are denoted in table 1.10.

Table1.10. Biologically significant plants belong to Simaroubaceae family

Plant	Properties
Ailanthus altissima	Cytotoxic (Yang et al., 2014)
Ailanthus excelsa	Antioxidant, cytotoxic, antibacterial, haemolytic (Deepika et al., 2017), anticancer (Lavhale et al., 2009)
Ailanthus grandis	Antineoplastic (Polonsky et al., 1980)
Ailanthus integrifolia	Cytotoxic and antitumour (Seida et al., 1978)
Ailanthus triphysa	Cytotoxic (Thongnest et al., 2017)
Brucea antidysenterica	Antitumour (Okano et al., 1985)
Brucea javanica	Cytotoxic (Ohnishi et al., 1995) Antimalarial (O'Neill et al., 1987)
Brucea mollis	Cytotoxic (Tung et al., 2012)
Castela texana	Cytotoxic and antiprotozoal (Dou et al., 1996)
Cedronia granatensis	Cytotoxic (Tischler et al., 1992)
Eurycoma harmandiana	Cytotoxic (Vieira Torquato et al., 2017)
Eurycoma longifolia	Antimalarial (Ang et al., 1995), cytotoxic (Park et al., 2014)
Hannoa chlorantha,	Antimalarial and cytotoxic (Francois et al., 1998)

Hannoa klaineana	Antitumour (Lumonadio et al., 1991)
Picrasma crenata	Anti-ulcer, anti-diabetic (Novello, 2008)
Picrasma javanica	Cytotoxic, abtibacterial (Prema et al., 2019), antiviral (Win et al., 2016), antimalarial (Saiin et al., 2003)
Simaba cedron	Antimalarial (Helmstadter, 2019)
Simaba cuspidate	Antineoplastic (Polonsky et al., 1980)
Simaba ferruginea	Anti-ulcer (de Souza Almeida et al., 2011)
Simaba guianensis	Antimalarial (Cabral et al., 1993)
Simaba multiflora	Antimalarial (Cabral et al., 1993)
Simaba orinocensis	Antimalarial (Muhammad et al., 2004)
Simarouba amara	Antineoplastic (Polonsky et al., 1978) Antimalarial (O'Neill et al., 1988)
Simarouba berteroana	Antiproliferative (Devkota et al., 2014)
Soulamea tomentosa	Antileukemic (Van Tri et al., 1981)
Quassia africana	Antimalarial (Cabral et al., 1993), larvicidal (Sama et al., 2014)
Quassia undulata	Antimalarial (Ajaiyeoba et al., 1999), improved cognitive functions (Odubanjo et al., 2018), antibacterial and antifungal (Ajaiyeoba and Krebs, 2003)

Several members of this plant family have been the subject of many research studies with respect to their chemical constitution and numerous compounds were purified and isolated. The major phytochemicals with profound biological properties detected in the members of Simaroubaceae belong to quassinoids, alkaloids, flavonoids, terpenoids, and phenolics.

The key active group of chemical in Simarouba is known as quassinoids, which comes under triterpenes (degraded triterpenes). The compounds of such chemical nature were known by the term “quassin” after the physician “Quassi” who used the bark of plants from family Simaroubaceae for the treatment of fever (Phillipson et al., 1995). Studies on quassinoids have proved their promising role as therapeutic agents

as an antitumor (Lavhale and Mishra, 2007), antiviral (Polonsky, 1985, Apers et al., 2002) like anti-HIV (Chakraborty and Pal, 2013), anti-inflammatory (Lavhale and Mishra, 2007), antiamoebic, antimalarial (Spencer et al., 1947), insecticidal (Sama et al., 2014), antitubercular, antiulcer, herbicidal, etc.

The other important groups of phytochemicals detected in this family members are flavonoids, alkaloids, steroids, coumarins and anthraquinones (Barbosa et al., 2011). The different compounds isolated from Simaroubaceae family members are given in table 1.11.

Table 1.11. Potential compounds isolated from Simaroubaceae family plants

Compound/s	Plant/s	Properties
6 alpha-tigloyloxychaparrinone, 6 alpha-tigloyloxychaparrin	*Simaba cuspidate, Ailanthus grandis*	Inhibits the growth of murine P388 lymphocytic leukaemia cell line (Polonsky et al., 1980)
11-O-trans-p-coumaroyl amarolide, amarolide, chaparrinone, chaparrin, glaucarubolone, holacanthone, 15-O-beta-D-glucopyranosyl glaucarubol	*Castela texana*	Cytotoxic and antiprotozoan (Dou et al., 1996)
15-desacetylundulatone15-O-beta-D-glucopyranosyl-21-hydrozy-glaucarubolone	*Hannoa klaineana*	Antitumour (Lumonadio et al., 1991)
(16R)-methoxyjavanicin B, (16S)-methoxyjavanicin B	*Picrasma javanica*	Cytotoxic and antibacterial (Prema et al., 2019)
Picrajavanicins A-G	*Picrasma javanica*	Antiproliferative (Win et al., 2015)

Ailanaltiolides A-J	*Ailanthus altissima*	Cytotoxic (Bai et al., 2018)
Apigenin, luteolin, kaempferol, quercetin,	*Ailanthus excelsa*	Antioxidant and antiproliferative (Said et al., 2010)
Soularubinone	*Soulamea tomentosa*	Inhibits the proliferation of P388 (Van Tri et al., 1981)
Bruceanol-A, Bruceanol-B,	*Brucea antidysenterica*	Antileukemic (Okano et al., 1985)
Bruceanol-C	*Brucea antidysenterica*	Cytotoxic (Fukamiya et al., 1988)
Bruceanol-D, Bruceanol-E, Bruceanol-F	*Brucea antidysenterica*	Cytotoxic (Imamura et al., 1993)
Bruceanol-G, Bruceanol-H,	*Brucea antidysenterica*	Cytotoxic (Imamura et al., 1995)
Bruceantin	*Brucea antidysenterica*	Antitumour (Cuendet and Pezzuto, 2004)
Bruceanthinoside C	*Brucea antidysenterica*	Cytotoxic (Fukamiya et al., 1987)
Bruceoside-D, Bruceoside-E, Bruceoside-F	*Brucea javanica*	Cytotoxic (Ohnishi et al., 1995)
Cendronolactone A	*Simaba cedron*	Cytotoxic (Ozeki et al., 1998)
Cycloapotirucallanes, ailanthusins A-E, malabaricanes, ailanthusins F-G	*Ailanthus triphysa*	Cytotoxic (Thongnest et al., 2017)
Eurycomanol	*Eurycoma longifolia*	Antimalarial (Ang et al., 1995)
Glaucarubine	*Ailanthus excelsa*	Antiamoebic (Duriez et al., 1962)

Glaucarubinone	*Ailanthus excelsa*	Anticancer (Huynh et al., 2015a)
Glaucarubolone	*Ailanthus excelsa*	Antineoplastic (Mata-Greenwood et al., 2001)
Isobruceine B, soulameanone, niloticine, bruceolline, bombiprenone, α-tocopherol, inosine, Apigenin 7-O-β-D-glucopyranoside, 9-methoxy-canthin-6-one	*Brucea mollis*	Cytotoxic (Tung et al., 2012)
Sergiolide, isobrucein B	*Cedronia granatensis*	Cyctotoxic (Tischler et al., 1992)
Shinjulactone O	*Ailanthus altissima*	Cytotoxic (Yang et al., 2014)
Simalikalactone D	*Quassia africana*	Antiviral (Apers et al., 2002)
Altissinol A, altissinol b	*Ailanthus altissima*	Cytotoxic (Wang et al., 2013)
Tirucallane, Apotirucallane	*Picrasma sps.*	Cytotoxic (Xu et al., 2016)
Yadanzioside M, Yadanzioside P	*Brucea antidysenterica*	Antitumour (Okano et al., 1989)

1.8.1. Biologically potent plants belong to genus Simarouba

This genus of trees and shrubs belongs to the family Simaroubaceae, native to the neotropical realm of the world. Generally, the plants of this group have compound leaves, with between 1 and 12 pairs of alternately pinnate leaflets. *Simarouba amara, S. berteroana, S. glauca, S. tulae, S. versicolor*, etc. are the important species belongs to the genus Simarouba show antimalarial, antiamoebic, cytotoxic, antiproliferative and antitumour potentialities.

Extracts of *Brucea javanica* fruits and *Simarouba amara* stems along with some quassinoids were proved as novel antiamoebic drugs (Wright et al., 1988). Crude extracts of *Simarouba tulae* has established high cytotoxic and antitumour activities (Claudio-Campos et al., 2015). A detailed list of major phytochemicals isolated from different species belongs to genera Simarouba with their biological action is given in table 1.12.

Table 1.12. The major chemicals isolated from different *Simarouba sps.* with biological action

Chemical	Plant	Action
13, 18-dehydroglaucarubinone	*Simarouba amara*	Antineoplastic (Polonsky et al., 1978)
Ailanthinone, 2'-acetylglaucarubinone, glaucarubinone, holacanthone	*Simarouba amara*	Antimalarial (O'Neill et al., 1988)
Apotirucallane, tirucallane, octanorapotirucallane	*Simarouba amara*	Cytotoxic (Grosvenor et al., 2006, Xu et al., 2016)
Canthin-6-one-9-methozy-5-O-β-D-glucopyranoside, Canthine alkaloids, Quassinoids	*Simarouba berteroana*	Inhibits the proliferation of cancer cells (Devkota et al., 2014, Vieira Torquato et al., 2017)
Glaucarubinone	*Simarouba versicolor*	Cytotoxic and antileukemic (Ghosh et al., 1977), Antiproliferative (Yeo et al., 2016, de Mesquita et al., 2009)

Simarouba glauca DC (Laxmitaru or paradise tree) occupies the first position among the different species of medicinally important plants belongs to genera Simarouba. Different parts of this plant, like leaves, twigs, roots, bark, etc have been extensively

used in traditional medicine. Recently several incidents on the cure of cancer of various types by the consumption of decoction of leaves of *S. glauca* have got wide publicity in the southern states of India over media (Narendran, 2013). However many people support the anti-cancer properties of this no scientific study has been conducted so far.

1.9. *Simarouba glauca* DC.

1.9.1. Description

1.9.1.1. Taxonomic classification

Scientific name:		*Simarouba glauca* DC.
Synonyms	:	*Simarouba medicinalis* Endl., *Simarouba officinalis* Macfad.
Kingdom	:	Plantae
Phylum	:	Tracheophyta
Class	:	Magnoliopsida
Order	:	Sapindales
Family	:	Simaroubaceae
Genus	:	*Simarouba*
Species	:	*glauca*

1.9.1.2. Common name

Simarouba glauca DC. is known in dissimilar names in different parts of the world as follows:-

Paradise tree, bitter wood, dysentery bark, Aceituno, bitter ash, princess tree, bitter damson	: English
Bois amer, bois blance, bois frene, bois negresse	: French
Acajou blanc, daguilla, gavilan, juan primero, olivio, palo amargo	: Spanish
Lakshmi Taru	: Hindi
Sourga Maram	: Tamil
Lakshmi Taru	: Malayalam

Figure 1.6. *Simarouba glauca* DC.

Figure 1.7. Inflorescence of *Simarouba glauca* DC

1.9.1.3. General characters/botanical description

S. glauca is an evergreen tree. Chromosome number is found to be 2n = 30 in *S. glauca* (Baratakke and Patil, 2010). The mature tree attains a height of 25-27 m and a stem diameter of 40-50 cm, often with a clear, cylindrical trunk up to 9 m. The crown is slender, with a width averaging 4-6 m, and a crown width-to-Diameter at Breast Height (DBH) ratio of 22:25. A full-grown tree has cracked and grey coloured outer bark while the inner bark is cream coloured (Figure1.6). The plant has a shallow taproot system generally suitable for mountain soils. The specific name of the plant ('glauca', originated from the Greek word 'glaukos') refers to the bluish-green foliage. The plant produces imparipinnate compound leaves (20 to 50 cm in length) with 13 to 23 shiny thick leaflets, which are dark green above; oblong, and often notched or smooth at the apex. The tree begins flowering and fruiting at 3-6 years of age. Flowering is annual starting in December and continuing up to February. The inflorescence of *S. glauca* is a panicle with ultimate branches bearing dichasial cymes (Figure 1.7). The plants belong this species are polygamodioecious (Armour, 1959) with about 1-5% of the population producing exclusively male flowers and 40-50% producing mainly male flowers and a few bisexual flowers and the remaining 40-50% producing only the female flowers. Sex identification of *S. glauca* at the pre-flowering stage is a difficult task as both sexes bear similar morphological characters (Baratakke and Patil, 2010). The plants are protandrous (male flowers attain maturity before the female flowers), flowering is annual and the flowers are white or pale yellow in colour. The flowers are pollinated by bees. The fruits (ellipsoid drupe, 2-3 cm long) are blackish purple in pink genotypes (Kaali variety) and brownish yellow in green genotypes (in Gauri variety) and are ready for harvest by April-May (Joshi and Hiremath, 2000). Reproductive season and duration may differ according to location and climate. The individual fruits required a period of one to two months for development and ripening. The ripened fruits are juicy and covered with thin but hard cuticle. The sweet pulp of mature fruits attracts many animals and natural propagation by seed dispersal is done mainly by cuckoos, mynas, bulbuls, squirrels, porcupines, etc (Joshi and Joshi, 2002). Generally cattle, sheep, goat and other herbivores do not browse on *S. glauca*. No major pests and diseases are recorded at present in its native places and also in India (Armour, 1959).

1.9.1.4. Habitat

S. glauca is a versatile tree which thrives well up to 1,000 meters above sea level in all types of well-drained soil and is found to grow in places with 250 to 2,500 mm annual rainfall and temperature going up to 45^0C. The pH of the soil this plant prefers ranges from 5.5 to 8.0. It can easily withstand dry and semi-arid conditions and are cultivated in areas where no other plants of economic value can be grown. The plant has already shown its capability to grow well even in the degraded soils (Joshi and Hiremath, 2000, Govindaraju et al., 2009). Since it can adapt very well in areas of adverse conditions, it is an excellent candidate for promoting as an oilseed crop in rural and tribal areas (Rout et al., 2014).

1.9.1.4.1. Geographical distribution

S. glauca DC is a native of Central and South America and found from Southern Florida to Costa Rica, Caribbean islands, Bahamas, Cuba, Hispaniola, Puerto Rico, Jamaica, Nicaragua, Mexico, EI Salvador, etc (Baratakke and Patil, 2010).

1.9.1.4.2. In India

S. glauca was first introduced in India from El Salvador (EC-19701) by Indian Council of Agricultural Research (ICAR), New Delhi, in 1961(Juyal et al., 1991, Bhagmal, 1994) as a budding source of vegetable oil in Orissa. During the seventies, the cultivation of this plant was spread to semi-arid, dry, saline and wasteland areas of some other Indian states like Gujarat, Maharashtra, Tamil Nadu, Karnataka, Andhra Pradesh, etc (Govindaraju et al., 2009). In 1986 it was brought into the campus of University of Agricultural Sciences, Bangalore and systematic research on this plant began from 1992 onwards (Joshi and Joshi, 2002). Currently, large scale plantations have been taken up in Karnataka, Tamil Nadu, Goa and Andhra Pradesh and other states of India (Rout et al., 2014).

1.9.2. Uses of *S. glauca* DC.

S. glauca DC is a unique tree that all of its parts are used in some way or the other (Govindaraju et al., 2009).

1.9.2.1. General use

Because of its speedy adaptability to diverse types of soil and climatic conditions, *S. glauca* has gained attention for large scale cultivation both for soil conservation, afforestation and reforestation programs. The well-developed tap root system and thick evergreen canopy of this plant are highly efficient in checking the soil erosion, support to soil microbial life, and improvement of soil fertility and groundwater recharging. So plant is well suitable for wasteland reclamation and is ideal for watershed management programme (Joshi and Hiremath, 2000, Joshi and Joshi, 2002).

The trunk of single ten-year-old *S. glauca* may yield 5-10 cubic feet of wood. The wood is light in weight, attractively grained, moderately strong and interestingly insect-resistant. The wood is highly used in making light furniture, packing material, toys and matches. The trunk is also used for the production of pulp for the paper industry. It makes good fuel too (Joshi and Joshi, 2002).

Leaf litter of *S. glauca* (on average 20 kg/tree/year) is an excellent feed for earthworms and it makes good manure, so it is suitable for the production of vermicompost (Govindaraju et al., 2009).

A full-grown *S. glauca* tree produces about 20 kg fruit pulp per year. It constitutes about 60% of the fresh fruit by weight. The fruit pulp is semi-sweet in taste because of 11-12% of sugars (Rath et al., 1987) and it can be a good source for making squash, juice and jam (Joshi and Joshi, 2002) or in the fermentation/beverage industry (Joshi and Hiremath, 2000, Joshi and Joshi, 2002). All such products will have wide acceptance among people because of their attractive natural colour, aroma and taste. The fruits, especially its peel can be used as a source of natural colouring agent (Joshi and Joshi, 2002).

The seeds of *S. glauca* are considered economically significant as they contain 60-75% edible oil (Armour, 1959, Severen, 1953, Ham et al., 1954). Since 1950 onwards, in El Salvador and some other Central American countries the oil extracted from the seeds of *S. glauca* is marketed for edible purposes under the trade name ‘Manteca Vegetal Nieve’, (Manteca = butter; Vegetal = vegetable; Nieve = snow) and demand for this product has progressively increased (Armour, 1959, Govindaraju et

al., 2009). According to Govindaraju et al (2009), the seed oil is rich in both unsaturated and saturated fatty acids and can be used in the production of vanaspati and/or margarine (Govindaraju et al., 2009). According to Jeyarani and Reddy (2001) seed oil consists of oleic acid (56%), stearic acid (27%) and palmitic acid (12.5%), as major fatty acids.

The oil of *S. glauca* seeds is mainly used for industrial purpose. Apart from consumption, the filtered crude oil can be used to blend with diesel @ 5-10%. The crude oil can be subjected to transesterification to manufacture biodiesel, a 100% substitute for diesel (Joshi and Joshi, 2002).

The filtered seed oil is well suited for the manufacture of lubricants, plasticizers, surfactants, stabilizers, grease, emulsifiers, varnishes, quality soaps, shampoos, cosmetics, candles, paints, polishes, pharmaceuticals, etc. (Govindaraju et al., 2009, Joshi and Joshi, 2002).

The oil cake which obtained as a by-product after seed oil extraction is rich in nitrogen (7.7 – 8.1 %), phosphorus (1.07%), potash (1.24 %) and is valuable organic manure. The endocarp of the seed of *S. glauca* can be used in the cardboard industry. They can also pulverize and added to enrich the compost since they contain potash. The cake obtains from oil extraction from seeds is rich in proteins, 32-37 % (Severen, 1953) but cannot be used for cattle feed unless the toxic and bitter particles are removed (Monseur and Motte, 1983).

The leaf litter, fruit pulp, oil-cake and unwanted wood can be used to generate biogas. The endocarp of the seed and waste wood can be used in thermal power generation. The lignocelluloses contained in biomass produced (about 15 tonnes/ha/year) can be used as feedstock for manufacturing second-generation bio fuels (Joshi and Joshi, 2002).

1.9.2.2. Ethnobotanical uses

The traditional use of *S. glauca* has been recorded in herbal medicine systems in the countries like Belize, Brazil, Cuba, French Guyana, Guiana, Haiti and Peru. Bark, wood, roots, leaves, etc. of this plant have been used in their traditional herbal medicine as amoebicide, analgesic, anthelmintic, antibacterial (Caceres et al., 1990),

antidysenteric, antimalarial (Franssen et al., 1997), antimicrobial, astringent, febrifuge, stomachic, sudorific, tonic and vermifuge. *S. glauca* was first imported into France from Guyana in 1713 as a remedy for dysentery (Patil and Gaikwad, 2011). Indigenous tribes in the Guyana rainforest used the bar of this tree as an effective medicine for the treatment of dysentery and malaria. In Cuba, the plant is known as gavilan, people use an infusion of the bark or leaves of *S. glauca* as an astringent and used as digestion and menstrual stimulant. The decoction they consume internally for diarrhoea, dysentery, colitis and malaria. It is externally applied as a remedy for wounds and sores (Patil and Gaikwad, 2011). In Belize, *S. glauca* is popularly known as negrito or dysentery bark. People in this country extensively use the bark (and occasionally the root) of this tree to prepare a hot water decoction which is used to wash sores and taken internally for treating dysentery, diarrhoea, stomach and bowel disorders. They have followed the same protocol regarding the preparation of astringent by using *S. glauca* bark for haemorrhages and internal bleeding. In a South American country Brazil, the plant is used much the same way against malaria, diarrhoea, dysentery, intestinal parasites, indigestion and anaemia. The bark of *S. glauca* has been considered the most efficient natural remedy against chronic and acute dysentery in Brazilian herbal medicine. In some countries, the seeds of this plant are extracted in alcohol and are used against snake bites (Patil and Gaikwad, 2011). Similar properties of this plant are reported in other Latin American countries. In a Central American country Guatemala, people traditionally use this plant for treating malaria (Franssen et al., 1997). According to Caceres et al., (1990) and Giron et al., (1991) the extract of *S. glauca* has been used in Guatemala for the treatment of gastrointestinal disorders.

1.9.2.3. Pharmacological properties

The different phytochemicals present in leaf, bark, wood, root, fruit pulp and seed of *S. glauca* possess antibacterial, amoebicide, antimalarial, analgesic, anthelmintic, antidysenteric, antileukemic, antitumoral, antiviral, antiherpetic, astringent, cytotoxic, emmenagogue, febrifuge, skin hydrating, stomachic, sudorific, tonic (Joshi and Joshi, 2002, Sharma and Sriram, 2014) properties. According to Lakshmi et al., (2014) the methanolic extract of leaves of *S. glauca* showed significant antimicrobial action and the most susceptible micro-organisms were found to be *Stenotrophomonas*

maltophilia, (gram-negative bacteria) and *Enterococcus faecalis* (gram-positive bacteria).

The major phytochemicals extracted from the seeds of *S. glauca* are glaucarubine (Ham et al., 1954) and glaucarubinone (Monseur and Motte, 1983), which is derived from glaucarubine by oxidation (Gaudemer and Polonsky, 1965). Valdes et al.,(2008) isolated glaucarubin, a quassinoid from *S. glauca* and found to have amoebicidal action *in vitro* and in experimental animal amoebiasis were evaluated and found effective.

Glaucarubinone, a quassinoid natural product found inhibited colorectal cancer growth and metastasis by suppression of hypoxia-inducible factor 1 α and β-catenin via a p-21 activated kinase 1-dependent pathway (Huynh et al., 2015b). Glaucarubinone and gemcitabine (a front-line chemotherapeutic agent) were synergistically reduced pancreatic cancer growth via down regulation of P21-activated kinases (Yeo et al., 2014). The potential cytotoxicity of paclitaxel, an anticancer drug was increased by glaucarubinone administration in KB (keratin forming human oral squamous carcinoma cell line) cells (Karthikeyan et al., 2016). In another study, synergic inhibitory action by glaucarubinone administered with gemcitabine was observed on the murine pancreatic cancer cell lines and also improved survival of immunocompetent orthotopic murine animals (Yeo et al., 2016). Tricaproin isolated from the leaves of *S. glauca* found inhibited the growth of human colorectal carcinoma cell line in time and dose-dependent manner (Jose et al., 2018).

Another important quassinoid glaucarubolone in nanomolar and subnanomolar concentrations is found suppressing the growth of HeLa cells by inhibiting the action of NADH oxidase associated with its plasma membrane (Morre et al., 1998).

Canthin-6-one, 2-methoxycanthin-6-one, 9-methoxycanthin-6-one, 2-hydroxycanthin-6-one, melianodiol, 14-deacetyleurylene, etc. isolated from the *S. glauca* were found exhibited cytotoxic activity against several human cancer cell line (Rivero-Cruz et al., 2005).

Chapter 2

Materials and Methods

Contents

2.1. Materials

2.1.1. Plant material

2.1.1.1. Taxonomical classification

2.1.1.2. Collection and authentication of plant

2.1.2. Chemicals

2.1.3. Diagnostic kits

2.1.4. Instruments

2.1.5. Reagents and stains

2.1.6. Animals

2.1.7. Cell lines and their maintenance

2.2. Methods

2.2.1. Preparation of plant extract

2.2.2. Phytochemical analysis

2.2.2.1. Preliminary phytochemical screening

2.2.2.1.1. Test for carbohydrates

2.2.2.1.2. Test for tannins

2.2.2.1.3. Test for coumarins

2.2.2.1.4. Test for terpenoids

2.2.2.1.5. Test for phenols

2.2.2.1.6. Test for saponins

2.2.2.1.7. Test for alkaloids

2.2.2.1.8. Test for flavonoids

2.2.2.1.9. Test for resins

2.2.2.1.10. Test for glycosides

2.2.2.1.11 Test for proteins and amino acids

2.2.2.1.12. Test for steroids

2.2.2.1.13. Test for anthraquinones

2.2.2.2. Thin Layer Chromatographic profiling

2.2.2.3. UPLC-Q-TOF-MS analysis of the extract

2.2.2.4. Quantitative analysis

2.2.2.4.1 Estimation of total phenolic content

2.2.2.4.2. Estimation of total flavonoid content

2.2.3. Cytotoxicity analysis *in vitro*

2.2.3.1. Short term cytotoxicity

2.2.3.1.1. Isolation of spleenocytes

2.2.3.1.2. Trypan blue dye exclusion method

2.2.3.2. Long term cytotoxicity

2.2.3.2.1. 3-(4,5-dimethylthiazole-2-yl)-2,5-diphenyltetrazolium bromide (MTT assay)

2.2.4. *In vitro* antioxidant assays

2.2.4.1. Hydroxyl radical scavenging activity

2.2.4.2. DPPH radical scavenging activity

2.2.4.3. Nitric oxide radical inhibition assay

2.2.4.4. Ferric reducing/antioxidant power (FRAP) assay

2.2.4.5. Inhibition of lipid peroxidation

2.2.4.6. Total antioxidant capacity determination

2.2.4.7. Lipoxygenase inhibition assay

2.2.5. *In vivo* toxicity studies

2.2.5.1. Acute toxicity study

2.2.5.2. Sub acute toxicity study

2.2.5.2.1. Determination of haematological parameters

2.2.5.2.1.1. Estimation of haemoglobin (Hb)

2.2.5.2.1.2. Determination of red blood cells (RBCs)

2.2.5.2.1.3. Determination of total leucocytes count (TC)

2.2.5.2.1.4. Determination of differential leucocyte count (DC)

2.2.5.2.1.5. Determination of platelet count (PLT)

2.2.5.2.1.6. Determination of packed cell volume (PCV)

2.2.5.2.2. Estimation of serum markers

2.2.5.2.2.1. Estimation of serum electrolytes

2.2.5.2.2.1.1. Determination of sodium and potassium

2.2.5.2.2.1.2. Determination of chloride

2.2.6. Analysis of hepatic function

2.2.6.1. Estimation of serum glutamic oxaloacetic transaminase (SGOT) activity

2.2.6.2. Estimation of serum glutamic pyruvic transaminase (SGPT) activity

2.2.6.3. Estimation of alkaline phosphatase (ALP) activity

2.2.6.4. Estimation of total bilirubin

2.2.6.5. Estimation of total protein

2.2.7. Analysis of renal function

2.2.7.1. Estimation of serum creatinine

2.2.7.2. Estimation of serum urea

2.2.8. Determination of lipid profile

2.2.8.1. Estimation of serum total cholesterol

2.2.8.2. Estimation of serum triglycerides

2.2.8.3. Estimation of serum high-density lipoprotein cholesterol

2.2.8.4. Estimation of serum low-density lipoprotein and very-low-density lipoprotein

2.2.9. *In vivo* antioxidant activity analysis

2.2.9.1. Evaluation of antioxidant activity of HE

2.2.9.1.1. Estimation of reduced glutathione (GSH)

2.2.9.1.2. Estimation of superoxide dismutase (SOD) activity

2.2.9.1.3. Estimation of catalase activity (CAT) in liver and kidney tissue

2.2.9.1.4. Estimation of catalase activity (CAT) in haemolysate

2.2.9.1.5. Estimation of lipid peroxidation in tissue

2.2.9.1.6. Estimation of total protein in tissue, blood and haemolysate

2.2.9.2. Protective effect of HE on sodium fluoride induced oxidative damage

2.2.9.3. Effect of HE on phorbol-12-merystate-13-acetate (PMA) induced superoxide radical scavenging activity

2.2.10. *In vivo* anti-inflammatory activity analysis

2.2.10.1. Carrageenan induced acute paw oedema in mice

2.2.10.2. Vascular permeability assessment by Evans blue dye extravasation method

2.2.10.3. Dextran induced acute paw oedema in mice

2.2.10.4. Formalin induced chronic paw oedema in mice

2.2.11. Antitumour studies

2.2.11.1. Determination of the antitumour effect of HE on ascites tumour model

2.2.11.1.1. Simultaneous administration of HE with the inoculation of ascites tumour

2.2.11.1.2. Pre and simultaneous administration of HE with the inoculation of ascites tumour

2.2.11.1.3. Administration of HE to the ascites tumour bearing mice

2.2.11.1.4. Simultaneous administration of HE in combination with cyclophosphamide with the inoculation of ascites tumour

2.2.11.2. Determination of the antitumour effect of HE on solid tumour model

2.2.11.2.1. Simultaneous administration of HE with the inoculation of solid tumour

2.2.11.2.2. Pre and simultaneous administration of HE with the inoculation of solid tumour

2.2.11.2.3. Administration of HE to the solid tumour bearing mice

2.2.11.2.4. Simultaneous administration of HE in combination with cyclophosphamide with the inoculation of solid tumour

2.2.12. Study on the protective effect of HE in systemic toxicity by chemotherapeutic drugs

2.2.12.1. Protective effect on cisplatin induced nephrotoxicity

2.2.12.2. Protective effect on cyclophosphamide induced systemic toxicity

2.2.12.3. Protective effects on cyclophosphamide induced systemic toxicity in tumour bearing mice.

2.2.13. Study on the effect of HE on DMBA induced breast cancer

2.2.14. Statistical analysis

2.1. Materials

2.1.1. Plant material

2.1.1.1. Taxonomical classification

(As per section 1.9.1.1., Chapter 1)

2.1.1.2. Collection and authentication of plant

Twigs from mature *S. glauca* were collected from herbal medicine garden maintained by Amala Ayurvedic Hospital, Thrissur and was identified by a plant taxonomist, Dr. C. N. Sunil, Research guide & Associate professor, Post Graduate & Research Department of Botany, Sree Narayana Mangalam College, Maliankara, Ernakulam, Kerala. A voucher specimen (No.SNMH-7128, dated on 24.02.2014) of this plant is deposited in the herbarium of the said college.

2.1.2. Chemicals

The various chemicals and substances used in the current study with the name of their suppliers are given in table 2.1. All the chemicals used in the study were of analytical grade.

Table 2.1. List of chemicals used

Sl. No.	Chemicals	Suppliers
1	1-naphthol	MERK specialties Pvt. Ltd., Mumbai
2	2, 2-diphenyl-1-picrylhydrazyl (DPPH)	Sigma-Aldrich Inc., St Louis, USA
3	2,4,6-Tris(2-pyridyl)-*s*-triazine (TPTZ)	Sisco Research Laboratories (SRL) Pvt. Ltd., Mumbai, India.
4	3-(4,5-dimethylthiazol-2-yl)-2,5-diphenyltetrazolium bromide (MTT)	Sigma-Aldrich Inc., St Louis, USA
5	5-5'Dithiobis (2-nitrobenzoic acid) (DTNB)	Sisco Research Laboratories (SRL) Pvt. Ltd., Mumbai, India.
6	7,12- Dimethyl benz[a]anthracene (DMBA)	Sigma-Aldrich Inc., St Louis, USA
7	15-lipoxidase	Sigma-Aldrich Inc., St Louis, USA
8	Acetone	Merck India Pvt. Ltd., Mumbai, India
9	Acetic acid glacial 99 - 100%	Merck India Pvt. Ltd., Mumbai, India
10	Aluminium potassium sulphate	Merck India Pvt. Ltd., Mumbai, India

11	Alpha naphthayl acetate	Sisco Research Laboratories (SRL) Pvt. Ltd., Mumbai, India.
12	Ammonium molybdate tetrahydrate	Sisco Research Laboratories (SRL) Pvt. Ltd., Mumbai, India.
13	Ascorbic acid	Sisco Research Laboratories (SRL) Pvt. Ltd., Mumbai, India.
14	Bovine serum albumin (BSA)	Merck India Pvt. Ltd., Mumbai, India
15	Cadmium acetate	Merck India Pvt. Ltd., Mumbai, India
16	Caesine	Himedia Laboratories Pvt. Ltd, Mumbai, India
17	Carboxymethyl cellulose	Sisco Research Laboratories (SRL) Pvt. Ltd., Mumbai, India.
18	Carmine	Merck India Pvt. Ltd, Mumbai, India
19	Carrageenan	Sigma-Aldrich Inc., St Louis, USA
20	Chloroform	Merck India Pvt. Ltd, Mumbai, India
21	Cisplatin	Sigma-Aldrich Inc., St Louis, USA
22	Copper sulphate	Merck India Pvt. Ltd, Mumbai, India
23	Cyclohexane	Merck India Pvt. Ltd, Mumbai, India
24	Cyclophosphamide (i.p.) (Cytoxan)	Sigma-Aldrich Inc., St Louis, USA
25	Deoxy ribose	Sisco Research Laboratories (SRL) Pvt. Ltd., Mumbai, India.
26	Dextran	Himedia Laboratories Pvt. Ltd, Mumbai, India
27	Dextrose	Merck India Pvt. Ltd, Mumbai, India
28	Di Potassium hydrogen phosphate	Merck India Pvt. Ltd, Mumbai, India
29	Di Sodium hydrogen phosphate	Merck India Pvt. Ltd, Mumbai, India
30	Eosin	Sigma-Aldrich Inc., St Louis, USA
31	Ethylene diamine tetra acetic acid (EDTA)	Merck India Pvt. Ltd, Mumbai, India
32	Evans blue	Sisco Research Laboratories (SRL) Pvt. Ltd., Mumbai, India.
33	Ferrric chloride	Merck India Pvt. Ltd, Mumbai, India
34	Ferrous sulphate	Merck India Pvt. Ltd, Mumbai, India
35	Folin's reagent (FCR)	Merck India Pvt. Ltd, Mumbai, India
36	Formaldehyde	Merck India Pvt. Ltd, Mumbai, India
37	Glutathione reduced (GSH)	Sisco Research Laboratories (SRL) Pvt. Ltd., Mumbai, India.
38	Haematoxylin	Sigma-Aldrich Inc., St Louis, USA
39	Hydrochloric acid	Merck India Pvt. Ltd, Mumbai, India
40	Hydrogen peroxide	Merck India Pvt. Ltd, Mumbai, India

41	Isoamyl alcohol	Merck India Pvt. Ltd, Mumbai, India
42	Isopropanol	Sisco Research Laboratories (SRL) Pvt. Ltd., Mumbai, India.
43	Leishman's stain	Himedia Laboratories Pvt. Ltd, Mumbai, India
44	Methanol (HPLC grade)	Merck India Pvt. Ltd, Mumbai, India
45	Nitrobluetetrazolium (NBT)	Sisco Research Laboratories (SRL) Pvt. Ltd., Mumbai, India.
46	Orthophosphoric acid	Merck India Pvt. Ltd, Mumbai, India
47	Pararosaniline hydrochloride	Sigma-Aldrich Inc., St Louis, USA
48	Phenol	Merck India Pvt. Ltd, Mumbai, India
49	Phorbol 12-myristate 13-acetate	Sigma-Aldrich Inc., St Louis, USA
50	Potassium chloride	Merck India Pvt. Ltd, Mumbai, India
51	Potassium dihydrogen phosphate	Merck India Pvt. Ltd, Mumbai, India
52	Potassium hydroxide	Merck India Pvt. Ltd, Mumbai, India
53	Potassium iodide	Sigma-Aldrich Inc., St Louis, USA
54	Riboflavin	Sisco Research Laboratories (SRL) Pvt. Ltd., Mumbai, India.
55	Schiff reagent	Nice chemicals, Ernakulam, Kerala
56	Silymarin	Sigma-Aldrich Inc., St Louis, USA
57	Sodium acetate anhydrous	Merck India Pvt. Ltd, Mumbai, India
58	Sodium azide	Merck India Pvt. Ltd, Mumbai, India
59	Sodium bicarbonate	Merck India Pvt. Ltd, Mumbai, India
60	Sodium carbonate anhydrous	Merck India Pvt. Ltd, Mumbai, India
61	Sodium chloride	Merck India Pvt. Ltd, Mumbai, India
62	Sodium cyanide	Merck India Pvt. Ltd, Mumbai, India
63	Sodium dihydrogen phosphate	Merck India Pvt. Ltd, Mumbai, India
64	Sodium dodecyl sulfate	Merck India Pvt. Ltd, Mumbai, India
65	Sodium fluoride	Merck India Pvt. Ltd, Mumbai, India
66	Sodium hydroxide	Merck India Pvt. Ltd, Mumbai, India
67	Sodium nitrate	Merck India Pvt. Ltd, Mumbai, India
68	Sodium potassium tartarate	Merck India Pvt. Ltd, Mumbai, India
69	Sodium sulphate	Merck India Pvt. Ltd, Mumbai, India
70	Sulphuric acid	Merck India Pvt. Ltd, Mumbai, India
71	Tamoxifen	Sigma-Aldrich Inc., St Louis, USA
72	Thiobarbituric acid (TBA)	Himedia Laboratories Pvt. Ltd, Mumbai, India
73	Trichloro acetic acid (TCA)	Merck India Pvt. Ltd, Mumbai, India
74	Tris hydrochloride (Tris HCl)	Merck India Pvt. Ltd, Mumbai, India
75	Tri sodium citrate	Merck India Pvt. Ltd, Mumbai, India

2.1.3. Diagnostic kits

The diagnostic reagent kits used for the detection of various biomolecules in the study and the name of their providers/suppliers are given below (Table 2.2).

Table 2.2. List of diagnostic kits used

Sl. No.	Diagnostic kit	Supplier
1	Albumin	Agappe Diagnostics Ltd., Ernakulam
2	Alkaline phosphatase (ALP)	Agappe Diagnostics Ltd., Ernakulam
3	Bicarbonates	Agappe Diagnostics Ltd., Ernakulam
4	Chloride	Agappe Diagnostics Ltd., Ernakulam
5	Cholestrol	Agappe Diagnostics Ltd., Ernakulam
6	Creatinine	Euro Diagnostic Systems Pvt. Ltd., Chennai.
7	HDL	Agappe Diagnostics Ltd., Ernakulam
8	Hemoglobin (Hb)	Agappe Diagnostics Ltd., Ernakulam
9	LDL	Agappe Diagnostics Ltd., Ernakulam
10	Potassium	Agappe Diagnostics Ltd., Ernakulam
11	Serum glutamate oxaloacetate transaminase (SGOT)	Agappe Diagnostics Ltd., Ernakulam
12	Serum glutamate pyruvate transaminase (SGPT)	Agappe Diagnostics Ltd., Ernakulam
13	Sodium	Agappe Diagnostics Ltd., Ernakulam
14	Total Bilirubin	Euro Diagnostic Systems Pvt. Ltd., Chennai.
15	Total protein	Euro Diagnostic Systems Pvt. Ltd., Chennai.
16	Triglycerides	Agappe Diagnostics Ltd., Ernakulam
17	Urea	Euro Diagnostic Systems Pvt. Ltd., Chennai.

2.1.4. Instruments

Instruments and their providers are given below (Table 2.3).

Table 2.3. List of instruments used

Sl. No.	Instrument	Provider
1	Deep freezer (-20ºC)	Remi Laboratory Instruments, Mumbai, India
2	Deep freezer (-80ºC)	Eppendorf, Germany

3	Electronic weighing balance	Shimadzu Corporation Ltd, India
4	High-speed cooling centrifuge	Remi Laboratory Instruments, Mumbai, India
5	Hotplate	Rotex Instruments Pvt. Ltd., India
6	Hot air oven	Rotex Instruments Pvt. Ltd., India
7	Incubator	Rotex Instruments Pvt. Ltd., India
8	Laboratory centrifuge	Remi Laboratory Instruments, Mumbai, India
9	Laminar flow hood (Horizontal)	Cleanair, Chennai, India
10	Magnetic stirrer	Remi Laboratory Instruments, Mumbai, India
11	Micro centrifuge	Tarsons Products Pvt. Ltd., Kolkata
12	Microtome	Remi Laboratory Instruments, Mumbai, India
13	pH meter	Elico Limited, Hyderabad, India
14	Phase-contrast microscope	Magnus, INVI, New Delhi, India
15	Tissue homogenizer	Remi Laboratory Instruments, Mumbai, India
16	Upright research microscope	Leica German radicle, Ambala
17	UV chamber	Remi Laboratory Instruments, Mumbai, India
18	UV/Visible spectrophotometer	PG instruments, UK
19	Vacuum concentrator	Eppendorf, Germany
20	Vortex mixer	Remi Laboratory Instruments, Mumbai, India

2.1.5. Reagents and stains

a) Dragendorff's reagent

Stock solution: 1.7 gm of bismuth subnitrate was mixed in a blend of 80 mL water and 20 mL glacial acetic acid. 100 mL of potassium iodide solution (50% w/v) was also added and stirred well until the bismuth nitrate dissolved. The solution thus obtained was kept in a dark bottle.

Working solution: 100 mL stock solution with 200 mL of glacial acetic acid was made up to 1 L with distilled water. The working solution thus prepared was also stored in a dark bottle.

b) Mayer's reagent

2.72 gm of mercuric chloride was dissolved in 120 mL distilled water. 10 gm of potassium iodide was dissolved in 40 mL distilled water separately. These two solutions were mixed together and made up to a total volume of 200 mL with distilled water.

c) Wagner's reagent (Iodo-potassium iodide)

2 gm of iodine and 6 gm of potassium iodide were dissolved in 100 mL of distilled water.

d) Phosphate buffered saline (PBS)

NaCl	- 8.00 gm
KCl	- 0.20 gm
KH_2PO_4	- 0.24 gm
Na_2HPO_4	- 1.44 gm

The contents were dissolved in 800 mL distilled water and the pH was adjusted to 7.4 with HCl and a final volume of 1000 mL was prepared by adding distilled water. The solution was sterilized by autoclaving at 15 lbs for15 min.

e) Trypan Blue dye (0.1% solution)

Trypan blue	- 0.1 gm
PBS	- 100 mL

Trypan blue dye was dissolved in 100 mL PBS and was stirred with a magnetic stirrer for overnight. The solution was filtered with Whatman No. 1 filter paper.

f) Tris-HCl buffer (pH 7.4, 0.1 M)

Tris-HCl	- 1.576 gm
Distilled water	- 100 mL

The Tris-HCl was dissolved in distilled water.

g) Formalin solution (neutral buffered, 10%)

Sodium phosphate, monobasic - 4.0 gm
Sodium phosphate, dibasic - 6.5 gm
Formaldehyde, 37% - 100 mL
Distilled water - 900 mL

All ingredients were mixed well and stored at room temperature.

h) Hayem's fluid

Mercuric chloride - 0.25 gm
Sodium sulphate - 2.50 gm
Sodium chloride - 0.50 gm
Distilled water - 100 mL
Final pH (25ºC) - 5.9 ± 0.1

i) Turk's fluid

Glacial acetic acid - 2.00 mL
Gentian Violet (1% w/v) - 1.00 mL
Distilled water - 97.00 mL

The solution was stirred overnight; filtered and final pH was adjusted to 2.2 ± 0.2 (at 25ºC)

j) Carnoy fluid

The Carnoy fluid was prepared by adding ethanol, chloroform and acetic acid in a ratio of 6:3:1 and stored in room temperature.

k) Carmine solution

Carmine (2%) and Aluminium potassium sulphate (5%) were added into 100 mL of boiling distilled water and boiled for 20 minutes. After cooling the solution was filtered and kept in room temperature.

2.1.6. Animals

Swiss albino and BALB/c mice (25 ± 3 gm, 7 - 8 weeks old) and Wistar rats (150-180 gm) were used for the *in vivo* studies and they were purchased from Small Animal Breeding Station (SABS), Kerala Veterinary and Animal Science University, Thrissur, Kerala, India. The animals were kept in well-ventilated polypropylene cages with rice hull bedding under standardized conditions such as temperature (25 ± 3 ºC), relative humidity (60 – 70%) and 12 hours dark/light cycle. They were fed with standard rat feed bought from Sai Durga Feeds and Foods, Bangalore, India and water *ad libitum*. The animals were acclimatized for seven days to the laboratory environment before each and every experiment. All the animal experiments in this research study were carried out with the prior approval of the Institutional Animal Ethics Committee (Approval no. ACRC/IAEC/16-06/11) and were conducted strictly according to the guidelines of Committee for the Purpose of Control and Supervision of Experiments on Animals (CPCSEA) which belongs to Department of Animal Husbandry and Dairying, Ministry of Agriculture and Farmers Welfare, Government of India.

2.1.7. Cell lines and their maintenance

Murine cancer cell lines like Ehrlich Ascites Carcinoma (EAC) and Dalton's Lymphoma Ascites (DLA) were purchased from Cancer Institute (WIA), Chennai, Tamil Nadu and the cell lines were maintained in the peritoneal cavity of mice at Amala Cancer Research Centre, Thrissur. For maintaining the stock of these cells, the cells were aspirated from the peritoneal cavity of the inoculated mice, washed with PBS and were counted and adjusted to $1x10^6$ cells and injected into the peritoneal cavity of healthy mice around 14 days intervals.

Human cancer cell lines, like cervical carcinoma (HeLa), liver cancer (HepG2), colorectal adenocarcinoma (HCT-15), estrogen and progesterone receptor-positive breast cancer (MCF-7), triple-negative breast cancer (MDA-MB-231); a murine macrophage (RAW-264.7) and an African monkey kidney (Vero E6) were purchased from the National Centre for Cell Science (NCCS), Pune, India. The cell lines were maintained in T25 cell culture flasks (at a temperature of 37ºC and under 5% CO_2 atmosphere) with specific culture medium supplemented with 10% fetal bovine serum

(FBS) and antibiotics in a CO_2 incubator. Aseptic conditions were maintained throughout the period. Inoculated cell culture flasks were inspected in regular time intervals for change in colour of the medium or contamination. Cells were sub-cultured soon after they attain around 80% confluence in growth.

For sub-culturing, the exhausted medium was removed and the cells were washed thrice with PBS with minimum disturbance to the cells. The cells were detached from the surface by adding 1 mL trypsin solution (0.25% trypsin in 0.001% EDTA) and kept the flask for a few minutes at 37°C in the incubator. The cell culture flask was gently tapped on the sides to ensure the speedy detachment of the adhering cells. 1 mL of fresh culture medium was added immediately to the flask in order to inactivate the excessive action of trypsin and mixed gently by a pipette to ensure the formation of a single cell suspension. The cells were counted and adjusted to $1x10^6$ cells and were inoculated into new culture flask containing an adequate amount of fresh culture medium.

2.2. Methods

2.2.1. Preparation of the plant extract

Hot water extract (HE) was prepared from mature leaves of *S. glauca*. The hot water extract was prepared as per the protocol (origin of this protocol is unknown) used by many patients in south India, especially in Kerala who consume this decoction as adjuvant therapy and as a treatment for cancer.

Accordingly, in this study, the extract was prepared by using 18 fresh mature leaflets (approximately 5 gm in weight) in 200 mL drinking water by taking consideration that the average human body weight is 60 kg. The extract was filtered and collected separately in a clean glass beaker. In the same way extract was prepared two more times by using the same plant matter. The extract thus prepared were pooled together, centrifuged (at 3000 rpm for 15 minutes) and filtered by using Whatman no. 1 filter paper. The supernatant was collected and evaporated in a hot air oven at 40ºC. The dry residue thus obtained after complete evaporation was used as the HE in this study. This procedure was repeated for obtaining more extract for the study. The extract was dark brown in colour and average yield of the dry residue was 15.70 ± 0.50%.

For the preparation of methanolic extract (ME), mature plant leaves were collected, washed and shade dried. The dried leaves were ground into a coarse powder with the help of a mixer grinder. The powdered sample was stored in an airtight container and kept in a cool, dark and dry place until used for the preparation of the extract. The powdered material (30 gm) was taken in a clean, conical flask (1000 mL) and extracted using methanol (99.9%) with the help of a magnetic stirrer. After 24 hours the supernatant was collected and centrifuged (at 3000 rpm for 15 minutes) and filtered by using Whatman no. 1 filter paper. The filtrate thus obtained was kept for evaporation and dried in a hot air oven at 40^{o}C. The extraction procedure was repeated for many days by using the same plant matter in fresh solvent until the solvent has not developed any colour. The extract obtained in each extraction were pooled together to make the final product. The ME thus obtained had a dark green colour and the average yield was 23.15 ± 0.06%

Both extracts (HE and ME) thus obtained were stored in separate airtight amber coloured bottles at 4^{o}C and used for further experiments.

For *in vivo* studies, a lower (LDHE: 160 mg/kg b. wt) and higher (HDHE: 260 mg/kg b. wt) of extract were used. The lower dose (LDHE) is equal to the human equivalent dose according to the existing practice of consumption of hot water extract. The animal equivalent dose was calculated by considering the body surface area Nair and Jacob, (2016). The extract (HE) was dissolved in 1% food-graded propylene glycol for animal administration.

2.2.2. Phytochemical analysis

2.2.2.1. Preliminary phytochemical screening

For phytochemical analysis, the HE and ME were dissolved in distilled water and methanol respectively. Qualitative analysis for the detection of phytochemicals present in the extracts (HE and ME) was completed according to the standard protocols (Harborne, 1984, Sofowora, 1993, Evans, 2009). Different phytochemicals like carbohydrates, tannins, coumarins, terpenoids, phenols, saponins, alkaloids, flavonoids, resins, glycosides, proteins and amino acids, steroids, sterols, anthraquinones, leucoanthocyanins, emodins, phlobatamins, etc are tested using specific methods and compared with control; for HE distilled water and for ME, 70% methanol.

2.2.2.1.1. Test for carbohydrates

i. Molisch test: The extract was treated with few drops of 1% alcoholic alpha-naphthol in a test tube and mixed well. 0.5 mL of concentrated sulphuric acid was added slowly along the sides of this test tube. A purple violet appeared at the junction of two solutions indicated the presence of carbohydrates.

ii. Benedict's test: To 1mL of extract, 3 mL of Benedict's reagent was added and heated for a few minutes in a boiling water bath. The appearance of orange-red precipitate confirmed the presence of carbohydrates.

iii. Fehling's test: A volume of 1 mL of Fehling's A and Fehling's B reagents were mixed and few drops of the extract are added and boiled for a few minutes. A brick-red coloured precipitate appeared, hence confirmed the presence of carbohydrates.

2.2.2.1.2. Test for tannins

i. Lead acetate test: Few drops of 10% lead acetate were added to 2 mL of the extract. The formation of bulky white or yellowish precipitate indicated the presence of tannins.

ii. Ferric Chloride Test: The extracts were heated for 10 minutes in a water bath and filtered by Whatman filter paper. About 2 to 3 drops of 0.1% ferric chloride was added to 5 mL of the extract. A brownish-green or blue-black colouration indicated the presence of tannins.

iii. Potassium hydroxide test: A volume of 4 mL of freshly prepared 10% potassium hydroxide solution was added to an equal volume of extract. Presence of dirty white precipitate indicated the presence of tannins.

2.2.2.1.3. Test for coumarins

A volume of 3 mL of 10% sodium hydroxide was added to 2 mL of the extract and mixed well by a vortex mixer. Formation of yellow color indicated the presence of coumarins in the extracts.

2.2.2.1.4. Test for terpenoids

Salkowski test: The extract was mixed with 2 mL of chloroform and 3 mL of concentrated sulphuric acid is added carefully to form a layer in a test tube. A reddish-brown colouration of the interface is appeared to indicate a positive test result of the presence of terpenoids.

2.2.2.1.5. Test for phenols

i. Ferric chloride test: To 2 mL of extract, 2 mL of 5% aqueous ferric chloride was added. Formation of deep color indicated the presence of phenols.

ii. Ammonium hydroxide test: To 2 mL of the extract, 1 mL of 1% gelatin and 10% sodium hydroxide were added. The appearance of white precipitate confirmed the presence of phenols.

2.2.2.1.6. Test for saponins

Froth test: About 0.2 gm of the plant extract was mixed with 5 mL of distilled water and shaken vigorously for 10 minutes. The appearance of froth that persists for 5 minutes indicated the presence of saponins.

2.2.2.1.7. Test for alkaloids

A volume of 10 mL of 1% of aqueous hydrochloric acid was added to about 0.5 gm of dry extract and mixed thoroughly by the vortex. The filtrate was separated by Whatman no. 1 filter paper and it was used for detecting the presence of alkaloids by the following tests

i. Dragendorff’s test: A volume of 1 mL of freshly prepared Dragendorff’s reagent was added to 2 mL of the filtrate and noted the formation of yellow to orange precipitate, indicated the presence of alkaloids.

ii. Mayer's test: Few drops of Mayer’s reagent were added to 2 mL of the filtrate and observed the formation of a creamy white coloured precipitate.

iii. Wagner's test: To 2 mL of the extract few drops Wagner's reagent was added. A reddish-brown precipitate appeared which also confirmed the presence of alkaloids in the extract.

2.2.2.1.8. Test for flavonoids

i. Sodium hydroxide test: To 2 mL of extract was added with 3-5 drops of 20% sodium hydroxide solution, the formation of intense yellow colour was noted. To this solution, few drops of dilute HCl (70%) were added and the yellow hue is disappeared. The formation and disappearance of yellow colour indicated the presence of flavonoids in the extract.

ii. A small quantity of the extract was heated with 10 mL of ethyl acetate in boiling water bath for 3 minutes. The mixture was filtered and the filtrate thus obtained is used for the following tests.

A. Ammonium test: A volume of 2 mL of the filtrate was shaken with 1 mL of 1% ammonia solution. The layers of the solution were allowed to separate. The yellow colour was noted at ammonia layer which indicated the presence of flavonoids.

B. Aluminum chloride test: The filtrate were shaken with 1 mL of 1% aluminum chloride solution and observed a yellow colour. When dilute sodium hydroxide and hydrochloric acid is added the yellow solution turned into colourless, which confirmed the presence of flavonoids.

2.2.2.1.9. Test for resins

A volume of 1 mL of extract was treated with a few drops of acetic anhydride solution followed by 1 mL of concentrated sulphuric acid. The solution gave colouration ranging from orange to yellow indicated the presence of resins in HE.

2.2.2.1.10. Test for glycosides

Keller-Kiliani Test: A volume of 2 mL plant extract were taken in a test tube, 2 mL glacial acetic acid, one drop of 5% aqueous ferric chloride solution and concentrated sulphuric acid were added into this. The reddish-brown colour appeared at the junction of the two liquid layers and the upper layer appeared in bluish-green colour confirmed the presence of glycosides in ME.

2.2.2.1.11. Test for proteins and amino acids

i. Biuret test: To 2 mL of extract 1 mL of 40% sodium hydroxide and a few drops of 1% copper sulphate were added to the plant extract. The appearance of violet color indicates the presence of peptide linkage molecules in the sample extract.

ii. Ninhydrin test: A volume of 2 mL ninhydrin (2,2-dihydroxyindane-1,3dione) reagent (0.05% in acetone) was added to 2 mL of extract. The appearance of purple colour indicates the presence of amino acids.

iii. Xanthoprotein test: A volume of 2 mL extract was taken in a test tube and 0.5 mL of concentrated nitric acid was added to it. The yellow colour is obtained if proteins are present.

iv. Heat coagulation test*:* About 2 mL of the extract was heated for five minutes in boiling water bath. Proteins get coagulation while heating.

2.2.2.1.12. Test for steroids

i. Liebermann Burchard test or acetic anhydride test: Acetic anhydride (1 mL) was added to 1 mL of chloroform and chilled to 0°C. Few drops of concentrated sulphuric acid was added to the ice-cold mixture followed by 1 mL of the extract. The solution turns to deep green colour which starts as a purplish, pink colour blue, and progressed to light green and finally dark green colour for the presence of steroids.

ii. Salkowski test: The extract was mixed with 2 mL of chloroform and 3 mL of concentrated sulphuric acid is added carefully to form a layer in a test tube. A reddish-brown colouration of the interface shows a positive test result for the presence of steroids.

2.2.2.1.13. Test for anthraquinones

Borntrager's test: Extract (0.5 gm) was heated with 5 mL of dilute sulphuric acid in a boiling water bath. Then the solution was filtered. 10 mL of benzene was added to 2 mL of the filtrate and shaken well. The solution is again filtered and to which 5 mL of 10% ammonia solution was added slowly and mixed well. Formation of pink or red colour in the ammonia layer (lower) indicates the presence of anthraquinones.

2.2.2.2. Thin Layer Chromatographic profiling

For Thin Layer Chromatographic (TLC) analysis leaf extracts (10 μL of 10 mg/mL concentration) were applied on the TLC aluminium sheets (from Merck KGaA, Darmstadt, Germany) of 11 cm length and developed with the solvent system containing n-butanol: glacial acetic acid: distilled water (60:15:25, v/v/v) for HE and chloroform: ethyl acetate: formic acid (8:2:0.2, v/v/v) for ME. The samples were applied 2 cm above its bottom with the help of capillary tubes. After the application of samples on the TLC plate, the plates were kept in glass chamber (solvent saturated) then the mobile phase was allowed to pass through the adsorbent phase up to 3/4th of the plate. The separated bands were visualized under visible light, UV (254 nm) and under visible light after exposure to iodine vapour. The retardation factor (Rf) value was calculated for each band by using the following formula.

$$\mathrm{Rf} = \frac{\text{Distance traveled by the substance}}{\text{Distance traveled by the solvent front}}$$

Suitable spray reagents were adopted for the detection of a significant group of plant compounds like flavonoids, terpenoids, alkaloids and phenolics present in the extracts.

Identification of the group of plant compounds by using spray reagents

i. Terpenoids by using Vanillin sulphuric acid reagent

An aqueous solution of Vanillin (10 %) was mixed with a solution of ethanolic acid and concentrated sulphuric acid (2:1) was sprayed on the TLC plates. The plates were kept in hot air for 15 minutes. The appearance of brown, dark green or purple coloured bands on the TLC indicated the presence of terpenoids.

ii. Alkaloids by Dragendorff's reagent

Stock solution: About 2.6 gm bismuth carbonate and 7.0 gm sodium iodide were boiled together with 25 mL of glacial acetic acid for a few minutes. After 12 hours the precipitated sodium acetate was filtered off. 20 mL of red-brown filtrate thus obtained was mixed with 80 mL ethyl acetate and 0.5 mL distilled water was added to this. The solution was stored in a dark bottle.

Spray solution: A volume of 10 mL of the stock solution was mixed with 100 mL glacial acetic acid and 240 mL ethyl acetate.

The alkaloids and other nitrogen compounds appeared in green and blue colour bands on a yellow background on TLC plates.

iii. Flavonoids

Flavonoids were detected as fluorescent bands under UV light after applying 1% ethanolic solution of aluminium chloride solution on the TLC plates.

iv. Phenolic compounds

Preparation of the reagent: About 0.1 gm of ferric chloride and 0.1 gm of potassium ferrocyanide were taken and dissolved 10 mL of distilled water respectively in separate glass beakers. These two solutions were mixed together just before to apply on the TLC plates. The TLC plates were incubated for 110^{o}C for few minutes. The phenolic compounds appeared in blue or brown colour.

2.2.2.3. UPLC-Q-TOF-MS Analysis of the extract

High resolution liquid chromatographic-mass separation of HE was carried out with the instrument 1290 Infinity UHPLC System, 1260 infinity Nano HPLC with Chipcube, 6550 iFunnel Q-TOFs (Agilent Technologies, USA) with HiP sampler (Model: G4226A), binary pump (Model: G4220B), column comp. (Model: G1316C), z and MS Q-TOF (Model: G6550A). The separation of HE was performed on Orbax eclipse column 18 (2.1 x 150 mm 5 μ) using a binary mobile phase consisting of 100% water containing 0.1% formic acid (A) and 100% acetonitrile containing 90% acetonitrile in 10% water and 0.1% formic acid (B). Elution was done under the following conditions: 5.0 μL injection volume; 0.2 mL/min flow rate with temperature set at 25^{o}C; 95.0% A and 0.0% B (2 min), 5.0% A and 95.0% B (20 min), 95% A and 5% B (26-30 min). The ESI-Q-TOF-MS detection was performed in positive ionisation mode with the following parameters: mass range 50-1000 (m/z), gas

temperature 250ºC, gas flow 13 L/min, nebulizer pressure 35 psig, capillary voltage 3500 V, skimmer 65 V, fragmentor energy 175 V.

2.2.2.4. Quantitative analysis

2.2.2.4.1. Estimation of total phenolic content

Total phenolic content of the extracts (HE and ME) was determined by using Folin-Ciocalteu reagent following the method of Ainsworth (Ainsworth and Gillespie, 2007) with some modification.

Principle

The transfer of electrons occurs from phenolic compounds to phosphomolybdic /phosphotungstic acid complexes present in Folin-Ciocalteu reagent in alkaline medium and form blue complexes and that can be determined spectroscopically at 765 nm.

Procedure

Approximately 0.5 mL of the extracts (1 mg/mL) was mixed with 2 mL of 10% Folin-Ciocalteu reagent and incubated at the darkness for six minutes. 4 mL of 7.5% sodium carbonate solution was then added to the reaction mixture. The test tubes were further incubated at room temperature for 30 minutes with intermittent shaking. The absorbance of the solution was taken at 765 nm, and total phenolic contents present in HE and ME was expressed as mg gallic acid equivalent (GAE) per gm of plant extract.

2.2.2.4.2. Estimation of total flavonoid content

Estimation of the total flavonoid content of HE and ME was determined by colourimetrically using aluminum chloride colorimetric method (Chang et al., 2002).

Principle

The aluminum chloride creates acid-stable complexes with the C-4 keto group and either the C-3 or C-5 hydroxyl groups of flavonoid compounds like flavones and flavonols. Moreover, aluminum chloride forms acid-labile complexes with the

orthodihydroxy groups present in the A or B rings of flavonoids and the absorbance of this can be measured spectroscopically at 415 nm.

Procedure

A volume of 0.5 mL of extracts (1 mg/mL) was mixed thoroughly with 1.5 mL of methanol, 0.1 mL of 10% aluminum chloride and finally 0.1 mL of 1 M potassium acetate. The final volume of the reaction mixture was adjusted to 5 mL by adding distilled water. The mixture was incubated at 25 ºC for 30 minutes. The absorbance of the solution was detected by spectrophotometer at 415 nm. A standard curve was prepared by using quercetin (0.50 – 0.25 mg/mL). The results are expressed as mg of quercetin equivalents (QE)/gm extract.

2.2.3. Cytotoxicity analysis *in vitro*

2.2.3.1. Short term cytotoxicity

2.2.3.1.1. Isolation of spleenocytes

Spleenocytes were used as normal cells to analyze the toxicity of HE. A male Wistar rat (180 gm) was anesthetized with chloroform. The spleen was isolated surgically in aseptic condition and washed in phosphate-buffered saline (PBS). The spleen was then minced and gently ground on a sterile stainless steel sieve, which was placed over a petridish containing PBS. The disaggregated spleen cells were transferred to a test tube and centrifuged at 3000 rpm for 10 minutes at 25ºC. The debris-free cell pellet was resuspended in hypotonic buffer containing 0.75% sodium chloride in order to make the lysis of erythrocytes. The spleenocytes were washed and were suspended in RPMI 1640 medium. The cell number was adjusted to 1×10^6 cells/mL using a haemocytometer (Ma et al., 2006).

2.2.3.1.2. Trypan blue dye exclusion method

This experiment is conducted based on the principle that the intact cell membrane of live cells prevent the entry of trypan blue dye to their interior, whereas the dead or damaged cells permit the trypan blue to get deeper in to the cell and stain their nucleus, which can be easily observed under a compound microscope (Moldeus et al., 1978). For the assay, 1×10^6 cells (DLA and EAC) and the extracts at different

concentrations were made up into a final volume of 1 mL PBS and incubated for 3 hrs at 37ºC in an incubator. For spleenocytes, a final volume of 1 mL was made using RPMI 1640 medium. Untreated cells were served as control. After incubation 100 μL of 0.1%, trypan blue was added to the tubes and mixed. After 2 minutes, 10 μL sample was dispensed into the counting chamber with care. Live and dead cell numbers were counted by a compound microscope and the % cell death was calculated according to the following formula.

$$\text{Percentage cell death} = \frac{\text{Number of dead cells}}{\text{Total number of cells counted}} \times 100$$

2.2.3.2. Long term cytotoxicity

2.2.3.2.1. 3-(4,5-dimethylthiazol-2-yl)-2,5-diphenyltetrazolium bromide (MTT) assay

Long term cytotoxicity of HE extract of *S. glauca* was determined by the MTT assay (Mosmann, 1983). This assay primarily intended to detect living cells, not the dead cells. A tetrazolium dye used in the experiment enters the cells, then to mitochondria of each and every cell. In live cells, the mitochondrial NAD(P)H- dependent cellular oxidoreductase enzyme reduces the tetrazolium salt into insoluble purple formazan crystals. The formazan crystals can dissolve in an organic solvent such as isopropanol, and the intensity of colour develops can be measured spectrophotometrically at 570 nm. This method is widely employed to measure cytotoxicity, proliferation or activation.

Cells at its log phase were inoculated in 24 well plate to an approximate count of 1×10^5 per mL and incubated at 37ºC under a 5% CO_2 and 95% humid atmosphere to facilitate adherence. When the seeded cells attained 80% confluence, the medium of each well was discarded and fresh medium which contain different concentrations of the extract was added to the well. Cells were then allowed to grow for 48 hours. After this incubation period, the medium was replaced with fresh medium containing 100 μL of MTT (5 mg/mL in PBS). The well plate was incubated at 37ºC for 4 hours. After that, formazan crystals developed were dissolved by adding 1 mL of the solubilizing solution (isopropanol, concentrated HCl and Triton X-100 prepared in a ratio of 50:0.43:5 (v/v/v)). The absorbance of the solution was read against a blank

solution at 570 nm. The experiments were performed at least three times, for each cell by using a different concentration of HE and the cell viability was calculated using the following formula.

$$\text{Percentage cell viability} = \frac{\text{Absorbance of treated}}{\text{Absorbance of control}} \times 100$$

2.2.4. *In vitro* antioxidant assays

The HE and ME of *S. glauca* were tested for its *in vitro* antioxidant activity by using standard methods. In all the methods performed the absorbance was measured against a blank solution which containing the extract or standard chemical substance and any reagents. A control test was conducted without the extract or standard substance. All *in vitro* antioxidant assays were conducted out in triplicate of each extract. The percentage scavenging activity and IC_{50} values ± SD were calculated.

2.2.4.1. Hydroxyl radical scavenging activity

The scavenging activity of extracts on hydroxyl radicals was evaluated using its competition with 2-deoxy-D-ribose (Saldanha et al., 1990).

Principle

Hydroxyl radicals are generated from Fenton reaction using Fe^{2+}/EDTA/ascorbate/H_2O_2 system. Then the degraded product of 2-deoxy-D-ribose was quantified in terms of a pink coloured chromogen generated by heating with TBA at low pH.

Procedure

The reaction mixture contained 100 μL of $FeCl_3$ (100 μM), EDTA (100 μM), 2-deoxy-D-ribose (2800 μM), phosphate buffer (100 μM, pH 7.4), H_2O_2 (100 μM), ascorbic acid (100 μM) and extract of different concentrations (20-100 μg/mL) were incubated at 37°C for 1 hr. At the end of incubation, 0.2 mL of SDS (8.1%) and 1.5 mL of acetic acid (20%, pH 3.5) and TBA (0.8%) were added and incubated this reaction mixture in boiling water bath for 1 hr and TBARs formation was measured at 532 nm. All the experiments were carried out in triplicate. Vitamin E was used as a positive control. The percentage of inhibition of hydroxyl radical generation at each volume was calculated using the following formula;

$$\% \text{ inhibition } = \frac{Ac - At}{Ac} \times 100$$

Here Ac = Absorbance of control without test sample and At = Absorbance of test

2.2.4.2. DPPH radical scavenging activity

The synthetic stable free radical, 2,2-diphenyl-1-picrylhydrazyl (DPPH) was taken to verify the electron-donating ability of extracts. (Kumar et al., 2012).

Principle

The DPPH method depends on the reduction of DPPH radical (DPPH*) which has purple colour in the presence of antioxidants to a yellow coloured diphenyl picrylhydrazine and the remaining DPPH shows maximum absorption at 517 nm.

Procedure

A volume of 0.187 mL of freshly prepared DPPH reagent (3 mg/25 mL methanol) and extract in different concentrations (2-10 μg/mL) were mixed together in separate test tubes and each reaction mixture was made to a final volume of 1 mL by methanol. These test tubes were incubated in dark condition for 20 minutes at 37 ^{O}C. After 20 min, the absorbance of the reaction mixture was measured at 517 nm using UV/Vis spectrophotometer and methanol was used as blank. DPPH reagent (3 mg/25 mL methanol) was taken as control. Vitamin C was used as a standard for comparing the efficacy of the extracts. Percentage inhibition of free DPPH radicals by the extracts was calculated by the following formula and the resulted was plotted. The concentration of extracts required to scavenge 50% of free DPPH radicals was calculated.

$$\% \text{ free radical scavenging activity} = \frac{Ac - As}{As} \times 100$$

Where Ac = Absorbance of Control and As = Absorbance of the sample

2.2.4.3. Nitric oxide radical inhibition assay

Nitric oxide radical inhibition property of the extracts was evaluated by Greiss reaction (Marcocci et al., 1994).

Principle

At physiological pH (7.4), spontaneous decomposition of Sodium nitroprusside in aqueous solutions produces nitric oxide which interacts with oxygen to produce stable products like nitrate and nitrite. Nitric oxide scavengers make competition with oxygen, leading to decreased production of nitrite. The concentration of nitrite in aqueous solution can be detected spectrophotometrically by using Greiss reagent, with which nitrite ions react to provide a stable product which maximum absorption at 542 nm.

Procedure

500 μL of sodium nitroprusside (10 mM) and extracts (20 – 100 μg/mL) were incubated at 25°C for 3 hrs. After incubation, the reaction mixture was mixed with an equal volume (1 mL) of freshly prepared Griess reagent (1% sulphanilamide and 0.1% naphthyl ethylene diamine dihydrochloride in 2.5% phosphoric acid). The contents were mixed and allowed to stand for 30 minutes in diffused light. Diazotization of nitrite with sulphanilamide and consequent reaction with naphthyl ethylene diamine results in the formation of a pink chromogen with was read at 546 nm. Along with that, control samples were prepared without a test sample in a similar way as done for the test. The percentage nitrite radical scavenging activity of samples was determined. The results were compared with data obtained by using Vitamin C as standard.

2.2.4.4. Ferric reducing/antioxidant power (FRAP) assay

The reducing activity of plant extracts was determined according to the method developed by Pulido et al., (2000).

Principle

By the action of electron-donating antioxidants, a ferric-tripyridyltriazine complex (colourless) may reduce into the blue coloured ferrous state at low pH. This complex has an absorption maximum at 595 nm. High absorbance of the reaction mixture indicates the high reducing capacity of the test compound.

Procedure

FRAP reagent was prepared by mixing 2.0 mL of a 10 mmol/L 2, 4, 6-Tri (2-pyridyl)-s-triazine (TPTZ) in 40 mmol/L HCl, 2.5 mL of $FeCl_3.6H_2O$ (20 mml/L) and 25 mL of acetate buffer (0.3 mol/L, pH 3.6). 0.9 mL of freshly prepared FRAP reagent, freshly prepared and warmed at 37ºC, was then mixed with 0.09 mL of distilled water and 0.03 mL of the test sample, water, or methanol as appropriate for the reagent blank. The final dilution of the extracts in the reaction mixture is kept to 1/34. The reaction mixture was then incubated for 20 min at 37°C and taken absorbance at 595 nm in a spectrophotometer. The percentage increase in the rate of reduction of ferric ion (Fe^{3+}) to ferrous ion (Fe^{2+}) was calculated by plotting a standard graph of ferrous sulfate heptahydrate with varying concentrations from 0.1 to 1.0 μM. Vitamin C was used as the standard. Half maximal effective concentration (EC_{50}) for each extract was determined by the formula given below.

$$EC_{50} = \frac{As - Ac}{As} \times 100$$

Where, As = Absorbance of the sample, Ac = Absorbance of control

2.2.4.5. Inhibition of lipid peroxidation

Lipid peroxidation inhibition of HE and ME in rat liver homogenate was performed according to the colorimetric method of Biswas et al. (2010).

Principle and procedure

A homogenate (10% w/v) of rat liver tissue (male Wistar rat) was prepared with 40 mM Tris-HCl buffer (pH 7.0) and centrifuged at 3000 rpm for 10 minutes. 0.5 mL of the clear supernatant was taken and into that 0.1 mL of each of 0.15 M KCl, 15 mM $FeSO_4$ and 6 mM ascorbic acid and HE and ME of different concentrations (10-50 μg /mL) were added. The reaction mixture was incubated at 37ºC for 1 hour. 1.0 mL of 1% ice-cold trichloroacetic acid (TCA) was added to the mixture and it was centrifuged at 3000 x g for 20 min at 4ºC. 2.0 mL of the supernatant was taken in another test tube and 1.0 mL of 0.8% thiobarbituric acid (TBA) was added and heated the mixture at 90ºC for 20 minutes in a water bath. After bringing to room temperature, the absorbance was measured at 532 nm by a spectrophotometer. The %

inhibition was calculated by using the formula given below. Ascorbic acid was used as a positive control.

$$\% \text{ inhibition} = \frac{Ac - As}{Ac} \times 100$$

Where, As = Absorbance of the sample, Ac = Absorbance of control

2.2.4.6. Total antioxidant capacity determination

The total antioxidant capacity of *S. glauca* extracts was spectrophotometrically determined by the phosphomolybdenum assay described by Prieto et al. (1999).

Principle

This assay is based on the reduction of phosphate-molybdenum (VI) into green coloured phosphate-molybdenum (V) complex by test compounds exhibiting antioxidant property.

Procedure

A volume of 1.0 mL of phosphomolybdenum reagent solution (prepared by mixing sulphuric acid (0.6 M), Na_2PO_4 (28 mM) and ammonium molybdate (4 mM) was incubated with extract solution (10-100 μg/mL) and incubated in capped test tubes in a water bath at 95^{o}C for 90 minutes. After incubation, samples were cooled and the absorbance of the solution was taken at 765 nm against a blank (without plant extract). Total antioxidant activity (in % inhibition) was calculated using the following formula;

$$\% \text{ inhibition} = \frac{As - Ac}{As} \times 100$$

Where, As = Absorbance of the test sample, Ac = Absorbance of the control.

2.2.4.7. Lipoxygenase inhibition assay

Principle

Lipoxygenase (LOX) is a heterogeneous category of lipid peroxidizing enzymes which catalyze the dioxygenation of polyunsaturated fatty acids which contain the 1, 4-cis, cis system to their subsequent hydroperoxy derivatives. One of the primary

targets of LOX is linoleic acid and its action on linoleic acid leads to the formation of a conjugated diene and its rate of conjugated diene produced can be measured spectrophotometrically at 234 nm.

Procedure

The reaction mixture was prepared by taking lipoxygenase (50 U), linoleic acid (100 nmoL) and extracts (10 -100 μg/mL) into a total volume of 1.0 mL of phosphate-buffered saline (pH 7.4). The reaction system was mixed and incubated at room temperature for 1 hour. The formation of conjugated diene was measured at 234 nm by a spectrophotometer. The positive control used in the study was vitamin C. The percentage inhibition of lipoxygenase enzyme by plant extracts were calculated by the formula given below.

$$\% \text{ inhibition} = \frac{Ac - As}{Ac} \text{x } 100$$

Where, As = Absorbance of the sample, Ac = Absorbance of control

2.2.5. *In vivo* toxicity studies

2.2.5.1. Acute toxicity study

Forty two adult healthy Swiss albino mice with similar weight (25 ± 3 gm) were categorized into 7 groups of 6 animals (3 males and 3 females) and maintained in different cages based on sex. The animals were subjected for a fasting period of 12 hours. A single dose of HE was administered by oral gavage to the animals belongs to Group III (0.1 gm/kg b. wt.), IV (0.25 gm/kg b. wt.), V (0.50 gm/kg b. wt.), VI (1.0 gm/kg b. wt.) and VII (2.0 gm/kg b. wt.). The animals in the vehicle group (Group II) were received 0.2 mL 1% food-grade propylene glycol (CAS number 57-55-6). Group I animals were administered 200 μL saline and considered as untreated (normal). All the animals were provided with food and water after 30 minutes of the drug administration. All changes in general behaviour related to the administration of extract in mice were observed continuously for 5 hours after dosing. The monitoring of mice was continued for 14 successive days for any visible changes in behaviour (like aggressiveness or drowsiness, noisy breathing), body weight, water and food intake, hair loss, oozing out of any discharges from their eye and ear and mortality. The changes in body weight and feed and water consumption rate were recorded

within every two days during the experiment time. At the end of experimental period animals were sacrificed and the internal organs were examined for any sign of change by conducting a necropsy. The experiment was conducted as per the Organization for Economic Cooperation and Development (OECD) guidelines (guideline no. 423) (OECD, 2001).

2.2.5.2. Sub-acute toxicity study

Subacute toxicity evaluation was performed as per the OECD test guideline no. 407 (OECD, 2008). Healthy adult male and female Swiss albino mice (25 ± 3 gm) were randomly divided into five experimental groups; an untreated group, administered 200 μL saline (group I), vehicle control (200 μL of 1% propylene glycol) group (group II) and HE treated (group III: 0.200 gm/kg b. wt., group IV: 0.300 gm/kg b. wt. and group V: 0.400 gm/kg b. wt) groups. Each group consisted of ten mice, five of each sex and they were maintained in separate cages. HE was administered once daily in the morning by oral gavage and continued for twenty eight days. The animals were monitored for behavioral and clinical symptoms such as immobility, diarrhea, hair loss, neuromuscular problems and mortality during the entire experimental period. Body weight, consumption of water and food were also monitored on a regular basis. At the end of the treatment period, animals fasted overnight but provided water in *ad libitum*. They were anesthetized with anesthetic ether and sacrificed by cervical decapitation for further examination. Blood was collected by direct cardiac puncture for hematological and biochemical analysis with and without anticoagulant ethylene diamine tetra acetic acid (EDTA) coated tubes, respectively. Haematological parameters were determined by using blood collected in EDTA coated tubes. For Serum biochemical analysis, blood was centrifuged at 3000 rpm for 5 minutes to obtain serum, which was stored at $^{-}20^{o}$C until performing assays. The serum was used for determining liver function tests (LFT) like serum aspartate transaminase (SGOPT/AST), serum glutamate pyruvate transaminase (SGPT/ALT), alkaline phosphatase (ALP) and total bilirubin. The lipid profiling test such as total cholesterol, triglycerides, HDL, LDL and VLDL levels and kidney function tests such as total creatinine and urea level were estimated by using commercially available diagnostic reagent kits. Various electrolytes present in serum such as sodium, potassium, chloride, bicarbonate, etc were also determined. Necropsies of the animals were performed. The weight of important organs like the brain, liver, stomach,

kidneys, and spleen was determined and organosomatic index in relation to the final body weight was calculated. A portion of the selected organs like brain, stomach, intestine, liver, kidney, spleen, lungs, heart and reproductive organs (testis in male and ovary in female) of animals of untreated, vehicle control and treated group (400 mg/kg b. wt.) were fixed in 10% neutral buffered formalin for 24 hours. Paraffin wax embedded organ tissue samples were cut into slices of 2-5 μm and stained with hematoxylin and eosin and the sections were observed under a (20X) objective lens and photographs were taken using Magnus inverted laboratory microscope. Histopathological examination was conducted out by a veterinary pathologist who was blind to the study.

2.2.5.2.1. Determination of haematological parameters

2.2.5.2.1.1. Estimation of Haemoglobin (Hb)

The haemoglobin level in the blood samples was determined by the method of Drabkin and Austin (1935).

Principle

Hemoglobin and its derivatives (except sulhemoglobin) oxidized into methemoglobin in the presence of alkaline potassium ferrocyanide. The methemoglobin then reacts with potassium cyanide and form cyanmethemoglobin, which has a maximum absorption at 546 nm. The absorbance of cyanmethemoglobin is directly proportional to the total haemoglobin concentration.

Procedure

A volume of 20 μL of fresh anticoagulant added blood was mixed with 5 mL of Drabkin's cyanmethemoglobin reagent and incubated for 5 minutes at room temperature. The absorbance of the reaction mixture was taken at 546 nm after incubation. The absorbance of the standard solution (provided in the reagent kit) equivalent to 60 mg/dL haemoglobin was also detected along with sample. The total haemoglobin content in blood was calculated using the following formula.

$$\text{Total haemoglobin (g/dL)} = \frac{\text{Absorbance of Test}}{\text{Absorbance of Standard}} \times \frac{251}{1000} \times 60$$

Where 251 is the dilution factor i.e Total reagent volume (5.02 mL/ sample volume (0.02 mL), 1000 is the multiplication factor to convert milligrams to grams. And 60 is the concentration of the Hb standard in mg%

2.2.5.2.1.2. Determination of red blood cells (RBCs)

The red blood cells are counted using the method of Cheesbrough and McArthur (1976).

Principle

Dilute the blood samples with Hayem's fluid (RBC diluting fluid) in a ratio of 1:200. This fluid is isotonic with blood and no haemolysis may occur. This does not remove the white cells but allows rouleaux formation. The samples are counted under high power (40X objective) by using a counting chamber. The number of cells in undiluted blood is calculated and reported as the number of red blood cells per cu mm of whole blood.

Procedure

Took blood up to the mark of 0.5 in RBC pipette and made up to the mark of 101 by taking RBC diluting fluid. This solution was mixed well by rotating the pipette for 2-3 minutes between palms. The solution was then added to the Neubauer counting chamber without air bubbles and allowed the cells to settle down for 3 minutes. The cells were counted under high power (40X) in the five squares of the central square as four corners squares and one central square of the large central square and of the chamber. The RBC count was determined by the formula

$$\text{RBC count (cells/mm}^3\text{)} = \frac{\text{Number of cells counted x dilution factor}}{\text{Depth factor x Area counted}}$$

Where the dilution factor is 200

The area is 5/25 (out of the 25 squares (1 sq.mm) of the larger central square, RBCs of 5 squares are counted)

Depth of counting chamber is 0.1mm

So, total RBC count = Number of cells × 10,000/mm^3

2.2.5.2.1.3. Determination of total leucocyte count (TC)

Total leucocyte count was estimated by the method of Cheesbrough and McArthur (1976).

Principle

When blood diluted with Turk's fluid (0.2 mL glacial acetic acid, 0.1 mL of 1% gentian violet and 99.7 mL water) may result in lysis of red blood and white blood cells. Though the WBC cells lose their cytoplasm, they show their nuclei prominently fixed by the glacial acetic acid and stained by gentian violet. The number of white blood cells is easily counted by this way under the low power of a compound microscope.

Procedure

The blood was drawn up to the 0.5 marks in WBC pipette and diluted with Turk's fluid up to the mark 11. The solution was mixed well by rotating the pipette in a horizontal position between palms and then allowed the cells to settle by keeping it 3 minutes. The mixture was then dispensed into a Neubauer counting chamber and kept to settle. Then the number of white blood cells in the four large corner squares was counted by using the low power objective. The total WBC count was determined by the formula.

$$\text{Total number of cells (per } \mu\text{L)} = \frac{\text{Counted cells}}{\text{Counted surface (mm}^2\text{) x Chamber depth (mm) x Dilution}}$$

Where Area counted = 1 mm^2 x 4 = 4 mm^2, Depth = 1/10 mm, Dilution = 1:20

Hence

Total WBC (cells/mm^3) = Number of cells counted × 50

2.2.5.2.1.4. Determination of differential leucocyte count (DC)

Differential leucocyte count helps the determination of the relative number of different types of leucocytes present in the blood and it was done by the method of Wintrobe and Greer (2009).

Principle

Leishman stain (blue coloured solution) is used in microscopy for staining blood smears. The different types WBCs can be easily differentiated from each other by observing the size of the cell, shape of the nucleus, presence or absence of granules, etc. in a compound microscope with 40X objective lens. Under Leishman staining, WBC cells perform the following characters. Neutrophil cells appear with purple coloured nuclei (multilobed) with pink cytoplasm, Eosinophil with purple nucleus (dumbbell-shaped), faint pink cytoplasm and orange-red granules, Basophils have an irregular purple nucleus and dark blue granules and monocytes have a purple colour nucleus (horseshoe shaped) and pink cytoplasm. Lymphocytes have a dark blue circular nucleus with light blue cytoplasm. Platelets usually appear as violet coloured granules.

Procedure

The blood smear was prepared with a drop of blood using a slide and a spreader. The smear was allowed to dry by waving in the air. The staining was done with 1 mL of Leishman stain (0.15 gm/100 mL methanol) for 2 to 3 minutes. Then added an equal amount of distilled water for diluting the stain and kept it for 3 more minutes. The slide was washed under tap water to remove the excess stain and air-dried. It was observed under the microscope objective lens with 40X magnification. The slide was examined by moving in a zig-zag manner to count different leucocytes. The percentages of different leucocytes counted were calculated by counting up to 100 cells.

2.2.5.2.1.5. Determination of platelet count (PLT)

The platelets in the blood samples were counted by using a manual method developed by Cheesbrough and McArthur (1976).

Principle

The blood is diluted with a 1% ammonium oxalate solution. The isotonic balance of the diluents is such that all erythrocytes are lysed while the leucocytes and platelets remain intact. The dilution is mixed well and incubated to permit lysis of the erythrocytes. After the incubation period, the dilution is mounted on a Neubauer

counting chamber. The cells are allowed to settle and then are counted in a specific area of the Neubauer counting chamber under the microscope.

Procedure

Using an RBC pipette, prepared a 1:200 dilution of blood as for RBC counting with diluting fluid (1% ammonium oxalate). Mixed gently for 2 minutes and charged the Neubauer counting chamber and observed under a compound microscope 40X objective. The platelets count is calculated by the formula

$$\text{Platelet count (cells/mm}^3\text{)} = \frac{\text{Number of cells counted (N) x dilution factor}}{\text{Depth factor x Area counted}}$$

Where the dilution factor is 200

The area is 5/25 (out of the 25 squares (1 sq.mm) of the larger central square, platelets of 5 squares are counted)

Depth of counting chamber is 0.1mm

So, the total number of platelets per mm^3 = N x 10,000

2.2.5.2.1.6. Determination of packed cell volume (PCV)

The PCV was determined by the method of Wintrobe and Greer (2009).

Principle

When the whole blood (mixed with anticoagulant) loaded into a Wintrobe tube and centrifuged at a standard speed, erythrocytes sediments at the bottom of the tube. This sedimented red cell column is known as haematocrit or packed red cell volume and expressed as percentage fraction of the whole blood.

Procedure

The anticoagulated whole blood after mixing thoroughly was filled in the Wintrobe tube using a Pasteur pipette. The tubes were centrifuged at 3000 rpm for 30 minutes. Mix blood sample thoroughly. The length of the red cell column was noted and the percentage of the red column to the total volume of the blood sample was calculated.

2.2.5.2.2. Estimation of serum markers

2.2.5.2.2.1. Estimation of serum electrolytes

2.2.5.2.2.1.1. Determination of sodium and potassium

Principle

Flame photometry method is the most commonly used method for the determination of sodium and potassium. If an alkali metal in solution is aspirated into a low-temperature flame in an aerosol form, it will alter excitation by the flame; emit a discrete frequency of light which is selected by an optical filter and reached in the photodetector in the flame photometer. The light emission is proportional to the concentration of the alkali in the sample (Deal, 1954).

Procedure

Sodium (1000 mEq/L) and potassium (100 mEq/L) standard stock solutions were prepared and by mixing these solutions, working standards were prepared as of 120 /2 mEq/L (S1), 140 / 4 mEq/L (S2), 160/6 mEq/L (S3). Four reaction systems – test sample (serum) and working standards (standard1, standard 2 and standard 3) were maintained. First, 10 mL of distilled water was pipette into each tube. A volume of 100 μL of serum and 100 μL of serum and working standards S1, S2, S3 solutions were added to respective tubes. The solutions in each tube were mixed thoroughly and transferred to bulbs for flame photometric determination of the samples. Flame emission intensity for each tube was determined and with a calibration curve prepared, the concentration of the sample was determined.

2.2.5.2.2.1.2. Determination of chloride

Serum electrolyte chloride estimation was done by mercuric thiocyanate method of Schoenfeld and Lewellen (1964) and Levinson (1976) using electrolyte diagnostic reagent kit with a flame photometer.

Principle

Chloride reacts with a solution of mercuric thiocyanate and ferric nitrate to form red-brown ferric thiocyanate and stable mercuric chloride. The intensity of the reddish-

brown colour developed is proportional to the concentration of chloride present in the serum sample.

Procedure

Four test tubes namely blank, control, standard, and sample, set and added 2.0 mL of chloride reagent. Then, to the blank 10 μL of deionized water was added and to standard, 10 μL of standard chloride reagent (100 mmol/L) was added. About 10 μL plasma from control and experimental groups was added to control and test tubes, respectively. The contents in the tubes were mixed thoroughly and incubated at room temperature for 2 minutes. The absorbance of standard, control and sample were measured at 505 nm against blank using Photometer system. The concentration of the chloride is calculated by the formula.

$$\text{Chloride (mmol/L)} = \frac{\text{Absorbance of sample}}{\text{Absorbance of standard}} \text{ x } 100$$

2.2.6. Analysis of hepatic function

The liver function tests were conducted using blood serum. Serum was separated and used to determine the serum glutamate oxaloacetate transaminase (SGOT), glutamate pyruvate transaminase (SGPT), alkaline phosphatase (ALP), bilirubin and total protein by commercially available kits.

2.2.6.1. Estimation of serum glutamic oxaloacetic transaminase (SGOT) activity

SGOT or aspartate aminotransferase (AST) was determined spectrophotometrically by IFCC (International Federation of Clinical Chemistry) kinetic method by using SGOT kit supplied by Agappe Diagnostics Ltd, Ernakulam, Kerala, India.

Principle

AST catalyzes the transfer of an amino group between L-Aspartate and alpha-ketoglutarate. The oxaloacetate formed in this reaction is then reacted with NADH + H^+ in the presence of malate dehydrogenase (MDH) to NAD^+. Since NADH + H^+ absorbs light at 340 nm and NAD^+ does not, the rate of decrease of absorbance is directly related to the AST activity in the sample (Thefeld et al., 1974, Bergmeyer et al., 1976).

$$\text{L-Aspartate + alpha-ketoglutarate} \xrightarrow{\text{AST}} \text{Oxaloacetate + L-Glutamate}$$

$$\text{Oxaloacetate + NADH + H}^{+} \xrightarrow{\text{MDH}} \text{L-Malate + NAD}^{+}$$

Procedure

Reagent kit consisted of two reagents.

Reagent 1 consists of Tris Buffer (pH 7.8 – 88 mmol/L), L-Aspartate (260 mmol/L), LDH (>1500U/L) and MDH (> 900U/L)

Reagent 2 consists of alpha - ketoglutarate (12 mmol/L) and NADH (0.24 mmol/L).

A working reagent was prepared for the assay by mixing reagent 1 with reagent 2 in ratio 4:1 (v/v). To a volume of 1000 μL working reagent 100 μL test sample was added mixed. The reaction mixture was incubated at 37^{o}C for 1 minute. The absorbance of this mixture was recorded at 340 nm with 60 seconds interval for 3 minutes. Calculated the average change in absorbance per minute (ΔA/min) subtracting each reading from the previous one and found the average of these values. The formula used for calculating SGOT activity is given below.

Calculation

$$\text{SGOT activity (U/L)} = (\Delta\text{A/min}) \times 1745$$

Where, 1745 is the calculation factor.

2.2.6.2. Estimation of serum glutamic pyruvic transaminase (SGPT) activity

SGPT or Alanine aminotransferase (ALT) was determined spectrophotometrically by IFCC (International Federation of Clinical Chemistry) kinetic method by using the SGPT kit supplied by Agappe Diagnostics Ltd, Ernakulam, Kerala, India.

Principle

ALT catalyzes the transfer of the amino group from L-alanine to alpha-ketoglutarate giving pyruvate and L-Glutamate. Produced pyruvate and NADH+ H^{+} reacts in the presence of Lactate dehydrogenase (LDH) to give L-lactate and NAD^{+}. Since NADH+ H^{+} absorbs light at 340 nm and NAD does not, the rate of decrease of

absorbance is directly proportional to the ALT activity in the sample (Thefeld et al., 1974).

$$\text{L-Alanine + alpha-ketoglutarate} \xrightarrow{\text{ALT}} \text{L-Glutamate + Pyruvate}$$

$$\text{Pyruvate + NADH + } H^{+} \xrightarrow{\text{LDH}} \text{L-Lactate + } NAD^{+}$$

Procedure

Reagent kit consisted of two reagents.

Reagent 1 consists of Tris Buffer, (pH 7.5 – 110 mmol/L), L-Alanine (600 mmol/L) and LDH (>1500U/L).

Reagent 2 consists of alpha -ketoglutarate (16 mmol/L) and NADH (0.24 mmol/L).

A working reagent was prepared for the assay by mixing reagent 1 with reagent 2 in ratio 4:1 (v/v). The working reagent is stable for 30 days at 2-8ºC. To a volume of 1000 μL working reagent 100 μL test sample was added mixed. The reaction mixture was incubated at 37ºC for 1 minute. The absorbance of this mixture was recorded at 340 nm with 60 seconds interval for 3 minutes. Calculated the average change in absorbance per minute (ΔA/min) subtracting each reading from the previous one and found the average of these values. The formula used for calculating SGPT activity is given below.

Calculation

$$\text{SGPT activity (U/L)} = (\Delta A/\text{min}) \times 1745$$

Where, 1745 is the calculation factor.

2.2.6.3. Estimation of alkaline phosphatase (ALP) activity

Alkaline phosphatase activity was determined spectrophotometrically by the method of kinetic reaction using ALP reagent kit supplied by Agappe Diagnostics Ltd, Ernakulam, Kerala, India.

Principle

Alkaline phosphatase (ALP) catalyzes the hydrolysis of Para-nitrophenyl phosphate in the presence of water, at pH 10.2 and liberates p-nitrophenol and inorganic phosphate, according to the following reaction:

$$\text{Para-nitrophenyl phosphate} + H_2O \xrightarrow{\text{ALP}} \text{p-nitrophenol} + \text{Inorganic phosphate}$$

The rate of p-nitrophenol formation can be measured spectrophotometrically (at 405 nm) is proportional to the catalytic concentration of alkaline phosphatase present in the sample (Schlebusch et al., 1974).

Procedure

Reagent kit consisted of two reagents.

Reagent 1 consists of Diethanolamine Buffer, (pH 10.2 – 125 mmol/L) and magnesium chloride (0.625 mmol/L).

Reagent 2 consists of Para-nitrophenyl phosphate (50 mmol/L).

A working reagent was prepared for the assay by mixing reagent 1 with reagent 2 in ratio 4:1 (v/v). The working reagent is stable for 30 days at 2-8ºC. To a volume of 1000 μL working reagent 20 μL test sample was added mixed. The reaction mixture was incubated at 37ºC for 1 minute. The absorbance of this mixture was recorded at 405 nm with 60 seconds interval for 3 minutes. Calculated the average change in absorbance per minute (ΔA/min) subtracting each reading from the previous one and found the average of these values. The formula used for calculating ALP activity is given below.

Calculation

$$\text{ALP activity (U/L)} = \Delta A/\text{min} \times 2750$$

Where, 2750 is the calculation factor.

2.2.6.4. Estimation of total bilirubin

Total bilirubin was determined spectrophotometrically by Walters and Gerarde method (1970) by using Bilirubin kit supplied by Agappe Diagnostics Ltd, Ernakulam, Kerala, India.

Principle

4-aminobenzenesulfonic acid (sulfanilic acid) reacts with sodium nitrate and form diazotized sulfanilic acid. Bilirubin reacts with this diazotized sulfanilic acid in the presence of diazo reagent (TAB) forms azobilirubin with pink colour which can be measured spectrophotometrically at 546 nm.

Procedure

A volume of 1000 μL bilirubin agent was taken (4-aminobenzenesulfonic acid -28.9 mmol/L and TAB – 9 mmol/L) in a test tube. Activator total (20 μL) was added to this and followed by 50 μL sample (serum). A reagent blank was also prepared similar to the test sample except for serum. Mixed carefully and they were incubated at room temperature for 5 minutes. The absorbance was measured at 546 nm and total bilirubin level was calculated by using the following formula.

Calculation

$$\text{Concentration of bilirubin (mg/dL)} = \text{OD of the Test} - \text{OD of reagent blank} \times 25$$

Where, 25 = calculation factor.

2.2.6.5. Estimation of total protein

The total quantity of protein present in the tissue and blood was determined by the colorimetric method of Lowry et al., (1951).

Principle

Tyrosine and tryptophan, the amino acids present in proteins may reduce the phosphomolybdate and phosphotungstate components of Folin-Ciocalteu phenol reagent in alkaline medium and produce a bluish-purple colour with maximum absorbance at 660 nm.

Procedure

Tissue homogenate (10% w/v, 10 μL) or serum (10 μL) was diluted with 990 μL of distilled water and added 5.0 mL of alkaline copper sulphate (50 mL of 2% sodium carbonate (Na_2CO_3) in 0.1N NaOH and 1 mL of 0.5% $CuSO_4$ in 1% sodium potassium tartarate). The reaction mixture was mixed well and incubated at room temperature for 10 minutes. Folin-Ciocalteu reagent (0.5 mL) in water (1:1) was added to the reaction mixture, mixed well and incubated at room temperature for 30 minutes. The absorbance of the reaction mixture was measured at 660 nm. Total protein content was calculated from the standard graph prepared by using bovine serum albumin (BSA, 10-100 μg/mL).

2.2.7. Analysis of renal function

The renal function tests were conducted by using blood serum. Serum was separated and used to determine the serum creatinine and serum urea by commercially available kits.

2.2.7.1. Estimation of serum creatinine

The level of serum creatinine was determined by Jaffe's kinetic method by using kit reagents supplied by Euro Diagnostic Systems Pvt. Ltd., Chennai, India.

Principle

The creatinine present in the sample reacts with sodium picrate (which originates from the picric acid present in the reagent), in alkaline condition and generates an orange coloured complex (creatinine picrate complex). This complex gives maximum absorbance at 520 nm and can be measured spectrophotometrically (Bones and Tausky, 1945, Toro and Ackermann, 1975). The reaction is represented below in the form of a formula.

$$\text{Creatinine} + \text{Sodium picrate} \xrightarrow{\text{Alkali}} \text{Orange coloured creatinine picrate complex}$$

Procedure

A working reagent was prepared by taking equal volumes of picric acid (>8mmol/L), and alkaline buffer, which contains NaOH (>475mmol/L), EDTA (> 2mmol/L), surfactants and stabilizers. A volume of 50 μL of serum was mixed with 1 mL working reagent. A volume of 50 μL of standard creatinine solution supplied with the kit was mixed with 1mL working reagent in another test tube and considered as standard. The absorbance of both solutions was measured at 520 nm against distilled water as blank after 30 seconds (A_0) and 90 seconds (A_1). The calculation was done using the following formula.

Calculation

ΔA was calculated for standard (S) and test sample (T)

$\Delta A_s = A_{s1} - A_{s0}$

$\Delta A_T = A_{T1} - A_{T0}$

$$\text{Serum Creatinine (mg/dL)} = \Delta A_T / \Delta A_S \times 2$$

Where A_T = Absorbance of test and A_S = Absorbance of standard, 2 = (standard concentration).

2.2.7.2. Estimation of serum urea

Serum urea concentration was estimated by Urease-GLDH (Enzymatic UV) method (Young et al., 1975) by using a reagent kit supplied by Euro Diagnostic Systems Pvt. Ltd., Chennai, India.

Principle

Urea in the sample is converted into ammonia and carbon dioxide by enzyme urease. In this method (modified), ammonium ions react with alpha-ketoglutarate and NADH to form glutamate and NAD. The rate of oxidation of NADH to NAD can be measured at 340 nm as a decrease in absorbance in a fixed time, which is proportional to the concentration of urea present in serum.

Procedure

Reagent kit contained two reagents. Prepared working reagent by mixing R1 (enzyme reagent) and R2 (Starter) in 4:1 ratio. A volume of 1 mL of working reagent was mixed with 10 μL of serum in a cuvette at 37^0C and measured absorbance (A_1) exactly after 30 seconds at 340 nm. Exactly after 60 seconds after A_1, recorded the absorbance (A_2) of the reaction mixture after 60 seconds. The change in absorbance (ΔA_T and A_S) was calculated by subtracting A_2-A_1. The same experiment was conducted with a standard sample (10 μL) provided with the kit with a concentration of 40 mg/dL urea.

Calculation

$$\text{Urea (mg/dL)} = \Delta A_T/\Delta A_S \times 40$$

Where ΔA_T = change in absorbance of the test, ΔA_S = change in absorbance of standard, 40 = concentration of standard.

2.2.8. Determination of lipid profile

2.2.8.1. Estimation of serum total cholesterol

The total cholesterol present in the serum was estimated by CHOD-PAP method (Allain et al., 1974) by using a reagent kit purchased from Agappe Diagnostic Ltd., Ernakulam, Kerala.

Principle

Enzymatic colorimetric estimation of total cholesterol (TC) can do according to the following reactions.

$$\text{Cholesterol ester} + H_2O_2 \xrightarrow{\text{Cholesterol esterase}} \text{Cholesterol} + \text{fatty acids}$$

$$\text{Cholesterol} + O_2 \xrightarrow{\text{Cholesterol oxidase}} \text{4-Cholesten-3-one} + H_2O_2$$

$$2H_2O_2 + \text{Phenol} + \text{4-Aminoantipyrien} \xrightarrow{\text{Peroxidase}} \text{Red quinone} + 4H_2O$$

The red coloured quinone shows maximum absorbance at 505 nm.

Procedure

The working reagent consists of a) Pipes buffer (pH 6.70) - 50 mmol/L, b) Phenol-24 mmol/L, c) Sodium Cholate - 0.5 mmol/L, d) 4-aminoantipyrien – 0.5 mmol/L e) Cholesterol Esterase - >180 U/L, f) Cholesterol Oxidase - > 200 U/L and g) Peroxidase - >1000 U/L. A volume of 10 μL serum sample was taken in test tube marked as 'T" and 10 μL of the standard solution provided with the kit (200 mg/dL) into test tube labeled as 'S' along with 1 mL of working reagent in each tube. The solution was mixed well and incubated at 37 °C for 5 minutes. After the incubation period, the absorbance of sample and standard were detected against reagent blank at 505 nm.

Calculation

$$\text{Total cholesterol (mg/dL)} = \frac{\text{Absorbance of sample}}{\text{Absorbance of Standard}} \text{ x } 200$$

Where, 200 = calculation factor.

2.2.8.2. Estimation of serum triglycerides

Total serum triglycerides (TG) was estimated by GPO-TOPS methodology (Schettler and Nussel, 1975) by using a commercial kit purchased from Agappe Diagnostics Ltd.

Principle

The enzymatic determination of triglyceride is based on the following reactions.

$$\text{Triglyceride} + H_2O \xrightarrow{\text{Lipoprotein Lipase}} \text{Glycerol} + \text{Fatty acid}$$

$$\text{Glycerol} + \text{ATP} \xrightarrow[Mg2+]{\text{Glycerol Kinase}} \text{Glycerol -3-phosphate} + \text{ADP}$$

$$\text{Glycero-3-phosphate} + O_2 \xrightarrow{\text{Glycerol-3-phosphate Oxidase}} \text{Dihydroxyacetone phosphate} + H_2O_2$$

$$2H_2O_2 + \text{4-Aminoantipyrine} + \text{TOPS} \xrightarrow{\text{Peroxidase}} \text{Violet coloured complex}$$

The final violet coloured complex gives maximum absorbance at 546 nm.

Procedure

About 10 μL serum in test tube 'T' and 10 μL of standard (200 mg/ dL) in test tube 'S' were added along with 1 mL of triglyceride reagent (Pipes-buffer, pH 7.00,- 5 mmol/L, TOPS - 5.3 mmol/L, potassium ferrocynate - 10 mmol/L, Magnesium Salt - 17 mmol/L, 4-Aminoantipyrine - 0.9 mmol/L, Adenosine Tri Phosphate - 3.15mmol/L, Lipoprotein Lipase - > 1800 U/L, Glycerol Kinase - > 450 U/L, Glycerol – 3- phosphate oxidase - > 3500 U/L, and Peroxidase - > 450 U/L). The content in the tubes was mixed well and incubated for 5 min at 37°C and the change in absorbance in standard and sample were determined against reagent blank at 546 nm. Total triglycerides (TG) was calculated using the formula,

Calculation

$$\text{Triglycerides (mg/dL)} = \frac{\text{Absorbance of Sample}}{\text{Absorbance of Standard}} \text{ x } 200$$

Where, 200 = calculation factor.

2.2.8.3. Estimation of serum high-density lipoprotein cholesterol

Quantitative determination of high density lipoprotein cholesterol (HDL) in serum was done by means of the photometric method (Naito, 1985) with a commercial kit purchased from Euro Diagnostic Systems Pvt. Ltd., Chennai, India.

Principle

The detergent (<2%) present in the reagents solubilizes only the HDL cholesterol present in the sample. The HDL cholesterol thus released will react with the cholesterol esterase, cholesterol oxidase and finally with chromogens and develop colour. The non HDL lipoproteins like low-density lipoproteins (LDL), very low-density lipoproteins (VLDL) and chylomicrons are inhibited from reacting with the enzymes present in the reagents due to absorption of the detergents on their surfaces. So the intensity of the colour formed is proportional to the HDL-c concentration in the serum sample and its maximum absorbance is at 600 nm.

Procedure

The kit consists of two reagents and a calibrator solution (lyophilized human serum). Reagent 1 consists of Cholesterol oxidase (<1000 U/L), peroxidase (<1300 U/L) and DSBmT (<1mM). Reagent 2 consists of Cholesterol esterase (<1500 U/L), 4-Aminoantipyrine (<1mM), detergent (2%) and Ascorbic oxidase (<3000 U/L).

A volume of 10 μL serum was added to 450 μL of R1. The same volume of R1 was added to 10 μL of HDL Calibrator. These two tubes with a blank tube (450 μL of R1) were incubated for 5 min at 37°C after mixing the contents of each tube. A volume of 150 μL of R2 is added into all the tubes. The reaction mixture was mixed well and incubated again at 37°C for 5 minutes and immediately after the incubation period, the absorbance of calibrator and sample at 600 nm against reagent blank. HDL in the sample was calculated using the following formula.

$$\text{HDL (mg/dL)} = \frac{\Delta A \text{ Sample}}{\Delta A \text{ Calibrator}} \text{ x Concentration of Calibrator}$$

2.2.8.4. Estimation of serum low-density lipoprotein and very-low-density lipoprotein

The LDL value was calculated using Friedewald's formula (Friedewald et al., 1972), which is stated below.

$$\text{LDL (mg/dL)} = \text{TC} - \text{HDL} - (\text{TG}/5)$$

Where, TC = Total cholesterol in sample, HDL = high density lipoprotein cholesterol, TG = Triglycerides.

VLDL level was also calculated by using formula,

VLDL (mg/dL) = Triglycerides (mg/dL)/ 5

2.2.9. *In vivo* antioxidant activity analysis

2.2.9.1. Evaluation of antioxidant activity of HE

Experimental design

The *in vivo* antioxidant activity of HE was evaluated according to the method of Liu et al. (2013). A total number of thirty female Swiss albino mice (25 ± 3 gm) were

used in this experiment. After acclimated for one week, the mice were randomly divided into five groups (six animals per group). Group I was kept as normal and treated with 200 μL saline. Group II was treated with 200 μL of 1% propylene glycol by gavage and considered as vehicle control. Group III animals were administered with 200 μL of ascorbic acid (15 mg/kg b. wt., p.o.) as standard drug. Mice in HE treatment groups (Group IV and Group V) were administered with HE in two different doses (160 and 260 mg/kg b. wt per day) by gavage. The treatment was continued for thirty consecutive days. One day after the last drug administration, the mice were sacrificed by ether anesthesia following overnight fasting.

Preparation of haemolysate

The blood was collected by cardiac puncture into EDTA coated tubes. The tubes were then centrifuged at 2000 rpm for 10 minutes. The supernatant was removed and the packed RBC collected was washed with saline. The haemoglobin concentration of the packed RBC was determined by the method developed by Drabkin and Austin (1935).

For haemolysis, a known volume of packed RBC cells (0.1 mL) was allowed to undergo lysis with hypotonic phosphate buffer (0.9 mL). The tubes were centrifuged after vigorous shaking at 10,000 rpm for 60 minutes in a refrigerated centrifuge for removing the debris of RBC and collected haemolysate was immediately used for the estimation of glutathione and to measure the activities of enzymes like superoxide dismutase and catalase.

Preparation of tissue homogenate

Soon after blood collection, the liver and kidney were dissected out and washed in ice-cold saline (0.9% NaCl) and weighed. The homogenate of these organs was prepared (10% w/v in 0.1M Tris hydrochloric acid buffer, pH 7.4) by a motor homogenizer in ice-cold conditions and used for the estimation of lipid peroxidation and total protein. The homogenates were further centrifuged at 8,600 rpm for 20 minutes at 4 °C. The supernatant was collected and used for the estimation of superoxide dismutase, catalase, glutathione peroxidase, reduced glutathione and total protein.

2.2.9.1.1. Estimation of reduced glutathione (GSH)

The reduced GSH content in the tissue and blood was determined by adopting the method of Moron et al., (1979)

Principle

GSH is measured by its reaction with DTNB which produces a yellow coloured complex and which can be measured spectrophotometrically with maximum absorption at 412 nm.

Procedure

About 100 μL of liver tissue supernatant or blood was taken along with 125 μL of 25% TCA (ice cooled) and kept on ice for 5 minutes. 0.6 mL of 5% TCA was added to the reaction mixture and centrifuged at 1500 rpm for 10 minutes. 100 μL of supernatant was taken from this reaction mixture and added 667 μL of 0.6 mM DTNB and solution was made up to a final volume of 1.0 mL with phosphate buffer (0.2 M, pH 8). The absorbance was measured immediately at 412 nm against phosphate buffer as blank. The level of reduced GSH was calculated by plotting a standard graph. The results are expressed as nmol/mg tissue protein (liver) or nmol/gm Hb (blood)

Calculation

$$\text{GSH (nmol/mg protein) level in liver tissue} = \frac{\text{Value from the graph (X)}}{\text{mg protein}}$$

From standard graph prepared, Y = 0.005X + 0.013.

2.2.9.1.2. Estimation of superoxide dismutase (SOD) activity

The estimation of SOD was determined as per the protocol of McCord and Fridovich (1969).

Principle

This assay is based on the ability of superoxide dismutase (SOD) to inhibit the reduction of nitro blue tetrazolium (NBT). SOD present in the tissue or serum uses the photochemical reduction of riboflavin as oxygen generating system and catalyzes the

inhibition of NBT reduction, the extent which can be assayed using a spectrophotometer.

Procedure

The reaction system was prepared by mixing 100 μL of the tissue (liver or blood sample), 2550 μL phosphate buffer (67 mM K-Na phosphate buffer, pH 7.8), 200 μL KCN in 0.1M of EDTA, 100 μL of 1.5 mM NBT and 50 μL riboflavin (0.12 mM) into a test tube. The same reaction mixture without the test sample was served as control. The initial absorbance of the solution was determined at 560 nm. The test tubes containing the reaction mixture was then exposed to an illuminating incandescent lamp for 20 minutes. Final absorbance of the reaction mixture was taken immediately after this procedure at 560 nm. First, the percentage inhibition was calculated as the percentage change of As (absorbance of the sample) with that of Ac (absorbance of control). The activity was of SOD was calculated by the following formula,

$$\text{SOD (U/mg protein) activity in liver tissue} = \frac{\text{Percentage inhibition}}{50 \text{ x protein (mg) (in 100 µL)}}$$

$$\text{Where, percentage inhibition} = \frac{\text{Ac - As}}{\text{As}} \text{ x } 100$$

2.2.9.1.3. Estimation of catalase (CAT) activity in liver and kidney tissue

The antioxidant enzyme, catalase activity in liver and kidney tissue was determined by the method developed by Beers and Sizer (1952).

Principle

The decomposition of hydrogen peroxide (H_2O_2) catalyzed by catalase can be measured by spectrophotometrically. At 240 nm, the molar extinction coefficient for H_2O_2 is 43.6/min and shown maximum absorbance in the region (240 nm). The absorbance decreases with the decomposition of H_2O_2.

Procedure

A volume of 2.7 mL of phosphate buffer (pH 7, 0.5 M) was taken in a quartz cuvette and 300 μL of H_2O_2 was added. The absorbance was measured against buffer blank.

Removed a volume of 50 μL reaction mixture from this and 50 μL of tissue supernatant was added and decrease in absorption of peroxide solution was measured at 25ºC at 240 nm for 1 minute with 15-second intervals. The activity of the enzyme in liver tissue was calculated by the formula given below.

Calculation

$$\text{Specific activity of catalase (U/mg protein)} = \frac{\Delta A/\text{min} \times 3000}{43.6 \text{ x protein (mg)}}$$

Here; ΔA /min = A2 - A1

A1 = Absorbance at 240, in t = 0 sec

A2 = Absorbance at 240, in t = 15 sec

3000 = dilution factor

43.6 = Molar extinction coefficient of H_2O_2

2.2.9.1.4. Estimation of catalase activity (CAT) in haemolysate

Catalase activity in the haemolysate was estimated by the protocol of Aebi et al., (1965)

Procedure

A volume of 10 μL haemolysate was made up to 5.0 mL with phosphate buffer solution (pH 7.0). To 2.0 mL of the above mixture, added 1.0 mL of phosphate buffer and considered as reference tube. To another 2.0 mL of the mixture (taken in quartz cuvette) 1.0 mL of H_2O_2 (30 mM) was added. The decrease in the absorption of peroxide solution was measured at 25ºC at 240 nm for 1 minute with 15 second time intervals. The activity of the enzyme in blood was calculated by the formula given below.

Calculation

$$\text{Specific activity of catalase (U/gm Hb)} = \frac{2.303 \text{ x } (\log A1/\log A2) \text{ x } 3000}{15 \text{ x Hb (g/dL)}}$$

Here; ΔA /min = A2 - A1

A1 = Absorbance at 240, in t = 0 sec, A2 = Absorbance at 240, in t = 15 sec

3000 = dilution factor

2.2.9.1.5. Estimation of lipid peroxidation in tissue

The level of lipid peroxidation in the tissue was determined by thiobarbituric acid reacting substance (TBARS) formation by the method by Ohkawa et al., (1979).

Principle

This assay is based on the reactivity of a secondary product of lipid peroxidation, molondialdehyde (MDA) with thiobarbituric acid (TBA) to produce a red pigment at acidic pH, which was measured spectrophotometrically at 532 nm.

Procedure

Incubated the reaction mixture, which containing 400 μL tissue homogenate, 200 μL SDS (8%), 1.5 mL acetic acid (20%, pH 3.5), 1.5 mL TBA (0.8%) and 400 μL distilled water at 95^{o}C for 1 hour in a water bath. After incubation, the test tubes were and 1000 μL of distilled water was added to the reaction mixture. The mixture was mixed well and then centrifuged at 1500 rpm for 10 minutes. The supernatant was collected and its absorbance was measured at 532 nm using distilled water as the blank. The concentration of MDA formed was calculated from the standard graph plotted at concentrations ranges between 1 to 10 nmol and expressed as nmol of MDA equivalent/mg protein.

Calculation

$$\text{Lipid peroxidation was expressed in terms of MDA} = \frac{\text{Value from the graph (X)}}{\text{Protein (mg)}}$$

Y = 0.0182X

2.2.9.2. Protective effect of HE on sodium fluoride-induced oxidative damage

Experimental design

Swiss albino female mice (25 ± 3gm) were used in this study. Thirty six mice were divided into six groups of six animals each. The first group of animals (Group I) was kept as normal (administered 200 μL saline). Animals in Group II (control group) were provided NaF (600 ppm; 60 mg/100 mL) through drinking water and Group III animals received 200 μL of 1% propylene glycol (p.o) + NaF (600 ppm; 60 mg/100

mL) through drinking water was vehicle control. Group IV animals given NaF (600 ppm: 60 mg/100 mL), were treated with 200 μL of ascorbic acid, as standard drug (15 mg/kg b. wt., p.o.) daily. Animals in Group V were given 200 μL of HE extract of *S. glauca* at a low dose (160 mg/kg b. wt., p.o.) and group VI animals were given 200 μL of the same extract in a higher dose (260 mg/kg b. wt., p.o.) along with NaF (600 ppm: 60 mg/100 mL). The animals belong to group II and III were pretreated with propylene glycol and ascorbic acid respectively for seven consecutive days Group IV and V animals were pretreated with respective doses of drugs for the same period of time. Except for animals in Group I, all the animals provided NaF (600 ppm; 60 mg/100 mL) through drinking water from 8th day onwards. Animals belong to all groups were sacrificed on the 15th day following overnight fasting (Nabavi et al., 2012)

Preparation of haemolysate

The blood was collected by cardiac puncture into EDTA coated tubes. The tubes were then centrifuged at 2000 rpm for 10 minutes. The supernatant was removed and the packed RBC collected was washed with saline. The haemoglobin concentration of the packed RBC was determined by the method developed by Drabkin and Austin (1935).

For haemolysis, a known volume of packed RBC cells (0.1 mL) was allowed to undergo lysis with hypotonic phosphate buffer (0.9 mL). The tubes were centrifuged after vigorous shaking at 10,000 rpm for 60 minutes in a refrigerated centrifuge for removing the debris of RBC and collected haemolysate was immediately used for the estimation of glutathione and to measure the activities of enzymes like superoxide dismutase and catalase.

Preparation of tissue homogenate

Soon after blood collection the liver was dissected out and washed in ice-cold saline (0.9% NaCl) and weighed. The liver homogenate was prepared (10% w/v in 0.1M Tris hydrochloric acid buffer, pH 7.4) by a motor homogenizer in ice-cold conditions and used for the estimation of lipid peroxidation and total protein. The homogenates were further centrifuged at 8,600 rpm for 20 minutes at 4 °C. The supernatant was collected and used for the estimation of superoxide dismutase, catalase, glutathione peroxidase, reduced glutathione and total protein.

Histological analysis

Tissues from the liver, was fixed in 10% neutral buffered formalin for histological studies. The slides were stained by haematoxylin and eosin. They were observed under 200X and photographs were taken.

2.2.9.3. Effect of HE on Phorbol-12-merystate-13-acetate (PMA) induced superoxide radical scavenging activity

Twenty four male BALB/c mice (25 ± 3 gm) were selected for the study and divided into 4 groups of 6 animals each. Group, I was treated with 200 μL saline (p.o.) and considered as the control group. Group II was assigned as a vehicle control group and animals in this group were given 200 μL of 1% propylene glycol (p.o). Group III animals (LDHE) was given a lower of a dose of HE; 160 mg/kg b. wt (p.o.) and Group IV, (HDHE) were supplied a higher dose of HE; 260 mg/kg b. wt., (p.o). All animals in Group II, III and III were administered with respective drugs for five consecutive days. On the first day, 200 μL of sodium caseinate (5% intraperitoneal) was injected to each animal elicit peritoneal macrophages. On fifth day the peritoneal macrophages were activated *in vivo* by injecting 100 μL PMA (100 ng/animal, i.p.). After three hours macrophages were collected by injecting 5 mL of PBS into the peritoneal cavity. The harvested cells were centrifuged at 2000 rpm for 10 minutes. The cells were then washed and resuspended in PBS to get a number of $1x10^6$ macrophages/mL. From these five-tenths of a milliliter of the macrophages were mixed with 0.5 mL of the reaction mixture which contains NBT (0.2% in PBS), dextrose (7.5%) and Hanks balanced salt solution prepared in the ratio of 6:2:4. The reaction mixture was then incubated for 45 minutes at room temperature. The mixture was then centrifuged and the pellet was then boiled with 2 mL of pyridine for 10 minutes. The absorbance values of treated animals were compared with untreated control (measured at 515 nm) and found out the percentage inhibition (Sheeja et al., 2006).

2.2.10. *In vivo* anti-inflammatory activity analysis

2.2.10.1. Carrageenan induced acute paw oedema in mice

Male BALB/c mice (25-28 gm) were divided into 5 groups. Group I was kept as control (carrageenan alone) and treated with 200 μL saline (p.o.) and Group II received 200 μL 1% propylene glycol/ animal/ day were considered as vehicle control. Group III received diclofenac (25 mg/kg b. wt) as a positive control. Group IV (LDHE) and group V (HDHE) were treated 160 mg and 260 mg/kg b. wt of HE respectively. The animals were pre-treated with doses of respective drug or diclofenac or propylene glycol, orally for four consecutive days. On 5th day 1 hr after HE or diclofenac or propylene glycol administration, inflammation was induced by intraplantar injection of 0.05 mL of 1% carrageenan in 0.1% carboxy methylcellulose (CMC) into the right hind paw of all the animals (Winter et al., 1962). Paw thickness was measured using vernier caliper, 1 hour prior and for every hour up to 6th hour after carrageenan injection. The percentage of inflammatory inhibition was calculated according to the following formula. After the experiment, the animals were sacrificed and the paw tissue was collected. It was kept in 10% neutral buffered formalin and histopathological analysis was conducted. The tissue architecture was analysed with respect to normal and control with treatment groups.

Calculation

$$\% \text{ inhibition} = \frac{[(PT - P0) \text{ control} - (PT - P0) \text{ treated}]}{(P\,T - P0) \text{ control}} \times 100$$

Where PT = paw thickness at a various time interval and P0 = initial paw thickness.

2.2.10.2. Vascular permeability assessment by Evans blue dye extravasation method

This experiment was designed to measure the inhibitory action of HE on vascular permeability, evoked by carrageenan-induced paw inflammation in mice with the help of Evans blue dye (Gupta et al., 2015). Evans blue is an azo dye that has a high affinity for serum albumin. Usually, serum albumin cannot come out of the blood vessels, unless inflammation occurs. So it is considered as a marker for determining the vascular permeability *in vivo.*

Thirty male BALB/c (25-28 gm) mice were used in the study and grouped into five groups. Group I was kept as control (carrageenan alone) and was administered with 200 μL saline (p.o.) and Group II received 200 μL 1% propylene glycol/ animal/ day were considered as vehicle control. Group III received diclofenac (25 mg/kg b. wt) as standard. Group IV (LDHE) and group V (HDHE) were treated 160 mg and 260 mg/kg b. wt of HE respectively. The animals were pre-treated with respective doses of drug or diclofenac or propylene glycol, orally for four consecutive days. On 5th day 1 hr after HE or diclofenac or propylene glycol administration, inflammation was induced by intraplantar injection of 0.05 mL of 1% carrageenan in 0.1% carboxy methyl cellulose (CMC) into the right hind paw of all the animals (Winter et al., 1962). Evans blue dye (25 mg/ kg b. wt) was injected into the tail vein of all mice after 3.5 hours of carrageenan injection. Photographs of the right hind paw of all animals were taken 30 minutes after Evans blue dye injection. After 4 hours of carrageenan injection, all animals were sacrificed by cervical dislocation and paw tissues were dissected and an equal weight of paw tissue from each mouse was sliced out. The paw tissue was homogenized in 1.0 mL of acetone and 1% sodium sulfate prepared in a ratio of 4:1 and incubated for 24 hours at 37ºC. This procedure allowed the extraction of Evans blue dye from the paw tissues. The solution containing tubes were centrifuged at 2000 rpm for 10 minutes and supernatants were collected and the absorbance was determined at 620 nm using a spectrophotometer. The percentage inhibitory effect of different doses of HE and diclofenac in comparison to the control was calculated according to the following formula. The quantity of Evans blue extracted from the Group I mice were also calculated.

$$\% \text{ inhibition} = \frac{\text{The absorbance of control-Absorbance of treated}}{\text{Absorbance control}} \text{ x } 100$$

2.2.10.3. Dextran induced acute paw oedema in mice

Male BALB/c mice (25-28 gm) grouped and were pre-treated with respective drug doses or diclofenac or 1% propylene glycol for 4 days similar to the study of carrageenan-induced acute paw oedema in mice. On 5th day 1 hr after HE or diclofenac (25 mg/kg b. wt; standard) or propylene glycol (1% propylene glycol; vehicle control) administration, inflammation was induced by intraplantar injection of 0.05 mL of 1% dextran in 0.1% carboxy methylcellulose (CMC) into the right hind

paw of all the animals (Maity et al., 1998). Paw thickness was measured using vernier caliper, 1 hour prior and continued for every hour up to 6th hour after dextran injection. The percentage of inhibition was calculated according to the formula used for the carrageenan-induced acute paw oedema in mice.

2.2.10.4. Formalin induced chronic paw oedema in mice

Male BALB/c mice (25-28 gm) were grouped similar to the grouping pattern followed in carrageenan-induced acute paw oedema model. They were pre-treated orally, for 7 consecutive days with respective drug doses or (25 mg/kg b. wt; standard) or propylene glycol (1% propylene glycol; vehicle control). On the 8th day, chronic inflammation was induced by intraplantar injection of 0.05 mL of 1% formalin on the right hind paw of all animals 1 hour after HE or diclofenac or propylene glycol administration (Chau, 1989). The oral administration of drug or diclofenac or propylene glycol continued for six consecutive days. Paw thickness was measured using vernier caliper, 1 hour prior and continued for the next 6 consecutive days after formalin injection. Photographs of the right hind paw of all animals were taken at the end of the experiment. The percentage of inhibition of chronic inflammation was calculated according to the formula used in the carrageenan model. After the experiment the animals were sacrificed and the paw tissue was collected. It was kept in 10% neutral buffered formalin and histopathological analysis was conducted. The tissue architecture was analysed with respect to normal and control with treatment groups.

2.2.11. Antitumour studies

2.2.11.1. Determination of the antitumour effect of HE on ascites tumour model

The effect of HE of *S. glauca* on ascites tumour (inoculate with EAC cells) bearing male Swiss albino mice was conducted in four different ways to determine the antitumor effects. The HE of *S. glauca* was administered orally to the experimental animals in all experimental setup. Cyclophosphamide (15 mg/kg b. wt) was administered (p.o.) as standard drug in this experiment. The treatment was done for 10 successive days. The death rate of animals due to tumour burden was noted and the percentage of increase in life span of mice was calculated using the following formula (Mazumdar et al., 1997).

$$\% \text{ increase in lifespan} = \frac{T\text{-}C}{C} \times 100$$

Where T = Average number of days the treated animals survived, C = Average number of days the animals in the control group survived.

2.2.11.1.1. Simultaneous administration of HE with the inoculation of ascites tumour

Ascites tumour was inoculated by injecting EAC cells ($1x10^6$ cells/animal) in the peritoneal cavity of male Swiss albino mice (30 numbers). They were divided into five groups (six animals/group). Animals in the first group (group I) received 200 μL saline and served as the control group. Animals in group II were given 200 μL 1% propylene glycol orally was the vehicle control. Animals in groups III were administered cyclophosphamide (15 mg/kg b. wt) orally. Groups IV (LDHE) and V (HDHE) animals were administered HE of *S. glauca* at 160 and 260 mg/kg b. wt. All animals in the treatment groups received respective treatment for ten successive days one day after tumour inoculation (Jose et al., 2016).

2.2.11.1.2. Pre and simultaneous administration of HE with the inoculation of ascites tumour

Eighteen animals were divided into three groups (six animals/group). Animals in group I were administered with 200 μL propylene glycol (1%, vehicle control) five days before and ten days after the inoculation of EAC cells ($1x10^6$ cells/animals) in their peritoneal cavity. Similarly, animals in group II (LDHE) and III (HDHE) were given HE of *S. glauca* 160 and 260 mg/kg b. wt respectively five days before and ten days after the tumor inoculation.

2.2.11.1.3. Administration of HE to ascites tumour bearing mice

Ascites tumour was inoculated by injecting EAC cells ($1x10^6$ cells/animals) in the peritoneal cavity of twenty four male Swiss albino mice. They were divided into four groups (six animals/group). Animals in the first group (group I; vehicle control) received were given 200 μL 1% propylene glycol orally for 10 days from 11^{th} day of inoculation of ascites tumour. Animals in groups II were administered cyclophosphamide as standard drug (15 mg/kg b. wt), Groups II (LDHE) and III

(HDHE) animals were administered HE of *S. glauca* at 160 and 260 mg/kg b. wt. respectively similar to the treatment protocol adopted for the group I mice.

2.2.11.1.4. Simultaneous administration of HE in combination with cyclophosphamide with the inoculation of ascites tumour

Twenty four animals were divided into four groups (six animals/group). Animals in group I was administered with 200 μL propylene glycol orally (1%, vehicle control) along with cyclophosphamide (15 mg/kg b. wt) for ten days after 24 hours of the inoculation of EAC cells ($1x10^6$ cells/animals) in their peritoneal cavity. Animals in group II, III and IV were given HE of *S. glauca* (LDHE; 160 mg/kg b. wt) along with cyclophosphamide in concentration of 15, 10 and 5 mg/kg b. wt respectively for ten days, 24 hours after tumor inoculation. An interval of 6 hours was observed between the oral administration of LDHE and CTX in each group.

2.2.11.2. Determination of the antitumour effect of HE on solid tumour model

The antitumor effect of HE of *S. glauca* on solid tumour bearing male Swiss albino mice was conducted in four different ways. The HE of *S. glauca* was administered orally to the experimental animals in all experimental setup. Cyclophosphamide (15 mg/kg b. wt) was used as the standard drug (p.o.) in this study. The tumor development in mice in each group was determined by measuring the diameter of tumour growth in two perpendicular planes using a digital vernier caliper before tumor inoculation and from the third day of tumor inoculation up to 28th day. The tumor size (cm^3) was calculated by using formula $4/3*\pi*a^2b/2$, where 'a' is the minor diameter and 'b' is the major diameter (Ma et al., 1991). Total weight of the animals and tumour size were measured on regular intervals. On the 28th day on tumor inoculation after tumor measurement, the animals were sacrificed and the tumor was isolated and weighed. Photographs of the isolated tumour were taken. A small part of the tumour was fixed in 10% neutral buffered formalin for histological study. Percentage inhibition of tumour weight was calculated by the formula

$$\% \text{ inhibition} = \frac{Wc\text{-}Wt}{Wc} \times 100$$

Where, Wc = Average weight of solid tumour in the control group, Wt = Average weight of solid tumour in the experiment group.

Hematological parameters like Hb and total leucocyte count were determined on the initial day, 14th day and 28th day. On the initial day and 14th day blood was collected by tail snip procedure and 28th by direct cardiac puncture (Thummar et al., 2015). Haematoxylin and Eosin staining procedure adopted for staining the histological preparations of the tumour part and analysis was done with the help of microscope (Magnus inverted laboratory microscope) and photographs were taken. The comparative study of tissue samples collected from different treatment groups were done with the architecture of normal tissue (a histological slide of right hind limb of untreated mice were used) and control group tissue samples

2.2.11.2.1. Simultaneous administration of HE with the inoculation of solid tumour

The solid tumour was induced by injecting DLA cells (1x10^6 cells/animals) subcutaneously to the right hind limb of Swiss albino mice (30 no). They were divided into five groups (six animals/group). Animals in the first group (group I) received 200 μL saline and served as the control group. Animals in group II were given 200 μL 1% propylene glycol orally was the vehicle control. Animals in groups III were administered cyclophosphamide (15 mg/kg b. wt) orally. Groups IV and V animals were administered HE of *S. glauca* at 160 and 260 mg/kg b. wt. respectively for ten successive days one day after tumor inoculation.

2.2.11.2.2. Pre and simultaneous administration of HE with the inoculation of solid tumour

Eighteen animals were divided into three groups (six animals/ group). Animals in group I were administered with 200 μL propylene glycol (1%, vehicle control) five days before and ten days after the inoculation of DLA cells (1x10^6 cells/animals) to their right hind limb. Similarly, animals in group II and III were given HE of *S. glauca* 160 and 260 mg/kg b. wt respectively five days before and ten days after inoculation of DLA cells.

2.2.11.2.3. Administration of HE to the solid tumour bearing mice

Twenty four animals were divided into four groups (six animals/ group). Animals in group I were administered with 200 μL propylene glycol (1%, vehicle control) for ten

consecutive days after ten days of inoculation of DLA to their right hind limb. Similarly, animals in groups II were administered cyclophosphamide (15 mg/kg b. wt), Groups II and III animals were administered HE of *S. glauca* at 160 and 260 mg/kg b. wt. respectively similar to the treatment protocol adopted for the group I mice.

2.2.11.2.4. Simultaneous administration of HE in combination with cyclophosphamide with the inoculation of solid tumour

Twenty four animals were divided into four groups (six animals/group). Animals in group I were administered with 200 μL propylene glycol (1%, vehicle control) along with cyclophosphamide (15 mg/kg b. wt) for ten days after 24 hours of the inoculation of DLA cells (1 x 10^6 cells/animals) to their right hind limb. Animals in group II, III and IV were given HE of *S. glauca* (160 mg/kg b. wt) along with cyclophosphamide in a concentration of 15, 10 and 5 mg/kg b. wt respectively for ten days, 24 hours after tumor inoculation. An interval of 6 hours was observed between the administration of LDHE and CTX in each group.

2.2.12. Study on the protective effect of HE in systemic toxicity by chemotherapeutic drugs

2.2.12.1. Protective effect on cisplatin induced nephrotoxicity

2.2.12.1.1. Experimental design

Thirty six male Swiss albino mice (25-28 gm) were equally divided into six groups – normal, control, vehicle control, standard, low dose (LDHE) and high dose (HDHE). During the study, the normal group animals were administered with 200 μL of saline. The control group animals were administered with 200 μL of saline and the vehicle control group was treated with 200 μL of 1% propylene glycol for seven days before and three days after cisplatin (CDDP) administration. The animals in the standard group were provided silymarin (100 mg/kg b. wt.) and LDHE and HDHE groups were administered hot water extract of *S. glauca*, at a dose of 160 and 260 mg/kg b. wt respectively by oral gavage for seven days before and three days after cisplatin administration. All the animals in groups except normal group were treated with a single dose of cisplatin (16 mg/kg b. wt, ip.) to induce renal damage (Somani et al.,

2000) on the eighth day of the experiment. All animals were sacrificed at the end of the experiment after overnight fasting.

2.2.12.1.2. Sample collection

Blood was collected in heparin-coated tubes directly from the heart after sacrificing animals with ether anesthesia for hematological analysis. For biochemical analysis blood was collected in non-heparinised tubes and serum is separated. Kidneys were removed, washed in PBS. Kidney homogenate (10% w/v) was prepared for every animal of each group in ice-cold 0.1M Tris buffer (pH7.4). Femur bones of the animals were collected for the determination of bone marrow cellularity and *α*-esterase activity.

Parameters studied

2.2.12.1.3. Haematological profile

Haematological parameters such as haemoglobin and total leucocyte count were evaluated as per the standard protocols mentioned (section, 2.2.5.2.1.1 and 2.2.5.2.1.3).

2.2.12.1.4. Bone marrow cellularity and α-esterase activity

The effect of HE on bone marrow cellularity was done according to the method of Sredni et al. (1992). Bone marrow cells from both femurs of animals were flushed out into PBS containing 10% fetal bovine serum. In order to determine bone marrow cellularity, bone marrow cells were counted using the Neubauer counting chamber and expressed as total live cells (as per trypan blue exclusion)/femur/mL. From the above cell preparation of each animal, a smear of cells was prepared on a clean glass slide and dried by waving air. The smears were stained with *α*-naphthyl acetate and then counterstained with haematoxylin to determine the non-specific alpha esterase activity. Alpha esterase positive cells appeared in orange-pink colour which was counted and expressed as a number of positive cells/4000 bone marrow cells (Bancrofit and Cook, 1984).

2.2.12.1.5. Serum urea and creatinine

Serum urea was determined by Urease-GLDH (Enzymatic UV) method and creatinine by Jaffe's kinetic method using commercially available kits (Euro Diagnostic Pvt.

Ltd., Chennai, India) as per instructions of manufactures (Refer Chapter 2, section 2.2.7.2 and 2.2.7.1).

Oxidative stress in kidney tissue

The extent of lipid peroxidation was measured in terms of MDA using thiobarbituric acid method (Ohkawa et al., 1979) (Refer Chapter 2, section 2.2.9.1.5). Furthermore, conjugated dienes (CD) and tissue hydroperoxides (HPs) in the homogenate were determined according to the modified method of John and Steven, (1978).

2.2.12.1.6. Determination of conjugated dienes

Principle

Lipid peroxidation is accompanied by the rearrangement of double bonds in polyunsaturated fatty acids which lead to the formation of conjugated dienes and has absorption maxima at 233 nm.

Procedure

A volume of 1 mL of tissue homogenate was mixed with 5 mL of a mixture of chloroform and methanol prepared in a ratio of 2:1. This mixture was centrifuged at 1000 rpm for 5 minutes. After centrifugation 3 mL of solution from the lower layer was taken and evaporated. The lipid residue remained after evaporation was dissolved in 1 mL of cyclohexane and absorbance was taken at 233 nm using cyclohexane as blank. The amount of conjugated diene formed was calculated by the formula given below.

Calculation

The conjugated diene formed is expressed in Mm/100 g tissue.

$$\text{Conjugated diene formed} = \frac{\text{OD of test x The volume of system x The total volume of homogenate x } 10^5}{2.52 \times 10^4 \text{ x Volume of lower layer taken x weight of tissue}}$$

Where 2.52×10^4 $M^{-1}CM^{-1}$ is molar extinction coefficient

2.2.12.1.7. Determination of hydroperoxides

Principle

The experiment is based on the ability of iodide to reduce hydroperoxides by the following reaction

$$2H^{+} + ROOH + 3I^{-} \rightarrow H_2O + ROH + I^{-3}$$

Procedure

A volume of 1 mL of tissue homogenate was mixed with 5 mL of chloroform: methanol mixture prepared in 2:1 ratio. The mixture was centrifuged at 1000 rpm for 5 minutes. After centrifugation, 3 mL of the lower layer was taken and evaporated to dryness. A volume of 1 mL of acetic acid: chloroform (3:2) mixture was added to it and followed by quickly added 50 μL of KI. The contents in the test tubes were mixed well. The tubes were placed in the darkness at room temperature for 5 minutes. A volume of 3 mL cadmium acetate was added, mixed well and centrifuged at 1000 rpm for 10 minutes. The absorbance of the upper layer was detected at 353 nm. The concentration of tissue hydroperoxides formed (mM/gm tissue) was calculated by the following formula.

Calculation

$$\text{Tissue hydroperoxides formed} = \frac{\text{OD of test x The volume of system x The total volume of homogenate x } 10^5}{1.73 \times 10^4 \text{ x Volume of the lower layer x Weight of tissue}}$$

Where 1.73×10^4 $M^{-1}CM^{-1}$ is molar extinction coefficient.

Antioxidant enzyme profile of the kidney

The analysis of various antioxidant enzymes such as superoxide dismutase (McCord and Fridovich, 1969), catalase (Beers and Sizer, 1952) and glutathione peroxidase (Hafeman et al., 1974) was assessed. In addition to these, the activity of non-enzymatic antioxidant reduced glutathione (Moron et al., 1979) and total protein present in renal tissue were also evaluated measured (Lowry et al., 1951).

2.2.12.1.8. Determination of glutathione peroxidase (GPx) activity

The GPx activity was determined as per the protocol of Hafeman et al., (1974)

Principle

The GPx enzyme activity is determined by measuring the decrease in the concentration of GSH content after incubation of the sample with H_2O_2 and NaN_3.

$$H_2O_2 + 2GSH \rightarrow 2\ GSSG + 2H_2O$$

The remaining GSH was measured by its reaction with DTNB.

Procedure

Incubated the reaction mixture containing 100 μL tissue supernatant, 100 μL 5 mM GSH, 100 μL of 25 mM NaN_3, 100 μL H_2O_2 (1.25 mM) and phosphate buffer (0.05 mM, pH 7) in a total volume of 2.5 mL at 37^{o}C for 10 minutes. The reaction was stopped by adding 2 mL of H_3PO_4 (1.65%) and the mixture was centrifuged at 3000 rpm for 10 minutes to settle down the precipitate. A volume of 2 mL of supernatant was taken from this and mixed with 2 mL of Na_2HPO_4 (0.4 M) and 1 mL of 1mM DTNB and kept for incubation for 10 minutes at 37^{o}C. The absorbance of the yellow coloured complex developed in this reaction was detected at 412 nm using distilled water as blank. A sample without the tissue supernatant was processed in the same way and considered as control. One unit of enzyme activity (GPx) was defined as a decrease in log GSH by 0.001per minute after subtraction of the decrease in log GSH/ minute for the non-enzymatic reaction and is expressed as U/mg protein for tissue supernatant and the formula is given below.

$$\text{The GPx (U/mg protein) activity} = \frac{\text{OD of blank} - \text{OD of sample}}{\text{Protein (mg) x 10}}$$

2.2.12.1.9. Histological analysis

A small portion of a kidney from each group was taken and fixed in 10% neutral buffered formalin solution. Sections with a thickness of 5 μm were taken, deparaffinized, hydrated and stained using haematoxylin and eosin. The renal sections were examined for the extent of damages to glomeruli, tubules and interstitial space.

2.2.12.2. Protective effect on cyclophosphamide-induced systemic toxicity

2.2.12.2.1. Experimental design

The protective effect of HE of *S. glauca* on cyclophosphamide-induced systemic toxicity in mice was conducted. In this experiment, thirty male Swiss albino mice were divided into five groups (n=6). Group I was kept was administered with 200 μL of saline (p.o.) for ten days and considered as a normal group. Animals in Group II were treated with cyclophosphamide dissolved in 200 μL of saline (CTX; 25 mg/kg b. wt, p. o.) for ten consecutive days considered as a control group. Animals in Group III were treated with CTX (25 mg/kg b. wt, p. o.) and administered 200 μL of 1% food graded propylene glycol (p.o.) and considered as a vehicle control group. Group IV (LDHE) and Group V (HDHE) were administered with 160 and 260 mg/kg b. wt. of HE extract, dissolved in 1% food graded propylene glycol (p.o.) for ten days along with CTX (25 mg/kg b. wt, p. o.). A time interval of 6 hours was observed between the administrations of cyclophosphamide and respective drug in each group. The animals were maintained for twenty days. On the initial day, 5^{th}, 10^{th}, and 15^{th} day body weight were recorded and blood samples collected from the tail vein of the animals and haematological parameters were analyzed. On the twenty-first day all animals were sacrificed following overnight fasting by ether anaesthesia (Pratheeshkumar and Kuttan, 2010). Body weight was measured.

2.2.12.2.2. Sample collection

In every five days of the experiment, the blood was collected from the tail vein. On 21^{st} day, the blood was collected to heparinised tubes by cardiac puncture. The bone marrow was collected from the femur bones. Tissues from liver, kidney, spleen and small intestine were fixed in 10% neutral buffered formalin for histological studies. Relative organ weight of the dissected organs, haematological parameters, liver function analysis, renal function analysis, liver and kidney antioxidant status, etc. were analyzed by standard procedures. Histopathological analysis of liver, kidney, spleen and small intestine were done.

2.2.12.2.3. Relative organ weight

The relative organ weight for kidneys was calculated using the following formula (Peter et al., 2018).

$$\text{Relative organ weight} = \frac{\text{Organ weight}}{\text{Total body weight}} \times 100$$

2.2.12.3. Protective effect on cyclophosphamide-induced systemic toxicity in tumour bearing mice.

2.2.12.3.1. Experimental design

This study was done according to the method developed by Sun and Peng (2008) with modification. Tumour was induced in thirty male Swiss albino mice by injecting DLA cells ($1x10^6$ cells/ animal) into the right hind limb. 24 hours later, mice were randomly divided into five groups, each consisting of 6 mice. Group I animals were administered 200 μL of saline and considered as untreated. Group II, animals were administered 200 μL CTX (25 mg/kg b. wt, p. o.) for ten days and considered as a control group. The co-treated mice received the same dose of CTX for the same time period and 200 μL of 1% food graded propylene glycol (group III, vehicle control), 160 mg/kg b. wt. of HE (Group IV; LDHE) and 260 mg/kg b. wt. of HE (Group V;HDHE) orally. The animals were maintained for twenty days. Total body weight of animals was measured on 0, 5, 10, 15 and 21st day of the experiment. The tumour volume was measured on these days by using a vernier caliper. Blood samples were collected from each experiment group by tail bleeding method on the mentioned days and haematological parameters like total Hb count and total leucocyte count were analyzed. On the twenty-first day, mice were weighed and sacrificed by ether anesthesia. Blood was collected into heparin-coated tubes and haematological analysis was done. The blood samples collected into non-heparin coated tubes were used to collect serum for the analysis of liver and kidney function parameters. Body organs (liver, kidney and spleen) and solid tumours were isolated and weighed. Liver and kidney antioxidant status were determined by using standard procedures mentioned earlier.

2.2.13. Study on the effect of HE on DMBA-induced breast cancer

2.2.13.1. Experimental design

The Chemopreventive effect of HE on 7, 12-dimethylbenzanthracene-induced cell proliferation in the breast tissues of female Swiss albino mice was evaluated according to the protocol of Minari and Okeke (2014). Thirty six adult female Swiss

albino mice (25 ± 3 gm) were used in this study. The mice were divided into six groups, each group had six mice. Animals in Group I was received 200 μL of saline per day and was considered as normal. The animals in Group II were treated with DMBA and 200 μL saline, considered as the control group. Group III or the vehicle control group animals were treated with DMBA and 200 μL 1% food graded propylene glycol. Group IV members were administered DMBA and tamoxifen (20 mg/kg b. wt/day, i.o) and considered as a standard group. Group V and VI were administered DMBA and lower (LDHE; 160 mg/kg b. wt/200 μL/day) and higher concentration of HE (HDHE; 260 mg/kg b. wt/200 μL/day). The DMBA (3.3 mg/200μL/animal) was administered every week. Both DMBA and HE were administered by oral gavage. DMBA and HE were dissolved in sesame oil and 1% propylene glycol respectively for administration. The treatment of animals lasted for six weeks. The animals except in the normal group were observed daily and their mammary glands were checked by close inspection, touching and palpitation. The mice were fasted overnight at the end of the experimental period and sacrificed by cervical dislocation. Necropsy of each animal was conducted and photographs were taken and detailed analysis this was conducted by the help of a veterinary surgeon, who was blind to the study.

2.2.13.2. Sample collection

Blood samples were collected by direct cardiac puncture for both hematological and biochemical analysis with and without heparin coated tubes, respectively. The haematological parameters were evaluated by using blood collected in heparin coated tubes. The blood collected in heparin not coated tubes was centrifuged at 3000 rpm for 5 minutes to obtain serum for biochemical analysis. The weight of organs like mammary glands, liver and ovary was determined by an electronic weighing machine. Mouse mammary gland (third pair) whole mount were prepared, stained with Carmine alum solution and observed under microscope (20X) for detecting the neoplastic changes.

2.2.13.3. Parameters studied

Haematological parameters (Hb level and total leucocyte count), liver function parameters (AST, ALT, ALP and total bilirubin) and antioxidant status of the hepatic tissue (the activity of catalase, SOD, GPx and level of GSH and MDA) were

determined by standard procedures mentioned previously. Histopathological analysis of mammary glands, liver and ovary was done with haematoxylin and eosin stains.

2.2.14. Statistical analysis

The *in vitro* assays were performed at least thrice in duplicate tubes and data represented are mean ± SD six values. For *in vivo* experiments the values are expressed as mean ± SD six animals. The mean values were statistically analyzed using one-way analysis of variance using graph pad Instat 3 software (Graph Pad Software, Inc. La Jolla, USA) traced by Dunnett multiple comparison test. $P < 0.05$ was considered statistically significant.

Chapter 3

Phytochemical and pharmacological screening of *Simarouba glauca* DC

Contents

3.1. Introduction

3.2. Materials and methods

3.2.1. Collection and authentication of plant

3.2.2. Preparation of extracts

3.2.3. Phytochemical screening of extracts

3.2.3.1. Qualitative analysis

3.2.3.2. Thin layer chromatographic profiling

3.2.4. *In vitro* cytotoxicity analysis

3.2.4.1. Cell lines

3.2.4.2. Short term cytotoxicity assay

3.2.4.3. Antiproliferative study

3.2.5. *In vitro* antioxidant assays

3.2.5.1. Hydroxyl radical scavenging activity

3.2.5.2. DPPH radical scavenging activity

3.2.5.3. Nitric oxide radical inhibition assay

3.2.5.4. Ferric reducing/antioxidant power (FRAP) assay

3.2.5.5. Total antioxidant capacity

3.2.5.6. Inhibition of lipid peroxidation

3.2.5.7. Lipoxygenase inhibition assay

3.2.6. Quantitative analysis of the extracts

3.2.6.1. Estimation of total phenolic content

3.2.6.2. Estimation of total flavonoid content

3.2.7. UPLC-Q-TOF-MS analysis of the extract

3.2.8. Statistical analysis

3.3. Results

3.3.1. The percentage yield of *S. glauca* leaf extracts

3.3.2. Phytochemical screening

3.3.3. Thin layer chromatographic profiling

3.3.3.1. Thin layer chromatographic profiling of HE

3.3.3.2. Thin layer chromatographic profiling of ME

3.3.4. Short term *in vitro* cytotoxicity

3.3.4.1. Cytotoxic effect of HE

3.3.4.2. Cytotoxic effect of ME

3.3.5. Antiproliferative efficacy of HE and ME

3.3.6. *In vitro* antioxidant action

3.3.6.1. Hydroxyl radical scavenging activity

3.3.6.2. DPPH radical scavenging activity

3.3.6.3. Nitric oxide radical inhibition activity

3.3.6.4. Ferric reducing/antioxidant power (FRAP) activity

3.3.6.5. Total antioxidant capacity

3.3.6.6. Inhibition of lipid peroxidation

3.3.6.7. Lipoxygenase inhibition activity

3.3.7. Quantitative analysis of extracts

3.3.8. UPLC-Q-TOF-MS analysis of HE

3.4. Discussion

3.1. Introduction

Herbal medicines are used in the treatment of different diseases including cancer in the world for a long time. There are claims that some traditional healers can cure cancer using herbal drugs (Vijayalakshmi et al., 2013). Currently, drug development from medicinal herbs is considered as an important aspect in the treatment of cancer. Even though many pharmacologically potent molecules are identified from traditionally used herbs (Xu et al., 2016) still research is going on to discover new anticancer agents from plants. Phytochemicals belong to flavonoids (Yao et al., 2011), terpenoids (Lu et al., 2012b), quinones (Lu et al., 2013), alkaloids (Lu et al., 2012a), phenolics (George et al., 2017), saponins (Xu et al., 2016), quassinoids (Tung et al., 2017), etc. have shown promising anticancer properties. The plant molecules either prevent the cancer formation or execute the curative effect on cancer in different ways.

Plant molecules with the cytotoxic property directly prevent cell metabolism or cell division and forcing cells to undergo apoptosis (Jamkhande and Wattamwar, 2015). Interestingly, several phytochemicals show prooxidant action, especially in the presence of transition metal ions and thus induce apoptosis indirectly in cancer cells. Several phytochemicals that act as antioxidants at particular concentrations behave like prooxidants at other concentrations (Zubair et al., 2016). This is the way in which phytochemicals can cure cancer progression.

In an alternative way, many plant molecules act as antioxidant substances, which scavenge free radicals and reduce oxidative stress. Oxidative stress and related inflammatory responses are major causes of cancer cell formation (Athreya and Xavier, 2017). Thus the nullification of reactive oxygen species (ROS) by plant molecules prevents the formation of cancer cells (Prasad et al., 2017). At the same time, these phytochemicals are greatly useful to prevent recurrence of cancer and reduce various health hazards associated with different conventional cancer therapy techniques.

Phytochemical analysis of Simaroubaceae plants has revealed the presence of many potential biomolecules in different parts of their body. Several constituents have been isolated from these plants. Alkaloids isolated from Simaroubaceae plants have shown

high cytotoxicity (Jiang and Zhou, 2008). Bark and leaves of *Simarouba* are reported to contain triterpenes useful in curing amoebiasis, diarrhoea and malaria (Patil and Gaikwad, 2011). Quassinoids, the bitter principles of the plants of this family have exhibited promising anticancer activity (Devkota et al., 2014).

Simarouba glauca DC. (Laxmitaru) commonly called 'paradise tree' belonging to the family Simaroubaceae has gained much importance due to its wide spectrum of biological properties. Many cancer patients in southern states of India, especially Kerala and Karnataka believe this tree as a magical tree and its decoction can cure cancer. Several incidents on the cure of cancer of various types by the consumption of decoction of *S. glauca* leaves have got wide publicity in recent time in these states over media. Another group of patients vouches that the decoction made out of the leaves of *S. glauca* can alleviate side effects induced by chemotherapy. Because of this, people have started cultivating the plant in various states of South India, particularly in Kerala. However, there is no scientific basis are available on the so-called magical anticancer and anti-tumour properties of *S. glauca.*

In this study, a preliminary phytochemical screening of two different extracts; hot water extract (HE) and methanolic extract (ME) prepared by using mature leaves of *S. glauca* was done. The HE was prepared according to the protocol exists among the cancer patients who use the leaves of *S. glauca* for cancer treatment. ME is prepared by using methanol because methanol is a polar solvent like water which is used for the preparation of HE. The main intention of this study was to evaluate the efficacy of HE in the context of cytotoxic and antioxidant effects in comparison with ME. It is decided to select the extract which shows pharmacological potential for further analysis.

3.2. Materials and methods

3.2.1. Collection and authentication of plant

The collection and authentication of leaves of *S. glauca* were done as mentioned in Chapter 2, section 2.1.1.2.

3.2.2. Preparation of extracts

Two different types of extracts; hot water extract (HE) and methanolic extract (ME) were prepared by the leaves of *S. glauca.* Detailed procedure regarding the preparation of these extracts is explained in section 2.2.1 under Chapter 2.

3.2.3. Phytochemical screening of extracts

3.2.3.1. Qualitative analysis

Phytochemical screening for the presence of various categories of plant compounds like carbohydrates, tannins, coumarins, terpenoids, phenols, saponins, alkaloids, flavonoids, resins, glycosides, proteins and amino acids, steroids and anthraquinones were done with appropriate tests as described in Chapter 2, section 2.2.2.1.

3.2.3.2. Thin layer chromatographic profiling

One dimensional TLC analysis was performed with pre-coated TLC aluminium sheets. Different solvent systems were used for different extracts. The procedure is narrated in Chapter 2, section 2.2.2.2.

3.2.4. *In vitro* cytotoxicity analysis

3.2.4.1. Cell lines

DLA, EAC and spleenocytes were used for the short term *in vitro* cytotoxicity study. Maintenance and collection of tumour cells and isolation of spleenocytes were done as per the procedure mentioned in Chapter 2, section 2.1.7 and 2.2.3.1.

3.2.4.2. Short term cytotoxicity assay

Chapter 2, section 2.2.3.1.2 explains the detailed protocol regarding the conduct of *in vitro* short term cytotoxicity analysis by using trypan blue dye exclusion method.

3.2.4.3. Antiproliferative study

The antiproliferative effect of HE and ME of *S. glauca* were evaluated by using human cervical carcinoma cell (HeLa), human hepatocarcinoma cell line (HepG2), human colorectal adenocarcinoma cell line (HCT-15), estrogen and progesterone

receptor-positive human breast cancer cell line (MCF-7), a triple-negative human breast cancer cell line (MDA-MB-231), a murine macrophage cancer cell line (RAW-264.7) and an African monkey kidney cell line (Vero E6). The maintenance of cells and experiment procedure are explained in Chapter 2, section 2.1.7 and 2.2.3.2.

3.2.5. *In vitro* antioxidant assays

3.2.5.1. Hydroxyl radical scavenging activity

Chapter 2, section 2.2.4.1 describes the principle and procedure regarding the experiment used for estimating the hydroxyl radical scavenging activity of plant extracts. Vitamin E was used as the standard in this experiment.

3.2.5.2. DPPH radical scavenging activity

The stable DPPH radical was used to assess the antioxidant property of HE and ME. Vitamin C was used as the standard in this experiment (Chapter 2, section 2.2.4.2).

3.2.5.3. Nitric oxide radical inhibition assay

Nitric oxide radical scavenging activity of the extracts was assessed by Greiss reaction as mentioned in Chapter 2, section 2.2.4.3. The result was compared with Vitamin C used as the standard.

3.2.5.4. Ferric reducing/antioxidant power (FRAP) assay

The percentage increase in the ferric reducing action of the extracts was conducted by a standard procedure mentioned in Chapter 2, section 2.2.4.4. Vitamin C was used as the standard.

3.2.5.5. Total antioxidant capacity

Chapter 2, section 2.2.4.6 explains the principle and procedure regarding the estimation of total antioxidant capacity (% inhibition) of HE and ME in detail.

3.2.5.6. Inhibition of lipid peroxidation

Murine liver tissue homogenate was used in this experiment to assess the inhibitory action of plant extracts on lipid peroxidation. Ascorbic acid was used as the standard in this experiment (Chapter 2, section 2.2.4.5.)

3.2.5.7. Lipoxygenase inhibition assay

The percentage inhibition of lipoxygenase enzyme by HE and ME of *S. glauca* were estimated by the protocol mentioned in Chapter 2, section 2.2.4.7. The results were analysed with the % inhibition showed by Vitamin C used as a standard drug.

3.2.6. Quantitative analysis of the extracts

3.2.6.1. Estimation of total phenolic content

The estimation of total phenolic content in the extracts (HE and ME) was done by using Folin-Ciocalteu reagent. The principle and procedure regarding the experiment are explained in section 2.2.2.4.1 of Chapter 2.

3.2.6.2. Estimation of total flavonoid content

Pharmacologically significant plant compound, flavonoid were estimated by aluminum chloride colourimetric method (Refer Chapter 2, section 2.2.2.4.2).

3.2.7. UPLC-Q-TOF-MS analysis of the extract

The high-resolution liquid chromatographic-mass separation of HE was carried out by using 1290 Infinity UHPLC system. The details regarding the instrument and procedure are explained in Chapter 2, section 2.2.2.3.

3.2.8. Statistical analysis

All assays were performed minimum thrice in duplicate and values represented as mean ± SD. Statistical analysis was done by one way ANOVA using Graph pad Instat software. The level of significance was fixed to $p<0.05$.

3.3. Results

3.3.1. The percentage yield of *S. glauca* leaf extracts

The HE obtained was dark brown in colour and the average yield of the dry residue was 15.70 ± 0.50%. The ME obtained had a dark green colour and the average yield was 23.15 ± 0.06%. The difference in percentage yield of both extracts was found at 47.45%.

3.3.2. Phytochemical screening

The different chemical tests conducted, unraveled the presence of phytochemicals like tannins, coumarins, terpenoids, phenols, saponins, alkaloids, flavonoids and carbohydrates in HE and ME of *S. glauca*. Organic molecules like proteins and free amino acids, steroids, sterols, anthraquinones and phlobatannins showed negative reaction for their specific identification tests. Resins were detected in HE but absent in ME. Glycosides were unable to detect in HE but the positive response for the same phytochemical was noted in ME (Table 3.1).

Table 3.1. Phytochemical screening of different extracts of *S. glauca* leaves

Sl. No.	Phytochemicals	Extract	
		HE	ME
1	Carbohydrates	+	+
2	Tannins	+	+
3	Coumarins	+	+
4	Terpenoids	+	+
5	Phenols	+	+
6	Saponins	+	+
7	Alkaloids	+	+
8	Flavonoids	+	+
9	Resins	+	-
10	Glycosides	-	+
11	Proteins & Amino acids	-	-
12	Steroids	-	-
13	Anthraquinones	-	-
14	Phlobatannins	-	-

+, presence and -, absence of phytochemicals

3.3.3. Thin layer chromatographic profiling

3.3.3.1. Thin layer chromatographic profiling of HE

Total twenty-three bands were developed while the HE of *S. glauca* was eluted by TLC. The number of bands observed under visible light and visualized under visible

light, after exposure to iodine vapour was six. But, under UV light (254nm) eleven bands were noticed (Figure 3.1). All the bands with similar Rf values were noted under visible light after exposure to iodine vapour. Band with Rf value 0.15, 0.24, 0.35, 0.54 and 0.68 were observed as common bands under visible light, iodine vapour and UV light (254 nm). Bands with high Rf value 0.43, 0.59, 0.63, 0.84, 0.89 and 0.96 were present only in UV light (254 nm) (Table 3.2).

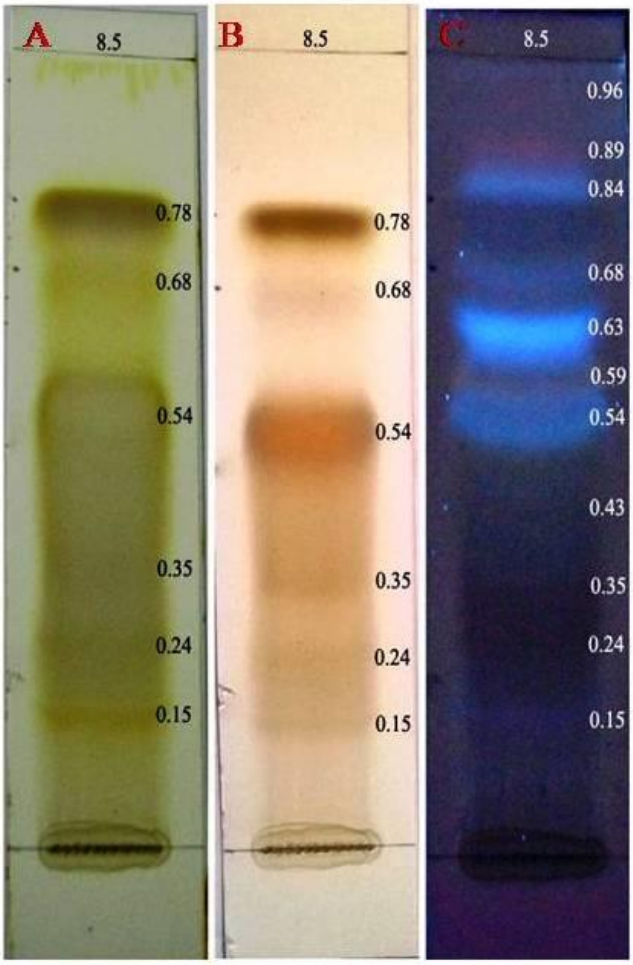

Figure 3.1. TLC of HE: Approximately 10 μL (100 μg) HE was applied on precoated thin layer chromatographic aluminium sheets of 11 cm length and developed using mobile phase, n-butanol: glacial acetic acid: distilled water (60:15:25, v/v/v) and observed under (A) visible light (B) visible light after exposed to iodine vapour and (C) UV (254 nm)

Table 3.2. Rf values of fractions obtained in TLC of HE of *S. glauca* viewed under visible light, visible light after exposure to iodine vapour and UV (254 nm)

Sl. No.	Band	Rf value		
		Normal light	Normal light, after exposure to Iodine vapour	UV (254 nm)
1	Band – I	0.15	0.15	0.15
2	Band - II	0.24	0.24	0.24
3	Band – III	0.35	0.35	0.35
4	Band – IV	0.54	0.54	0.43
5	Band - V	0.68	0.68	0.54
6	Band – VI	0.78	0.78	0.59
7	Band – VII	-	-	0.63
8	Band – VIII	-	-	0.68
9	Band – IX	-	-	0.84
10	Band – X	-	-	0.89
11	Band – XI	-	-	0.96

Pharmacologically significant components like flavonoids, triterpenoids, terpenoids, alkaloids and phenolics of HE of *S. glauca* were detected by different spraying reagents in separate TLC plates (Figure 3.2). Among the different phytochemicals analysed with suitable reagents, seven fluorescent bands (with Rf values 0.24, 0.35, 0.63, 0.68, 0.76, 0.81 and 0.89) were observed under UV (254 nm) while the TLC plates were treated with 1% ethanolic solution of aluminium chloride for flavonoids. Triterpenoids revealed their presence with three bands when the TLC plates were treated with the anisaldehyde-sulphuric acid reagent. The Rf value of these bands were 0.29, 0.54 and 0.81. Band with Rf value 0.81 was found common in flavonoids and triterpenoids. Terpenoids and alkaloids were found positive with their respective reagents and developed four bands. Bands with Rf value 0.24 and 0.63 were noted common for both. The other bands found positive for terpenoids have Rf value 0.54 and 0.68 respectively. Bands with Rf value 0.65 and 0.90 were the other bands found positive for alkaloids. Four bands (Rf values 0.15, 0.22, 0.54 and 0.89) were visualized when treated with ferric chloride reagent and revealed the presence of

phenolics. Band with Rf value 0.54 was found positive for triterpenoids, terpenoids and phenolics. Band with Rf value 0.89 gave a positive response for flavonoid and phenolics. Another band with Rf value 0.63 was found present in flavonoids, terpenoids and alkaloids.

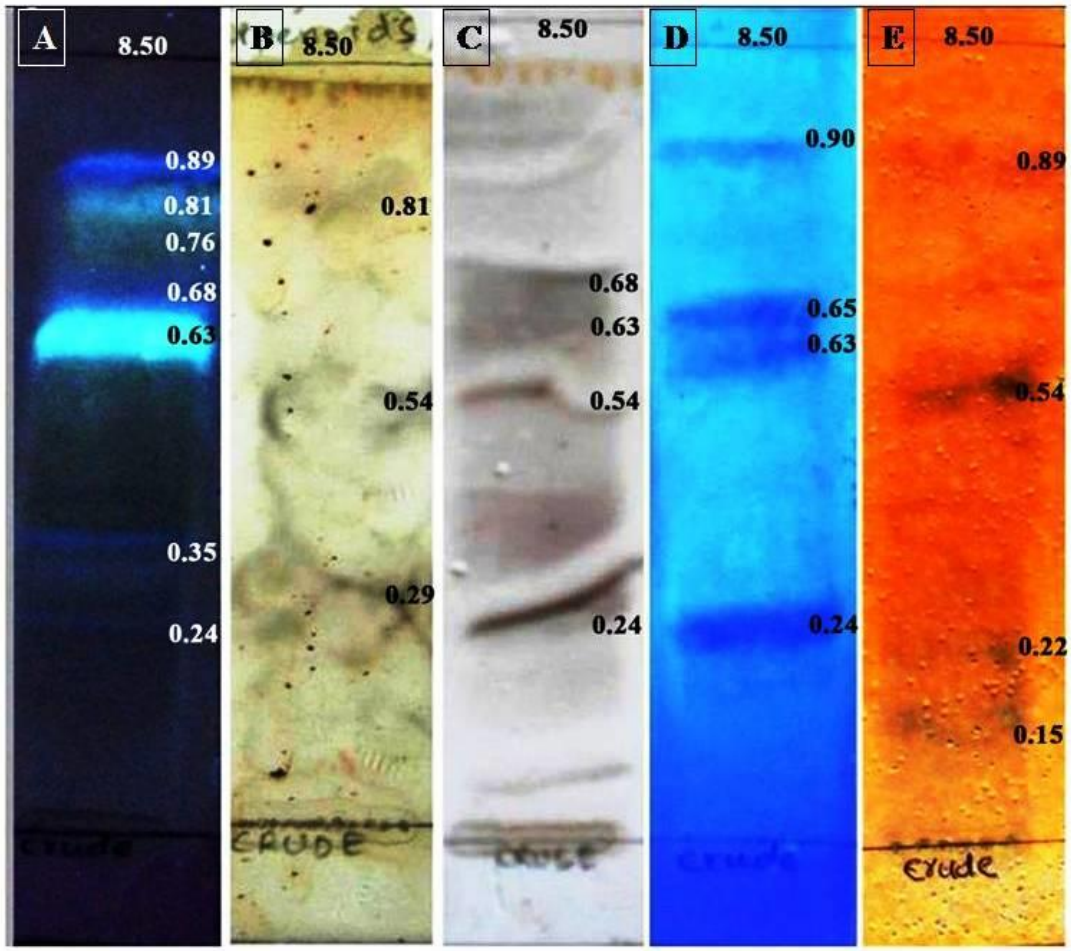

Figure 3.2. Phytochemical profile of HE: Approximately 10 μL (100 μg) HE was applied on precoated thin layer chromatographic aluminium plates of 11 cm length and developed using mobile phase, n-butanol: glacial acetic acid: distilled water (60:15:25, v/v/v) and sprayed with (A) 1% ethanolic solution of aluminium chloride for flavonoids and observed under UV (B) anisaldehyde-sulphuric acid reagent for triterpenoids (C) vanillin sulphuric acid reagent for terpenoids (D) Dragendorff's reagent for alkaloids and (E) ferric chloride reagent for phenolics

3.3.3.2. Thin layer chromatographic profiling of ME

Total twenty-eight bands were developed while the ME of *S. glauca* was eluted by TLC. The number of bands observed under visible light was eleven. But, the number of bands could visualize under visible light after exposure to iodine vapour were nine and under UV light (254 nm) eight bands were noticed (Figure 3.3). Three bands with

similar Rf values (0.83, 0.92 and 0.94) were noted under visible light and iodine vapour. Band with Rf value 0.98 was observed as a common one under iodine vapour and UV light (254 nm). Another band with Rf value 0.23 was obtained under visible light and UV light (254 nm). Band with high Rf value (0.92) was present under all the conditions are taken for visualizing the bands (Table 3.3).

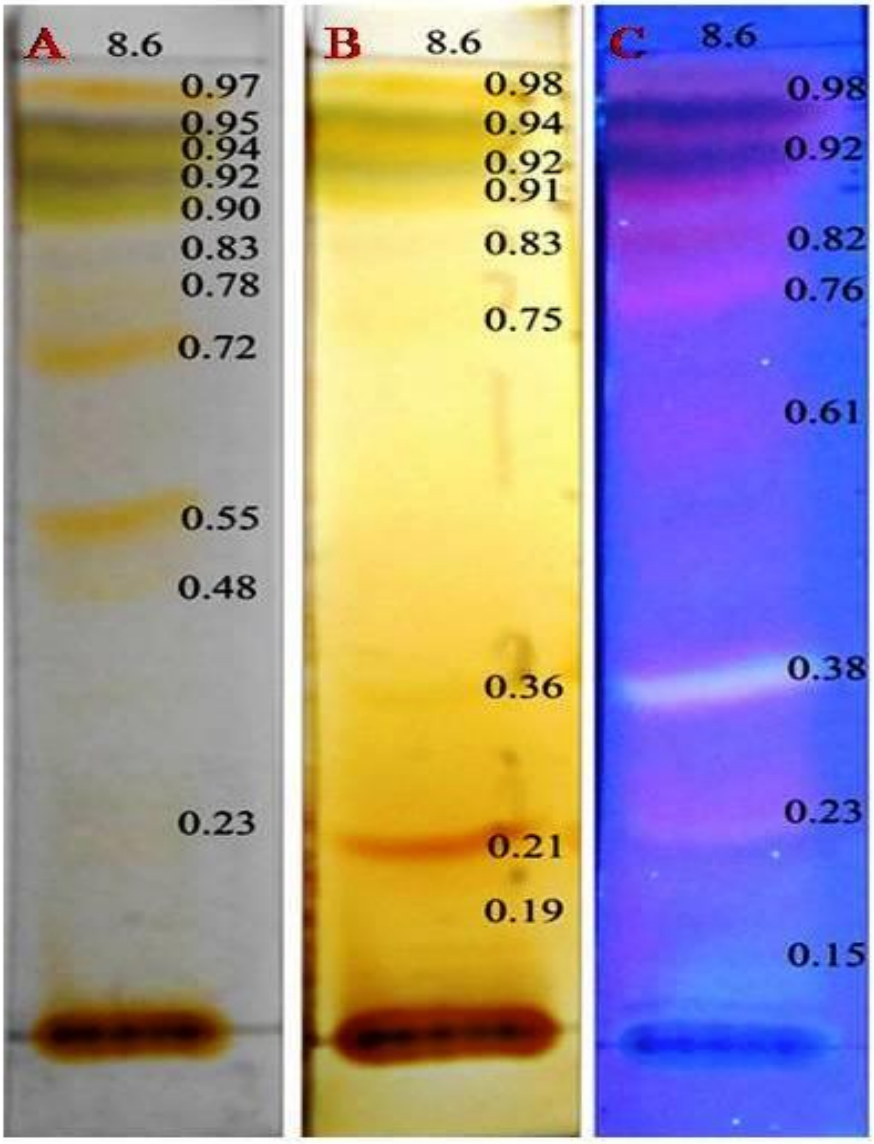

Figure 3.3. TLC of ME: Approximately 10 μL (100 μg) ME was applied on precoated thin layer chromatographic aluminium plate of 11 cm length and developed using mobile phase, chloroform: ethyl acetate: formic acid (8:2:0.2, v/v/v) and observed under (A) visible light (B) visible light after exposed to iodine vapour and (C) UV (254 nm)

Table 3.3. Rf values of fractions obtained in TLC of ME of *S. glauca* viewed under visible light, visible light after exposure to iodine vapour and UV (254 nm)

Sl. No.	Band	Rf value		
		Normal light	Normal light, after exposure to Iodine vapour	UV (254 nm)
1	Band – I	0.23	0.19	0.15
2	Band – II	0.48	0.21	0.23
3	Band – III	0.55	0.36	0.38
4	Band – IV	0.72	0.75	0.61
5	Band – V	0.78	0.83	0.76
6	Band – VI	0.83	0.91	0.82
7	Band – VII	0.90	0.92	0.92
8	Band – VIII	0.92	0.94	0.98
9	Band – IX	0.94	0.98	--
10	Band – X	0.95	--	--
11	Band – XI	0.97	--	--

Similar to HE pharmacologically important phytochemicals like flavonoids, triterpenoids, terpenoids, alkaloids and phenolics of ME of *S. glauca* were detected by different spraying reagents to separate TLC plates (Figure 3.4). The maximum number of bands (8 number) were observed in the TLC under UV (254 nm) after treated with 1% ethanolic solution of aluminium chloride for flavonoids. The Rf value of these bands were 0.09, 0.50, 0.55, 0.62, 0.64, 0.72, 0.78 and 0.95. When treated with the anisaldehyde-sulphuric acid reagent for triterpenoids, five bands gave a positive response; they are with Rf value 0.13, 0.64, 0.77, 0.78 and 0.91. Band with Rf value 0.78 found common for both flavonoids and triterpenoids. A total number of six bands (Rf values of 0.10, 0.54, 0.64, 0.79, 0.87 and 0.95) were observed in TLC treated with vanillin sulphuric acid reagent for terpenoids. Band with Rf value 0.95 appeared as common for both flavonoids and terpenoids. For alkaloids and phenolic compounds, only two bands were observed with respective reagents. Band with Rf value 0.70 and 0.86 were found to be positive for alkaloids by Dragendorff's reagent.

Phenolic compounds were coloured with ferric chloride reagent and developed two bands with following Rf values; 0.64 and 0.79. Band with Rf value 0.79 were found common for both terpenoids and phenolic compounds. Similar to this band with Rf value 0.64 could observe in flavonoids, triterpenoids, terpenoids and phenolics.

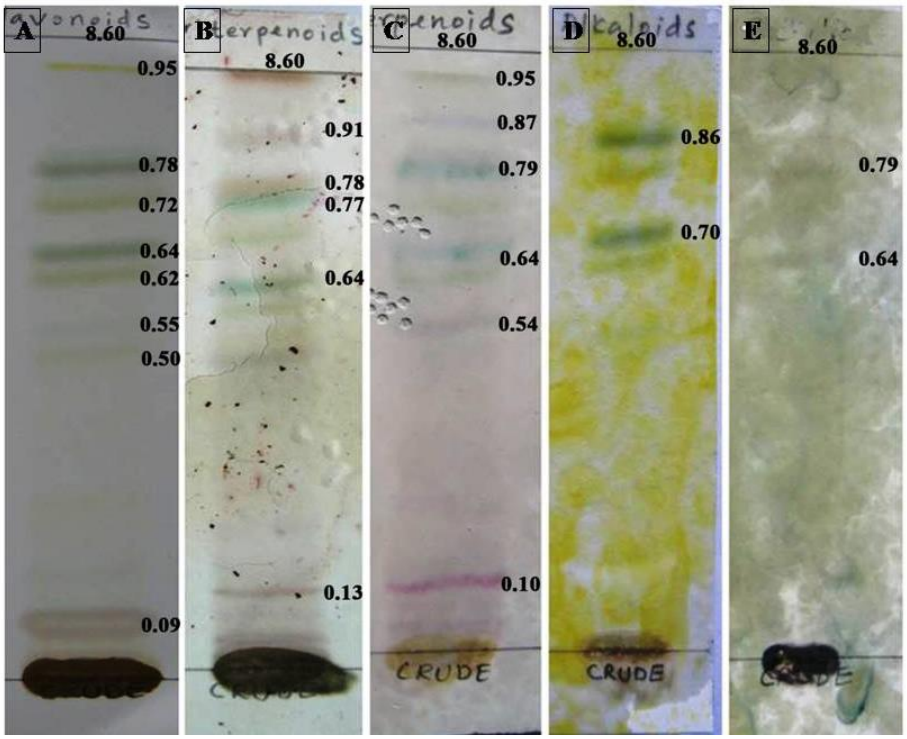

Figure 3.4. Phytochemical profile of ME: Approximately 10 μL (100 μg) ME was applied on precoated thin layer chromatographic aluminium plate of 11 cm and developed using mobile phase, chloroform: ethyl acetate: formic acid (8:2:0.2, v/v/v). The plates were then sprayed with (A) 1% ethanolic solution of aluminium chloride for flavonoids and observed under UV (B) anisaldehyde-sulphuric acid reagent for triterpenoids (C) vanillin sulphuric acid reagent for terpenoids (D) Dragendorff's reagent for alkaloids and (E) ferric chloride reagent for phenolics and photographed

3.3.4. Short term *in vitro* cytotoxicity

3.3.4.1. Cytotoxic effect of HE

The HE showed a dose-dependent increase in the cytotoxicity towards all the cell lines used.-In the maximum concentration of drug used in the study (100 μg/mL), the EAC cells showed only 12.41 ± 1.25% cell death. In the same concentration of HE, DLA cells showed 37.55 ± 0.93% cell death. The percentage of cell death among normal cells (spleenocytes) was found minuscule (4.97 ± 0.18). It is noted that the cancer cells are more affected by the cytotoxic nature of HE than the normal cells

(Figure 3.5). The IC_{50} value of HE for all the cells studied was found to be >100 μg/mL.

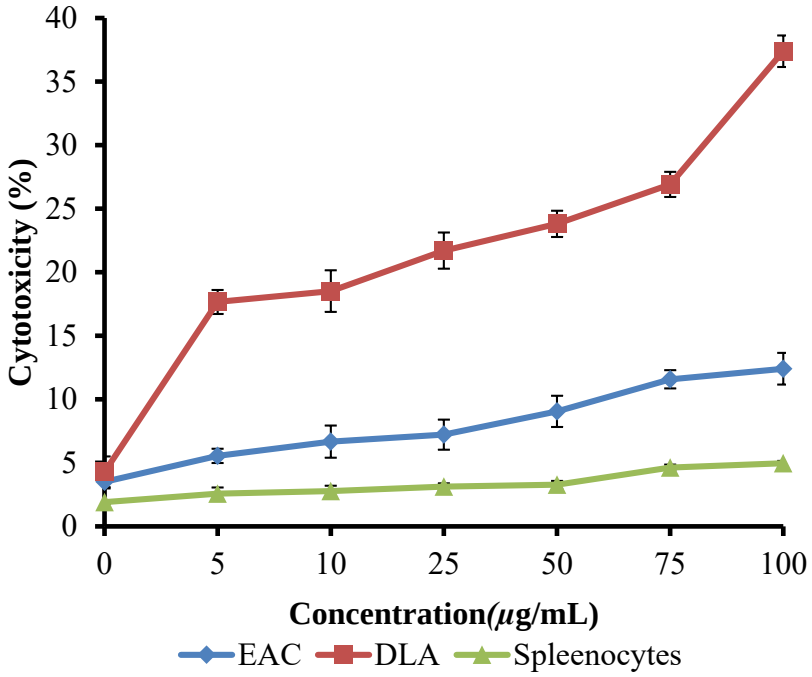

Figure 3.5. Toxicity of HE towards DLA, EAC and spleenocytes: Cells ($1x10^6$) in 1mL PBS, (spleenocytes in RPMI 1640 medium) were exposed to various concentration of HE as indicated in figure for 3 hr and the cytotoxicity was evaluated by Trypan blue method. Values are expressed as mean ± SD of at least three experiments done in duplicate tubes

3.3.4.2. Cytotoxic effect of ME

The short term cytotoxicity of ME of *S. glauca* at various concentrations (5-100 μg/mL) is depicted in figure 3.6. The maximum percentage of cytotoxicity for EAC cells (35.32 ± 2.35) could be observed at 100 μg/mL concentration. At the same concentration (100 μg/mL) the percentage cytotoxicity obtained with DLA cell suspension was 43.34 ± 1.71%. Towards spleen cells, the action of ME of *S. glauca* (100 μg/mL) was found to be feeble (16.26 ± 1.71% inhibition). The IC_{50} value of ME extract of *S. glauca* in these cells was supposed to be >100 μg/mL. Like the earlier experiment, the cytotoxic action of ME was more prominent towards the cancer cells than normal body cell.

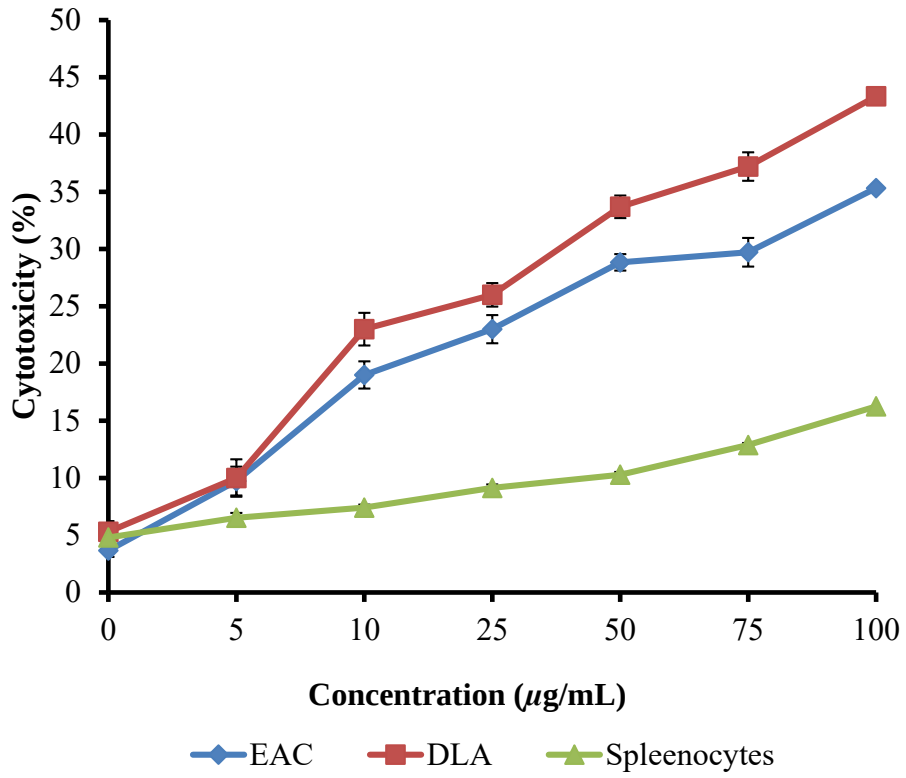

Figure 3.6 Toxicity of ME towards DLA, EAC and spleenocytes: Cells ($1x10^6$) in 1mL PBS (spleenocytes in RPMI 1640 medium) were exposed to various concentration of ME for 3 hr and the cytotoxicity was evaluated by Trypan blue method. Values are expressed as mean ± SD of at least three experiments done in duplicate tubes

3.3.5. Anti-proliferative effect of HE and ME

HE and ME were used to analysing their antiproliferative effect by using various cell lines. Both extracts were showed antiproliferative activity in a dose-dependent manner (Figure 3.7, 3.8, 3.9 and 3.10). HE showed lower IC_{50} (<100 μg/mL) for three cell lines studied (HCT-15, RAW 264.7 and HeLa). In all other cell lines, the IC_{50} value for HE and ME was found >100 μg/mL (Table 3.4).

Table 3.4. Antiproliferative effect of extracts of *S. glauca* on various cell lines

Cell line	IC_{50} (μg/mL)	
	HE (μg/mL)	ME (μg/mL)
HCT-15	71.53 ± 0.72	>100
RAW 264.7	85.32 ± 3.17	>100
HeLa	98.33 ± 7.35	>100
HepG2	>100	>100
MDA-MB-231	>100	>100
MCF-7	>100	>100
Vero-E6	>100	>100

Values are expressed as mean ± SD for three experiments

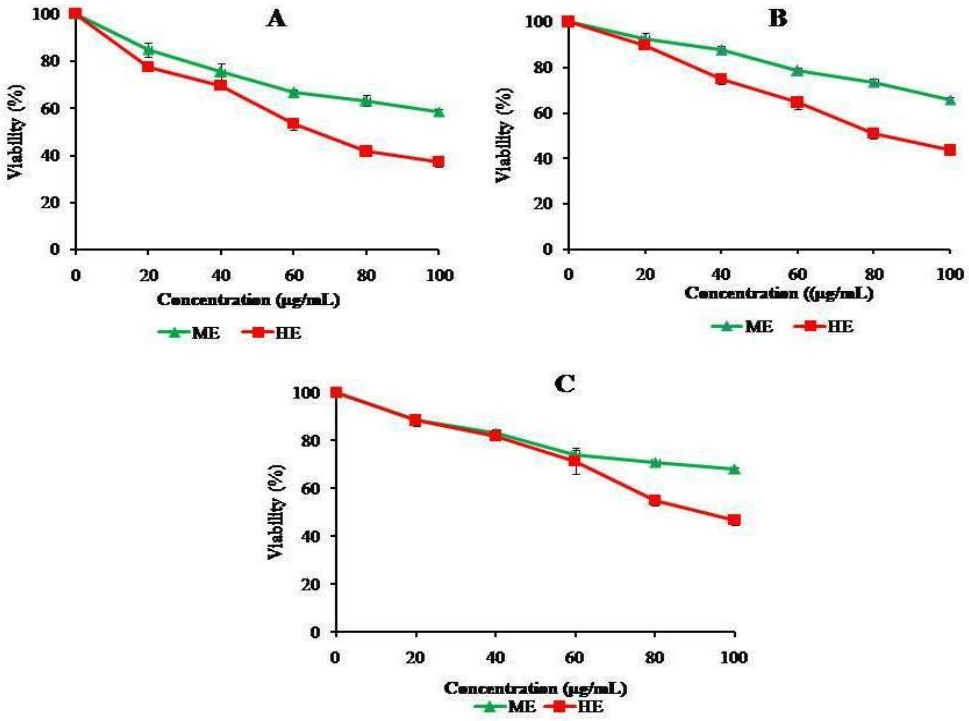

Figure 3.7. Antiproliferative activity of leaf extracts (ME and HE) of *S. glauca* against A) HCT-15, B) RAW 264.7 and HeLa cells: Cells ($1x10^5$) at it log phase in 24 well plates were exposed to HE and ME extracts at concentration given in figure over 48 hr. The cell viability was then measured using the MTT assay. Values are expressed as mean ± SD for three independent experiments

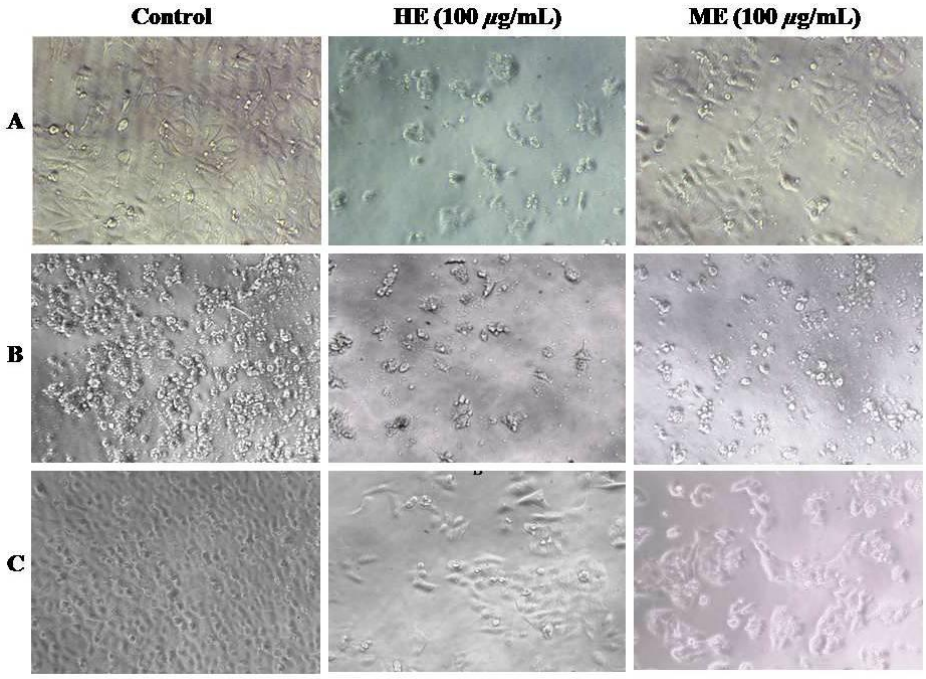

Figure 3.8. Morphological changes observed under a phase-contrast microscope (200X) in A) HCT 15, B) RAW 264 and C) HeLa cells: Cells ($1x10^5$) at it log phase in 24 well plates were exposed to HE and ME extracts at concentration given in figure over 48 hr.

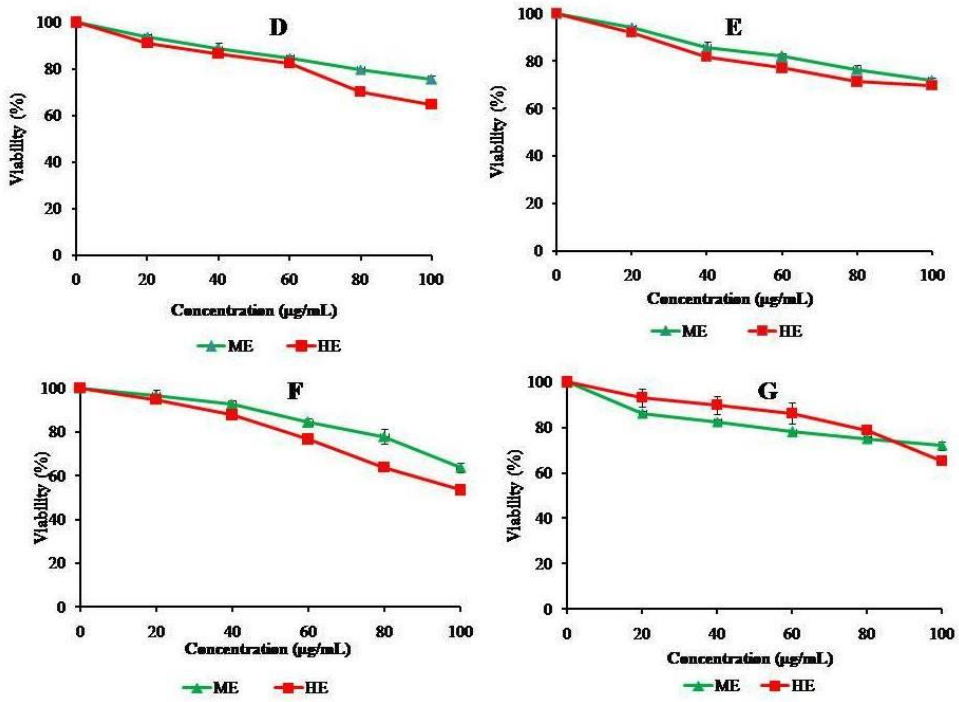

Figure 3.9. Antiproliferative activity of leaf extracts (ME and HE) of *S. glauca* against D) HepG2 E) MDA-MB-231 F) MCF-7, and G) Vero-E6 cells: Cells ($1x10^5$) at it log phase in 24 well plates were exposed to HE and ME extracts at concentration given in figure over 48 hr. The cell viability was then measured using the MTT assay. Values are expressed as mean ± SD for three experiments

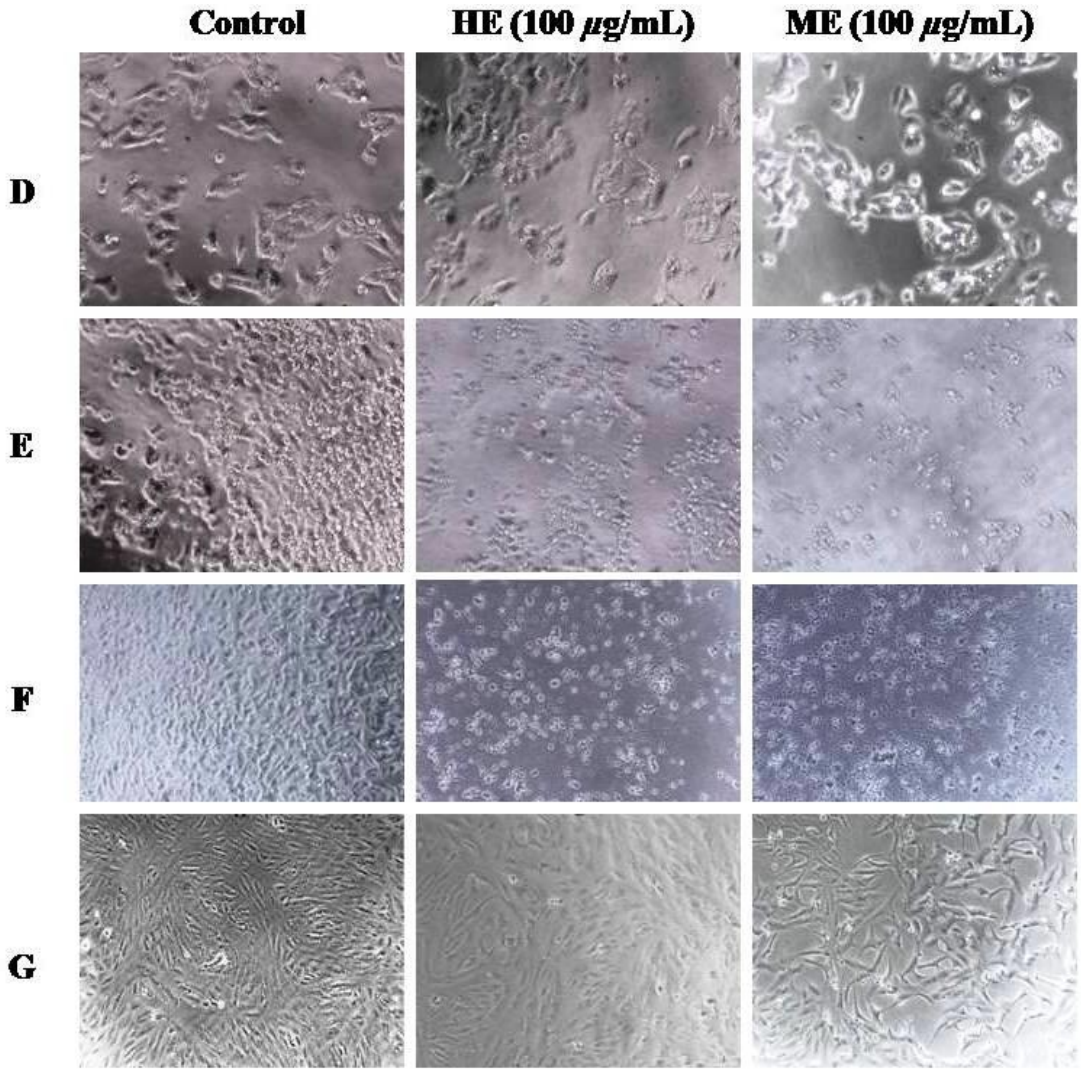

Figure 3.10. Morphological changes observed under an inverted microscope using phase-contrast objectives (200X) in D) HepG2 E) MDA-MB-231 F) MCF-7, and G) Vero-E6 cells: Cells ($1x10^5$) at it log phase in 24 well plates were exposed to HE and ME extracts at concentration given in figure over 48 hr. The cells were observed under an inverted microscope using phase contrast objective.

3.3.6. *In vitro* antioxidant action

3.3.6.1. Hydroxyl radical scavenging activity

The hydroxyl radical scavenging efficacy of extracts of *S. glauca* used in the study is shown in figure 3.11.A. Both HE and ME was found to inhibit hydroxyl radical generation in a dose-dependent manner (20-100 μg/mL). The IC_{50} values obtained for the extracts were <100 μg/mL. Among the extracts, HE was found more effective

(77.88 ± 2.75 μg/mL) than ME (82.64 ± 3.02 μg/mL). Vitamin E was used as the standard in this experiment and obtained an IC_{50} value of 0.49 ± 0.05 μg/mL.

3.3.6.2. DPPH radical scavenging activity

DPPH radical scavenging activity of HE and ME is depicted in figure 3.11. Both the extracts showed a dose-dependent reduction of DPPH free radical within a concentration range from 1 - 10 μg/mL. The IC_{50} value for HE and ME was 7.47 ± 0.48 μg/mL and 7.08 ± 0.32 μg/mL respectively. The IC_{50} value obtained for DPPH radical scavenging activity by using different extracts of *S. glauca* was found very close to each other. The IC_{50} value documented for vitamin C used in this experiment as standard was 2.4 ± 0.12 μg/mL.

3.3.6.3. Nitric oxide radical inhibition activity

The nitric oxide radical scavenging activity of leaf extracts of *S. glauca* is illustrated in figure 3.11.C. The extracts used in this experiment were ranged from 20 to 100 μg/mL. The HE and ME were effective in inhibiting noted in nitric oxide scavenging action a dose-dependent manner. The IC_{50} value for ME was found greater (94.16 ± 3.45 μg/mL) than the HE (63.13 ± 2.34 μg/mL). In other words, the HE was found to be more effective in scavenging the nitric oxide radical. The standard drug used in this experiment (vitamin C) showed an IC_{50} value of 10.20 ± 2.34 μg/mL, which is 6.19 fold higher in comparison with nitric oxide scavenging action of HE.

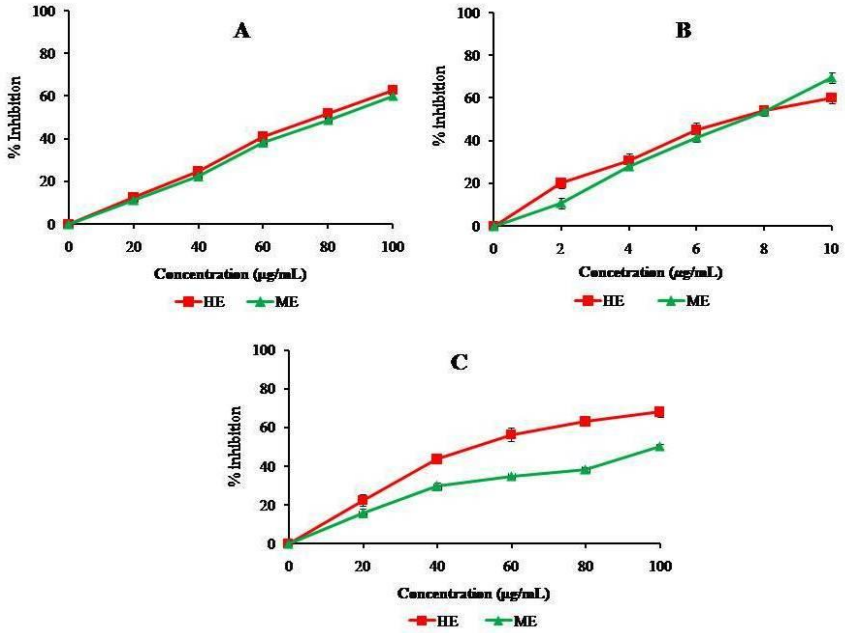

Figure 3.11. The *in vitro* free radical scavenging activities of HE and ME of *S. glauca* leaves: A) Hydroxyl radical scavenging assay, B) DPPH radical scavenging assay and C) Nitric oxide scavenging assay. Values are expressed as mean ± SD for three experiments

3.3.6.4. Ferric reducing/antioxidant power (FRAP) activity

The antioxidant capacity of a compound is related to its reducing power. The ferric reducing antioxidant capacity of extracts of *S. glauca* was thoroughly evaluated and found effective. The extracts used in this study exhibited ferric reducing action in a dose-dependent way. The half-maximal effective concentration (EC_{50}) was found 3.66 ± 0.29 μg/mL for HE. The ME extract showed an EC_{50} of 5.54 ± 0.72 μg/mL (Figure 3. 12.D).

3.3.6.5. Total antioxidant capacity

Total antioxidant capacity of extract was assessed by adopting the standard protocol and the data showed a half-maximal effective concentration (EC_{50}) <100 μg/mL for both HE and ME (Figure 3.12. E). The EC_{50} value was found to be 77.85 ± 3.45 μg/mL for HE and 88.65 ± 4.25 μg/mL for ME. For both extracts, the total antioxidant capacity was noted in a dose dependent manner.

3.3.6.6. Inhibition of lipid peroxidation

In this assay, the highest rate of inhibition of lipid peroxidation was performed by ME rather than HE (Figure 3.12.F). It showed an IC_{50} value of 19.74 ± 1.67 μg/mL. The HE extract was found less effective compare to ME and IC_{50} value was 37.82 ± 2.54 μg/mL. Vitamin C used as a standard in this experiment and IC_{50} value obtained is 30.23 ± 1.14 μg/mL. ME extract showed a greater percentage of inhibition of lipid peroxidation in comparison with standard drug.

3.3.6.7. Lipoxygenase inhibition activity

The inhibitory action of lipoxygenase enzyme by plant extracts showed good antioxidant capacity. In this experiment, HE showed lower IC_{50} value than ME (Figure 3.12.G). The IC_{50} value for HE was 32.57 ± 1.64 μg/mL. The IC_{50} value for ME was 74.85 ± 2.32 μg/mL. The IC_{50} value of vitamin C used in this study was 30.12 ± 2.32 μg/mL which is close to the IC_{50} value of HE in this experiment.

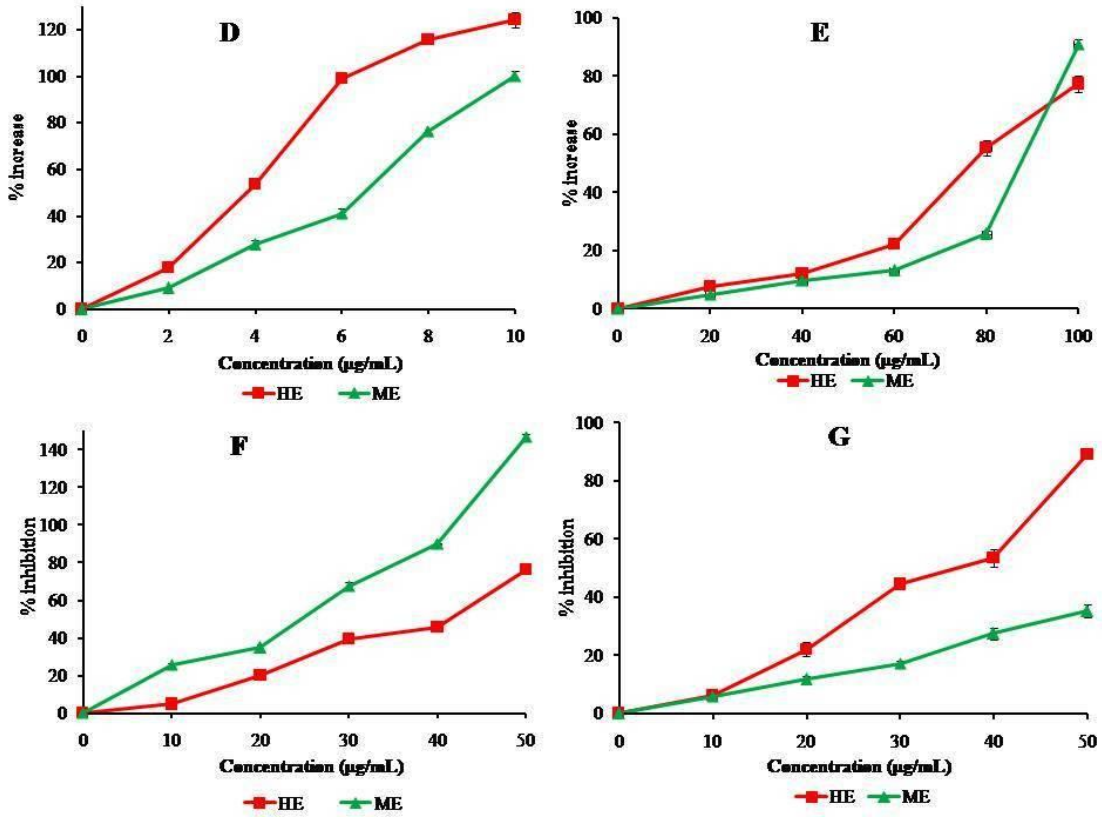

Figure 3.12. The *in vitro* free radical scavenging activities of HE and ME of *S. glauca* leaves: D) FRAP assay, E) total antioxidant capacity assay F) inhibition of lipid peroxidation and G) lipoxygenase inhibition assay. Values are expressed as mean ± SD for three experiments

3.3.7. Quantitative analysis of extracts

Apart from the qualitative analysis for phytochemicals, quantitative estimation of pharmacologically significant compounds like phenols and flavonoids were done. The total phenolic content of the extracts is expressed in gallic acid equivalents (mg GAE/ gm extract) and total flavonoid content in mg quercetin per gm extract (mg QTE/gm extract). The total phenolic content in HE was 77.58 ± 0.65 mg GAE/ gm extract. The total phenolic content in ME was found very close to HE (78.17 ± 0.43 mg GAE/ gm extract). The total flavonoid content was found more in HE (27.13 ± 2.65 mg QTE/gm extract) than ME (16.0 ± 1.06 mg QTE/gm extract). Table 3.5 shows the data obtained from the quantitative analysis of extracts of *S. glauca*.

Table 3. 5. Total phenol and flavonoid content of different extracts of *S. glauca*

Extract	Total phenol content (mg GAE/gm extract)	Total flavonoid content (mg QTE/gm extract)
HE	77.58 ± 0.65	27.13 ± 2.65
ME	78.17 ± 0.43	16.0 ± 1.06

Values are expressed as mean ± SD for three experiments

3.3.8. UPLC-Q-TOF-MS analysis of HE

UPLC-Q-TOF-MS analysis of HE revealed as many as 93 constituents out of which 79 compounds were able to identify. The name of these compounds with their retention time, mass and DB diff (ppm) are described in table 3.6 and the spectrum has depicted in figure 3.13. Twenty-one peaks were unable to identify. Out of this, nine active components with antioxidant, anti-inflammatory and anticancer properties were identified. They are Chlorogenic acid (with RT 6.308, 7.081 min and mass 354.0918, 354.0923 kDa), loganin (with RT 6.816 min and mass 390.1499 kDa), acetylsalicylic acid (with RT 7.102 min and mass 180.041 kDa), irigenin (with RT 7.152 min and mass 450.134), dihydrorobinetin (with RT 9.078, 9.457 min and mass 304.0557, 304.0563 kDa), gitoxin (with RT 10.972 min and mass 780.4169 kDa), oleandrin (with RT 11.208, 11.523, 11.887, 13.09, 13.8, 13.868 min and mass 576.3267, 576.3272, 576.3275, 576.3263, 576.3268, 576.3265 kDa), cucurbitacin L (with RT 11.901, 13.804 min and mass 516.3062, 516.3055 kDa) and cucurbitacin B (with RT 15.492 min and mass 558.3163 kDa).

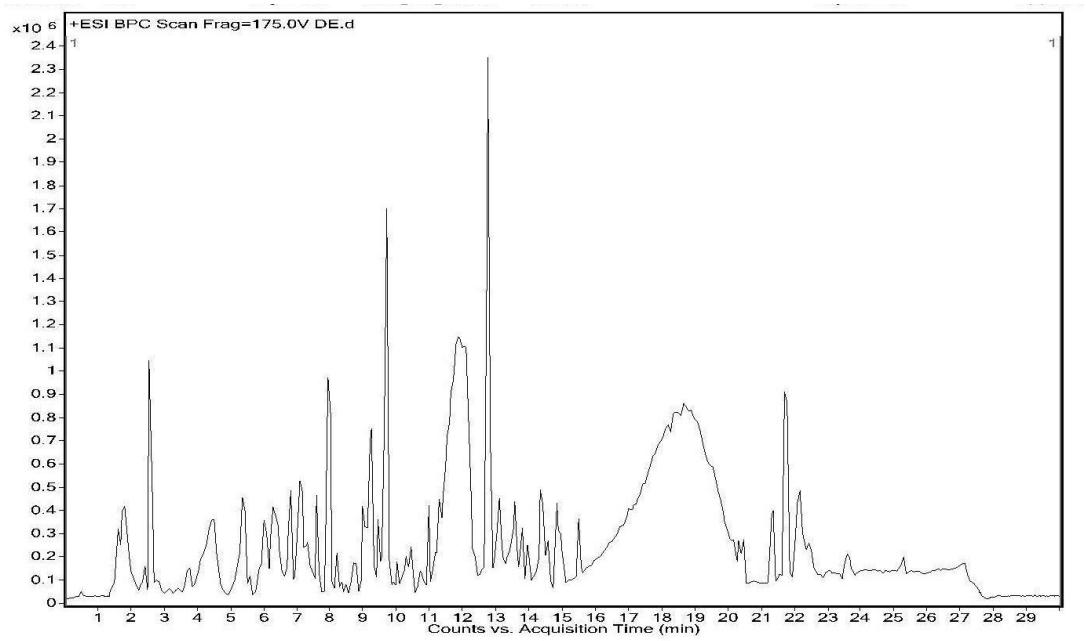

Figure 3.13. Total ion chromatogram of the HE of *S. glauca* when subjected to UPLC-Q-TOF-MS analysis

Table 3.6. Different constituents of HE of *S. glauca* identified by UPLC-Q-TOF-MS

RT	Mass	DB diff (ppm)	Name
1.755	162.1114	10.23	Carnitine
1.816	133.1113	-7.8	Bis (2-hydroxypropyl) amine
2.57	267.0942	4.53	Neuraminic acid
2.572	135.0533	-1.26	4-Hydroxy-L-threonine
4.401	138.0907	8.38	nn-Dimethylaniline-n-oxide
5.38	350.1187	0.18	Estrone 3-sulfate
5.87	380.1283	2.89	2-Methoxyestrone 3-sulfate
5.945	310.0291		
6.01	382.1447	0.91	2-Methoxyestradiol-17beta 3-sulfate
6.063	183.054	-4.44	4-Pyridoxic acid
6.14	293.1153	3.96	7-Acetamidonitrazepam
6.213	152.0574	7.43	N-Methyl-2-pyridone-5-carboxamide (Nudifloramide)
6.308	354.0918	9.14	Chlorogenic acid
6.312	158.059	-7.01	4,6-dioxoheptanoic acid

6.451	414.1709	-5.8	His Gln Met
6.598	394.1451	9.6	Asn Asp Phe
6.816	390.1499	6.83	Loganin
6.993	390.1832	2.8	11-Dehydrodexamethasone
7.013	384.1605	0.52	3b,16b- Dihydroxyandrostenone
7.081	354.0923	7.98	Chlorogenic acid
7.086	730.1685		
7.102	180.041	6.99	Acetylsalicylic acid (aspirin)
7.152	450.134	-5.55	IRIGENIN, 7-BENZYL ETHER
7.155	252.1108	0.65	Tyr Ala
7.159	224.1169	-3.76	butalbital
7.166	339.1521	6.39	Pro His Ser
7.271	346.1135	1.7	S 26191
7.475	288.0477	-4.05	N-1-Desalkylflurazepam
7.608	202.1574	-2.64	3S-hydroxy-undecanoic acid
7.612	404.202	-0.24	GluArgThr
7.882	143.0954	-5.11	1-Aminocyclohexanecarboxylic
7.882	171.0902	-3.92	3-Methylcrotonyl)glycine methyl ester
7.97	236.1165	-1.8	PheAla
8.215	406.1342	8.43	3,5-Pyridinedicarboxylic acid, 1,4-dihydro-2,6-dimethyl-4-(2nitrophenyl)-, 2-hydroxy-2-methylpropyl
8.745	243.1602	8.54	3-Hydroxymorphinan
9.078	304.0557	8.45	DIHYDROROBINETIN
9.137	404.2015	1.52	7alpha-(Thiomethyl)spironolactone
9.23	210.1604	-5.48	Altretamine
9.456	418.0869		
9.457	304.0563	6.59	DIHYDROROBINETIN
9.695	492.1968		
9.702	452.2044	3.43	ThrPheTrp

10.029	476.222	2.26	Loperamide
10.031	514.2589	-4.27	DIHYDROFISSINOLIDE
10.283	760.3608		
10.406	94.0074	15.41	Dimethyl sulfone
10.776	680.2925		
10.972	780.4169	16.24	GITOXIN
11.092	666.2254	-5.25	Glycogen
11.208	576.3267	5.51	OLEANDRIN
11.297	670.3694	22.15	Saquinavir
11.383	286.0956	-0.88	5-(3,4-Dihydroxy-1,5-cyclohexadien-1-yl)-5-phenylhydantoin
11.523	576.3272	4.57	OLEANDRIN
11.887	576.3275	4.09	OLEANDRIN
11.901	516.3062	4.76	Cucurbitacin L
11.917	480.2851	0.24	GPA(10:0/10:0)[U]
11.923	480.2844	1.57	GPA(10:0/10:0)
12.377	273.2644	8.73	C16 Sphinganine
12.59	518.321	6.46	Cucurbitacin F
12.767	568.271	-6.68	SWIETENINE
12.771	567.287	-1	Dihydrodeoxystreptomycin
13.035	273.2647	7.59	C16 Sphinganine
13.09	576.3263	6.09	OLEANDRIN
13.104	338.3144	11.96	2,4-dimethyl-2-eicosenoic acid
13.105	239.223		
13.287	644.2624		
13.476	658.2969		
13.558	440.2916	-3.21	26,26,26-trifluoro-25-hydroxy-27-norvitamin D3 / 26,26,26- trifluoro-25-hydroxy-27- norcholecalciferol
13.8	576.3268	5.26	OLEANDRIN
13.804	516.3055	6.26	Cucurbitacin L

13.832	412.1468	3.28	N-Carboxytocainideglucuronide
13.868	576.3265	5.8	OLEANDRIN
14.264	652.3437		
14.293	647.3286		
14.345	372.2461	6.4	Arg Val Val
14.384	815.3722		
14.835	304.2979	8.39	Acetylpyridinium
14.883	700.3442		
14.975	285.2643	8.77	C17 Sphingosine
14.977	366.3452	12.39	Nervonic acid
15.492	558.3163	5.25	Cucurbitacin B
15.492	480.2847	1	GPA(10:0/10:0)
16.233	331.3209		
16.879	532.3722		
17.113	332.2532	9.23	9R,10S,18-trihydroxy-stearic acid
17.264	548.3288		
19.365	290.1626	1.64	PROCATEROL
20.072	568.3941	6.65	1-dodecanoyl-2-tridecanoyl- sn-glycero-3-phosphate (ammonium salt)
20.152	296.16	7.86	Lactone of PGF-MUM
20.16	166.0255	6.53	Benzoquinoneacetic acid
20.374	367.4148		
20.468	608.3301		
20.468	603.374	-20.2	Benzonatate (2,5,8,11,14,17,20,23,26-Nonaoxaoctacosan-28-yl p-(butylamino)-benzoate
21.334	402.2226	0.14	Leu Asp Arg
21.535	484.2793	1.64	GPGro(16:0/0:0)[U]
21.739	552.3998		
22.133	606.2816	-4.5	Trandolaprilglucuronide
22.369	567.4166		
23.594	408.2843	8.04	3beta,6alpha,7alpha- Trihydroxy-5beta-cholan-24- oic Acid
25.852	521.586		

Table 3.7. The important chemical constituents of HE of *S. glauca* detected by UPLC-Q-TOF-MS and their properties

Sl. No.	Constituent	Properties
1	Chlorogenic acid	Antibacterial (Lou et al., 2011), antioxidant and anti-inflammatory (Tajik et al., 2017), anticancer (Yamagata et al., 2018), antiproliferative (Hou et al., 2017), antihypertensive (Hakkou et al., 2017), inhibits angiogenesis (Zhong et al., 2017), hepatoprotective, neuroprotective and cardioprotective (Naveed et al., 2018)
2	Loganin	Anti-inflammatory (Li et al., 2016), anti-osteoporosis (Yang et al., 2019) and brain tonic (Hwang et al., 2017, Yao et al., 2017)
3	Acetylsalicylic acid	Anti-inflammatory(Kata et al., 2017), antinociceptive (Bednarczyk-Cwynar et al., 2016), anticancer (Alfonso et al., 2014) and cardioprotective (Kim and Becker, 2016)
4	Irigenin	Antioxidant and anti-inflammatory (Ahn et al., 2006), Antimetastatic (Amin et al., 2016) and anticancer (Xu et al., 2018)
5	Dihydrorobinetin	Analgesic, anti-inflammatory and antiarthritic (Ficarra et al., 1995)
6	Gitoxin	Antitumour (Lopez-Lazaro et al., 2003)
7	Oleandrin	Anticancer (Ko et al., 2018), anti-inflammatory (Sreenivasan et al., 2003), induce apoptosis (Pan et al., 2017) and antitumour (Elmaci et al., 2018)
8	Cucurbitacin B	Anticancer (Garg et al., 2018b), cardioprotective (Xiao et al., 2017), anti-inflammatory (Ma et al., 2014), antiproliferative (Duangmano et al., 2012) and anti-stress effect (Garg et al., 2018a)
9	Cucurbitacin L	Induce apoptosis (Abdelwahab et al., 2012)

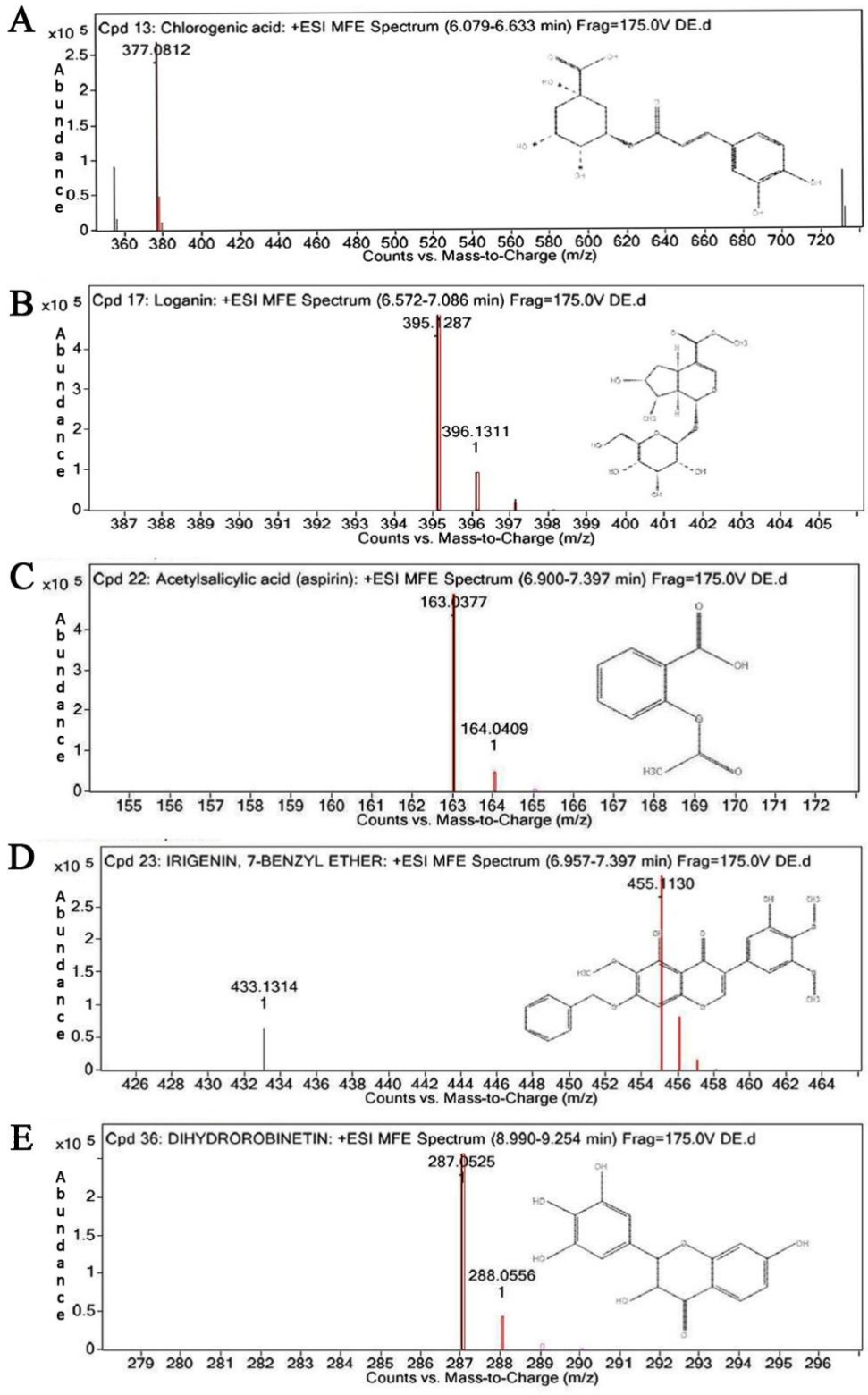

Figure 3.14. The compounds identified from HE of *S. glauca* by UPLC-Q-TOF-MS analysis: (A) Chlorogenic acid, (B) Loganin, (C) Acetylsalicylic acid, (D) Irigenin, and (E) Dihydrorobinetin

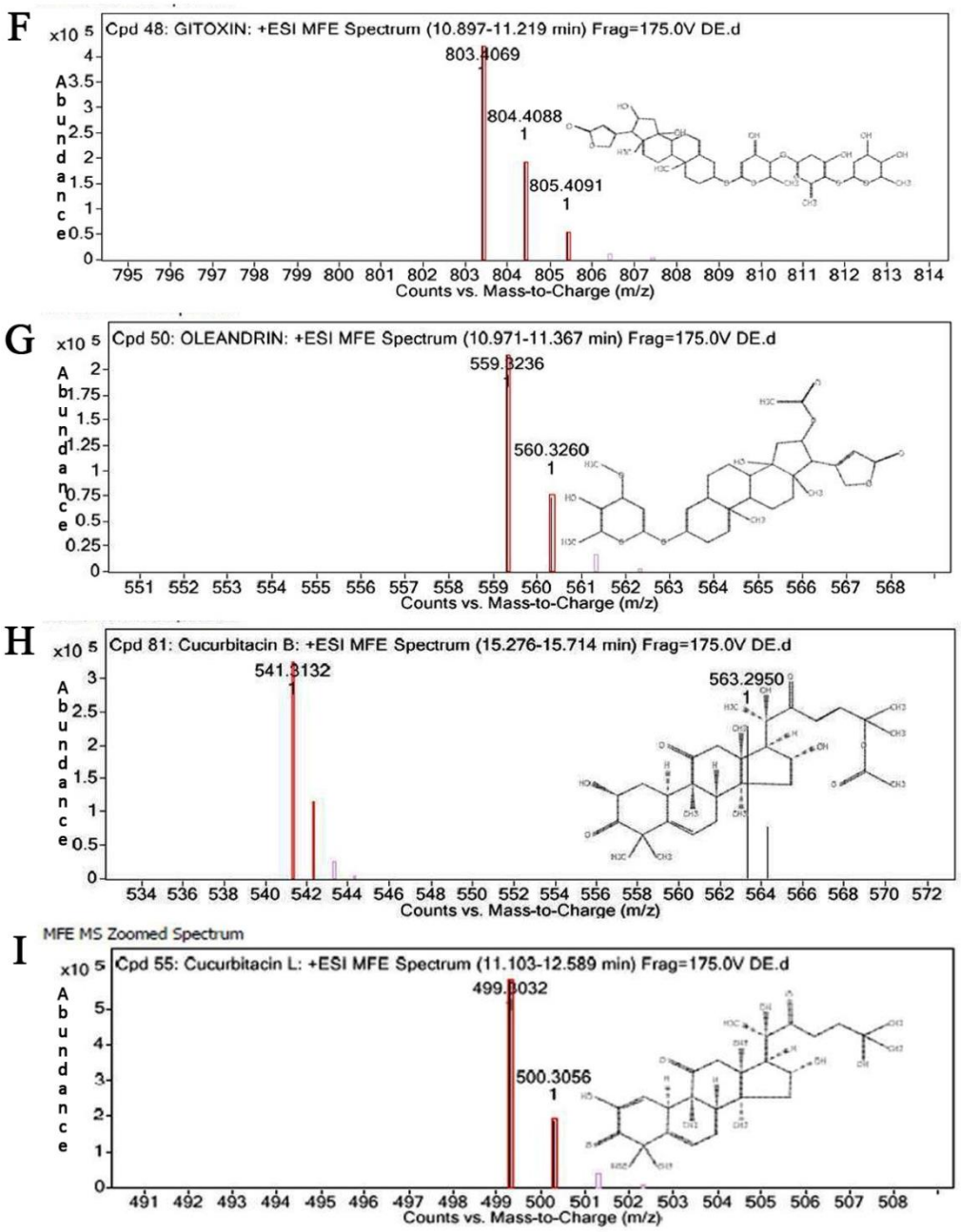

Figure 3.15. The compounds tentatively identified from HE of *S. glauca* by UPLC-Q-TOF-MS analysis: (F) Gitoxin, (G) Oleandrin, (H) Cucurbitacin B, and (I) Cucurbitacin L

3.4. Discussion

Preparing a decoction by using different parts of medicinal herbs for consumption is easy and is considered as a general practice in traditional medicine in many countries on the world. This is the same protocol used by the cancer patients in S. India who consume *S. glauca* decoction as part of their treatment. Methanolic extract (ME) was

prepared by using methanol (99.9%) for more scientific support and also for comparison. It was found that the yield of HE extract was less with respect to ME. It is reported that different solvents have significant effects on the yield of extractable. In general, water can extract around half of the extractable solids in comparison with extraction by absolute methanol (Ngo et al., 2017). As the study was concentrated on the anticancer properties of the plant leaf extracts, phytochemical screening, cytotoxic effects on cancer cells and normal cells, quantitative estimation of phenolic and flavonoids and *in vitro* antioxidant capacity (Ngo et al., 2017) of HE and ME were thoroughly analyzed.

Initial phytochemical screening of HE and ME unravelled the presence of a similar group of compounds between the extracts. TLC analysis of the individual extracts with spraying agents for different phytochemicals also revealed the presence of potential phytochemicals like phenolics, flavonoids, triterpenoids, terpenoids and alkaloid shared among HE and ME. Polyphenols are a huge and diverse group of phytochemicals extensively consumed by man. Flavonoids are plant secondary metabolites included under polyphenols and abundantly seen in commonly consumed vegetable and fruits. They show excellent antioxidant, anti-inflammatory and anticancer properties (Foti, 2007). Many studies have pointed out the fact that the consumption of diet enriched with flavonoids is directly connected to a decreased risk of cancer formation (Magne Nde et al., 2015). Terpenoids are considered as the largest group of phytochemicals (Thoppil and Bishayee, 2011), traditionally used for medicinal purposes in Asian countries. The alkaloids present in plants have excellent antioxidant and anticancer potential (Khare et al., 2019).Terpenoids and triterpenoids are found useful in the prevention and therapy of several dreadful diseases, including cancer (Sharma et al., 2017). Quassinoids, the important category of phytochemicals present in Simaroubaceae family members are degraded triterpenes lactones (Fiaschetti et al., 2011). Since the extraction procedure for quassinoids is different, no specific tests were conducted in this study to detect the presence of this particular group of phytochemical in HE and ME.

The short term cytotoxicity analysis done by using cancer cell lines like DLA and EAC showed that the extracts are less toxic to them. The IC_{50} value obtained in this

study was >100 μg/mL. It is noticed that cytotoxic effect on normal cells (spleenocytes) was minuscule and both extracts are safe for using *in vivo* experiments.

The antiproliferative activity of HE was found better than ME since it showed a lower IC_{50} value on three cell lines studied (HCT-15, RAW 264.7 and HeLa). The IC_{50} value was found above 100 μg/mL for ME in all the cell lines studied, indicating its less cytotoxic nature. By considering the results of both short term and long term cytotoxicity assays it is concluded that HE extract of *S. glauca* possess higher cytotoxic potential than ME.

It is revealed from this study that both extracts possess an excellent antioxidant capacity. In comparison, HE is found to be more active. The antioxidant quality may be attributed to the presence of different phytochemicals present in these extracts. The alkaloids, carotenoids and polyphenols hold high antioxidant activity (Xu et al., 2017). Along with the earlier mentioned compounds, terpenoids are very effective antioxidant molecules (Grassmann, 2005). The quantitative estimation of polyphenols and flavonoids among the HE and ME indicated the presence of these phytochemicals in abundance in HE then ME.

Since HE showed more antioxidant potential in comparison with ME, the phytochemical analysis of HE was done with UPLC-Q-TOF-MS. The UPLC-Q-TOF-MS analysis unravelled the presence of many potent antioxidants, anti-inflammatory and anticancer molecules like chlorogenic acid, loganin, acetylsalicylic acid, irigenin, dihydrorobinetin, gitoxin, oleandrin, cucurbitacin L and cucurbitacin B. In conclusion the present study revealed the differential cytotoxicity of HE and its excellent antioxidant potential with respect to ME. So the HE of *S. glauca* has been selected for further studies.

Chapter 4

Safety evaluation of hot water extract of *Simarouba glauca* DC

Contents

4.1. Introduction

4.2. Materials and methods

4.2.1. Collection and authentication of plant

4.2.2. Animals

4.2.3. Preparation of extract

4.2.4. Acute toxicity study

4.2.5. Sub-acute toxicity study

4.2.6. Statistical analysis

4.3. Results

4.3.1. Effect of acute oral administration of HE

4.3.2. Effect of sub-acute administration of oral doses of HE

4.4. Discussion

4.1. Introduction

Many herbs, either in the form of an extract, pure compound or as derivative, provide unlimited chances for the discovery of novel drugs. Most plants or plant products used in the form of medicine are not scientifically tested or documented for their toxicity and efficacy. Only little knowledge or evidence is available regarding the potential toxicity that medicinal herbs may cause to the consumers. The general public is primarily interested in the fast access of these plants and totally unaware of the potential health hazards associated with consumption of these plants. More than this, based on the long term use by human beings many people have false belief that plants used in traditional medicine are nontoxic. However, many instances have exposed that a lot of plants used in traditional medicine are toxic (Koduru et al., 2006). Therefore it is obvious that the conventional use of any herbs for treatments, by no means, assures the safety of that plant.

Apart from these in a scientific drug development programme it is mandatory that the test material be evaluated for its safety before being used in *in vivo* experiments. OECD guideline is widely accepted in several laboratories. Toxicological screening is an integral part of drug development strategy As per Code of Federal Regulations, Title 21 of FDA, (US Food and Drug Administration) it is highly essential to evaluate new drugs for pharmacological activity and toxicity potential in animals (Part 314, 2019). In this century, toxicological evaluation of food substances, food additives, plant toxins, cosmetics, pharmaceuticals, chemicals, etc., have attained great importance (Parasuraman, 2011).

Simarouba glauca DC. (Laxmitaru, Paradise tree) belonging to the family Simaroubaceae has been extensively used in traditional medicine in different parts of the world (Jose et al., 2018). So far several constituents have been isolated from this plant, mainly quassinoids with a promising antimalarial (O'Neill et al., 1986) and anticancer (Karthikeyan et al., 2016) activity. Glaucarubinone, a quassinoid isolated from *S. glauca* has great potential as an anticancer molecule (Yeo et al., 2016, Karthikeyan et al., 2016). Recently *S. glauca* has become a ‘tree of solace’ for many cancer patients in South India, especially in Kerala (Narendran, 2013). Several reports on the cure of cancer of various types at their initial stages by the consumption of decoction of leaves of *S. glauca* have got wide publicity in this state over media.

Added to this many patients vouch that the decoction made out of the leaves of *S. glauca* could alleviate side effects while undergoing chemotherapy and minimize the appetite loss. In fact, no scientific information is available on the chemical composition and toxicity profile of decoction of *S. glauca* leaves. It has been noted that the profuse and injudicious consumption of plant materials as such and their decoction made out of different plants as medicine for various diseases can cause hazardous effects on health (Nair et al., 2014). Since it is an exotic plant, it is crucial to pay more attention to find the chemical composition and scrutinize the safety of *S. glauca* before recommending it for therapeutic purposes. The current study focuses on the detailed toxicity analysis of oral administration of hot water extract of *S. glauca* leaves (HE), which is prepared as per the protocol followed by its advocates in Swiss albino mice.

The primary phytochemical screening of HE unveiled the presence of potential phytochemicals like flavonoids, phenolics, terpenoids, triterpenoids and alkaloids in it. The short term cytotoxicity analysis showed moderate action of HE but, the antiproliferative activity of HE was found better on cell lines like HCT-15, RAW 267 and HeLa. Moreover the HE showed excellent antioxidant activity in different *in vitro* experiments conducted. The quantitative estimation revealed the presence of a good amount of polyphenols and flavonoids in HE. Apart from this, the UPLC-Q-TOF-MS analysis of HE revealed the presence of many antioxidant, anti-inflammatory and anticancer molecules like chlorogenic acid, loganin, dihydrorobinetin, oleandrin, gitoxin, acetylsalicylic acid, cucurbitacin L, Cucurbitacin B, etc. All these results gave a positive node for conducting *in vivo* studies of HE of *S. glauca*. Conducting acute and sub-acute toxicity analysis is inevitable for determining LD_{50} and dose fixation for further *in vivo* studies. In this context, it is decided to conduct a detailed toxicity evaluation (both acute and sub-acute) of HE of *S. glauca* in murine models.

4.2. Materials and methods

4.2.1. Collection and authentication of plant

Leaves of *S. glauca* DC were collected from the herbal medicine garden located at the campus of Amala Ayurvedic Hospital, Thrissur. The authentication of the plant was done by Dr. C. N. Sunil. (Refer Chapter 2, section 2.1.1.2)

4.2.2. Animals

Female and male Swiss albino mice (25-28 gm) were purchased and maintained as explained in Chapter 2, section 2.1.6.

4.2.3. Preparation of extract

The detailed procedure regarding the preparation of HE of *S. glauca* is described in Chapter 2, section 2.2.1.

4.2.4. Acute toxicity study

Forty-two adult and healthy Swiss albino mice (25 ± 3 gm) of both sexes were grouped into seven categories and used to conduct the acute toxicity study. The study was done as per the number 423 of OECD guidelines (OECD, 2001). The duration of the study was fourteen days. This study is inevitable to find the 50% lethal dose (LD_{50}) of HE of *S. glauca* for Swiss albino mice (Parasuraman, 2011). The detailed procedure regarding this study is explained in Chapter 2, section 2.2.5.1.

4.2.5. Sub-acute toxicity study

OECD guideline number 407 was followed for this study (OECD, 2008). Similar to acute toxicity analysis, Swiss albino mice (25 ± 3 gm) of both sexes were used in this study. The animals (50 numbers; 25 males and 25 females) were randomly divided into five experimental groups like an untreated group (group I, administered 200 μL saline, p.o.), vehicle treated control (administered 200 μL 1% propylene glycol, p.o.) (group II) and HE treated (group III: 0.200 gm/kg b. wt., group IV: 0.300 gm/kg b. wt. and group V: 0.400 gm/kg b. wt) groups. They were housed in different cages based on dose, treatment and sex. The dose 0.200 gm/kg b. wt administered to animals in group III is near to human equivalent dose (160 mg/kg b. wt) as per the treatment practice followed by the people. The animal equivalent dose calculation was done based on body surface area (Nair and Jacob, 2016). The animals were given HE doses orally for 28 days and there after animals were sacrificed following overnight fasting. The blood and tissues were collected and biochemical analysis was done. The detailed procedure regarding the administration of drug and data collection is explained in Chapter 2, section 2.2.5.2.

4.2.6. Statistical analysis

Each *in vitro* assay was performed at least thrice and the data were expressed as Mean value ± SD. Statistical analysis of the data was done by one-way analysis of variance (ANOVA) followed by Dunnett multiple comparison tests using Graph Pad Instat software. Data on vehicle control and HE treated animals were compared with the untreated animal group. A probability level lower than 5% ($p < 0.05$), was considered significant.

4.3. Results

4.3.1. Effect of acute oral administration of HE

Swiss albino mice administered (p.o.) a single dose of 0.1, 0.25, 0.5, 1.0, and 2.0 gm/kg b. wt. of HE of *S. glauca* were observed for 14 consecutive days showed no morbidity and mortality. Evaluation of skin, fur, eyes and ears of treated animals showed no abnormality in appearance with respect to an untreated group of animals. No hair loss was seen. Respiratory and central nervous system effects (tremor), autonomic effects (salivation) were not observed. No abnormal changes in behavior (aggression, self-mutilation, drowsiness, gait, changes in body posture, locomotor disability, etc.) were noticed. Water and food consumption rates were close to the normal group of animals. The animals were active during the study period. A steady increase in the gain of body weight was noted in all treated animals. The final body weight of mice in all treated groups was increased and no significant difference was noted with respect to untreated animals during the study period (Table 4.1). Necropsy studies were conducted at the end of the experiment revealed no abnormal change in size, colour and texture of visceral organs with respect to untreated animals. Result obtained from this study is summarized and represented in the form of a table (Table 4.2).

Table 4.1. Effect of acute administration of HE on body weight (gm) of mice

Group	Day		
	1	7	14
Male			
Untreated	26.20 ± 0.96	27.43 ± 1.12	28.73 ± 1.21
Vehicle control [a]	26.17 ± 0.89	27.33 ± 0.91	28.67 ± 0.91
0.100 gm/kg b. wt.	26.20 ± 0.96	27.47 ± 0.76	28.67 ± 0.98
0.250 gm/kg b. wt.	26.27 ± 0.75	27.53 ± 1.02	28.77 ± 1.02
0.500 gm/kg b. wt.	25.87 ± 1.05	27.13 ± 0.99	28.37 ± 1.05
1 gm/kg b. wt.	26.10 ± 0.65	27.33 ± 1.29	28.47 ± 1.25
2 gm/kg b. wt.	25.80 ± 0.80	27.03 ± 1.15	28.17 ± 1.43
Female			
Untreated	25.93 ± 0.81	26.57 ± 0.63	27.53 ± 0.95
Vehicle control [a]	25.63 ± 1.07	26.13 ± 0.97	27.30 ± 1.15
0.100 gm/kg b. wt.	25.60 ± 0.83	26.13 ± 0.77	27.20 ± 1.05
0.250 gm/kg b. wt.	25.50 ± 0.95	26.20 ± 1.09	27.10 ± 0.45
0.500 gm/kg b. wt.	25.57 ± 1.10	26.30 ± 1.08	27.23 ± 1.15
1 gm/kg b. wt.	25.50 ± 0.75	26.23 ± 0.95	27.00 ± 1.25
2 gm/kg b. wt.	25.80 ± 0.76	26.57 ± 1.34	27.40 ± 1.15

[a] Vehicle control (1% propylene glycol)
Values are mean ± standard deviation of three animals per sex in each group

Table 4.2. Effect of acute administration of HE on general appearance and behaviour of mice

Observation	Group						
	Untreated	Vehicle control [a]	HE (gm/kg b. wt.)				
			0.1	0.25	0.50	1.0	2.0
Feed consumption	Normal	Normal	Normal	Normal	Normal	Normal	Normal
Water consumption	Normal	Normal	Normal	Normal	Normal	Normal	Normal
Change in skin	No effect	No effect	No effect	No effect	No effect	No effect	No effect
Drowsiness	Not observed	Not observed	Not observed	Not observed	Not observed	Not observed	Not observed
Sedation	Not observed	Not observed	Not observed	Not observed	Not observed	Not observed	Not observed
Eye color	No effect	No effect	No effect	No effect	No effect	No effect	No effect
Diarrhoea	Not observed	Not observed	Not observed	Not observed	Not observed	Not observed	Not observed
General Physique	Normal	Normal	Normal	Normal	Normal	Normal	Normal
Mortality	Nil	Nil	Nil	Nil	Nil	Nil	Nil

[a] Vehicle control (1% propylene glycol)

4.3.2. Effect of sub-acute administration of oral doses of HE

General appearance and behaviour of both sexes of Swiss albino mice were not adversely affected by the administration of HE of *S. glauca* at doses of 200, 300 and 400 mg/kg b wt for 28 days. No toxicity signs like drowsiness and alternation in the locomotor activity were noted in the mice. In all treated group animals, the appearance of the skin, fur, eyes, ear, etc. was found during the study period. No abnormal behaviour was noticed in any treatment groups. Mortality was not observed in any of the group members, they remained active and healthy during the entire period of study. Further, administration of HE did not produce any abnormal change in the body weight of both male and female mice with respect to normal mice (Figure 4.1a and 4.1b). The body weight of animals was found increasing in a steady manner. When compared to the normal group of animals, the rate of feed consumption of male and female mice in the treated group was found same (Figure 4.2a and b). Similar to the above the water consumption rate was found normal (Figure 4.3a and b). No digestive system disorders were noticed in the drug-treated animals in the entire period of the experiment.

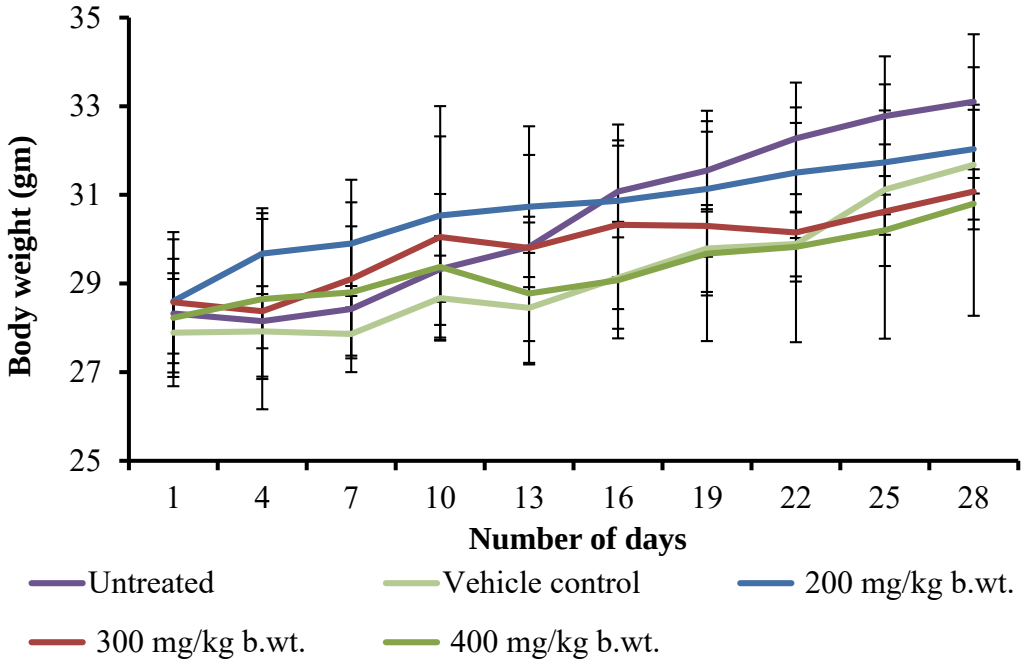

Figure 4.1a. Effect of sub-acute administration of 200, 300 and 400 mg/kg b. wt. of HE on body weight (gm) of male mice: The extract was administered orally to the particular group on a daily basis for twenty-eight days

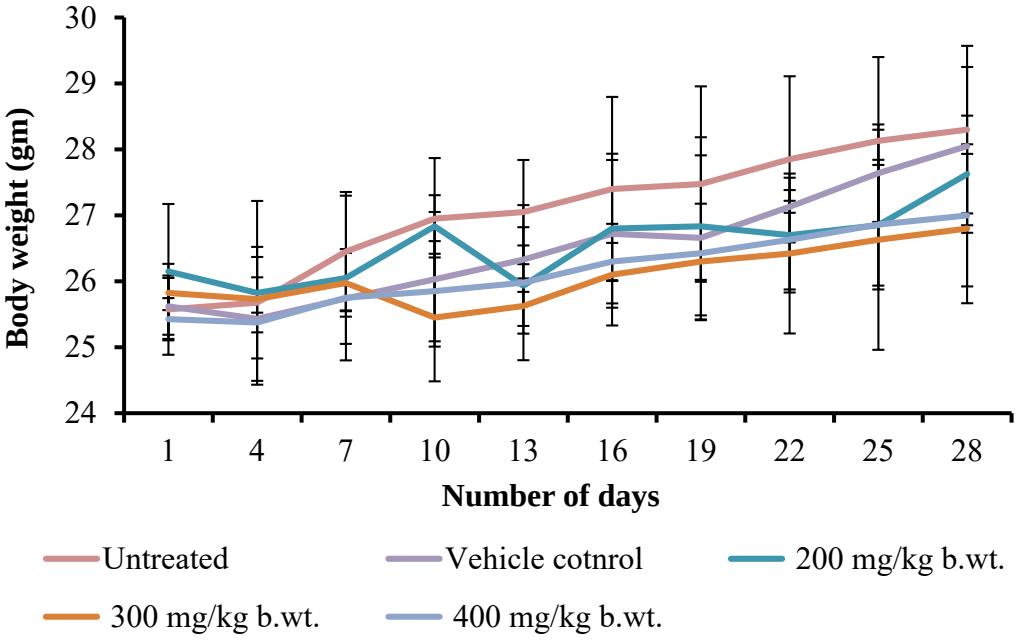

Figure 4.1b. Effect of sub-acute administration of 200, 300 and 400 mg/kg b. wt. of HE on body weight (gm) of female mice: The extract was administered orally to the particular group on a daily basis for twenty-eight days

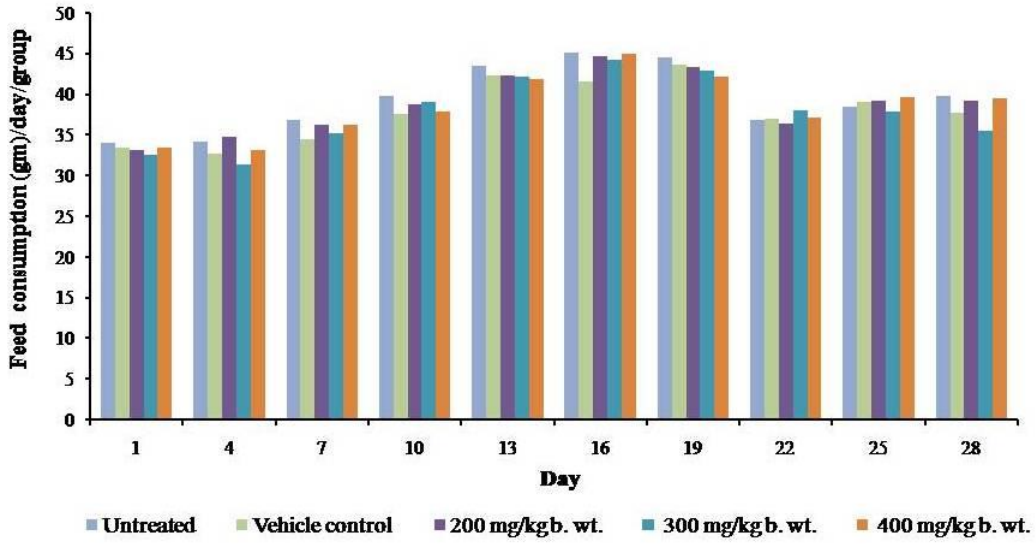

Figure 4.2a. Effect of sub-acute administration of 200, 300 and 400 mg/kg b. wt. of HE on feed consumption (gm/day/group) of male mice: The extract was administered orally to the particular group on a daily basis for twenty-eight days

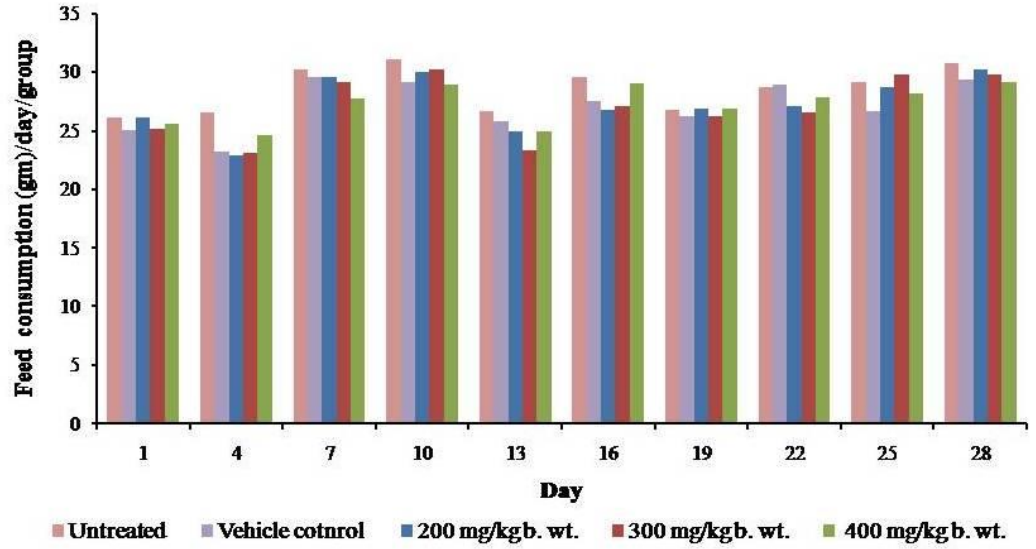

Figure 4.2b. Effect of sub-acute administration of 200, 300 and 400 mg/kg b. wt. of HE on feed consumption (gm/day/group) of female mice: The extract was administered orally to the particular group on a daily basis for twenty-eight days

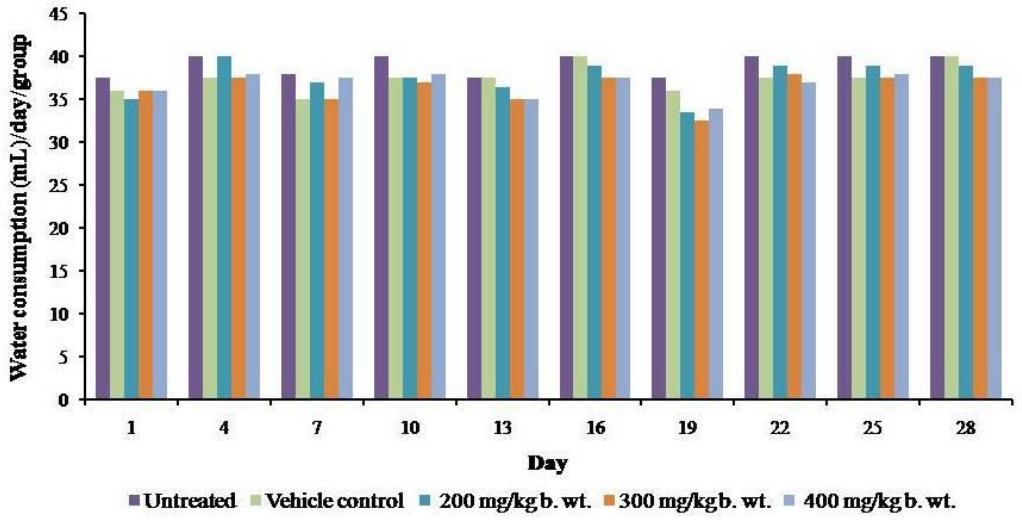

Figure 4.3a. Effect of sub-acute administration of 200, 300 and 400 mg/kg b. wt. of HE on water consumption (mL/day/group) of male mice: The extract was administered orally to the particular group on a daily basis for twenty-eight days

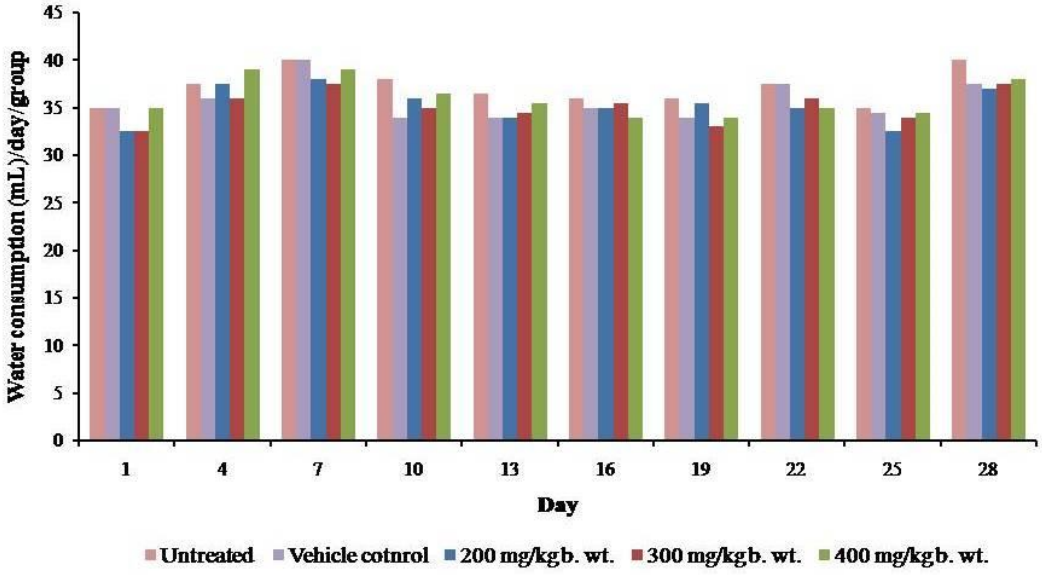

Figure 4.3b. Effect of sub-acute administration of 200, 300 and 400 mg/kg b. wt. of HE on water consumption (mL/day/group) of female mice: The extract was administered orally to the particular group on a daily basis for twenty-eight days

Necropsy analysis of treated animals was found normal and no pathological abnormalities like change in organ colour, lesions, etc. were found in any of the treated animals (Figure 4.4). No significant changes (at $p>0.05$ level) were observed in the organosomatic index of major organs like liver, kidney, spleen, stomach, small intestine, heart, lungs, brain, testes (in the male) and ovaries (in female) of HE administered animals in comparison with untreated mice (Table 4.3 a & b). The haematological parameters were found unaffected in HE administered animals in comparison to untreated animals at $p>0.05$ level during the study period (Table 4.4).

Figure 4.4. Effect of sub-acute administration of HE on the viscera of male (A) and female (B) Swiss albino mice: (Vehicle = 1 % propylene glycol, HE treated = 400 mg/kg b. wt.; highest concentration administered). The propylene glycol and HE were administered orally on a daily basis for 28 days

Table 4.3a. Effect of sub-acute administration of HE on relative organ weight of male and female Swiss albino mice: The extract was administered for 28 days

Group	Liver	Kidneys	Spleen	Stomach	Small intestine
Male					
Untreated	4.74 ± 0.21	1.28 ± 0.15	0.40 ± 0.01	0.98 ± 0.08	4.33 ± 0.62
Vehicle control [a]	4.83 ± 0.28^{ns}	1.41 ± 0.05^{ns}	0.44 ± 0.18^{ns}	1.02 ± 0.04^{ns}	4.51 ± 0.34^{ns}
200 mg/kg b. wt.	4.81 ± 0.35^{ns}	1.33 ± 0.23^{ns}	0.43 ± 0.14^{ns}	0.86 ± 0.04^{ns}	4.24 ± 0.07^{ns}
300 mg/kg b. wt.	4.89 ± 0.21^{ns}	1.41 ± 0.18^{ns}	0.51 ± 0.06^{ns}	0.94 ± 0.35^{ns}	4.19 ± 0.46^{ns}
400 mg/kg b. wt.	4.97 ± 0.34^{ns}	1.31 ± 0.02^{ns}	0.57 ± 0.20^{ns}	1.13 ± 0.20^{ns}	4.06 ± 0.35^{ns}
Female					
Untreated	5.14 ± 0.03	1.13 ± 0.11	0.50 ± 0.08	0.89 ± 0.16	4.65 ± 0.30
Vehicle control [a]	5.19 ± 0.13^{ns}	1.14 ± 0.07^{ns}	0.53 ± 0.02^{ns}	1.03 ± 0.21^{ns}	4.53 ± 0.49^{ns}
200 mg/kg b. wt.	5.17 ± 0.93^{ns}	1.13 ± 0.01^{ns}	0.49 ± 0.17^{ns}	0.87 ± 0.22^{ns}	4.38 ± 0.58^{ns}
300 mg/kg b. wt.	5.15 ± 0.01^{ns}	0.97 ± 0.34^{ns}	0.48 ± 0.02^{ns}	0.95 ± 0.22^{ns}	4.40 ± 0.51^{ns}
400 mg/kg b. wt.	5.13 ± 0.19^{ns}	1.22 ± 0.08^{ns}	0.57 ± 0.02^{ns}	1.04 ± 0.39^{ns}	4.72 ± 0.15^{ns}

[a] Vehicle control (1% propylene glycol)

Values are mean ± standard deviation of 5 animals/sex/group calculated by formula, (organ weight /body weight) x100

^{ns} $p>0.05$ between untreated and treated groups

Table 4.3b. Effect of sub-acute administration of HE on relative organ weight of male and female Swiss albino mice: The extract was administered for 28 days

Group	Heart	Lungs	Brain	Testes
Male				
Untreated	0.50 ± 0.30	0.71 ± 0.08	0.83 ± 0.06	0.58 ± 0.03
Vehicle control [a]	0.53 ± 0.09^{ns}	0.78 ± 0.12^{ns}	0.98 ± 0.14^{ns}	0.61 ± 0.05^{ns}
200 mg/kg b. wt.	0.53 ± 0.10^{ns}	0.70 ± 0.18^{ns}	0.85 ± 0.06^{ns}	0.59 ± 0.09^{ns}
300 mg/kg b. wt.	0.54 ± 0.08^{ns}	0.64 ± 0.07^{ns}	0.87 ± 0.19^{ns}	0.60 ± 0.08^{ns}
400 mg/kg b. wt.	0.56 ± 0.12^{ns}	0.74 ± 0.08^{ns}	0.92 ± 0.20^{ns}	0.60 ± 0.05^{ns}
Female				**Ovaries**
Untreated	0.45 ± 0.03	0.66 ± 0.02	0.84 ± 0.32	0.30 ± 0.06
Vehicle control [a]	0.47 ± 0.02^{ns}	0.64 ± 0.04^{ns}	0.85 ± 0.27^{ns}	0.35 ± 0.05^{ns}
200 mg/kg b. wt.	0.49 ± 0.02^{ns}	0.62 ± 0.01^{ns}	0.89 ± 0.04^{ns}	0.40 ± 0.10^{ns}
300 mg/kg b. wt.	0.50 ± 0.07^{ns}	0.68 ± 0.15^{ns}	0.92 ± 0.22^{ns}	0.33 ± 0.07^{ns}
400 mg/kg b. wt.	0.44 ± 0.01^{ns}	0.69 ± 0.02^{ns}	0.86 ± 0.04^{ns}	0.34 ± 0.08^{ns}

[a] Vehicle control (1% propylene glycol)

Values are mean ± standard deviation of 5 animals/sex/group calculated by formula, (organ weight /body weight) x100

^{ns} $p>0.05$ between untreated and treated groups

Table 4.4. Effect of sub-acute administration of HE on hematological parameters of Swiss albino mice: The extract was administered for 28 days

Group	Hb (gm/dL)	RBC ($x10^6$/cu mm)	Platelet ($x10^5$/cu mm)	WBC (cells/ cu mm)	Neutrophil (%)	Lymphocyte (%)	Eosinophil (%)	PCV (%)
Male								
Untreated	13.2 ± 0.45	9.2 ± 0.36	2.6 ± 0.14	8900 ± 345.09	42.0 ± 3.56	53.0 ± 1.21	5.0 ± 0.43	37.0 ± 1.24
Vehicle control [a]	13.1 ± 0.23[ns]	9.5 ± 0.31 [ns]	2.5 ± 0.29 [ns]	9000 ± 284.21 [ns]	43.0 ± 2.87 [ns]	52.0 ± 1.54 [ns]	5.0 ± 0.32 [ns]	38.0 ± 1.43 [ns]
200 mg/kg b. wt.	13.6 ± 0.64 [ns]	9.5 ± 0.54 [ns]	2.5 ± 0.32 [ns]	9200 ± 265.65 [ns]	43.0 ± 4.30 [ns]	52.0 ±1.31 [ns]	5.0 ± 0.52 [ns]	38.0 ± 1.76 [ns]
300 mg/kg b. wt.	13.2 ± 0.93 [ns]	9.3 ± 1.21 [ns]	2.4 ± 0.25 [ns]	9350 ± 313.26 [ns]	41.0 ± 3.21 [ns]	54.0 ± 0.98 [ns]	5.0 ± 0.31 [ns]	38.0 ± 1.54 [ns]
400 mg/kg b. wt.	14.0 ± 0.34 [ns]	10.2 ± 0.54 [ns]	2.6 ± 0.16 [ns]	9200 ± 360.89 [ns]	43.0 ± 4.85 [ns]	52.0 ± 1.85 [ns]	5.0 ± 0.12 [ns]	39.0 ± 1.23 [ns]
Female								
Untreated	12.9 ± 0.38	8.1 ± 0.87	2.1 ± 0.18	7500 ± 408.43	44.0 ± 1.37	51.0 ± 1.01	5.0 ± 1.41	32.0 ± 1.31
Vehicle control [a]	12.7 ± 0.17 [ns]	8.4 ± 0.57 [ns]	2.2 ± 0.21 [ns]	7900 ± 421.87 [ns]	43.0 ± 1.76 [ns]	52.0 ± 0.97 [ns]	6.0 ± 1.23 [ns]	32.0 ± 1.34 [ns]
200 mg/kg b. wt.	12.8 ± 0.38 [ns]	8.3 ± 0.45 [ns]	2.1 ± 0.33 [ns]	7200 ± 512.21 [ns]	41.0 ± 2.54 [ns]	53.0 ± 1.32 [ns]	6.0 ± 0.78 [ns]	33.0 ± 0.97 [ns]
300 mg/kg b. wt.	13.1 ± 0.35 [ns]	8.9 ± 0.49 [ns]	2.2 ± 0.28 [ns]	7500 ± 671.23 [ns]	42.0 ± 4.24 [ns]	52.0 ± 2.83 [ns]	6.0 ± 1.23 [ns]	33.0 ± 1.75 [ns]
400 mg/kg b. wt.	13.2 ± 0.42 [ns]	9.0 ± 0.65 [ns]	2.3 ± 0.28 [ns]	7900 ± 439.88 [ns]	42.0 ± 1.22 [ns]	53.0 ± 0.97 [ns]	5.0 ± 0.89 [ns]	32.0 ± 1.93 [ns]

[a] Vehicle control (1% propylene glycol)

Values are mean ± standard deviation of 5 animals/sex/group.

Abbreviations: Hb, hemoglobin; RBC, red blood corpuscle; WBC, white blood corpuscle; PCV, packed cell volume

[ns] $p>0.05$ between untreated and treated groups

Liver and renal function parameters did not show any variation than the untreated animals in the HE treated groups of animals (Table 4.5 and Table 4.6). There were no significant (at $p>0.05$ level) changes noted in the levels of serum electrolytes (Table 4.7) in HE treated animals with respect to the untreated group of animals. The lipid profile parameters of the treated groups did not show any significant differences from (at $p>0.05$ level) the untreated group of animals (Table 4.8). The histological examination of the organs such as liver, kidneys, brain, stomach, small intestine, spleen, heart, lungs and reproductive organs (testes in male and ovaries in female) of animals treated with various doses of HE did not show any adverse toxicological effects when compared with untreated group animals (Figure 4.5a and 4.5b).

Table 4.5. Effect of sub-acute administration of HE on liver function parameters of Swiss albino mice: The extract was administered for 28 days

Group	Total bilirubin (mg/dL)	AST (U/L)	ALT (U/L)	ALP (U/L)	Total protein (gm/dL)
Male					
Untreated	0.32 ± 0.05	106.0 ± 22.54	52.0 ± 7.34	67.0 ± 11.24	6.5 ± 0.25
Vehicle control [a]	0.33 ± 0.06^{ns}	107.0 ± 15.34^{ns}	52.0 ± 5.83^{ns}	69.0 ± 16.76^{ns}	6.5 ± 0.32^{ns}
200 mg/kg b. wt.	0.32 ± 0.08^{ns}	108.0 ± 15.83^{ns}	51.0 ± 4.37^{ns}	63.0 ± 15.23^{ns}	6.3 ± 0.41^{ns}
300 mg/kg b. wt.	0.33 ± 0.12^{ns}	122.0 ± 12.93^{ns}	52.0 ± 5.23^{ns}	67.0 ± 19.27^{ns}	6.4 ± 0.32^{ns}
400 mg/kg b. wt.	0.35 ± 0.03^{ns}	130.0 ± 15.84^{ns}	55.0 ± 5.73^{ns}	73.0 ± 17.87^{ns}	6.8 ± 0.05^{ns}
Female					
Untreated	0.31 ± 0.05	120.0 ± 10.23	33.0 ± 2.32	65.0 ± 18.19	5.8 ± 0.28
Vehicle control [a]	0.34 ± 0.07^{ns}	123.0 ± 11.56^{ns}	33.0 ± 3.27^{ns}	68.0 ± 12.43^{ns}	5.9 ± 0.27^{ns}
200 mg/kg b. wt.	0.35 ± 0.01^{ns}	129.0 ± 13.77^{ns}	37.0 ± 3.78^{ns}	68.0 ± 17.87^{ns}	6.1 ± 0.34^{ns}
300 mg/kg b. wt.	0.35 ± 0.04^{ns}	132.0 ± 16.17^{ns}	35.0 ± 6.12^{ns}	67.0 ± 16.29^{ns}	6.1 ± 0.24^{ns}
400 mg/kg b. wt.	0.38 ± 0.08^{ns}	139.0 ± 15.21^{ns}	36.0 ± 8.17^{ns}	70.0 ± 10.28^{ns}	6.0 ± 0.09^{ns}

[a] Vehicle control (1% propylene glycol)

Values are mean ± standard deviation of 5 animals/sex/group

Abbreviations: AST, aspartate aminotransferase; ALT, alanine aminotransferase; ALP, alkaline phosphatase

^{ns} $p>0.05$ between untreated and treated groups

Table 4.6. Effect of sub-acute administration of HE on renal function parameters: The extract was administered for 28 days

Group	Serum Urea (mg/dL)	Serum creatinine (mg/dL)
Male		
Untreated	24.38 ± 2.42	0.40 ± 0.02
Vehicle control [a]	23.13 ± 0.72[ns]	0.42 ± 0.02 [ns]
200 mg/kg b. wt.	24.27 ± 2.16 [ns]	0.38 ± 0.02 [ns]
300 mg/kg b. wt.	23.75 ± 2.95 [ns]	0.38 ± 0.04 [ns]
400 mg/kg b. wt.	23.33 ± 1.81 [ns]	0.41 ± 0.03 [ns]
Female		
Untreated	22.27 ± 0.48	0.42 ± 0.03
Vehicle control [a]	23.42 ± 1.37 [ns]	0.42 ± 0.06 [ns]
200 mg/kg b. wt.	23.43 ± 0.33 [ns]	0.42 ± 0.07 [ns]
300 mg/kg b. wt.	22.37 ± 1.45 [ns]	0.41 ± 0.09 [ns]
400 mg/kg b. wt.	23.42 ± 1.40 [ns]	0.43 ± 0.08 [ns]

[a] Vehicle control (1% propylene glycol)
Values are mean ± standard deviation of 5 animals/sex/group
[ns] $p>0.05$ between untreated and treated groups

Table 4.7. Effect of sub-acute administration of HE on serum electrolytes of Swiss albino mice: The extract was administered for 28 days

Group	Bicarbonate (mmol/L)	Sodium (mmol/L)	Potassium (mmol/L)	Chloride (mmol/L)
Male				
Untreated	22.47 ± 0.81	143.67 ± 1.53	5.27 ± 0.25	105.67 ± 2.08
Vehicle control [a]	23.07 ± 0.61 [ns]	143.00 ± 4.04 [ns]	5.53 ± 0.25 [ns]	106.67 ± 1.53 [ns]
200 mg/kg b. wt.	23.38 ± 0.58 [ns]	145.40 ± 3.08 [ns]	5.47 ± 0.21 [ns]	106.00 ± 1.00 [ns]
300 mg/kg b. wt.	23.33 ± 1.53 [ns]	146.43 ± 3.50 [ns]	5.50 ± 0.06 [ns]	107.45 ± 0.58 [ns]
400 mg/kg b. wt.	23.66 ± 1.73 [ns]	142.60 ± 1.22 [ns]	5.43 ± 0.15 [ns]	107.33 ± 0.58 [ns]
Female				
Untreated	21.33 ± 0.76	140.37 ± 2.03	5.14 ± 0.36	102.00 ± 2.00
Vehicle control [a]	21.47 ± 0.57 [ns]	142.17 ± 2.94 [ns]	5.16 ± 0.06 [ns]	103.33 ± 1.53 [ns]
200 mg/kg b. wt.	20.33 ± 1.15 [ns]	142.33 ± 2.52 [ns]	5.13 ± 0.87 [ns]	103.33 ± 0.58 [ns]
300 mg/kg b. wt.	21.11 ± 1.54 [ns]	141.80 ± 1.71 [ns]	5.27 ± 0.32 [ns]	103.00 ± 1.00 [ns]
400 mg/kg b. wt.	21.00 ± 1.00 [ns]	142.67 ± 2.08 [ns]	5.24 ± 0.14 [ns]	103.67 ± 1.53 [ns]

[a] Vehicle control (1% propylene glycol)

Values are mean ± standard deviation of 5 animals/sex/group

[ns] $p>0.05$ between untreated and treated groups

Table 4.8. Effect of sub-acute administration of HE on lipid profile of Swiss albino mice: The extract was administered for 28 days

Group	Cholesterol (mg/dL)	Triglycerides (mg/dL)	HDL (mg/dL)	LDL (mg/dL)	VLDL (mg/dL)
Male					
Untreated	56.25 ± 2.77	117.50 ± 1.80	27.25 ±1.48	15.75 ± 2.49	13.25 ± 1.30
Vehicle control [a]	56.00 ± 3.00 [ns]	117.60 ± 1.12 [ns]	28.50 ± 1.80 [ns]	14.50 ± 1.50 [ns]	13.00 ± 0.71 [ns]
200 mg/kg b. wt.	57.75 ± 1.48 [ns]	118.50 ± 2.60 [ns]	27.50 ± 1.12 [ns]	16.75 ± 1.64 [ns]	12.50 ± 0.50 [ns]
300 mg/kg b. wt.	59.25 ± 2.95 [ns]	118.50 ± 2.50 [ns]	29.75 ± 1.48 [ns]	17.00 ± 1.00 [ns]	12.50 ± 1.12 [ns]
400 mg/kg b. wt.	58.50 ± 1.66 [ns]	118.90 ± 2.95 [ns]	29.50 ± 2.60 [ns]	16.75 ± 1.30 [ns]	12.25 ± 1.09 [ns]
Female					
Untreated	51.50 ± 1.12	114.25 ± 2.54	27.25 ± 1.30	14.25 ± 1.48	10.00 ± 0.00
Vehicle control [a]	51.00 ± 1.58 [ns]	114.25 ± 3.96 [ns]	26.75 ± 0.43 [ns]	14.00 ± 1.58 [ns]	10.25 ± 0.43 [ns]
200 mg/kg b. wt.	52.00 ± 2.55 [ns]	114.45 ± 2.59 [ns]	27.50 ± 1.50 [ns]	14.00 ± 1.22 [ns]	10.50 ± 0.50 [ns]
300 mg/kg b. wt.	51.75 ± 2.28 [ns]	115.25 ± 5.00 [ns]	26.75 ± 1.09 [ns]	14.50 ± 1.66 [ns]	10.50 ± 0.50 [ns]
400 mg/kg b. wt.	52.00 ± 1.58 [ns]	115.65 ± 5.30 [ns]	27.25 ± 1.09 [ns]	14.00 ± 0.71 [ns]	10.75 ± 0.83 [ns]

[a] Vehicle control (1% propylene glycol)

Values are mean ± standard deviation of 5 animals/sex/group.

Abbreviations: HDL, high-density lipoprotein; LDL, low-density lipoprotein; VLDL, very-low-density lipoprotein

[ns] $p>0.05$ between untreated and treated groups

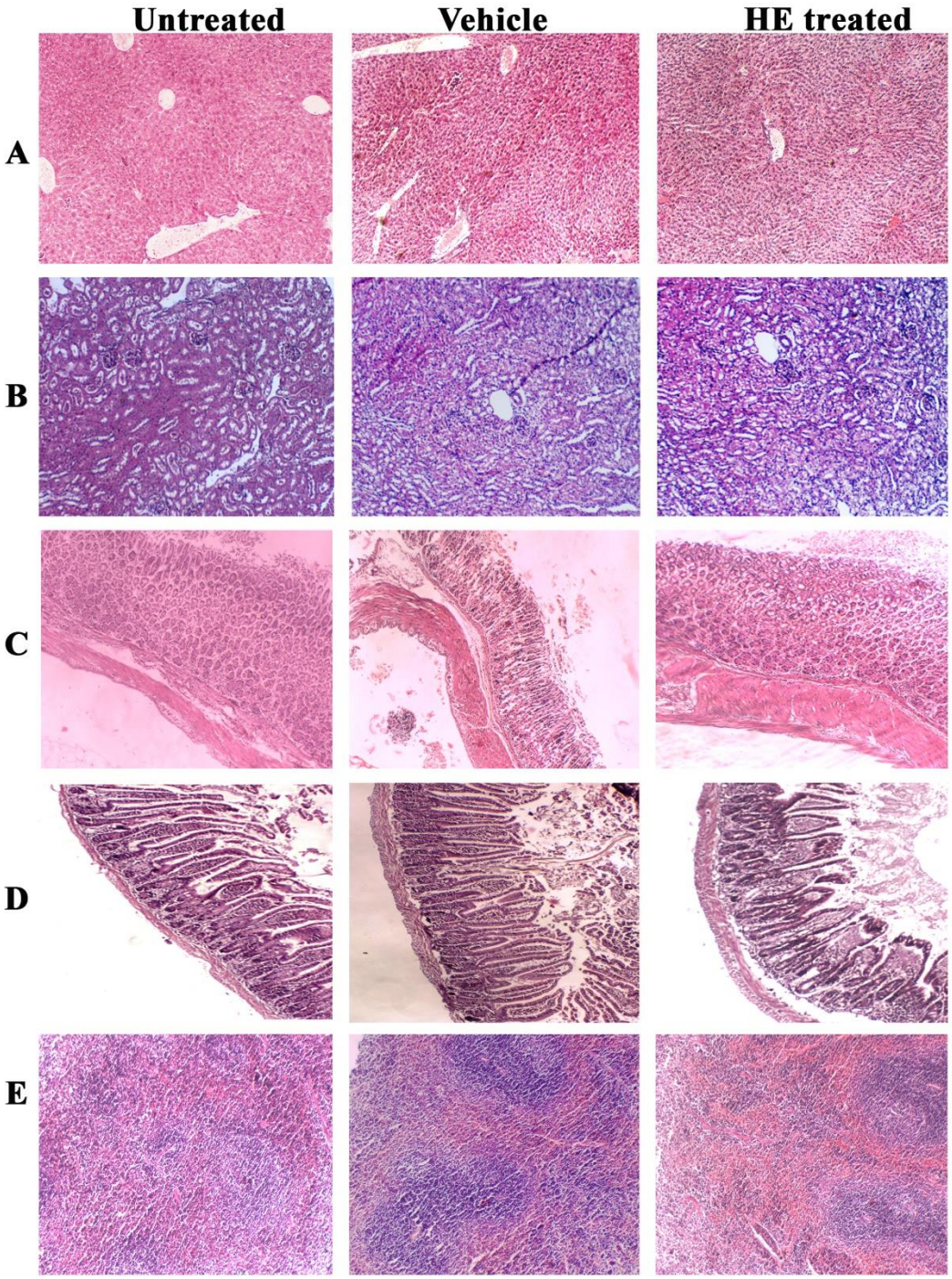

Figure 4.5a. Histological analysis of different organs of female Swiss albino mice received orally HE (400 mg/kg b. wt.) of *S. glauca:* The animals received test material (untreated: 200 μL saline, vehicle: 200 μL 1% propylene glycol and HE treated: 200 μL HE (400 mg/kg b. wt)) orally for 28 consecutive days. The animals were then sacrificed after overnight fasting and various organs such as (A) Liver, (B) Kidney, (C) Stomach, (D) Small intestine, and (E) Spleen were subjected histological evaluation under haematoxylin and eosin staining. The images (200X) were taken under an inverted microscope

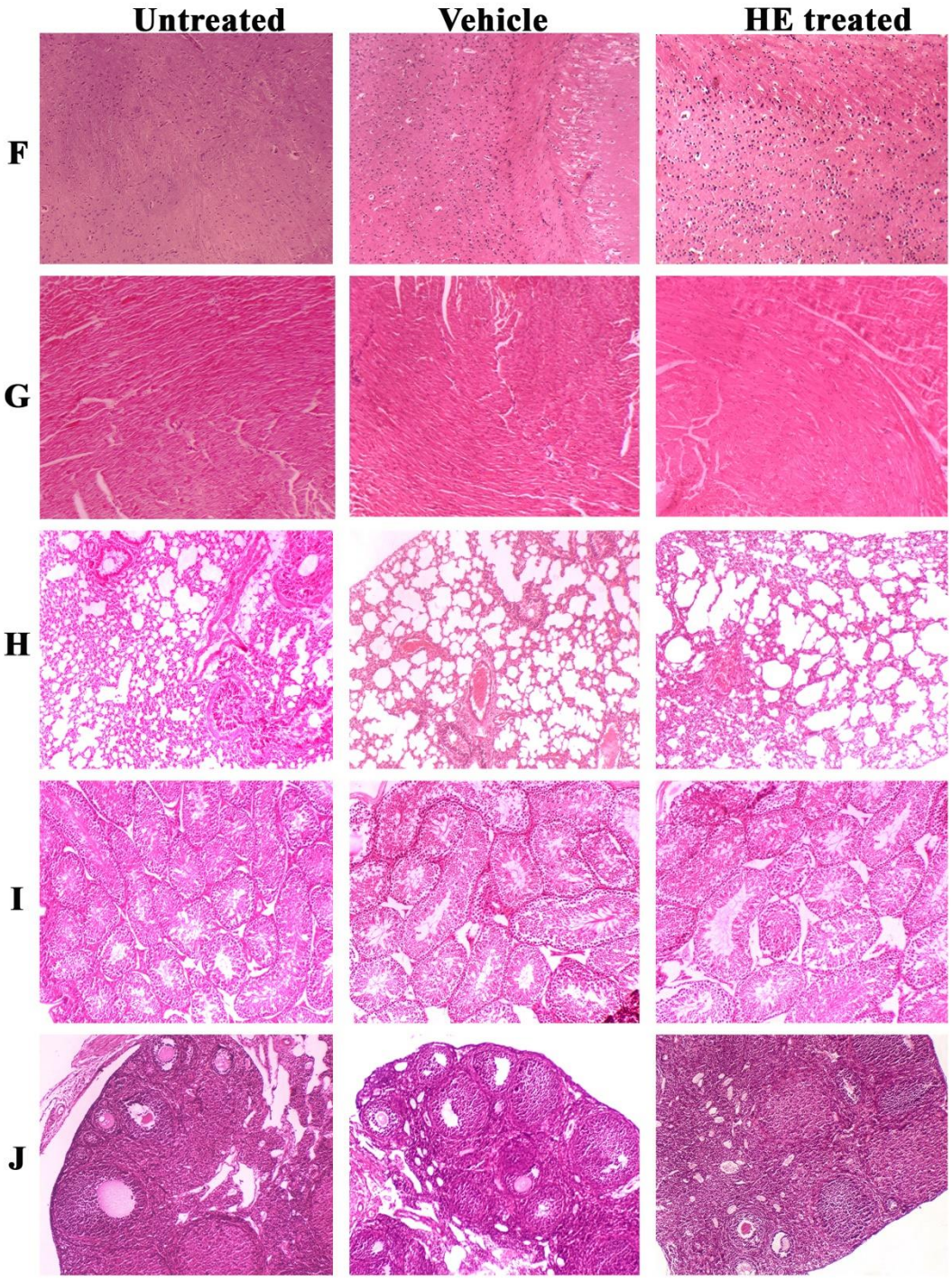

Figure 4.5b. Histological analysis of different organs of female Swiss albino mice received HE (400 mg/kg. b. wt.) of *S. glauca:* The animals received test material (untreated: 200 μL saline, vehicle: 200 μL 1% propylene glycol and HE treated: 200 μL HE (400 mg/kg b. wt)) orally for 28 consecutive days. The animals were then sacrificed after overnight fasting and various organs such as (F) Brain, (G) Heart, (H) Lungs, (I) Testes (male) and (J) Ovary were subjected histological evaluation under haematoxylin and eosin staining. The images (200X) were taken under an inverted microscope

4.4. Discussion

Although a large number of people use hot water extract of leaves of *S. glauca* as health tonic or medicine for different diseases including cancer, only scanty evaluation reports on the toxicity of this plant are available. In the present study, we used the hot water extract of *S. glauca* leaves, which is similar to the preparation that the people of the southern part of India, especially in Kerala, recently started to, consume as a part of adjuvant therapy for cancer treatment.

Phytotoxicity and cytotoxicity of *S. glauca* are mainly related to a group of bitter toxic compounds called quassinoids. A dichloromethane extract of the bark of *S. glauca* was found to be toxic to brine shrimp (Rivero-Cruz et al., 2005). Vaughan (1970) has reported toxicity in *Simarouba* meal. According to Severn (1953) and Rath et al., (1987), it is the bitter principle related to quassine in the residual cake of Simarouba, which is found to be toxic to livestock. Govindaraju et al., (2009) have reported that even if the de-oiled meal of *S. glauca* is a rich source of nutrients, it requires detoxification of compounds like saponin, alkaloid, phenolics and phytic acid before using it as a feed or food constituent. Another study conducted by Solis et al., (1993), the toxic nature of quassinoids varies from nontoxicity to high toxicity in the analysis conducted by using brine shrimp. Though the quassinoids have a polar affinity (Rout et al., 2014), HE of *S. glauca* requires a thorough formal toxicological evaluation for its safety.

The primary intention of conducting acute toxicity test was the determination of the effect of a single dose of HE of *S. glauca* on Swiss albino mice. Swiss albino mice were used in the study because animals belong to order Rodentia are generally used as test animals in this type of study (Parasuraman, 2011). Mice of both sexes were used to study the sex-based differentiation in response to the treatment. As a routine practice in acute toxicity test, the investigational substance was administered at various dosage levels and the consequence was observed for 14 consecutive days. No changes were found in body weight, behavior, food, and water consumption rate of the treated group animals. A change in body weight of treated animals with respect to untreated animals is considered as a sign of adverse effects of an investigational substance (Teo et al., 2002). Since no significant changes were observed in general behavior and body weight in the treated groups as compared to the untreated group of

animals, it is suggested that the acute doses of HE of *S. glauca* administered up to 2000 mg/kg b. wt. is safe on the normal metabolism in these animals.

Further, acute toxicity evaluation allowed the determination of 50% lethal dose (LD_{50}) of HE of *S. glauca* in Swiss albino mice, which is very essential for future studies. Since no ill effects and mortality were reported from animals treated with HE *S. glauca* at various doses up to 2000 mg/kg b. wt., it can be assumed that the 50% lethal dose (LD_{50}) of HE of *S. glauca* for Swiss albino mice is >2000 mg/kg b. wt.

Similar to acute toxicity study, no morbidities and mortalities were noted by the investigational substance (HE) in both sexes of Swiss albino mice at various levels of concentrations. Symptoms related to toxicity like tremor, locomotor difficulties, weight loss and hypo-activity (Bourhia et al., 2019) was not shown by any animals of the treated groups.

Analysis of blood parameters is very much applicable for risk assessment, as any changes in the hematological and biochemical systems have a higher predictive value for human toxicity when data are translated from animal studies (Olson et al., 2000). According to Mukinda and Syce (2007), the hematopoietic system is one of the most responsive targets for lethal compounds and an indispensable indicator of physiological and pathological conditions in man and animal. In the 28 days sub-acute toxicity study, HE, up to 400 mg/kg b. wt. did not make any change in the hematological parameters in comparison to an untreated group of animals. Biochemical parameters analyzed remained within the reference range for the species (Serfilippi et al., 2003) indicating that HE has no harmful effects on the haematopoietic system.

The lack of significant effects on liver function parameters like total bilirubin, AST, ALT, ALP and total protein, after 28 days administration of HE in animals of all treated groups with respect to the untreated group of animals showed that liver function was normal. The activity of AST, ALT, and ALP of 200 mg/kg b. wt/day treated mice; equal to the human dose were found very close to the levels of untreated groups. According to Rahman et al., (2001), the AST and ALT are popular enzymes used as biomarkers, which can predict possible liver injury. Usually, if any toxicity challenges occur in the body, the levels of these enzymes may be elevated due to the

damage of parenchymal cells of the liver (Wolf et al., 1972, Wang et al., 2014). Considering the levels of AST, ALT and ALP noted in this study, ushers the nontoxic nature of HE of *S. glauca* in mice.

Any changes in the level of major lipids like total cholesterol, high-density lipoprotein cholesterol, low-density lipoprotein cholesterol and very high-density lipoprotein cholesterol can give a clear view on lipid metabolism and its predisposition of heart to arteriosclerosis and atherosclerosis. Elevated levels of all lipids except the high-density lipoprotein are associated with an increased risk of atherosclerosis. High levels of triglycerides and low-density lipoproteins are associated with coronary artery diseases. In the present study, the lipid profile of animals was also not affected by the ingestion of HE for 28 days, indicating that the extract did not affect the lipid metabolism of animals.

Serum urea and creatinine are known indicators of renal function. The abnormal increase or decrease in the level of urea and creatinine in blood suggests obvious damage to kidneys (Rahman et al., 2001). An abnormal increase in urea concentration in serum indicates acute kidney failure (Rosner and Bolton, 2006). In this study, the creatinine and urea levels were found within the normal range after the sub-acute administration of HE attesting that the administration of different doses of HE not related to any toxicity.

In addition, the levels of serum electrolytes like bicarbonate, chloride, potassium and sodium were found unchanged by the oral administration of HE regardless of the dose given. Electrolytes help the inward movement of nutrients and out ward movements of wastes in body cells. They sustain a healthy water balance and support the body to maintain a stabilized pH level.

Sub-acute oral administration of HE did not adversely affect the morphology of mice's internal organs confirming the hematological and biochemical parameters results and that this extract, in doses up to 400 mg/kg b. wt/ day was well tolerated by the mice. In this study, the relative organ weight in female and male mice was not affected by the administration of HE. An increase in relative organ weight is an indication of inflammation while a decrease in the same can be attributed to cellular constriction (Moore and Dalley, 1999).

The histological analysis of major organs of HE treated animal did not reveal any significant changes in the tissue architecture of the organs studied. The current study indicates that HE did not cause any inflammation or cell constriction to the organs of treated mice. Both the macroscopic and microscopic evaluations of the various organs of HE-treated mice also indicated the plant extract to be safe.

In conclusion acute toxic administration of HE at a dose of 2000 mg/kg. b. wt. and sub-acute oral administration of HE up to 400 mg/kg b. wt. is found to be non-toxic and safe to mice. If the finding of this study extrapolates to humans, the regular consumption of hot water extract of leaves of *S. glauca* can be considered comparatively safe. The study results also provide a positive nod to the use of HE of *S. glauca* for conducting animal experiments to evaluate its medicinal efficacy.

Chapter 5

Evaluation of antitumour efficacy of *Simarouba glauca* DC

Contents

5.1. Introduction

5.2. Materials and methods

5.2.1. Collection of plant

5.2.2. Animals

5.2.3. Preparation of hot water extract of *S. glauca*

5.2.4. Antitumour studies

5.2.4.1. Determination of the antitumour effect of HE on the ascites tumour model

5.2.4.1.1. Simultaneous administration of HE with the inoculation of ascites tumour

5.2.4.1.2. Pre and simultaneous administration of HE with the inoculation of ascites tumour

5.2.4.1.3. Administration of HE to the ascites tumour bearing mice

5.2.4.1.4. Simultaneous administration of HE in combination with cyclophosphamide with the inoculation of ascites tumour

5.2.4.2. Determination of the antitumour effect of HE on the solid tumour model

5.2.4.2.1. Simultaneous administration of HE with the inoculation of solid tumour

5.2.4.2.2. Pre and simultaneous administration of HE with the inoculation of solid tumour

5.2.4.2.3. Administration of HE to the solid tumour bearing mice

5.2.4.2.4. Simultaneous administration of HE in combination with cyclophosphamide with the inoculation of solid tumour

5.2.5. Histological analysis

5.2.6. Statistical analysis

5.3. Results

5.3.1. Effect of HE on the ascites tumour model

5.3.1.1. Simultaneous administration of HE in ascites tumour development

5.3.1.2. Pre and simultaneous administration of HE in ascites tumour development

5.3.1.3. Administration of HE to the ascites tumour bearing mice

5.3.1.4. Simultaneous administration of HE in combination with cyclophosphamide in ascites tumour development

5.3.2. Effect of HE on the solid tumour model

5.3.2.1. Simultaneous administration of HE in solid tumour development

5.3.2.2. Pre and simultaneous administration of HE in the solid tumour development

5.3.2.3. Administration of HE to the solid tumour bearing mice

5.3.2.4. Simultaneous administration of HE in combination with cyclophosphamide in solid tumour development

5.4. Discussion

5.1. Introduction

Preliminary phytochemical analysis of the HE of *Simarouba glauca* conducted in the present study revealed several groups of pharmacologically potential compounds like alkaloids, flavonoids, carbohydrates, phenolics, tannins, terpenes, saponins, and coumarins. Presence of flavonoids, terpenoids, alkaloids, and phenolics has been confirmed by TLC profiling. UPLC-Q-TOF-MS analysis of HE revealed as many as 93 constituents in which 79 compounds are identified and out of this 9 compounds have detected with significant pharmacological roles. Chlorogenic acid, loganin, acetylsalicylic acid, irigenin, dihydrorobinetin, gitoxin, oleandrin, procaterol, cucurbitacin B are the molecules detected in HE with established pharmacological properties like antioxidant, anti-inflammatory, cytotoxicity, antitumour and anticancer effects.

Because *S. glauca* is a widely publicised plant with anticancer potential and no scientific basis has been attributed to its potential, it is essential that parallel to *in vitro* methods, *in vivo* studies, have to be carried out. *In vivo* mouse models are widely employed in cancer drug development. Even if these models do not create reliable complications of human tumours, the main benefit is that it offers an immuno-competent background for the tumour growth as in real life. The National Cancer Institute (NCI) of United States, stands first in the list of agencies which included the preclinical cancer models for the adoption of potential cancer therapeutics (Voskoglou-Nomikos et al., 2003).

Murine lymphoma models are comparatively inexpensive and easy to conduct. Because of its reliability, DLA and EAC lymphoma models are widely used in cancer studies for evaluating the efficacy of new drugs (Koiri et al., 2017). These models require a short duration of time to study the effectiveness of drugs. DLA and EAC lymphoma is a kind of transplantable T-cell lymphoma with spontaneous origin in the primary endocrine organ thymus of murine animals. They are also capable of developing ascites and solid tumours. DLA model is highly effective in concern with its genetic constancy and heterogeneity of the transplanted cell line. Lymphoma cells such as DLA and EAC are quickly growing cancer cells with aggressive behaviour (Segura et al., 2000). The inoculation of DLA and EAC cells induces an inflammatory reaction. The sustained inflammatory responses increase vascular permeability, which finally results in ascetic fluid accumulation (Fecchio et al., 1990).

Since the HE extract possesses various significant biomolecules, it is necessary to carry out *in vivo* studies to establish its antitumour efficacy. The primary objective of

conducting *in vivo* antitumour studies is a collection of preliminary data to select substances with anticancer activity for further advanced studies.

5.2. Materials and methods

5.2.1. Collection of plant

Leaves of *S. glauca* were collected from the herbal medicine garden located at the campus of Amala Ayurvedic Hospital, Thrissur and authenticated (Chapter 2, section 2.1.1.2).

5.2.2. Animals

Male Swiss albino mice (25-27 gm) were purchased and maintained as described in Chapter 2, section 2.1.6.

5.2.3. Preparation of hot water extract of *S. glauca*

The detailed procedure regarding the preparation of hot water extract (HE) of *S. glauca* is described in Chapter 2, section 2.2.1.

5.2.4. Antitumour studies

Antitumour effects of HE of *S. glauca* were conducted in both ascites and solid tumour bearing mice. Ehrlich's Ascites cells (EAC) and Dalton's Lymphoma Ascites (DLA) cells were used respectively for inoculating ascites and solid tumour in mice. The methods regarding the maintenance and preparation of stock of cell for inoculation are explained in Chapter 2, section 2.1.7.

5.2.4.1. Determination of the antitumour effect of HE on the ascites tumour model

The detailed protocol regarding the analysis of antitumour efficacy of HE on ascites bearing tumour is given in Chapter 2, section 2.2.11.1.

5.2.4.1.1. Simultaneous administration of HE with the inoculation of ascites tumour

This study is designed to evaluate the effect of HE administered orally for ten consecutive days, 24 hours after the inoculation of tumour cells into the peritoneal cavity of mice. The detailed procedure is explained in Chapter 2, section 2.2.11.1.1.

5.2.4.1.2. Pre and simultaneous administration of HE with the inoculation of ascites tumour

Chapter 2, section 2.2.11.1.2 describes the detailed procedure regarding the administration of HE. In this study, HE is administered orally for 5 successive days before the inoculation of ascites tumour (pre-treatment) and for 10 consecutive days, after tumour inoculation.

5.2.4.1.3. Administration of HE to the ascites tumour bearing mice

In this study, the various concentrations of HE were administered orally for ten consecutive days to the ascites tumour bearing mice from 11^{th} day of tumour inoculation i.e., after the development of tumour into a noticeable size. The detailed methodology is stated in Chapter 2, section 2.2.11.1.3.

5.2.4.1.4. Simultaneous administration of HE in combination with cyclophosphamide with the inoculation of ascites tumour

In this experiment, a combination of HE (160 mg/kg b. wt) and cyclophosphamide (standard drug) was administered orally for ten days after 24 hours of the inoculation of tumour cells. An interval of six hours was maintained between the administration of LDHE and cyclophosphamide in each group. The protocol of this experiment is explained in Chapter 2, section 2.2.11.1.4.

5.2.4.2. Determination of the antitumour effect of HE on the solid tumour model

The detailed protocol regarding the analysis of antitumour efficacy of HE (administered orally) on solid tumour bearing mice narrated in Chapter 2, section 2.2.11.2. Haematological parameter like total Hb (2.2.5.2.1.1), total leucocyte count (2.2.5.2.1.3) and differential leucocyte count (2.2.5.2.1.4) of the experiment animals were determined according to the protocol mentioned in the bracket.

5.2.4.2.1. Simultaneous administration of HE with the inoculation of solid tumour

Chapter 2, section 2.2.11.2.1 provides a detailed sketch regarding the administration of HE along with inoculation of solid tumour in male Swiss albino mice.

5.2.4.2.2. Pre and simultaneous administration of HE with the inoculation of solid tumour

In this experiment system, the animals were pre-treated with various concentration of HE for five days before the inoculation of solid tumour in their right hind limb. Then they had administered the same concentration of HE for ten more days (refer Chapter 2, section 2.2.11.2.2).

5.2.4.2.3. Administration of HE to the solid tumour bearing mice

In this experiment regime, animals were administered with different drug doses only for ten days after the inoculation of solid tumour. Chapter 2, section 2.2.11.2.3 discloses the details of the experimental procedure.

5.2.4.2.4. Simultaneous administration of HE in combination with cyclophosphamide with the inoculation of solid tumour

In this experiment, various combinations of cyclophosphamide (15, 10 and 5 mg/kg b. wt.) with HE (160 mg/kg b. wt) were administered orally for ten days to mice after 24 hours of tumour inoculation. A period of 6 hours was maintained between the administration of LDHE and cyclophosphamide (Chapter 2, section 2.2.11.2.4).

5.2.5. Histological analysis

The solid tumor developed was excised out and a small portion from each group was taken and fixed in 10% neutral buffered formalin solution. Microtome sections with a thickness of 5 μm were taken, deparaffinised, hydrated and stained using haematoxylin and eosin. The proliferation of cancer cells was observed under (20 X) objective of Magnus inverted laboratory microscope lens and photographs were taken. The histological examination was conducted out by a veterinary pathologist who was blind to the study.

5.2.6. Statistical analysis

The data expressed as mean ± SD of six animals per group. The mean values were statistically analyzed by Graph Pad Instat 3 software (Chapter 2, section 2.2.14.)

5.3. Results

5.3.1. Effect of HE on the ascites tumour model

5.3.1.1. Simultaneous administration of HE in ascites tumour development

The antitumour effect of different doses of HE, 1% propylene glycol (vehicle in which HE dissolved) and CTX (standard drug) was evaluated among EAC inoculated ascites tumour bearing mice. The study groups were compared with the untreated (control) group of ascites bearing mice. In the control group and vehicle group first mortality due to tumour burden was noted on 15th day after tumour inoculation but, in HE treated group the first death was noted on 19th day. In the standard drug-treated group, the first mortality was reported on 24th day after tumour inoculation. The whole number of animals died on day 18th and 19th in control and vehicle control groups. In the LDHE, the last animal died on 21st day but it was on 22nd in HDHE treated group. But in the standard group, the animals were alive for more days and the last animal died on day 28 after tumour inoculation. The per cent survival of animals in different groups during the experiment was plotted and given below (Figure 5.1.)

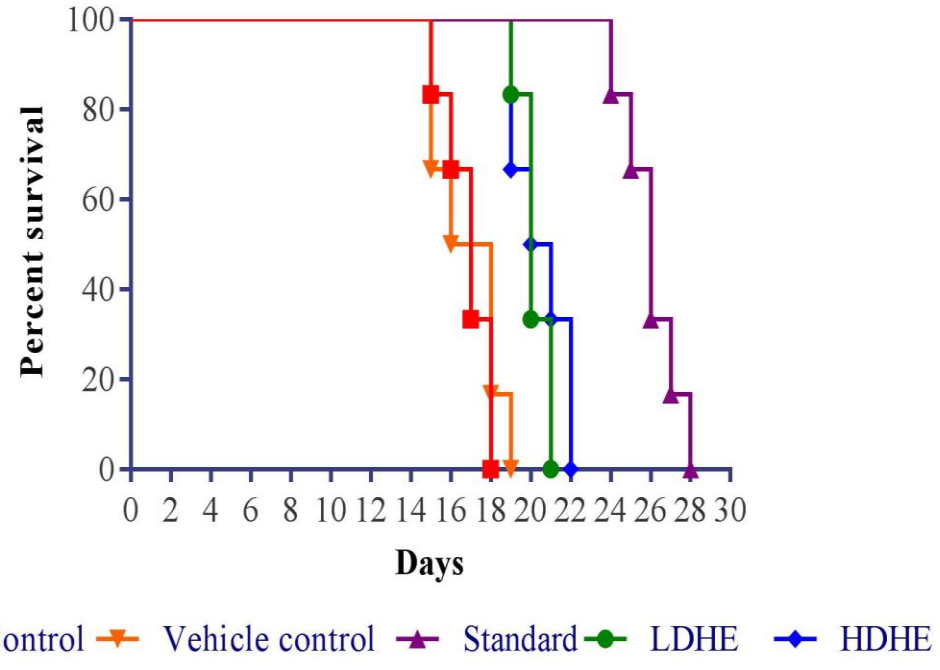

Figure 5.1. Percent survival of mice administered with HE along with the inoculation of ascites tumour: Ascites tumour was inoculated by injecting EAC cells (1x10^{6}cells/animal) in the peritoneal cavity of Swiss albino mice. The animals, except control, were received test material orally (vehicle control; 200 μL 1% propylene glycol, standard; cyclophosphamide (15 mg/kg b. wt), LDHE; 160 mg/kg b. wt, and HDHE; 260 mg/kg b. wt) for ten consecutive days one day after tumour inoculation

Table 5.1. Effect of HE on the mean survival days and percentage increase in the life span of Swiss albino mice along with the inoculation of ascites tumour: Ascites tumour was inoculated by injecting EAC cells ($1x10^6$cells/animal) in the peritoneal cavity of Swiss albino mice. The animals, except control, were received test material orally (vehicle control; 200 μL 1% propylene glycol, standard; cyclophosphamide (15 mg/kg b. wt), LDHE; 160 mg/kg b. wt, and HDHE; 260 mg/kg b. wt) for ten consecutive days one day after tumour inoculation

Group	Mean survival days	% increase in the life span
Control	16.80 ± 1.17	-
Vehicle control (1% propylene glycol)	16.83 ± 1.72^{ns}	0
Standard (CTX: 15 mg/kg b. wt)	26.00 ± 1.41**	54.68
LDHE (160 mg/kg b. wt)	20.17 ± 0.75**	19.80
HDHE (260 mg/kg b. wt)	20.50 ± 1.38**	21.78

Values are mean ± standard deviation of six animals per group
^{ns} $p>0.05$, ** $P < 0.01$ when compared to control

5.3.1.2. Pre and simultaneous administration of HE in the ascites tumour development

Administration of different doses of HE five days before and ten days after the inoculation of the tumour were increased the mean survival time and percentage increase in life span with respect to the vehicle control group (Figure 5.2 & Table 5.2).

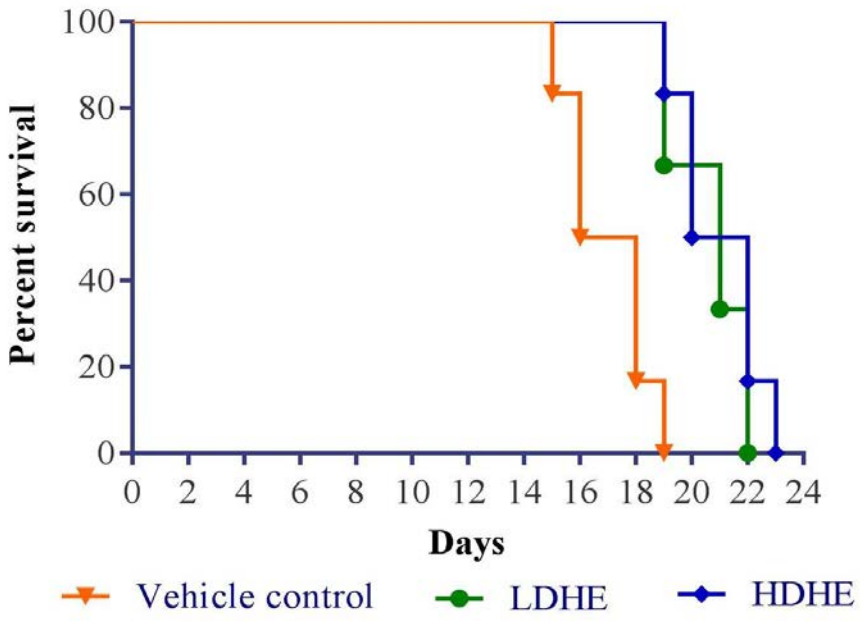

Figure 5.2. Percent survival of mice administered with HE before and after the inoculation of ascites tumour: Ascites tumour was inoculated by injecting EAC cells (1x10^{6}cells/animal) in the peritoneal cavity of Swiss albino mice. The animals were received test material orally (vehicle control; 200 μL 1% propylene glycol, LDHE; 160 mg/kg b. wt, and HDHE; 260 mg/kg b. wt) five successive days before and ten consecutive days after tumour inoculation

Table 5.2. Effect of HE on the mean survival days and percentage increase in the life span of Swiss albino mice before and after the inoculation of ascites tumour: Ascites tumour was inoculated by injecting EAC cells (1x10^{6}cells/animal) in the peritoneal cavity of Swiss albino mice. The animals were received test material orally (vehicle control; 200 μL 1% propylene glycol, LDHE; 160 mg/kg b. wt, and HDHE; 260 mg/kg b. wt) five successive days before and ten consecutive days after tumour inoculation

Group	Mean survival days	% increase in the life span
Vehicle control (1% propylene glycol)	17.00 ± 1.55	-
LDHE (160 mg/kg b. wt)	20.67 ± 1.37**	21.53
HDHE (260 mg/kg b. wt)	22.00 ± 1.55**	23.53

Values are mean ± standard deviation of six animals per group
** P < 0.01, when compared to vehicle control

5.3.1.3. Administration of HE to the ascites tumour bearing mice

Analysis of results obtained after the administration of different doses of HE, ten days after the inoculation of ascites tumour is depicted below (Figure 5.3 and Table 5.3).

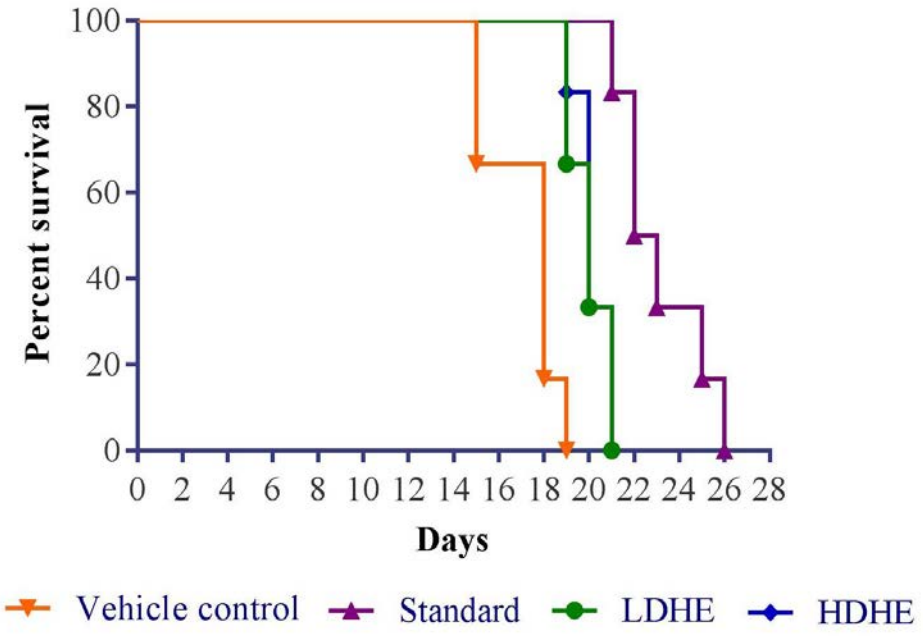

Figure 5.3. Percent survival of mice administered with HE ten days after the inoculation of ascites tumour: Ascites tumour was inoculated by injecting EAC cells ($1x10^6$cells/animal) in the peritoneal cavity of Swiss albino mice: The animals were received test material orally (vehicle control; 200 μL 1% propylene glycol, standard; cyclophosphamide (15 mg/kg b. wt), LDHE; 160 mg/kg b. wt, and HDHE; 260 mg/kg b. wt) for ten consecutive days after ten days of tumour inoculation

Table 5.3. Effect of HE on the mean survival days and percentage increase in the life span of Swiss albino mice ten days after the inoculation of ascites tumour: Ascites tumour was inoculated by injecting EAC cells ($1x10^6$cells/animal) in the peritoneal cavity of Swiss albino mice. The animals were received test material orally (vehicle control; 200 μL 1% propylene glycol, standard; cyclophosphamide (15 mg/kg b. wt), LDHE; 160 mg/kg b. wt, and HDHE; 260 mg/kg b. wt) for ten consecutive days after ten days of tumour inoculation

Group	Mean survival days	% increase in the life span
Vehicle control (1% propylene glycol)	17.20 ± 1.72	-
Standard (CTX: 15 mg/kg b. wt)	23.17 ± 1.94**	34.95
LDHE (160 mg/kg b. wt)	20.00 ± 0.89**	16.50
HDHE (260 mg/kg b. wt)	20.17 ± 0.75**	17.48

Values are mean ± standard deviation of six animals per group
** $P < 0.01$, when compared to vehicle control

5.3.1.4. Simultaneous administration of HE in combination with cyclophosphamide in ascites tumour development

The effectiveness of combinations of HE along with CTX was conducted. The per cent survival rate and mean survival time were found increasing. Animals in the treated groups were survived more than 50 days but, the mice treated with a combination of CTX (15 mg/kg b. wt) and drug vehicle found died within 28 days (Figure 5.4 & Table 5.4).

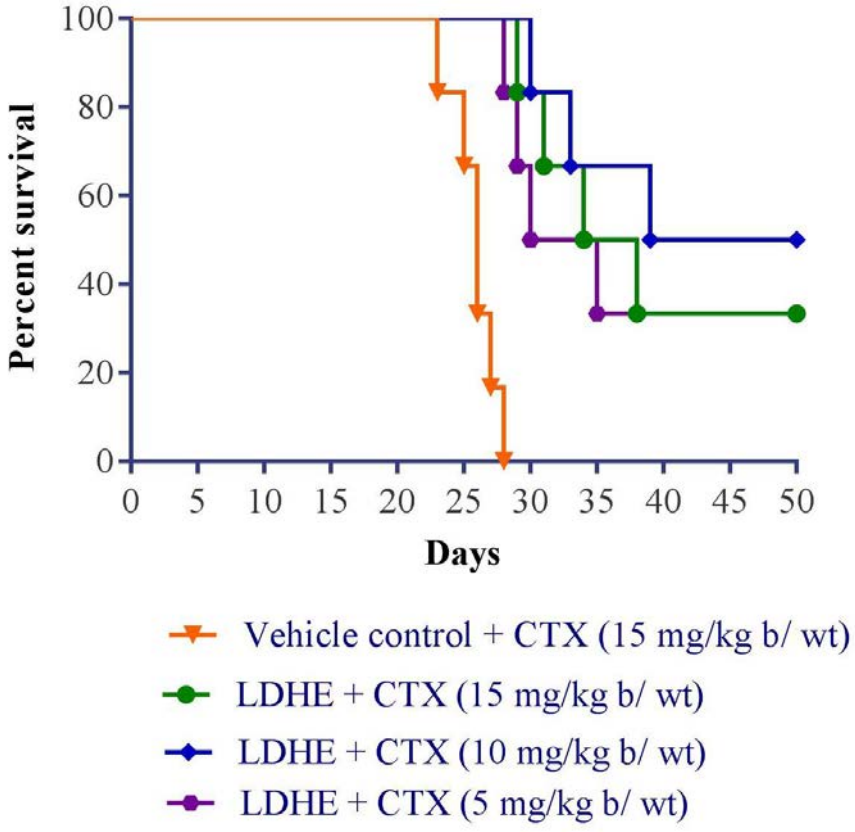

Figure 5.4. Percent survival of mice administered with HE in a combination of cyclophosphamide, one day after the inoculation of ascites tumour: Ascites tumour was inoculated by injecting EAC cells ($1x10^6$cells/animal) in the peritoneal cavity of Swiss albino mice. The animals were received test material orally for ten consecutive days one day after tumour inoculation

Table 5.4. Mean survival days of mice administered with HE in a combination of cyclophosphamide, one day after the inoculation of ascites tumour: Ascites tumour was inoculated by injecting EAC cells ($1x10^6$cells/animal) in the peritoneal cavity of Swiss albino mice. The animals were received test material orally for ten consecutive days one day after tumour inoculation

Group	Mean survival days
Vehicle control + CTX (15 mg/kg b. wt)	25.83 ± 1.72
LDHE + CTX (15 mg/kg b. wt)	2 survived after 50 days
LDHE + CTX (10 mg/kg b. wt)	3 survived after 50 days
LDHE + CTX (5 mg/kg b. wt)	2 survived after 50 days

Vehicle control (1% propylene glycol), LDHE (160 mg/kg b. wt)
Values are mean ± standard deviation of six animals per group

5.3.2. Effect of HE on the solid tumour model

5.3.2.1. Simultaneous administration of HE in solid tumour development

Oral administrations of sub-lethal concentrations of HE (160 and 260 mg/kg b. wt) was found to reduce the DLA induced solid tumour development in mice. Compared to the standard drug (CTX), the tumour inhibiting the action of the HE extract was less. It is also found that the vehicle control has no influence on tumour development and the data was very close to the untreated (control) animal group. All animals were survived until the end of the experiment period in the entire groups.

The tumour volume measured during the experiment was found increasing. Maximum volume (8.69 ± 0.73cm^3) was noted in the control group which was followed by the vehicle control group (8.49 ± 0.84 cm^3). In comparison with the control group of animals, the tumour volume was showed a significant reduction in the entire drug-treated groups and found more reduction in CTX treated group of animals. The tumour volume measured during the experiment period is depicted in figure 5.5.

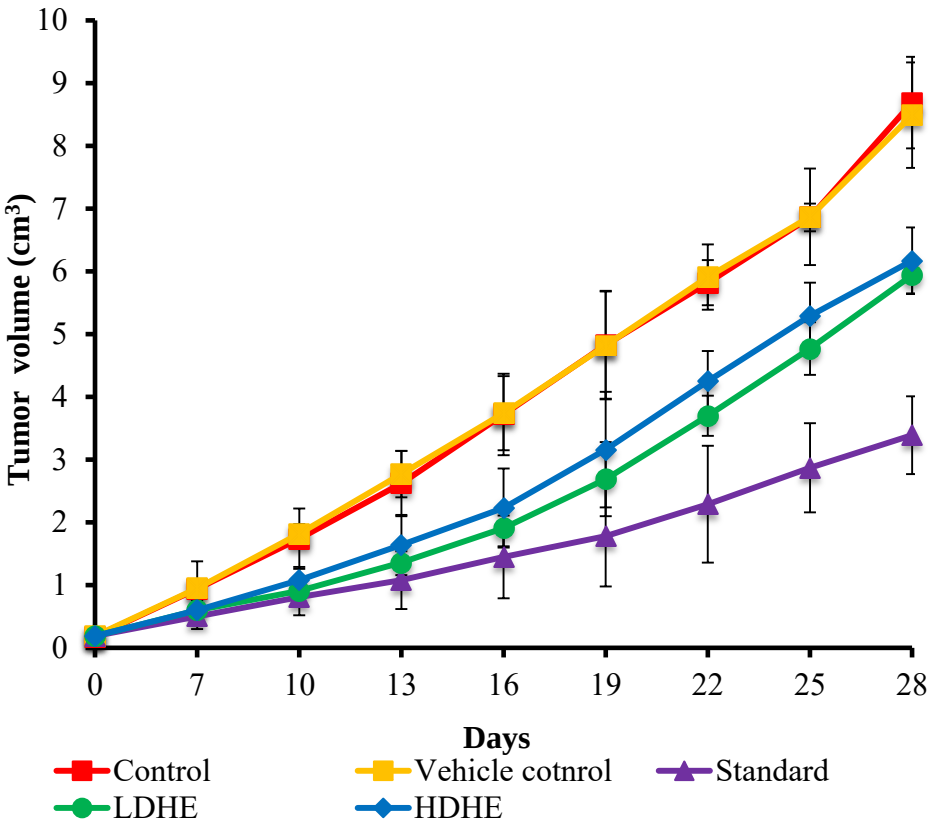

Figure 5.5. Tumour volume of mice administered with HE along with the inoculation of solid tumour: Solid tumour was inoculated by injecting DLA cells (1x10^{6}cells/animal) subcutaneously to the right hind limb of Swiss albino mice. The animals, except control, were received test material orally (vehicle control; 200 μL 1% propylene glycol, standard; cyclophosphamide (15 mg/kg b. wt), LDHE; 160 mg/kg b. wt, and HDHE; 260 mg/kg b. wt) for ten successive days one day after tumour inoculation

The increase in tumour volume was evident from the gross morphology of animals in different treatment groups with respect to control group of animals (Figure 5.6 and 5.7). The average gain in body weight found varying between the treatment groups. In control, vehicle control and standard group the average gain in body weight was negative. The maximum gain in body weight (gm) was noted in LDHE (1.02 gm) followed by HDHE (0.92 gm). The percentage of inhibition in tumour weight was found high in the standard group (46.43). It was 22.96 and 20.41 gm respectively in LDHE and HDHE. The general characteristics are summarised in table 5.5.

The effect of HE on haematological parameters like total Hb level and leucocyte count was also found changing in the treated groups with respect to control group animals. Hb level in control, vehicle control and the standard group were found decreasing during the experiment period. A drastic reduction was noted in the Hb

level of the CTX treated group from an initial level of 15.08 ± 0.43 to 8.32 ± 0.13 gm/dL at the end of the experiment. In LDHE and HDHE, the Hb level was found increasing slightly from the initial level (Figure 5.9). A similar trend was noted in total leucocyte count of drug-treated animals (both LDHE and HDHE). The total WBC count was found to decreasing in control, vehicle control and standard group, among these groups an extreme reduction was observed in the standard group (Table 5.6).

Histological evaluation of tumour tissues revealed a massive proliferation of tumour cells and necrosis in control and vehicle control groups. The cell proliferation was least in the standard group and was followed by LDHE and HDHE treated groups. The change in cellular architecture made by DLA tumour cells was evaluated with a tissue sample collected from normal (not treated with any drug) mice (Figure 5.8).

Table 5.5. Characteristics of mice administered with HE along with the inoculation of solid tumour: Solid tumour was inoculated by injecting DLA cells ($1x10^6$cells/animal) subcutaneously to the right hind limb of Swiss albino mice: The animals, except control were received test material orally (vehicle control; 200 μL 1% propylene glycol, standard; cyclophosphamide (15 mg/kg b. wt), LDHE; 160 mg/kg b. wt, and HDHE; 260 mg/kg b. wt) for ten successive days one day after tumour inoculation

Parameters	Group				
	Control	Vehicle control	Standard	LDHE	HDHE
Initial body weight (gm) (at 0 day)	27.55 ± 0.40	27.73 ± 0.97	27.35 ± 0.32	27.35 ± 0.33	27.17 ± 0.42
Number of mice	6	6	6	6	6
Final body weight (gm) (at 28 day)	30.47 ± 0.47	30.64 ± 0.83 ^{ns}	28.96 ± 0.61**	31.39 ± 0.29*	31.19 ± 0.59^{ns}
Number of mice	6	6	6	6	6
Tumour weight (gm) (at 28 day)	3.92 ± 0.34	3.80 ± 0.33^{ns}	2.10 ± 0.09**	3.02 ± 0.12**	3.12 ± 0.21**
% inhibition in tumour weight	-	8.16	46.43	22.96	20.41
Net final body weight (gm)	26.55 ± 0.45	26.84 ± 0.82 ^{ns}	26.86 ± 0.54^{ns}	28.37 ± 0.31**	28.07 ± 0.77**
Body weight gain (gm)	-1.00	-0.89	-0.49	1.02	0.90
Change from the initial body weight (%)	-3.77	-3.32	-1.85	3.58	3.18

Values are mean ± standard deviation of six animals per group
% inhibition in tumour weight = (Average weight of solid tumour in the control group – Average weight of solid tumour in the experiment group.)/ The average weight of solid tumour in the control group x 100
Net final body weight = (Final body weight – Tumour weight)
Body weight gain = (Net final body weight – Initial body weight)
Change from the initial body weight = (Body weight gain)/Net final bodyweight x 100
^{ns} $p>0.05$, * $p<0.05$, ** $p<0.01$ between control and treated groups

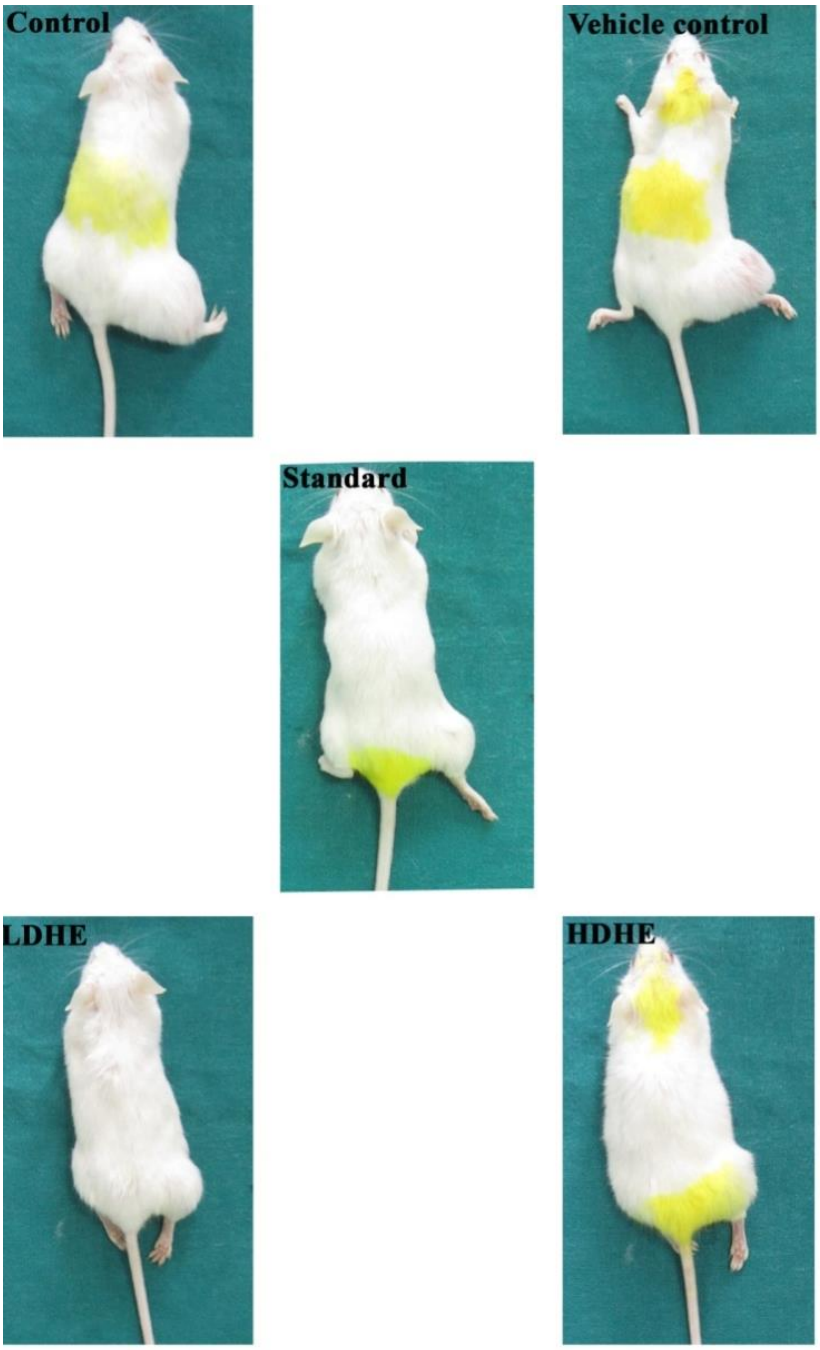

Figure 5.6. Morphology of mice administered with HE along with the inoculation of solid tumour: Solid tumour was inoculated by injecting DLA cells ($1x10^6$cells/animal) subcutaneously to the right hind limb of Swiss albino mice. The animals, except control, were received test material orally (vehicle control; 200 μL 1% propylene glycol, standard; cyclophosphamide (15 mg/kg b. wt), LDHE; 160 mg/kg b. wt, and HDHE; 260 mg/kg b. wt) for ten successive days one day after tumour inoculation

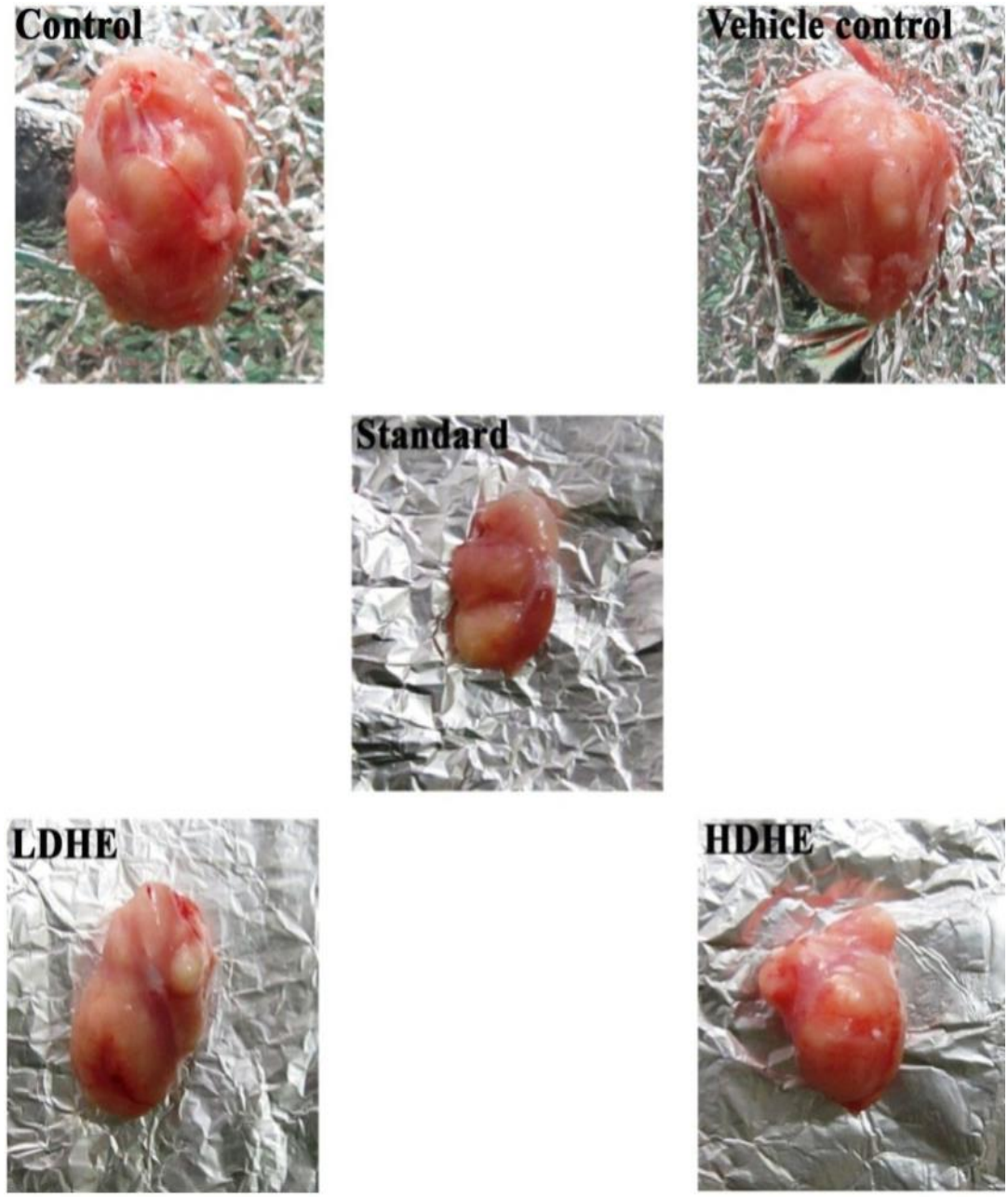

Figure 5.7. Tumour isolated from the mice administered with HE along with the inoculation of solid tumour: Solid tumour was inoculated by injecting DLA cells ($1x10^6$cells/animal) subcutaneously to the right hind limb of Swiss albino mice. The animals, except control, were received test material orally (vehicle control; 200 μL 1% propylene glycol, standard; cyclophosphamide (15 mg/kg b. wt), LDHE; 160 mg/kg b. wt, and HDHE; 260 mg/kg b. wt) for ten successive days one day after tumour inoculation

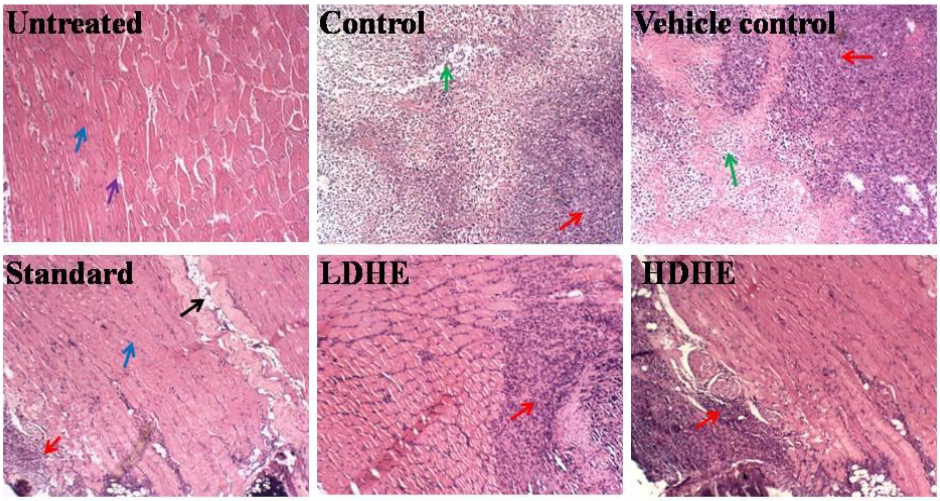

Figure 5.8. Histology of H & E stained section of solid tumour from the mice administered with HE along with the inoculation of solid tumour: Solid tumour was inoculated by injecting DLA cells ($1x10^6$cells/animal) subcutaneously to the right hind limb of Swiss albino mice. The animals, except control, were received test material orally (vehicle control; 200 μL 1% propylene glycol, standard; cyclophosphamide (15 mg/kg b. wt), LDHE; 160 mg/kg b. wt, and HDHE; 260 mg/kg b. wt) for ten successive days one day after tumour inoculation. The green arrow indicates necrosis, the red arrow denotes tumour cells, the violet arrow represents endomysial connective tissue, the black arrow indicates adipocytes and the blue arrow denotes muscle cells. The images (200X) were taken under an inverted microscope

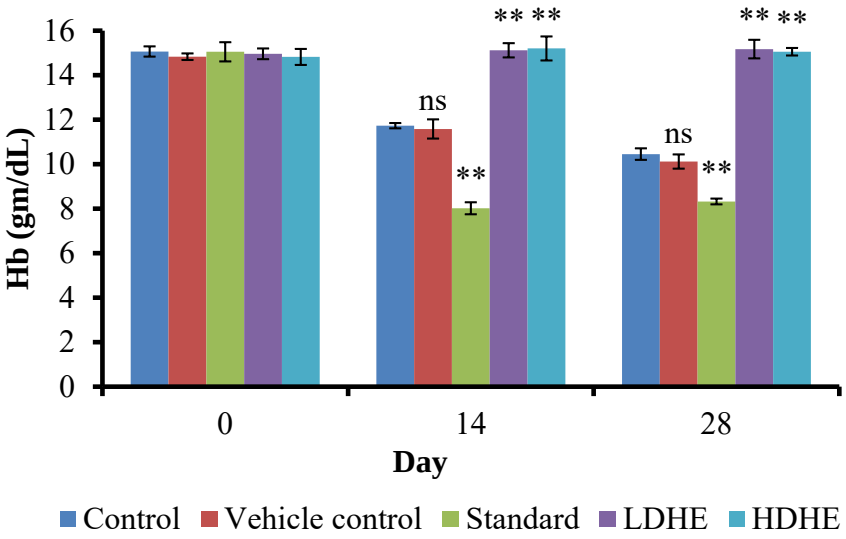

Figure 5.9. Effect of HE on Hb in mice administered with HE along with the inoculation of solid tumour: Solid tumour was inoculated by injecting DLA cells ($1x10^6$cells/animal) subcutaneously to the right hind limb of Swiss albino mice. The animals, except control, were received test material orally (vehicle control; 200 μL 1% propylene glycol, standard; cyclophosphamide (15 mg/kg b. wt), LDHE; 160 mg/kg b. wt, and HDHE; 260 mg/kg b. wt) for ten successive days one day after tumour inoculation

Table 5.6. Effect of HE on total leucocyte count of mice administered with HE along with the inoculation of solid tumour: Solid tumour was inoculated by injecting DLA cells ($1x10^6$cells/animal) subcutaneously to the right hind limb of Swiss albino mice. The animals, except control, were received test material orally (vehicle control; 200 μL 1% propylene glycol, standard; cyclophosphamide (15 mg/kg b. wt), LDHE; 160 mg/kg b. wt, and HDHE; 260 mg/kg b. wt) for ten successive days one day after tumour inoculation

Day	Group				
	Control	**Vehicle control**	**Standard**	**LDHE**	**HDHE**
0 day	11220 ± 280	10700 ± 760^{ns}	10600 ± 340^{ns}	11030 ± 760 ^{ns}	11600 ± 530^{ns}
14th day	9300 ± 360	9400 ± 510^{ns}	8300 ± 320**	11600 ± 290**	11300 ± 420**
28th day	8700 ± 270	8500 ± 120^{ns}	6300 ± 420**	11000 ± 670**	11200 ± 420**

Values are mean ± standard deviation of six animals per group
^{ns} $p>0.05$, ** $p<0.01$ between control and treated groups for different days

5.3.2.2. Pre and simultaneous administration of HE in the solid tumour development

The administration of HE at different doses for 5 successive days earlier to tumour inoculation and 10 consecutive days after the inoculation of the tumour was found effective with respect to the vehicle control group of animals. The tumour volume was noted to be 8.42 ± 0.76 in vehicle control. A significant reduction was noted in the tumour volume of LDHE (5.09 ± 0.46) and HDHE (4.99 ± 0.53) at the end of the experiment period. The reduction in tumour volume was found close to each other in the drug-treated groups at varying time intervals (Figure 5.10)

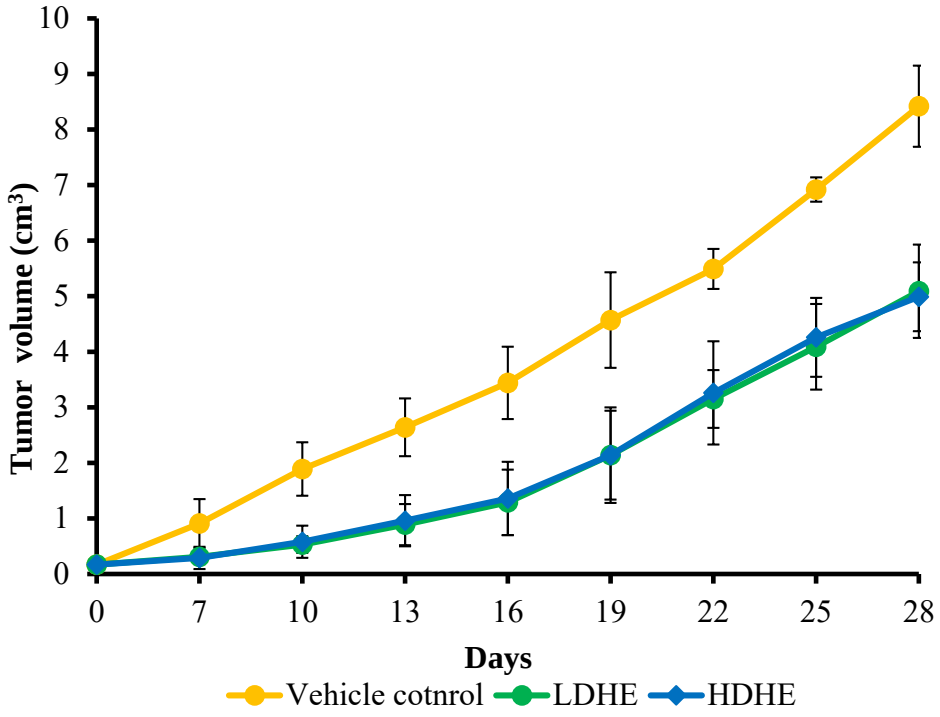

Figure 5.10. Tumour volume of mice administered with HE before and after the inoculation of solid tumour: Solid tumour was inoculated by DLA cells ($1x10^6$cells/animal) subcutaneously to the right hind limb of Swiss albino mice. The animals were received test material orally (vehicle control; 200 μL 1% propylene glycol, LDHE; 160 mg/kg b. wt, and HDHE; 260 mg/kg b. wt) five successive days before and ten consecutive days after tumour inoculation

All mice were survived in the entire period of study. The net final body weight (gm) of vehicle control group animals was found decreased (26.25 ± 0.41) and percentage change from the initial body weight was found -3.87. Unlike this, in LDHE (27.87 ± 0.49) and HDHE (28.46 ± 0.64) net final body weight found increased and it was

significantly different from the control group of animals. The tumour weight (gm) was 3.73 ± 0.30, 2.82 ± 0.36 and 2.75 ± 0.29 in vehicle control, LDHE and HDHE respectively at the 28th day of the experiment. The percentage inhibition of tumour weight was slightly more in HDHE (26.27%) with respect to LDHE (24.40%) with respect to the control group (Table 5.7).

Table 5.7. Characteristics of mice administered with HE before and after the inoculation of solid tumour: Solid tumour was inoculated by DLA cells (1x10^{6}cells/animal) subcutaneously to the right hind limb of Swiss albino mice. The animals were received test material orally (vehicle control; 200 μL 1% propylene glycol, LDHE; 160 mg/kg b. wt, and HDHE; 260 mg/kg b. wt) five successive days before and ten consecutive days after tumour inoculation

Parameters	Group		
	Vehicle control	LDHE	HDHE
Initial body weight (gm) (at 0 day)	27.76 ± 0.29	26.83 ± 0.53	27.47 ± 0.35
Number of mice	6	6	6
Final body weight (gm) (at 28 day)	29.98± 0.35	30.69 ± 0.24*	31.21 ± 0.64**
Number of mice	6	6	6
Tumour weight (gm) (at 28 day)	3.73 ± 0.30	2.82 ± 0.36**	2.75 ± 0.29**
% inhibition in tumour weight	-	24.40	26.27
Net final body weight (gm)	26.25 ± 0.41	27.87 ± 0.49**	28.46 ± 0.64**
Body weight gain (gm)	-1.01	1.04	1.00
Change from the initial body weight (%)	-3.87	3.70	3.47

Values are mean ± standard deviation of six animals per group
% inhibition in tumour weight = (Average weight of solid tumour in the vehicle control group – Average weight of solid tumour in the experiment group.)/ The average weight of solid tumour in the vehicle control group x 100
Net final body weight = (Final body weight – Tumour weight)
Body weight gain = (Net final body weight – Initial body weight)
Change from the initial body weight = (Body weight gain)/Net final body weight x 100
* $p<0.05$, ** $p<0.01$ between Vehicle control and treated groups

Morphological changes of body and the size of tumour occurred in the drug-treated animals with respect to control group is depicted in figure 5.11 and 5.12. In the vehicle control group animals, the solid tumour was found enlarged. A reduction in the tumour size was noted in the drug treated animals with respect to vehicle control group. Microscopic analysis done with the tissue preparations of drug-treated animals showed a marked improvement in the inhibition of tumour progression with respect to vehicle control group animals (Figure 5.13). In the vehicle control group the micro architecture of muscle tissue was found deteriorated. The shape and appearance of muscle tissue were fully changed due to the progression of cancer cells. Necrosis was found in vehicle control tissue. In LDHE treated animals the progression of cancer cells were found less with respect to HDHE Haemoglobin level in the vehicle control group animals was progressively reduced from the beginning to the end of the experiment. At the initial day of the experiment level of Hb was 14.82 ± 0.27 gm/dL) but, the 28^{th} day it was found 10.47 ± 0.20 gm/dL. Interestingly, in HE treated groups the Hb level was found constant (Figure 5.14). A similar result was obtained with respect to the total leucocyte count of animals and it is summarised in table no. 5.8. The haematological parameters analysed in drug-treated animals showed a significant change ($p<0.01$) in their level during the observation days (0, 14 and 28) with respect to vehicle control group animals.

Figure 5.11. Morphology of mice administered with HE before and after the inoculation of solid tumour. Solid tumour was inoculated by DLA cells ($1x10^6$cells/animal) subcutaneously to the right hind limb of Swiss albino mice: The animals were received test material orally (vehicle control; 200 μL 1% propylene glycol, LDHE; 160 mg/kg b. wt, and HDHE; 260 mg/kg b. wt) five successive days before and ten consecutive days after tumour inoculation

Figure 5.12. Tumour isolated from the mice administered with HE before and after the inoculation of solid tumour. Solid tumour was inoculated by DLA cells ($1x10^6$cells/animal) subcutaneously to the right hind limb of Swiss albino mice: The animals were received test material orally (vehicle control; 200 μL 1% propylene glycol, LDHE; 160 mg/kg b. wt, and HDHE; 260 mg/kg b. wt) five successive days before and ten consecutive days after tumour inoculation

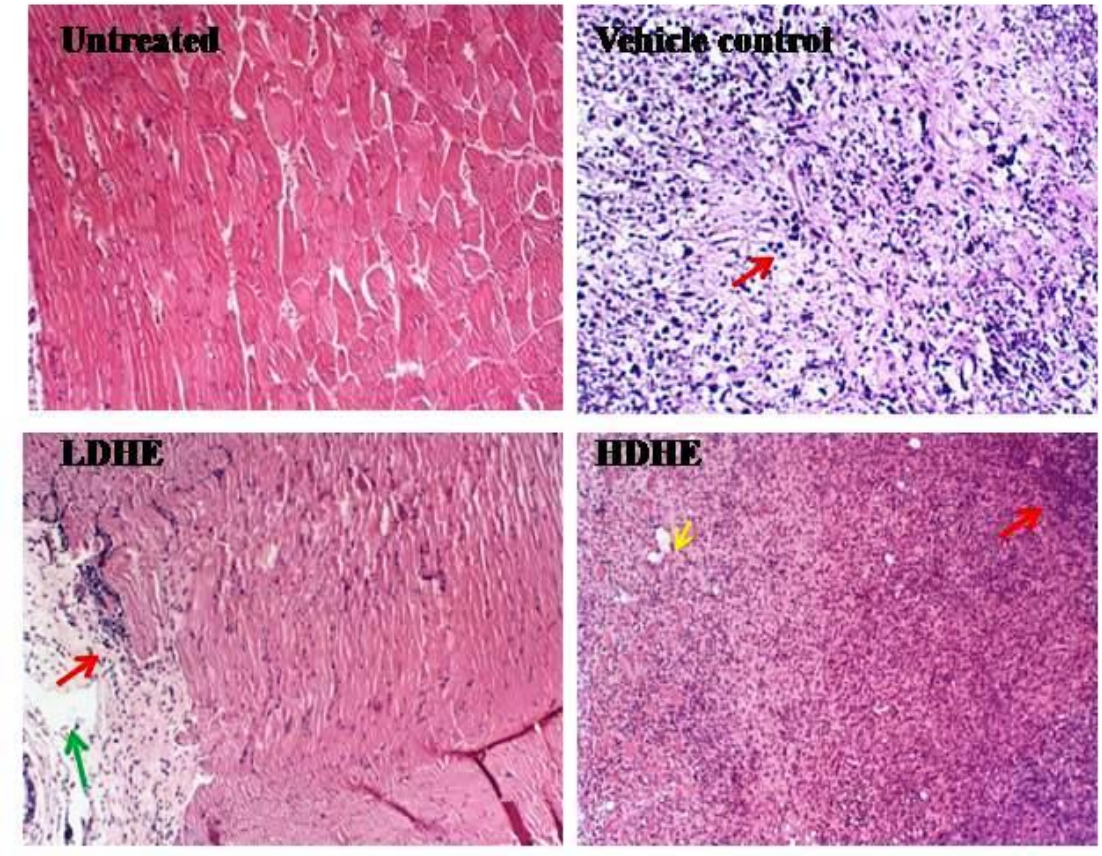

Figure 5.13. Histology of H & E stained section of solid tumour from the mice administered with HE before and after the inoculation of solid tumour: Solid tumour was inoculated by DLA cells ($1x10^6$cells/animal) subcutaneously to the right hind limb of Swiss albino mice. The animals were received test material orally (vehicle control; 200 μL 1% propylene glycol, LDHE; 160 mg/kg b. wt, and HDHE; 260 mg/kg b. wt) five successive days before and ten consecutive days after tumour inoculation. The images (200X) were taken under an inverted microscope. The green arrow indicates necrosis, the red arrow denotes tumour cells and the yellow arrow represents blood vessel

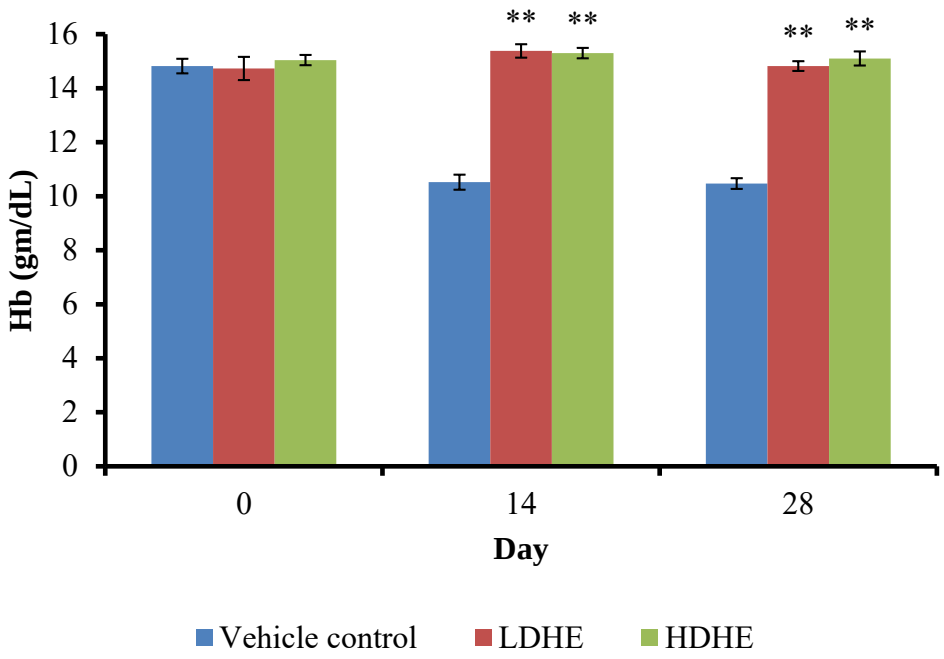

Figure 5.14. Effect of HE on Hb in mice administered with HE before and after the inoculation of solid tumour: Solid tumour was inoculated by DLA cells ($1x10^6$cells/animal) subcutaneously to the right hind limb of Swiss albino mice. The animals were received test material orally (vehicle control; 200 μL 1% propylene glycol, LDHE; 160 mg/kg b. wt, and HDHE; 260 mg/kg b. wt) five successive days before and ten consecutive days after tumour inoculation

Table 5.8. Effect of HE on total leucocyte count of mice administered with HE before and after the inoculation of solid tumour: Solid tumour was inoculated by DLA cells ($1x10^6$cells/animal) subcutaneously to the right hind limb of Swiss albino mice. The animals were received test material orally (vehicle control; 200 μL 1% propylene glycol, LDHE; 160 mg/kg b. wt, and HDHE; 260 mg/kg b. wt) five successive days before and ten consecutive days after tumour inoculation

Day	Group		
	Vehicle control	**LDHE**	**HDHE**
0 day	11500 ± 480	11200 ± 390 ^{ns}	11600 ± 290 ^{ns}
14th day	10200 ± 320	11000 ± 240**	11200 ± 460**
28th day	9500 ± 340	11300 ± 250**	11500 ± 410**

Values are mean ± standard deviation of six animals per group
^{ns} $p>0.05$, ** $p<0.01$ between vehicle control and treated groups for different days

5.3.2.3. Administration of HE to the solid tumour bearing mice

Antitumour efficacy of HE administered orally at different concentrations (160 and 260 mg/kg b. wt) ten days after the inoculation of solid tumour in mice generated the following data. A hundred percentages (100%) of animals in the treatment groups were survived in the experiment period. The tumour volume of the mice in all groups was found increasing during the period of time. A maximum reduction of volume of the solid tumour was noted in animals treated with CTX (42.55%) with respect to the vehicle control group. In LDHE and HDHE treated group of animals, the tumour volume was reduced to 19.45% and 22.41% at the end of the study (Figure 5.15). Bodyweight of animals in all groups was increased. However, net final body weight in-vehicle control and the standard group were lower. The percentage change from the initial body weight was -2.24 in the standard group and 7.82, 7.65 in LDHE and HDHE treated groups respectively (Table 5.9). The tumour with maximum weight was noted in-vehicle control-treated animals and the average weight was 4.13 ± 0.25. The average tumour weight was very less in animals treated with CTX (2.73 ± 0.20). The average tumour weight in LDHE and HDHE were higher than the CTX treated group and found close to each other. General morphological changes occurred in the different group animals administered with HE after ten days of tumour inoculation is depicted in figure 5.16. The animals administered with standard drug found to become weak and thin during the treatment. Increase in tumour size is obvious from the photographs taken from the isolated tumours from various groups of animals (Figure 5.17). Histological observations of the tissue prepared from the groups showed less proliferation of tumour cells in the standard group (Figure 5.18) with respect to the vehicle control group. Haematological parameters like total Hb count and total leucocyte count were found constant in LDHE and HDHE treated animals. A steady decrease in Hb level was noted in CTX treated animal from 15.05 ± 0.31 to 7.43 ± 0.43 gm/dL. A similar trend was noted in the vehicle control group of animals; it was 14.82 ± 0.28 gm/dL in the initial day of the experiment but, came to a lower level of 9.05 ± 0.14 gm/dL at the 28^{th} day of the experiment (Figure 5.19). Total leucocyte count was 11300 ± 320 in the standard group of animals during the initial day of the study and lowered to 6320 ± 210 at the end day. It was noted that in LDHE and HDHE treated groups, total WBC cells were marginally increased from the first day to last day of the experiment (Table 5.10).

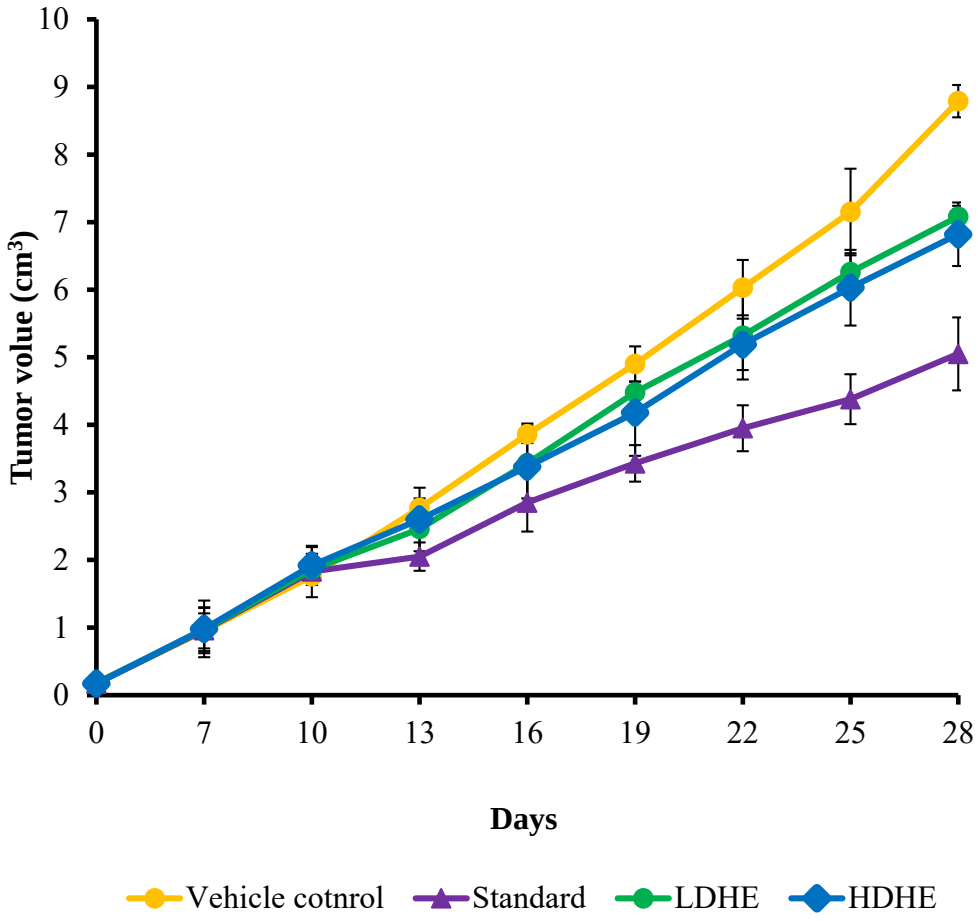

Figure 5.15. Tumour volume of mice administered with HE, ten days after the inoculation of solid tumour: Solid tumour was inoculated by injecting DLA cells ($1x10^6$cells/animal) subcutaneously to the right hind limb of Swiss albino mice: The animals were received test material orally (vehicle control; 200 μL 1% propylene glycol, standard; cyclophosphamide (15 mg/kg b. wt), LDHE; 160 mg/kg b. wt, and HDHE; 260 mg/kg b. wt) for ten consecutive days after ten days of tumour inoculation

Table 5.9. Characteristics of mice administered with HE, ten days after the inoculation of solid tumour: Solid tumour was inoculated by injecting DLA cells ($1x10^6$cells/animal) subcutaneously to the right hind limb of Swiss albino mice. The animals were received test material orally (vehicle control; 200 μL 1% propylene glycol, standard; cyclophosphamide (15 mg/kg b. wt), LDHE; 160 mg/kg b. wt, and HDHE; 260 mg/kg b. wt) for ten consecutive days after ten days of tumour inoculation

Parameters	Group			
	Vehicle control	Standard	LDHE	HDHE
Initial body weight (gm) (at 0 day)	27.27 ± 0.64	27.21 ± 0.32	27.18 ± 0.45	27.41 ± 0.29
Number of mice	6	6	6	6
Final body weight (gm) (at 28 day)	30.16 ± 0.48	29.35 ± 0.56^{ns}	32.91 ± 0.90**	33.04 ± 0.62**
Number of mice	6	6	6	6
Tumour weight (gm) (at 28 day)	4.13 ± 0.25	2.73 ± 0.20**	3.42 ± 0.48**	3.35 ± 0.28**
% inhibition in tumour weight	-	33.90	17.19	18.89
Net final body weight (gm)	26.02 ± 0.57	26.61 ± 0.49^{ns}	29.42 ± 0.52**	29.69 ± 0.38**
Body weight gain (gm)	-1.25	-0.59	2.31	2.27
Change from the initial body weight (%)	-4.81	-2.24	7.82	7.65

Values are mean ± standard deviation of six animals per group
% inhibition in tumour weight = (Average weight of solid tumour in the control group – Average weight of solid tumour in the experiment group.)/ The average weight of solid tumour in the control group x 100
Net final body weight = (Final body weight – Tumour weight)
Bodyweight gain = (Net final body weight – Initial body weight)
Change from the initial body weight = (Body weight gain)/Net final body weight x 100
^{ns} $p>0.05$, ** $p<0.01$ between vehicle control and treated groups

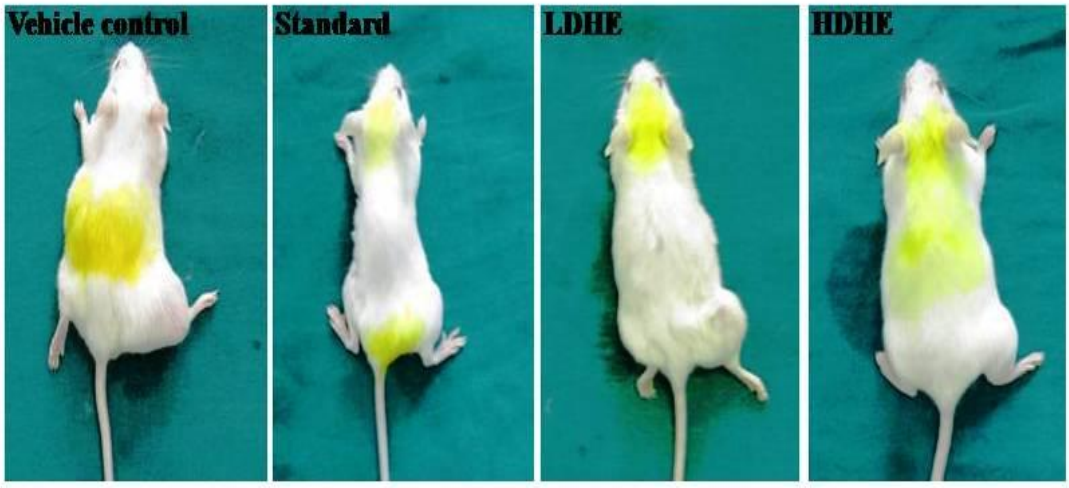

Figure 5.16. Morphology of mice administered with HE, ten days after the inoculation of solid tumour: Solid tumour was inoculated by injecting DLA cells ($1x10^6$cells/animal) subcutaneously to the right hind limb of Swiss albino mice: The animals were received test material orally (vehicle control; 200 μL 1% propylene glycol, standard; cyclophosphamide (15 mg/kg b. wt), LDHE; 160 mg/kg b. wt, and HDHE; 260 mg/kg b. wt) for ten consecutive days after ten days of tumour inoculation

Figure 5.17. Tumour isolated from the mice administered with HE, ten days after the inoculation of solid tumour: Solid tumour was inoculated by injecting DLA cells ($1x10^6$cells/animal) subcutaneously to the right hind limb of Swiss albino mice: The animals were received test material orally (vehicle control; 200 μL 1% propylene glycol, standard; cyclophosphamide (15 mg/kg b. wt), LDHE; 160 mg/kg b. wt, and HDHE; 260 mg/kg b. wt) for ten consecutive days after ten days of tumour inoculation

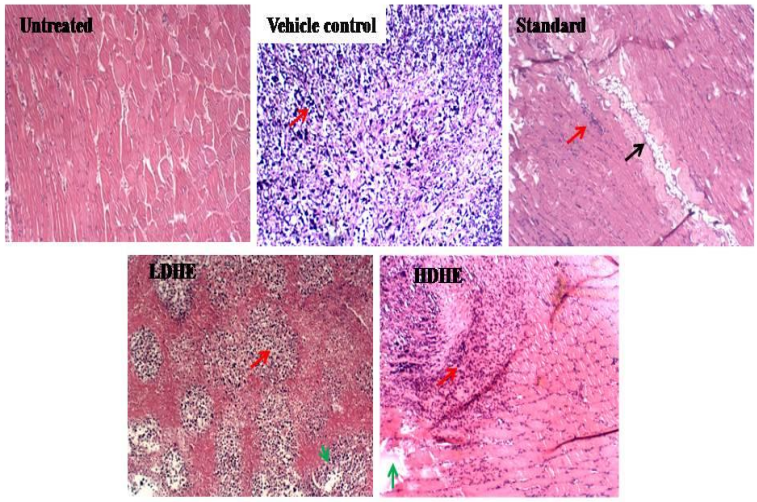

Figure 5.18. Histology of H & E stained section of solid tumour from the mice administered with HE, ten days after the inoculation of solid tumour: Solid tumour was inoculated by injecting DLA cells ($1x10^6$cells/animal) subcutaneously to the right hind limb of Swiss albino mice. The animals except untreated, were received test material orally (vehicle control; 200 μL 1% propylene glycol, standard; cyclophosphamide (15 mg/kg b. wt), LDHE; 160 mg/kg b. wt, and HDHE; 260 mg/kg b. wt) for ten consecutive days after ten days of tumour inoculation. The green arrow indicates necrosis, the red arrow represents tumour cells and the black arrow denotes adipocytes. The images (200X) were taken under an inverted microscope

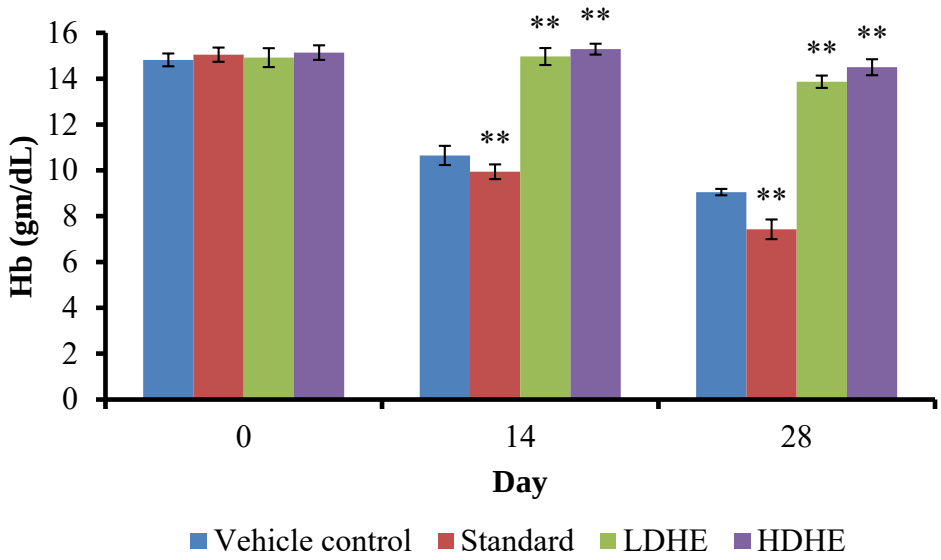

Figure 5.19. Effect of HE on Hb in mice administered with HE, ten days after the inoculation of solid tumour: Solid tumour was inoculated by injecting DLA cells ($1x10^6$cells/animal) subcutaneously to the right hind limb of Swiss albino mice. The animals were received test material orally (vehicle control; 200 μL 1% propylene glycol, standard; cyclophosphamide (15 mg/kg b. wt), LDHE; 160 mg/kg b. wt, and HDHE; 260 mg/kg b. wt) for ten consecutive days after ten days of tumour inoculation

Table 5.10. Effect of HE on total leucocyte count of mice administered with HE, ten days after the inoculation of solid tumour: Solid tumour was inoculated by injecting DLA cells ($1x10^6$cells/animal) subcutaneously to the right hind limb of Swiss albino mice. The animals were received test material orally (vehicle control; 200 μL 1% propylene glycol, standard; cyclophosphamide (15 mg/kg b. wt), LDHE; 160 mg/kg b. wt, and HDHE; 260 mg/kg b. wt) for ten consecutive days after ten days of tumour inoculation

Day	Group			
	Vehicle control	**Standard**	**LDHE**	**HDHE**
0 day	10900 ± 480	11300 ± 320 ^{ns}	11010 ± 260 ^{ns}	11200 ± 540 ^{ns}
14th day	11200 ± 540	8340 ± 320 **	11900 ± 380*	12300 ± 360**
28th day	11400 ± 230	6320 ± 210**	12000 ± 480*	12200 ± 530**

Values are mean ± standard deviation of six animals per group
^{ns} $p>0.05$, * $p<0.05$, ** $p<0.01$ between control and treated groups for different days

5.3.2.4. Simultaneous administration of HE in combination with cyclophosphamide in solid tumour development

A combination of various doses of CTX with LDHE administered mice showed the following results. The tumour volume was found decreased in the drug-treated groups in comparison with vehicle and CTX combination. The tumour volume was measured 3.69 cm^3 at the end of the experiment in vehicle and CTX group. A maximum reduction (38.75%) in tumour volume was noted in the group which was administered a combination of LDHE and CTX (10 mg/kg b. wt). Second to this (31.98%) reduction of tumour volume was noted in mice treated with LDHE in combination with CTX (15 mg/kg b. wt). A combination of LDHE with CTX (5 mg/kg b. wt) treated animals was showed only 24.12% reduction in the tumour volume (Figure 5.20).

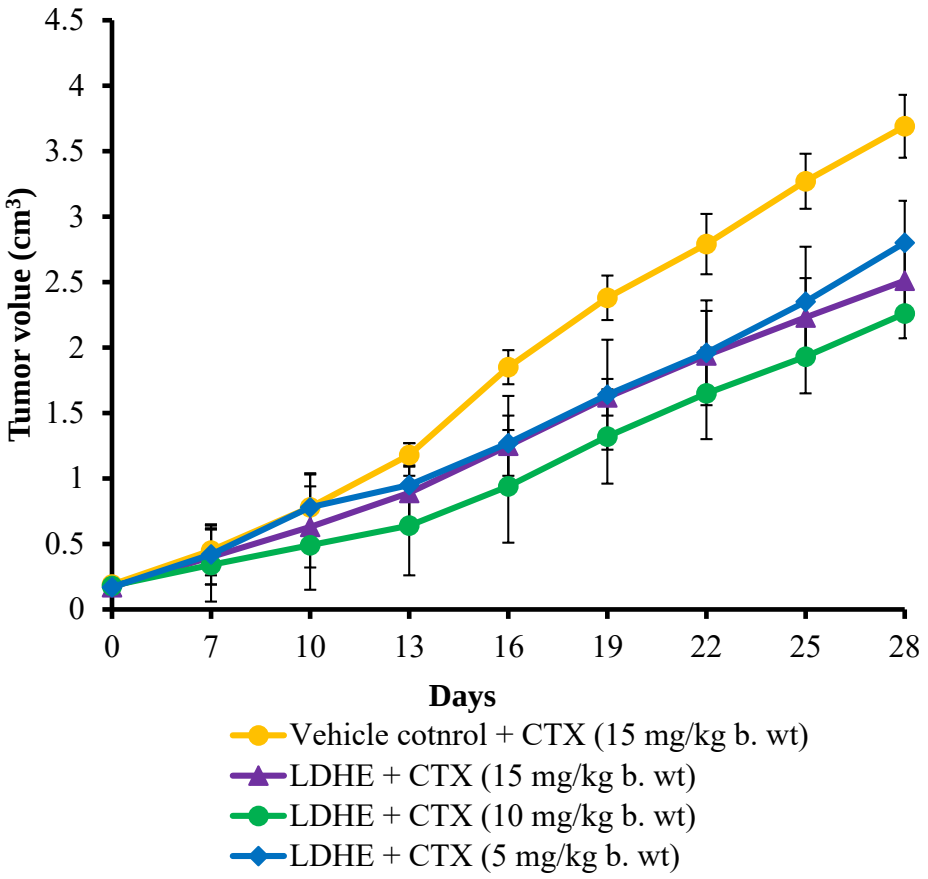

Figure 5.20. Tumour volume of mice administered with HE in combination with cyclophosphamide one day after the inoculation of solid tumour: Solid tumour was inoculated by injecting DLA cells ($1x10^6$cells/animal) subcutaneously to the right hind limb of Swiss albino mice. The animals were received test material orally for ten consecutive days one day after tumour inoculation

All animals in the experimental groups were showed 100 percentage survival capacities in the experiment period. The maximum net body weight gain (gm) was noted in animals treated with LDHE + CTX (10 mg/kg b. wt) and it was only 0.81 gm. The net gain in body weight was 0.57 gm in animals treated with LDHE + CTX (15 mg/kg b. wt) followed by the only 0.49 gm in LDHE + CTX (5 mg/kg b. wt) treated animals. The average net weight of vehicle + LDHE treated animals was found to be a negative value (Table 5.11). 19.28% of tumour weight reduction was noted in LDHE + CTX (15 mg/kg b. wt) treated group. The percentage tumour reduction was 25.30 and 20.88 respectively in LDHE + CTX (10 mg/kg b. wt) and LDHE + CTX (5 mg/kg b. wt) treated animals (Figure 5.22). The reduction in body weight in the first and second group of animals was obvious from their external appearance (Figure 5.21).

Micrographs of solid tumour tissues isolated from different groups are depicted in figure 5.23. The micrographs were analysed with the normal architecture of the muscle tissue. The tumour cell proliferation and related necrosis were found more in LDHE + CTX (15 mg/kg b. wt) treated group and LDHE + CTX (5 mg/kg b. wt) groups.

The haemoglobin level was found reduced in all drug-treated animals with respect to their level at the initial day of the experiment. A maximum decrease in Hb level was noted in vehicle + CTX (15 mg/kg b. wt) treated group at the 28^{th} day of the experiment (8.21 ± 0.14 gm/dL) and it was 42.8% less in comparison with total Hb level in initial day. The percentage reduction in total Hb level was 28.3%, 21.5% and 28.3% in group II, group III and group IV animals respectively (Figure 5.24).

Total leucocyte count of drug-treated animals showed a similar response like total Hb level. Compare with the initial day in all treated groups the total leucocyte count found decreased. The maximum reduction was noted in group I (vehicle + CTX (15 mg/kg b. wt) treated mice on the 28^{th} day of the experiment. In day 14 and 28, compared to group I the total leucocyte count significantly increased in all drug-treated animals. (Table 5.12).

Table 5.11. Characteristics of mice administered with HE in combination with cyclophosphamide after the inoculation of solid tumour: Solid tumour was inoculated by injecting DLA cells ($1x10^6$cells/animal) subcutaneously to the right hind limb of Swiss albino mice. The animals were received test material orally for ten consecutive days one day after tumour inoculation

Parameters	Group			
	Vehicle control + CTX (15 mg/kg b. wt)	**LDHE + CTX (15 mg/kg b. wt)**	**LDHE + CTX (10 mg/kg b. wt)**	**LDHE + CTX (5 mg/kg b. wt)**
Initial body weight (gm) (at 0 day)	26.77 ± 0.36	27.02 ± 0.21	26.95 ± 0.63	27.09 ± 0.39
Number of mice	6	6	6	6
Final body weight (gm) (at 28 day)	28.34 ± 0.16	29.60 ± 0.21**	29.62 ± 0.43**	29.55 ± 0.51**
Number of mice	6	6	6	6
Tumour weight (gm) (at 28 day)	2.49 ± 0.34	2.01 ± 0.19**	1.86 ± 0.20**	1.97 ± 0.16**
% inhibition in tumour weight	-	19.28	25.30	20.88
Net final body weight (gm)	25.85 ± 0.20	27.59 ± 0.35**	27.76 ± 0.45**	27.59 ± 0.48**
Body weight gain (gm)	-0.92	0.57	0.81	0.49
Change from the initial body weight (%)	-3.56	2.07	2.92	1.79

Values are mean ± standard deviation of six animals per group

% inhibition in tumour weight = (Average weight of solid tumour in-vehicle control + CTX (15 mg/kg b. wt) group – Average weight of solid tumour in the experiment group)/ Average weight of solid tumour in-vehicle control + CTX (15 mg/kg b. wt) group x 100

Net final body weight = (Final body weight – Tumour weight), Body weight gain = (Net final body weight – Initial body weight)

Change from the initial body weight = (Body weight gain)/Net final body weight x 100

** $p<0.01$ between vehicle control + CTX (15 mg/kg b. wt) and treated groups

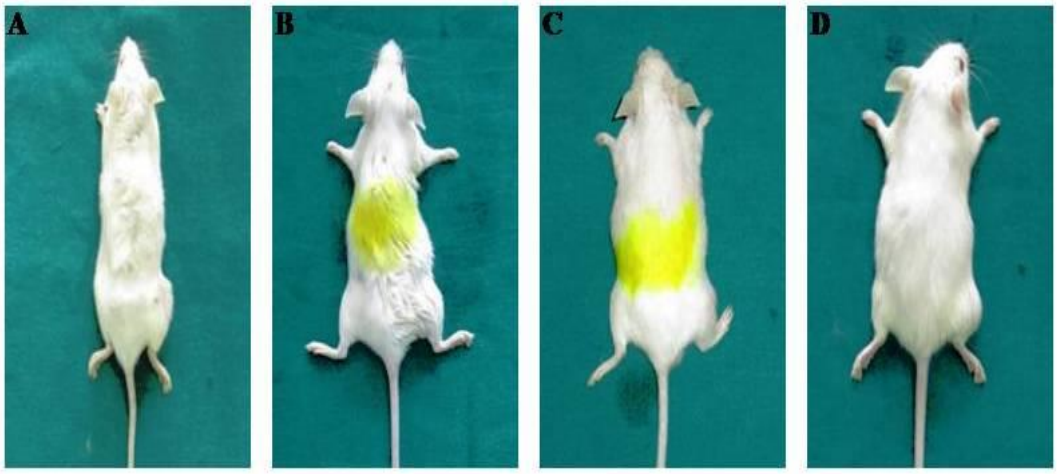

Figure 5.21. Morphology of mice administered with HE in combination with cyclophosphamide after the inoculation of solid tumour: Solid tumour was inoculated by injecting DLA cells ($1x10^6$cells/animal) subcutaneously to the right hind limb of Swiss albino mice. The animals were received test material orally for ten consecutive days one day after tumour inoculation. A) vehicle control (200 μL 1% propylene glycol) + CTX (15 mg/kg b. wt), B) LDHE (160 mg/kg b. wt) + CTX (15 mg/kg b. wt), C) LDHE (160 mg/kg b. wt) + CTX (10 mg/kg b. wt) and D) LDHE (160 mg/kg b. wt) + CTX (5 mg/kg b. wt)

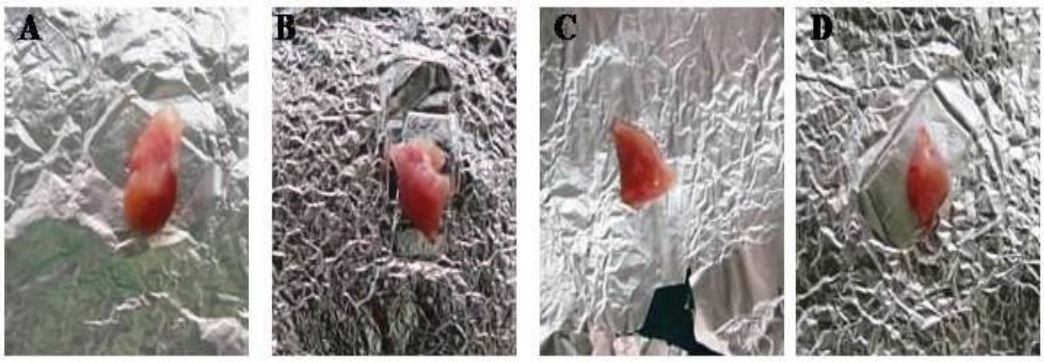

Figure 5.22. Tumour isolated from the mice administered with HE in combination with cyclophosphamide after the inoculation of solid tumour: Solid tumour was inoculated by injecting DLA cells ($1x10^6$cells/animal) subcutaneously to the right hind limb of Swiss albino mice. The animals were received test material orally for ten consecutive days one day after tumour inoculation. A) vehicle control (200 μL 1% propylene glycol) + CTX (15 mg/kg b. wt), B) LDHE (160 mg/kg b. wt) + CTX (15 mg/kg b. wt), C) LDHE (160 mg/kg b. wt) + CTX (10 mg/kg b. wt) and D) LDHE (160 mg/kg b. wt) + CTX (5 mg/kg b. wt)

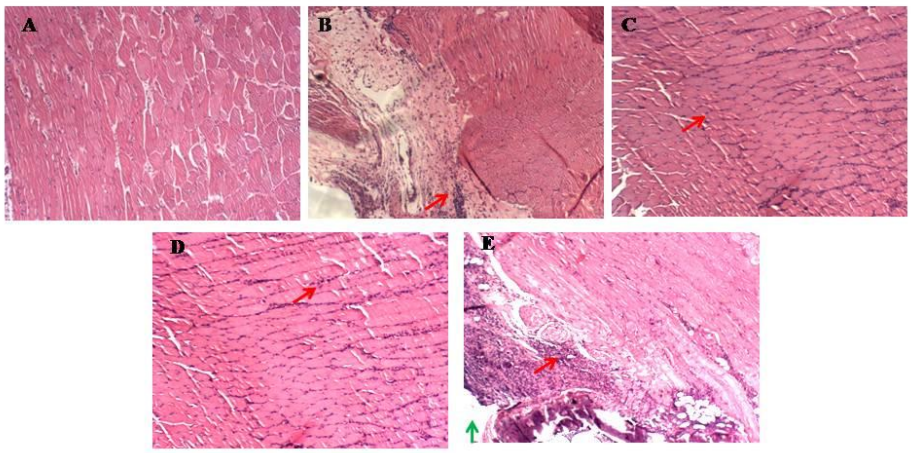

Figure 5.23. Histology of H & E stained section of solid tumour from the mice administered with HE in combination with cyclophosphamide after the inoculation of solid tumour: Solid tumour was inoculated by injecting DLA cells (1x10^{6}cells/animal) subcutaneously to the right hind limb of Swiss albino mice. The animals were received test material orally for ten consecutive days one day after tumour inoculation. A) normal B) vehicle control (200 μL 1% propylene glycol) + CTX (15 mg/kg b. wt), C) LDHE (160 mg/kg b. wt) + CTX (15 mg/kg b. wt), D) LDHE (160 mg/kg b. wt) + CTX (10 mg/kg b. wt) and E) LDHE (160 mg/kg b. wt) + CTX (5 mg/kg b. wt). The green arrow indicates necrosis and the red arrow represents tumour cells. The images (200X) were taken under an inverted microscope

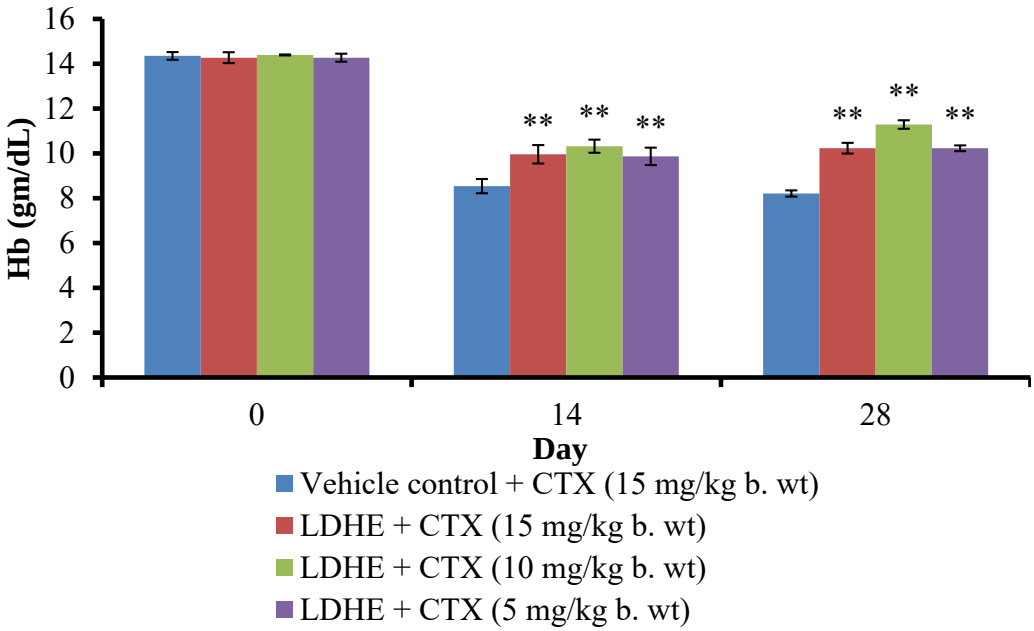

Figure 5.24. Effect of HE on Hb in mice administered with HE in combination with cyclophosphamide after the inoculation of solid tumour: Solid tumour was inoculated by injecting DLA cells (1x10^{6}cells/animal) subcutaneously to the right hind limb of Swiss albino mice. The animals were received test material orally for ten consecutive days one day after tumour inoculation

Table 5.12. Effect of HE on total leucocyte count of mice administered with HE in combination with cyclophosphamide after the inoculation of solid tumour: Solid tumour was inoculated by injecting DLA cells ($1x10^6$cells/animal) subcutaneously to the right hind limb of Swiss albino mice. The animals were received test material orally for ten consecutive days one day after tumour inoculation

Day	Group			
	Vehicle control + CTX (15 mg/kg b. wt)	**LDHE + CTX (15 mg/kg b. wt)**	**LDHE + CTX (10 mg/kg b. wt)**	**LDHE + CTX (5 mg/kg b. wt)**
0 day	10040 ± 290	10300 ± 340^{ns}	10100 ± 260^{ns}	10200 ± 220^{ns}
14th day	7200 ± 340	8200 ± 760*	9300± 330**	8000 ± 560*
28th day	6430± 330	8120 ± 430**	8650 ± 380**	7430 ± 230**

Values are mean ± standard deviation of six animals per group
^{ns} $p>0.05$, * $p<0.05$, ** $p<0.01$ between vehicle control + CTX (15mg/kg b. wt) and treated groups for different days

5.4. Discussion

This study evaluated the antitumour efficacy of the HE extract of *S. glauca* in transplantable tumour-bearing mice. Ascites and solid tumours were developed in mice by using EAC and DLA cells respectively. These cells are rapidly growing cancer cells with the ability to make local inflammatory responses. These inflammatory responses are followed by a sequence of reactions like the escalation of permeability of blood vessels, forceful oedema formation, cellular migration and finally, results in progressive ascetic fluid formation. The ascetic fluid thus formed plays a crucial role in tumour growth as it acts as a nutritional source for tumour cells. Antitumour activity evaluation of test compounds in mice with EAC and DLA cell inoculation is considered as effective and reliable (Kumar et al., 2014).

Antitumour activity of HE on ascites tumour was conducted in four different ways. In the first experiment, the drug was administered 24 hours after inoculation of the tumour. In the second experiment was assigned to see whether the earlier administration of HE can make any antitumour effect. So in this experiment, the animals were pre-treated with lower and higher doses of HE for five days before the inoculation of tumour and treatment was continued for ten consecutive days. The third experiment was designed to study the antitumour activity of HE in animals with serious tumour burden. The extract at different doses was administered to mice for ten days only after ten days of tumour inoculation. In order to assess the synergetic effect of HE with CTX, the fourth experiment was conducted. In this experiment, the animals were received various combinations of CTX with HEDE. In all experiments, the duration was fixed to 28 days. These experiment protocols were adopted for checking the antitumour activity of solid tumour bearing mice.

In ascites tumour studies, the HE treated tumour bearing mice showed a marginal increase in their life span and mean survival days. Prolongation of life period is an important and reliable measure for the primary evaluation of antitumour efficacy of a test material (Haldar et al., 2010). In control and vehicle control mice, EAC inoculation caused 100% mortality within 18 days. The maximum increase in the life span of animals was noted in experiment condition four were which the animals were treated with a combination of LDHE + various doses of CTX; like 15, 10 and 5 mg/kg b. wt. In these groups, the animals were survived even after 50 days of inoculation of

ascites tumour cells. In all other experimental conditions, the percentage increase in survival of animals was < 25% and standard drug used in respective experiments (CTX) found more effective than HE. As per the NCI criteria, it is asserted that in ascites tumour model of antitumour studies, if a test compound increases the life span of test animals by 25% or more over that of the control it may be considered with significant antitumour activity (Hazra et al., 2002). Treatment of HE at different doses in different experiment setup delayed the onset of mortality. Except for the fourth experiment condition, in rest all experiments consider together the LDHE showed a maximum percentage of increase in life span to 21.57% and HDHE showed a maximum of 23.53%. This result was obtained in the experiment were which the animals were pre-treated with the respective drugs for 5 days, before tumour inoculation. The mean survival capacity of animals in both LDHE and HDHE treated mice were found close to each other and were not significantly varied. So it is concluded that except experiment number four, the antitumour efficacy of HE extract is not favourable in relationship with CTX.

In solid tumour models, a similar trend was noted with respect to tumour volume, tumour weight, net body weight gain, etc. The HE, when administered with CTX (10 mg/kg b wt) made 25.30% inhibition of tumour weight on 28^{th} day of the experiment. In experiment setup two (five days pre-administration and ten days administration of drug after tumour inoculation), LDHE and HDHE showed 24.40% and 26.27% of tumour weight reduction respectively. These results suggest the antitumour potential of HE of *S. glauca*. The probable reason for obtaining such results is the stimulatory effect of HE on the immune system of mice. The results of experiment four indicated that HE is capable to inhibit the side effects of CTX when administered in combination. Results of haematological parameters validate the possible hypothesis mentioned regarding the potential action of HE.

In almost all experiment regimes, the total Hb count and leucocyte count were found lowering in control, vehicle control and standard drug-treated groups. The incidence of EAC and DLA induced anaemia was reported in mice by many researchers (Price and Greenfield, 1958, Kumar et al., 2014). It is well known that the development of anaemia is a trouble with the majority of the cancer chemotherapy drugs. The cause of anaemia in cancer is myelosuppression induced by chemotherapeutic agents (Thummar et al., 2015). The mice treated with different doses of HE showed a

protective effect in haemoglobin levels. Along with this the total leucocyte count in the HE treated group were found constant. This indicates that the HE protects the defensive mechanism of the body and reduces the tumour burden indirectly. If the HE had a direct toxic effect on tumour cells that could have reduced the Hb and WBC count by acting on bone marrow cells. The drastic reduction in Hb and total leucocyte count noted in CTX treated mice and this is because of the direct toxic effect of CTX on bone marrow precursors (Thummar et al., 2015).

Histopathological examinations of the section from the solid tumour of control and vehicle control animals revealed typical malignant features. Numerous cancer cells were found infiltrating to muscular tissue. This indicates the high proliferative action of DLA cells. More wide necrotic regions were noted in the tissues of mice belongs to control and vehicle control group with respect to HE and CTX treated mice.

In conclusion the *in vivo* experiments conducted to find the antitumour efficacy of HE extract of *S. glauca* indicate the therapeutic potential of this plant with no side effects. However, it is well clear that the HE prevent the development of solid and ascites tumor in mice and as result increase the life span of these animals. This may be due to its high antioxidant and anti-inflammatory potential of HE, which has been proved by different *in vitro* experiments in this study and also due the identification of phytomolecules possessing this potential. Even though, in already developed tumors the HE is not at all effective in reducing the tumor burden. So far, a cancer preventive potential not curative potential of *S. glauca* has been suggested by these results. This necessitates further studies *in vivo* to establish its antioxidant, anti-inflammatory and chemopreventive actions of HE.

Chapter 6

Antioxidant and anti-inflammatory aspects of *Simarouba glauca* DC

Contents

6.1. Introduction

6.2. Materials and methods

6.2.1. Animals

6.2.2. *In vivo* antioxidant activity analysis

6.2.2.1. Evaluation of the antioxidant activity of HE

6.2.2.2. Determination of the protective effect of HE on sodium fluoride-induced oxidative damage

6.2.2.3. Determination of the protective effect of HE on phorbol-12-merystate-13-acetate (PMA) induced superoxide radical scavenging activity

6.2.3. *In vivo* anti-inflammatory analysis

6.2.3.1. Carrageenan induced acute paw oedema in mice

6.2.3.2. Vascular permeability assessment by Evans blue dye extravasation method

6.2.3.3. Dextran induced acute paw oedema in mice

6.2.3.4. Formalin induced chronic paw oedema in mice

6.2.4. Statistical analysis

6.3. Results

6.3.1. *In vivo* antioxidant activity of HE

6.3.1.1. Antioxidant potentials of HE

6.3.1.2. Protective effect of HE on sodium fluoride-induced oxidative damage

6.3.1.3. Protective effect of HE on phorbol-12-merystate-13-acetate (PMA) induced superoxide radical scavenging activity

6.3.2. *In vivo* anti-inflammatory properties of HE

6.3.3.1. Effect of HE on carrageenan-induced acute paw oedema in mice

6.3.3.2. Effect of HE on extravasation of Evans blue dye

6.3.3.3. Effect of HE on dextran induced acute paw oedema in mice

6.3.3.4. Effect of HE on formalin-induced chronic paw oedema in mice

6.4. Discussion

6.1. Introduction

Antioxidants and prooxidants are substances they can prevent the damage induced by the ROS (Milkovic et al., 2014). Even though many synthetic antioxidants are widely used in nutrition, but their structural instability manifests serious side effects in the body (Chen et al., 1992). Botanicals are considered as the major source of natural antioxidants. Many plant compounds like phenolics, flavonoids, terpenoids, sesquiterpene lactones and coumarins are considered as excellent antioxidants (Augustyniak et al., 2010).

The data reported in the earlier chapter of this study (regarding phytochemical screening) of HE of *S. glauca* revealed that the presence of plant compounds which are considered as an excellent antioxidant and anti-inflammatory substances. Among the different phytochemicals detected polyphenols (flavonoids and phenolic acids) possess antioxidant, anti-inflammatory as well as anticancer activities (Hazafa et al., 2019). Along with polyphenols, the other plant compounds terpenoids, triterpenoids, alkaloids etc. detected also have a positive influence in cancer management. The chemopreventive action of terpenoids includes a combination of antioxidant, immune-enhancing, anti-inflammatory and anti-hormonal effects (Rabi and Bishayee, 2009). The different *in vitro* antioxidant studies are also showed a promising antioxidant action of HE. In this context, a detailed investigation on the HE for it's *in vivo* antioxidant and anti-inflammatory potential was planned to conduct. The study includes the evaluation of the antioxidant potential of HE in mice, the protective effect on the sodium fluoride (NaF) induced oxidative damage in mice and protective effect of HE on PMA induced superoxide radical scavenging activity in mice peritoneal macrophages. This chapter also includes experiments evaluating the anti-inflammatory potential of HE by using carrageenan and dextran induced acute and formalin-induced chronic inflammatory mice models.

6.2. Materials and methods

6.2.1. Animals

Female Swiss albino mice and male BALB/c mice were used for different *in vivo* antioxidant and anti-inflammatory studies. For evaluating the protective effect of HE on sodium fluoride-induced oxidative damage female Swiss albino mice (25 ± 3 gm)

were used. Male BALB/c mice (25-28 gm) were used for the evaluation of the protective effect of HE on Phorbol-12-myristate-13-acetate (PMA) induced superoxide radical scavenging activity. Male BALB/c mice (25-28 gm) were used to evaluate the *in vivo* anti-inflammatory activity of HE. The animals were maintained in standardized conditions and the animals were acclimatized for seven days before the commencement of the experiment. The experiments were conducted with the prior permission of IAEC (ACRC/IAEC/16-06/11).

6.2.2. *In vivo* antioxidant activity analysis

The *in vivo* antioxidant capacity of HE was analysed in three different ways.

6.2.2.1. Evaluation of the antioxidant activity of HE

The antioxidant activity of HE was evaluated as per the protocol of Liu et al. (2013). Female Swiss albino mice were used in this experiment. The HE was administered orally in two doses (LDHE: 160 mg/kg b. wt and HDHE: 260 mg/kg b. wt). The experiment lasted for thirty days. Antioxidant status of haemolysate, liver and kidney were analysed. The detailed procedure of this experiment is given in Chapter 2, section 2.2.9.1.

6.2.2.2. Determination of the protective effect of HE on sodium fluoride-induced oxidative damage

The protective effect of HE was determined by inducing oxidative stress in female Swiss albino mice using sodium fluoride (Nabavi et al., 2012). The oxidative damage was induced with sodium fluoride (600 ppm/L/day; 60 mg/100 mL), which provided along with the drinking water. Ascorbic acid (15 mg/kg b. wt) was used as the standard drug in this experiment. All the animals were administered with respective doses of drugs orally. The detailed protocol of the experiment is given in Chapter 2, section 2.2.9.2.

6.2.2.3. Determination of the protective effect of HE on phorbol-12-myristate-13-acetate (PMA) induced superoxide radical scavenging activity

Evaluation of the protective effect of HE on PMA induced superoxide radical production was studied as per the procedure explained in Chapter 2, section 2.2.9.3.

6.2.3. *In vivo* anti-inflammatory analysis

The *in vivo* anti-inflammatory activity of the HE was analysed by three different methods. Among these two were acute inflammatory models and the last one was a chronic inflammatory model. In all the methods, diclofenac (25 mg/kg b. wt, p.o.) was used as the standard. The vehicle control group were administered 200 μL of 1% propylene glycol orally. The drug was administered orally (p.o.) to the respective group of animals in the experiments.

6.2.3.1. Carrageenan induced acute paw oedema in mice

The detailed procedure regarding the anti-inflammatory action of HE on carrageenan-induced acute paw oedema in mice is explained in Chapter 2, section 2.2.10.1.

6.2.3.2. Vascular permeability assessment by Evans blue dye extravasation method

In this study, the paw oedema was induced by using carrageenan. The administration of Evans blue dye in mice body and determination of its concentration in the inflammation site were done according to the procedure explained in Chapter 2, section 2.2.10.2.

6.2.3.3. Dextran induced acute paw oedema in mice

The anti-inflammatory action of HE was analysed by using another acute paw oedema model in mice. In this experiment, dextran was used to induce oedema in hind paw of mice. The procedure of this experiment is narrated in Chapter 2, section 2.2.10.3.

6.2.3.4. Formalin induced chronic paw oedema in mice

Chronic model for the evaluation of the anti-inflammatory effect of HE was done by using formalin. (Refer to Chapter 2, section 2.2.10.4).

6.2.4. Statistical analysis

Values are expressed as mean ± SD of six animals per group. The data were analyzed by one way ANOVA and Dunnett post hoc test. The data were considered to be

significant at the $p<0.05$ level. The statistical analysis was done by Graph Pad Instat 3 software.

6.3. Results

6.3.1. *In vivo* antioxidant activity of HE

6.3.1.1. Antioxidant potentials of HE

The aim of this study was to investigate the influence of HE in the normal antioxidant system of normal animals over a period of thirty days. The blood and tissue (liver and kidney) Catalase, SOD and GSH levels found increasing in different doses of HE administered animals. The data obtained from the different treated groups were found comparable to the ascorbic acid, the standard drug used in this study.

The blood antioxidant status of HE administered animals were found improved during the study period (Figure 6.1). The catalase activity was noted 34.20 ± 0.87 U/gm Hb in the normal group and 34.13 ± 1.33 U/gm Hb in the vehicle group. In the standard group, the catalase activity was elevated to 38.59 ± 1.33 U/gm Hb and it was found significant ($p<0.01$). The catalase activity in the LDHE treated group was found 36.98 ± 1.78 U/gm Hb ($p<0.01$) and in HDHE the data was found 36.63 ± 1.25 ($p<0.05$) U/gm Hb with respect to the normal group. The SOD activity also showed a similar trend with respect to the administration of HE. The SOD activity was found 1.27 ± 0.08 U/gm Hb and 1.22 ± 0.04 U/gm Hb in normal and vehicle control group respectively. In LDHE and HDHE, the activity of SOD was detected as 1.39 ± 0.05 U/gm Hb and 1.37 ± 0.04 U/gm Hb. These values were significantly different ($p<0.01$) with respect to the normal group. SOD activity in the standard drug-treated group was 1.73 ± 0.04 U/gm Hb. The level of reduced glutathione in the blood of the normal group of animals was 7.48 ± 0.35 nmol/gm Hb. A little decrease in GSH was observed in the vehicle control group (7.18 ± 0.10 nmol/gm Hb) and it was found non-significant ($p>0.05$) with respect to the normal group. In the standard group, the value was increased up to 8.23 ± 0.14. The LDHE (8.34 ± 0.45 nmol/gm Hb) and HDHE (8.31 ± 0.35 nmol/gm Hb) administered group were produced a higher concentration of GSH than the standard group. GSH level observed in standard, LDHE and HDHE groups were statistically significant ($p<0.01$) from the normal group.

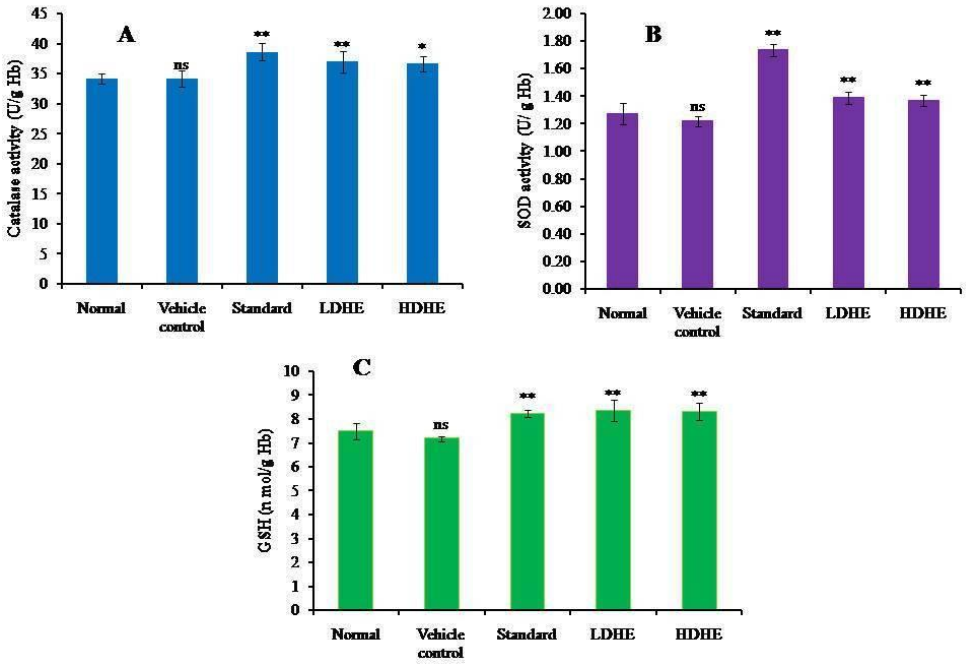

Figure 6.1. Effect of HE on the antioxidant status of blood: Female Swiss albino mice were given orally 200 μL of 1% propylene glycol; vehicle control, 200 μL of Ascorbic acid (15 mg/kg b. wt); HE at lower (160 mg/kg b. wt) and higher (260 mg/kg b. wt) dose over a period of thirty consecutive days. The animals were sacrificed and liver tissues were excised. The activity of A) catalase and B) superoxide dismutase and concentration of C) GSH were determined. Values are expressed as mean ± SD, ^{ns} $p>0.05$, * $p<0.05$, ** $p<0.01$ between normal and treated groups

The antioxidant status of the liver tissue after the administration of HE was examined in detail and the graphical representation of the result obtained is depicted in figure 6.2 and 6.3. A maximum increase in catalase activity was found in standard (13.31 ± 0.41 U/mg protein) followed by HDHE (11.98 ± 0.43 U/mg protein) and LDHE (11.95 ± 0.26 U/mg protein) and found significantly different from the normal group ($p<0.01$). The catalase activity in normal and vehicle control groups was 10.84 ± 0.43 U/mg protein and 10.50 ± 0.41 U/mg protein respectively. The activity of SOD was increased in standard (1.02 ± 0.06 U/mg protein), LDHE (1.00 ± 0.03 U/mg protein) and HDHE (1.00 ± 0.04 U/mg protein) with respect to normal group (0.91 ± 0.04 U/mg protein). The SOD activity in the vehicle control group was shown a marginal increase (0.92 ± 0.01 U/mg protein) but it was not significant with respect to normal group ($p>0.05$).

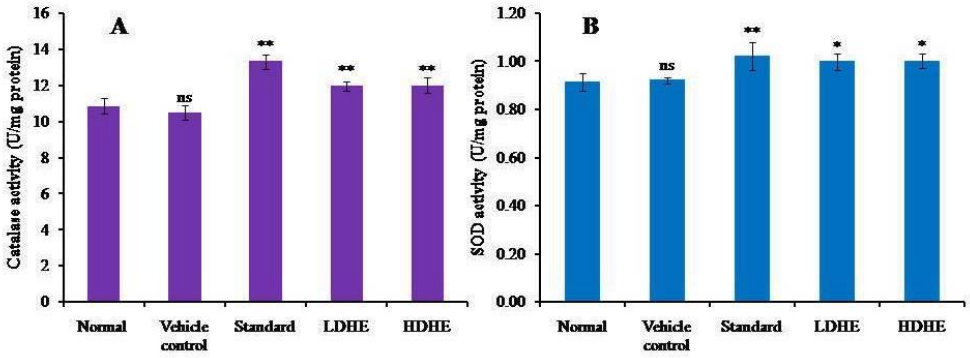

Figure 6.2. Effect of HE on the antioxidant status of liver: Female Swiss albino mice were given orally 200 μL of 1% propylene glycol; vehicle control, 200 μL of Ascorbic acid (15 mg/kg b. wt); HE at lower (160 mg/kg b. wt) and higher (260 mg/kg b. wt) dose over a period of thirty consecutive days. The animals were sacrificed and liver tissues were excised. The activity of A) catalase and B) superoxide dismutase were determined. Values are expressed as mean ± SD, ^{ns} $p>0.05$, * $p<0.05$, ** $p<0.01$ between normal and treated groups

The activity of another antioxidant enzyme GPx, evaluated in this study was showed a better response to HE administration. In the normal group, the GPx activity was found 33.32 ± 0.96 U/mg protein and in-vehicle control 32.38 ± 0.59 U/mg protein. In the ascorbic acid-treated group (standard) the activity was 43.35 ± 0.98 U/mg protein. The HE treated groups were exhibited a higher enzymatic activity which was 42.85 ± 0.73 U/mg protein and 42.50 ± 0.60 U/mg protein respectively in LDHE and HDHE groups. The values were found significant with respect to the normal group at $p<0.01$ level. The concentration of GSH molecule was found increased in LDHE (16.11 ± 0.72 nmol/mg protein) and HDHE (16.01 ± 0.52 nmol/mg protein) treated groups like standard drug administered group (18.08 ± 0.67 nmol/mg protein). The values were significantly different ($p<0.01$) from normal group (11.19 ± 0.58 nmol/mg protein). The GSH level was found lower in the vehicle control group (10.71 ± 0.87 nmol/mg protein) but it was not significant ($p>0.05$) with respect to the normal group. The inhibition of lipid peroxidation was found increased ($p<0.01$) as depicted in figure 6.3E in standard (1.12 ± 0.04 MDA nmol/mg protein), LDHE (1.17 ± 0.06 MDA nmol/mg protein) and HDHE (1.18 ± 0.04 MDA nmol/mg protein) when compared to normal (1.25 ± 0.03 MDA nmol/mg protein) and vehicle control (1.25 ± 0.02 MDA nmol/mg protein).

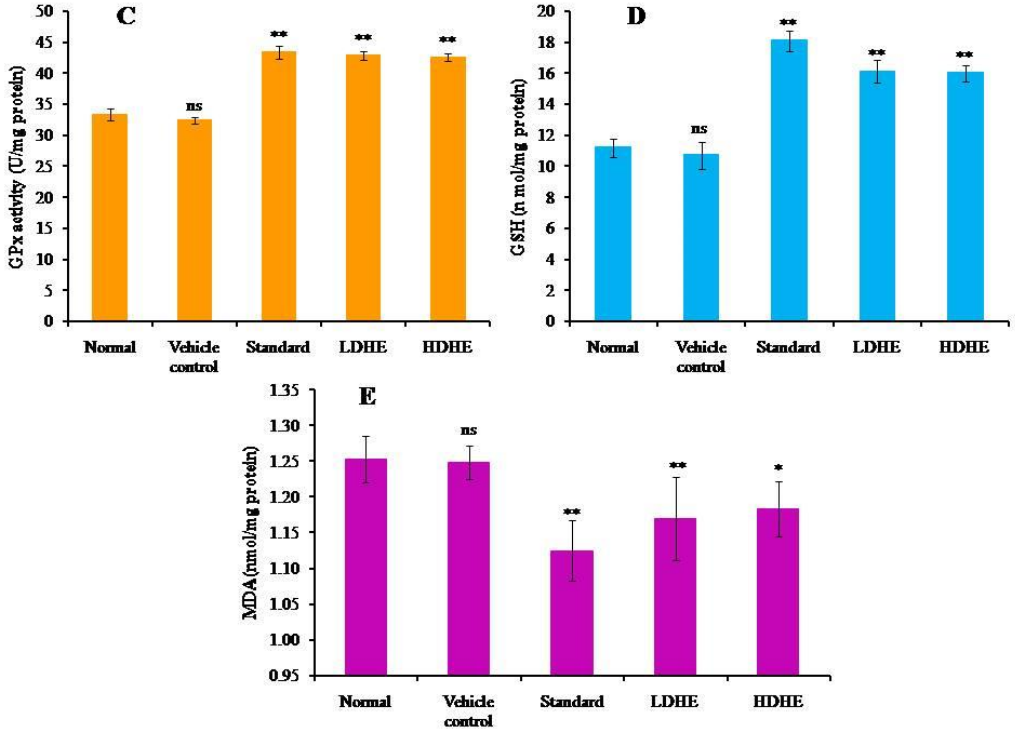

Figure 6.3. Effect of HE on the antioxidant status of liver: Female Swiss albino mice were given orally 200 μL of 1% propylene glycol; vehicle control, 200 μL of Ascorbic acid (15 mg/kg b. wt); HE at lower (160 mg/kg b. wt) and higher (260 mg/kg b. wt) dose over a period of thirty consecutive days. The animals were sacrificed and liver tissues were excised. The C) GPx, D) GSH and E) lipid peroxidation were determined. Values are expressed as mean ± SD, ^{ns} $p>0.05$, * $p<0.05$, ** $p<0.01$ between normal and treated groups

In kidney tissue, the administration of HE was found escalating its antioxidant status. The activity of catalase enzyme in the renal tissue was 23.41 ± 1.69 U/mg protein. The administration of standard drug increased catalase activity to 30.26 ± 0.23 U/mg protein, LDHE to 26.44 ± 0.74 U/mg protein and HDHE to 25.64 ± 1.55 U/mg protein. The catalase activity in the vehicle control group was found decreasing (21.71 ± 0.53 U/mg protein) but not significant at $p>0.05$ level. A similar response was noted in the activity for renal SOD. The data obtained in different treatment groups were as follows, standard (1.16 ± 0.06 U/mg protein), LDHE (1.14 ± 0.05 U/mg protein) and HDHE (1.14 ± 0.06 U/mg protein). The activity of SOD found significantly elevated from the normal group (1.02 ± 0.01 U/mg protein) at $p<0.01$ level.

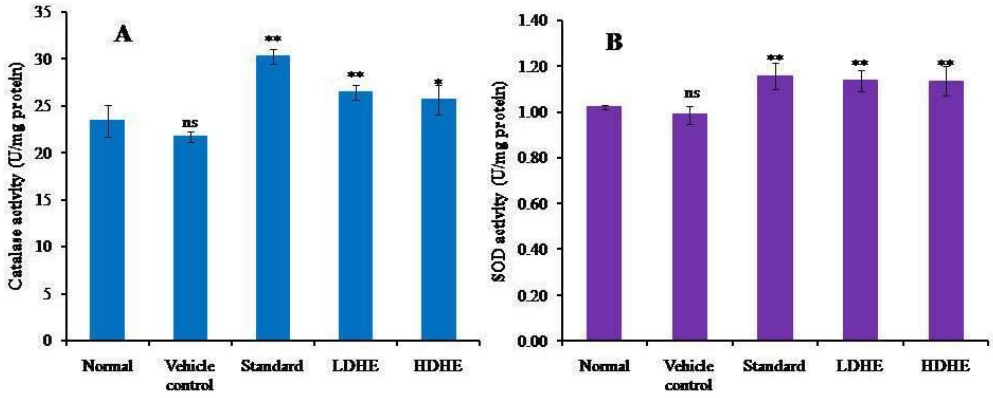

Figure 6.4. Effect of HE on the antioxidant status of kidney: Female Swiss albino mice were given orally 200 μL of 1% propylene glycol; vehicle control, 200 μL of Ascorbic acid (15 mg/kg b. wt); HE at lower (160 mg/kg b. wt) and higher (260 mg/kg b. wt) dose over a period of thirty consecutive days. The animals were sacrificed and liver tissues were excised. The activity of A) catalase and B) superoxide dismutase were determined. Values are expressed as mean ± SD, ^{ns} $p>0.05$, * $p<0.05$, ** $p<0.01$ between normal and treated groups

The renal tissue GPx activity was increased in LDHE (42.44 ± 2.21 U/mg protein) and HDHE (41.89 ± 1.96 U/mg protein) and standard group (43.83 ± 0.53 U/mg protein). These values were found significantly different ($p<0.01$) from the normal group (34.24 ± 1.54 U/mg protein). As depicted in figure 6.5 D, the GSH level was found rising in LDHE (17.22 ± 0.71 nmol/mg protein) and HDHE (17.60 ± 0.44 nmol/mg protein). The maximum level of GSH was noted in the standard group (18.30 ± 0.78 nmol/mg protein). The GSH level was 10.99 ± 0.68 nmol/mg protein in the vehicle control group and 10.90 ± 0.40 nmol/mg protein in the normal group. Regarding the lipid peroxidation, the MDA content in normal and vehicle control group was 3.10 ± 0.08 MDA nmol/mg protein and 3.16 ± 0.25 MDA nmol/mg protein. The lipid peroxidation rate was found decreasing in the standard administered group animals (2.98 ± 0.15 MDA nmol/mg protein). The MDA content was decreased in LDHE (2.32 ± 0.06 MDA nmol/mg protein) and HDHE (2.63 ± 0.11 MDA nmol/mg protein) treated animals and the values were found less than the standard group.

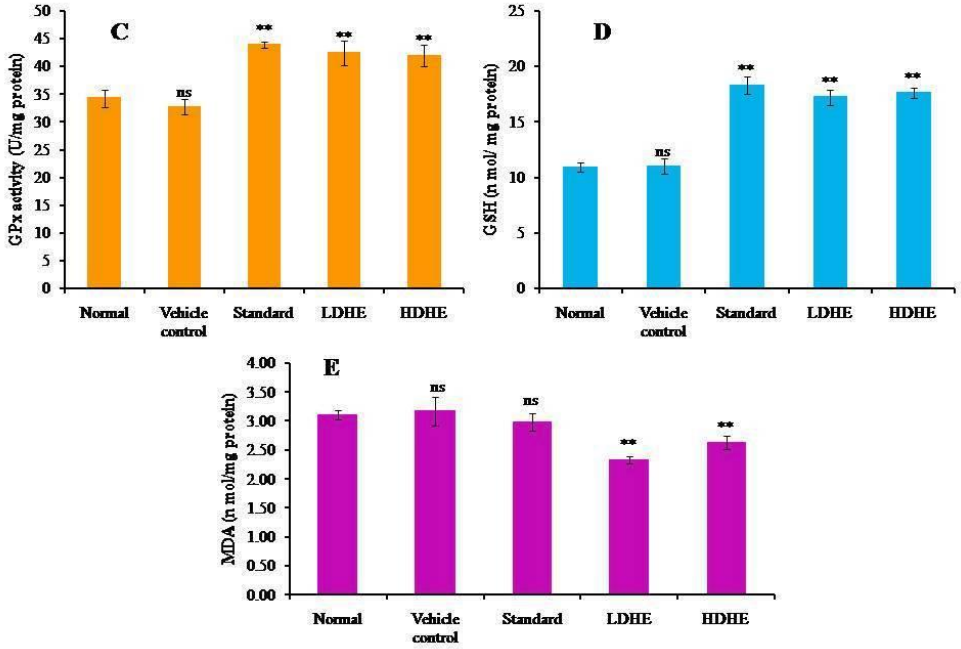

Figure 6.5. Effect of HE on the antioxidant status of kidney: Female Swiss albino mice were given orally 200 μL of 1% propylene glycol; vehicle control, 200 μL of Ascorbic acid (15 mg/kg b. wt); HE at lower (160 mg/kg b. wt) and higher (260 mg/kg b. wt) dose over a period of thirty consecutive days. The animals were sacrificed and liver tissues were excised. The activity of C) GPx, D) GSH concentration and E) lipid peroxidation rate were determined. Values are expressed as mean ± SD, ^{ns} $p>0.05$, ** $p<0.01$ between normal and treated groups

6.3.1.2. Protective effect of HE on sodium fluoride-induced oxidative damage

Compared to the control group, the antioxidant markers in the blood of drug-treated animals were elevated significantly ($p<0.01$) the levels of catalase, superoxide dismutase and reduced glutathione (Figure 6.6). The administration of NaF reduced the catalase activity in control group (24.37 ± 2.76 U/gm Hb) and vehicle control group (25.32 ± 2.34 U/gm Hb) in comparison with the normal group (54.53 ± 3.71 U/gm Hb). But the catalase activity was found significantly increased ($p<0.01$) in LDHE (43.85 ± 3.27 U/gm Hb) and HDHE (43.26 ± 4.35 U/gm Hb) along with the ascorbic acid (standard) administered animals (44.48 ± 2.50 U/gm Hb). The activity of catalase was found less in HDHE with respect to LDHE but, the values were found very close to each other. The superoxide dismutase activity was found elevated in the standard group (2.25 ± 0.12 U/gm Hb) which appeared close to the normal group (2.40 ± 0.16 U/gm Hb). Similar to the standard group, LDHE (1.67 ± 0.10 U/gm Hb) and HDHE (1.69 ± 0.06 U/gm Hb) showed a significant increase ($p<0.01$) in SOD

activity. The SOD activity in control group (0.78 ± 0.15 U/gm Hb) and vehicle control group (0.80 ± 0.18 U/gm Hb) was found very low when administered with NaF in comparison with the normal group (2.40 ± 0.16 U/gm Hb). The glutathione level was found decreased significantly ($p<0.01$) in control group (2.25 ± 0.15 nmol/gm Hb) and vehicle control group (2.44 ± 0.08 nmol/gm Hb) with respect to normal group (4.30 ± 0.14 nmol/gm Hb). The HE administered groups, LDHE (3.93 ± 0.32 nmol/gm Hb) and HDHE (3.53 ± 0.34 nmol/gm Hb) showed a significantly enhanced level ($p<0.01$) in the GSH. It was noted that LDHE was showed a marginal increase in the level of GSH in comparison to HDHE.

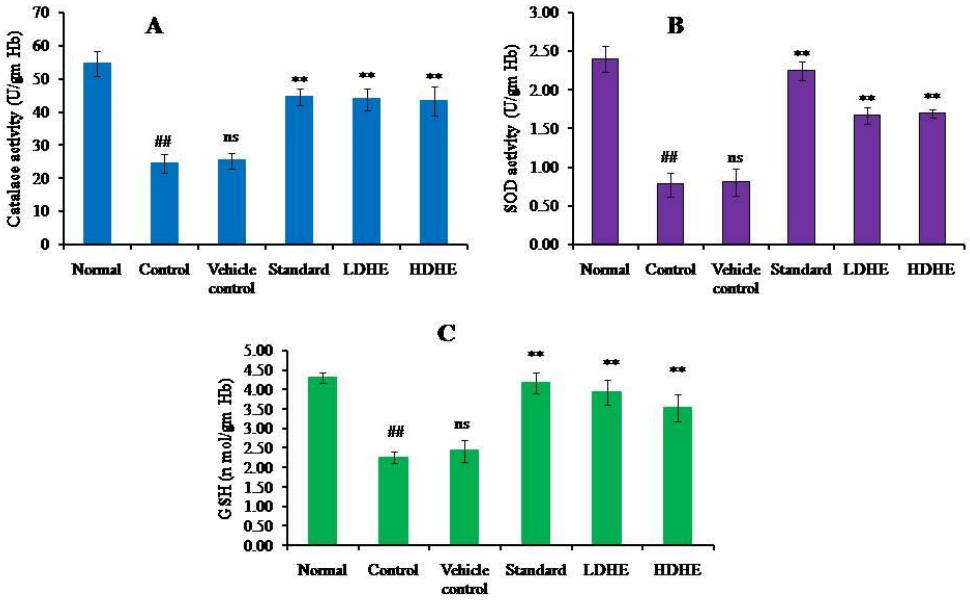

Figure 6.6. Protective effect of HE on the antioxidant status of blood following NaF-induced oxidative damage: A) catalase, B) superoxide dismutase and C) GSH. Normal; animals treated with 200 μL saline, control; animals administered with NaF (60 mg/ 100 mL) for seven days through drinking water, vehicle control: animals administered with 200 μL of 1% propylene glycol, standard: animals treated with 200 μL ascorbic acid (15 mg/kg b. wt, p.o.), LDHE: animals treated HE (160 mg/kg b. wt, p.o.), HDHE: animals treated with HE (260 mg/kg b. wt, p.o.). propylene glycol, standard, LDHE and HDHE were pre-administered for seven days and continued with NaF (60 mg/ 100 mL) for seven more days. Values are expressed as mean ± SD. ##: $p<0.01$ (control compared to normal), ^{ns}: $p>0.05$(vehicle control compared to control), **: $p<0.01$(standard, LDHE and HDHE compared to control)

Like in the blood, the antioxidant status of liver tissue was negatively affected by the administration of NaF but, the administration of standard and different doses of HE have proved their protective effect. The antioxidant enzyme catalase activity was found low in control (22.08 ± 2.87 U/mg protein) and vehicle control (23.12 ± 2.57

U/mg protein) after the administration of NaF. In the normal group, the catalase activity was noted at about 44.47 ± 2.22 U/mg protein. The administration of ascorbic acid could elevate the catalase activity up to 41.49 ± 3.33 U/mg protein (at $p<0.01$ level). The different doses of HE administered groups showed an increase in catalase activity in a dose-dependent manner. The catalase activity in LDHE treated mice was 32.57 ± 3.36 U/mg protein and it was found significant ($p<0.01$). A higher dose of HE (HDHE; 260 mg/kg b. wt) administered group resulted in a value of 38.08 ± 3.33 U/mg protein in this experiment. A similar response was noted in the activity of superoxide dismutase. The SOD activity was found 0.52 ± 0.12 U/mg protein and 0.50 ± 0.13 U/mg protein in control and vehicle control group respectively at the end of the experiment with respect to normal group (1.49 ± 0.17 U/mg protein). The administration of standard, LDHE and HDHE increased the SOD activity up to 1.41 ± 0.16, 1.33 ± 0.07 and 1.37 ± 0.10 U/mg protein respectively and the values were noted significant at $p<0.01$ level when compared with the control group.

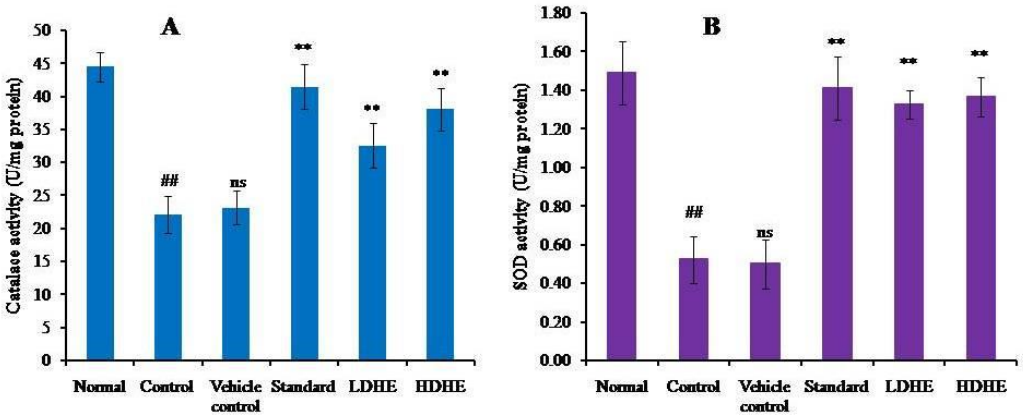

Figure 6.7. Protective effect of HE on the antioxidant status of the liver following NaF-induced oxidative damage: A) catalase and B) superoxide dismutase. Normal; animals treated with 200 μL saline, control; animals administered with NaF (60 mg/100 mL) for seven days through drinking water, vehicle control: animals administered with 200 μL of 1% propylene glycol, standard: animals treated with 200 μL ascorbic acid (15 mg/kg b. wt, p.o.), LDHE: animals treated HE (160 mg/kg b. wt, p.o.), HDHE: animals treated with HE (260 mg/kg b. wt, p.o.). propylene glycol, standard, LDHE and HDHE were pre-administered for seven days and continued with NaF (60 mg/100 mL) for seven more days. Values are expressed as mean ± SD. ##: $p<0.01$ (control compared to normal), ^{ns}: $p>0.05$(vehicle control compared to control), **: $p<0.01$(standard, LDHE and HDHE compared to control)

Activity status of antioxidant enzyme GPx and level of antioxidant molecule GSH in liver tissue were also showed a positive change when HE was administered along with NaF in mice. The lipid peroxidation was found decreased with respect to NaF administered animals (Figure 6.8). The GPx activity was found 34.10 ± 1.25 U/mg protein in the normal group. In the control group and vehicle control group the GPx activity was 19.88 ± 2.05 U/mg protein and 19.53 ± 2.13 U/mg protein respectively. Ascorbic acid used as a standard in this experiment could increase the said enzyme activity up to 31.35 ± 1.82 U/mg protein ($p<0.01$) with respect to the control group. The LDHE (28.19 ± 2.22 U/mg protein) and HDHE (28.94 ± 1.78) increased the GPx activity significantly at $p<0.01$ level with respect to control group of animals. It is noted that the activity of GPx of LDHE and HDHE group was close to each other. The antioxidant molecule reduced glutathione level was found lowered in control (7.89 ± 1.68 nmol/mg protein) and vehicle control group (8.96 ± 1.06 nmol/mg protein). The administration of standard drug (14.20 ± 2.12 nmol/mg protein) and lower (13.98 ± 1.21 nmol/mg protein) and higher doses (14.03 ± 1.38 nmol/mg protein) of HE made a significant increase ($p<0.01$) in the concentration of GSH with respect to control group and it was close to the normal group (15.36 ± 1.33 nmol/mg protein). The MDA content in liver tissue was significantly elevated in control group (0.85 ± 0.10 nmol MDA/mg protein) and vehicle control group (0.84 ± 0.02 nmol MDA/mg protein) of animals after NaF administration with respect to normal group (0.50 ± 0.04 nmol MDA /mg protein). In the standard drug-treated group the MDA concentration was noted to be 0.52 ± 0.06 nmol MDA/mg protein. The LDHE (0.54 ± 0.02 nmol MDA/mg protein) and HDHE (0.57 ± 0.02 nmol MDA/mg protein) were found low and close to the standard drug-treated group and were significantly ($p<0.01$) different from the control group.

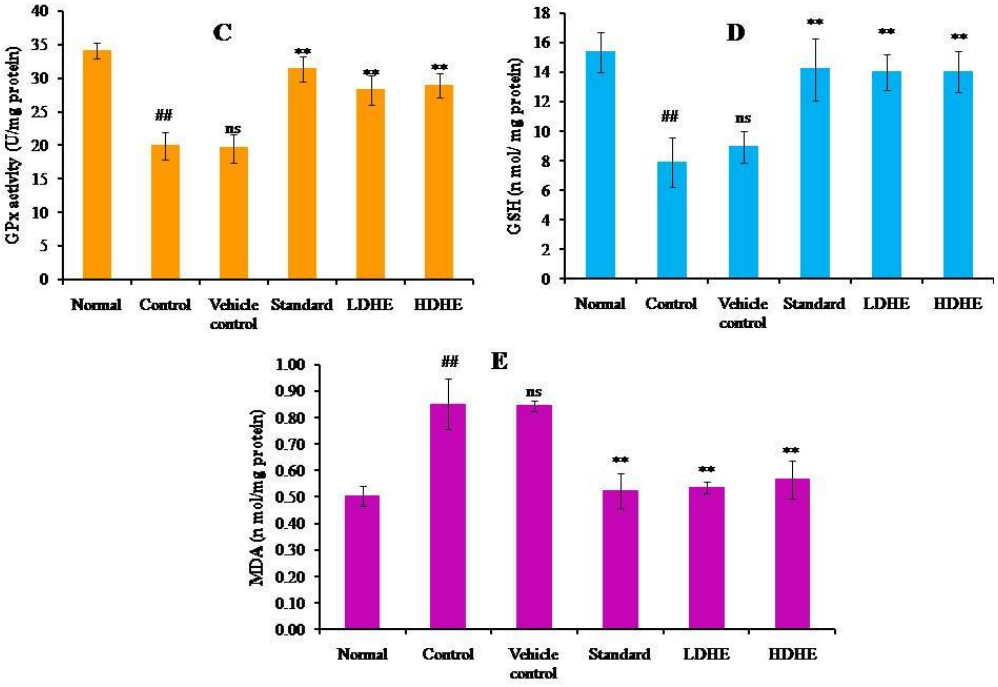

Figure 6.8. Protective effect of HE on the antioxidant status of the liver following NaF-induced oxidative damage: C) GPx, D) GSH, and E) lipid peroxidation. Normal; animals treated with 200 μL saline, control; animals administered with NaF (60 mg/100 mL) for seven days through drinking water, vehicle control: animals administered with 200 μL of 1% propylene glycol, standard: animals treated with 200 μL ascorbic acid (15 mg/kg b. wt, p.o.), LDHE: animals treated HE (160 mg/kg b. wt, p.o.), HDHE: animals treated with HE (260 mg/kg b. wt, p.o.) propylene glycol, standard, LDHE and HDHE were pre-administered for seven days and continued with NaF (60 mg/100 mL) for seven more days. Values are expressed as mean ± SD. ##: $p<0.01$ (control compared to normal), ^{ns}: $p>0.05$ (vehicle control compared to control), **: $p<0.01$(standard, LDHE and HDHE compared to control)

Histological examination of the liver tissue isolated from the control group and vehicle group animals showed damage in their architecture (Figure 6.9). Infiltration of blood cells was found in different regions of the liver tissue. Apart from the infiltration of blood cells, necrosis was observed in the control and vehicle control group indicating the severe destructive effect of NaF in liver tissue. Similar to the results of different biochemical tests mentioned earlier, the histological analysis of liver tissue samples taken from the LDHE and HDHE group mice have revealed their healing efficacy on the liver damage caused by NaF. The standard drug-treated mice liver tissue was also showed better curative action.

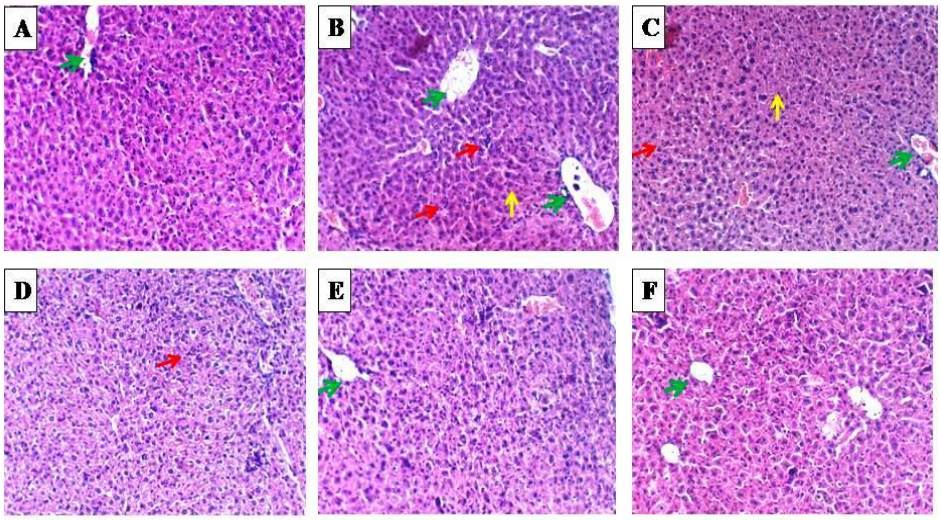

Figure 6.9. Protective effect of HE on the histology of the liver following NaF-induced oxidative damage: A) normal, B) control C) vehicle control, D) standard, E) LDHE and F) HDHE. Normal; animals treated with 200 μL saline, control; animals administered with NaF (60 mg/100 mL) for seven days through drinking water, vehicle control: animals administered with 200 μL of 1% propylene glycol, standard: animals treated with 200 μL ascorbic acid (15 mg/kg b. wt, p.o.), LDHE: animals treated HE (160 mg/kg b. wt, p.o.), HDHE: animals treated with HE (260 mg/kg b. wt, p.o.). propylene glycol, standard, LDHE and HDHE were pre-administered for seven days and continued with NaF (60 mg/100 mL) for seven more days. All histological micrographs were stained with haematoxylin and eosin (H & E) and observed under 200X. The green arrow represents central vein, the red arrow denotes blood cell infiltration, and the yellow arrow indicates necrosis

6.3.1.3. Protective effect of HE on phorbol-12-myristate-13-acetate (PMA) induced superoxide radical scavenging activity

PMA induced superoxide radicals in mice macrophages, which was induced by sodium caseinate provided with another reliable data regarding the antioxidant efficacy of different doses of HE. The LDHE (160 mg/kg b. wt) showed 74.18% efficacy in inhibiting superoxide radical generation The administration of HDHE (260 mg/kg b. wt) was effective in producing 73.57% (which is close to the value of LDHE), efficacy in inhibition of superoxide radical generated in the macrophages in mice peritoneum. Both the values were found significant ($p<0.01$) with the control group. The vehicle control group showed a minimum action (4.81%) and was found insignificant with control group data (Figure 6.10 and Table 6.1).

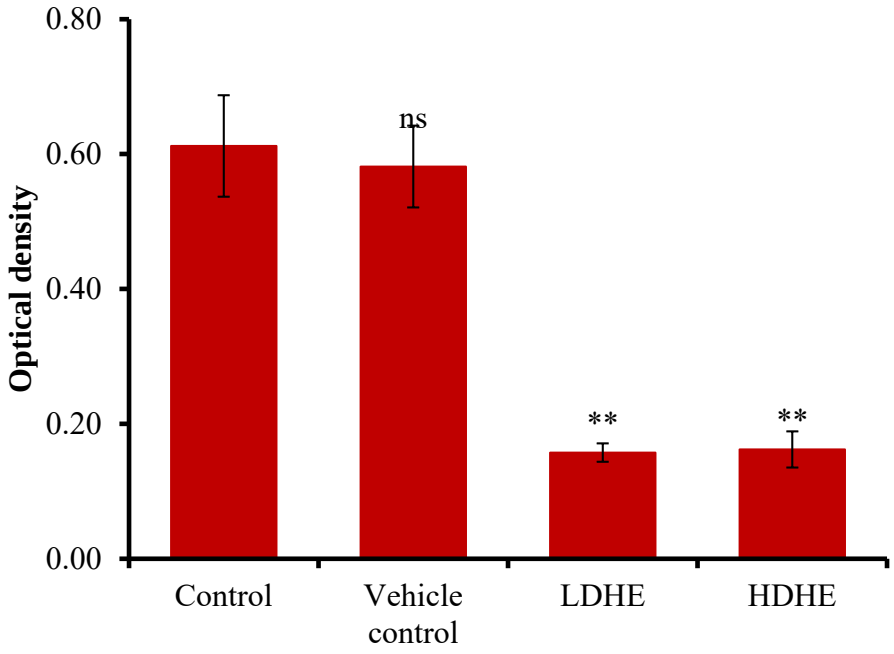

Figure 6.10. Effect of HE on PMA-induced superoxide radical generation in mice peritoneal macrophages: control group: animals treated with 200 μL of saline, vehicle control: animals treated with given 200 μL 1% propylene glycol (p.o), LDHE: animals treated with 200 μL of HE (160 mg/kg b. wt (p.o.)) and HDHE: animals treated with 200 μL of HE (260 mg/kg b. wt., (p.o)). All animals in vehicle control, LDHE and HDHE were administered with respective drugs for five consecutive days. On the first day, 200 μL of sodium caseinate (5% intraperitoneal) was injected to each animal elicit peritoneal macrophages. On fifth day the peritoneal macrophages were activated *in vivo* by injecting 100 μL PMA (100 ng/animal, i.p.). After three hours macrophages were collected by injecting 5 mL of PBS into the peritoneal cavity. Values are expressed as mean ± SD. ^{ns} $p>0.05$, ** $p<0.01$ between control and treated groups

Table 6.1. Percentage inhibition by HE on PMA induced superoxide radical generation in mice peritoneal macrophages

Group	Percentage inhibition
Vehicle control (1% propylene glycol)	4.81 ± 0.15^{ns}
LDHE (160 mg/kg b. wt)	$74.18 \pm 1.77^{**}$
HDHE (260 mg/kg b. wt)	$73.57 \pm 2.20^{**}$

Values are expressed as mean ± SD
^{ns} $p>0.05$, ** $p<0.01$ between vehicle control and treated groups

6.3.2. *In vivo* anti-inflammatory properties of HE

6.3.3.1. Effect of HE on carrageenan-induced acute paw oedema in mice

Administration of 160 and 260 mg/kg b. wt of HE of *S. glauca* made a significant reduction on paw oedema induced by carrageenan. One hour before injecting the carrageenan the right hind paw thickness of mice in all groups together was 1.76 ± 0.02 mm. While injecting carrageenan the paw thickness was increased to an average of 3.16 ± 0.25 mm at 0 hour. The paw thickness was found decreasing in LDHE and HDHE administered animals. The percentage of oedema formation in 3rd hr after intraplantar injection of carrageenan was 43.70 and 39.51% in LDHE and HDHE groups respectively compared to the control group. The percentage inhibition in diclofenac treated group was found to be 42.72% during the same time (Figure 6. 11 & Table 6a). The oedema was found decreasing in all the treated groups up to the 6th hour. At 6th hour an average paw thickness of 1.93 ± 0.04 mm (72.36% of inhibition) of oedema was noted in the standard group. The percentage inhibition of oedema was 79.40 (1.84 ± 0.09 mm paw thickness) and 73.37% (1.97 ± 0.05 paw thickness) respectively in LDHE and HDHE group. The morphological changes occurred in the right hind paw of mice at the third hour of the paw oedema is depicted in figure 6.12. The histological examination conducted in the skin tissue of right hind paw of mice from the experiment groups confirmed the anti-inflammatory potential of HE. In control and vehicle control group, infiltration of inflammatory cells was prominent but such infiltration was minimum in HE and standard drug-treated groups. The alternations occurred in tissue architecture was compared with the help of a skin tissue isolated from normal mice.

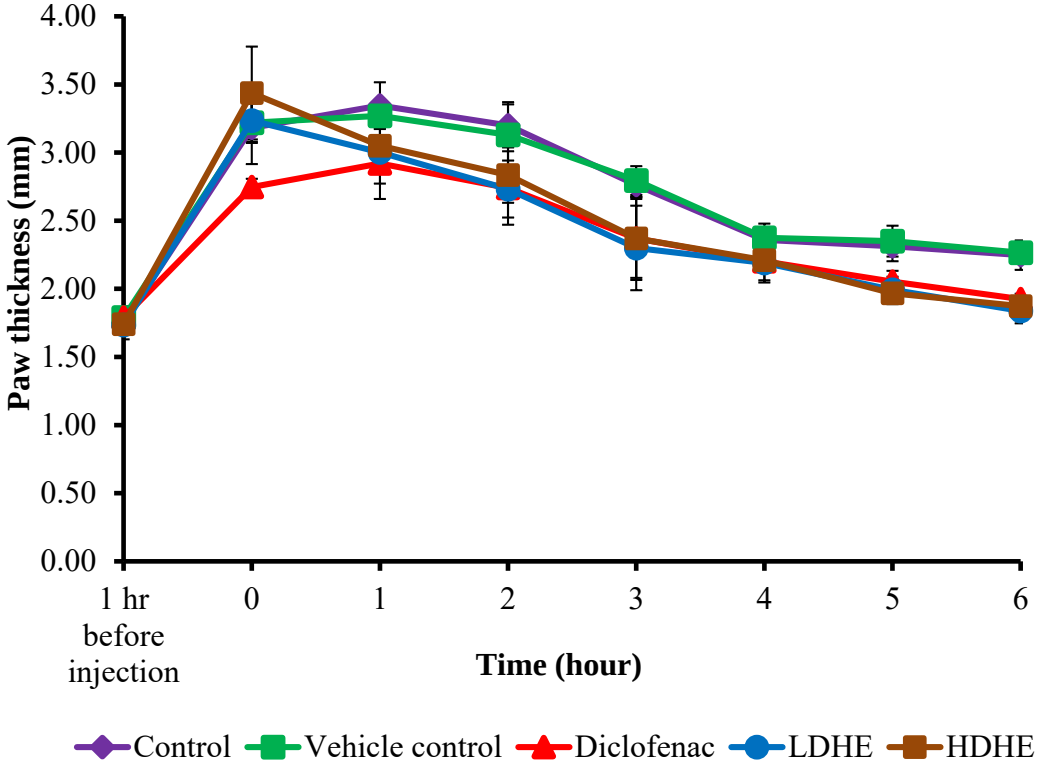

Figure 6.11. *In vivo* anti-inflammatory effect of HE on carrageenan-induced acute paw oedema in mice: control: animals treated 200 μL saline and injected carrageenan, vehicle control: animals treated with 200 μL 1% propylene glycol/ animal/ day, diclofenac (standard): animals treated with diclofenac (25 mg/kg b. wt), LDHE and HDHE were treated 160 mg and 260 mg/kg b. wt of HE respectively. The animals were pre-treated doses of respective drug or diclofenac or propylene glycol, orally for four consecutive days. On 5th day 1 hour after saline or HE or diclofenac or propylene glycol administration in respective groups, the inflammation was induced by intraplantar injection of 0.05 mL of 1% carrageenan in 0.1% CMC into the right hind paw of the all animals. Paw thickness was measured using vernier caliper, 1 hour prior and for every hour up to 6th hour after carrageenan injection. Values are expressed as mean ± SD of six animals per group.

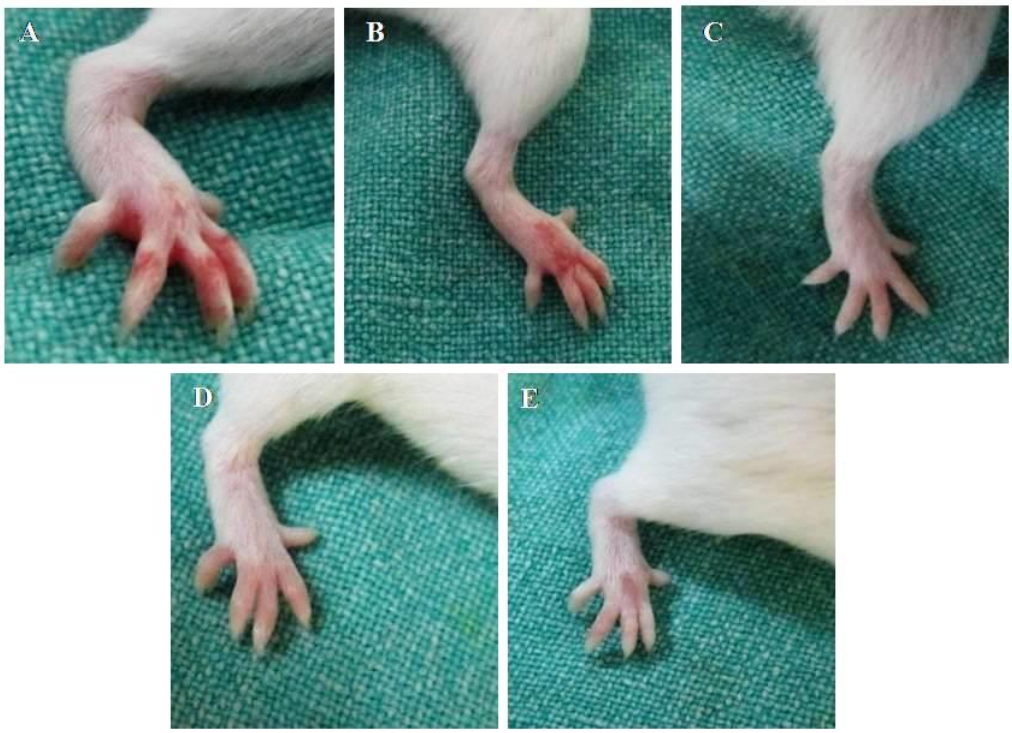

Figure 6.12. Morphological changes occurred at the third hour on the hind paw of mice belongs to various experimental groups in acute oedema induced by carrageenan: A) control: animals treated with 200 μL saline and injected carrageenan, B) vehicle control: animals treated with 200 μL 1% propylene glycol/ animal/ day, C) diclofenac (standard): animals treated with diclofenac (25 mg/kg b. wt), D) LDHE and E) HDHE were treated 160 mg and 260 mg/kg b. wt of HE respectively. The animals were pre-treated with doses of respective drug or diclofenac or propylene glycol, orally for four consecutive days. On 5th day 1 hour after saline or HE or diclofenac or propylene glycol administration in the respective groups, the inflammation was induced by intraplantar injection of 0.05 mL of 1% carrageenan in 0.1% CMC into the right hind paw of the all animals.

Table 6.2. Anti-inflammatory effect (% inhibition) of HE of *S. glauca* in comparison with other treatments on carrageenan-induced acute paw oedema in mice

Category	**Time (hour)**					
	1	**2**	**3**	**4**	**5**	**6**
Vehicle control (1 % propylene glycol)	7.21 ± 0.04	7.59 ± 0.27	0.74 ± 0.06	4.10 ± 0.27	0.44 ± 0.08	4.52 ± 0.18
Diclofenac (25 mg/kg b. wt)	29.00 ± 1.79**	34.31 ± 1.35**	42.72 ± 1.11**	32.38 ± 2.00**	53.33 ± 1.86**	72.36 ± 1.89**
LDHE (160 mg/kg b. wt)	20.53 ± 1.75**	31.21 ± 1.79**	43.70 ± 2.93**	25.41 ± 3.11**	54.22 ± 3.40**	79.40 ± 4.83**
HDHE (260 mg/kg b. wt)	18.18 ± 1.80**	24.48 ± 2.41**	39.51 ± 1.91**	22.95 ± 1.65**	59.56 ± 2.33**	73.37 ± 2.39**

** $p<0.01$ between control and treated groups

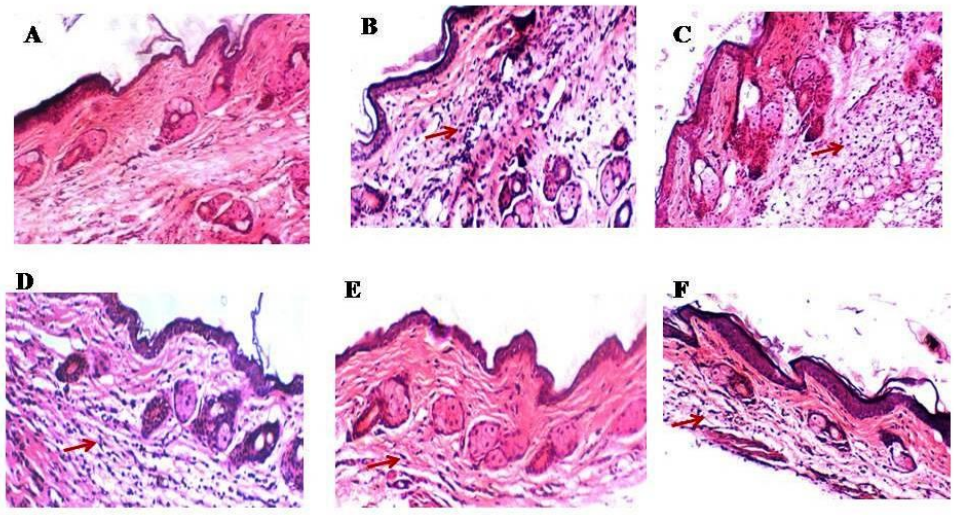

Figure 6.13. Anti-inflammatory effect of HE on histological changes in skin tissue of the plantar region of mouse paw: control: animals treated with 200 μL saline and injected carrageenan, vehicle control: animals treated with 200 μL 1% propylene glycol/ animal/ day, diclofenac (standard): animals treated with diclofenac (25 mg/kg b. wt), LDHE and HDHE were treated 160 mg and 260 mg/kg b. wt of HE respectively. The animals were pre-treated with doses of respective drug or diclofenac or propylene glycol, orally for four consecutive days. On 5th day 1 hour after saline or HE or diclofenac or propylene glycol administration, inflammation was induced by intraplantar injection of 0.05 mL of 1% carrageenan in 0.1% CMC into the right hind paw of the all animals. After the experiment the animals were sacrificed and the paw tissue was collected. It was kept in 10% neutral buffered formalin and histopathological analysis was conducted. The tissue architecture were analysed with respect to normal and control with treatment groups. Red arrow indicates the infiltration of inflammatory cells (H & E staining, 200X)

6.3.3.2. Effect of HE on extravasation of Evans blue dye

Anti-inflammatory effect of HE on the extravasation of Evans blue dye in oedema induced by carrageenan was conducted. A morphological change observed in the paw tissue of different group of animals in this experiment is depicted in figure 6.14. It was found that the diclofenac and HE extracts significantly reduced ($p<0.01$) extravasation of Evans blue dye in the paw of mice. The percentage inhibition of the retention of Evans Blue dye in the paw tissue of vehicle control (1% propylene glycol) administered animals were found to be 3.48 %. The percentage inhibition of the retention of Evans Blue dye in the paw tissue of standard drug, LDHE and HDHE treated mice were found 86.77%, 80.78% and 82.04% respectively with respect to control group. Data obtained during the quantification of Evans Blue dye extracted

from carrageenan-induced paw oedema of mice belong to different groups is given in figure 6.15a and 6.15b.

Figure 6.14. Morphological changes occurred on the hind paw of mice belongs to various experimental groups in the Evans blue extravasation assay: A) control, animals treated with 200 μL of saline and injected carrageenan B) vehicle control: animals administered 200 μL 1% propylene glycol, C) diclofenac: animals treated with diclofenac (standard: 25 mg/kg b. wt), D) LDHE E) HDHE: animals administered 160 mg and 260 mg/kg b. wt of HE respectively. The animals in particular group were pre-treated with respective doses of drug or diclofenac or propylene glycol, or saline (p.o) for four consecutive days. On 5th day 1 hr after HE or diclofenac or propylene glycol administration, inflammation was induced by intraplantar injection of 0.05 mL of 1% carrageenan in 0.1% CMC into the right hind paw of all the animals. Evans blue dye (25 mg/ kg b. wt) was injected into the tail vein of all mice after 3.5 hours of carrageenan injection. Photographs of the right hind paw of all animals were taken 30 minutes after Evans blue dye injection

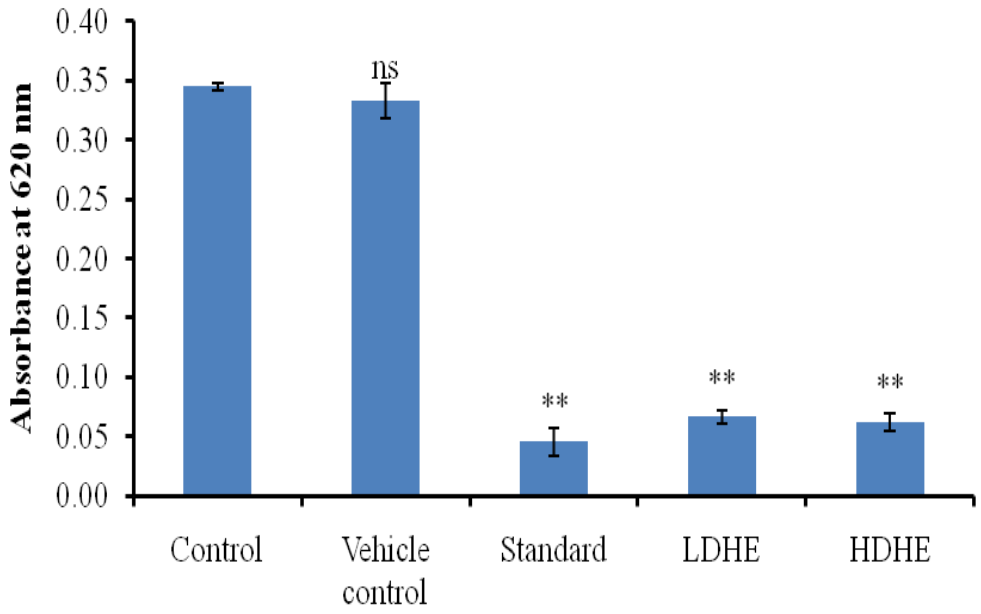

Figure 6.15a. Quantification of Evans blue dye extracted from carrageenan-induced paw oedema in mice from various groups: A) control, animals treated with 200 μL of saline and injected carrageenan B) vehicle control: animals administered 200 μL 1% propylene glycol, C) diclofenac: animals treated with diclofenac (standard: 25 mg/kg b.wt), D) LDHE E) HDHE: animals administered 160 mg and 260 mg/kg b. wt of HE respectively. The animals in particular group were pre-treated with respective doses of drug or diclofenac or propylene glycol, or saline (p.o) for four consecutive days. On 5th day 1 hr after HE or diclofenac or propylene glycol administration, inflammation was induced by intraplantar injection of 0.05 mL of 1% carrageenan in 0.1% CMC into the right hind paw of all the animals. Evans blue dye (25 mg/ kg b. wt) was injected into the tail vein of all mice after 3.5 hours of carrageenan injection. After 4 hours of carrageenan injection, all animals were sacrificed by cervical dislocation and paw tissues were dissected and an equal weight of paw tissue from each mouse was sliced out. The paw tissue was homogenized in 1.0 mL of acetone and 1% sodium sulfate prepared in a ratio of 4:1 and incubated for 24 hours at 37^{o}C. This procedure allowed the extraction of Evans blue dye from the paw tissues. The solution containing tubes were centrifuged at 2000 rpm for 10 minutes and supernatants were collected and the absorbance was determined at 620 nm using a spectrophotometer. Values are expressed as mean ± SD of six animals per group. ^{ns} $p>0.05$, ** $p<0.01$ between control and treated groups

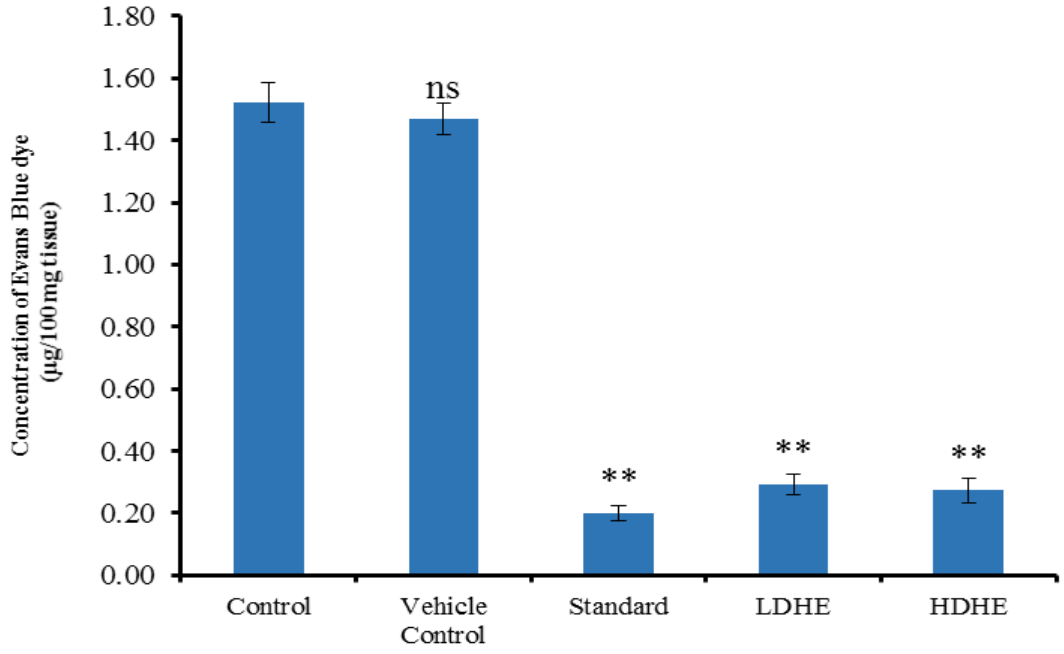

Figure 6.15b. Quantification of Evans blue dye extracted from carrageenan-induced paw oedema in mice from various groups: A) control, animals treated with 200 μL of saline and injected carrageenan B) vehicle control: animals administered 200 μL 1% propylene glycol, C) diclofenac: animals treated with diclofenac (standard: 25 mg/kg b. wt), D) LDHE E) HDHE: animals administered 160 mg and 260 mg/kg b. wt of HE respectively. The animals in particular group were pre-treated with respective doses of drug or diclofenac or propylene glycol, or saline (p.o) for four consecutive days. On 5th day 1 hr after HE or diclofenac or propylene glycol administration, inflammation was induced by intraplantar injection of 0.05 mL of 1% carrageenan in 0.1% CMC into the right hind paw of all the animals. Evans blue dye (25 mg/ kg b. wt) was injected into the tail vein of all mice after 3.5 hours of carrageenan injection. Values are expressed as mean ± SD of six animals per group. After 4 hours of carrageenan injection, all animals were sacrificed by cervical dislocation and paw tissues were dissected and an equal weight of paw tissue from each mouse was sliced out. The paw tissue was homogenized in 1.0 mL of acetone and 1% sodium sulfate prepared in a ratio of 4:1 and incubated for 24 hours at 37°C. This procedure allowed the extraction of Evans blue dye from the paw tissues. The solution containing tubes were centrifuged at 2000 rpm for 10 minutes and supernatants were collected and the absorbance was determined at 620 nm using a spectrophotometer. ^{ns} $p>0.05$, ** $p<0.01$ between control and treated groups

6.3.3.3. Effect of HE on dextran induced acute paw oedema in mice

In this acute oedema model, the HE administration inhibited the paw oedema caused by dextran. Compared to the control group, on the third hour of dextran administration, the percentage inhibition in LDHE group was 29.35% and HDHE group was 28.67% (Table 6.3). In diclofenac (25 mg/kg b. wt) treated group percentage inhibition was found to be 38.15% at the same duration of time. Only

6.32% of inhibition was noted in the vehicle control group on the 3rd hour of dextran administration. At the 6th hour of dextran administration, the percentage inhibition in the vehicle control group was found 0.65%. In the standard, LDHE and HDHE administered groups; the percentage inhibition was 71.66%, 49.84% and 43.3% respectively. Figure 6. 16 represents the *in vivo* anti-inflammatory effect of HE on dextran induced acute paw oedema in mice.

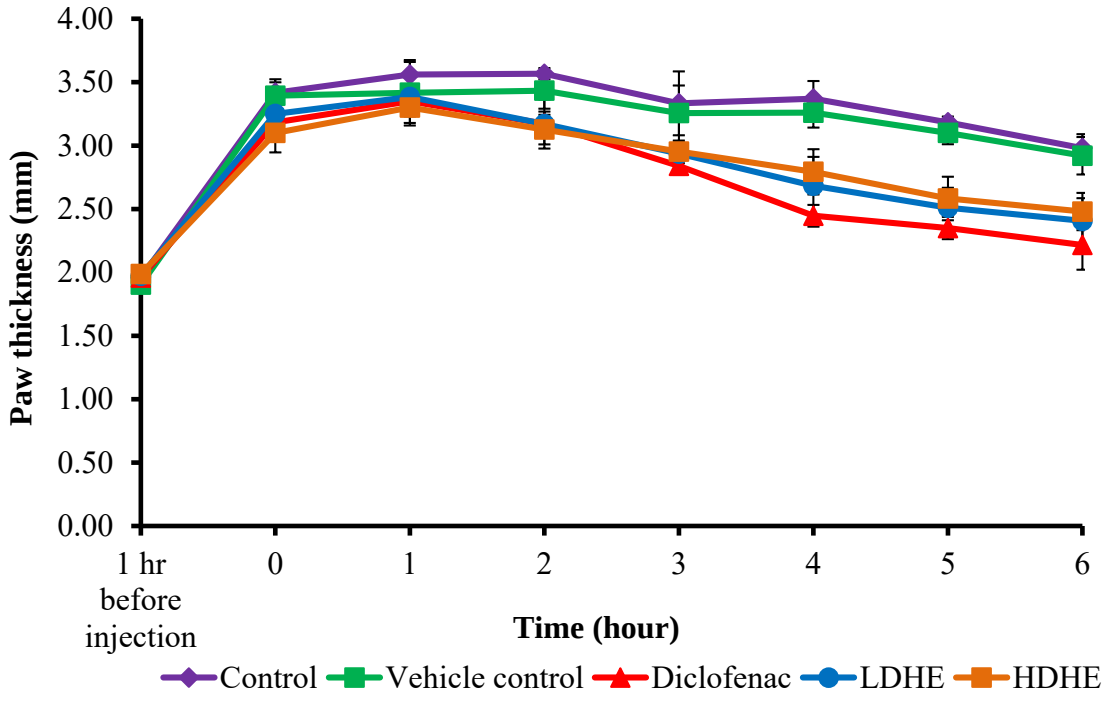

Figure 6.16. *In vivo* anti-inflammatory effect of HE on dextran induced acute paw oedema in mice: control: animals treated 200 μL saline and injected dextran, vehicle control: animals treated with 200 μL 1% propylene glycol/ animal/ day, diclofenac (standard): animals treated with diclofenac (25 mg/kg b. wt), LDHE and HDHE were treated 160 mg and 260 mg/kg b. wt of HE respectively. The animals were pre-treated doses of respective drug or diclofenac or propylene glycol, orally for four consecutive days. On 5th day 1 hour after saline or HE or diclofenac or propylene glycol administration in respective groups, the inflammation was induced by intraplantar injection of 0.05 mL of 1% dextran in 0.1% CMC into the right hind paw of the all animals. Paw thickness was measured using vernier caliper, 1 hour prior and for every hour up to 6th hour after carrageenan injection. Values are expressed as mean ± SD of six animals per group.

Table 6.3. Anti-inflammatory effect (% inhibition) of HE of *S. glauca* in comparison with other treatments on dextran induced acute paw oedema in mice

Category	Time (hour)					
	1	**2**	**3**	**4**	**5**	**6**
Vehicle control (1 % propylene glycol)	5.61	4.97	6.32	4.01	2.45	0.65
Diclofenac (25 mg/kg b. wt)	11.23	22.57	38.15	53.77	65.49	71.66
LDHE (160 mg/kg b. wt)	7.07	20.70	29.35	44.10	49.73	49.84
HDHE (260 mg/kg b. wt)	12.68	23.81	28.67	36.79	44.29	43.32

6.3.3.4. Effect of HE on formalin-induced chronic paw oedema in mice

Administration of HE inhibited the chronic paw oedema caused by intraplantar injection of formalin compared to control (Figure 6.17 and 6.18). During the third day, the percentage inhibition in LDHE treated group was 21.60% and HDHE group was 20.61%. Diclofenac (25 mg/kg b. wt) treated group was shown 26.43% inhibition in paw thickness. But on the sixth day of formalin injection, drug-treated groups were showed 44.39% and 39.39% inhibition in LDHE and HDHE respectively. In the same time interval, the diclofenac treated group showed 42.63% reduction in chronic inflammation (Table 6. 4). Histological observations were confirmed the anti-inflammatory action of various doses of HE extract (Figure 6. 19). The infiltration of inflammatory cells was found less in standard; LDHE and HDHE treated groups in comparison with control and vehicle control groups.

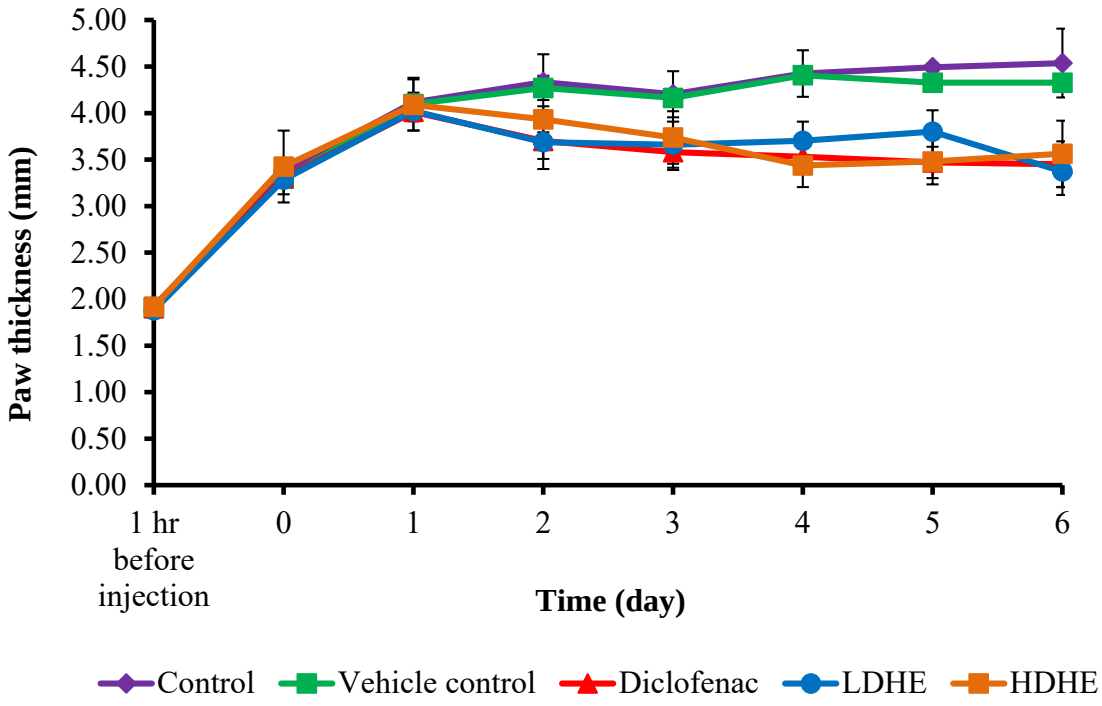

Figure 6.17. *In vivo* anti-inflammatory effect of HE on formalin-induced chronic paw oedema in mice: control: animals treated 200 μL saline and injected formalin, vehicle control: animals treated with 200 μL 1% propylene glycol/ animal/ day, diclofenac (standard): animals treated with diclofenac (25 mg/kg b. wt), LDHE and HDHE were treated 160 mg and 260 mg/kg b. wt of HE respectively. They animals were pre-treated orally, for 7 consecutive days with respective drug doses or (25 mg/kg b. wt; standard) or propylene glycol (1% propylene glycol; vehicle control). On the 8th day, chronic inflammation was induced by intraplantar injection of 0.05 mL of 1% formalin on the right hind paw of all animals 1 hour after HE or diclofenac or propylene glycol administration. The oral administration of drug or diclofenac or propylene glycol continued for six consecutive days. Paw thickness was measured using vernier caliper, 1 hour prior and continued for the next 6 consecutive days after formalin injection. Values are expressed as mean ± SD of six animals per group

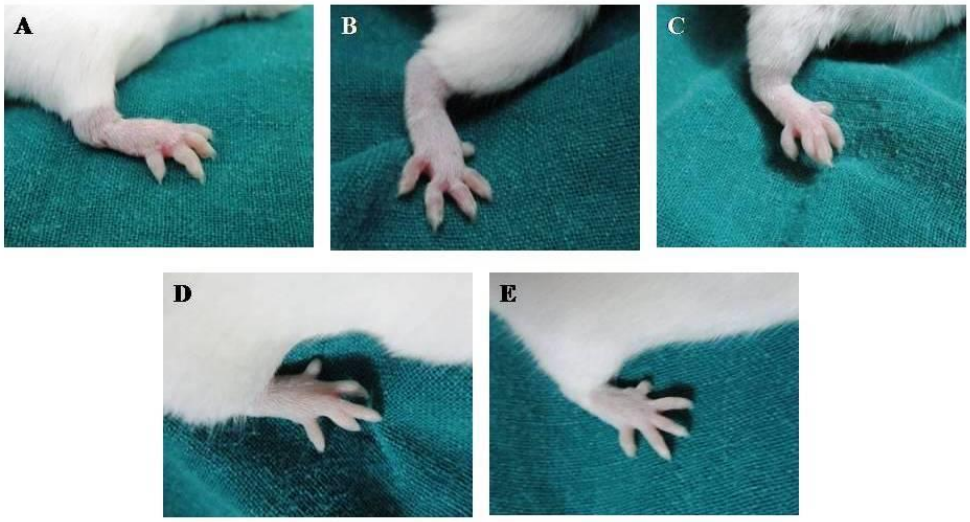

Figure 6.18. Morphological changes occurred on the hind paw of mice belongs to various experimental groups in chronic oedema induced by formalin: A) control, B) vehicle control, C) standard (diclofenac, 25 mg/kg b. wt), D) LDHE and E) HDHE A) control: animals treated 200 μL saline and injected formalin, B) vehicle control: animals treated with 200 μL 1% propylene glycol/ animal/ day, C) diclofenac (standard): animals treated with diclofenac (25 mg/kg b. wt), D) LDHE and E) HDHE were treated 160 mg and 260 mg/kg b. wt of HE respectively. They animals were pre-treated orally, for 7 consecutive days with respective drug doses or (25 mg/kg b. wt; standard) or propylene glycol (1% propylene glycol; vehicle control). On the 8th day, chronic inflammation was induced by intraplantar injection of 0.05 mL of 1% formalin on the right hind paw of all animals 1 hour after HE or diclofenac or propylene glycol administration. The oral administration of drug or diclofenac or propylene glycol continued for six consecutive days. Photographs of the right hind paw of all animals were taken at the end of the experiment

Table 6.4. Anti-inflammatory effect (% inhibition) of HE of *S. glauca* in comparison with other treatments on formalin-induced chronic paw oedema in mice

Category	Time (day)					
	1	2	3	4	5	6
Vehicle control (1 % propylene glycol)	0.11	1.94	1.02	0.10	5.84	10.29
Diclofenac (25 mg/kg b. wt)	3.76	25.41	26.43	34.97	39.01	42.63
LDHE (160 mg/kg b. wt)	1.94	24.69	21.60	26.87	25.00	44.39
HDHE (260 mg/kg b. wt)	1.48	16.80	20.61	39.66	40.08	39.39

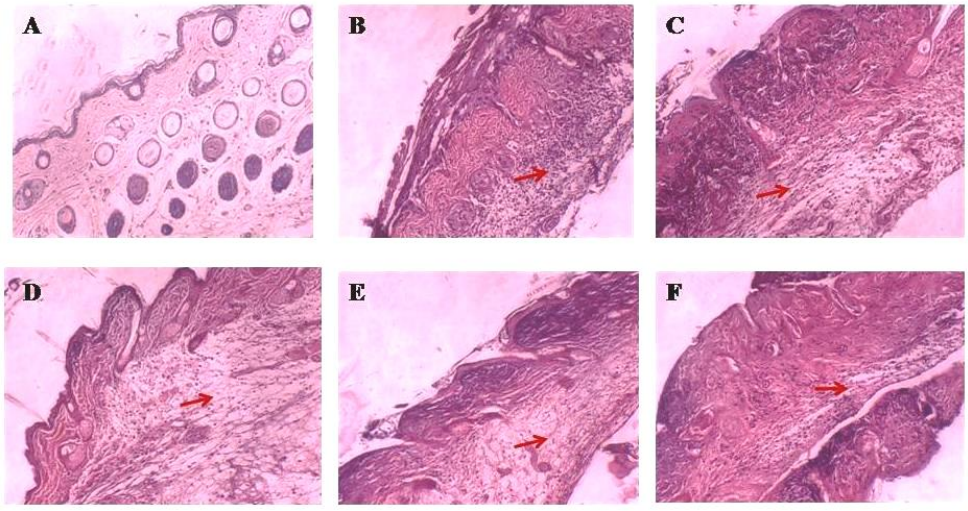

Figure 6.19. Anti-inflammatory effect of HE on histological changes in skin tissue of the plantar region of mouse paw: A) normal, B) control: animals treated 200 μL saline and injected formalin, C) vehicle control: animals treated with 200 μL 1% propylene glycol/ animal/ day, D) diclofenac (standard): animals treated with diclofenac (25 mg/kg b. wt), E) LDHE and F) HDHE were treated 160 mg and 260 mg/kg b. wt of HE respectively. They animals were pre-treated orally, for 7 consecutive days with respective drug doses or (25 mg/kg b. wt; standard) or propylene glycol (1% propylene glycol; vehicle control). On the 8^{th} day, chronic inflammation was induced by intraplantar injection of 0.05 mL of 1% formalin on the right hind paw of all animals 1 hour after HE or diclofenac or propylene glycol administration. The oral administration of drug or diclofenac or propylene glycol continued for six consecutive days. After the experiment the animals were sacrificed and the paw tissue was collected. It was kept in 10% neutral buffered formalin and histopathological analysis was conducted. The tissue architecture were analysed with respect to normal and control with treatment groups. Red arrow indicates the infiltration of inflammatory cells (H & E staining, 200X)

6.4. Discussion

Oral administration of either ascorbic acid or extract for 30 days was found to increase antioxidant enzymes and molecules (catalase, SOD, GPx and level of GSH and MDA) in normal animals. Catalase plays an important role in the protection of cells against the poisonous effects of hydrogen peroxide. The catalase is implicated in diverse pathological and physiological conditions (Kodydkova et al., 2014). The activity of catalase was found increased in the different tissues studied when administered with ascorbic acid and different doses of HE. SOD is considered as one of the major antioxidant enzymes in the body that can prevent the oxidative damage of macromolecules (Miao and St Clair, 2009). Here in this study the SOD activity in the blood, hepatic tissue and renal tissue was found increased significantly after the mice were ingested with ascorbic acid and HE extracts. GPx, another enzyme studied in this work is considered as an important antioxidant enzyme that catalyzes the reduction of H_2O_2 and organic hydroperoxides by glutathione (Bortoli et al., 2017). The GPx level was also found increased in the study indicating that the HE is supporting the antioxidant system. In the antioxidant status of the body (Traverso et al., 2013), the GSH, plays an important role and also connected with many cellular functions. The concentration of GSH was found elevated during the administration of HE and standard in the different tissues studied. The antioxidant efficacy of HE and ascorbic acid was found associated with the decrease of MDA levels. MDA is reported as a major indicator of lipid peroxidation (Zhang et al., 2003). In general, the study indicated that the different doses of HE extract and ascorbic acid reacted the enzymatic and non-enzymatic antioxidant defence system of the body. The study also noted that the effects of HE are very close to the response generated by the ascorbic acid for the majority of parameters analyzed and in some situations, the HE activity was found more. This may be due to the reason that ascorbic acid has both prooxidant and antioxidant capacity which can reduce its ability to protect the body from oxidation damage. Another possible reason for better antioxidant capacity of HE is the presence of flavonoids as reported in the previous chapters, which are more excellent antioxidant substances when compared with ascorbic acid (Jensen et al., 2008).

Sodium fluoride (NaF) is an inorganic salt, which is a potent oxidative chemical and causes direct damage to DNA. NaF can break DNA strand and can induce apoptosis (Herrera-Calderon et al., 2019). In the current study, the administration of NaF made a deleterious effect on both enzymatic and non-enzymatic antioxidant status of blood and liver of control and vehicle control group of animals. However, in LDHE and HDHE treated animals, considerable improvement in both enzymatic and non-enzymatic antioxidant systems were noted. Antioxidants present in LDHE and HDHE may be compete with fluoride ions thereby increase the activity of enzymes may be another reason for its excellent antioxidant capacity. There is another possibility of the promotion of synthesis of antioxidant enzymes by HE of *S. glauca*

Phorbol myristate acetate (PMA) is considered as a potent activator of neutrophils and macrophages, which result in the production of large amounts of oxygen-free radicals. The administration of PMA can induce tissue injury by making deleterious effects on the immune system (Rehan et al., 1985). In the present study, the administration of different doses of HE could ameliorate the PMA induced superoxide radical generation in mice peritoneal macrophages.

The *in vivo* antioxidant efficacy of HE is very much correlated with *in vitro* antioxidant studies, which already narrated in Chapter 3. This beneficial activity of HE on NaF induced oxidative damage of liver and blood tissue of mice may owe to the presence of antioxidants phytochemicals in the extract, which was unveiled in the phytochemical screening and UPLC-Q-TOF-MS analysis. According to Pandiyan and Prabu (2013), plant-derived chemicals like polyphenols and flavonoids can subsidize the fluoride-induced damage in cells. One of the possible reasons for the antioxidant efficacy of HE may be attributed to the immunomodulatory effect of phytochemicals present in it.

In the present study, the HE extract inhibited on the acute paw oedema induced by carrageenan and dextran. The chronic paw oedema induced by the injection of formalin was also found decreased by the administration of HE when compared with the control group. Mouse paw oedema is widely used to test the novel anti-inflammatory drugs. A number of mediators are found involved in inflammation. In the early phase of carrageenan-induced inflammation, histamine, serotonin and bradykinin are acting as mediators. Prostaglandins are connected with the second

phase of inflammation and associated with increased vascular permeability (Cuzzocrea et al., 1999) and intense leukocyte infiltration (Pires et al., 2019). Histamine and serotonin secreted from the mast cells is the primary reason for oedema in the acute model of dextran induced paw oedema in mice (Pires et al., 2019). The reduced rate of Evans blue dye extravasation in HE administered animals, in carrageenan-induced paw oedema may be related with the anti-inflammatory activity of HE. The retention of Evans blue dye in the paw tissue was less with respect to the control group because the HE might have reduced the permeability of blood vessels present in the paw region. Histological examinations of paw tissue demonstrated reduction of the infiltration of inflammatory cells in HE treated mice which had induced paw oedema by carrageenan. Formalin induced chronic paw oedema is widely used to evaluate the anti-inflammatory and antinociceptive activity of chemicals (Fikry et al., 2018). According to Azab et al., (2016), the phytochemicals like phenolic acids, flavonoids, carotenoids, terpenes and sulphides are possessing anti-inflammatory activity. The HE extract, presently used in the study is detected with the presence of said phytochemicals, possibly attributed to the findings in the study.

The results of the different experiments conducted in this chapter have established the working hypothesis that HE of *S. glauca* is capable of showing excellent antioxidant and anti-inflammatory action. Through comparison with standards (vitamin C for antioxidant experiments and diclofenac for anti-inflammatory experiments), the positive effect of HE on various aspects studied in the experiments was proven.

Chapter 7

Chemoprotective effects of *Simarouba glauca* DC

Contents

7.1. Introduction

7.2. Materials and methods

7.2.1. Animals

7.2.2. Determination of chemoprotective effects of HE

7.2.2.1. Cisplatin-induced renal toxicity

7.2.2.2. Cyclophosphamide-induced systemic toxicity

7.2.2.3. Cyclophosphamide-induced systemic toxicity in tumour bearing mice

7.2.2.3.1. Parameters studied

7.2.3. Statistical analysis

7.3. Results

7.3.1. Effect of HE on cisplatin-induced renal toxicity

7.3.2. Effect of HE on cyclophosphamide-induced systemic toxicity

7.3.3. Effect of HE on cyclophosphamide-induced systemic toxicity in tumour-bearing mice

7.4. Discussion

7.1. Introduction

The hot water decoction of S*imarouba glauca* has also been advocated by the common people of southern part of India as a remedy for cancer and chemotherapeutic drug induced secondary toxicity. Lack of scientific validation for such use always reduces its clinical acceptance. The results so far acquired and described in the previous chapters, indicate the antioxidant and anti-inflammatory efficacy (both *in vitro* and *in vivo*) of HE extract of *S. glauca* which is comparable to vitamin C and diclofenac, scientifically approved drugs. Along with these findings the *in vivo* experiments conducted to determine the antitumour efficacy of the HE extract indicated that the HE of *S. glauca* prevent tumour development in Solid and ascites tumour models without generating any side effects. In these studies it was observed that HE is capable of increasing the life span of DLA and EAC induced tumour-bearing animals. When the HE was administered to tumour bearing mice along with cyclophosphamide (standard drug), was found to reduce cyclophosphamide induced myelosuppression. These results prompted to evaluate the chemoprotective efficacy of HE against the toxicity induced by cisplatin and cyclophosphamide used in chemotherapy.

Cisplatin is a popular cytostatic agent used extensively for treating a variety of malignant tumours, encompassing breast, urinary bladder, prostate, head, neck, colon, ovary and testes carcinomas (Arafa and Atteia, 2019, Podratz et al., 2011). The anticancer effect of cisplatin is mediated by interfering with DNA damage which affects its replication and repair mechanisms. Apart from this, the damaged DNA affects the normal transcription process of protein synthesis and finally results in oxidative stress which initiates apoptosis through the mitochondrial pathway (Podratz et al., 2011). Cell death associated with oxidative stress causes many inflammatory responses and highly significant (Peres and da Cunha, 2013). This mechanism of cisplatin action makes toxicity to many non-targeted organs including brain (Shabani et al., 2012), ear (Sergi et al., 2003), kidney, and gastrointestinal tract (Sindhu and Kuttan, 2013). Cisplatin is excreted by kidneys, and a high quantity of cisplatin can accumulate in renal tissue because of basolateral organic cation system (Ciarimboli et al., 2010). Cisplatin also settles in cell organelle; mitochondria and affects bioenergetics of the cell (Santos et al., 2008). The accumulation of cisplatin in other

cell organelles like endoplasmic reticulum, nucleus, cell membranes, lysosomes causes inflammation and finally the death of cell (Peres and da Cunha, 2013).

Cyclophosphamide is considered as a potent cytotoxic agent and it belongs to the category of alkylating drugs and has been used widely as a drug for more than three decades for the treatment of different ailments like chronic systemic rheumatic diseases (Woytala et al., 2016), autoimmune diseases, various tumours and also used in organ transplantations (Sharma et al., 2017a). Because of the multiple adverse effects like cytotoxic and immunosuppressive effects (Shirani et al., 2015), the administration of this drug is limited. Hepatotoxicity (Mahmoud, 2014), nephrotoxicity, urotoxicity, teratogenicity, mutagenicity (Caglayan et al., 2018), toxic effects on the male reproductive system (Kaya et al., 2019) and peripheral neuropathy (Sharma et al., 2017b) are the major side effects associated with cyclophosphamide administration. The other common side effects of this drug include digestive system disorders like diarrhoea, vomiting and nausea. It also causes bone marrow suppression, hemorrhagic cystitis, cardiotoxicity, lethargy and alopecia (Ejaz et al., 2018), Cyclophosphamide can be administered both orally and intravenously in an inactive cytostatic form (Woytala et al., 2016). The cyclophosphamide is activated by liver microsomal cytochrome P450 mixed oxidase system and leads to the production of reactive substances like acrolein and phosphoramide mustard, which are capable to enter many body cells and there they acquire alkylating property by further chemical transformation reactions (Zarei and Shivanandappa, 2013). The metabolites mainly react with DNA molecules and cause their fragmentation which finally leads to the death of the cells. Cyclophosphamide is capable to work in all different phases of the cell cycle. It can prevent the formation of immune cells like T and B lymphocytes and decrease the concentration of antibody synthesis. Apart from making oxidative stress (Zhai et al., 2018), cyclophosphamide is capable to induce inflammatory responses by raising the levels of biomolecules like tumour necrosis factor – alpha, nuclear factor kappa B, interleukin-6, etc (Caglayan et al., 2018).

In this context, there is an urgent need to develop efficient substances that can protect the body from the adverse effects of chemotherapy based toxicity. It is essential to elevate the body's antioxidant defences with natural and safe antioxidants to reduce or

to prevent the toxic effects of cyclophosphamide or cisplatin or other chemotherapeutic drugs.

7.2. Materials and methods

7.2.1. Animals

Male Swiss albino mice (25 ± 3 gm) were used for the study. They were kept in standard conditions in the animal house of Amala Cancer Research Centre during the experimental period. The animals were acclimatized for a period of seven days before the commencement of the study. The experiments were done with the permission of the Institutional Animal Ethics Committee (IACE) as per order number ACRC/IAEC/16-06/11.

7.2.2. Determination of chemoprotective effect of HE

7.2.2.1. Cisplatin-induced renal toxicity

Experimental design

Thirty-six animals were equally divided into six groups – normal, control, vehicle control, standard, low dose (LDHE) and high dose (HDHE). During the study, the normal group of animals were administered 200 μL of saline (p.o.) per day for 10 days. The control group animals were administered with 200 μL of saline (p.o.) and the vehicle control group animals were treated with 200 μL of 1% propylene glycol (p.o.) for seven days before and three days after cisplatin administration. The animals in the standard group were provided silymarin (100 mg/kg b. wt.) and LDHE and HDHE groups were administered hot water extract of *S. glauca*, at dose of 160 and 260 mg/kg b. wt respectively by oral gavage for seven days before and three days after cisplatin administration. All the animals except in the normal group were treated with single dose of cisplatin (16 mg/kg b. wt, ip.) to induce renal damage (Somani et al., 2000) on eighth day of the experiment. All animals were sacrificed at the end of the experiment after overnight fasting (Refer Chapter 2, section 2.2.12.1).

Sample collection

Blood was collected in heparin-coated tubes directly from the heart after sacrificing the animals for haematological analysis. For biochemical analysis blood was collected

in non-heparinised tubes and separated the serum. Kidneys were removed, washed in saline solution. Kidney homogenate (10% w/v) was prepared for every animal of each group in ice-cold 0.1M Tris buffer (pH 7.4). Femur bones of the animals were collected for the determination of bone marrow cellularity and *α*-esterase activity.

Parameters studied

Haematological profile

Haematological parameters such as haemoglobin (Drabkin and Austin, 1935) and Total WBC (Cheesbrough and McArthur, 1976) count were evaluated (Refer Chapter 2, section 2.2.5.2.1.1. and 2.2.5.2.1.3).

Bone marrow cellularity and α-esterase activity

Bone marrow cells from both femurs of animals were flushed out into PBS containing 10% foetal bovine serum (Mehara and Vaidya, 1984). In order to determine bone marrow cellularity, bone marrow cells were counted using a Neubauer counting chamber and expressed as cells/femur/mL. From the above cell preparation of each animal, a smear of cells was prepared on a clean glass slide and dried by waving air. The smears were stained with *α*-naphthyl acetate and then counterstained with haematoxylin (Bancrofit and Cook, 1984). α-esterase positive cells appeared in orange-pink colour which was counted and expressed as the number of positive cells/4000 bone marrow cells (Refer Chapter 2, section 2.2.12.1.4).

Serum urea and creatinine

Serum urea was determined by Berthelot reaction method (Young et al., 1975) and creatinine by Jaffe's reaction method (Bones and Tausky, 1945) using commercially available kits (Euro Diagnostics, Chennai, India) as per instructions of manufactures (Refer Chapter 2, section 2.2.7.2 and 2.2.7.1).

Oxidative stress status in kidney tissue

The extent of lipid peroxidation was measured in terms of MDA equivalent carbonyls using the thiobarbituric acid method (Ohkawa et al., 1979) (Refer Chapter 2, section 2.2.9.1.5). Furthermore, conjugated dienes (CD) and tissue hydroperoxides (HPs) in

the homogenate were determined according to the modified method of John and Steven, (1978) (Refer Chapter 2, section 2.2.12.1.6 and 2.2.12.1.7).

Antioxidant enzyme profile of the kidney

The analysis of various antioxidant enzymes such as superoxide dismutase (McCord and Fridovich, 1969) (Refer Chapter 2, section 2.2.9.1.2), catalase (Beers and Sizer, 1952) (Refer Chapter 2, section 2.2.9.1.3) and glutathione peroxidase (Hafeman et al., 1974) (Refer Chapter 2, section 2.2.12.1.8) was carried out. In addition to these, the level of non-enzymatic antioxidant, reduced glutathione (Moron et al., 1979) (Refer Chapter 2, section 2.2.9.1.1) and total protein present in renal tissue were also evaluated (Lowry et al., 1951) (Refer Chapter 2, section 2.2.6.5).

Histological analysis

A small portion of the kidney from each group was taken and fixed in 10% neutral buffered formalin solution, Sections with a thickness of 5 μm were taken, deparaffinized, hydrated and stained using haematoxylin-eosin. The stained renal sections were examined for the extent of damages to glomeruli, tubules and interstitial space.

7.2.2.2. Cyclophosphamide-induced systemic toxicity

The effect of different doses of HE on cyclophosphamide-induced systemic toxicity was evaluated by using male Swiss albino mice. The animals (30 numbers) were divided into five groups of six animals each. Group I was kept as normal and administered 200 μL of saline (p.o.) per day for ten consecutive days. Oral administration of cyclophosphamide was done (25 mg/kg b. wt) for ten consecutive days to animals belongs to rest all groups. Group II animals were considered as the control group and were administered only CTX. The vehicle control group (Group III) was administered with 200 μL of 1% food graded propylene glycol (p.o.) for ten consecutive days. Group IV and Group V animals were treated with 160 and 260 mg/kg b. wt of HE extract (p.o.) for ten consecutive days. A minimum of 6 hour time interval was observed between the administrations of cyclophosphamide and respective drug. The animals were maintained for twenty days. The collection for various body tissues for different studies is described in Chapter 2, section 2.2.12.2.

Parameters studied

Body weight and organ weight

Body weight of the animals in each group was measured on 0, 5, 10, 15 and 21st day of the experiment. The weight of different organs like liver, kidney and spleen was measured by an electronic weighing machine after washing with normal saline.

Relative organ weight

Relative organ weight of liver, kidneys and spleen were calculated by the formula given in Chapter 2, section. 2.2.12.2.3.

Bone marrow cellularity and alpha esterase activity

The bone marrow cellularity and alpha esterase activity of the animals were conducted by using bone marrow collected from the femur bones of the animals. The detailed procedure is given in Chapter 2, section 2.2.12.1.4.

Haematological parameters

The level of Hb (Refer Chapter 2, section 2.2.5.2.1.1) and total leucocyte count (Chapter 2, section 2.2.5.2.1.3) of the animals in different groups were evaluated as per standard protocol on 0, 5, 10, 15 and 21st day of the experiment.

Liver function parameters

The hepatic function of the animals was analysed by using blood serum. The principle and procedure regarding the estimation of AST (2.2.6.1), ALT (2.2.6.2), ALP (2.2.6.3), total bilirubin (2.2.6.4) and total protein (2.2.6.5) is provided in Chapter 2 as per the reference number indicated in the bracket.

Renal function parameters

The analysis of renal function parameters like serum creatinine and serum urea was carried out as per the procedure is given in Chapter 2, section 2.2.7.1 and 2.2.7.2 respectively.

Antioxidant status of liver and kidney

For the analysis of the antioxidant status of liver and kidney, 10% (w/v in 0.1 M Tris hydrochloric acid buffer, pH 7.4) tissue homogenate was prepared. The enzymatic and non-enzymatic antioxidant status of the said tissues was evaluated as per the protocol given in chapter 2 and section number of each one is cited in bracket Catalase (2.2.9.1.3), SOD (2.2.9.1.2), GPx (2.2.12.1.8), GSH (2.2.9.1.1) and TBARS (2.2.9.1.5).

Histological studies

Tissue samples from liver, kidney, spleen and small intestine were collected from animals in the experimental groups and fixed in 10% neutral buffered formalin solution. Sections (5 μm thickness) were taken and stained with haematoxylin and eosin. They were observed in a microscope (200X) and photographs were taken. The tissue architecture of the drug-treated animals was compared with the control group.

7.2.2.3. Cyclophosphamide-induced systemic toxicity in tumour bearing mice

The chemoprotective effect of HE was evaluated by using cyclophosphamide-induced toxicity in tumour-bearing mice. The solid tumour was inoculated in the right hind limb of the mice by using DLA cells. The experimental design is narrated in Chapter 2, section 2.2.12.3.1.

Parameters studied

Body weight and organ weight

Body weight of each group members was measured on 0, 5, 10, 15 and 21st day of the experiment by using an electronic weighing machine. The weight of liver, kidney and spleen were measured after washing by normal saline solution.

Relative organ weight

The relative organ weight of major organs like liver, kidneys and spleen were calculated by the formula given in Chapter 2, section. 2.2.12.2.3.

Tumour volume and weight

The tumour volume of all the animals in the experiment was determined by measuring the diameter of tumour growth in two perpendicular planes using a digital vernier calliper in every three days from the beginning of the experiment (Refer Chapter 2, section 2.2.11.2). On the 21st day, the tumour was isolated and weighed by using an electronic weighing balance.

Haematological parameters

Important haematological parameters like the level of Hb and total leucocyte count of the animals in different groups were evaluated as per standard protocol (Hb - Chapter 2, section 2.2.5.2.1.1., Total leucocyte count - Chapter 2, section 2.2.5.2.1.3) on 0, 5, 10, 15 and 21st day of the experiment.

Liver function parameters

Different liver function markers of the animals were analysed as per the protocol mentioned as follows, AST – Chapter 2, section 2.2.6.1, ALT – Chapter 2, section 2.2.6.2, ALP – Chapter 2, section 2.2.6.3, total bilirubin – Chapter 2, section 2.2.6.4 and total protein – Chapter 2, section 2.2.6.5.

Renal function parameters

The renal function status was analysed by checking the concentration of serum creatinine and serum urea as per the procedure is given in Chapter 2, section 2.2.7.1 and 2.2.7.2 respectively.

Antioxidant status of liver and kidney

The antioxidant status of liver and kidney tissues was evaluated as per the protocol is given Chapter 2. The section number for each of the parameters detected is noted in bracket, Catalase (2.2.9.1.3), SOD (2.2.9.1.2), GPx (2.2.12.1.8), GSH (2.2.9.1.1) and TBARS (2.2.9.1.5).

7.2.3. Statistical analysis

The values are expressed as mean ± SD six animals. The mean values were statistically analyzed using one-way analysis of variance using Graph Pad Instat 3 software (Graph Pad Software, Inc. La Jolla, USA) traced by Dunnett multiple comparison test. $P < 0.05$ was considered to be statistically significant.

7.3. Results

7.3.1. Effect of HE on cisplatin-induced renal toxicity

Haematological parameters

Cisplatin administration reduced the Hb content and total WBC count of control and vehicle control group animals. The administration of 160 and 260 mg/kg b. wt of HE significantly ($p<0.01$) prevented this drop in the level of Hb content and total WBC count in comparison with the control group of animals. The Hb level was 9.2 ± 1.10 and 9.4 ± 1.01 (gm/dL) in control group and vehicle control group respectively in comparison with normal group of animals (14.4 ± 1.09 gm/dL) at the end of the experiment. But the significant rise in the level of Hb was noted in HELD (15.2 ± 1.09 gm/dL) and HEHD (15.4 ± 0.90 gm/dL) group animals. In the silymarin treated group the Hb level was 12.2 ± 1.04 gm/dL (Figure 7.1A). A similar tendency was noted in the level of WBC count (cells/cu.mm) of HE administered groups, (9500 ± 463 and 9250 ± 512 in HELD and HEHD respectively) in comparison with control (4100 ± 643) and vehicle control (4500 ± 589) group animals (Figure 7.1B). In silymarin group, the total number of WBC was 5800 ± 603.

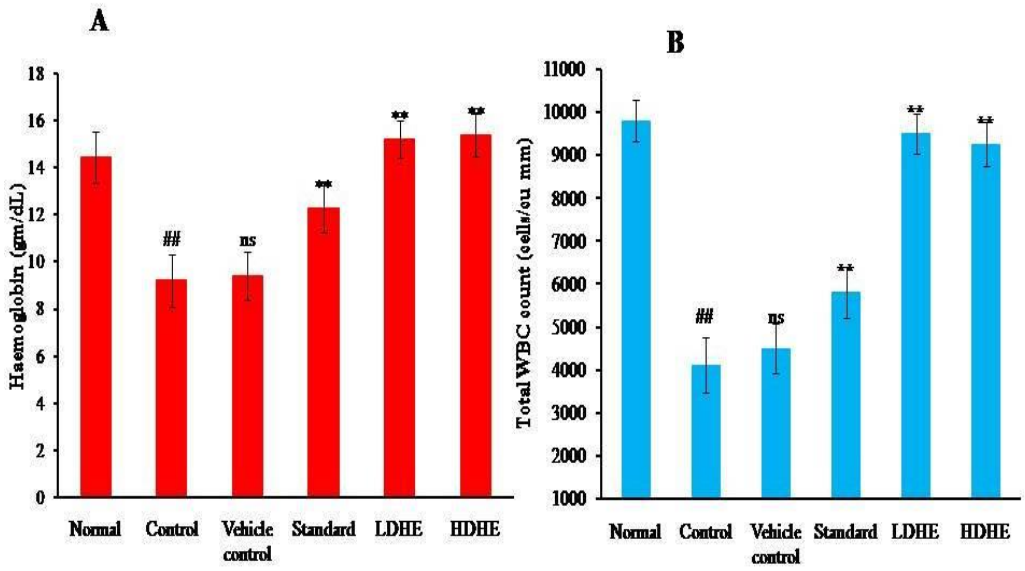

Figure 7.1. Effect of HE on haematological parameters in cisplatin-induced renal toxicity in mice: A) Haemoglobin level and B) Total WBC count. Normal; animals treated with 200 μL saline (p.o.) per day for ten days, control; animals treated with 200 μL saline (p.o.) per day for 7 days before and 3 days after CDDP administration, vehicle control; animals treated with 200 μL 1% food graded propylene glycol (p.o.) for 7 days before and 3 days after CDDP administration, standard; animals treated with silymarin (100 mg/kg b. wt, p.o.) for 7 days before and 3 days after CDDP administration, LDHE and HDHE; animals treated with HE at 160 and 260 mg/kg b. wt (p.o.) respectively for 7 days before and 3 days after CDDP administration. CDDP (16 mg/kg b. wt, ip) administered on 7th day. Values are mean ± standard deviation of six animals per group. ##: $p<0.01$ (control compared to normal), ^{ns} $p>0.05$: non-significant (vehicle control compared to control), ** $p<0.01$ (standard, LDHE and HDHE compared to control)

Bone marrow cellularity and the number of α-esterase positive cells

Bone marrow cellularity and the number of α-esterase positive cells were decreased in both the cisplatin-treated group and vehicle control group (Figure 7.2A and 2B). HE treatment (both low dose and high dose) increased bone marrow cellularity in a dose-dependent manner, but the number of α-esterase positive cells (number of positive cells per four thousand bone marrow cells) were more in LDHE (813.33 ± 37.86) than HDHE (793.33 ± 15.28).

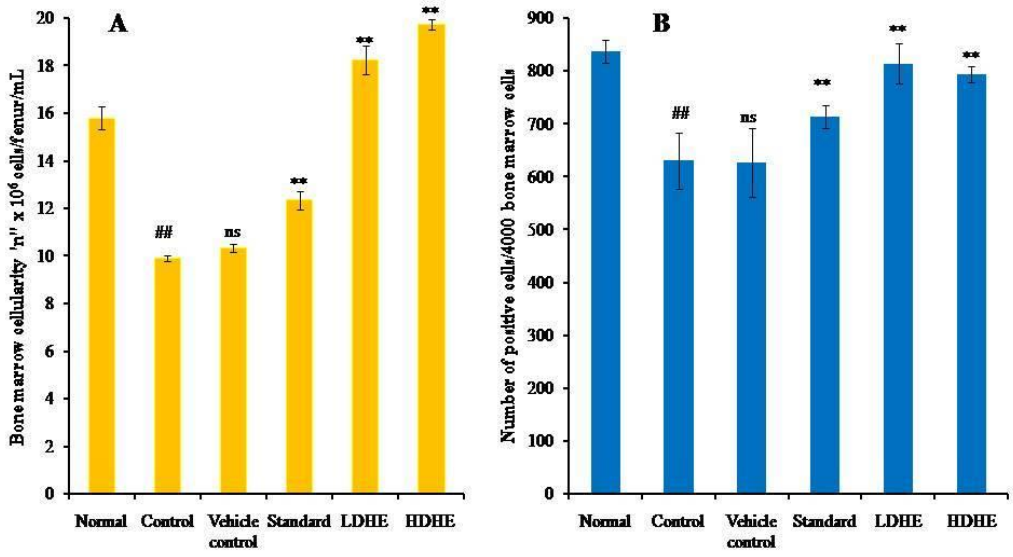

Figure 7.2. Effect of HE on A) bone marrow cellularity and B) alpha esterase positive cells in cisplatin-induced renal toxicity in mice: Normal; animals treated with 200 μL saline (p.o.) per day for ten days, control; animals treated with 200 μL saline (p.o.) per day for 7 days before and 3 days after CDDP administration, vehicle control; animals treated with 200 μL 1% food graded propylene glycol (p.o.) for 7 days before and 3 days after CDDP administration, standard; animals treated with silymarin (100 mg/kg b. wt, p.o.) for 7 days before and 3 days after CDDP administration, LDHE and HDHE; animals treated with HE at 160 and 260 mg/kg b. wt (p.o.) respectively for 7 days before and 3 days after CDDP administration. CDDP (16 mg/kg b. wt, ip) administered on 7th day. Values are mean ± standard deviation of six animals per group. ##: $p<0.01$ (control compared to normal), ^{ns} $p>0.05$: non-significant (vehicle control compared to control), ** $p<0.01$ (standard, LDHE and HDHE compared to control)

Renal function parameters

Serum creatinine and serum urea levels (mg/dL) significantly improved in the HE ($p<0.01$), in a dose-dependent manner (Figure 7.3A and 3B). A profound increase in the level of serum creatinine and serum urea was noted in cisplatin (1.87 ± 0.09, 93.17 ± 1.67) and vehicle control groups (1.77 ± 0.08, 91.83 ± 1.26). Silymarin treated animals shown a lower level of serum creatinine (0.39 ± 0.02) and serum urea (21.83 ± 1.67).

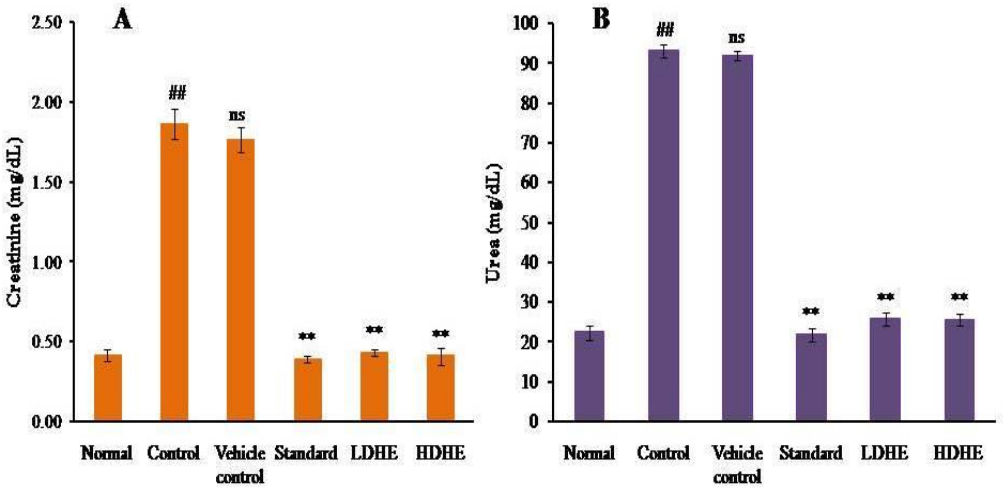

Figure 7.3. Effect of HE on renal function markers in cisplatin-induced renal toxicity in mice: A) Creatinine and B) Urea. Normal; animals treated with 200 μL saline (p.o.) per day for ten days, control; animals treated with 200 μL saline (p.o.) per day for 7 days before and 3 days after CDDP administration, vehicle control; animals treated with 200 μL 1% food graded propylene glycol (p.o.) for 7 days before and 3 days after CDDP administration, standard; animals treated with silymarin (100 mg/kg b. wt, p.o.) for 7 days before and 3 days after CDDP administration, LDHE and HDHE; animals treated with HE at 160 and 260 mg/kg b. wt (p.o.) respectively for 7 days before and 3 days after CDDP administration. CDDP (16 mg/kg b. wt, ip) administered on 7th day. Values are mean ± standard deviation of six animals per group. ##: $p<0.01$ (control compared to normal), ^{ns} $p>0.05$: non-significant (vehicle control compared to control), ** $p<0.01$ (standard, LDHE and HDHE compared to control)

Antioxidant status in kidney

Superoxide dismutase, catalase, glutathione peroxidase and non-enzymatic reduced glutathione level were found to be decreased in cisplatin and vehicle control-treated groups in comparison with the normal group. However, the pre-treatment of HE in lower and higher doses significantly ($p<0.01$) improved the level of antioxidant enzymes similar to the increase observed in silymarin treated group (Figure 7.4 and 7.5).

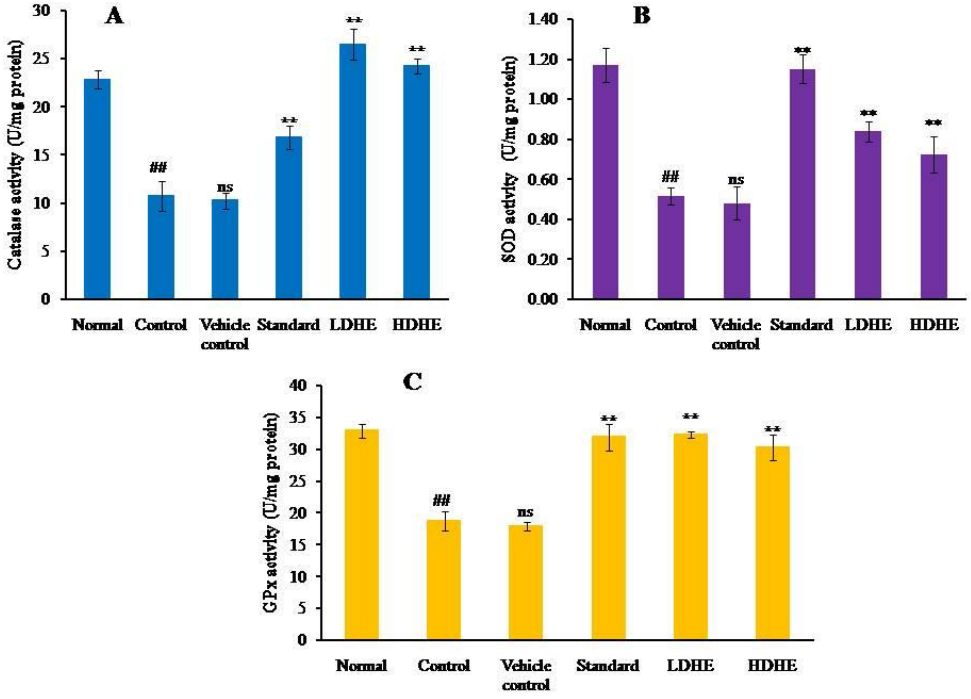

Figure 7.4. Effect of HE on renal antioxidant enzymes in cisplatin-induced renal toxicity in mice: A) catalase, B) SOD and C) GPx. Normal; animals treated with 200 μL saline (p.o.) per day for ten days, control; animals treated with 200 μL saline (p.o.) per day for 7 days before and 3 days after CDDP administration, vehicle control; animals treated with 200 μL 1% food graded propylene glycol (p.o.) for 7 days before and 3 days after CDDP administration, standard; animals treated with silymarin (100 mg/kg b. wt, p.o.) for 7 days before and 3 days after CDDP administration, LDHE and HDHE; animals treated with HE at 160 and 260 mg/kg b. wt (p.o.) respectively for 7 days before and 3 days after CDDP administration. CDDP (16 mg/kg b. wt, ip) administered on 7th day. Values are mean ± standard deviation of six animals per group. ##: $p<0.01$ (control compared to normal), ^{ns} $p>0.05$: non-significant (vehicle control compared to control), ** $p<0.01$ (standard, LDHE and HDHE compared to control)

TBARS levels (nmol MDA/mg protein) were found significantly increased in the renal cortex of mice in the cisplatin (4.98 ± 0.48) and vehicle control group (4.81 ± 0.20) in comparison with that of normal group animals (1.30 ± 0.36). Treatment of LDHE (2.04 ± 0.19) and HDHE (2.38 ± 0.14) significantly decreased the extent of lipid peroxidation as observed in the silymarin treated group animals (2.26 ± 0.28). The levels of other tissue damage markers such as hydroperoxides and conjugated diene were showed a prominent increase in cisplatin and vehicle administered group, while the different doses of HE administered group documented hydroperoxides and conjugated diene levels which were close to normal and silymarin treated group.

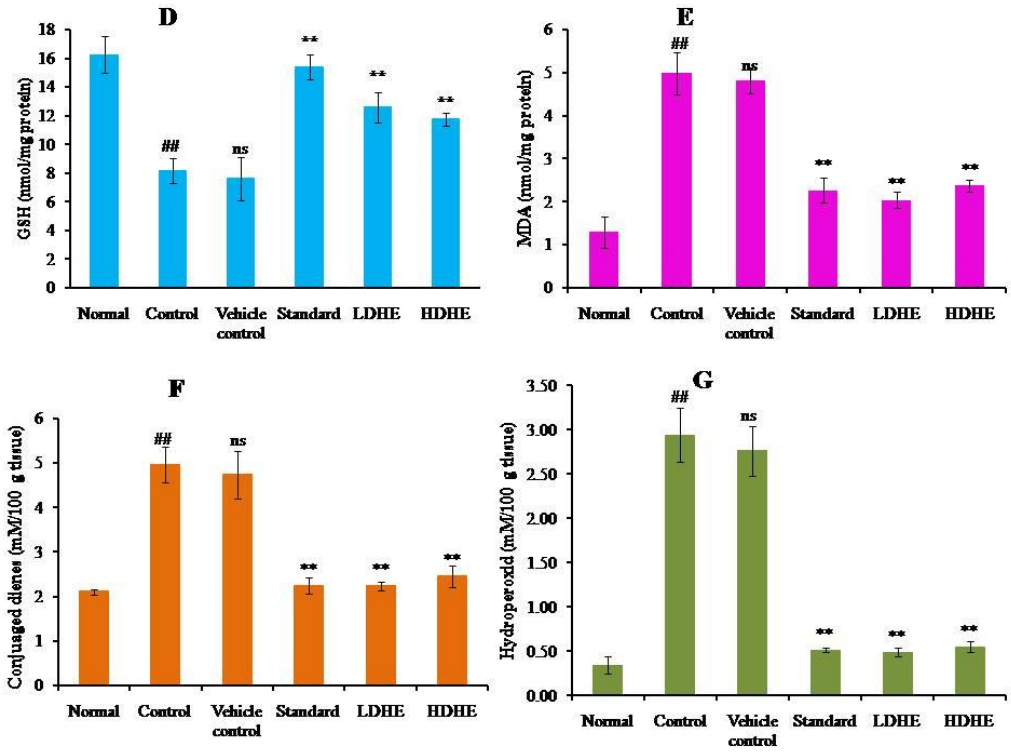

Figure 7.5. Effect of HE on biomarkers in cisplatin-induced renal toxicity in mice: D) GSH, E) MDA, F) conjugated diene and G) hydroperoxides level. Normal; animals treated with 200 μL saline (p.o.) per day for ten days, control; animals treated with 200 μL saline (p.o.) per day for 7 days before and 3 days after CDDP administration, vehicle control; animals treated with 200 μL 1% food graded propylene glycol (p.o.) for 7 days before and 3 days after CDDP administration, standard; animals treated with silymarin (100 mg/kg b. wt, p.o.) for 7 days before and 3 days after CDDP administration, LDHE and HDHE; animals treated with HE at 160 and 260 mg/kg b. wt (p.o.) respectively for 7 days before and 3 days after CDDP administration. CDDP (16 mg/kg b. wt, ip) administered on 7th day. Values are mean ± standard deviation of six animals per group. ##: $p<0.01$ (control compared to normal), ^{ns} $p>0.05$: non-significant (vehicle control compared to control), ** $p<0.01$ (standard, LDHE and HDHE compared to control)

Histological observations

Compared with the normal group, the histological details of kidney tissue of cisplatin and vehicle control group animals showed profound damages. Shrunken renal corpuscle, infiltration of cells, haemorrhage and necrosis were the major harmful changes noted in these groups. In HE (both low dose and high dose) treated groups these events were minuscule, similar to silymarin treated group (Figure 7.6).

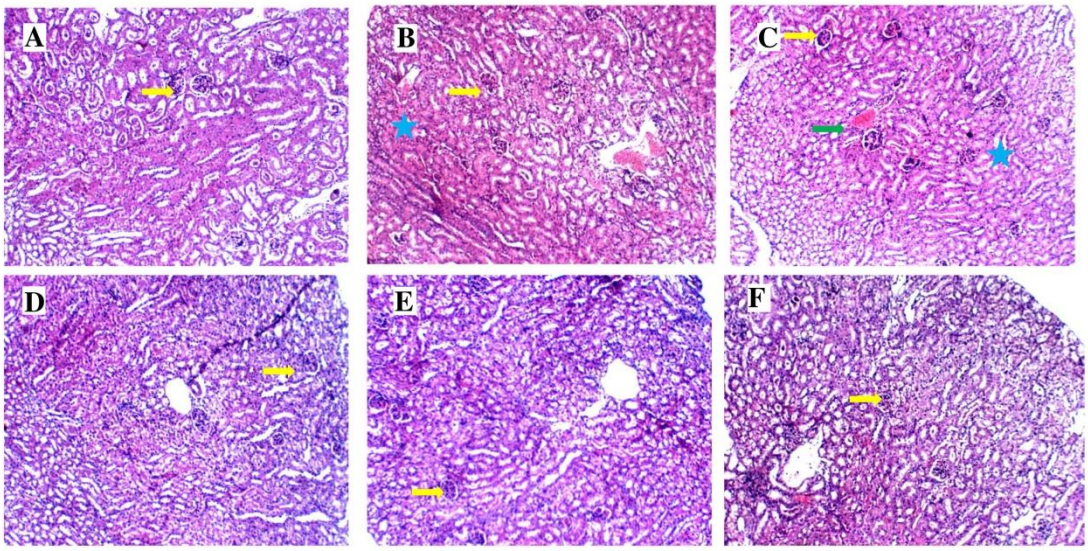

Figure 7.6. Effect of HE on the histology of kidney tissue in cisplatin-induced mice: A) normal; animals treated with 200 μL saline (p.o.) per day for ten days, B) control; animals treated with 200 μL saline (p.o.) per day for 7 days before and 3 days after CDDP administration, C) vehicle control; animals treated with 200 μL 1% food graded propylene glycol (p.o.) for 7 days before and 3 days after CDDP administration, standard; animals treated with silymarin (100 mg/kg b. wt, p.o.) for 7 days before and 3 days after CDDP administration, D) LDHE and E) HDHE; animals treated with HE at 160 and 260 mg/kg b. wt (p.o.) respectively for 7 days before and 3 days after CDDP administration. CDDP (16 mg/kg b. wt, ip) administered on 7th day. The yellow arrow indicates renal corpuscle, the green arrow represents cast formation, and the star denotes necrosis in renal tissue (H & E staining, 200X)

7.3.2. Effect of HE on cyclophosphamide-induced systemic toxicity

Body weight

The average body weight of animals (gm) was found decreased in all the treated group of animals with respect to the normal group of animals. At the 0 day, the average body weight of animals in all groups was 26.45 ± 0.51 gm. The average weight of animals in normal reference group was 26.0 ± 0.78 gm at the 0 days, but it was increased to 30.28 ± 1.32 gm on day of sacrifice. In control and vehicle control group the average body weight was reduced to 21.36 ± 0.68 and 22.03 ± 0.68 gm respectively from the initial average body weight of 25.70 ± 0.81 and 26.52 ± 0.66 gm. On the other hand only moderate reduction of average body weight was noted in LDHE (from 26.92 ± 0.80 to 25.63 ± 0.74 gm) and HDHE (from 26.97 ± 0.82 to 25.16 ± 1.13 gm) during this experiment. The decrease in body weight of animals was noted from the 5th day onwards in all treated group (Figure 7.7).

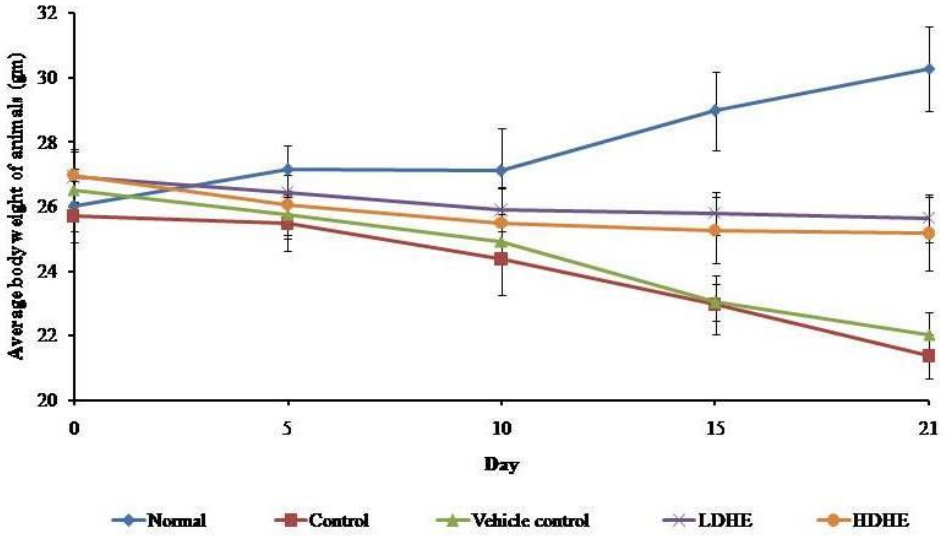

Figure 7.7. Protective effect of HE treatment on the average body weight of cyclophosphamide-induced mice: normal; animals treated with 200 μL of saline (p.o.) for ten days, control; animals treated with 200 μL of CTX (25 mg/kg b. wt, p.o.) for ten days, vehicle control, animals treated with 200 μL of 1% food graded propylene glycol (p.o.) and CTX (25 mg/kg b. wt, p.o) for ten days, LDHE; animals treated with 200 μL of 160 mg/kg b. wt of HE and (p.o.) and CTX (25 mg/kg b. wt, p.o.) for ten days, HDHE; animals treated with 200 μL of 260 mg/kg b. wt of HE and (p.o) and CTX (25 mg/kg b. wt, p.o) for ten days. Values are mean ± standard deviation of six animals per group

Organosomatic index of liver, kidney and spleen

The detailed analysis of organosomatic index of liver, kidney and spleen of different groups in this experiment is given in table 7.1.The organosomatic index of liver and kidney of control group animals showed a moderate decrease and not significant ($p>0.05$) with respect to normal group. The organosomatic index of liver and kidney was 5.38 ± 0.21 and 1.50 ±0.19 respectively in control group. The organosomatic index of liver and kidney was 5.67 ± 0.33 and 1.57 ± 0.33 respectively in normal group. The organosomatic index of liver, kidney and spleen of vehicle control group was found close to the control group. The organosomatic index of spleen of HE treated groups showed significant change with respect to the control group at $p<0.01$ level. The organosomatic index of spleen was decreased in control (0.41 ± 0.05) and vehicle control (0.43 ± 0.02) with respect to normal group (0.63 ± 0.03). The organosomatic index of spleen in LDHE and HDHE was 0.64 ± 0.04 and 0.66 ± 0.04 respectively.

Table 7.1. Protective effect of HE on the organosomatic index of liver, kidney and spleen of cyclophosphamide-induced mice

Group	Liver	Kidney	Spleen
Normal	5.67 ± 0.33	1.57 ± 0.33	0.63 ± 0.03
Control	5.38 ± 0.21[a]	1.50 ± 0.19[a]	0.41 ± 0.05[##]
Vehicle control (1 % propylene glycol)	5.34 ± 0.34 [ns]	1.42 ± 0.21 [ns]	0.43 ± 0.02 [ns]
LDHE (160 mg/kg b. wt)	5.50 ± 0.91 [ns]	1.53 ± 0.31 [ns]	0.64 ± 0.04[**]
HDHE (260 mg/kg b. wt)	5.47 ± 0.65 [ns]	1.51 ± 0.38 [ns]	0.66 ± 0.04[**]

Values are mean ± standard deviation of six animals per group
[a]p>0.05:non significant, [##]p<0.01 control compared to normal
[ns] p>0.05, [**] p<0.01 between control and treated groups

Bone marrow cellularity and the number of alpha esterase positive cells

The number of bone marrow cells (cells x 10^6/ femur/mL) documented in the normal animals was 17.74 ± 0.56. Compared to this the cells were lower in control (8.53 ± 0.71) and vehicle control (8.88 ± 0.40) group animals. This drop in cellularity was not observed in the treated groups and documented significantly higher ($p<0.01$) number than control group animals. The bone marrow cellularity documented with LDHE and HDHE were 13.73 ± 0.85 and 13.06 ± 0.44 (Figure 7.8A). The number of alpha esterase positive cells was found to be 928.45 ± 28.14 in the normal group of animals (Figure 7.8B). In control and vehicle control group, the number of alpha esterase positive cells was found decreased to 509.54 ± 14.32 and 497.21 ± 19.23 respectively. The HE of *S. glauca* treated groups had values which are higher than the control values (LDHE - 786.38 ± 13.42 and HDHE - 756.87 ± 23.76).

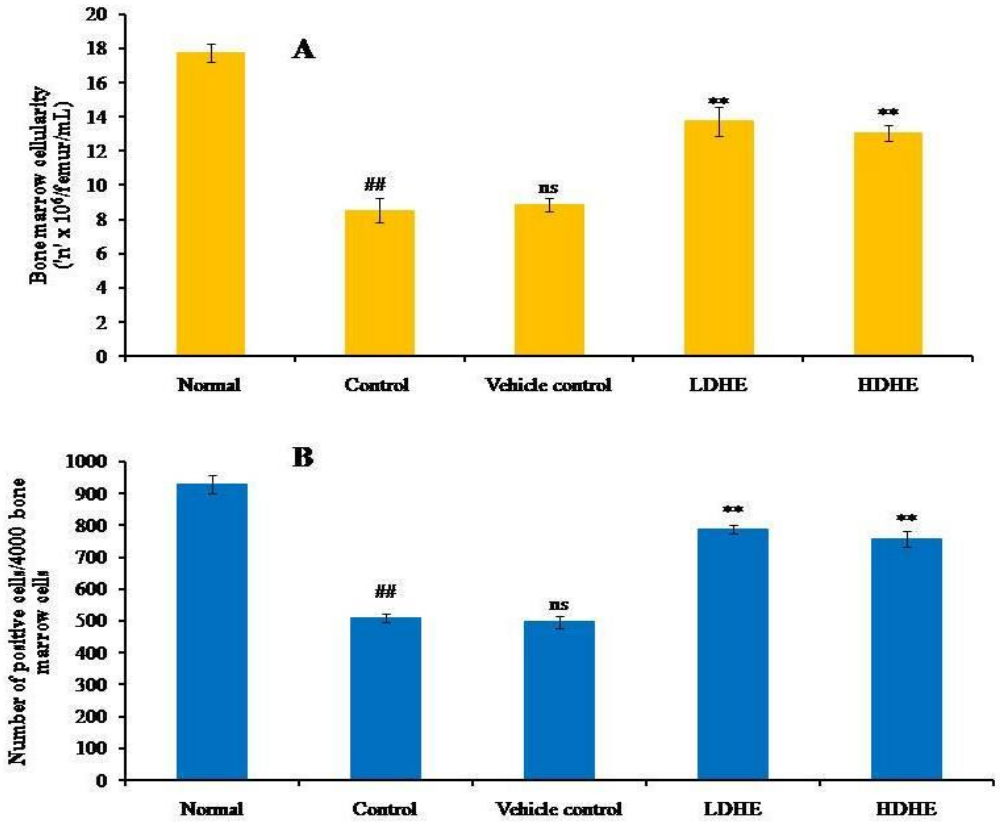

Figure 7.8. Protective effect of HE treatment on (A) the bone marrow cellularity and (B) Number of alpha esterase positive cells in cyclophosphamide-induced mice: normal; animals treated with 200 μL of saline (p.o.) for ten days, control; animals treated with 200 μL of CTX (25 mg/kg b. wt, p.o.) for ten days, vehicle control, animals treated with 200 μL of 1% food graded propylene glycol (p.o.) and CTX (25 mg/kg b. wt, p.o.) for ten days, LDHE; animals treated with 200 μL of 160mg/kg b. wt of HE and (p.o.) and CTX (25 mg/kg b. wt, p.o.) for ten days, HDHE; animals treated with 200 μL of 260 mg/kg b. wt of HE and (p.o.) and CTX (25 mg/kg b. wt, p.o.) for ten days. Values are mean ± standard deviation of six animals per group. $^{\#\#}$: $p<0.01$ (control compared to normal), ^{ns} $p>0.05$, ** $p<0.01$ between control and treated groups

Haematological parameters

Figure 7.9 depicts the protective effect of HE on the haematological parameters in cyclophosphamide-induced toxicity in mice. Over the entire period of time the Hb level in the normal group animals were remained almost the same. However the Hb level (gm/dL) was found decreased in control (from 14.0 ± 0.76 to 10.30 ± 0.43) and vehicle control group (13.8 ± 0.71 to 10.2 ± 0.54). The administration of HE could not prevent the drop however did not allow such a prominent loss in Hb level. A drastic decrease in total leucocyte level was observed in the control (from 10200 ± 103 to

3200 ± 178) and vehicle control group (from 10100 ± 120 to 3200 ± 173) from 0 to 21st day. The decrease in total leucocyte level (cells/cu. mm) was noted from 5th day onwards in all the treated groups. In the entire period of study, the leucocyte count was found constant in the normal group. As shown in figure 7.9B, in LDHE treated group, the total leucocyte count was 8500 ± 174, followed by HDHE 6800 ± 127 on the 21st day of the experiment.

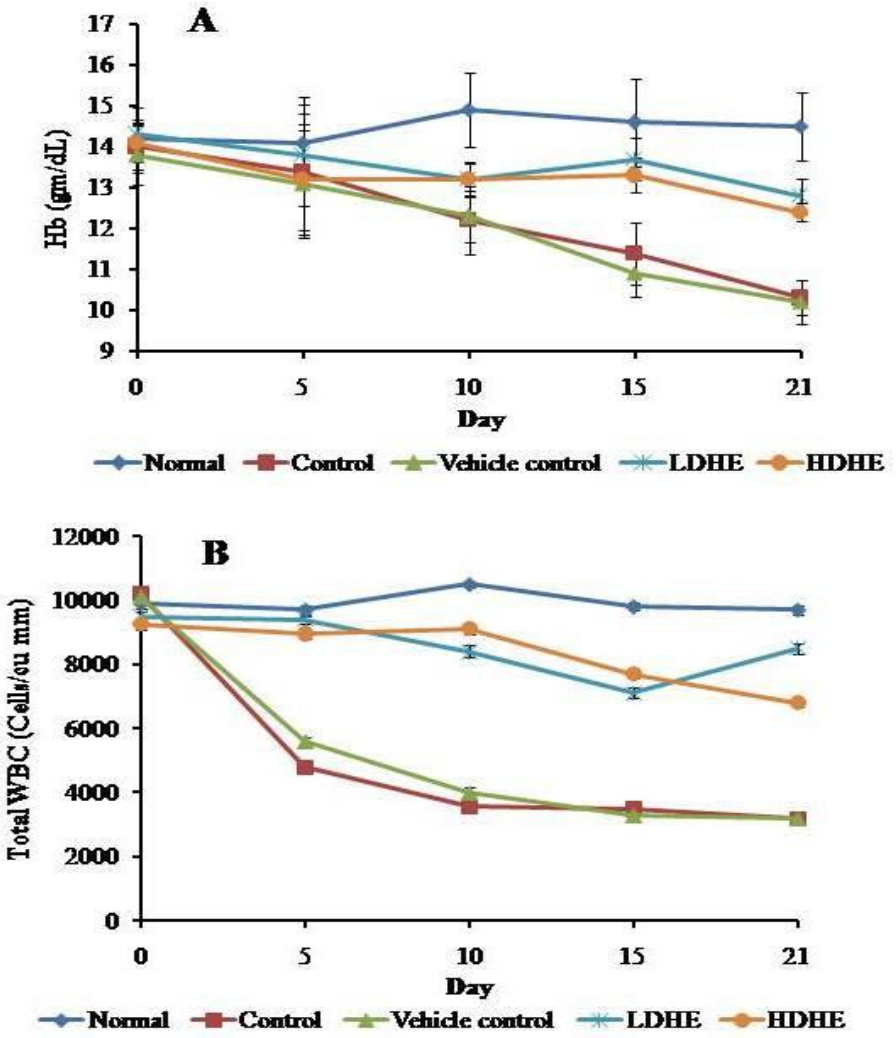

Figure 7.9. Protective effect of HE treatment on the haematological parameters in cyclophosphamide-induced mice: A) Hb and B) total leucocyte count. normal; animals treated with 200 μL of saline (p.o.) for ten days, control; animals treated with 200 μL of CTX (25 mg/kg b. wt, p.o.) for ten days, vehicle control, animals treated with 200 μL of 1% food graded propylene glycol (p.o.) and CTX (25 mg/kg b. wt, p.o.) for ten days, LDHE; animals treated with 200 μL of 160 mg/kg b. wt of HE and (p.o.) and CTX (25 mg/kg b. wt, p.o.) for ten days, HDHE; animals treated with 200 μL of 260 mg/kg b. wt of HE and (p.o.) and CTX (25 mg/kg b. wt, p.o.) for ten days. Values are mean ± standard deviation of six animals per group

Liver function parameters

The protective effect of HE on liver function parameters in cyclophosphamide-induced mice is summarized in table 7.2. In general the level of total bilirubin, AST, ALT, ALP and total protein were significantly varied from the control group and HE treated groups. In normal group the total bilirubin level (mg/dL) was found 0.32 ± 0.04 and in the cyclophosphamide administered group it increased to 0.65 ± 0.05. In the LDHE and HDHE the values were found 0.33 ± 0.05 and 0.33 ± 0.55 respectively and were significantly different ($p<0.01$). The liver AST, ALT and ALP activities were found increased in control group with respect to normal group but, in all, HE treated groups the values were found close to normal group. It was found that the total protein level (gm/dL) decreased in control group (5.1 ± 0.26) and vehicle control group (5.3 ± 0.25) with respect to normal group (6.7 ± 0.22). The total protein level was found 6.8 ± 0.32 and 6.9 ± 0.24 (gm/dL) respectively in LDHE and HDHE treated groups.

Renal function parameters

In this experiment, similar to liver function parameters the level of renal function parameters was found close to the normal group. Urea and creatinine values (mg/dL) were found increased in control and vehicle control group animals (Table 7.3). But, these parameters were significantly ($p<0.01$) lower in LDHE [urea (31 ± 0.76) and creatinine (0.58 ± 0.02)] and HDHE [urea (34 ± 1.23), at $p<0.05$ level and creatinine (0.59 ± 0.03) at $p<0.05$ level] groups

Antioxidant status in liver

The antioxidant status is shown in figure 7.10 and 7.11. The administration of different doses of HE enhanced the antioxidant status of the liver of experimental animals. In cyclophosphamide control group animals, the activity of antioxidant enzymes (U/mg protein) like catalase (6.78 ± 0.64), SOD (0.50 ± 0.08), GPx (14.87 ± 1.47) were found decreased compared with normal group. In normal group catalase, SOD and GPx activity was found 16.36 ± 0.34, 1.21 ± 0.08, and 30.26 ± 2.31 respectively. In the same way the level of GSH was reduced to 6.84 ± 0.56 (nmol/mg protein) in control group from normal group (15.24 ± 0.30). The lipid peroxidation rate was found elevated in the control group (7.58 ± 0.45 MDA nmol/mg protein) in

comparison with the normal group (1.63 ± 0.14 MDA nmol/mg protein). In vehicle control group the activity of antioxidant enzymes (U/mg protein) like catalase, SOD, GPx were 6.87 ± 0.48, 0.53 ± 0.08 and 15.67 ± 1.32 and the GSH level was found 6.51 ± 0.70 (nmol/mg protein). The lipid peroxidation rate was 7.44 ± 0.57(MDA nmol/mg protein) in vehicle control group. The administration of LDHE and HDHE increased catalase activity in to 12.65 ± 0.47 and 12.69 ± 0.64 (U/mg protein) respectively. SOD and GPx level (U/mg protein) was found elevated in LDHE, (0.85 ± 0.07, 27.75 ± 1.03) and HDHE (0.85 ± 0.05, 27.82 ± 1.21) administered animals with respect to control animals in this experiment. The level of GSH in liver tissue was found increased significantly ($p<0.05$) in LDHE (11.70 ± 0.43) and HDHE (11.38 ± 0.76) treated animals with respect to control group of animals. The MDA level was found significantly lowered at $p<0.05$ level in LDHE (1.80 ± 0.21) and HDHE (1.76 ± 0.08) treated animals in comparison with vehicle control.

Table 7.2. Protective effect of HE treatment on liver function parameters in cyclophosphamide-induced mice

Group	Total Bilirubin (mg/dL)	AST (U/L)	ALT (U/L)	ALP (U/L)	Total Protein (gm/dL)
Normal	0.32 ± 0.04	140 ± 20.14	46 ± 2.15	46.25 ± 10.14	6.7 ± 0.22
Control	0.65 ± 0.05$^{\#\#}$	210 ± 16.34$^{\#\#}$	71 ± 3.11$^{\#\#}$	92.75 ± 13.65$^{\#\#}$	5.1 ± 0.26$^{\#\#}$
Vehicle control (1 % propylene glycol)	0.58 ± 0.06^{ns}	205 ± 18.12 ^{ns}	69 ± 2.02 ^{ns}	96.32 ± 13.18 ^{ns}	5.3 ± 0.25 ^{ns}
LDHE (160 mg/kg b. wt)	0.33 ± 0.05**	135 ± 14.80**	48 ± 2.24**	50.27 ± 12.29**	6.8 ± 0.32**
HDHE (260 mg/kg b.wt)	0.33 ± 0.05**	139 ± 18.23**	51 ± 2.52**	53.18 ± 13.49**	6.9 ± 0.24**

Values are mean ± standard deviation of six animals per group
$^{\#\#}$:p<0.01 between normal and control group ^{ns} p>0.05, ** p<0.01 between control and treated groups

Table 7.3. Protective effect of HE treatment on renal function parameters in cyclophosphamide-induced mice

Group	Urea (mg/dL)	Creatinine (mg/dL)
Normal	28 ± 0.03	0.41 ± 0.02
Control	51 ± 0.12$^{\#\#}$	0.98 ± 0.04$^{\#\#}$
Vehicle control (1 % propylene glycol)	49 ± 0.17^{ns}	0.95 ± 0.02 ^{ns}
LDHE (160 mg/kg b. wt)	31 ± 0.06**	0.58 ± 0.02**
HDHE (260 mg/kg b. wt)	34 ± 0.08*	0.59 ± 0.03**

Values are mean ± standard deviation of six animals per group.
$^{\#\#}$:p<0.01 between normal and control group ^{ns} p>0.05, *p<0.05,** p<0.01 between control and treated groups

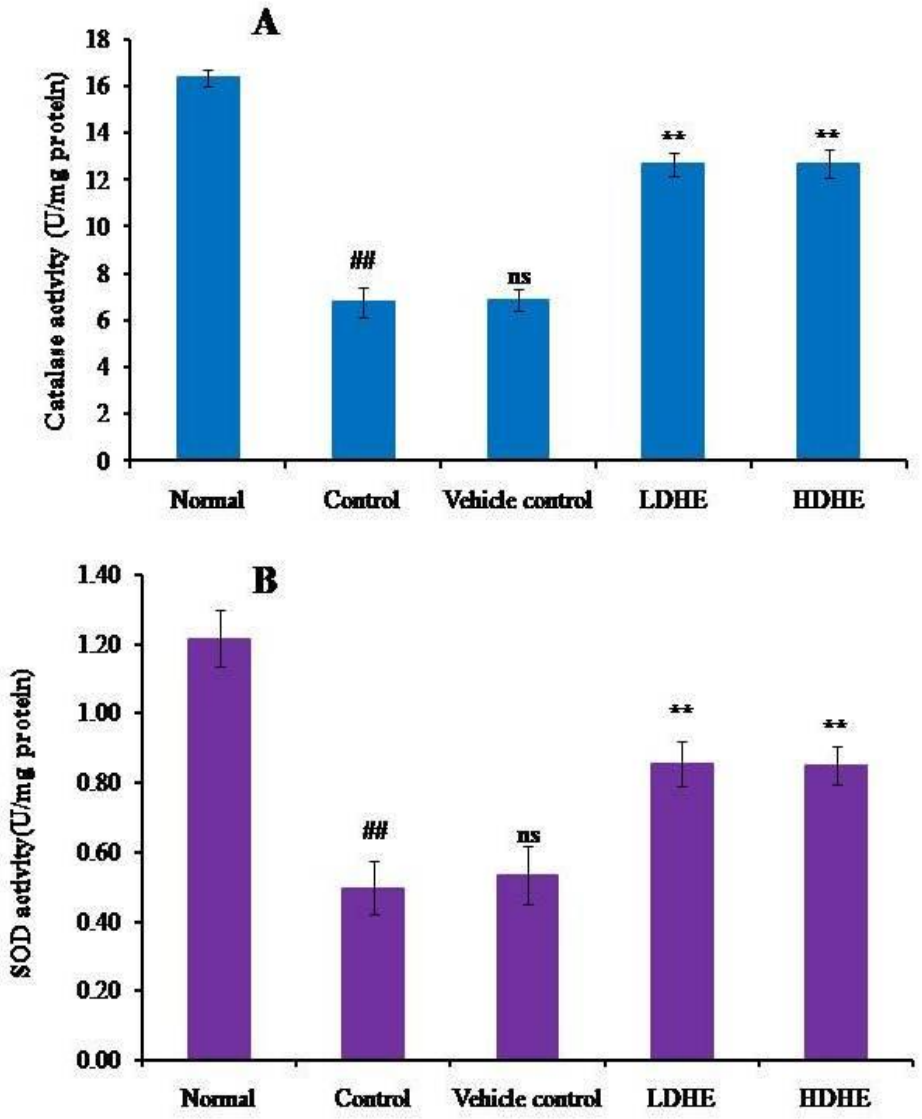

Figure 7.10. Protective effect of HE treatment on the liver antioxidant status in cyclophosphamide-induced mice: A) catalase and B) SOD activity. normal; animals treated with 200 μL of saline (p.o.) for ten days, control; animals treated with 200 μL of CTX (25 mg/kg b. wt, p.o.) for ten days, vehicle control, animals treated with 200 μL of 1% food graded propylene glycol (p.o.) and CTX (25 mg/kg b. wt, p.o.) for ten days, LDHE; animals treated with 200 μL of 160 mg/kg b. wt of HE and (p.o.) and CTX (25 mg/kg b. wt, p.o.) for ten days, HDHE; animals treated with 200 μL of 260 mg/kg b. wt of HE and (p.o.) and CTX (25 mg/kg b. wt, p.o.) for ten days. Values are mean ± standard deviation of six animals per group. $^{\#\#}$: $p<0.01$ (control compared to normal), ^{ns} $p>0.05$, ** $p<0.01$ between control and treated groups

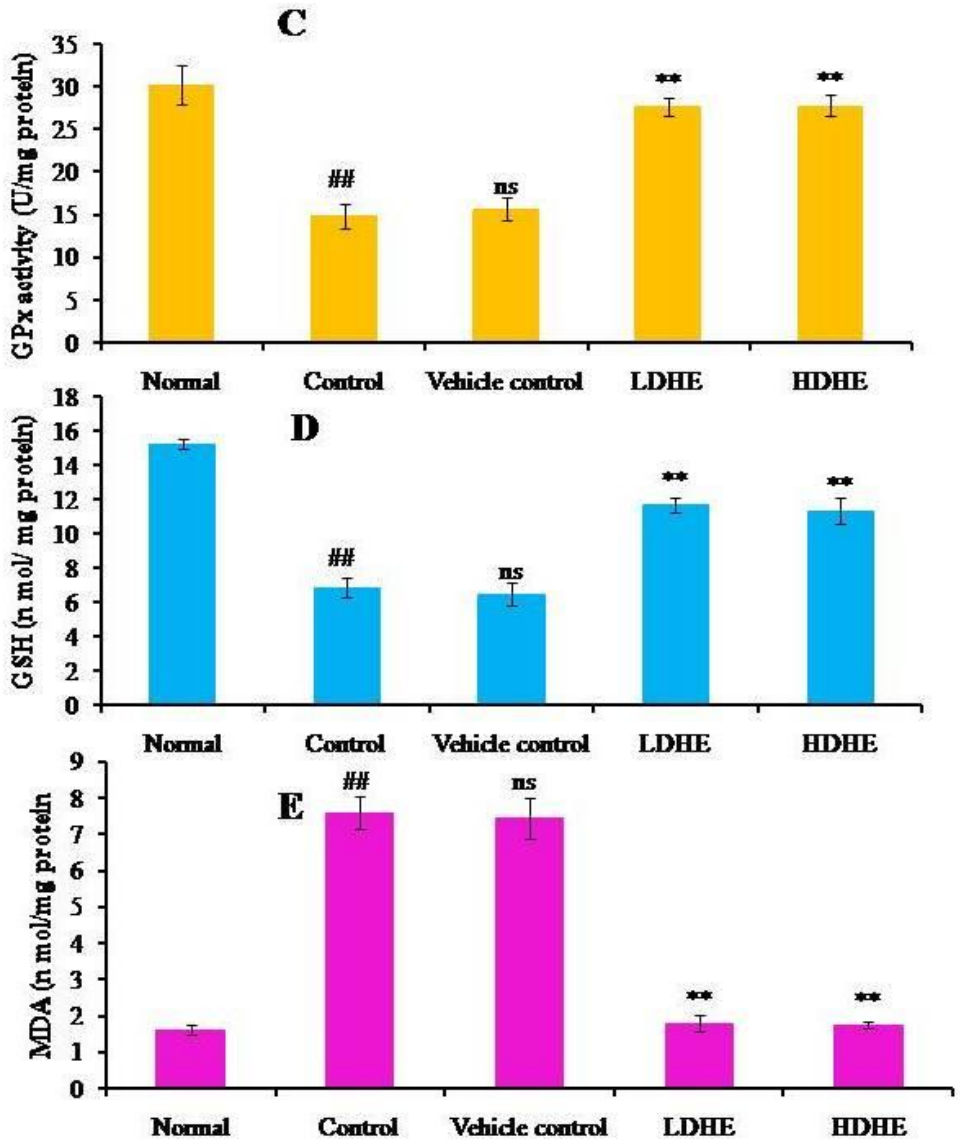

Figure 7.11. Protective effect of HE treatment on the liver antioxidant status in cyclophosphamide-induced mice: C) GPx D) GSH and E) MDA. normal; animals treated with 200 μL of saline (p.o.) for ten days, control; animals treated with 200 μL of CTX (25 mg/kg b. wt, p.o.) for ten days, vehicle control, animals treated with 200 μL of 1% food graded propylene glycol (p.o.) and CTX (25 mg/kg b. wt, p.o.) for ten days, LDHE; animals treated with 200 μL of 160 mg/kg b. wt of HE and (p.o.) and CTX (25 mg/kg b. wt, p.o.) for ten days, HDHE; animals treated with 200 μL of 260 mg/kg b. wt of HE and (p.o.) and CTX (25 mg/kg b. wt, p.o.) for ten days. Values are mean ± standard deviation of six animals per group. $^{\#\#}$: $p<0.01$ (control compared to normal), ^{ns} $p>0.05$, ** $p<0.01$ between control and treated groups

Antioxidant status in kidney

Similar to the protective effect of HE on the liver antioxidant status, the antioxidant status of the renal tissue was also found better in cyclophosphamide-induced mice

(7.12 and 7.13). In the renal tissue of the normal group, the activity of catalase enzyme (U/mg protein) was found 21.71 ± 1.14. It was 13.37 ± 0.80, 12.01 ± 1.17, 21.28 ± 1.61 and 21.40 ± 1.45 in control, vehicle control, LDHE and HDHE respectively. A similar trend was noted in the activity of SOD and GPx of renal tissue. The concentration of GSH (nmol/mg protein) was found 14.63 ± 0.45 in the normal group. In control and vehicle control group the GSH level was estimated only to 5.60 ± 0.94 and 6.07 ± 0.50 respectively. In the LDHE and HDHE, the GSH level was noted to be 13.56 ± 0.58 and 13.52 ± 0.83 nmol/ mg protein respectively and was significant at $p<0.01$ level with respect to control. In this experiment LDHE and HDHE values were found close to each other. The lipid peroxidation rate (in MDA equivalent/mg protein) of renal tissue was found elevated in control (5.65 ± 0.07) and vehicle control (5.72 ± 0.29) with respect to normal group (2.33 ± 0.12). In the treatment groups, LDHE and HDHE the levels were 2.44 ± 0.03 and 2.76 ± 0.08 respectively and it was found significant with control at $p<0.01$ level.

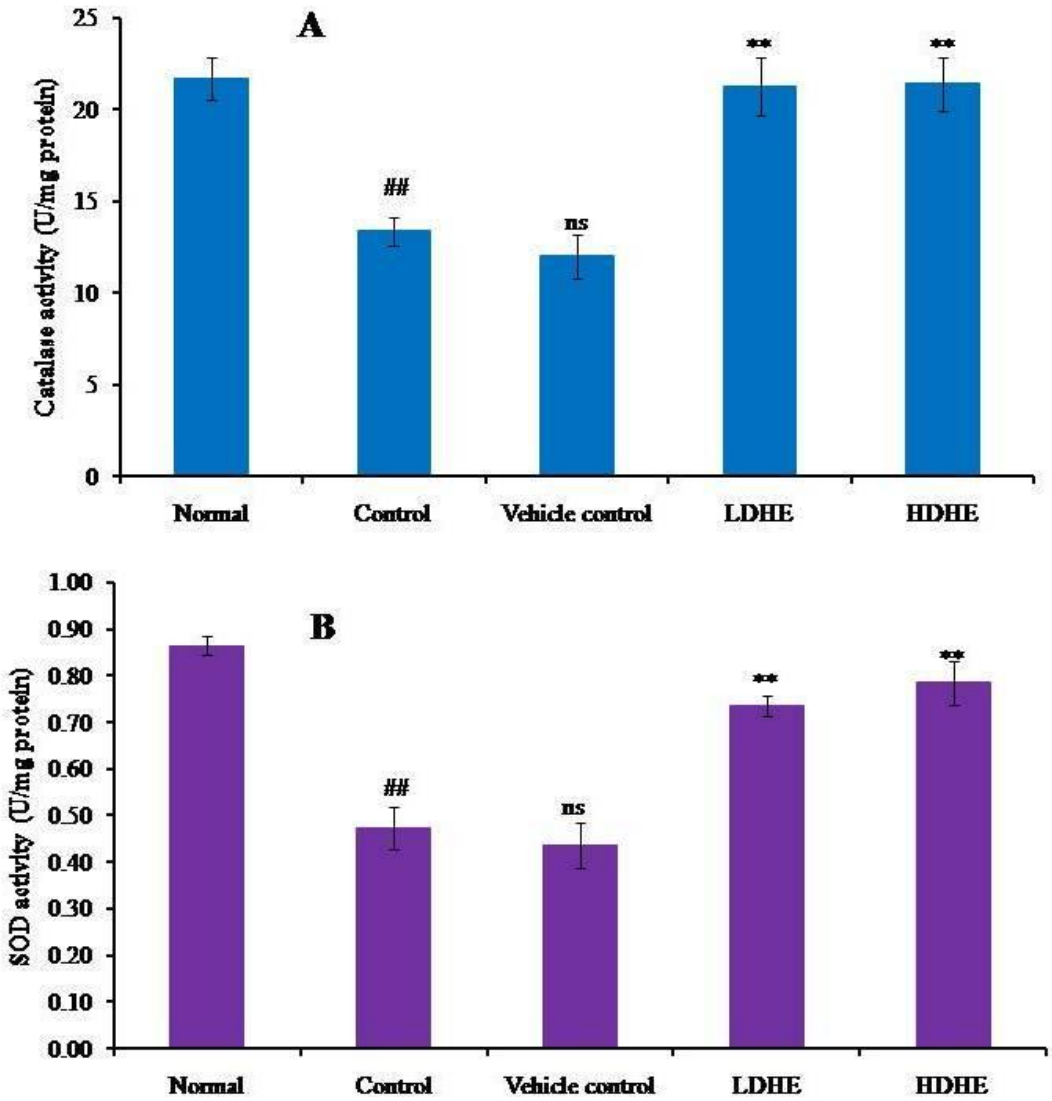

Figure 7.12. Protective effect of HE treatment on the kidney antioxidant status in cyclophosphamide-induced mice: A) catalase and B) SOD activity. normal; animals treated with 200 μL of saline (p.o.) for ten days, control; animals treated with 200 μL of CTX (25 mg/kg b. wt, p.o.) for ten days, vehicle control, animals treated with 200 μL of 1% food graded propylene glycol (p.o.) and CTX (25 mg/kg b. wt, p.o.) for ten days, LDHE; animals treated with 200 μL of 160 mg/kg b. wt of HE and (p.o.) and CTX (25 mg/kg b. wt, p.o.) for ten days, HDHE; animals treated with 200 μL of 260 mg/kg b. wt of HE and (p.o.) and CTX (25 mg/kg b. wt, p.o.) for ten days. Values are mean ± standard deviation of six animals per group. $^{\#\#}$: $p<0.01$ (control compared to normal), ^{ns} $p>0.05$, ** $p<0.01$ between control and treated groups

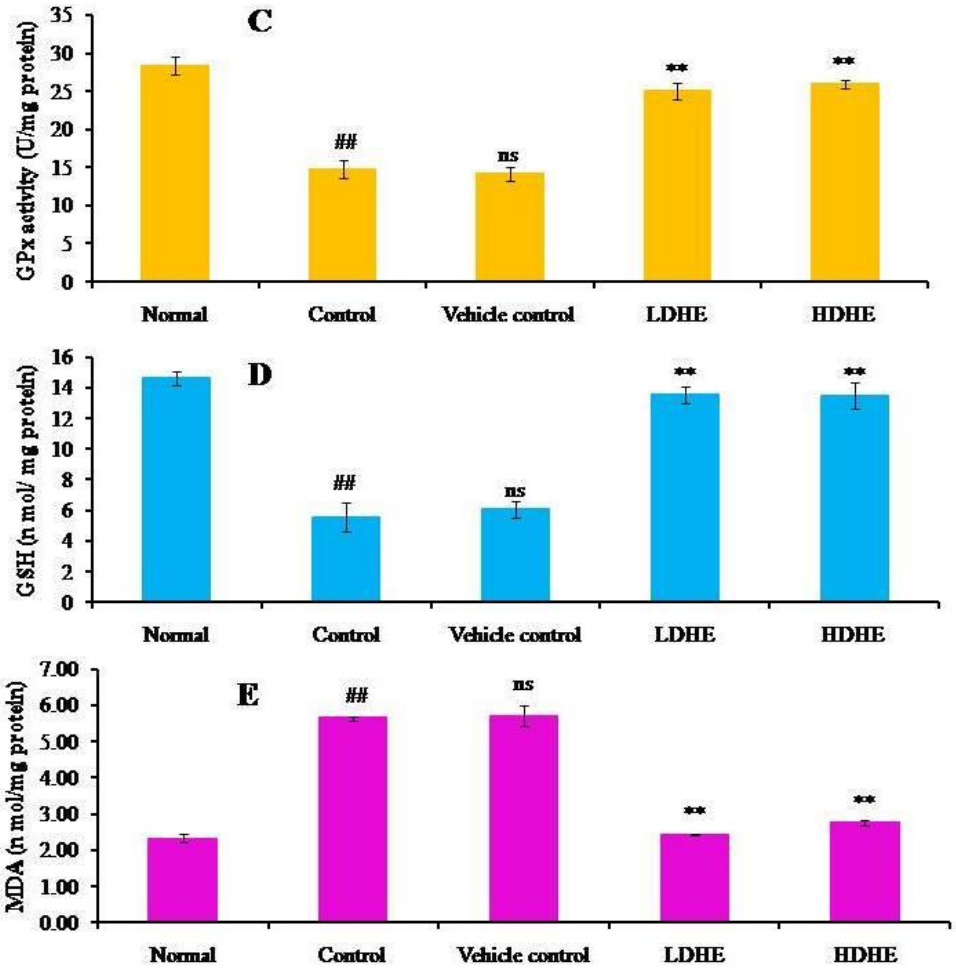

Figure 7.13. Protective effect of HE treatment on the kidney antioxidant status in cyclophosphamide-induced mice: C) GPx D) GSH and E) MDA. normal; animals treated with 200 μL of saline (p.o.) for ten days, control; animals treated with 200 μL of CTX (25 mg/kg b. wt, p.o.) for ten days, vehicle control, animals treated with 200 μL of 1% food graded propylene glycol (p.o.) and CTX (25 mg/kg b. wt, p.o.) for ten days, LDHE; animals treated with 200 μL of 160 mg/kg b. wt of HE and (p.o.) and CTX (25 mg/kg b. wt, p.o.) for ten days, HDHE; animals treated with 200 μL of 260 mg/kg b. wt of HE and (p.o.) and CTX (25 mg/kg b. wt, p.o.) for ten days. Values are mean ± standard deviation of six animals per group. $^{\#\#}$: $p<0.01$ (control compared to normal), ^{ns} $p>0.05$, ** $p<0.01$ between control and treated groups

Histological observations

Liver tissue from control and vehicle control mice showed severe damage. Inflammation, dilation of blood vessels, haemorrhage and necrosis were observed in these tissues. Along with these fat depositions was also noted in the control and vehicle control group. The liver tissue of HE treated groups showed less damage in the histopathological analysis (Figure 7.14).

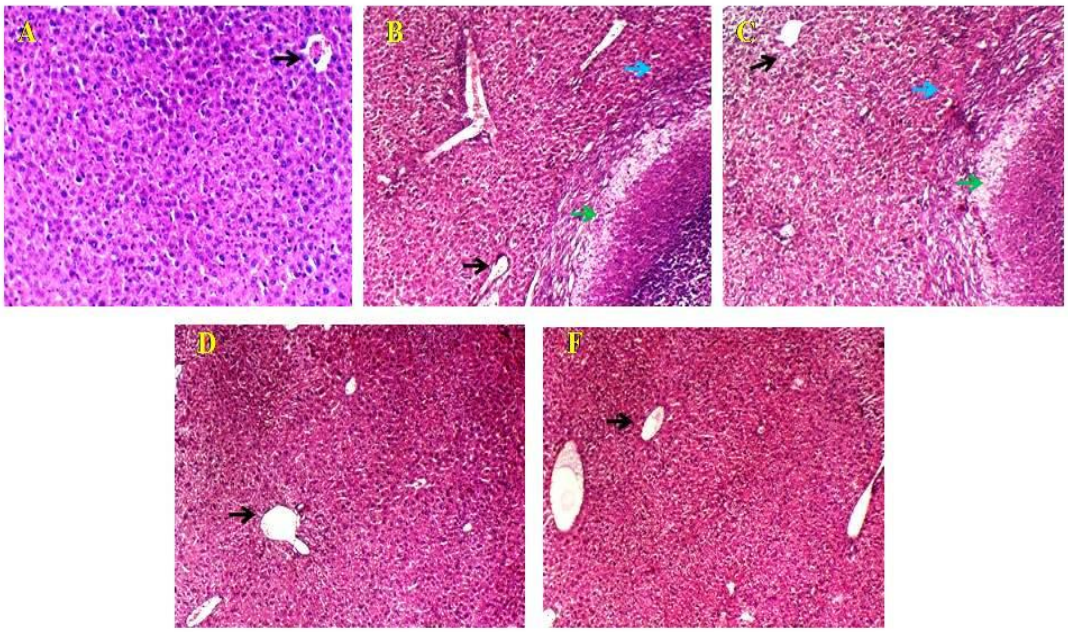

Figure 7. 14. Histological evaluation of the protective effect of HE treatment on the liver in cyclophosphamide administered mice: A) normal; animals treated with 200 μL of saline (p.o.) for ten days, B) control; animals treated with 200 μL of CTX (25 mg/kg b. wt, p.o.) for ten days, C) vehicle control, animals treated with 200 μL of 1% food graded propylene glycol (p.o.) and CTX (25 mg/kg b. wt, p.o.) for ten days, D) LDHE; animals treated with 200 μL of 160 mg/kg b. wt of HE and (p.o.) and CTX (25 mg/kg b. wt, p.o.) for ten days and E) HDHE; animals treated with 200 μL of 260 mg/kg b. wt of HE and (p.o.) and CTX (25 mg/kg b. wt, p.o.) for ten days. The black arrow represents the vein, the blue arrow represents necrosis, and the green arrow represents fat deposition, (H & E staining, 200 X)

The histological analysis of kidney tissue of control and vehicle control group animals showed many abnormal changes in renal tissue architecture (Figure 7.15). The abnormality in the size and shape of renal corpuscles were observed in control and vehicle control group. Haemorraghage and necrosis were observed in control and vehicle group. The HE treated group showed tendency to heal the damage caused by cyclophosphamide but, a small number of haemorrhage was noted in HDHE group.

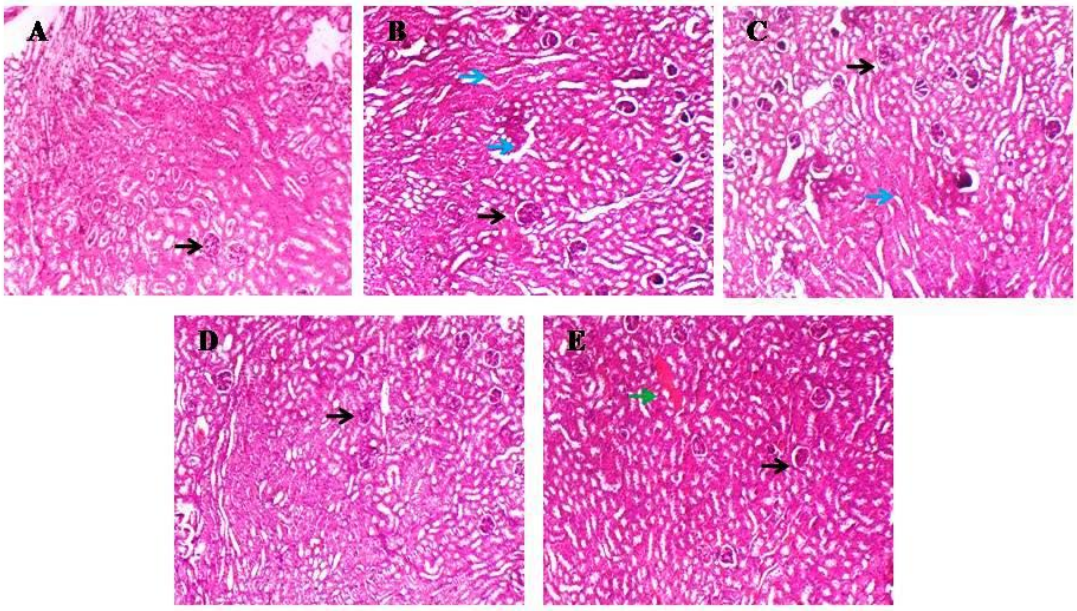

Figure 7.15. Histological evaluation of the protective effect of HE treatment on the kidney in cyclophosphamide administered mice: A) normal; animals treated with 200 μL of saline (p.o.) for ten days, B) control; animals treated with 200 μL of CTX (25 mg/kg b. wt, p.o.) for ten days, C) vehicle control, animals treated with 200 μL of 1% food graded propylene glycol (p.o.) and CTX (25 mg/kg b. wt, p.o.) for ten days, D) LDHE; animals treated with 200 μL of 160 mg/kg b. wt of HE and (p.o.) and CTX (25 mg/kg b. wt, p.o.) for ten days, E) HDHE; animals treated with 200 μL of 260 mg/kg b. wt of HE and (p.o.) and CTX (25 mg/kg b. wt, p.o.) for ten days. The black arrow represents the Bowman's capsule, the blue arrow represents necrosis and the green arrow represents haemorrhage, (H & E staining, 200X)

H and E staining showed the disrupted structure of spleen in control and vehicle control group (Figure 7.16). The distinguishing marks between red pulp and white pulp were not seen in these groups. Apart from a lot of necrosis were found in these two groups. The number of cells in the control and vehicle control group was found decreased. In LDHE and HDHE group the boundary between red pulp and white pulp were observed very clearly. The lymphocytes in HE treated group were found situated closely.

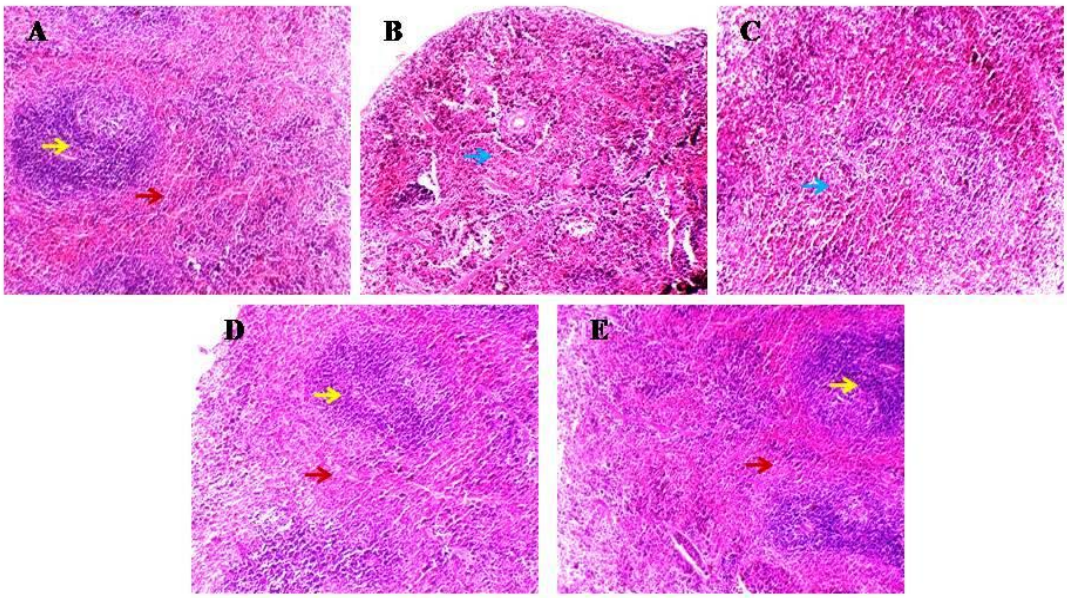

Figure 7.16. Histological evaluation of the protective effect of HE treatment on the spleen in cyclophosphamide administered mice: A) normal; animals treated with 200 μL of saline (p.o.) for ten days, B) control; animals treated with 200 μL of CTX (25 mg/kg b. wt, p.o.) for ten days, C) vehicle control, animals treated with 200 μL of 1% food graded propylene glycol (p.o.) and CTX (25 mg/kg b. wt, p.o.) for ten days, D) LDHE; animals treated with 200 μL of 160 mg/kg b. wt of HE and (p.o.) and CTX (25 mg/kg b. wt, p.o.) for ten days, E) HDHE; animals treated with 200 μL of 260 mg/kg b. wt of HE and (p.o.) and CTX (25 mg/kg b. wt, p.o.) for ten days. The red arrow represents the red pulp, the yellow arrow represents white pulp and the blue arrow represents disrupted tissue in spleen, (H & E staining, 200X)

Histological analysis of small intestine of cyclophosphamide treated control showed severe damage to the intestinal villi when compared to normal group animal tissue (Figure 7.17). The same type of response was noted in the vehicle control group. The length of the villi found decreased and mutilated. The crypt architecture was found destroyed heavily by the cyclophosphamide. In LDHE and HDHE treated groups a prominent improvement was noted. The villi were found normal and complete.

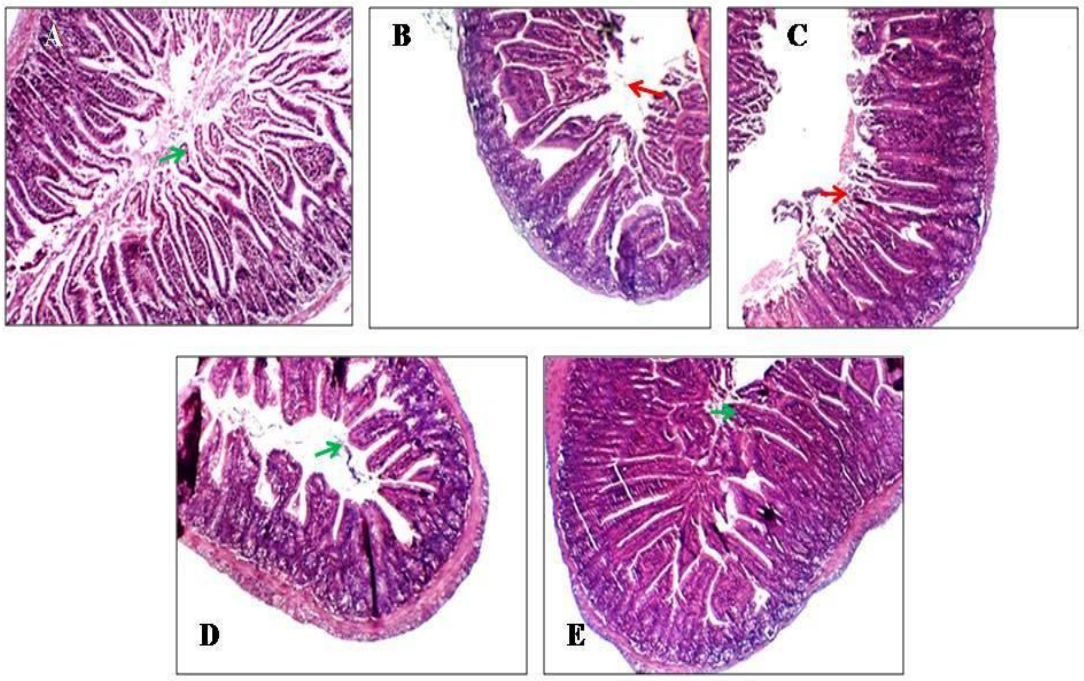

Figure 7.17. Histological evaluation of the protective effect of HE treatment on the small intestine in cyclophosphamide administered mice: A) normal; animals treated with 200 μL of saline (p.o.) for ten days, B) control; animals treated with 200 μL of CTX (25 mg/kg b. wt, p.o.) for ten days, C) vehicle control, animals treated with 200 μL of 1% food graded propylene glycol (p.o.) and CTX (25 mg/kg b. wt, p.o.) for ten days, D) LDHE; animals treated with 200 μL of 160 mg/kg b. wt of HE and (p.o.) and CTX (25 mg/kg b. wt, p.o..) for ten days, E) HDHE; animals treated with 200 μL of 260 mg/kg b. wt of HE and (p.o.) and CTX (25 mg/kg b. wt, p.o.) for ten days. The red arrow represents the disrupted villi and the green arrow represents normal villi, (H & E staining, 200X)

7.3.3. Effect of HE on cyclophosphamide-induced systemic toxicity in tumour-bearing mice

Body weight

The average body weight (gm) of mice was found decreased in control (from 28.13 ± 0.76 to 22.30 ± 1.27) and vehicle control (from 28.53 ± 0.49 to 22.57 ± 0.39) and it

started decreasing from the 5th day onwards. The average body weight in LDHE and HDHE treated groups was started decreasing from the 10th day of the experiment period (Figure 7.18). In the untreated (tumour alone) animal group, the body weight was found increasing from 28.34 ± 0.32 to 33.32 ± 1.43.

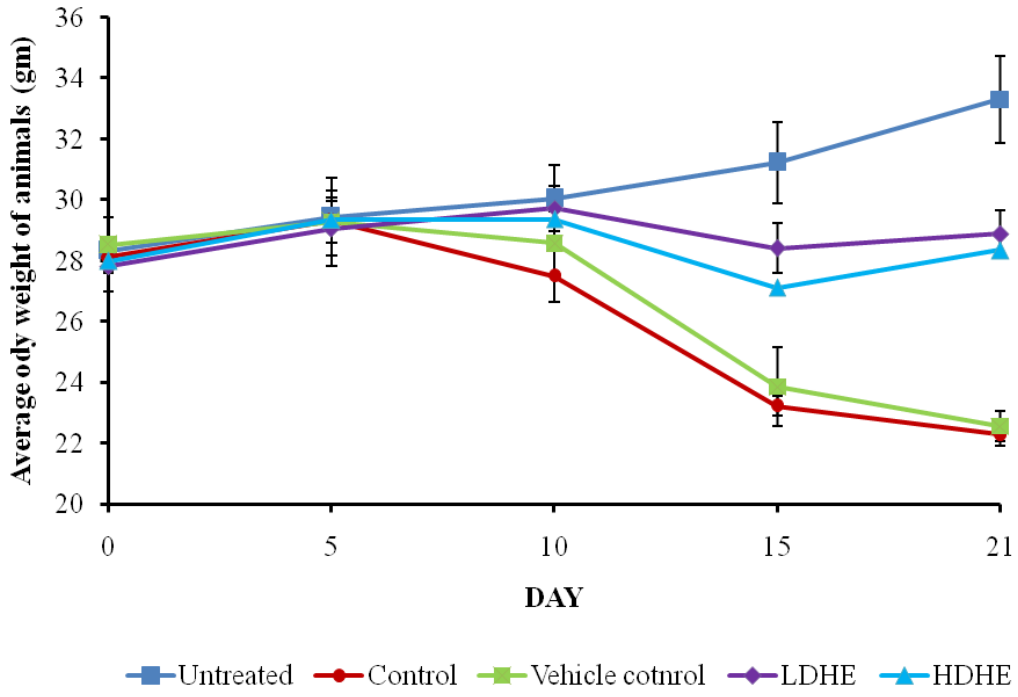

Figure 7.18. Protective effect of HE treatment on the average body weight of cyclophosphamide-induced toxicity in tumour-bearing mice: untreated; animals administered with 200 μL of saline (p.o.) for ten days, control; animals treated with 200 μL of CTX (25 mg/kg b. wt, p.o.) for ten days, vehicle control, animals treated with 200 μL of 1% food graded propylene glycol (p.o.) and CTX (25 mg/kg b. wt, p.o.) for ten days, LDHE; animals treated with 200 μL of 160 mg/kg b. wt of HE and (p.o.) and CTX (25 mg/kg b. wt, p.o.) for ten days, HDHE; animals treated with 200 μL of 260 mg/kg b. wt of HE and (p.o.) and CTX (25 mg/kg b. wt, p.o.) for ten days. Tumour was inoculated by injecting DLA cells (1x10^6 cells) into right hind limb of animals in all groups one day prior to the administration of drugs. Values are mean ± standard deviation of six animals per group

Tumour volume and tumour weight

The tumour volume (cm^3) of the experimental animals in all groups was found decreasing (Figure 7.19) except the untreated (tumour alone) group. At the end of the experiment, the tumour volume was observed as 0.85 ± 0.05 in LDHE and 0.92 ± 0.13 in HDHE with respect to control (1.13 ± 0.09). In-vehicle control group the tumour volume was found increasing and the maximum value was observed on the 21st day of

the experiment (1.15 ± 0.13). The tumour volume was 1.15 ± 0.13 in the vehicle control group. In the untreated (tumour alone) group the tumour volumes were increased steadily and end up with 5.45 ± 0.21 cm^3 on the 21st day. The average tumour weight (gm) of the untreated animal was 2.76 ± 0.05. The average tumour weight was 1.42 ± 0.06, 1.40 ± 0.13, 0.63 ± 0.09 and 0.64 ± 0.08 in control, vehicle control, LDHE and HDHE respectively (Figure 7.20). The percentage inhibition in tumour weight was observed as 48.55 and 49.28 in control group and vehicle control group respectively in comparison with untreated group. But, the percentage inhibition of tumour weight was 77.17 and 76.81 respectively in LDHE and HDHE administered groups.

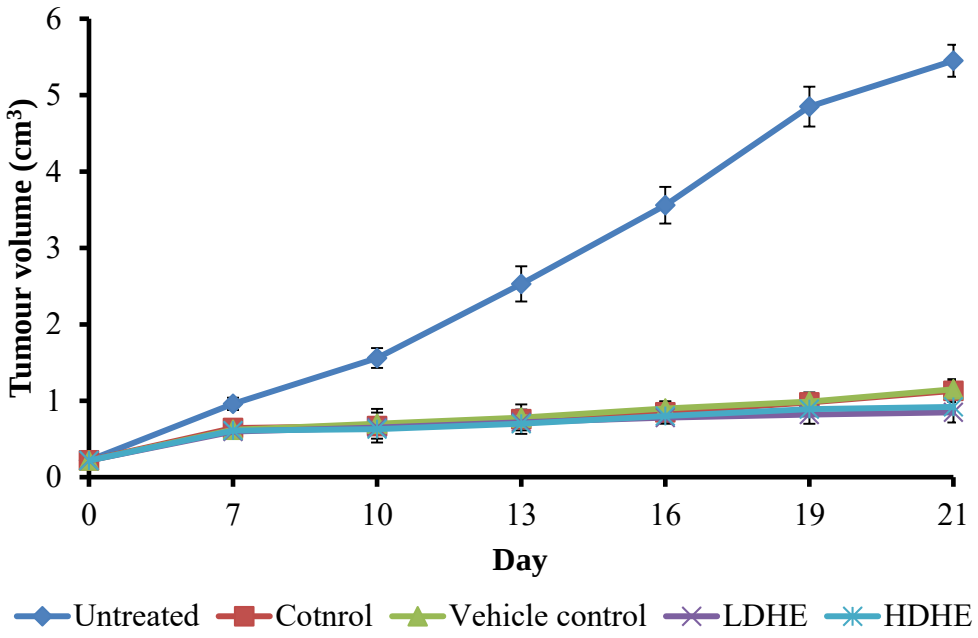

Figure 7.19. Protective effect of HE treatment on the average tumour volume (cm^3) of cyclophosphamide-induced toxicity in tumour-bearing mice: untreated; animals administered with 200 μL of saline (p.o.) for ten days, control; animals treated with 200 μL of CTX (25 mg/kg b. wt, p.o.) for ten days, vehicle control, animals treated with 200 μL of 1% food graded propylene glycol (p.o.) and CTX (25 mg/kg b. wt, p.o.) for ten days, LDHE; animals treated with 200 μL of 160 mg/kg b. wt of HE and (p.o.) and CTX (25 mg/kg b. wt, p.o.) for ten days, HDHE; animals treated with 200 μL of 260 mg/kg b. wt of HE and (p.o.) and CTX (25 mg/kg b. wt, p.o.) for ten days. Tumour was inoculated by injecting DLA cells (1x10^6 cells) into right hind limb of animals in all groups one day prior to the administration of drugs. Values are mean ± standard deviation of six animals per group

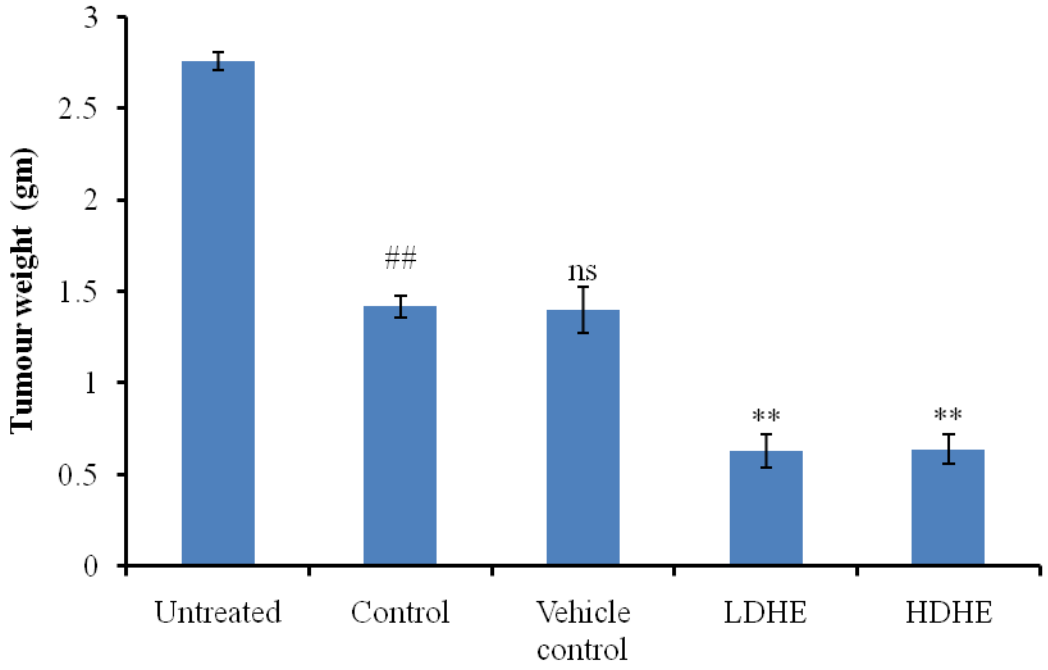

Figure 7.20. Protective effect of HE treatment on the average tumour weight of cyclophosphamide-induced toxicity in tumour-bearing mice: untreated; animals administered with 200 μL of saline (p.o.) for ten days, control; animals treated with 200 μL of CTX (25 mg/kg b. wt, p.o.) for ten days, vehicle control, animals treated with 200 μL of 1% food graded propylene glycol (p.o.) and CTX (25 mg/kg b. wt, p.o.) for ten days, LDHE; animals treated with 200 μL of 160 mg/kg b. wt of HE and (p.o.) and CTX (25 mg/kg b. wt, p.o.) for ten days, HDHE; animals treated with 200 μL of 260 mg/kg b. wt of HE and (p.o.) and CTX (25 mg/kg b. wt, p.o.) for ten days. Tumour was inoculated by injecting DLA cells ($1x10^6$ cells) into right hind limb of animals in all groups one day prior to the administration of drugs. Values are mean ± standard deviation of six animals per group. $^{\#\#}$: $p<0.01$ between untreated and control, ns $p>0.05$, ** $p<0.01$ between control and treated groups

Organosomatic index of liver, kidney and spleen

The organosomatic index of vital organs like liver, kidney and spleen were studied in this experiment and the data is summarised into table 7.4. A moderate decrease in the organosomatic index of liver and kidney of different experimental groups were observed with respect to the control group. The organosomatic index of liver in untreated (tumour alone) group, LDHE and HDHE was 5.10 ± 0.45, 4.98 ± 0.24 and 4.87 ± 0.10 respectively. A similar observation was noted in the organosomatic index of kidney of experimental animals (untreated - 1.35 ± 0.23, control – 1.04 ± 0.20, vehicle control – 1.09 ± 0.31, LDHE – 1.27 ± 0.13 and HDHE – 1.28 ± 0.11). The organosomatic index of spleen of untreated group was 0.72 ± 0.05. A significant increase ($p<0.01$) in the organosomatic index of spleen was noted in LDHE (0.68 ±

0.01) and HDHE (0.69 ± 0.04) with respect to control group (0.52 ± 0.05). The organosomatic index of spleen of vehicle control group (0.53 ± 0.05) was found close to control group and not significant at p>0.05 level.

Table 7.4. Protective effect of HE on the organosomatic index of liver, kidney and spleen of cyclophosphamide-induced toxicity in tumour bearing mice

Group	Liver	Kidney	Spleen
Untreated	5.10 ± 0.45	1.35 ± 0.23	0.72 ± 0.05
Control	4.59 ± 0.25[a]	1.04 ± 0.20 [a]	0.52 ± 0.05[##]
Vehicle control (1 % propylene glycol)	4.58 ± 0.18 [ns]	1.09 ± 0.31 [ns]	0.53 ± 0.05 [ns]
LDHE (160 mg/kg b. wt)	4.98 ± 0.24 [ns]	1.27 ± 0.13 [ns]	0.68 ± 0.01[**]
HDHE (260 mg/kg b.wt)	4.87 ± 0.10 [ns]	1.28 ± 0.11 [ns]	0.69 ± 0.04[**]

Values are mean ± standard deviation of six animals per group.
[a]: p>0.05 between untreated and control group
[##]: p<0.01 between untreated and control group
[ns] p>0.05, [**] p<0.01 between control and treated groups

Haematological parameters

A notable change was observed in the haematological parameters like Hb and total leucocyte count of the treated animals as depicted in figure 7.21. In the untreated (tumour alone) group, the Hb level (gm/dL) was found increasing during the experiment period (from 13.8 ± 0.23 to 14.53 ± 0.34). In control and vehicle control group the Hb level (gm/dL) shifted to 8.12 ± 0.41 and 8.09 ± 0.24 from 13.6 ± 0.15 and 13.7 ± 0.34 respectively. The fall in Hb level was noted from the 5th day of the experiment. A marginal decrease in the level of Hb was noted in LDHE and HDHE. In LDHE the Hb level was 14.0 ± 0.35 gm/dL on the initial day of the experiment and decreased to 12.95 ± 0.25 gm/dL on the 21st day. Similar to this in HDHE group, the Hb level was 13.9 ± 0.38 gm/dL on the beginning of the experiment and at the last day, it was declined into 12.83 ± 0.17 gm/dL. The average total leucocyte count (cells/cu mm) was 9900 ± 130 in control group on 0 days and decreased into 4600 ± 130 at the end of the experiment. A similar trend was noted in the leucocyte count of vehicle control group (from 10100 ± 125 to 4800 ± 120). Similar to Hb level, a marginal decrease in total leucocyte count was noted in both LDHE and HDHE but, the untreated group (tumour alone) maintained a steady state of increase in the leucocyte count.

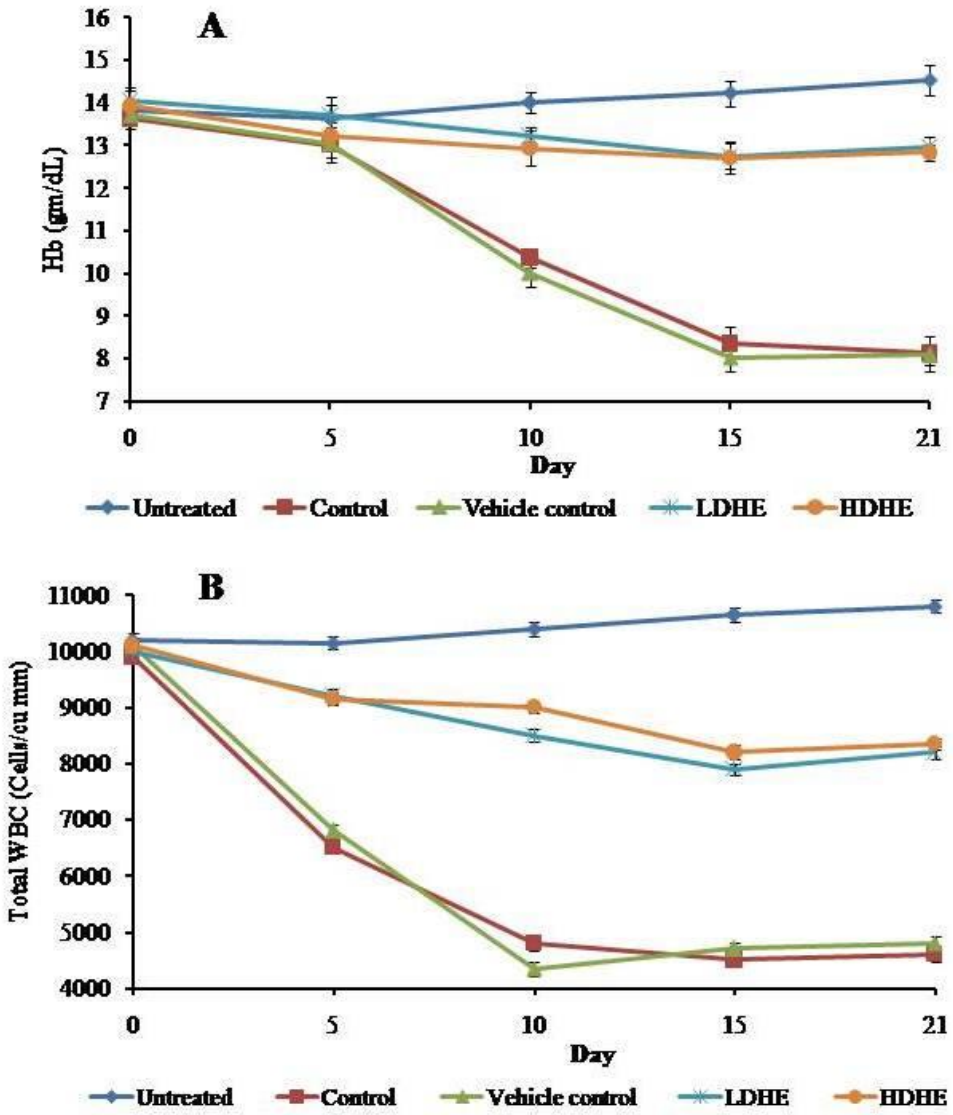

Figure 7.21. Protective effect of HE treatment on the haematological parameters of cyclophosphamide-induced toxicity in tumour-bearing mice: A) Hb level and B) total leucocyte count: untreated; animals administered with 200 μL of saline (p.o.) for ten days, control; animals treated with 200 μL of CTX (25 mg/kg b. wt, p.o.) for ten days, vehicle control, animals treated with 200 μL of 1% food graded propylene glycol (p.o.) and CTX (25 mg/kg b. wt, p.o.) for ten days, LDHE; animals treated with 200 μL of 160 mg/kg b. wt of HE and (p.o.) and CTX (25 mg/kg b. wt, p.o.) for ten days, HDHE; animals treated with 200 μL of 260 mg/kg b. wt of HE and (p.o.) and CTX (25 mg/kg b. wt, p.o.) for ten days. Tumour was inoculated by injecting DLA cells ($1x10^6$ cells) into right hind limb of animals in all groups one day prior to the administration of drugs. Values are mean ± standard deviation of six animals per group.

Liver function parameters

The effect of administration of different doses of HE on the liver function parameters in cyclophosphamide-induced toxicity in tumour bearing mice showed a promising effect (Table 7.5). In untreated (tumour alone) group of animals the total bilirubin value (mg/dL) was found to be less (0.40 ± 0.03) with respect to control (0.76 ± 0.08), vehicle control (0.82 ± 0.02), LDHE (0.51 ± 0.04) and HDHE (0.53 ± 0.02). The activity of different enzymes like AST, ALT and ALP was found increased in control and vehicle control group but, in the drug-treated groups, the values were found close to the untreated animals. Total protein level (gm/dL) was also found decrease in the control (4.34 ± 0.43) and vehicle control group (4.45 ± 0.65) with respect to the untreated group of animals (6.94 ± 0.26). The total protein level of LDHE (5.67 ± 0.23) and HDHE (5.87 ± 0.38) was found close to untreated group of animals.

Renal function parameters

Serum urea and creatinine values (mg/dL) were found elevated in control (64 ± 0.05, 0.94 ± 0.07) and vehicle control group (64 ± 0.05, 0.97 ± 0.04). In the untreated group, the serum urea and creatinine level were 34 ± 0.04 and 0.45 ± 0.05 respectively. The data regarding serum urea and creatinine of vehicle control group was not significantly different from the control group at $p>0.05$ level. In HE treated groups, the urea and creatinine level were not elevated significantly (at $p<0.01$ level) with respect to the control group (Table 7.6).

Table 7.5. Protective effect of HE treatment on liver function parameters in cyclophosphamide-induced toxicity in tumour-bearing mice

Group	Total Bilirubin (mg/dL)	AST (U/L)	ALT (U/L)	ALP (U/L)	Total protein (gm/dL)
Untreated	0.40 ± 0.03	120 ± 12.34	52 ± 1.67	48.23 ± 2.54	6.94 ± 0.26
Control	0.76 ± 0.08$^{\#\#}$	220 ± 15.64$^{\#\#}$	82 ± 2.18$^{\#\#}$	93.56 ± 3.54$^{\#\#}$	4.34 ± 0.43$^{\#\#}$
Vehicle control (1 % propylene glycol)	0.82 ± 0.02 ^{ns}	214 ± 17.88 ^{ns}	83 ± 1.98 ^{ns}	92.92 ± 2.39 ^{ns}	4.45 ± 0.65 ^{ns}
LDHE (160 mg/kg b. wt)	0.51 ± 0.04**	145 ± 14.32**	62 ± 2.12**	58.89 ± 3.21**	5.67 ± 0.23**
HDHE (260 mg/kg b.wt)	0.53 ± 0.02**	152 ± 13.21**	63 ± 2.76**	59.23 ± 3.54**	5.87 ± 0.38**

Values are mean ± standard deviation of six animals per group.
$^{\#\#}$P<0.01, between untreated and control group
^{ns} p>0.05, ** p<0.01 between control and treated groups

Table 7.6. Protective effect of HE treatment on renal function parameters in cyclophosphamide-induced toxicity in tumour-bearing mice

Group	Urea (mg/dL)	Creatinine (mg/dL)
Untreated	34 ± 0.04	0.45 ± 0.05
Control	64 ± 0.07$^{\#\#}$	0.94 ± 0.07$^{\#\#}$
Vehicle control (1 % propylene glycol)	64 ± 0.05 ^{ns}	0.97 ± 0.04 ^{ns}
LDHE (160 mg/kg b. wt)	48 ± 0.04**	0.57 ± 0.07**
HDHE (260 mg/kg b.wt)	48 ± 0.05**	0.58 ± 0.05**

Values are mean ± standard deviation of six animals per group.
$^{\#\#}$P<0.01, between untreated and control group
^{ns} p>0.05, ** p<0.01 between control and treated groups

Antioxidant status in liver

The liver antioxidant parameters were analysed in detail and the results are depicted in figure 7.22 and 7.23. The catalase activity (U/mg protein) of the liver tissue was found decreased in control (6.56 ± 0.44) and vehicle control group (6.50 ± 0.31) with respect to the untreated (tumour alone) group (17.41 ± 0.77). A significant increase ($p<0.01$) was noted in LDHE (13.73 ± 0.80) and HDHE (12.69 ± 0.64). The SOD activity (U/mg protein) was found 1.23 ± 0.06 in the untreated (tumour alone) group. The SOD activity was 0.46 ± 0.03, 0.43 ± 0.12, 0.68 ± 0.04 and 0.68 ± 0.14 in the control, vehicle control, LDHE and HDHE respectively. The change in SOD activity level was significant ($p<0.01$) between control and HE treated groups. GPx activity (U/mg protein) in liver tissue was affected adversely in control (12.34 ± 0.72) and vehicle control group (12.47 ± 1.24) in comparison with untreated (tumour alone) group (40.32 ± 1.39).A significant elevation (at $p<0.01$ level) in GPx activity was noted in LDHE (32.19 ± 1.58) and HDHE (33.16 ± 1.48). The concentration of GSH (nmol/mg protein) in untreated, control, vehicle control, LDHE and HDHE was 16.31 ± 1.22, 5.71 ± 0.70, 5.89 ± 1.08, 15.12 ± 0.83 and 15.11 ± 0.85 respectively. The lipid peroxidation rate (MDA nmol/mg protein) was found increased in control (6.09 ± 0.67) and vehicle control group (6.15 ± 0.37) with respect to untreated group (1.70 ± 0.20). The lipid peroxidation rate of LDHE was found 2.01 ± 0.19 in LDHE group and 2.21 ± 0.37 in HDHE, both values are significantly different from control group ($p<0.05$).

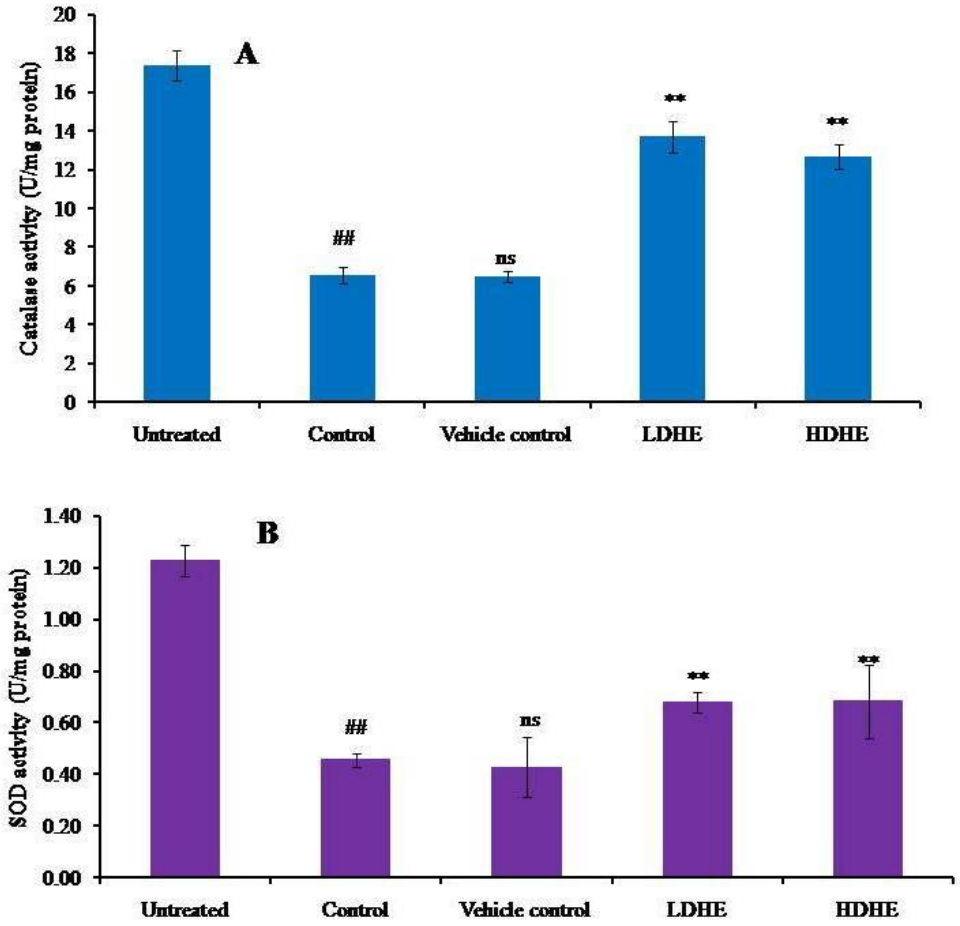

Figure 7.22. Protective effect of HE treatment on the liver antioxidant status of cyclophosphamide-induced toxicity in tumour-bearing mice: A) catalase and B) SOD activity. untreated; animals administered with 200 μL of saline (p.o.) for ten days, control; animals treated with 200 μL of CTX (25 mg/kg b. wt, p.o.) for ten days, vehicle control, animals treated with 200 μL of 1% food graded propylene glycol (p.o.) and CTX (25 mg/kg b. wt, p.o.) for ten days, LDHE; animals treated with 200 μL of 160 mg/kg b. wt of HE and (p.o.) and CTX (25 mg/kg b. wt, p.o.) for ten days, HDHE; animals treated with 200 μL of 260 mg/kg b. wt of HE and (p.o.) and CTX (25 mg/kg b. wt, p.o.) for ten days. Tumour was inoculated by injecting DLA cells ($1x10^6$ cells) into right hind limb of animals in all groups one day prior to the administration of drugs. Values are mean ± standard deviation of six animals per group. $^{\#\#}p<0.01$ between control and untreated, ^{ns} $p>0.05$, ** $p<0.01$ between control and treated groups

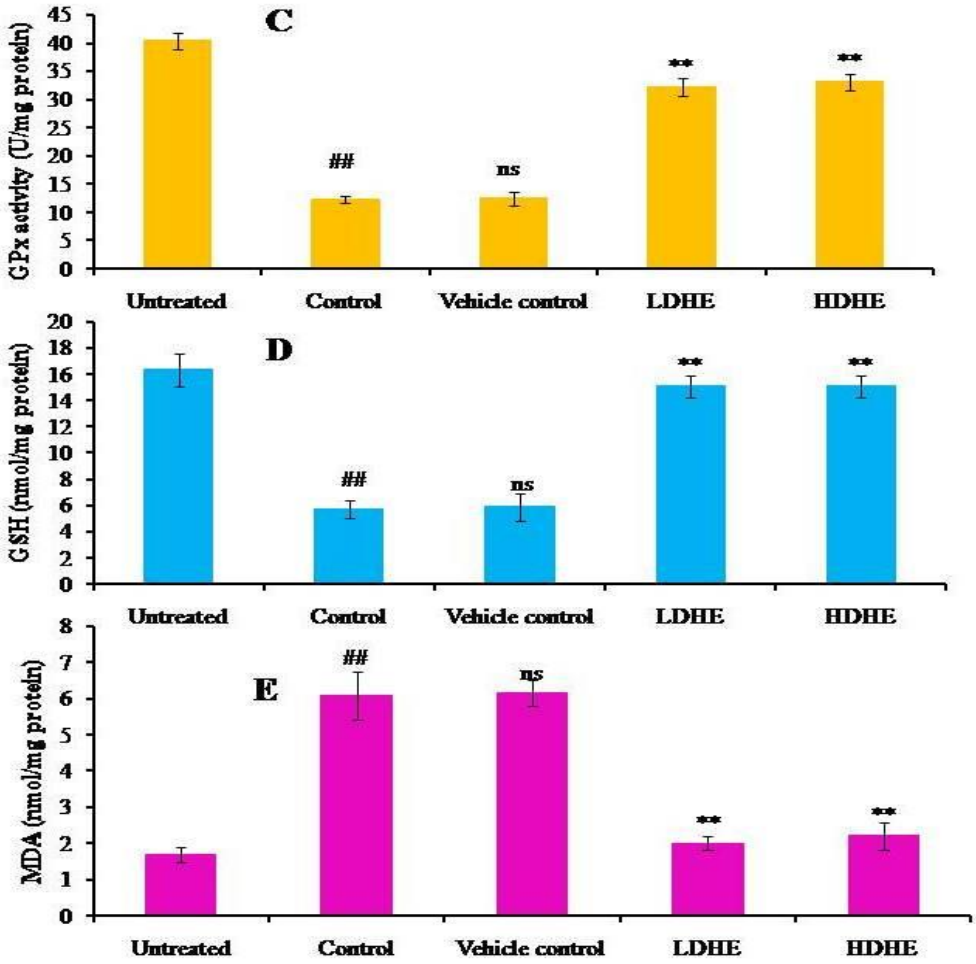

Figure 7.23. Protective effect of HE treatment on the liver antioxidant status of cyclophosphamide-induced toxicity in tumour-bearing mice: C) GPx, D) GSH and E) MDA. untreated; animals administered with 200 μL of saline (p.o.) for ten days, control; animals treated with 200 μL of CTX (25 mg/kg b. wt, p.o.) for ten days, vehicle control, animals treated with 200 μL of 1% food graded propylene glycol (p.o.) and CTX (25 mg/kg b. wt, p.o.) for ten days, LDHE; animals treated with 200 μL of 160 mg/kg b. wt of HE and (p.o.) and CTX (25 mg/kg b. wt, p.o.) for ten days, HDHE; animals treated with 200 μL of 260 mg/kg b. wt of HE and (p.o.) and CTX (25 mg/kg b. wt, p.o.) for ten days. Tumour was inoculated by injecting DLA cells ($1x10^6$ cells) into right hind limb of animals in all groups one day prior to the administration of drugs. Values are mean ± standard deviation of six animals per group. $^{\#\#}p<0.01$ between control and untreated, ^{ns} $p>0.05$, ** $p<0.01$ between control and treated groups

Antioxidant status of kidney

On biochemical evaluation, the kidney tissue isolated from control group and vehicle control group revealed low levels of activity of antioxidant enzymes, GSH concentration and high level of lipid peroxidation, when compared with the untreated group. The activity of catalase, SOD and GPx was found increased significant level

($p<0.01$) in both LDHE and HDHE treated animals when compared with the control group. The GSH concentration (nmol/mg protein) was improved to 13.18 ± 0.53 and 12.99 ± 0.41 in LDHE and HDHE respectively. The lipid peroxidation rate (MDA nmol/mg protein) in untreated (tumour alone) renal tissue was 2.33 ± 1.22 but, in control and vehicle control group the MDA level was elevated to 6.64 ± 0.44 and 6.70 ± 0.27 respectively. The administration of different doses of HE, decreased the MDA level of renal tissue into 2.56 ± 0.26 (LDHE) and 3.72 ± 0.33 (HDHE) respectively and change was found significant at $p<0.01$ level. Figure 7.24 and 7.25 depict the antioxidant status of renal tissue.

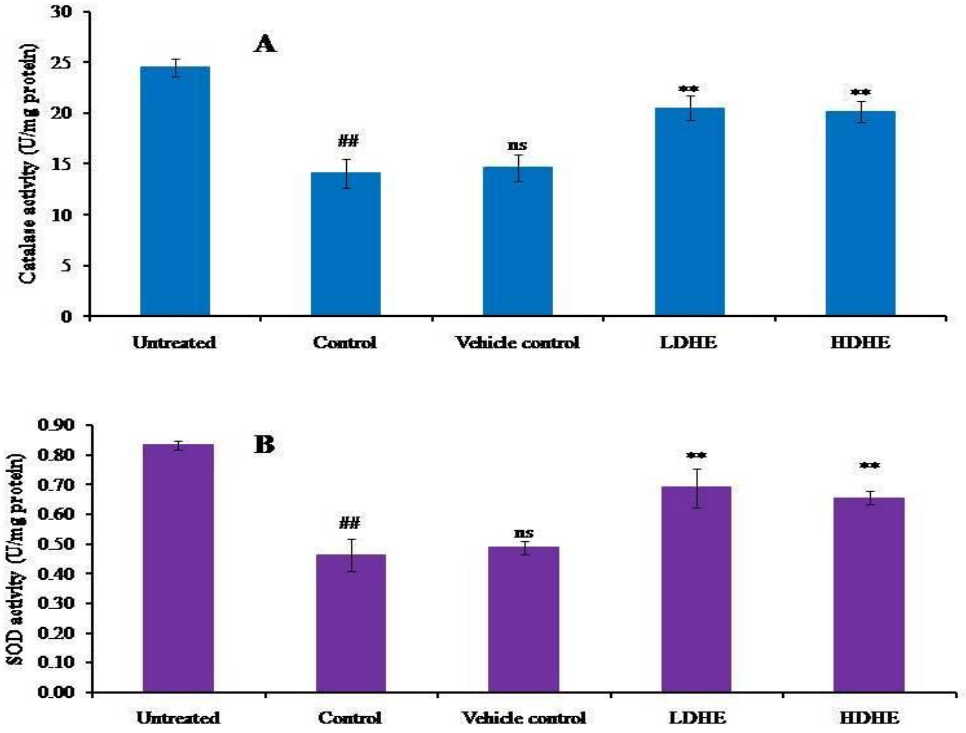

Figure 7.24. Protective effect of HE treatment on the kidney antioxidant status of cyclophosphamide-induced toxicity in tumour-bearing mice: A) catalase and B) SOD activity. untreated; animals administered with 200 μL of saline (p.o.) for ten days, control; animals treated with 200 μL of CTX (25 mg/kg b. wt, p.o.) for ten days, vehicle control, animals treated with 200 μL of 1% food graded propylene glycol (p.o.) and CTX (25 mg/kg b. wt, p.o.) for ten days, LDHE; animals treated with 200 μL of 160 mg/kg b. wt of HE and (p.o.) and CTX (25 mg/kg b. wt, p.o.) for ten days, HDHE; animals treated with 200 μL of 260 mg/kg b. wt of HE and (p.o.) and CTX (25 mg/kg b. wt, p.o.) for ten days. Tumour was inoculated by injecting DLA cells ($1x10^6$ cells) into right hind limb of animals in all groups one day prior to the administration of drugs. Values are mean ± standard deviation of six animals per group. $^{\#\#}p<0.01$ between control and untreated, ^{ns} $p>0.05$, ** $p<0.01$ between control and treated groups

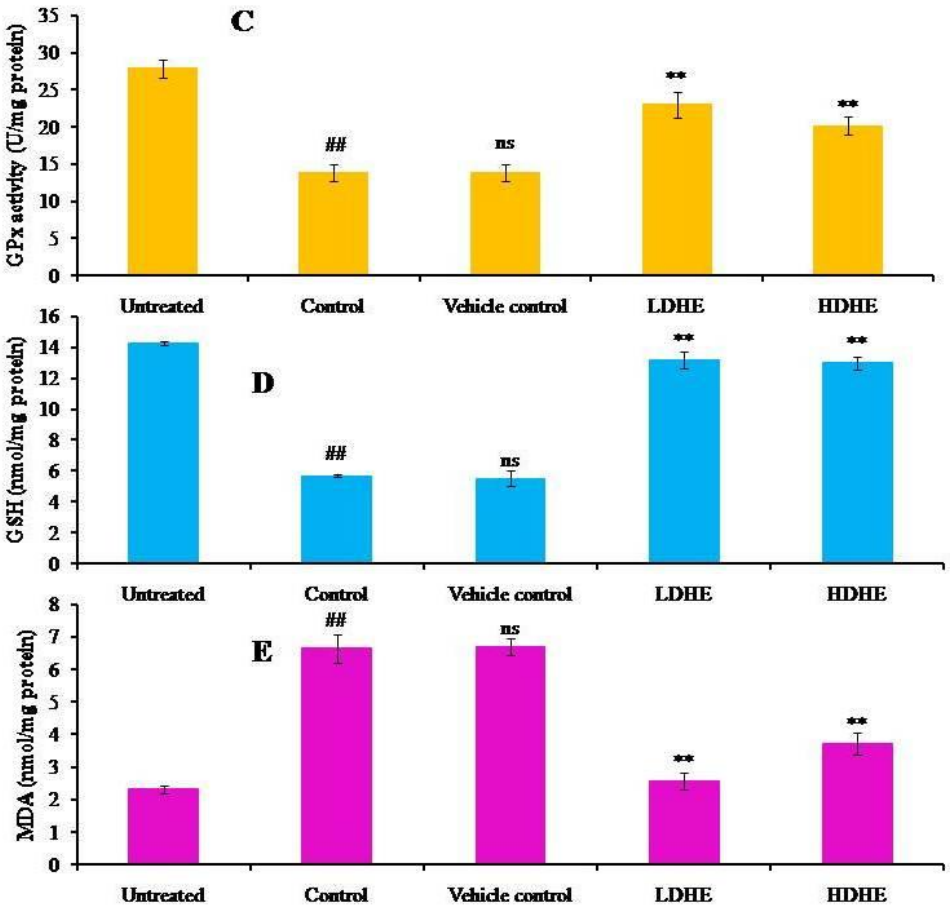

Figure 7. 25. Protective effect of HE treatment on the kidney antioxidant status of cyclophosphamide-induced toxicity in tumour-bearing mice: C) GPx, D) GSH and E) MDA. untreated; animals administered with 200 μL of saline (p.o.) for ten days, control; animals treated with 200 μL of CTX (25 mg/kg b. wt, p.o.) for ten days, vehicle control, animals treated with 200 μL of 1% food graded propylene glycol (p.o.) and CTX (25 mg/kg b. wt, p.o.) for ten days, LDHE; animals treated with 200 μL of 160 mg/kg b. wt of HE and (p.o.) and CTX (25 mg/kg b. wt, p.o.) for ten days, HDHE; animals treated with 200 μL of 260 mg/kg b. wt of HE and (p.o.) and CTX (25 mg/kg b. wt, p.o.) for ten days. Tumour was inoculated by injecting DLA cells ($1x10^6$ cells) into right hind limb of animals in all groups one day prior to the administration of drugs. Values are mean ± standard deviation of six animals per group. $^{\#\#}p<0.01$ between control and untreated, ^{ns} $p>0.05$, ** $p<0.01$ between control and treated groups

7.4. Discussion

In general, the study has unveiled the chemoprotective efficacy of HE of *S. glauca* against cisplatin-induced organ-specific toxicity and cyclophosphamide-induced systemic toxicity. Here in this study it is clear that the HE of *S. glauca* reduces the myelosuppression induced by both cisplatin and cyclophosphamide as indicated by the biochemical and histological details of individual organs. In addition, the toxic effect of cyclophosphamide treated tumor bearing animals has been reduced significantly. This strongly indicates the chemoprotective efficacy of HE.

In the current study, the renal protective effect of HE was compared with silymarin, which is a natural antioxidant extracted from the seeds of milk thistle. It is used in the treatment of inflammatory liver disease and hepatic cirrhosis. The hepato-protective effect of silymarin is attributed to the antioxidant properties (which have a role in cisplatin-induced nephrotoxicity) and increasing intracellular concentration of GSH (Tamayo and Diamond, 2007). According to Ibrahim et al., (2018) and Divya et al., (2016) silymarin made significant improvement in kidney function tests and renal histopathology as protective mechanism in cisplatin-induced acute renal failure. Herein cisplatin-induced myelosuppression was confirmed in control and vehicle control groups in contrast with normal group. Bone marrow cellularity and the number of α esterase positive cell were decreased significantly in these groups due to the action of cisplatin, which coincides with the decreasing level of WBC and Hb. The pre-treatment of HE in low and high doses increased (actually preventing the loss) the level of bone marrow cellularity and the number of α esterase positive cell. The increase in level of Hb and WBC count in the HE administered groups ushers light to its ability to nullify the secondary toxicity of cisplatin in bone marrow. In this study, the mice treated with single dose of cisplatin showed significant increase in level of renal function markers and it is due to the reduction in glomerular filtration rate (Atessahin et al., 2007). The serum urea and creatinine levels were found to be decreased in treated animals, those who were orally administered lower and higher doses of HE. This effect was comparable to that of silymarin, the standard drug used in this study. According to Baek et al., (2003), oxidative stress is the major cause of kidney damage in cisplatin-induced nephrotoxicity. The formation of cisplatin-GSH conjugation is the foremost reason for oxidative stress initiates by cisplatin (Hanigan

and Devarajan, 2003). This cisplatin-GSH conjugation leads to the depletion of GSH level and disturbs the redox status in renal tissue and may cause an increase in production of superoxide and other oxygen radicals (Santos et al., 2007). This study shows that cisplatin causes acute nephrotoxicity through decrease in the levels of antioxidant enzymes like SOD, CAT, GPx and GSH and a relative increase in lipid peroxidation, conjugated diene and tissue hydroperoxides was observed. However, LDHE and HDHE treatment reversed these changes and ameliorates the adverse effects of cisplatin similar to the action of standard drug used in the study. Histopathological analysis of kidney tissue of control and vehicle control groups show severe renal tissue damage in this study. Haemorrhage, changes in size and shape of renal corpuscles and necrosis are prominent in these tissues. The devastating action of cisplatin was not severe in HE treated animals according to the histopathological observations and it indicates the chemoprotective effect of HE. The protective action of HE may be due to the presence of phytochemicals like alkaloids, flavonoids and terpenoids present in the extract, which can quench the oxidative radicals generated in the renal tissue due to cisplatin toxicity.

The toxicity of cyclophosphamide is attributed to acrolein and phosphoramide, two active metabolites of cyclophosphamide which interferes with the antioxidant defence system generate highly reactive oxygen free radicals. The ROS causes functional and structural alterations in enzymes (Kim et al., 2014).

The average body weight of the experimental animals was found decreased when treated with cyclophosphamide with respect to normal group, which is considered as the primary symptom of toxicity (Teo et al., 2002). But, in the HE treated groups and silymarin treated groups the average bodyweight reduction was less and indicates they can ameliorate the toxic effects of cyclophosphamide. The organosomatic index of liver and kidney was decreased in control and vehicle control group with respect to normal group. But, a significant decrease in the relative organ weight of spleen was noted in control and vehicle control group and this may be due to the toxic action of cyclophosphamide on liver, kidney and especially in spleen (Li et al., 2015). The restoration of organosomatic index of the spleen in HE treated groups showing its efficacy in supporting the immune system of the body. Wang et al., (2012) reported that the administration of cyclophosphamide can reduce the bone marrow cellularity and total leucocyte count in cyclophosphamide administered animals. In the present

experiment, the bone marrow cellularity and number of alpha esterase positive cells were found decreased in control and vehicle control group indicated the severe toxic action of cyclophosphamide in bone marrow. This result was authenticated by the less Hb content and total leucocyte level in the control and vehicle control group. The increased level of bone marrow cellularity and number of alpha esterase positive cells were found in HE treated groups. Coincide with these results in the HE treated group the Hb level and total leucocyte level were found increased. In the present study, the oral administration of cyclophosphamide demonstrated significant liver and renal toxicity, as confirmed by an elevated level of serum liver and serum kidney markers in the control and vehicle control group. The unusually high level of these markers noted in the study is the result of cyclophosphamide-induced hepatic and renal dysfunction and damage.

In the current study, cyclophosphamide administration decreased liver and kidney antioxidant status. The activities of catalase, SOD, GPx of liver and kidney tissue were found increased. MDA level was found increased while GSH level decreased. The significant decrease in the activities of catalase, SOD, GPx and depletion in the level of GSH in control and vehicle control group may be due to the direct conjugation of cyclophosphamide and its metabolites to free or protein-bound sulphur groups (Caglayan et al., 2018). Administration of HE in mice induced with cyclophosphamide toxicity significantly restored the levels of the enzymatic and non-enzymatic antioxidants. This indicates the hepatoprotective and nephroprotective effects of HE on cyclophosphamide-induced hepatic and renal injuries may be based on its antioxidant properties. These results agreed with the *in vitro* antioxidant study results. The histological investigation confirmed that cyclophosphamide causes liver damage as evidenced by the cell infiltration, sinusoidal dilation and necrosis. Alternations in size and shape of renal corpuscles, haemorrhage, necrosis etc. were observed in renal tissue of cyclophosphamide treated mice. The suppressive action of cyclophosphamide on the function of the immune system organs was verified from the structural disintegration and decrease in number of cell of spleen from the control and vehicle control group. Also, reduced number of villi, mutilation of villi and alternation in change of crypts were shown in the small intestine of cyclophosphamide treated control and the vehicle control group. However, HE administration improved the histological architecture of liver, kidney, spleen and small intestine. Thus, the

histopathological observations of liver, kidney and small intestine of HE treated groups confirmed protective effect of HE and the findings supported the results of biochemical analysis.

As described in Chapter 5, it was observed that the combination of HE (LDHE) and cyclophosphamide (in lower concentrations) could increase the life span of ascites tumour bearing mice. In solid tumour bearing mice, the administration of LDHE and cyclophosphamide had shown reduction in tumour volume and tumour weight. The earlier study confirmed the chemoprotective effect of HE in cyclophosphamide-induced toxicity in mice without tumour induction. Therefore in the present study, an attempt was made to analyse whether HE could check the toxicity induced by cyclophosphamide in tumour-bearing mice.

The average body weight of all animals groups in the experiment except the untreated (tumour alone) group found lowered during the period of study. This may be owing to the toxicity of cyclophosphamide (Yu et al., 2019). The administration of HE at different doses helped the animals of the respective groups to prevent excessive weight loss as noted in control group. This result ushers to the cyclophosphamide-induced toxicity reducing property of HE.

The tumour volume and tumour weight were found decreased in all the experimental groups except untreated (tumour alone) group. The primary reason for the reduction of tumour volume and weight may be attributed to the administration of cyclophosphamide. Cyclophosphamide is widely used as a standard drug in several animals experiments to compare the effectiveness of the test substances (Meng et al., 2018). In the present experiment, the tumour volume and weight of LDHE and HDHE treated animals along with cyclophosphamide were found significantly less rather than cyclophosphamide alone treated group. This may be due to the synergistic action of HE and cyclophosphamide and suggesting the possibility of utilizing HE for combinational therapy.

The haematological parameters like Hb level and total leucocyte count are two frequently studied experimental parameters to precisely reflect the chemotherapeutic injury. In order to study the effect of HE on cyclophosphamide-induced anaemia and leukopenia, the peripheral Hb level and the total WBC count in the solid tumour bearing mice administered with cyclophosphamide were measured. The experiment

results showed that HE significantly recover the reduced Hb and WBC count in tumour-bearing mice by cyclophosphamide, suggesting that HE could offer preferential protection against anaemia and leukopenia induced by cyclophosphamide. Liver dysfunction and associated troubles are the most common regimen-related toxicity reported in patients treated with cyclophosphamide (Kocahan et al., 2017). Liver tissues were the primary regions for the microsomal activation of the drugs. The hepatic activation of cyclophosphamide leading to the creation of poisonous metabolites caused injury to the liver tissues. Because of this damage, the liver function markers level found increase in blood, which was verified by increased activities in serum, when compared with untreated group of animals. The HE treatment brought back this increase in the levels of liver function marker enzymes in cyclophosphamide treated animals and indicates the protective efficacy of the HE towards liver.

The significant increase in the level of serum urea and creatinine are indicators for renal damage and nephrotoxicity (Mok, 2016). In the present study, the increased urea and creatinine in control and vehicle control group animals substantiate the renal toxicity due to cyclophosphamide. HE significantly reduced the serum urea and creatinine levels in the cyclophosphamide-treated animals, demonstrating the protection exercised by the HE which restored renal function. Cyclophosphamide is a potent chemotherapeutic drug which can disrupt the antioxidant status of liver and kidney (Zoheir et al., 2015). In the present study, the antioxidant status of liver and kidney of cyclophosphamide exposure associated toxicity in tumour-bearing mice were shown a similar effect. Both enzymatic and non-enzymatic antioxidant mechanisms were altered to a critical level in control and vehicle group with respect to untreated animal group. The supplementation of HE in different doses was made a significant improvement in the antioxidant status of both hepatic and renal tissue of cyclophosphamide-induced tumour-bearing mice. This chemoprotective and tumour reducing effects of HE may be due to the coordinated action of different antioxidant and anti-inflammatory phytochemicals present in it.

Puranik et al., (2017) have reported the anticancer activity of ethanolic extract of leaves of *S. glauca* against T-24 cells (bladder cancer cell line) via antioxidant mechanism. The anticancer efficacy of different compounds isolated from *S. glauca* was demonstrated by many authors (Rivero-Cruz et al., 2005, Reynertson et al., 2011,

Jose et al., 2018). According to Lakshmi et al., (2014), the leaf extracts of *S. glauca* (methanolic, chloroform and ethyl acetate extracts) show excellent antioxidant quality. They claim that the antioxidant status of these extracts is due to the hydroxyl groups existing in the phenolic compounds chemical structure that can provide the necessary component as a radical scavenger.

In conclusion, the results of this study show that HE greatly protects male Swiss albino mice from the toxic manifestation of cisplatin and cyclophosphamide therapy and warrant its use in combination chemotherapy with respective chemotherapeutic drugs in the treatment of malignancy.

Chapter 8

Anticarcinogenic effect of *Simarouba glauca* DC

Contents

8.1. Introduction

8.2. Materials and methods

8.2.1. Animals

8.2.2. Methodology

8.2.3. Parameters studied

8.2.3.1. Mouse mammary gland whole mount preparation and analysis

8.2.3.2. Haematological parameters

8.2.3.3. Liver function parameters

8.2.3.4. Antioxidant status of liver

8.2.3.5. Histopathological analysis

8.2.4. Statistical analysis

8.3. Results

8.3.1. Effect of HE on the survival rate of animals

8.3.2. Necropsy

8.3.3. Organ weight

8.3.4. Haematological parameters

8.3.5. Liver function parameters

8.3.6. Antioxidant status of liver

8.3.7. Histopathological analysis

8.4. Discussion

8.1. Introduction

The results so far discussed in the preceding chapters of this thesis have revealed that the HE of *S. glauca* leaves possesses a diverse group of phytochemicals with potential antioxidant, anti-inflammatory, antiproliferative and anticancer properties. The HE has shown inhibitory action on various cell lines in the antiproliferative study. Apart from these, a moderate decrease in tumour development (both ascites and solid tumour induced by cell lines) was also noted in HE of *S. glauca* administered animals and HE was found to be an excellent chemoprotective agent in different *in vivo* models. This insisted on a study of the ability of HE in the anticarcinogenic activity of HE on DMBA-induced breast cancer development in mice, which is the focus of this chapter. The advantages of mouse mammary tumours include the following. First of all the mammary tumors are located in a confined area under the skin and can be detected effortlessly. One of the great advantages for studying mouse mammary tumourigenesis is the capacity to differentiate morphologically dissimilar lesions which are forerunner to neoplastic lesions (Medina and Shepherd, 1981). Apart from this, the tumour can be easily removed for any kind of study. Furthermore in the preliminary studies, the HE of *S. glauca* has shown antiproliferative effect on breast cancer cell lines like MDA-MB-231 and MCF-7. The IC_{50} (μg/mL) of HE for MDA-MB-231 and MCF-7 was 145.21 ± 1.22 and 104.75 ± 3.83 respectively.

According to GLOBOCAN 2018, among the diverse cancer types, breast cancer represents the most common neoplastic disease in females. Women from economically developing countries have more number for breast cancer cases in comparison with developed countries (Bray et al., 2018). As per the same report, breast cancer is placed first among Indian females with high age-adjusted rate and mortality. According to Malvia et al., (2017) the age-adjusted rate of breast cancer is forty-one per one lakh women for Delhi and is followed by Chennai (38) and Bangalore (34). Thiruvananthapuram is ranked fourth in this list with an age-adjusted incidence rate of 33.7.

7, 12-dimethylbenz(a)anthracene (DMBA) is a polycyclic aromatic hydrocarbon that has been used to promote tumours in different laboratory animals (Karimi et al., 2019). Substantial evidence advocates that DMBA-induced mammary carcinogenesis in mice imitates human breast cancer in many aspects (Singhal et al., 2019). DMBA

can induce carcinogenesis either by initiating or promoting mutations in several genes. DMBA up-regulates its own aryl hydrocarbon receptors (AhR) present in cytosol and shifted into the nucleus where it joined to the aryl hydrocarbon receptor nuclear translocator protein (ARNT). The AhR-ARNT complex induces the up-regulation of cytochrome P450 enzymes that metabolizes DMBA into a mutagenic epoxide which makes mutations (Trombino et al., 2000).

8.2. Materials and methods

8.2.1. Animals

Thirty-six adult female Swiss albino mice (7-8 weeks old) of an average weight of 25 ± 3 gm were used in this study. The animals were kept in standard conditions (Chapter 2, section 2.1.6) and were acclimatized for a period of seven days before the commencement of the experiment.

8.2.2. Methodology

The current study was conducted as per the method used by Minari and Okeke (2014) with little modifications. DMBA was used for the induction of cell proliferation in the breast tissue of mice. The mice were grouped into six categories. Group I was considered as normal and treated with saline (200 μL/day). The control group (Group II) animals were administered DMBA (3.3 mg/200 μL/week) and 200 μL saline per day. In the vehicle control group (Group III), the animals were treated with 200 μL of 1% food graded propylene glycol (a solvent used for dissolving HE) per day along with DMBA administration (3.3 mg/200 μL/week). The group IV (standard) was treated with tamoxifen (20 mg/kg b. wt/day, p.o.) along with DMBA (3.3 mg/200 μL/week). Group V and VI animals were treated with low dose (160 mg/kg b. wt, p.o.) and high dose of HE (260 mg/kg b. wt, p.o.) with DMBA (3.3 mg/200 μL/week). The DMBA was dissolved in sesame oil and administered through oral gavage. The treatment lasted for six weeks. The animals were observed for four more weeks. The mammary glands of animals were carefully checked daily after fourth week by touching and palpitation (Barros et al., 2004). The survival rate of animals in each group was calculated. After the study period (10 weeks), the animals were sacrificed by ether anaesthesia after overnight fasting. Blood was collected by direct cardiac puncture. The organs like mammary glands, liver and ovary were separated and their

weight was noted. The detailed procedure regarding the experiment is narrated in Chapter 2, section 2.2.13.1.

8.2.3. Parameters studied

8.2.3.1. Mouse mammary gland whole mount preparation and analysis

The whole-mount preparation of mouse mammary glands was done as per the protocol of Tolg et al., (2018). The third pair of mammary glands of mice from each group were isolated and transferred to the glass slide. The gland was stretched over the glass slide without tearing the tissue and allowed to dry partially and stick to the glass surface. The slides were then submerged to Carnoy's solution for 24 hours at room temperature. The slides were then transferred to the coupling jar containing Carmine alum solution and stored there at room temperature for 3 days. The excess stain was removed by submerging the slides in de-staining solution at room temperature. The solution was changed in every 30 minutes until the solution remained clear. The slides were dehydrated by submerging slides in 70, 80, 95 and absolute ethanol for five minutes each. The slides were then placed into xylene in glass containers and mounted with Permount SP 15. The slides were observed under the microscope (20X objective) and photographs were taken.

8.2.3.2. Haematological parameters

Haematological parameters like Hb level and total leucocyte count were determined as per the protocol given in section 2.2.5.2.1.1 and 2.2.5.2.1.3 respectively.

8.2.3.3. Liver function parameters

Liver function parameters like AST (Chapter 2, section 2.2.6.1.), ALT (Chapter 2 section 2.2.6.2), ALP (Chapter 2, section 2.2.6.3) activities and total bilirubin (2.2.6.4) were estimated by using commercially available analytical reagent kits.

8.2.3.4. Antioxidant status of liver

Liver homogenate (10% w/v in 0.1M Tris hydrochloric acid buffer, pH 7.4) was prepared as described Chapter 2, section 2.2.9.1 for the analysis of various enzymatic and non-enzymatic parameters associated with the antioxidant status. The different parameters like catalase (Chapter 2, section 2.2.9.1.3), SOD (Chapter 2, section

2.2.9.1.2), GPx (Chapter 2, section 2.2.12.1.8), GSH (Chapter 2, section 2.2.9.1.1) and MDA (Chapter 2, section 2.2.9.1.5) were analysed as per the protocol given in bracket.

8.2.3.5. Histological analysis

A portion of the selected organs like mammary glands, liver and ovary of animals belong to each group were fixed in 10% buffered formalin for 24 hrs. Paraffin wax embedded tissue samples were cut into slices of 5 μm and stained with hematoxylin and eosin. The sections were observed under a 20X objective lens and photographs were taken by using Magnus inverted laboratory microscope. Histopathological examination was conducted out by a veterinary pathologist who is blind to the experiment plan.

8.2.4. Statistical analysis

The values are expressed as mean ± SD of six animals. The mean values were statistically analyzed using one-way ANOVA using Graph Pad Instat 3 software (Graph Pad Software, Inc. La Jolla, USA) followed by Dunnett multiple comparison test and $P<0.05$ was considered statistically significant.

8.3. Results

8.3.1. Effect of HE on survival rate of animals

The higher rate of mice's death throughout the experiment period was recorded in control (40%) and vehicle control group (40%). In the control group, the animals died on the 60^{th} and 68^{th} day of the experiment. In the vehicle control group, the death of animals occurred on 62^{th} and 67^{th} day. Animals treated with tamoxifen (as standard drug) and different doses of HE (LDHE and HDHE) were survived during the entire study period (Figure 8.1).

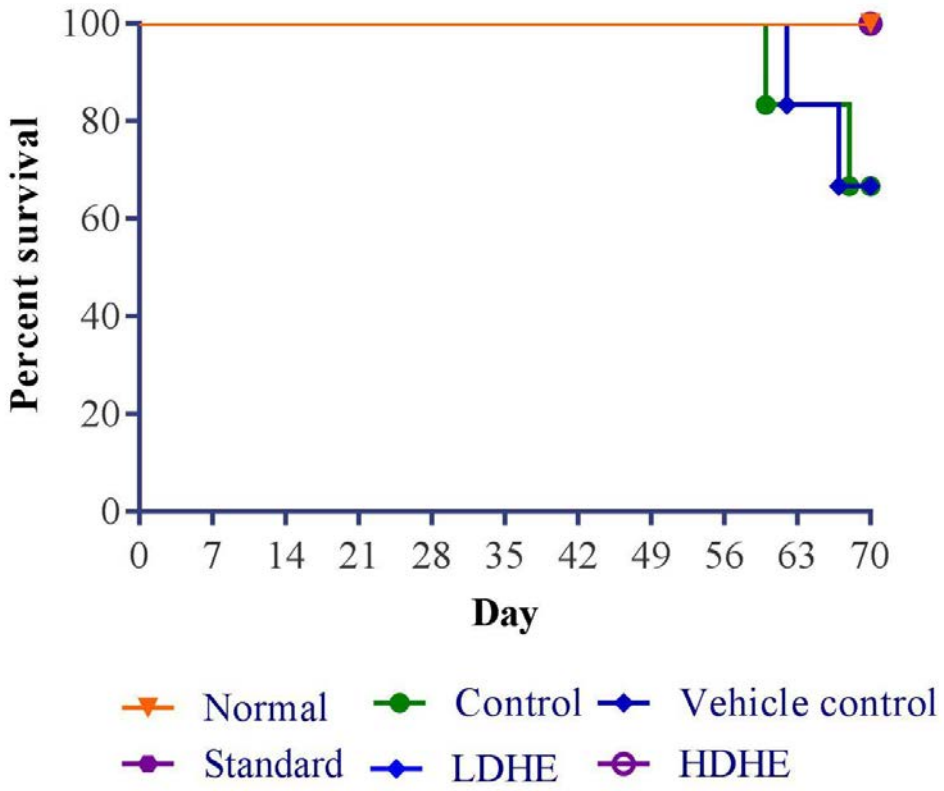

Figure 8.1. Kaplan Meir survival curve shows the anticarcinogenic effect of HE on the survival rate of experimental animals: normal, mice treated with 200 μL saline/day; control, animals treated with 200 μL saline/day; vehicle control, the animals administered 200 μL of 1% food graded propylene glycol/day; standard, animals treated with tamoxifen (20 mg/kg b. wt/day, p.o.), LDHE and HDHE, animals were treated with low dose (160 mg/kg b. wt/day p.o.) and high dose (260 mg/kg b. wt per/day p.o.) of HE. Except for normal group, all animals received intragastric dosage of DMBA at 3.3 mg/200 μL/week and respective drugs for 6 weeks

8.3.2. Necropsy

In this study, no palpable breast tumour was observed during the study period but, the isolated mammary glands (3rd pair) showed a tendency to increase in size in control and vehicle control group with respect to normal group animals (Figure 8.2). The size of the mammary glands was found more with respect to the normal group in standard and HE treated animals but, the change was found moderate. It was observed an increasing tendency of blood vessels formation around the mammary glands of mice treated with DMBA. The vascular nature was more prominent in the control and vehicle control group (Figure 8,2 B & C) in comparison with the normal group of mice (Figure 8.2 A). Because of high vascular nature the mammary glands isolated

from control and vehicle control group appeared deep red in colour. The vascular nature of mammary glands was less in other treatment groups like standard, LDHE and HDHE (Figure 8.2 D, E & F). The tumour size was also found less compared to control group animals.

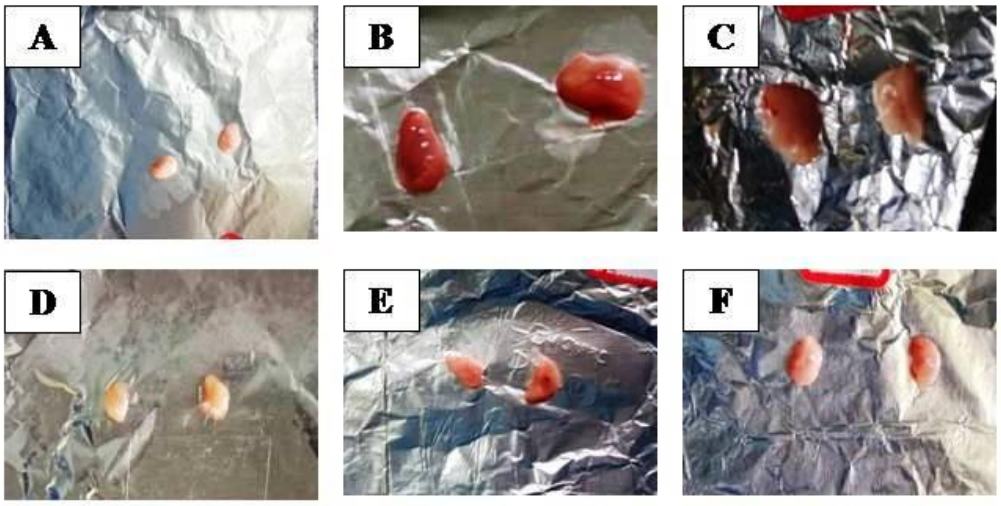

Figure 8.2. Effect of HE on the size of mammary gland tumors and its vascularisation: (A) normal, mice treated with 200 μL saline/day; (B) control, animals treated with 200 μL saline/day; (C) vehicle control, the animals administered 200 μL of 1% food graded propylene glycol/day; (D) standard, animals treated with tamoxifen (20 mg/kg b. wt/day, p.o.), (E) LDHE and (F) HDHE, animals were treated with low dose (160 mg/kg b. wt/day, p.o.) and high dose (260 mg/kg b. wt/day, p.o.) of HE. Except for normal group, all animals received intragastric dosage of DMBA at 3.3 mg/200 μL/week and respective drugs for 6 weeks

The third pair of mammary pads was showed lobulo-alveolar outgrowths in the control and vehicle control groups. Along with lobulo-alveolar outgrowths ductal outgrowths were also noted in control and vehicle control groups (Figure 8.3 B & C). But the outgrowths were not that much prominent in standard, LDHE and HDHE treated groups (Figure 8.3 D, E & F).

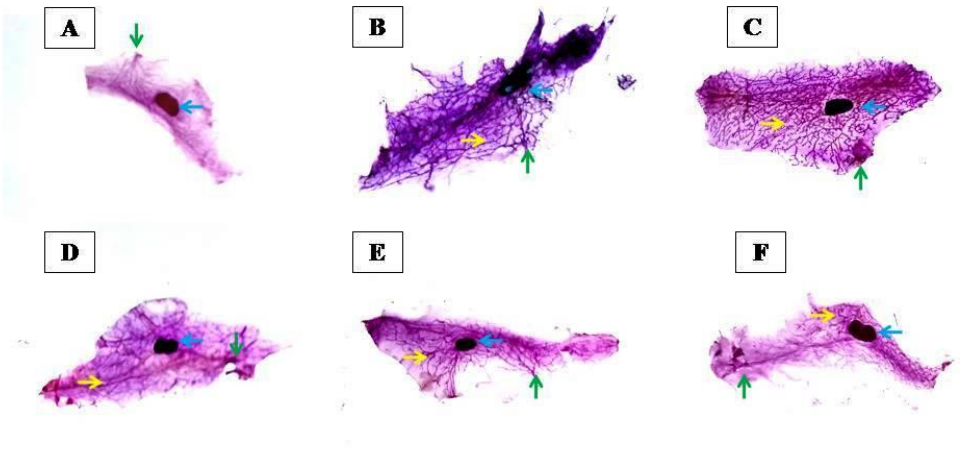

Figure 8.3. Effect of HE on the fat pad of mammary gland: (A) normal, mice treated with 200 μL saline/day; (B) control, animals treated with 200 μL saline/day; (C) vehicle control, the animals administered 200 μL of 1% food graded propylene glycol/day; (D) standard, animals treated with tamoxifen (20 mg/kg b. wt/day, p.o.), (E) LDHE and (F) HDHE, animals were treated with low dose (160 mg/kg b. wt/day, p.o.) and high dose (260 mg/kg b. wt/day, p.o.) of HE. Except for normal group, all animals received intragastric dosage of DMBA at 3.3 mg/200 μL/week and respective drugs for 6 weeks. The blue arrow indicates the lymph node, the green arrow indicates the nipple and yellow arrow indicating the proliferation

Tumour in the ovary was noted in the experimental groups except the normal group (Figure 8.4). Fifty percent (50%) ovarian tumour incidence was noted in animals belonged to control and vehicle control group as compared with the normal group. The tamoxifen was used as standard drug to control breast tumours in this study; however, the animals belonging to this category also showed tumour incidence (33%) as compared with normal group. But in this group, the tumour size was found less with respect to control and vehicle control group. Ovarian tumour burden was also noted in LDHE and HDHE treated animal groups and the percentage rate of tumour incidence was 33% in both the groups. The tumour size was found increased compare with the standard group but, was smaller than control and vehicle control group.

Moreover, the enlargement of uterine horns of the animals was observed in the control and vehicle control group members with ovarian tumours (Figure 8.4 B & C) with respect to the normal group (Figure 8.4 A). The uterine horns became short and stout in these group members. The similar changes in the size and shape of uterine horn were noted in animals those who developed tumours in ovaries from the standard, LDHE and HDHE groups (Figure 8.4 D, E & F) but, these changes were less

compared with control and vehicle control group animals. The necropsy analysis also revealed an increased number of blood vessels on the internal body wall of the experimental animals belongs to control and vehicle control groups with respect to normal group animals. The vascularisation was more prominent near to the mammary glands and ovaries of the experimental animals. Compared with blood vessels noted on the inner body wall and around the ovaries of control and vehicle control, fewer blood vessels were found in the tamoxifen and different doses of HE treated groups.

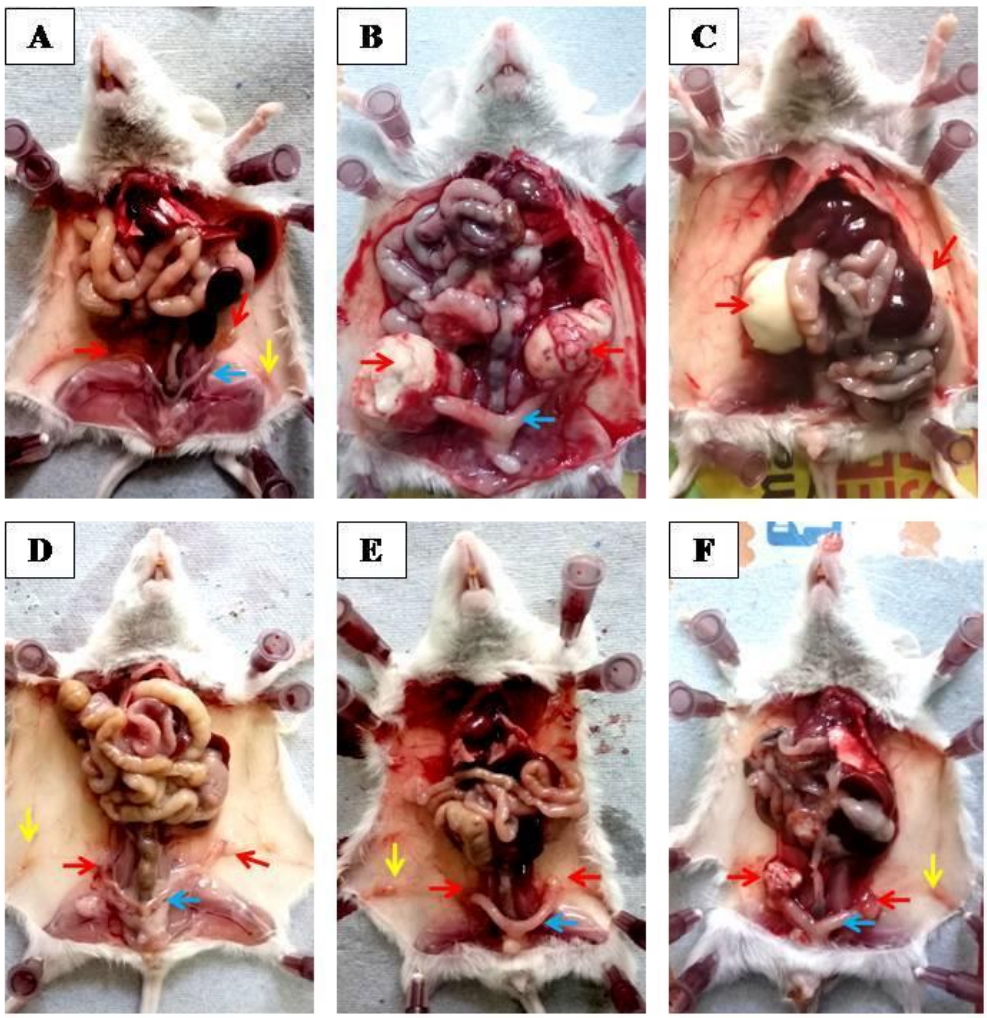

Figure 8.4. Effect of HE on ovarian tumour size: (A) normal, mice treated with 200 μL saline/day; (B) control, animals treated with 200 μL saline/day; (C) vehicle control, the animals administered 200 μL of 1% food graded propylene glycol/day; (D) standard, animals treated with tamoxifen (20 mg/kg b. wt/day, p.o.), (E) LDHE and (F) HDHE, animals were treated with low dose (160 mg/kg b. wt/day, p.o.) and high dose (260 mg/kg b. wt/day, p.o.) of HE. Except for normal group, all animals received intragastric dosage of DMBA at 3.3 mg/200 μL/week and respective drugs for 6 weeks. The red arrow indicates the ovary, the blue arrow indicates uterine horn and the yellow arrow indicates the mammary gland

8.3.3. Organ weight

Weight of 3rd pair of mammary glands, ovaries and liver were measured by the help of an electronic weighing machine and is provided in table 8.1. In the normal group, the average weight (gm) of mammary glands was found to be 0.027 ± 0.001 gm. In control and vehicle control group, the average weight of mammary gland was increased to 0.16 ± 0.003 and 0.16 ± 0.001 g respectively. The average weight of mammary glands was found elevated in standard (0.05 ± 0.002 gm), LDHE (0.09 ± 0.002 gm) and HDHE (0.09 ± 0.003 gm). A similar trend was noted in the average organ weight of ovary of the animals. The average weight of ovaries (right and left together) was 0.023 ± 0.002 (gm) in normal group of animals. The average ovary weight was found 3.17 ± 0.02 and 3.13 ± 0.03 gm in control and vehicle control group of animals. 0.46 ± 0.03, 0.68 ± 0.04 and 0.69 ± 0.03 gm were the average weight of ovaries observed in standard, LDHE and HDHE treated animals. The average weight of liver (gm) in normal group of animals was 1.32 ± 0.04 g in normal group. In control and vehicle control group, the average weight of liver found close to each other (1.67 ± 0.03 and 1.62 ± 0.03 gm). The average weight of liver in standard group was found increased (1.85 ± 0.03 gm). In LDHE and HDHE administered groups, the values were 1.56 ± 0.03 and 1.55 ± 0.02 gm and all the values were statistically significant from the control group at $p<0.01$ level.

Table 8.1. Anticarcinogenic effect of HE on the organ weight of DMBA-induced cancer development in Swiss albino mouse

Group	Organ weight (gm)		
	Mammary gland	**Ovary**	**Liver**
Normal	0.027 ± 0.001	0.023 ± 0.002	1.32 ± 0.04
Control	0.16± 0.003$^{\#\#}$	3.17 ± 0.02$^{\#\#}$	1.67 ± 0.03$^{\#\#}$
Vehicle control	0.16± 0.001^{ns}	3.13 ± 0.03 ^{ns}	1.62 ± 0.03 ^{ns}
Standard	0.05± 0.002**	0.46 ± 0.03**	1.85 ± 0.03**
LDHE	0.09± 0.002**	0.68 ± 0.04**	1.56 ± 0.03**
HDHE	0.09± 0.003**	0.69± 0.03**	1.55 ± 0.02**

Values are mean ± standard deviation of six animals per group (normal, standard, LDHE and HDHE) and four animals per control and vehicle control groups.
$^{\#\#}p<0.05$ between normal and control group
^{ns} $p>0.05$, ** $p<0.01$ between control and treated groups

8.3.4. Haematological parameters

The Hb level and total leucocyte count were analyzed at the end of the experiment period and the result obtained is depicted in figure 8.5. The Hb level (gm/dL) of the normal group was found to be 13.9 ± 0.33. The Hb value was found less in control (8.32 ± 0.3), vehicle control (8.45 ± 0.21) and standard group (8.92 ± 0.37). Compared with the control group a significant increase of Hb (at $p<0.01$ level) was noted in LDHE (12.7 ± 0.26) and HDHE (12.6 ± 0.21) treated groups. The total leucocyte count (cells/cu mm blood) was found to decrease in the control, vehicle control and the standard groups similar to their Hb level. The minimum value was noted in standard group (3100 ± 265) followed by control group (4200 ± 342) and vehicle control (4100 ± 320) group. The maximum value was observed in normal group (11700 ± 250) followed by HDHE (6800 ± 330) and LDHE (6600 ± 250).

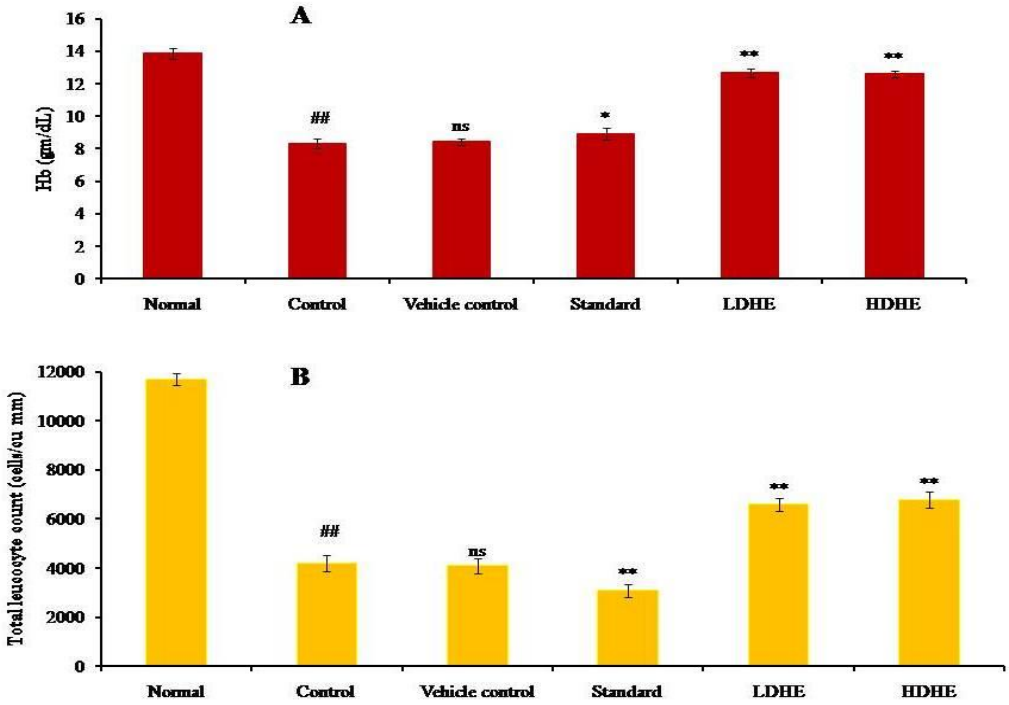

Figure 8.5. Effect of HE on haematological parameters of DMBA-induced breast cancer in mice: (A) Total Hb level and (B) total leucocyte count. normal, mice treated with 200 μL saline/day; control, animals treated with 200 μL saline/day; vehicle control, the animals administered 200 μL of 1% food graded propylene glycol/day; standard, animals treated with tamoxifen (20 mg/kg b. wt/day, p.o.), LDHE and HDHE, animals were treated with low dose (160 mg/kg b. wt/day, p.o.) and high dose (260 mg/kg b. wt/day, p.o.) of HE. Except for normal group, all animals received intragastric dosage of DMBA at 3.3 mg/200 μL/week and respective drugs for 6 weeks. Values are expressed as mean ± SD. ##: $p<0.01$ (control compared to normal), ns: non-significant $p>0.05$, *: $p<0.05$, **: $p<0.01$, (vehicle control, standard, LDHE and HDHE compared to control)

8.3.5. Liver function parameters

The liver function parameters were analysed in the present experiment and the result obtained is summarised into table 8.2. The total bilirubin (mg/dL) was found increased in all treated groups with respect to the normal group. In the normal group, the total bilirubin value was 0.30 ± 0.01. In control, vehicle control, standard, LDHE and HDHE the values were found 0.64 ± 0.03, 0.62 ± 0.03, 0.62 ± 0.02, 0.35 ± 0.03 and 0.36 ± 0.01 respectively. In statistical analysis, compared to control the values were found insignificant in the vehicle control and standard group at $p>0.05$ level. A similar trend was noted in the result of AST, ALP and ALP level (U/L). Compared with the normal group (129 ± 1.65), the AST level was found increased in control (165 ± 2.45), vehicle control (164 ± 1.76), standard (173 ± 2.03), LDHE (145 ± 1.86) and HDHE (143 ± 1.73) groups. Except for the vehicle control group, the data of all groups were significantly different from control group at $p>0.05$ level. The ALT level was 57 ± 1.65, 78 ± 1.44, 76 ± 2.06, 82 ± 2.21, 66 ± 2.32 and 70 ± 2.30 respectively in normal, control, vehicle control, standard, LDHE and HDHE groups respectively. In comparison with control the vehicle control value was found insignificant at $p>0.05$ level but, standard group data was found significantly ($p<0.05$ level) different from control group and rest all groups were showed significant level of difference at $p<0.01$ level. The ALP level of normal group was 51.34 ± 2.13. Control and vehicle control group values were found very close to each other and the values were 98.76 ± 2.07 and 99.76 ± 1.87. A significant change ($p<0.05$) was observed in the level of ALP in standard (93.32 ± 1.99), LDHE (65.43 ± 1.54) and HDHE groups (67.82 ± 2.55) with respect to control group. Total protein concentration (gm/dL) was found decreased in all treated groups with respect to normal group (6.54 ± 0.43). A maximum decrease in the level of protein was noted in control group (3.98 ± 0.36). The total protein concentration was found very close to each other in the vehicle control (4.32 ± 0.32) and standard group (4.32 ± 0.27) and was insignificant from control group ($p>0.05$ level). The LDHE (5.43 ± 0.14) and HDHE (5.49 ± 0.32) treated groups were showed increase in level of protein concentration with respect to control group and the data was significant at $p<0.05$ level.

Table 8.2. Anticarcinogenic effect of HE on the liver function parameters of DMBA-induced cancer development in Swiss albino mouse

Group	Total Bilirubin (mg/dL)	AST (U/L)	ALT (U/L)	ALP (U/L)	Total protein (gm/dL)
Normal	0.30 ± 0.01	129 ± 1.74	57 ± 1.65	51.34 ± 2.13	6.54 ± 0.43
Control	0.64 ± 0.03$^{\#\#}$	165 ± 2.45$^{\#\#}$	78 ± 1.44$^{\#\#}$	98.76 ± 2.07$^{\#\#}$	3.98 ± 0.36$^{\#\#}$
Vehicle control	0.62 ± 0.03 ^{ns}	164± 1.76 ^{ns}	76 ± 2.06 ^{ns}	99.76 ± 1.87 ^{ns}	4.32 ± 0.32 ^{ns}
Standard	0.62 ± 0.02 ^{ns}	173 ± 2.03**	82 ± 2.21*	93.32 ± 1.99**	4.32 ± 0.27 ^{ns}
LDHE	0.35 ± 0.03**	145 ± 1.86**	66 ± 2.32**	65.43 ± 1.54**	5.43 ± 0.14**
HDHE	0.36 ± 0.01**	143 ± 1.73**	70 ± 2.30**	67.82 ± 2.55**	5.49 ± 0.32**

Values are mean ± standard deviation of six animals per group (normal, standard, LDHE and HDHE) and four animals per control and vehicle control groups.

$^{\#\#}p<0.01$ between control compared to normal

^{ns} $p>0.05$, $^{*}p<0.05$, ** $p<0.01$ between control and treated groups

8.3.6. Antioxidant status of liver

The enzymatic and non-enzymatic antioxidant status of the liver was analysed in the study. The catalase enzyme activity (U/mg protein) was found to be 16.41 ± 1.21 in the normal group (Figure 8.6A). In the control, vehicle and standard groups the catalase activity was found decreased up to 9.16 ± 1.45, 9.15 ± 1.96 and 9.52 ± 1.63 respectively. With respect to control group, the activity of catalase in the LDHE (12.45 ± 1.44) and HDHE (12.32 ± 1.77) treated groups were found increased at significant ($p<0.01$) level. The activity of SOD (U/mg protein) was found affected badly in control (0.51 ± .06) and vehicle control (0.54 ± .07) groups with respect to normal group (1.39 ± .07). A significant difference ($p<0.01$) was noted in the activity of SOD in standard group (0.63 ± 0.04), LDHE (0.95 ± 0.05) and HDHE (1.015 ± 0.06) treated groups with respect to control group (Figure 8.6B).

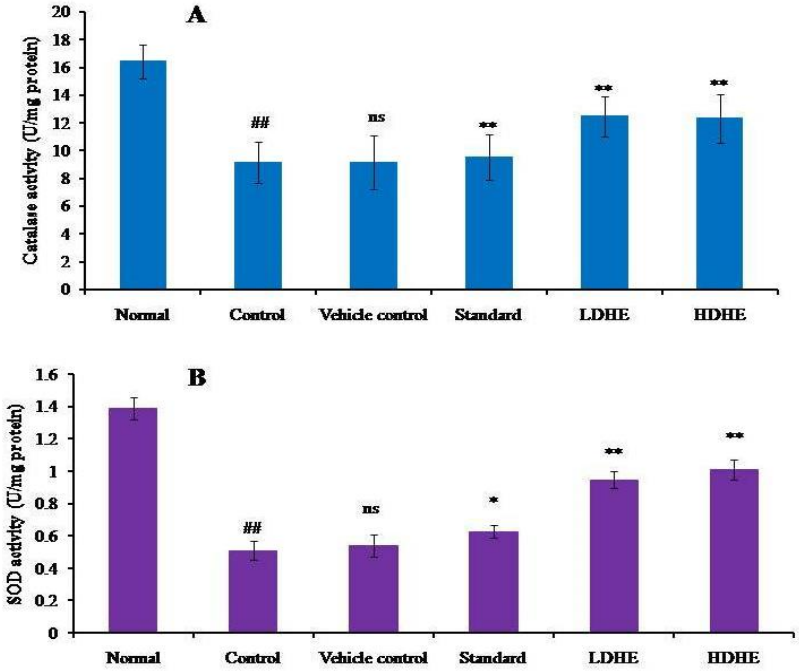

Figure 8.6. Effect of HE on the activity of (A) catalase and (B) SOD in the liver tissue of DMBA-induced breast cancer in mice: normal, mice treated with 200 μL saline/day; control, animals treated with 200 μL saline/day; vehicle control, the animals administered 200 μL of 1% food graded propylene glycol/day; standard, animals treated with tamoxifen (20 mg/kg b. wt/day, p.o.), LDHE and HDHE, animals were treated with low dose (160 mg/kg b. wt/day, p.o.) and high dose (260 mg/kg b. wt/day, p.o.) of HE. Except for normal group, all animals received intragastric dosage of DMBA at 3.3 mg/200 μL/week and respective drugs for 6 weeks. Values are expressed as mean ± SD. ##: $p<0.01$ (control compared to normal), ns: non-significant $p>0.05$, *: $p<0.05$, **: $p<0.01$, (vehicle control, standard, LDHE and HDHE compared to control)

The activity of GPx present in liver tissue was found to be 33.25 ± 1.96 (U/mg protein) in the normal group (Figure 8.6C). The activity of GPx (U/mg protein) was found decreased in control (14.29 ± 2.05), vehicle control (14.21 ± 2.1) and tamoxifen-treated (15.32 ± 2.31) groups. There was no such drop in activity observed in liver tissue of LDHE (25.71 ± 0.91) and HDHE (24.54 ± 3.12) treated group of animals. The activity was significantly ($p<0.05$) higher than the control group. The concentration of GSH molecule (nmol/mg protein) in hepatic tissue was showed a tendency to decline in control, vehicle control and standard groups and the values were noted as 8.51 ± 1.58, 8.45 ± 2.08 and 9.19 ± 0.8 respectively. The value noted in the vehicle control and the standard group was insignificant at $p>0.05$ level with respect to the control group. In the normal group, the value was found to be 16.71 ± 1.7 nmol/mg protein. A significant increase was noted in the level of GSH in LDHE (11.67 ± 1.38) and HDHE (11.85 ± 2.19) treated groups and values found to be significant at $p<0.05$ level when compared with control group (Figure 8.6D). The lipid peroxidation rate of hepatic tissue (nmol MDA/mg protein) of DMBA treated mice (control; 6.18 ± 0.13) was found increased with respect to the normal group of animals (1.09 ± 0.07). An elevation in the MDA level was noted in the vehicle control (6.13 ± 0.07) and the standard group (5.97 ± 0.11) with respect to the normal group. A significant level of decrease ($p<0.05$) in the concentration of MDA was noted in LDHE (2.73 ± 0.09) and HDHE (2.56 ± 0.19) with respect to control group (Figure 8.6E).

8.3.7. Histological analysis

Histological sections of the mammary gland from mice exposed to DMBA showed tumour growth. Along with tumour, hyperplasia, elongation and enlargement of ducts and lobes were noted as compared to animals of the normal group (Figure 8.7A). The microarchitecture of mammary glands of animals in the control and vehicle control group was found altered severely (Figure 8.7B & C). Compared to the control group and vehicle control group animals, the histological sections of the mammary glands of the tamoxifen (Figure 8.7 D) and HE treated animals (Figure 8.7 E & F) were shown a microarchitecture similar to normal animals.

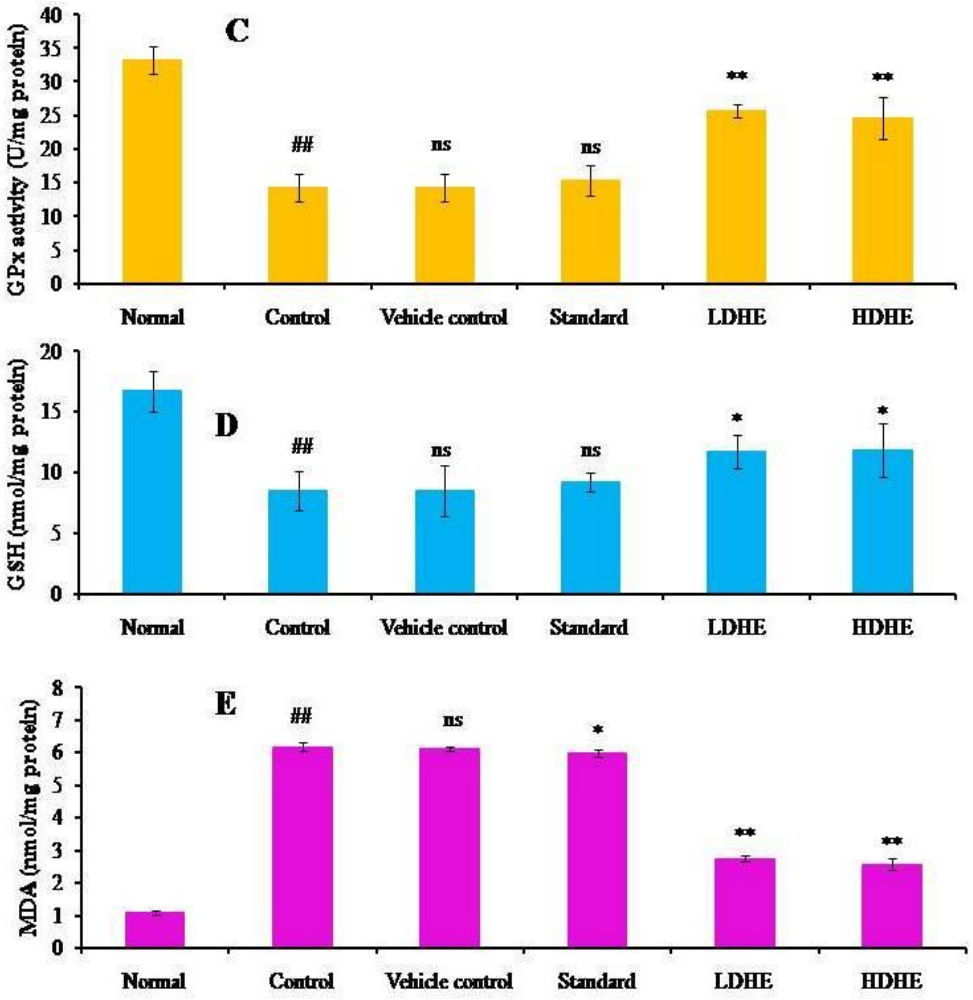

Figure 8.6. Effect of HE on the activity of (C) GPx, (D) the concentration of GSH and (E) MDA in the liver tissue of DMBA-induced breast cancer in mice: normal, mice treated with 200 μL saline/day; control, animals treated with 200 μL saline/day; vehicle control, the animals administered 200 μL of 1% food graded propylene glycol/day; standard, animals treated with tamoxifen (20 mg/kg b. wt/day, p.o.), LDHE and HDHE, animals were treated with low dose (160 mg/kg b. wt/day, p.o.) and high dose (260 mg/kg b. wt/day, p.o.) of HE. Except for normal group, all animals received intragastric dosage of DMBA at 3.3 mg/200 μL/week and respective drugs for 6 weeks. Values are expressed as mean ± SD. ##: $p<0.01$ (control compared to normal), ns: non-significant $p>0.05$, *: $p<0.05$, **: $p<0.01$, (vehicle control, standard, LDHE and HDHE compared to control)

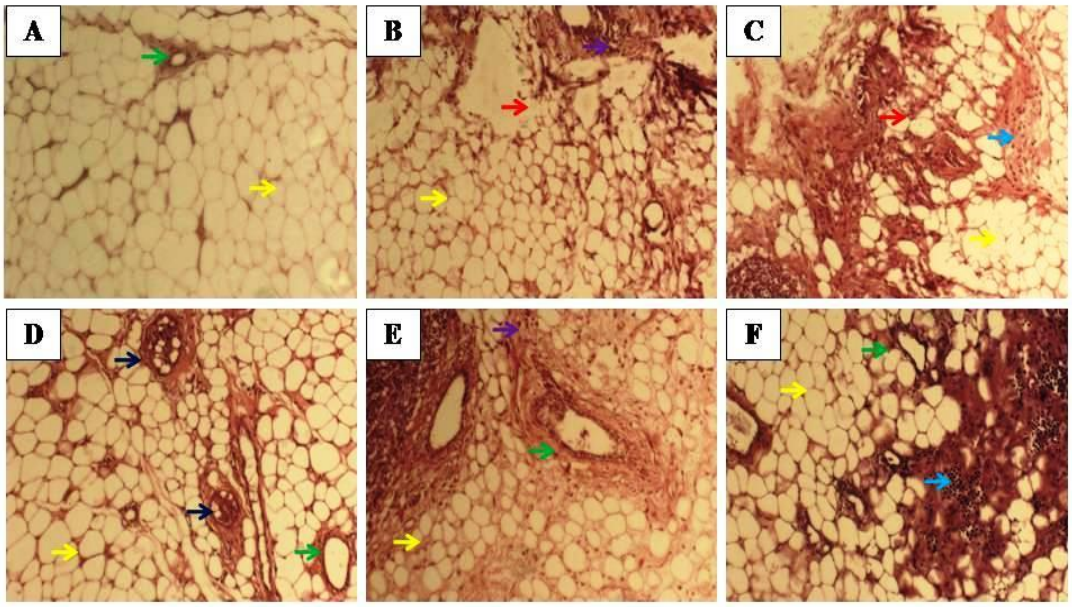

Figure 8.7. Anticarcinogenic effect of HE on the histology of DMBA-induced cancer in the mammary gland of Swiss albino mice: (A) normal, mice treated with 200 μL saline/day; (B) control, animals treated with 200 μL saline/day; (C) vehicle control, the animals administered 200 μL of 1% food graded propylene glycol/day; (D) standard, animals treated with tamoxifen (20 mg/kg b. wt/day, p.o.), (E) LDHE and (F) HDHE, animals were treated with low dose (160 mg/kg b. wt/day, p.o.) and high dose (260 mg/kg b. wt/day, p.o.) of HE. Except for normal group, all animals received intragastric dosage of DMBA at 3.3 mg/200 μL/week and respective drugs for 6 weeks. (H & E, 200X). The green arrow indicates the ducts in mammary glands, the blue arrow indicates cancer cells, the black arrow indicates cancer cells in ducts, the red arrow indicates necrosis and the yellow arrow indicates the adipose tissue

The histological analysis of the ovary (Figure 8.8) showed tumours with the varying percentage in DMBA treated groups. In the control and vehicle control group (Figure 8.8.B & C) the ovaries were found distorted. The ovary of tamoxifen and HE treated animals were also showed alternation in the structure of cortex and stroma. Change in size and shape follicle cells were noted in standard and HE treated animals (Figure 8.8.D, E & F).

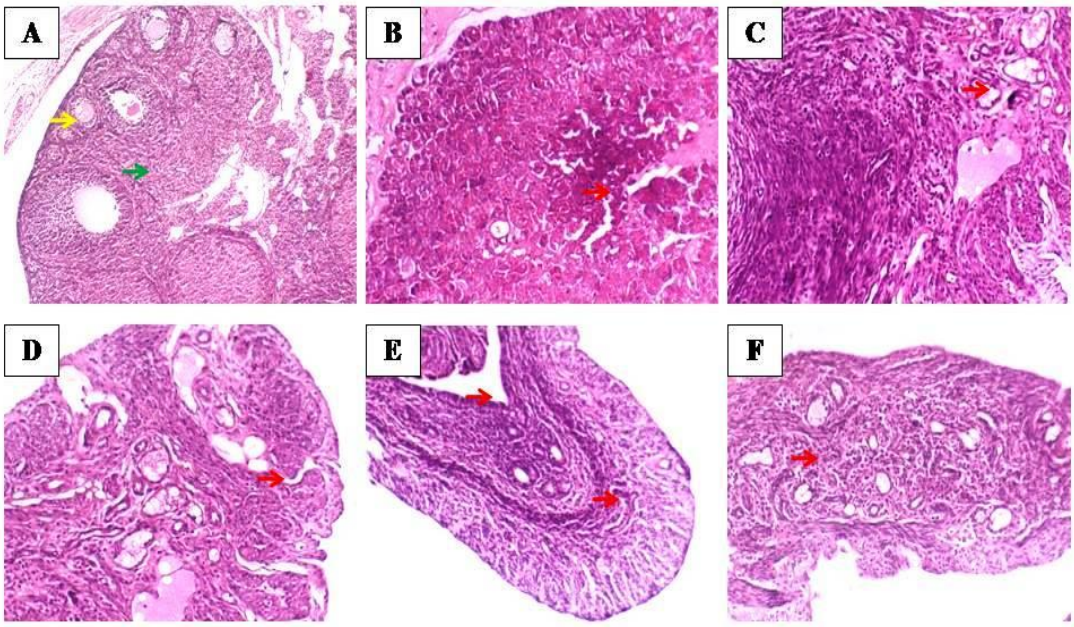

Figure 8.8. Anticarcinogenic effect of HE on the histology of DMBA-induced cancer in the mammary gland of Swiss albino mice: (A) normal, mice treated with 200 μL saline/day; (B) control, animals treated with 200 μL saline/day; (C) vehicle control, the animals administered 200 μL of 1% food graded propylene glycol/day; (D) standard, animals treated with tamoxifen (20 mg/kg b. wt/day, p.o.), (E) LDHE and (F) HDHE, animals were treated with low dose (160 mg/kg b. wt/day, p.o.) and high dose (260 mg/kg b. wt/day, p.o.) of HE. Except for normal group, all animals received intragastric dosage of DMBA at 3.3 mg/200 μL/week and respective drugs for 6 weeks. (H & E, 200X).The green arrow indicates the stroma, red arrow indicates necrosis and the yellow arrow indicates the follicle

Histological analysis of liver tissue in control and vehicle control group (Figure 8.9.B & C) was shown a drastic difference in their microarchitecture with respect to normal animal group (Figure 8.9A). Necrosis and tumour cell progression was noted in the control and vehicle control group. Sections of liver tissue from mice administered with tamoxifen (Figure 8.9.D) and HE at various doses (Figure 8.9E & F) were shown a microarchitecture which was close to normal group animals (Figure 8.9).

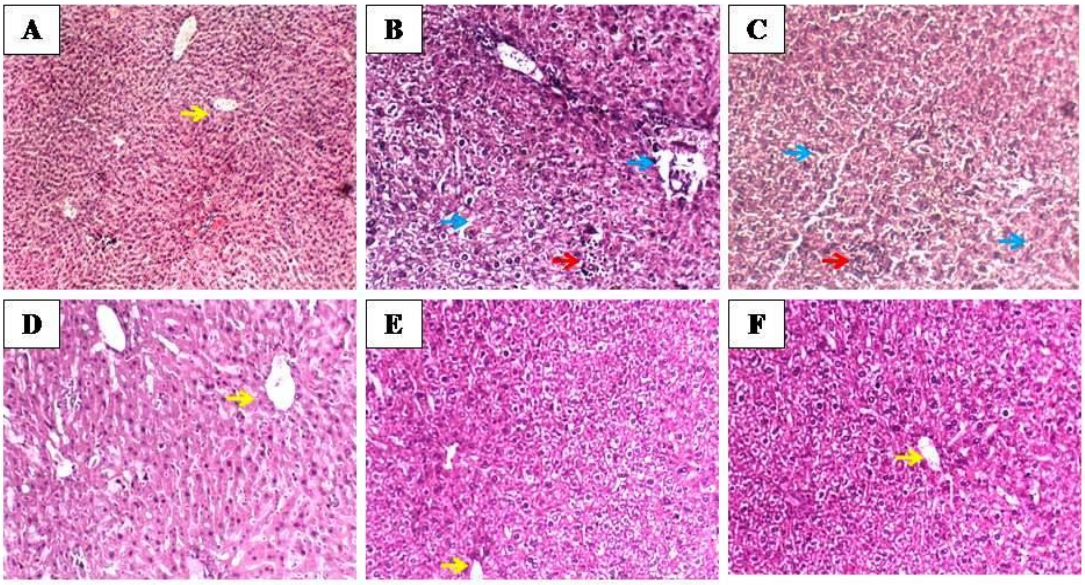

Figure 8.9. Anticarcinogenic effect of HE on the histology of DMBA-induced cancer in the mammary gland of Swiss albino mice: (A) normal, mice treated with 200 μL saline/day; (B) control, animals treated with 200 μL saline/day; (C) vehicle control, the animals administered 200 μL of 1% food graded propylene glycol/day; (D) standard, animals treated with tamoxifen (20 mg/kg b. wt/day, p.o.), (E) LDHE and (F) HDHE, animals were treated with low dose (160 mg/kg b. wt/day, p.o.) and high dose (260 mg/kg b. wt/day, p.o.) of HE. Except for normal group, all animals received intragastric dosage of DMBA at 3.3 mg/200 μL/week and respective drugs for 6 weeks. (H & E, 200X). The blue arrow indicates the necrosis, the red arrow indicates cancer cells and the yellow arrow indicates the vein

8.4. Discussion

In this study, the chemopreventive effect of HE on DMBA-induced tumour in mammary glands of female Swiss albino mice was documented which projected its anti-carcinogenic potential. DMBA is an organic pollutant generated by incomplete combustion of fossil fuels. DMBA is present in tobacco and various tobacco products and is documented to cause mammary tumours in humans (Silihe et al., 2017). DMBA is used to induce cancer in murine species, mainly mammary tumours. The mammary tumours developed in DMBA exposed rodents strongly imitate those of human breast cancer (Russo and Russo, 2000). In this study, the intragastric dose of 3.3 mg/animal/week of DMBA for 6 consecutive weeks was used to induce mammary tumours in female Swiss albino mice.

Tamoxifen (trans-1-(4-β-dimethylaminoethoxyphenyl)-1,2-diphenylbut-1-ene, was used as a standard drug in the present study. Tamoxifen is a regularly prescribed drug for decreasing recurrence rate and rising survival rate in estrogen receptor-positive breast cancers (Pan et al., 2016). In addition, tamoxifen is also used as a chemopreventive agent in women at high risk of developing breast cancer, especially ductal carcinoma (Fisher et al., 1999). Tamoxifen is considered as a pro-drug and the anticancer activity of tamoxifen occurs via 4-hydroxy tamoxifen, an active metabolite and its desmethyl analogue called endoxifen, which are produced by liver CYP 2D6 and CYP3A/3A5 isoenzymes (Wu et al., 2009).

The survival rate of animals was found decreased in the control and vehicle control group up by 66% during the experiment period. No immediate death was noted in the control group and vehicle control group due to the oral administration of DMBA. However, standard, LDHE and HDHE treated animals were survived during the entire period of the experiment. The decreased survival rate in control and vehicle control group may be attributed to the toxicity of DMBA as reported by many researchers (Ojeswi et al., 2010, Sahin et al., 2018). Form this data it became evident that different doses of HE administration could decrease the toxicity of DMBA and increased the life span of animals similar to standard drug used.

No palpable mammary tumours were observed during the study period. Mice of 7 - 8 weeks old age were used in the study may be one of the reasons for the slower

development of tumour in mammary glands of mice. Many researchers prefer mice in the lower age (between 3 - five weeks) for this type of study. Apart from this, so many researchers allowed the DMBA administered mice to do mating which oscillates their hormonal environment and facilitates tumour formation in mammary glands (Currier et al., 2005). The observation period was confined to a short period (10 weeks) in this study may be another reason for not detecting mammary tumours of non-palpable size. However, histopathological studies of mammary glands and mammary pad analysis of mice treated with DMBA showed proliferation of cells. Above to all, the average weight of mammary glands was found increased in DMBA administered group of animals. The proliferation of cells and change in tissue architecture of mammary glands were found severe in control and vehicle control groups. But, the histopathological studies of mammary glands of the standard group and HE administered groups showed the chemoprotective effect of tamoxifen and different doses of HE in respective group of animals. Moreover, the mammary pad analysis of standard drug and HE treated animals showed less progression of cells in mammary gland ducts suggested its chemoprotective efficacy of HE. The vascular nature of mammary glands and associated regions were found increasing in DMBA administered control group animals which was less in tamoxifen and HE treated animals. This result supporting the fact that tumour growth and metastasis directly depend on angiogenesis (Nishida et al., 2006).

Palpable growth was detected in the abdominal cavity of mice, especially in the control group and vehicle control group at the last two weeks of the experiment period and was found as ovarian tumours during the necropsy. It has been reported by many researchers that the DMBA can induce ovarian tumour along with mammary gland tumour. Kuwahara (1967) reported that single intragastric administration of 0.5 mL of 2% DMBA dissolved in sesame oil produced 59% of ovarian tumour in mice. According to Huang et al., (1998), oral administration of 1mg of DMBA once a week for five weeks in mice caused tumour formation in mammary glands, ovarian tumours and uterine tumours. The exact reason related to tumour formation in ovary and uterus of DMBA administered animals are not yet completely deciphered. Even then, many possible suggestions are provided by various researchers for this problem. Stewart et al., (2004) reported that the point

mutations occurred in the Tp53 and Ki-Ras genes are one of the main reasons for the formation of DMBA induced ovarian carcinoma in murine animals. They also noted an over expression of progesterone and estrogen receptors in the ovarian lesion formed by the administration of DMBA. The immunosuppressive effect of DMBA is related to enhanced production of prostaglandin E2. Point mutation, disturbance in cellular oxidant-antioxidant balance and activation of *ras* family genes are the proposed mechanism for DMBA carcinogenicity (Jezierska-Drutel et al., 2013). It was observed a less rate of ovarian tumour formation in standard and HE treated groups with respect to control and vehicle control groups. The ovarian tumour developed in these categories of animals was very small and non-palpable. This observation directly indicated the beneficial effect of LDHE and HDHE in the chemoprotection of DMBA-induced carcinogenic effect in mice.

An increase in the weight of the liver was noted in the control and vehicle control animals in the current study. In standard group, the average weight of the liver was found more with respect to another group of animals. The uterine horn of animals was found enlarged in control, vehicle control animals in comparison with normal group of animals. These observations coincide with the observation made by Huang et al., (1998). According to them, the average weight of liver and uterus was found increased in DMBA administered animals with respect to normal group. The increased weight of the liver in the standard group may be related to the toxicity of both DMBA and tamoxifen. It has been noted that tamoxifen causes liver damage (Ching et al., 1992). According to Pan et al., (2016), non-alcoholic fatty liver disease is an adverse effect caused by tamoxifen in breast cancer patients. The data regarding the liver function markers and antioxidant status of hepatic tissue from control, vehicle control and standard groups have substantiated this observation. The activity of liver function enzymes, enzymatic and non-enzymatic antioxidant status of liver tissue found altered in an alarming way in these groups. But, the HE treated group of animals had a data which was close to the normal group of animals indicating the chemoprotective effect of HE. This chemoprotective effect of HE was similar to the protective effect it showed in the systemic toxicity induced by cyclophosphamide and nephrotoxicity induced by cisplatin in mice.

The decrease in the level of Hb and total leucocyte count observed in the control and vehicle control group may be due to the immunosuppressive effects of DMBA (Karimi et al., 2019). The Hb and total leucocyte count of LDHE and HDHE treated animals were found close to the normal group animals indicating that they prevent the immunosuppressive effect of DMBA.

Histopathological studies of ovaries and liver of control and vehicle control animals revealed the carcinogenic nature of DMBA. Severe damage was noted in the tissue architecture of ovaries and liver of control and vehicle control group animals. The severity of change in micro-architecture of ovary and liver were found less in standard and HE treated animals.

The exact mechanism(s) of HE for the chemopreventive activity of DMBA-induced carcinogenesis is not yet clear. The earlier studies have indicated that the HE contains several phytochemicals with excellent antioxidant and anti-inflammatory potential. Moreover, the immense antioxidant and anti-inflammatory capacity of HE has been proved in both *in vitro* and *in vivo* conditions. The potent inhibitory activity of HE in DMBA-induced mammary carcinogenesis in mice may be attributed to its antioxidant and anti-inflammatory efficacy.

Summary

Summary

From the above studies, HE and ME extract of the plant *Simarouba glauca* DC was found to be a good source of pharmacologically important phytochemicals. The cytotoxic effect (short term) of HE and ME was found less to DLA and EAC cells (IC_{50}>100 μg/mL). Both HE and ME were found less toxic to normal cells (rat spleen cells) than the cancer cells in short term cytotoxicity assay. The antiproliferative study showed the greater efficacy of HE in comparison with ME. HE exerted more or equal *in vitro* antioxidant efficacy with respect to ME. Since the HE of *S. glauca* showed more pharmacological potentiality in respect of ME, it was selected for further studies. UPLC-Q-TOF-MS analysis revealed the presence of antioxidant, anti-inflammatory and antitumour molecules in HE. Acute oral administration of HE at a dose of 2000 mg/kg b. wt was found to be safe to Swiss albino mice. The sub-acute administration of HE up to 400 mg/kg b. wt was found non-toxic to Swiss albino mice. Simultaneous administration and pre and simultaneous administration of HE in EAC inoculated mice and simultaneous administration of HE in EAC induced ascites tumour bearing mice showed less antitumour efficacy. Both lower and higher doses of HE were found working in the same way. But, simultaneous administration of lower dose of HE with combination of CTX increased the life span of mice inoculated with EAC cells. A similar tendency of action was noted in DLA induced tumour studies. However, in both tumour model experiments, HE supported the Hb level and total leucocyte count in experimental animals. Administration of HE elevated the antioxidant status of normal mice. HE could ameliorate the oxidative stress created by NaF in mice. A high percentage inhibition of PMA induced superoxide radical generation in mice peritoneal macrophages were noted by HE. In the *in vivo* acute and chronic inflammation models, the HE worked well. HE inhibited the extravasation of Evans blue dye in acute inflammation model. Histological analysis showed reduced infiltration of inflammatory cells in paw tissue in all inflammatory models. The administration of HE significantly reduced the cisplatin-induced renal toxicity in mice. HE administration decreased the systemic toxicity developed by CTX in both normal and tumour-bearing mice. The antioxidant status of major organs found improved during HE administration. LDHE and HDHE showed similar rate of

action in all chemoprotective models. Administration of HE decreased the toxicity generated by DMBA in mice. HE administration slowed down the tumour development in breast and ovary of DMBA-induced mice and protected the antioxidant status of liver. In this experiment also both lower and higher concentration of HE exhibited a similar trend in action.

In conclusion, HE of *S. glauca* showed excellent antioxidant, anti-inflammatory, chemoprotective and anti-tumour efficacy and the administration of HE was found safe. HE showed a preventive nature towards cancer in the different models studied rather than curing the already formed tumour. Overall the study suggests that the plant *S. glauca* does not cure already formed tumours but might be useful in the prevention of cancer development.

Future Perspectives

Using different *in vivo* chemical-induced and graft models anticancer properties of *S. glauca* hot water extract need to ascertain. Studies need to be emphasized to understand the immunomodulatory role of this plant so that the Hot water extract could be better evaluated in the clinical situation.

Bibliography

2011. Cancer Facts/Treatment modalities/Surgery.

2015a. Hormone Therapy to Treat Cancer. Available: https://www.cancer.gov/about-cancer/treatment/types/hormone-therapy.

2015b. What is Cancer?

2016. How does chemotherapy work?

2017a. Gene therapy. *General cancer information* [Online].

2017b. General cancer information. *Homone therapy for cancer* [Online].

2017c. The genetics of cancer. Available: https://www.cancer.gov/about-cancer/causes-prevention/genetics.

2017d. Other treatments. *Treatment of cancer* [Online].

2017e. Radiation therapy to treat cancer. *National Cancer Institute* [Online]. Available: https://www.cancer.gov/about-cancer/treatment/types/radiation-therapy.

2018a. The burden of cancers and their variations across the states of India: the Global Burden of Disease Study 1990-2016. *Lancet Oncol,* 19**,** 1289-1306.

2018b. Cancer. Available: https://www.who.int/news-room/facts-in-pictures/detail/cancer [Accessed 14.02.2019].

2018c. Cancer Types. Available: https://www.cancer.gov/types [Accessed 14.02.2019].

2018d. Immunotherapy to treat cancer.

2018e. Radiation Therapy Basics. Available: https://www.cancer.org/treatment/treatments-and-side-effects/treatment-types/radiation/basics.html.

2019a. American Cancer Society. Cancer Facts & Figures 2019.

2019b. Cancer Types. *Cancer* [Online]. Available: https://www.verywellhealth.com/more-cancer-types-4158486.

ABDELWAHAB, S. I., HASSAN, L. E., ABDUL MAJID, A. M., YAGI, S. M., MOHAN, S., ELHASSAN TAHA, M. M., AHMAD, S., CHUEN, C. S., NARRIMA, P., RAIS, M. M., SYAM, S., MOHARAM, B. A. & HADI, A. H. 2012. Cucurbitacin L 2-O-beta-Glucoside Demonstrates Apoptogenesis in Colon Adenocarcinoma Cells (HT-29): Involvement of Reactive Oxygen and Nitrogen Species Regulation. *Evid Based Complement Alternat Med,* 490136**,** 26.

ADAMS, J. M. & CORY, S. 2007. The Bcl-2 apoptotic switch in cancer development and therapy. *Oncogene,* 26**,** 1324-37.

AEBI, H., CANTZ, M. & SUTER, H. 1965. Cellular distribution of catalase activity in red cells of homozygous and heterozygous cases of acatalasia. *Experientia,* 21**,** 713-4.

AHMED, S. I., HAYAT, M. Q., TAHIR, M., MANSOOR, Q., ISMAIL, M., KECK, K. & BATES, R. B. 2016. Pharmacologically active flavonoids from the anticancer, antioxidant and antimicrobial extracts of Cassia angustifolia Vahl. *BMC Complement Altern Med,* 16**,** 016-1443.

AHN, K. S., NOH, E. J., CHA, K. H., KIM, Y. S., LIM, S. S., SHIN, K. H. & JUNG, S. H. 2006. Inhibitory effects of Irigenin from the rhizomes of Belamcanda chinensis on nitric oxide and prostaglandin E(2) production in murine macrophage RAW 264.7 cells. *Life Sci,* 78**,** 2336-42.

AINSWORTH, E. A. & GILLESPIE, K. M. 2007. Estimation of total phenolic content and other oxidation substrates in plant tissues using Folin-Ciocalteu reagent. *Nat Protoc,* 2**,** 875-7.

AJAIYEOBA, E. O. & KREBS, H. C. 2003. Antibacterial and antifungal activities of Quassia undulata and Quassia amara extracts in vitro. *Afr J Med Med Sci,* 32**,** 353-6.

AJAIYEOBA, E. O., ABALOGU, U. I., KREBS, H. C. & ODUOLA, A. M. 1999. In vivo antimalarial activities of Quassia amara and Quassia undulata plant extracts in mice. *J Ethnopharmacol,* 67**,** 321-5.

ALFONSO, L., AI, G., SPITALE, R. C. & BHAT, G. J. 2014. Molecular targets of aspirin and cancer prevention. *Br J Cancer,* 111**,** 61-7.

ALLAIN, C. C., POON, L. S., CHAN, C. S., RICHMOND, W. & FU, P. C. 1974. Enzymatic determination of total serum cholesterol. *Clin Chem,* 20**,** 470-5.

ALLAVENA, P., GERMANO, G., MARCHESI, F. & MANTOVANI, A. 2011. Chemokines in cancer related inflammation. *Exp Cell Res,* 317**,** 664-73.

AMIN, A., CHIKAN, N. A., MOKHDOMI, T. A., BUKHARI, S., KOUL, A. M., SHAH, B. A., GHAREMIRSHAMLU, F. R., WAFAI, A. H., QADRI, A. & QADRI, R. A. 2016. Irigenin, a novel lead from Western Himalayan chemiome inhibits Fibronectin-Extra Domain A induced metastasis in Lung cancer cells. *Sci Rep,* 6.

ANG, H. H., CHAN, K. L. & MAK, J. W. 1995. *In vitro antimalarial activity of quassinoids from Eurycoma longifolia against Malaysian chloroquine-*

resistant Plasmodium falciparum isolates, Planta Med. 1995 Apr;61(2):177-8. doi: 10.1055/s-2006-958042.

APERS, S., CIMANGA, K., VANDEN BERGHE, D., VAN MEENEN, E., LONGANGA, A. O., FORIERS, A., VLIETINCK, A. & PIETERS, L. 2002. Antiviral activity of simalikalactone D, a quassinoid from Quassia africana. *Planta Med,* 68**,** 20-4.

ARAFA, M. H. & ATTEIA, H. H. 2019. Protective Role of Epigallocatechin Gallate in a Rat Model of Cisplatin-Induced Cerebral Inflammation and Oxidative Damage: Impact of Modulating NF-kappaB and Nrf2. *Neurotox Res,* 13**,** 019-00095.

ARMOUR, R. P. 1959. Investigations on Simarouba glauca Dc. in El Salvador. *Economic Botany,* 13**,** 41-66.

ASIF, M. 2012. A brief study of toxic effects of some medicinal herbs on kidney. *Adv Biomed Res,* 1**,** 2277-9175.

ATESSAHIN, A., CERIBASI, A. O., YUCE, A., BULMUS, O. & CIKIM, G. 2007. Role of ellagic acid against cisplatin-induced nephrotoxicity and oxidative stress in rats. *Basic Clin Pharmacol Toxicol,* 100**,** 121-6.

ATHREYA, K. & XAVIER, M. F. 2017. Antioxidants in the Treatment of Cancer. *Nutr Cancer,* 69**,** 1099-1104.

AUGUSTYNIAK, A., BARTOSZ, G., CIPAK, A., DUBURS, G., HORAKOVA, L., LUCZAJ, W., MAJEKOVA, M., ODYSSEOS, A. D., RACKOVA, L., SKRZYDLEWSKA, E., STEFEK, M., STROSOVA, M., TIRZITIS, G., VENSKUTONIS, P. R., VISKUPICOVA, J., VRAKA, P. S. & ZARKOVIC, N. 2010. Natural and synthetic antioxidants: an updated overview. *Free Radic Res,* 44**,** 1216-62.

AZAB, A., NASSAR, A. & AZAB, A. N. 2016. Anti-inflammatory Activity of Natural Products. *Molecules,* 21.

AZAD, N., IYER, A., VALLYATHAN, V., WANG, L., CASTRANOVA, V., STEHLIK, C. & ROJANASAKUL, Y. 2010. Role of oxidative/nitrosative stress-mediated Bcl-2 regulation in apoptosis and malignant transformation. *Ann N Y Acad Sci*.

BABA A. I., C., C. 2007. *Comparative Oncology*, Bucharest:The Publishing House of the Romanian Academy.

BABU, T. D., KUTTAN, G. & PADIKKALA, J. 1995. Cytotoxic and anti-tumour properties of certain taxa of Umbelliferae with special reference to Centella asiatica (L.) Urban. *J Ethnopharmacol,* 48**,** 53-7.

BAEK, S. M., KWON, C. H., KIM, J. H., WOO, J. S., JUNG, J. S. & KIM, Y. K. 2003. Differential roles of hydrogen peroxide and hydroxyl radical in cisplatin-induced cell death in renal proximal tubular epithelial cells. *J Lab Clin Med,* 142**,** 178-86.

BAERISWYL, V. & CHRISTOFORI, G. 2009. The angiogenic switch in carcinogenesis. *Semin Cancer Biol,* 19**,** 329-37.

BAI, W., YANG, H. Y., JIAO, X. Z., FENG, K. N., CHEN, J. J. & GAO, K. 2018. Structurally Diverse Highly Oxygenated Triterpenoids from the Roots of Ailanthus altissima and Their Cytotoxicity. *J Nat Prod,* 81**,** 1777-1785.

BALACHANDRAN, P. & GOVINDARAJAN, R. 2005. Cancer--an ayurvedic perspective. *Pharmacol Res,* 51**,** 19-30.

BANCROFIT, J. D. & COOK, H. C. 1984. *Manual of histologic techniques,* Churchill Living Stone, London.

BANCROFIT, J. D. & COOK, H. C. 1984. *Manual of histologic techniques,* Churchill Living Stone, London.

BARATAKKE, R. C. & PATIL, C. G. 2010. Cytological investigation in poly-gamo-dioecious tree *Simarouba glauca* DC. *Nucleus,* 53**,** 33-36.

BARBOSA, L. F., BRAZ-FILHO, R. & VIEIRA, I. J. 2011. Chemical constituents of plants from the genus Simaba (Simaroubaceae). *Chem Biodivers,* 8**,** 2163-78.

BARBUTI, A. M. & CHEN, Z. S. 2015. Paclitaxel Through the Ages of Anticancer Therapy: Exploring Its Role in Chemoresistance and Radiation Therapy. *Cancers,* 7**,** 2360-71.

BARROS, A. C., MURANAKA, E. N., MORI, L. J., PELIZON, C. H., IRIYA, K., GIOCONDO, G. & PINOTTI, J. A. 2004. Induction of experimental mammary carcinogenesis in rats with 7,12-dimethylbenz(a)anthracene. *Rev Hosp Clin Fac Med Sao Paulo,* 59**,** 257-61.

BAXEVANIS, C. N., PEREZ, S. A. & PAPAMICHAIL, M. 2009. Combinatorial treatments including vaccines, chemotherapy and monoclonal antibodies for cancer therapy. *Cancer Immunol Immunother,* 58**,** 317-24.

BEDNARCZYK-CWYNAR, B., WACHOWIAK, N., SZULC, M., KAMINSKA, E., BOGACZ, A., BARTKOWIAK-WIECZOREK, J., ZAPRUTKO, L. & MIKOLAJCZAK, P. L. 2016. Strong and Long-Lasting Antinociceptive and Anti-inflammatory Conjugate of Naturally Occurring Oleanolic Acid and Aspirin. *Front Pharmacol,* 7.

BEERS, R. F., JR. & SIZER, I. W. 1952. A spectrophotometric method for measuring the breakdown of hydrogen peroxide by catalase. *J Biol Chem,* 195**,** 133-40.

BERGMEYER, H. U., BOWERS, G. N., JR., HORDER, M. & MOSS, D. W. 1976. Provisional recommendations on IFCC methods for the measurement of catalytic concentrations of enzymes. Part 2. IFCC method for aspartate aminotransferase. *Clin Chim Acta,* 70**,** F19-29.

BERTRAM, J. S. 2000. The molecular biology of cancer. *Mol Aspects Med,* 21**,** 167-223.

BERX, G. & VAN ROY, F. 2009. Involvement of members of the cadherin superfamily in cancer. *Cold Spring Harb Perspect Biol,* 1**,** 23.

BHAGMAL 1994. *Sustainability in Oilseeds,* Hyderabad, Indian Society of Oilseeds Research.

BISWAS, M., HALDAR, P. K. & GHOSH, A. K. 2010. Antioxidant and free-radical-scavenging effects of fruits of Dregea volubilis. *Journal of natural science, biology, and medicine,* 1**,** 29-34.

BLASCO, M. A. 2005. Telomeres and human disease: ageing, cancer and beyond. *Nat Rev Genet,* 6**,** 611-22.

BONES, R. W. & TAUSKY, H. H. 1945. Colorimetric determination of creatinine by the Jaffe reaction. *Journal of Biological Chemistry***,** 581-591.

BORTOLI, M., TORSELLO, M., BICKELHAUPT, F. M. & ORIAN, L. 2017. Role of the Chalcogen (S, Se, Te) in the Oxidation Mechanism of the Glutathione Peroxidase Active Site. *Chemphyschem,* 18**,** 2990-2998.

BOURHIA, M., HAJ SAID, A. A., CHAANOUN, A., EL GUEDDARI, F., NAAMANE, A., BENBACER, L. & KHLIL, N. 2019. Phytochemical Screening and Toxicological Study of Aristolochia baetica Linn Roots: Histopathological and Biochemical Evidence. *Journal of toxicology,* 2019**,** 8203832-8203832.

BRAY, F., FERLAY, J., SOERJOMATARAM, I., SIEGEL, R. L., TORRE, L. A. & JEMAL, A. 2018. Global cancer statistics 2018: GLOBOCAN estimates of incidence and mortality worldwide for 36 cancers in 185 countries. *CA Cancer J Clin,* 68**,** 394-424.

CABRAL, J. A., MCCHESNEY, J. D. & MILHOUS, W. K. 1993. A new antimalarial quassinoid from Simaba guianensis. *J Nat Prod,* 56**,** 1954-61.

CACERES, A., CANO, O., SAMAYOA, B. & AGUILAR, L. 1990. Plants used in Guatemala for the treatment of gastrointestinal disorders. 1. Screening of 84 plants against enterobacteria. *J Ethnopharmacol,* 30**,** 55-73.

CAGLAYAN, C., TEMEL, Y., KANDEMIR, F. M., YILDIRIM, S. & KUCUKLER, S. 2018. Naringin protects against cyclophosphamide-induced hepatotoxicity and nephrotoxicity through modulation of oxidative stress, inflammation, apoptosis, autophagy, and DNA damage. *Environ Sci Pollut Res Int,* 25**,** 20968-20984.

CALIN, G. A., DUMITRU, C. D., SHIMIZU, M., BICHI, R., ZUPO, S., NOCH, E., ALDLER, H., RATTAN, S., KEATING, M., RAI, K., RASSENTI, L., KIPPS, T., NEGRINI, M., BULLRICH, F. & CROCE, C. M. 2002. Frequent deletions and down-regulation of micro- RNA genes miR15 and miR16 at 13q14 in chronic lymphocytic leukemia. *Proc Natl Acad Sci U S A,* 99**,** 15524-9.

CASAZZA, A., DI CONZA, G., WENES, M., FINISGUERRA, V., DESCHOEMAEKER, S. & MAZZONE, M. 2014. Tumor stroma: a complexity dictated by the hypoxic tumor microenvironment. *Oncogene,* 33**,** 1743-54.

CHAKRABORTY, D. & PAL, A. 2013. *Natural Products*

CHAKRABORTY, S. & RAHMAN, T. 2012. The difficulties in cancer treatment. *Ecancermedicalscience,* 14.

CHANG, C. C., YANG, M. H., WEN, H. M. & CHERN, J. C. 2002. Estimation of Total Flavonoid Content in Propolis by Two Complementary Colorimetric Methods. *Journal of Food and Drug Analysis,* 10**,** 178-182.

CHANG, F. R. & WU, Y. C. 2001. Novel cytotoxic annonaceous acetogenins from Annona muricata. *J Nat Prod,* 64**,** 925-31.

CHAU, T. T. 1989. *Pharmacological Methods in the Control of Inflammations,* Alan R Liss, Inc. New York.

CHEESBROUGH, M. & MCARTHUR, J. N. 1976. *Laboratory manual for rural tropical hospitals: a basis for training courses,* Edinburgh, Churchill Livingstone.

CHEN, C., PEARSON, A. M. & GRAY, J. I. 1992. Effects of synthetic antioxidants (BHA, BHT and PG) on the mutagenicity of IQ-like compounds. *Food Chemistry,* 43**,** 177-183.

CHEN, R. S., KO, J. C., CHIU, H. C., WO, T. Y., HUANG, Y. J., TSENG, S. C., CHEN, H. J., HUANG, Y. C., JIAN, Y. J., LEE, W. T. & LIN, Y. W. 2013.

Pemetrexed downregulates ERCC1 expression and enhances cytotoxicity effected by resveratrol in human nonsmall cell lung cancer cells. *Naunyn Schmiedebergs Arch Pharmacol,* 386**,** 1047-59.

CHENG, N., CHYTIL, A., SHYR, Y., JOLY, A. & MOSES, H. L. 2008. Transforming growth factor-beta signaling-deficient fibroblasts enhance hepatocyte growth factor signaling in mammary carcinoma cells to promote scattering and invasion. *Mol Cancer Res,* 6**,** 1521-33.

CHIH, H. J., LEE, A. H., COLVILLE, L., BINNS, C. W. & XU, D. 2013. A review of dietary prevention of human papillomavirus-related infection of the cervix and cervical intraepithelial neoplasia. *Nutr Cancer,* 65**,** 317-28.

CHIH, H. W., CHIU, H. F., TANG, K. S., CHANG, F. R. & WU, Y. C. 2001. Bullatacin, a potent antitumor annonaceous acetogenin, inhibits proliferation of human hepatocarcinoma cell line 2.2.15 by apoptosis induction. *Life Sci,* 69**,** 1321-31.

CHING, C. K., SMITH, P. G. & LONG, R. G. 1992. *Tamoxifen-associated hepatocellular damage and agranulocytosis*, Lancet. 1992 Apr 11;339(8798):940. doi: 10.1016/0140-6736(92)90991-b.

CHO, E., CHUNG, E. Y., JANG, H. Y., HONG, O. Y., CHAE, H. S., JEONG, Y. J., KIM, S. Y., KIM, B. S., YOO, D. J., KIM, J. S. & PARK, K. H. 2017. Anti-cancer Effect of Cyanidin-3-glucoside from Mulberry via Caspase-3 Cleavage and DNA Fragmentation in vitro and in vivo. *Anticancer Agents Med Chem,* 17**,** 1519-1525.

CIARIMBOLI, G., DEUSTER, D., KNIEF, A., SPERLING, M., HOLTKAMP, M., EDEMIR, B., PAVENSTADT, H., LANVERS-KAMINSKY, C., AM ZEHNHOFF-DINNESEN, A., SCHINKEL, A. H., KOEPSELL, H., JURGENS, H. & SCHLATTER, E. 2010. Organic cation transporter 2 mediates cisplatin-induced oto- and nephrotoxicity and is a target for protective interventions. *Am J Pathol,* 176**,** 1169-80.

CLAUDIO-CAMPOS, K., HERNANDEZ-RIVERA, J., RIVERA-GUTIERREZ, J., ORTIZ-RIVERA, I., CARVAJAL-VELEZ, A., PEREZ-TORRES, M., PAGAN-ORTIZ, M. & OSPINA-MILLAN, C. A. 2015. Biological screening of select Puerto Rican plants for cytotoxic and antitumor activities. *P R Health Sci J,* 34**,** 25-30.

COUSSENS, L. M. & WERB, Z. 2002. Inflammation and cancer. *Nature,* 420**,** 860-7.

CROCE, C. M. 2008. Oncogenes and Cancer. *New England Journal of Medicine,* 358**,** 502-511.

CUENDET, M. & PEZZUTO, J. M. 2004. Antitumor activity of bruceantin: an old drug with new promise. *J Nat Prod,* 67**,** 269-72.

CURRIER, N., SOLOMON, S. E., DEMICCO, E. G., CHANG, D. L., FARAGO, M., YING, H., DOMINGUEZ, I., SONENSHEIN, G. E., CARDIFF, R. D., XIAO, Z. X., SHERR, D. H. & SELDIN, D. C. 2005. Oncogenic signaling pathways activated in DMBA-induced mouse mammary tumors. *Toxicol Pathol,* 33**,** 726-37.

CUZZOCREA, S., SAUTEBIN, L., DE SARRO, G., COSTANTINO, G., ROMBOLA, L., MAZZON, E., IALENTI, A., DE SARRO, A., CILIBERTO, G., DI ROSA, M., CAPUTI, A. P. & THIEMERMANN, C. 1999. Role of IL-6 in the pleurisy and lung injury caused by carrageenan. *J Immunol,* 163**,** 5094-104.

DE BIASI, A. R., VILLENA-VARGAS, J. & ADUSUMILLI, P. S. 2014. Cisplatin-induced antitumor immunomodulation: a review of preclinical and clinical evidence. *Clin Cancer Res,* 20**,** 5384-91.

DE MESQUITA, M. L., DE PAULA, J. E., PESSOA, C., DE MORAES, M. O., COSTA-LOTUFO, L. V., GROUGNET, R., MICHEL, S., TILLEQUIN, F. & ESPINDOLA, L. S. 2009. Cytotoxic activity of Brazilian Cerrado plants used in traditional medicine against cancer cell lines. *J Ethnopharmacol,* 123**,** 439-45.

DE SOUZA ALMEIDA, E. S., FILHO, V. C., NIERO, R., CLASEN, B. K., BALOGUN, S. O. & DE OLIVEIRA MARTINS, D. T. 2011. Pharmacological mechanisms underlying the anti-ulcer activity of methanol extract and canthin-6-one of Simaba ferruginea A. St-Hil. in animal models. *J Ethnopharmacol,* 134**,** 630-6.

DEAL, S. B. 1954. Flame Photometric Determination of Sodium and Potassium. *Analytical Chemistry,* 26**,** 598-599.

DEBERARDINIS, R. J. & CHANDEL, N. S. 2016. Fundamentals of cancer metabolism. *Science advances,* 2**,** e1600200-e1600200.

DEEPIKA, S., HARISHKUMAR, R., DINESH, M., ABARNA, R., ANBALAGAN, M., ROOPAN, S. M. & SELVARAJ, C. I. 2017. Photocatalytic degradation of synthetic food dye, sunset yellow FCF (FD&C yellow no. 6) by Ailanthus excelsa Roxb. possessing antioxidant and cytotoxic activity. *J Photochem Photobiol B,* 177**,** 44-55.

DESAI, A. G., QAZI, G. N., GANJU, R. K., EL-TAMER, M., SINGH, J., SAXENA, A. K., BEDI, Y. S., TANEJA, S. C. & BHAT, H. K. 2008. Medicinal plants and cancer chemoprevention. *Curr Drug Metab,* 9**,** 581-91.

DEVI, K. P., MALAR, D. S., NABAVI, S. F., SUREDA, A., XIAO, J., NABAVI, S. M. & DAGLIA, M. 2015. Kaempferol and inflammation: From chemistry to medicine. *Pharmacol Res,* 99**,** 1-10.

DEVKOTA, K. P., WILSON, J. A., HENRICH, C. J., MCMAHON, J. B., REILLY, K. M. & BEUTLER, J. A. 2014. Compounds from Simarouba berteroana which inhibit proliferation of NF1-defective cancer cells. *Phytochem Lett,* 7**,** 42-45.

DIVYA, M. K., LINCY, L., RAGHAVAMENON, A. C. & BABU, T. D. 2016. Ameliorative effect of Apodytes dimidiata on cisplatin-induced nephrotoxicity in Wistar rats. *Pharmaceutical Biology,* 54**,** 2149-2157.

DOU, J., MCCHESNEY, J. D., SINDELAR, R. D., GOINS, D. K. & WALKER, L. A. 1996. A new quassinoid from Castela texana. *J Nat Prod,* 59**,** 73-6.

DRABKIN, D. L. & AUSTIN, J. H. 1935. Spectrophotometric studies: II Preparations from washed blood cells; nitric oxide hemoglobin and sulfhemoglobin. *Journal of Biological Chemistry,* 112**,** 51-65.

DRABKIN, D. L. & AUSTIN, J. H. 1935. Spectrophotometric studies: II Preparations from washed blood cells; nitric oxide hemoglobin and sulfhemoglobin. *Journal of Biological Chemistry,* 112**,** 51-65.

DUANGMANO, S., SAE-LIM, P., SUKSAMRARN, A., DOMANN, F. E. & PATMASIRIWAT, P. 2012. Cucurbitacin B inhibits human breast cancer cell proliferation through disruption of microtubule polymerization and nucleophosmin/B23 translocation. *BMC Complement Altern Med,* 12**,** 1472-6882.

DURIEZ, R., BAILLY, C. & ROUSTAN, R. 1962. [Glaucarubine in the treatment of intestinal amebiasis]. *Presse Med,* 70**,** 1291-2.

EDDERKAOUI, M., HONG, P., VAQUERO, E. C., LEE, J. K., FISCHER, L., FRIESS, H., BUCHLER, M. W., LERCH, M. M., PANDOL, S. J. & GUKOVSKAYA, A. S. 2005. Extracellular matrix stimulates reactive oxygen species production and increases pancreatic cancer cell survival through 5-lipoxygenase and NADPH oxidase. *Am J Physiol Gastrointest Liver Physiol,* 289**,** 21.

EGEBLAD, M., NAKASONE, E. S. & WERB, Z. 2010. Tumors as organs: complex tissues that interface with the entire organism. *Dev Cell,* 18**,** 884-901.

EIZNHAMER, D. A. & XU, Z. Q. 2004. Betulinic acid: a promising anticancer candidate. *IDrugs,* 7**,** 359-73.

EJAZ, K., RAZA, M. A., MAROOF, S. & HAIDER, M. W. 2018. *Cyclophosphamide-induced Atrial Fibrillation With Rapid Ventricular Rate*, Cureus. 2018 May 16;10(5):e2633. doi: 10.7759/cureus.2633.

ELKADY, A. I., HUSSEIN, R. A. & ABU-ZINADAH, O. A. 2014. Differential control of growth, apoptotic activity and gene expression in human colon cancer cells by extracts derived from medicinal herbs, Rhazya stricta and Zingiber officinale and their combination. *World J Gastroenterol,* 20**,** 15275-88.

ELMACI, I., ALTURFAN, E. E., CENGIZ, S., OZPINAR, A. & ALTINOZ, M. A. 2018. Neuroprotective and tumoricidal activities of cardiac glycosides. Could oleandrin be a new weapon against stroke and glioblastoma? *Int J Neurosci,* 128**,** 865-877.

ELZOGHBY, A. O., EL-LAKANY, S. A., HELMY, M. W., ABU-SERIE, M. M. & ELGINDY, N. A. 2017. Shell-crosslinked zein nanocapsules for oral codelivery of exemestane and resveratrol in breast cancer therapy. *Nanomedicine,* 12**,** 2785-2805.

EVANS, W. C. 2009. *Trease and Evans Pharmacognosy*, Saunders Elsevier.

FECCHIO, D., SIROIS, P., RUSSO, M. & JANCAR, S. 1990. Studies on inflammatory response induced by Ehrlich tumor in mice peritoneal cavity. *Inflammation,* 14**,** 125-32.

FIALKOW, L., WANG, Y. & DOWNEY, G. P. 2007. Reactive oxygen and nitrogen species as signaling molecules regulating neutrophil function. *Free Radic Biol Med,* 42**,** 153-64.

FIASCHETTI, G., GROTZER, M. A., SHALABY, T., CASTELLETTI, D. & ARCARO, A. 2011. Quassinoids: From Traditional Drugs to New Cancer Therapeutics. *Current Medicinal Chemistry,* 18**,** 316-328.

FICARRA, R., FICARRA, P., TOMMASINI, S., CALABRO, M. L., RAGUSA, S., BARBERA, R. & RAPISARDA, A. 1995. Leaf extracts of some Cordia species: analgesic and anti-inflammatory activities as well as their chromatographic analysis. *Farmaco,* 50**,** 245-56.

FIKRY, E. M., HASAN, W. A. & MOHAMED, E. G. 2018. Rutin and meloxicam attenuate paw inflammation in mice: Affecting sorbitol dehydrogenase activity. *J Biochem Mol Toxicol,* 32**,** 5.

FISHER, B., DIGNAM, J., WOLMARK, N., WICKERHAM, D. L., FISHER, E. R., MAMOUNAS, E., SMITH, R., BEGOVIC, M., DIMITROV, N. V., MARGOLESE, R. G., KARDINAL, C. G., KAVANAH, M. T.,

FEHRENBACHER, L. & OISHI, R. H. 1999. Tamoxifen in treatment of intraductal breast cancer: National Surgical Adjuvant Breast and Bowel Project B-24 randomised controlled trial. *Lancet,* 353**,** 1993-2000.

FOTI, M. C. 2007. Antioxidant properties of phenols. *J Pharm Pharmacol,* 59**,** 1673-85.

FRANCOIS, G., DIAKANAMWA, C., TIMPERMAN, G., BRINGMANN, G., STEENACKERS, T., ATASSI, G., VAN LOOVEREN, M., HOLENZ, J., TASSIN, J. P., ASSI, L. A., VANHAELEN-FASTRE, R. & VANHAELEN, M. 1998. Antimalarial and cytotoxic potential of four quassinoids from Hannoa chlorantha and Hannoa klaineana, and their structure-activity relationships. *Int J Parasitol,* 28**,** 635-40.

FRANSSEN, F. F. J., SMEIJSTERS, L. J. J. W., BERGER, I. & ALDANA, B. E. M. 1997. In vivo and in vitro antiplasmodial activities of some plants traditionally used in Guatemala against malaria. *Antimicrobial agents and chemotherapy,* 41**,** 1500-1503.

FRIEDEWALD, W. T., LEVY, R. I. & FREDRICKSON, D. S. 1972. Estimation of the concentration of low-density lipoprotein cholesterol in plasma, without use of the preparative ultracentrifuge. *Clin Chem,* 18**,** 499-502.

FU, L. & XIE, C. 2019. A lucid review of Helicobacter pylori-induced DNA damage in gastric cancer. *Helicobacter,* 11**,** 12631.

FUKAMIYA, N., OKANO, M., TAGAHARA, K., ARATANI, T. & LEE, K. H. 1988. Antitumor agents, 93. Bruceanol C, a new cytotoxic quassinoid from Brucea antidysenterica. *J Nat Prod,* 51**,** 349-52.

FUKAMIYA, N., OKANO, M., TAGAHARA, K., ARATANI, T., MURAMOTO, Y. & LEE, K. H. 1987. Antitumor agents, 90. Bruceantinoside C, a new cytotoxic quassinoid glycoside from Brucea antidysenterica. *J Nat Prod,* 50**,** 1075-9.

GAO, F., YUAN, Q., GAO, L., CAI, P., ZHU, H., LIU, R., WANG, Y., WEI, Y., HUANG, G., LIANG, J. & GAO, X. 2014. Cytotoxicity and therapeutic effect of irinotecan combined with selenium nanoparticles. *Biomaterials,* 35**,** 8854-8866.

GARG, S., KAUL, S. C. & WADHWA, R. 2018a. Anti-Stress and Glial Differentiation Effects of a Novel Combination of Cucurbitacin B and Withanone (CucWi-N): Experimental Evidence. *Ann Neurosci,* 25**,** 201-209.

GARG, S., KAUL, S. C. & WADHWA, R. 2018b. Cucurbitacin B and cancer intervention: Chemistry, biology and mechanisms (Review). *Int J Oncol,* 52**,** 19-37.

GAUDEMER, A. & POLONSKY, J. 1965. Structure de la glaucarubinone nouveau principe amer isole de Simaruba glauca. *Phytochemistry,* 4**,** 149-153.

GENTRIC, G., MIEULET, V. & MECHTA-GRIGORIOU, F. 2017. Heterogeneity in Cancer Metabolism: New Concepts in an Old Field. *Antioxid Redox Signal,* 26**,** 462-485.

GEORGE, B. P., ABRAHAMSE, H. & HEMMARAGALA, N. M. 2017. Phenolics from Rubus fairholmianus induces cytotoxicity and apoptosis in human breast adenocarcinoma cells. *Chem Biol Interact,* 275**,** 178-188.

GERSTEN, O. & WILMOTH, J. R. 2002. The cancer transition in Japan since 1951. *Demographic Research,* 7**,** 271-306.

GHOSH, P. C., LARRAHONDO, J. E., LEQUESNE, P. W. & RAFFAUF, R. F. 1977. Antitumor plants. IV. Constituents of Simarouba versicolor. *Lloydia,* 40**,** 364-9.

GIRON, L. M., FREIRE, V., ALONZO, A. & CACERES, A. 1991. Ethnobotanical survey of the medicinal flora used by the Caribs of Guatemala. *J Ethnopharmacol,* 34**,** 173-87.

GOCHEVA, V., WANG, H. W., GADEA, B. B., SHREE, T., HUNTER, K. E., GARFALL, A. L., BERMAN, T. & JOYCE, J. A. 2010. IL-4 induces cathepsin protease activity in tumor-associated macrophages to promote cancer growth and invasion. *Genes Dev,* 24**,** 241-55.

GOVINDARAJU, K., DARUKESHWARA, J. & SRIVASTAVA, A. K. 2009. Studies on protein characteristics and toxic constituents of Simarouba glauca oilseed meal. *Food Chem Toxicol,* 47**,** 1327-32.

GRASSMANN, J. 2005. Terpenoids as plant antioxidants. *Vitam Horm,* 72**,** 505-35.

GREGORY, C. D. & PATERSON, M. 2018. An apoptosis-driven 'onco-regenerative niche': roles of tumour-associated macrophages and extracellular vesicles. *Philos Trans R Soc Lond B Biol Sci,* 373.

GROSVENOR, S. N., MASCOLL, K., MCLEAN, S., REYNOLDS, W. F. & TINTO, W. F. 2006. Tirucallane, apotirucallane, and octanorapotirucallane triterpenes of Simarouba amara. *J Nat Prod,* 69**,** 1315-8.

GUO, Q., LIN, J., LIU, R., GAO, Y., HE, S., XU, X., HUA, B., LI, C., HOU, W., ZHENG, H. & BAO, Y. 2015. Review on the Applications and Molecular

Mechanisms of Xihuang Pill in Tumor Treatment. *Evid Based Complement Alternat Med,* 854307**,** 10.

GUPTA, A. K., PARASAR, D., SAGAR, A., CHOUDHARY, V., CHOPRA, B. S., GARG, R., ASHISH & KHATRI, N. 2015. Analgesic and Anti-Inflammatory Properties of Gelsolin in Acetic Acid Induced Writhing, Tail Immersion and Carrageenan Induced Paw Edema in Mice. *PLoS One,* 10.

HAFEMAN, D. G., SUNDE, R. A. & HOEKSTRA, W. G. 1974. Effect of dietary selenium on erythrocyte and liver glutathione peroxidase in the rat. *J Nutr,* 104**,** 580-7.

HAKKOU, Z., MACIUK, A., LEBLAIS, V., BOUANANI, N. E., MEKHFI, H., BNOUHAM, M., AZIZ, M., ZIYYAT, A., RAUF, A., HADDA, T. B., SHAHEEN, U., PATEL, S., FISCHMEISTER, R. & LEGSSYER, A. 2017. Antihypertensive and vasodilator effects of methanolic extract of Inula viscosa: Biological evaluation and POM analysis of cynarin, chlorogenic acid as potential hypertensive. *Biomed Pharmacother,* 93**,** 62-69.

HALDAR, P. K., KAR, B., BALA, A., BHATTACHARYA, S. & MAZUMDER, U. K. 2010. Antitumor activity of Sansevieria roxburghiana rhizome against Ehrlich ascites carcinoma in mice. *Pharm Biol,* 48**,** 1337-43.

HAM, E. A., SCHAFER, H. M., DENKEWALTER, R. G. & BRINK, N. G. 1954. Structural studies on Glaucarubin from Simarouba glauca. *Journal of American Chemical Society,* 76**,** 6066-6068.

HANAHAN, D. & FOLKMAN, J. 1996. Patterns and emerging mechanisms of the angiogenic switch during tumorigenesis. *Cell,* 86**,** 353-64.

HANAHAN, D. & WEINBERG, R. A. 2000. The hallmarks of cancer. *Cell,* 100**,** 57-70.

HANAHAN, D. & WEINBERG, R. A. 2011. Hallmarks of cancer: the next generation. *Cell,* 144**,** 646-74.

HANIGAN, M. H. & DEVARAJAN, P. 2003. Cisplatin nephrotoxicity: molecular mechanisms. *Cancer Ther,* 1**,** 47-61.

HARBORNE, J. B. 1984. *Phytochemical Methods A Guide to Modern Techniques of Plant Analysis,* Dordrecht, Springer.

HAZAFA, A., REHMAN, K. U., JAHAN, N. & JABEEN, Z. 2019. The Role of Polyphenol (Flavonoids) Compounds in the Treatment of Cancer Cells. *Nutr Cancer,* 9**,** 1-12.

HAZRA, B., SARKAR, R., BHATTACHARYYA, S. & ROY, P. 2002. Tumour inhibitory activity of chicory root extract against Ehrlich ascites carcinoma in mice. *Fitoterapia,* 73**,** 730-3.

HELMSTADTER, A. 2019. Traditional use and scientific investigations of the medicinal plant Simaba cedron Planch. *Pharmazie,* 74**,** 385-389.

HERNANDES, M. S. & BRITTO, L. R. 2012. NADPH oxidase and neurodegeneration. *Curr Neuropharmacol,* 10**,** 321-7.

HERRERA-CALDERON, O., CHACALTANA-RAMOS, L., YULI-POSADAS, R. A., PARI-OLARTE, B., ENCISO-ROCA, E., TINCO-JAYO, J. A., ROJAS-ARMAS, J. P., FELIX-VELIZ, L. M. V. & FRANCO-QUINO, C. 2019. Antioxidant and Cytoprotective Effect of Piper aduncum L. against Sodium Fluoride (NaF)-Induced Toxicity in Albino Mice. *Toxics,* 7.

HORNEBER, M., BUESCHEL, G., DENNERT, G., LESS, D., RITTER, E. & ZWAHLEN, M. 2012. How many cancer patients use complementary and alternative medicine: a systematic review and metaanalysis. *Integr Cancer Ther,* 11**,** 187-203.

HOU, N., LIU, N., HAN, J., YAN, Y. & LI, J. 2017. Chlorogenic acid induces reactive oxygen species generation and inhibits the viability of human colon cancer cells. *Anticancer Drugs,* 28**,** 59-65.

HUANG, M. T., LOU, Y. R., XIE, J. G., MA, W., LU, Y. P., YEN, P., ZHU, B. T., NEWMARK, H. & HO, C. T. 1998. Effect of dietary curcumin and dibenzoylmethane on formation of 7,12-dimethylbenz[a]anthracene-induced mammary tumors and lymphomas/leukemias in Sencar mice. *Carcinogenesis,* 19**,** 1697-700.

HUANG, S. S. & ZHENG, R. L. 2006. Rosmarinic acid inhibits angiogenesis and its mechanism of action in vitro. *Cancer Lett,* 239**,** 271-80.

HUYNH, N., BEUTLER, J. A., SHULKES, A., BALDWIN, G. S. & HE, H. 2015a. Glaucarubinone inhibits colorectal cancer growth by suppression of hypoxia-inducible factor 1alpha and beta-catenin via a p-21 activated kinase 1-dependent pathway. *Biochim Biophys Acta,* 1**,** 157-165.

HWANG, E. S., KIM, H. B., LEE, S., KIM, M. J., LEE, S. O., HAN, S. M., MAENG, S. & PARK, J. H. 2017. Loganin enhances long-term potentiation and recovers scopolamine-induced learning and memory impairments. *Physiol Behav,* 171**,** 243-248.

IBRAHIM, M. E., BANA, E. E. & EL-KERDASY, H. I. 2018. Role of Bone Marrow Derived Mesenchymal Stem Cells and the Protective Effect of

Silymarin in Cisplatin-Induced Acute Renal Failure in Rats. *Am J Med Sci,* 355**,** 76-83.

IKEZAKI, S., NISHIKAWA, A., FURUKAWA, F., KUDO, K., NAKAMURA, H., TAMURA, K. & MORI, H. 2001. Chemopreventive effects of curcumin on glandular stomach carcinogenesis induced by N-methyl-N'-nitro-N-nitrosoguanidine and sodium chloride in rats. *Anticancer Res,* 21**,** 3407-11.

IMAMURA, K., FUKAMIYA, N., NAKAMURA, M., OKANO, M., TAGAHARA, K. & LEE, K. H. 1995. Bruceanols G and H cytotoxic quassinoids from Brucea antidysenterica. *J Nat Prod,* 58**,** 1915-9.

IMAMURA, K., FUKAMIYA, N., OKANO, M., TAGAHARA, K. & LEE, K. H. 1993. Bruceanols D, E, and F three new cytotoxic quassinoids from Brucea antidysenterica. *J Nat Prod,* 56**,** 2091-7.

JAGETIA, G. C., NAYAK, V. & VIDYASAGAR, M. S. 1998. Evaluation of the antineoplastic activity of guduchi (Tinospora cordifolia) in cultured HeLa cells. *Cancer Lett,* 127**,** 71-82.

JAMKHANDE, P. G. & WATTAMWAR, A. S. 2015. Annona reticulata Linn. (Bullock's heart): Plant profile, phytochemistry and pharmacological properties. *Journal of traditional and complementary medicine,* 5**,** 144-152.

JANAKIRAM, N. B., MOHAMMED, A., MADKA, V., KUMAR, G. & RAO, C. V. 2016. Prevention and treatment of cancers by immune modulating nutrients. *Mol Nutr Food Res,* 60**,** 1275-94.

JENSEN, G. S., WU, X., PATTERSON, K. M., BARNES, J., CARTER, S. G., SCHERWITZ, L., BEAMAN, R., ENDRES, J. R. & SCHAUSS, A. G. 2008. In vitro and in vivo antioxidant and anti-inflammatory capacities of an antioxidant-rich fruit and berry juice blend. Results of a pilot and randomized, double-blinded, placebo-controlled, crossover study. *J Agric Food Chem,* 56**,** 8326-33.

JEYARANI, T. & REDDY, S. Y. 2001. Cocoa butter extender from *Simarouba glauca* fat. *Journal of the American Oil Chemists Society,* 78**,** 271-276.

JEZIERSKA-DRUTEL, A., ROSENZWEIG, S. A. & NEUMANN, C. A. 2013. Role of oxidative stress and the microenvironment in breast cancer development and progression. *Adv Cancer Res,* 119**,** 107-25.

JIANG, M.-X. & ZHOU, Y.-J. 2008. Canthin-6-one alkaloids from Picrasma quassioides and their cytotoxic activity. *Journal of Asian Natural Products Research,* 10**,** 1009-1012.

JOHN, A. B. & STEVEN, A. D. 1978. *Microsomal lipid peroxidation,* New York, Academic Press.

JOSE, A., CHAITANYA, M., KANNAN, E. & MADHUNAPANTULA, S. V. 2018. Tricaproin Isolated From Simarouba glauca Inhibits the Growth of Human Colorectal Carcinoma Cell Lines by Targeting Class-1 Histone Deacetylases. *Front Pharmacol,* 9**,** 127.

JOSE, J., DHANYA, A. T., HARIDAS, K. R., SUMESH KUMAR, T. M., JAYARAMAN, S., VARIYAR, E. J. & SUDHAKARAN, S. 2016. Structural characterization of a novel derivative of myricetin from Mimosa pudica as an anti-proliferative agent for the treatment of cancer. *Biomed Pharmacother,* 84**,** 1067-1077.

JOSHI, S. & HIREMATH, S. 2000. Simarouba - A potential oilseed tree. *Current Science,* 78**,** 694-697.

JOSHI, S. & JOSHI, S. 2002. Simarouba glauca DC (Paradise tree). *In:* SCIENCES, U. O. A. (ed.). Bangalore: GKVK Bangalore 65, India.

JUYAL, S. P., SINGH, R. V., LAL, U. M. & SINGH, J. P. 1991. *Strategies for making India Self-reliant in Vegetable Oils,* Hyderabad, Directorate of Oilseeds Research.

KABARY, D. M., HELMY, M. W., ELKHODAIRY, K. A., FANG, J. Y. & ELZOGHBY, A. O. 2018. Hyaluronate/lactoferrin layer-by-layer-coated lipid nanocarriers for targeted co-delivery of rapamycin and berberine to lung carcinoma. *Colloids Surf B Biointerfaces,* 169**,** 183-194.

KARIMI, B., ASHRAFI, M., SHOMALI, T. & YEKTASERESHT, A. 2019. Therapeutic effect of simvastatin on DMBA-induced breast cancer in mice. *Fundam Clin Pharmacol,* 33**,** 84-93.

KARTHIKEYAN, S., HOTI, S. L., NAZEER, Y. & HEGDE, H. V. 2016. Glaucarubinone sensitizes KB cells to paclitaxel by inhibiting ABC transporters via ROS-dependent and p53-mediated activation of apoptotic signaling pathways. *Oncotarget,* 7**,** 42353-42373.

KASCHULA, C. H., HUNTER, R., COTTON, J., TUVERI, R., NGARANDE, E., DZOBO, K., SCHAFER, G., SIYO, V., LANG, D., KUSZA, D. A., DAVIES, B., KATZ, A. A. & PARKER, M. I. 2016. The garlic compound ajoene targets protein folding in the endoplasmic reticulum of cancer cells. *Mol Carcinog,* 55**,** 1213-28.

KATA, D., FOLDESI, I., FEHER, L. Z., HACKLER, L., JR., PUSKAS, L. G. & GULYA, K. 2017. A novel pleiotropic effect of aspirin: Beneficial regulation

of pro- and anti-inflammatory mechanisms in microglial cells. *Brain Res Bull,* 132**,** 61-74.

KAYA, C., BARBAROS BASESKIOGLU, A., YIGITASLAN, S., YASEMIN OZATIK, F., OZATIK, O. & USLU, S. 2019. The therapeutic potential of amifostine on cyclophosphamide-induced testicular dysfunction in rats: An experimental study. *Int J Reprod Biomed,* 17.

KAZEROUNIAN, S., YEE, K. O. & LAWLER, J. 2008. Thrombospondins in cancer. *Cell Mol Life Sci,* 65**,** 700-12.

KERBEL, R. & FOLKMAN, J. 2002. Clinical translation of angiogenesis inhibitors. *Nat Rev Cancer,* 2**,** 727-39.

KESSENBROCK, K., PLAKS, V. & WERB, Z. 2010. Matrix metalloproteinases: regulators of the tumor microenvironment. *Cell,* 141**,** 52-67.

KHARE, R., UPMANYU, N. & JHA, M. 2019. Exploring the potential effect of Methanolic extract of Salvia officinalis against UV exposed skin aging: In vivo and In vitro model. *Curr Aging Sci,* 8**,** 187460981266619080814054 9.

KIM, J. & BECKER, R. C. 2016. Aspirin dosing frequency in the primary and secondary prevention of cardiovascular events. *J Thromb Thrombolysis,* 41**,** 493-504.

KIM, M. Y., CHOI, S. D. & RYU, A. 2015. Is complementary and alternative therapy effective for women in the climacteric period? *J Menopausal Med,* 21**,** 28-35.

KIM, S.-H., LEE, I.-C., BAEK, H.-S., SHIN, I.-S., MOON, C., BAE, C.-S., KIM, S.-H., KIM, J.-C. & KIM, H.-C. 2014. Mechanism for the protective effect of diallyl disulfide against cyclophosphamide acute urotoxicity in rats. *Food and chemical toxicology : an international journal published for the British Industrial Biological Research Association,* 64**,** 110-118.

KLYMKOWSKY, M. W. & SAVAGNER, P. 2009. Epithelial-mesenchymal transition: a cancer researcher's conceptual friend and foe. *Am J Pathol,* 174**,** 1588-93.

KO, Y. S., RUGIRA, T., JIN, H., PARK, S. W. & KIM, H. J. 2018. Oleandrin and Its Derivative Odoroside A, Both Cardiac Glycosides, Exhibit Anticancer Effects by Inhibiting Invasion via Suppressing the STAT-3 Signaling Pathway. *Int J Mol Sci,* 19.

KOCAADAM, B. & SANLIER, N. 2017. Curcumin, an active component of turmeric (Curcuma longa), and its effects on health. *Crit Rev Food Sci Nutr,* 57**,** 2889-2895.

KOCAHAN, S., DOGAN, Z., ERDEMLI, E. & TASKIN, E. 2017. Protective Effect of Quercetin Against Oxidative Stress-induced Toxicity Associated With Doxorubicin and Cyclophosphamide in Rat Kidney and Liver Tissue. *Iran J Kidney Dis,* 11**,** 124-131.

KODURU, S., GRIERSON, D. S. & AFOLAYAN, A. J. 2006. Antimicrobial Activity of Solanum aculeastrum. *Pharmaceutical Biology,* 44**,** 283-286.

KODYDKOVA, J., VAVROVA, L., KOCIK, M. & ZAK, A. 2014. Human catalase, its polymorphisms, regulation and changes of its activity in different diseases. *Folia Biol,* 60**,** 153-67.

KOIRI, R. K., MEHROTRA, A. & TRIGUN, S. K. 2017. Dalton's Lymphoma as a Murine Model for Understanding the Progression and Development of T-Cell Lymphoma and Its Role in Drug Discovery. *International Journal of Immunotherapy and Cancer Research,* 3**,** 1-6.

KOUL, I. B. & KAPIL, A. 1993. Evaluation of the liver protective potential of piperine, an active principle of black and long peppers. *Planta Med,* 59**,** 413-7.

KRYSTON, T. B., GEORGIEV, A. B., PISSIS, P. & GEORGAKILAS, A. G. 2011. Role of oxidative stress and DNA damage in human carcinogenesis. *Mutat Res,* 711**,** 193-201.

KUMAR, N., DHAMIJA, I., VASANTH RAJ, P., JAYASHREE, B. S., PARIHAR, V., MANJULA, S. N., THOMAS, S., GOPALAN KUTTY, N. & MALLIKARJUNA RAO, C. 2014. Preliminary investigation of cytotoxic potential of 2-quinolone derivatives using in vitro and in vivo (solid tumor and liquid tumor) models of cancer. *Arabian Journal of Chemistry,* 7**,** 409-417.

KUMAR, R. A., SRIDEVI, K., KUMAR, N. V., NANDURI, S. & RAJAGOPAL, S. 2004. Anticancer and immunostimulatory compounds from Andrographis paniculata. *J Ethnopharmacol,* 92**,** 291-5.

KUMAR, R. S., RAJKAPOOR, B. & PERUMAL, P. 2012. Antioxidant activities of Indigofera cassioides Rottl. Ex. DC. using various in vitro assay models. *Asian Pac J Trop Biomed,* 2**,** 256-61.

KUWAHARA, I. 1967. Experimental induction of ovarian tumors in mice treated with single administration of 7,12-dimethylbenz[a]anthracene, and its histopathological observation. *Gan,* 58**,** 253-66.

LAKSHMI, K. S., SANGEETHA, D., SIVAMANI, S., TAMILARASAN, M., RAJESH, T. P. & ANANDRAJ, B. 2014. In vitro antibactrial, antioxidant,

haemolytic, thrombolytic activities and phytochemical analysis of Simarouba glacuca leaves extracts. *International Journal of Pharmaceutical Sciences and Research,* 5**,** 432-437.

LAVHALE, M. S. & MISHRA, S. H. 2007. Nutritional and therapeutic potential of Ailanthus excelsa - A Review. *Pharmacognosy Reviews,* 1**,** 105-113.

LAVHALE, M. S., KUMAR, S., MISHRA, S. H. & SITASAWAD, S. L. 2009. A novel triterpenoid isolated from the root bark of Ailanthus excelsa Roxb (Tree of Heaven), AECHL-1 as a potential anti-cancer agent. *PLoS One,* 4**,** 28.

LEVINSON, S. S. 1976. Direct determination of serum chloride with a semiautomated discrete analyzer. *Clin Chem,* 22**,** 273-4.

LI, G., LEE, L.-S., LI, M., TSAO, S.-W. & CHIU, J.-F. 2011. Molecular changes during arsenic-induced cell transformation. *Journal of Cellular Physiology,* 226**,** 3225-3232.

LI, J., LI, S., WANG, X. & WANG, H. 2017. Esculetin induces apoptosis of SMMC-7721 cells through IGF-1/PI3K/Akt-mediated mitochondrial pathways. *Can J Physiol Pharmacol,* 95**,** 787-794.

LI, J., LIN, W., XU, P., ZHANG, J., YANG, H. & LING, X. 2015. Metabolic profiling study on potential toxicity and immunotoxicity-biomarker discovery in rats treated with cyclophosphamide using HPLC-ESI-IT-TOF-MS. *Biomed Chromatogr,* 29**,** 768-76.

LI, M., CHEN, J., YU, X., XU, S., LI, D., ZHENG, Q. & YIN, Y. 2019a. Myricetin Suppresses the Propagation of Hepatocellular Carcinoma via Down-Regulating Expression of YAP. *Cells,* 8.

LI, Q., FU, G. B., ZHENG, J. T., HE, J., NIU, X. B., CHEN, Q. D., YIN, Y., QIAN, X., XU, Q., WANG, M., SUN, A. F., SHU, Y., RUI, H., LIU, L. Z. & JIANG, B. H. 2013. NADPH oxidase subunit p22(phox)-mediated reactive oxygen species contribute to angiogenesis and tumor growth through AKT and ERK1/2 signaling pathways in prostate cancer. *Biochim Biophys Acta,* 12**,** 8.

LI, T., ZHAO, N., LU, J., ZHU, Q., LIU, X., HAO, F. & JIAO, X. 2019b. Epigallocatechin gallate (EGCG) suppresses epithelial-Mesenchymal transition (EMT) and invasion in anaplastic thyroid carcinoma cells through blocking of TGF-beta1/Smad signaling pathways. *Bioengineered,* 10**,** 282-291.

LI, Y., LI, Z., SHI, L., ZHAO, C., SHEN, B., TIAN, Y. & FENG, H. 2016. Loganin inhibits the inflammatory response in mouse 3T3L1 adipocytes and mouse model. *Int Immunopharmacol,* 36**,** 173-179.

LIN, T. H., HSU, W. H., TSAI, P. H., HUANG, Y. T., LIN, C. W., CHEN, K. C., TSAI, I. H., KANDASWAMI, C. C., HUANG, C. J., CHANG, G. D., LEE, M. T. & CHENG, C. H. 2017. Dietary flavonoids, luteolin and quercetin, inhibit invasion of cervical cancer by reduction of UBE2S through epithelial-mesenchymal transition signaling. *Food Funct,* 8**,** 1558-1568.

LIU, H., LV, L. & YANG, K. 2015. Chemotherapy targeting cancer stem cells. *Am J Cancer Res,* 5**,** 880-93.

LIU, H., ZENG, Z., WANG, S., LI, T., MASTRIANI, E., LI, Q. H., BAO, H. X., ZHOU, Y. J., WANG, X., LIU, Y., LIU, W., HU, S., GAO, S., YU, M., QI, Y., SHEN, Z., WANG, H., GAO, T., DONG, L., JOHNSTON, R. N. & LIU, S. L. 2017. Main components of pomegranate, ellagic acid and luteolin, inhibit metastasis of ovarian cancer by down-regulating MMP2 and MMP9. *Cancer Biol Ther,* 18**,** 990-999.

LIU, J., JIA, L., KAN, J. & JIN, C. H. 2013. In vitro and in vivo antioxidant activity of ethanolic extract of white button mushroom (Agaricus bisporus). *Food Chem Toxicol,* 51**,** 310-6.

LIU, Y., LAN, L., HUANG, K., WANG, R., XU, C., SHI, Y., WU, X., WU, Z., ZHANG, J., CHEN, L., WANG, L., YU, X., ZHU, H. & LU, B. 2014. Inhibition of Lon blocks cell proliferation, enhances chemosensitivity by promoting apoptosis and decreases cellular bioenergetics of bladder cancer: potential roles of Lon as a prognostic marker and therapeutic target in baldder cancer. *Oncotarget,* 5**,** 11209-24.

LOPEZ-LAZARO, M., PALMA DE LA PENA, N., PASTOR, N., MARTIN-CORDERO, C., NAVARRO, E., CORTES, F., AYUSO, M. J. & TORO, M. V. 2003. Anti-tumour activity of Digitalis purpurea L. subsp. heywoodii. *Planta Med,* 69**,** 701-4.

LOU, Z., WANG, H., ZHU, S., MA, C. & WANG, Z. 2011. Antibacterial activity and mechanism of action of chlorogenic acid. *J Food Sci,* 76**,** 1750-3841.

LOWRY, O. H., ROSEBROUGH, N. J., FARR, A. L. & RANDALL, R. J. 1951. Protein measurement with the Folin phenol reagent. *J Biol Chem,* 193**,** 265-75.

LU, J. J., BAO, J. L., CHEN, X. P., HUANG, M. & WANG, Y. T. 2012. Alkaloids isolated from natural herbs as the anticancer agents. *Evid Based Complement Alternat Med,* 485042**,** 4.

LU, J. J., BAO, J. L., WU, G. S., XU, W. S., HUANG, M. Q., CHEN, X. P. & WANG, Y. T. 2013. Quinones derived from plant secondary metabolites as anti-cancer agents. *Anticancer Agents Med Chem,* 13**,** 456-63.

LU, J. J., DANG, Y. Y., HUANG, M., XU, W. S., CHEN, X. P. & WANG, Y. T. 2012b. Anti-cancer properties of terpenoids isolated from Rhizoma Curcumae--a review. *J Ethnopharmacol,* 143**,** 406-11.

LUANPITPONG, S., TALBOTT, S. J., ROJANASAKUL, Y., NIMMANNIT, U., PONGRAKHANANON, V., WANG, L. & CHANVORACHOTE, P. 2010. Regulation of lung cancer cell migration and invasion by reactive oxygen species and caveolin-1. *J Biol Chem,* 285**,** 38832-40.

LUMONADIO, L., ATASSI, G., VANHAELEN, M. & VANHAELEN-FASTRE, R. 1991. Antitumor activity of quassinoids from Hannoa klaineana. *J Ethnopharmacol,* 31**,** 59-65.

LUO, Q. & ASHER, G. N. 2017. Complementary and Alternative Medicine Use at a Comprehensive Cancer Center. *Integr Cancer Ther,* 16**,** 104-109.

MA, J., ZHANG, Q., CHEN, S., FANG, B., YANG, Q., CHEN, C., MIELE, L., SARKAR, F. H., XIA, J. & WANG, Z. 2013. Mitochondrial dysfunction promotes breast cancer cell migration and invasion through HIF1alpha accumulation via increased production of reactive oxygen species. *PLoS One,* 8.

MA, J., ZI JIANG, Y., SHI, H., MI, C., LI, J., XING NAN, J., WU, X., JOON LEE, J. & JIN, X. 2014. Cucurbitacin B inhibits the translational expression of hypoxia-inducible factor-1alpha. *Eur J Pharmacol,* 723**,** 46-54.

MA, T., KANG, C., SHAO, H., QI, Q. & HU, W. 2006. Protective Effects of Ulinastatin on Proliferation and Cytokine Release of Splenocytes from Rats with Severe Acute Pancreatitis. *European Surgical Research,* 38**,** 445-450.

MA, Y., MIZINO, T. & ITO, H. 1991. Antitumor Activity of Some Polysaccharides Isolated from a Chinese Mushroom, "Huangmo", the Fruiting Body of Hohenbuehelia serotina. *Agricultural and Biological Chemistry,* 55**,** 2701-2710.

MADSEN, C. D. & SAHAI, E. 2010. Cancer dissemination--lessons from leukocytes. *Dev Cell,* 19**,** 13-26.

MAGNE NDE, C. B., ZINGUE, S., WINTER, E., CRECZYNSKI-PASA, T. B., MICHEL, T., FERNANDEZ, X., NJAMEN, D. & CLYNE, C. 2015. Flavonoids, Breast Cancer Chemopreventive and/or Chemotherapeutic Agents. *Curr Med Chem,* 22**,** 3434-46.

MAHMOUD, A. M. 2014. Hesperidin protects against cyclophosphamide-induced hepatotoxicity by upregulation of PPARgamma and abrogation of oxidative stress and inflammation. *Can J Physiol Pharmacol,* 92**,** 717-24.

MAITY, T. K., MANDAL, S. C., MUKHERJEE, P. K., SAHA, K., DAS, J., PAL, M. & SAHA, B. P. 1998. Studies on anti-inflammatory effect of *Cassia tora* leaf extract (Fam Leguminosae). *Phytotherapy Research,* 12**,** 221-223.

MALIK, F., KUMAR, A., BHUSHAN, S., KHAN, S., BHATIA, A., SURI, K. A., QAZI, G. N. & SINGH, J. 2007. Reactive oxygen species generation and mitochondrial dysfunction in the apoptotic cell death of human myeloid leukemia HL-60 cells by a dietary compound withaferin A with concomitant protection by N-acetyl cysteine. *Apoptosis,* 12**,** 2115-33.

MALVIA, S., BAGADI, S. A., DUBEY, U. S. & SAXENA, S. 2017. Epidemiology of breast cancer in Indian women. *Asia Pac J Clin Oncol,* 13**,** 289-295.

MANTOVANI, A., SAVINO, B., LOCATI, M., ZAMMATARO, L., ALLAVENA, P. & BONECCHI, R. 2010. The chemokine system in cancer biology and therapy. *Cytokine Growth Factor Rev,* 21**,** 27-39.

MARCOCCI, L., MAGUIRE, J. J., DROY-LEFAIX, M. T. & PACKER, L. 1994. The nitric oxide-scavenging properties of Ginkgo biloba extract EGb 761. *Biochem Biophys Res Commun,* 201**,** 748-55.

MARTIN, A., FUZER, A. M., BECCENERI, A. B., DA SILVA, J. A., TOMASIN, R., DENOYER, D., KIM, S. H., MCINTYRE, K. A., PEARSON, H. B., YEO, B., NAGPAL, A., LING, X., SELISTRE-DE-ARAUJO, H. S., VIEIRA, P. C., COMINETTI, M. R. & POULIOT, N. 2017. [10]-gingerol induces apoptosis and inhibits metastatic dissemination of triple negative breast cancer in vivo. *Oncotarget,* 8**,** 72260-72271.

MATA-GREENWOOD, E., DAEUBLE, J. F., GRIECO, P. A., DOU, J., MCCHESNEY, J. D., MEHTA, R. G., KINGHORN, A. D. & PEZZUTO, J. M. 2001. Novel esters of glaucarubolone as inducers of terminal differentiation of promyelocytic HL-60 cells and inhibitors of 7,12-dimethylbenz[a]anthracene-induced preneoplastic lesion formation in mouse mammary organ culture. *J Nat Prod,* 64**,** 1509-13.

MAULIK, N. & DAS, D. K. 2002. Redox signaling in vascular angiogenesis. *Free Radic Biol Med,* 33**,** 1047-60.

MAZUMDAR, U. K., GUPTA, M., MAITI, S. & MUKHERJEE, D. 1997. Antitumor activity of Hygrophila spinosa on Ehrlich ascites carcinoma and sarcoma-180 induced mice. *Indian J Exp Biol,* 35**,** 473-7.

MCCORD, J. M. & FRIDOVICH, I. 1969. Superoxide dismutase. An enzymic function for erythrocuprein (hemocuprein). *J Biol Chem,* 244**,** 6049-55.

MEDINA, D. & SHEPHERD, F. 1981. Selenium-mediated inhibition of 7,12-dimethylbenz[a]anthracene-induced mouse mammary tumorigenesis. *Carcinogenesis,* 2**,** 451-455.

MEHARA, E. & VAIDYA, M. C. 1984. *A hand book of practical and clinical immunology,* New Delhi, CBS Publishers.

MENG, Q., PAN, J., LIU, Y., CHEN, L. & REN, Y. 2018. Anti-tumour effects of polysaccharide extracted from Acanthopanax senticosus and cell-mediated immunity. *Exp Ther Med,* 15**,** 1694-1701.

MIAO, L. & ST CLAIR, D. K. 2009. Regulation of superoxide dismutase genes: implications in disease. *Free Radic Biol Med,* 47**,** 344-56.

MILKOVIC, L., SIEMS, W., SIEMS, R. & ZARKOVIC, N. 2014. Oxidative stress and antioxidants in carcinogenesis and integrative therapy of cancer. *Curr Pharm Des,* 20**,** 6529-42.

MINARI, J. B. & OKEKE, U. 2014. Chemopreventive effect of Annona muricata on DMBA-induced cell proliferation in the breast tissues of female albino mice. *Egyptian Journal of Medical Human Genetics,* 15**,** 327-334.

MITRA, A., CHAKRABARTI, J., BANERJI, A., CHATTERJEE, A. & DAS, B. R. 2006. Curcumin, a potential inhibitor of MMP-2 in human laryngeal squamous carcinoma cells HEp2. *J Environ Pathol Toxicol Oncol,* 25**,** 679-90.

MOHANAN, P., SUBRAMANIYAM, S., MATHIYALAGAN, R. & YANG, D. C. 2018. Molecular signaling of ginsenosides Rb1, Rg1, and Rg3 and their mode of actions. *J Ginseng Res,* 42**,** 123-132.

MOK, C. C. 2016. Con: Cyclophosphamide for the treatment of lupus nephritis. *Nephrol Dial Transplant,* 31**,** 1053-7.

MOLDEUS, P., HOGBERG, J. & ORRENIUS, S. 1978. Isolation and use of liver cells. *Methods Enzymol,* 52**,** 60-71.

MONSEUR, X. & MOTTE, J. C. 1983. Quantitative high-performance liquid chromatographic analysis of the bitter quassinoid compounds from Simaruba glauca seeds. *journal of Chromatography,* 264**,** 469-473.

MOORE, K. L. & DALLEY, A. F. 1999. *Clinically Oriented Anatomy,* Philadelphia, Lippincott Williams & Wilkins.

MORON, M. S., DEPIERRE, J. W. & MANNERVIK, B. 1979. Levels of glutathione, glutathione reductase and glutathione S-transferase activities in rat lung and liver. *Biochim Biophys Acta,* 582**,** 67-78.

MORRE, D. J., GRIECO, P. A. & MORRE, D. M. 1998. Mode of action of the anticancer quassinoids--inhibition of the plasma membrane NADH oxidase. *Life Sci,* 63**,** 595-604.

MOSMANN, T. 1983. Rapid colorimetric assay for cellular growth and survival: application to proliferation and cytotoxicity assays. *J Immunol Methods,* 65**,** 55-63.

MOUDI, M., GO, R., YIEN, C. Y. & NAZRE, M. 2013. Vinca alkaloids. *Int J Prev Med,* 4**,** 1231-5.

MUHAMMAD, I., BEDIR, E., KHAN, S. I., TEKWANI, B. L., KHAN, I. A., TAKAMATSU, S., PELLETIER, J. & WALKER, L. A. 2004. A new antimalarial quassinoid from Simaba orinocensis. *J Nat Prod,* 67**,** 772-7.

MUKINDA, J. T. & SYCE, J. A. 2007. Acute and chronic toxicity of the aqueous extract of Artemisia afra in rodents. *J Ethnopharmacol,* 112**,** 138-44.

MUKUND, V., MUKUND, D., SHARMA, V., MANNARAPU, M. & ALAM, A. 2017. Genistein: Its role in metabolic diseases and cancer. *Crit Rev Oncol Hematol,* 119**,** 13-22.

MUNIYAN, S., CHOU, Y.-W., TSAI, T.-J., THOMES, P., VEERAMANI, S., BENIGNO, B. B., WALKER, L. D., MCDONALD, J. F., KHAN, S. A., LIN, F.-F., LELE, S. M. & LIN, M.-F. 2015. p66Shc longevity protein regulates the proliferation of human ovarian cancer cells. *Molecular Carcinogenesis,* 54**,** 618-631.

NABAVI, S. M., NABAVI, S. F., ESLAMI, S. & MOGHADDAM, A. H. 2012. In vivo protective effects of quercetin against sodium fluoride-induced oxidative stress in the hepatic tissue. *Food Chemistry,* 132**,** 931-935.

NAIR, A. B. & JACOB, S. 2016. A simple practice guide for dose conversion between animals and human. *J Basic Clin Pharm,* 7**,** 27-31.

NAIR, S., GEORGE, J., KUMAR, S. & GRACIOUS, N. 2014. Acute Oxalate Nephropathy following Ingestion of Averrhoa bilimbi Juice. *Case Rep Nephrol,* 240936**,** 4.

NAITO, H. K. 1985. The association of serum lipids, lipoproteins, and apolipoproteins withcoronary artery disease assessed by coronary arteriography. *Annals of the New York Academy of Sciences,* 454**,** 230-238.

NARENDRAN, R. 2013. A tree of solace for cancer patients. *The New Indian Express*

NAVEED, M., HEJAZI, V., ABBAS, M., KAMBOH, A. A., KHAN, G. J., SHUMZAID, M., AHMAD, F., BABAZADEH, D., FANGFANG, X., MODARRESI-GHAZANI, F., WENHUA, L. & XIAOHUI, Z. 2018. Chlorogenic acid (CGA): A pharmacological review and call for further research. *Biomed Pharmacother,* 97**,** 67-74.

NGO, T. V., SCARLETT, C. J., BOWYER, M. C., NGO, P. D. & VUONG, Q. V. 2017. Impact of Different Extraction Solvents on Bioactive Compounds and Antioxidant Capacity from the Root of Salacia chinensis L. *Journal of Food Quality,* 2017**,** 8.

NING, D., JIN, M., XV, T., SUN, J. & LI, M. 2018. Homoisoflavanone-1 isolated from Polygonatum odoratum arrests the cell cycle and induces apoptosis in A549 cells. *Oncol Lett,* 16**,** 3545-3554.

NISHIDA, N., YANO, H., NISHIDA, T., KAMURA, T. & KOJIRO, M. 2006. Angiogenesis in cancer. *Vascular health and risk management,* 2**,** 213-219.

NOVAK, K. L. & CHAPMAN, G. E. 2001. Oncologists' and naturopaths' nutrition beliefs and practices. *Cancer Pract,* 9**,** 141-6.

NOVELLO, C. R., BAZOTTE, R. B., AMADO, C. A. B., MARQUES, L. C., CORTEZ. A. G. 2008. Toxicological and Parmacological Studies of *Picrasma crenata* (Vell.) Engler (Simaroubaceae) in Mice and Rats. *Latin American Journal of Pharmacy,* 27**,** 345-348.

ODUBANJO, V. O., IBUKUN, E. O., OBOH, G. & ADEFEGHA, S. A. 2018. Aqueous extracts of two tropical ethnobotanicals (Tetrapleura tetraptera and Quassia undulata) improved spatial and non-spatial working memories in scopolamine-induced amnesic rats: Influence of neuronal cholinergic and antioxidant systems. *Biomed Pharmacother,* 99**,** 198-204.

OECD 2001. OECD guideline for testing of chemicals. Acute Oral Toxicity-Acute Toxic Class method. 423.

OECD 2008. OECD guidelines for the testing of chemicals. Repeated Dose 28-Day Oral Toxicity Study in Rodents.

OHKAWA, H., OHISHI, N. & YAGI, K. 1979. Assay for lipid peroxides in animal tissues by thiobarbituric acid reaction. *Anal Biochem,* 95**,** 351-8.

OHNISHI, S., FUKAMIYA, N., OKANO, M., TAGAHARA, K. & LEE, K. H. 1995. Bruceosides D, E, and F, three new cytotoxic quassinoid glucosides from Brucea javanica. *J Nat Prod,* 58**,** 1032-8.

OJESWI, B. K., KHOOBCHANDANI, M., HAZRA, D. K. & SRIVASTAVA, M. M. 2010. Protective effect of Thuja occidentalis against DMBA-induced breast cancer with reference to oxidative stress. *Hum Exp Toxicol,* 29**,** 369-75.

OKANO, M., FUKAMIYA, N., ARATANI, T., JUICHI, M. & LEE, K. H. 1985. Antitumor agents, 74. Bruceanol-A and -B, two new antileukemic quassinoids from Brucea antidysenterica. *J Nat Prod,* 48**,** 972-5.

OKANO, M., FUKAMIYA, N., TOYOTA, T., TAGAHARA, K. & LEE, K. H. 1989. Antitumor agents, 104. Isolation of yadanziosides M and P from Brucea antidysenterica and identification of bruceantinoside B as a mixture of yadanzioside P and bruceantinoside C. *J Nat Prod,* 52**,** 398-401.

OLSON, H., BETTON, G., ROBINSON, D., THOMAS, K., MONRO, A., KOLAJA, G., LILLY, P., SANDERS, J., SIPES, G., BRACKEN, W., DORATO, M., VAN DEUN, K., SMITH, P., BERGER, B. & HELLER, A. 2000. Concordance of the toxicity of pharmaceuticals in humans and in animals. *Regul Toxicol Pharmacol,* 32**,** 56-67.

OMRAN, A. R. 2005. The Epidemiologic Transition: A Theory of the Epidemiology of Population Change. *The milbank memorial fund quarterly,* 83**,** 731-757.

O'NEILL, M. J., BRAY, D. H., BOARDMAN, P., CHAN, K. L., PHILLIPSON, J. D., WARHURST, D. C. & PETERS, W. 1987. Plants as sources of antimalarial drugs, Part 4: Activity of Brucea javanica fruits against chloroquine-resistant Plasmodium falciparum in vitro and against Plasmodium berghei in vivo. *J Nat Prod,* 50**,** 41-8.

O'NEILL, M. J., BRAY, D. H., BOARDMAN, P., PHILLIPSON, J. D., WARHURST, D. C., PETERS, W. & SUFFNESS, M. 1986. Plants as sources of antimalarial drugs: in vitro antimalarial activities of some quassinoids. *Antimicrob Agents Chemother,* 30**,** 101-4.

O'NEILL, M. J., BRAY, D. H., BOARDMAN, P., WRIGHT, C. W., PHILLIPSON, J. D., WARHURST, D. C., GUPTA, M. P., CORREYA, M. & SOLIS, P. 1988. Plants as sources of antimalarial drugs, Part 6: Activities of Simarouba amara fruits. *J Ethnopharmacol,* 22**,** 183-90.

OZEKI, A., HITOTSUYANAGI, Y., HASHIMOTO, E., ITOKAWA, H., TAKEYA, K. & DE MELLO ALVES, S. 1998. Cytotoxic quassinoids from Simaba cedron. *J Nat Prod,* 61**,** 776-80.

PALLIYAGURU, D. L., SINGH, S. V. & KENSLER, T. W. 2016. Withania somnifera: From prevention to treatment of cancer. *Mol Nutr Food Res,* 60**,** 1342-53.

PALUMBO, M., KAVAN, P., MILLER, W., PANASCI, L., ASSOULINE, S., JOHNSON, N., COHEN, V., PATENAUDE, F., POLLAK, M., JAGOE, R. & BATIST, G. 2013. Systemic cancer therapy: achievements and challenges that lie ahead. *Frontiers in Pharmacology,* 4.

PAN, H. J., CHANG, H. T. & LEE, C. H. 2016. Association between tamoxifen treatment and the development of different stages of nonalcoholic fatty liver disease among breast cancer patients. *J Formos Med Assoc,* 115**,** 411-7.

PAN, L., ZHANG, Y., ZHAO, W., ZHOU, X., WANG, C. & DENG, F. 2017. The cardiac glycoside oleandrin induces apoptosis in human colon cancer cells via the mitochondrial pathway. *Cancer Chemother Pharmacol,* 80**,** 91-100.

PANDIYAN, D. S. T. & PRABU, S. M. 2013. Molecular Mechanism of Fluoride Induced Oxidative Stress and Its Possible Reversal by Chelation Therapy. *Research and reviews:A Journal of Toxicology,* Volume 3.

PARASURAMAN, S. 2011. Toxicological screening. *J Pharmacol Pharmacother,* 2**,** 74-9.

PARK, M. H. & HONG, J. T. 2016. Roles of NF-kappaB in Cancer and Inflammatory Diseases and Their Therapeutic Approaches. *Cells,* 5.

PARK, S., NHIEM, N. X., KIEM, P. V., MINH, C. V., TAI, B. H., KIM, N., YOO, H. H., SONG, J. H., KO, H. J. & KIM, S. H. 2014. Five new quassinoids and cytotoxic constituents from the roots of Eurycoma longifolia. *Bioorg Med Chem Lett,* 24**,** 3835-40.

PART 314, C. O. F. R. T. 2019. Electroni Code of Federal Regulations e-CFR.

PATIL, M. S. & GAIKWAD, D. K. 2011. A critical review on medicinally important oil yielding plant laxmitaru (Simarouba glauca DC.). *Journal of Pharmaceutical Sciences and Research,* 3**,** 1195-1213.

PAULSEN, C. E. & CARROLL, K. S. 2013. Cysteine-mediated redox signaling: chemistry, biology, and tools for discovery. *Chem Rev,* 113**,** 4633-79.

PAVLOVA, N. N. & THOMPSON, C. B. 2016. The Emerging Hallmarks of Cancer Metabolism. *Cell metabolism,* 23**,** 27-47.

PELENGARIS, S., KAHN, M. 2006. *The Molecular Biology of Cancer.,* Victoria, Australia, Blackwell Publishing.

PERES, L. A. & DA CUNHA, A. D., JR. 2013. Acute nephrotoxicity of cisplatin: molecular mechanisms. *J Bras Nefrol,* 35**,** 332-40.

PETER, A. I., NAIDU, E. C., AKANG, E., OGEDENGBE, O. O., OFFOR, U., RAMBHAROSE, S., KALHAPURE, R., CHUTURGOON, A., GOVENDER, T. & AZU, O. O. 2018. Investigating Organ Toxicity Profile of Tenofovir and Tenofovir Nanoparticle on the Liver and Kidney: Experimental Animal Study. *Toxicol Res,* 34**,** 221-229.

PHILLIPSON, J. D., WRIGHT, C. W., KIRBY, G. C. & WRHURST, D. C. 1995. *Structure and biological activity of sesquiterpene and diterpene derivatices from medicinal plants.,* London, University Press. *Phytochemistry, Botany and Metabolism of Alkaloids, Phenolics and Terpenes,* Berlin, Heidelberg, Springer.

PICKUP, M. W., MOUW, J. K. & WEAVER, V. M. 2014. The extracellular matrix modulates the hallmarks of cancer. *EMBO Rep,* 15**,** 1243-53.

PIRES, A. F., MARQUES, G. F. O., ALENCAR, N. M. N., MARTINS, M. G. Q., SILVA, M., NASCIMENTO, K. S. D., CAVADA, B. S. & ASSREUY, A. M. S. 2019. Inhibitory effect of Lonchocarpus araripensis lectin in rat acute models of inflammation. *An Acad Bras Cienc,* 91**,** 0001-3765201920180991.

PODRATZ, J. L., KNIGHT, A. M., TA, L. E., STAFF, N. P., GASS, J. M., GENELIN, K., SCHLATTAU, A., LATHROUM, L. & WINDEBANK, A. J. 2011. Cisplatin induced mitochondrial DNA damage in dorsal root ganglion neurons. *Neurobiol Dis,* 41**,** 661-8.

POLJSAK, B. & DAHMANE, R. 2012. Free radicals and extrinsic skin aging. *Dermatol Res Pract,* 135206**,** 29.

POLONSKY, J. 1985. Quassinoid bitter principle-II. *Fortschritte der Chemie organischer Naturstoffe,* 47**,** 221-237.

POLONSKY, J., VARON, Z., MORETTI, C., PETTIT, G. R., HERALD, C. L., RIDEOUT, J. A., SAHA, S. B. & KHASTGIR, H. N. 1980. The antineoplastic quassinoids of Simaba cuspidata spruce and Ailanthus grandis Prain. *J Nat Prod,* 43**,** 503-9.

POLONSKY, J., VRON, Z., JACQUEMIN, H. & PETTIT, G. R. 1978. The isolation and structure of 13,18-dehydroglaucarubinone, a new antineoplastic quassinoid from Simarouba amara. *Experientia,* 34**,** 1122-1123.

PRASAD, S., GUPTA, S. C. & TYAGI, A. K. 2017. Reactive oxygen species (ROS) and cancer: Role of antioxidative nutraceuticals. *Cancer Lett,* 387**,** 95-105.

PRATHEESHKUMAR, P. & KUTTAN, G. 2010. Cardiospermum halicacabum inhibits cyclophosphamide induced immunosupression and oxidative stress in mice and also regulates iNOS and COX-2 gene expression in LPS stimulated macrophages. *Asian Pac J Cancer Prev,* 11**,** 1245-52.

PREMA, WONG, C. P., NUGROHO, A. E., AWOUAFACK, M. D., WIN, Y. Y., WIN, N. N., NGWE, H. & MORITA, H. 2019. Two new quassinoids and other constituents from Picrasma javanica wood, and their biological activities. *J Nat Med,* 73**,** 589-596.

PRICE, V. E. & GREENFIELD, P. E. 1958. *Anaemia in Cancer,* New York, Academic Press.

PRIETO, P., PINEDA, M. & AGUILAR, M. 1999. Spectrophotometric quantitation of antioxidant capacity through the formation of a phosphomolybdenum complex: specific application to the determination of vitamin E. *Anal Biochem,* 269**,** 337-41.

PULIDO, R., BRAVO, L. & SAURA-CALIXTO, F. 2000. Antioxidant activity of dietary polyphenols as determined by a modified ferric reducing/antioxidant power assay. *J Agric Food Chem,* 48**,** 3396-402.

PURANIK, S., GHAGANE, S., NERLI, R., JALALPURE, S. & HIREMATH, M. 2017. Evaluation of in vitro Antioxidant and Anticancer Activity of Simarouba glauca Leaf Extracts on T-24 Bladder Cancer Cell Line. *Pharmacognosy Journal,* 9**,** 906-912.

QIN, S. 2010. Suofu Qin's work on studies of cell survival signaling in cancer and epithelial cells. *World J Biol Chem,* 1**,** 369-76.

RABI, T. & BISHAYEE, A. 2009. Terpenoids and breast cancer chemoprevention. *Breast Cancer Res Treat,* 115**,** 223-39.

RAHMAN, M. F., SIDDIQUI, M. K. & JAMIL, K. 2001. Effects of Vepacide (Azadirachta indica) on aspartate and alanine aminotransferase profiles in a subchronic study with rats. *Hum Exp Toxicol,* 20**,** 243-9.

RAMASAMY, K. & AGARWAL, R. 2008. Multitargeted therapy of cancer by silymarin. *Cancer Lett,* 269**,** 352-62.

RATH, S. P., SRINIVASULU, C. & MAHAPATRA, S. N. 1987. Investigation on Simarouba glauca - a new oilseed of Indian Origin. *Journal Oil Technologists Association of India***,** 64-65.

REHAN, A., JOHNSON, K. J., KUNKEL, R. G. & WIGGINS, R. C. 1985. Role of oxygen radicals in phorbol myristate acetate-induced glomerular injury. *Kidney Int,* 27**,** 503-11.

REYNERTSON, K. A., CHARLSON, M. E. & GUDAS, L. J. 2011. Induction of murine embryonic stem cell differentiation by medicinal plant extracts. *Exp Cell Res,* 317**,** 82-93.

RIVERO-CRUZ, J. F., LEZUTEKONG, R., LOBO-ECHEVERRI, T., ITO, A., MI, Q., CHAI, H. B., SOEJARTO, D. D., CORDELL, G. A., PEZZUTO, J. M., SWANSON, S. M., MORELLI, I. & KINGHORN, A. D. 2005. Cytotoxic constituents of the twigs of Simarouba glauca collected from a plot in Southern Florida. *Phytother Res,* 19**,** 136-40.

ROSNER, M. H. & BOLTON, W. K. 2006. Renal Function Testing. *American Journal of Kidney Diseases,* 47**,** 174-183.

ROUT, P. K., RAO, Y. R., JENA, K. S., SAHOO, D. & ALI, S. 2014. Safety evaluation of Simarouba glauca seed fat. *J Food Sci Technol,* 51**,** 1349-55.

RUIZ-RAMOS, R., LOPEZ-CARRILLO, L., RIOS-PEREZ, A. D., DE VIZCAYA-RUIZ, A. & CEBRIAN, M. E. 2009. Sodium arsenite induces ROS generation, DNA oxidative damage, HO-1 and c-Myc proteins, NF-kappaB activation and cell proliferation in human breast cancer MCF-7 cells. *Mutat Res,* 674**,** 109-15.

RUSSO, J. & RUSSO, I. H. 2000. Atlas and histologic classification of tumors of the rat mammary gland. *J Mammary Gland Biol Neoplasia,* 5**,** 187-200.

SABRA, S. A., ELZOGHBY, A. O., SHEWEITA, S. A., HAROUN, M., HELMY, M. W., ELDEMELLAWY, M. A., XIA, Y., GOODALE, D., ALLAN, A. L. & ROHANI, S. 2018. Self-assembled amphiphilic zein-lactoferrin micelles for tumor targeted co-delivery of rapamycin and wogonin to breast cancer. *Eur J Pharm Biopharm,* 128**,** 156-169.

SAHIN, K., TUZCU, M., YABAS, M., ORHAN, C., SAHIN, N. & OZERCAN, I. H. 2018. LFM-A13, a potent inhibitor of polo-like kinase, inhibits breast carcinogenesis by suppressing proliferation activity and inducing apoptosis in breast tumors of mice. *Invest New Drugs,* 36**,** 388-395.

SAID, A., TUNDIS, R., HAWAS, U. W., EL-KOUSY, S. M., RASHED, K., MENICHINI, F., BONESI, M., HUEFNER, A., LOIZZO, M. R. & MENICHINIB, F. 2010. In vitro antioxidant and antiproliferative activities of flavonoids from Ailanthus excelsa (Roxb.) (Simaroubaceae) leaves. *Z Naturforsch C,* 65**,** 180-6.

SAIIN, C., RATTANAJAK, R., KAMCHONWONGPAISAN, S., INGKANINAN, K., SUKONTASON, K., BARAMEE, A. & SIRITHUNYALUG, B. 2003. Isolation and in vitro antimalarial activity of hexane extract from Thai

Picrasma javanica B1 stembark. *Southeast Asian J Trop Med Public Health,* 2**,** 51-5.

SALDANHA, L. A., ELIAS, G. & RAO, M. N. 1990. Oxygen radical scavenging activity of phenylbutenones and their correlation with antiinflammatory activity. *Arzneimittelforschung,* 40**,** 89-91.

SALEEM, M., ASIF, J., ASIF, M. & SALEEM, U. 2018. Amygdalin, from Apricot Kernels, Induces Apoptosis and Causes Cell Cycle Arrest in Cancer Cells: An Updated Review. *Anticancer Agents Med Chem,* 5**,** 187152061866618010516113 6.

SAMA, W., AJAIYEOBA, E. O. & CHOUDHARY, M. I. 2014. Larvicidal properties of simalikalactone D from Quassia africana (Simaroubaceae) Baill and Baill, on the malaria vector Anopheles gambiae. *Afr J Tradit Complement Altern Med,* 11**,** 84-8.

SANTOS, N. A., BEZERRA, C. S., MARTINS, N. M., CURTI, C., BIANCHI, M. L. & SANTOS, A. C. 2008. Hydroxyl radical scavenger ameliorates cisplatin-induced nephrotoxicity by preventing oxidative stress, redox state unbalance, impairment of energetic metabolism and apoptosis in rat kidney mitochondria. *Cancer Chemother Pharmacol,* 61**,** 145-55.

SANTOS, N. A., CATAO, C. S., MARTINS, N. M., CURTI, C., BIANCHI, M. L. & SANTOS, A. C. 2007. Cisplatin-induced nephrotoxicity is associated with oxidative stress, redox state unbalance, impairment of energetic metabolism and apoptosis in rat kidney mitochondria. *Arch Toxicol,* 81**,** 495-504.

SAREK, J., KVASNICA, M., URBAN, M., KLINOT, J. & HAJDUCH, M. 2005. Correlation of cytotoxic activity of betulinines and their hydroxy analogues. *Bioorg Med Chem Lett,* 15**,** 4196-200.

SCHETTLER, G. & NUSSEL, E. 1975. enzymatic colorimtric determination of high density lipoprotein cholestero by CHOD-PAP method. *Arav. Med,* 10**,** 25-29.

SCHILLACI, O., SCIMECA, M., TRIVIGNO, D., CHIARAVALLOTI, A., FACCHETTI, S., ANEMONA, L., BONFIGLIO, R., SANTEUSANIO, G., TANCREDI, V., BONANNO, E., URBANO, N. & MAURIELLO, A. 2019. Prostate cancer and inflammation: A new molecular imaging challenge in the era of personalized medicine. *Nucl Med Biol,* 19**,** 30323-8.

SCHLEBUSCH, H., RICK, W., LANG, H. & KNEDEL, M. 1974. [Standards in the activities of clinically important enzymes]. *Dtsch Med Wochenschr,* 99**,** 765-6.

SCHOENFELD, R. G. & LEWELLEN, C. J. 1964. A Colorimetric Method for Determination of Serum Chloride. *Clin Chem,* 10**,** 533-9.

SEGURA, J. A., BARBERO, L. G. & MÁRQUEZ, J. 2000. Ehrlich ascites tumour unbalances splenic cell populations and reduces responsiveness of T cells to Staphylococcus aureus enterotoxin B stimulation. *Immunology letters,* 74**,** 111-115.

SEIDA, A. A., KINGHORN, A. D., CORDELL, G. A. & FARNSWORTH, N. R. 1978. Potential anticancer agents IX. Isolation of a new simaroubolide, 6alpha-tigloyloxychaparrinone, from Ailanthus integrifolia ssp. calycina (Simaroubaceae). *Lloydia,* 41**,** 584-7.

SERFILIPPI, L. M., PALLMAN, D. R. & RUSSELL, B. 2003. Serum clinical chemistry and hematology reference values in outbred stocks of albino mice from three commonly used vendors and two inbred strains of albino mice. *Contemp Top Lab Anim Sci,* 42**,** 46-52.

SERGI, B., FERRARESI, A., TROIANI, D., PALUDETTI, G. & FETONI, A. R. 2003. Cisplatin ototoxicity in the guinea pig: vestibular and cochlear damage. *Hearing research,* 182**,** 56-64.

SEVEREN, M. L. 1953. Aceituno seed fat. *Journal of the American Oil Chemists Society,* 30**,** 124-126.

SHABANI, M., NAZERI, M., PARSANIA, S., RAZAVINASAB, M., ZANGIABADI, N., ESMAEILPOUR, K. & ABAREGHI, F. 2012. Walnut consumption protects rats against cisplatin-induced neurotoxicity. *Neurotoxicology,* 33**,** 1314-21.

SHANMUGAM, M. K., SHEN, H., TANG, F. R., ARFUSO, F., RAJESH, M., WANG, L., KUMAR, A. P., BIAN, J., GOH, B. C., BISHAYEE, A. & SETHI, G. 2018. Potential role of genipin in cancer therapy. *Pharmacol Res,* 133**,** 195-200.

SHAO, Z. M., SHEN, Z. Z., LIU, C. H., SARTIPPOUR, M. R., GO, V. L., HEBER, D. & NGUYEN, M. 2002. Curcumin exerts multiple suppressive effects on human breast carcinoma cells. *Int J Cancer,* 98**,** 234-40.

SHARMA, S. & SRIRAM, N. 2014. Anti-Ulcer activity of *Simarouba glauca* against Ethanol and Indomethacin induced ulcer in rats. *International Journal of Research in Pharmacology & Pharmacotherapeutics,* 3**,** 85-89.

SHARMA, S. H., THULASINGAM, S. & NAGARAJAN, S. 2017. Terpenoids as anti-colon cancer agents - A comprehensive review on its mechanistic perspectives. *Eur J Pharmacol,* 795**,** 169-178.

SHARMA, S., SHARMA, P., KULURKAR, P., SINGH, D., KUMAR, D. & PATIAL, V. 2017a. Iridoid glycosides fraction from Picrorhiza kurroa attenuates cyclophosphamide-induced renal toxicity and peripheral neuropathy via PPAR-gamma mediated inhibition of inflammation and apoptosis. *Phytomedicine,* 36**,** 108-117.

SHEEJA, K., SHIHAB, P. K. & KUTTAN, G. 2006. Antioxidant and anti-inflammatory activities of the plant Andrographis paniculata Nees. *Immunopharmacol Immunotoxicol,* 28**,** 129-40.

SHIRANI, K., HASSANI, F. V., RAZAVI-AZARKHIAVI, K., HEIDARI, S., ZANJANI, B. R. & KARIMI, G. 2015. Phytotrapy of cyclophosphamide-induced immunosuppression. *Environ Toxicol Pharmacol,* 39**,** 1262-75.

SILIHE, K. K., ZINGUE, S., WINTER, E., AWOUNFACK, C. F., BISHAYEE, A., DESAI, N. N., JOAO MELLO, L., MICHEL, T., TANKEU, F. N., NDINTEH, D. T., HONORINE RIWOM, S., NJAMEN, D. & CRECZYNSKI-PASA, T. B. 2017. Ficus umbellata Vahl. (Moraceae) Stem Bark Extracts Exert Antitumor Activities In Vitro and In Vivo. *Int J Mol Sci,* 18.

SINDHU, E. R. & KUTTAN, R. 2013. Carotenoid lutein protects the kidney against cisplatin-induced acute renal failure. *J Environ Pathol Toxicol Oncol,* 32**,** 21-8.

SINGHAL, S. S., HORNE, D., SINGHAL, J., VONDERFECHT, S., SALGIA, R. & AWASTHI, S. 2019. Synergistic efficacy of RLIP inhibition and 2'-hydroxyflavanone against DMBA-induced mammary carcinogenesis in SENCAR mice. *Mol Carcinog,* 58**,** 1438-1449.

SOFOWORA, A. 1993. *Medicinal Plants and Traditional Medicine in Africa,* Ibadan, Nigeria., Spectrum Books Ltd.

SOLIS, P. N., WRIGHT, C. W., ANDERSON, M. M., GUPTA, M. P. & PHILLIPSON, J. D. 1993. A microwell cytotoxicity assay using Artemia salina (brine shrimp). *Planta Med,* 59**,** 250-2.

SOMANI, S. M., HUSAIN, K., WHITWORTH, C., TRAMMELL, G. L., MALAFA, M. & RYBAK, L. P. 2000. Dose-dependent protection by lipoic acid against cisplatin-induced nephrotoxicity in rats: antioxidant defense system. *Pharmacol Toxicol,* 86**,** 234-41.

SPORN, M. B. 1996. The war on cancer. *Lancet,* 347**,** 1377-81.

SREDNI, B., ALBECK, M., KAZIMIRSKY, G. & SHALIT, F. 1992. The immunomodulator AS101 administered orally as a chemoprotective and radioprotective agent. *Int J Immunopharmacol,* 14**,** 613-9.

SREENIVASAN, Y., SARKAR, A. & MANNA, S. K. 2003. Oleandrin suppresses activation of nuclear transcription factor-kappa B and activator protein-1 and potentiates apoptosis induced by ceramide. *Biochem Pharmacol,* 66**,** 2223-39.

STEWART, S. L., QUEREC, T. D., OCHMAN, A. R., GRUVER, B. N., BAO, R., BABB, J. S., WONG, T. S., KOUTROUKIDES, T., PINNOLA, A. D., KLEIN-SZANTO, A., HAMILTON, T. C. & PATRIOTIS, C. 2004. Characterization of a carcinogenesis rat model of ovarian preneoplasia and neoplasia. *Cancer Res,* 64**,** 8177-83.

STYLOS, E., CHATZIATHANASIADOU, M. V., SYRIOPOULOU, A. & TZAKOS, A. G. 2017. Liquid chromatography coupled with tandem mass spectrometry (LC-MS/MS) based bioavailability determination of the major classes of phytochemicals. *J Chromatogr B Analyt Technol Biomed Life Sci,* 15**,** 15-38.

SUBRAMANI, R. & LAKSHMANASWAMY, R. 2017. Complementary and Alternative Medicine and Breast Cancer. *Prog Mol Biol Transl Sci,* 151**,** 231-274.

SUN, H. X. & PENG, X. Y. 2008. Protective effect of triterpenoid fractions from the rhizomes of Astilbe chinensis on cyclophosphamide-induced toxicity in tumor-bearing mice. *J Ethnopharmacol,* 119**,** 312-7.

SUNILA, E. S. & KUTTAN, G. 2004. Immunomodulatory and antitumor activity of Piper longum Linn. and piperine. *J Ethnopharmacol,* 90**,** 339-46.

TAI, C. J., LIU, C. H., PAN, Y. C., WONG, S. H., RICHARDSON, C. D. & LIN, L. T. 2019. Chemovirotherapeutic Treatment Using Camptothecin Enhances Oncolytic Measles Virus-Mediated Killing of Breast Cancer Cells. *Sci Rep,* 9**,** 019-43047.

TAJIK, N., TAJIK, M., MACK, I. & ENCK, P. 2017. The potential effects of chlorogenic acid, the main phenolic components in coffee, on health: a comprehensive review of the literature. *Eur J Nutr,* 56**,** 2215-2244.

TALIB, W. H. 2017. Consumption of garlic and lemon aqueous extracts combination reduces tumor burden by angiogenesis inhibition, apoptosis induction, and immune system modulation. *Nutrition,* 44**,** 89-97.

TALMADGE, J. E. & FIDLER, I. J. 2010. AACR centennial series: the biology of cancer metastasis: historical perspective. *Cancer Res,* 70**,** 5649-69.

TAMAYO, C. & DIAMOND, S. 2007. Review of clinical trials evaluating safety and efficacy of milk thistle (Silybum marianum [L.] Gaertn.). *Integr Cancer Ther,* 6**,** 146-57.

TEO, S., STIRLING, D., THOMAS, S., HOBERMAN, A., KIORPES, A. & KHETANI, V. 2002. A 90-day oral gavage toxicity study of D-methylphenidate and D,L-methylphenidate in Sprague-Dawley rats. *Toxicology,* 179**,** 183-96.

TERRY, P. & WOLK, A. 2001. Tea consumption and the risk of colorectal cancer in Sweden. *Nutr Cancer,* 39**,** 176-9.

THATTE, U., BAGADEY, S. & DAHANUKAR, S. 2000. Modulation of programmed cell death by medicinal plants. *Cell Mol Biol,* 46**,** 199-214.

THEFELD, W., HOFFMEISTER, H., BUSCH, E. W., KOLLER, P. U. & VOLLMAR, J. 1974. [Reference values for the determination of GOT, GPT, and alkaline phosphatase in serum with optimal standard methods (author's transl)]. *Dtsch Med Wochenschr,* 99**,** 343-4.

THONGNEST, S., BOONSOMBAT, J., PRAWAT, H., MAHIDOL, C. & RUCHIRAWAT, S. 2017. Ailanthusins A-G and nor-lupane triterpenoids from Ailanthus triphysa. *Phytochemistry,* 134**,** 98-105.

THOPPIL, R. J. & BISHAYEE, A. 2011. Terpenoids as potential chemopreventive and therapeutic agents in liver cancer. *World J Hepatol,* 3**,** 228-49.

THUMMAR, V. R., PARASURAMAN, S., BASU, D. & RAVEENDRAN, R. 2015. Evaluation of in vivo antitumor activity of cleistanthin B in Swiss albino mice. *J Tradit Complement Med,* 6**,** 383-388.

TISCHLER, M., CARDELLINA, J. H., 2ND, BOYD, M. R. & CRAGG, G. M. 1992. Cytotoxic quassinoids from Cedronia granatensis. *J Nat Prod,* 55**,** 667-71.

TOLG, C., COWMAN, M. & TURLEY, E. A. 2018. Mouse Mammary Gland Whole Mount Preparation and Analysis. *Bio-protocol,* 8**,** e2915.

TORO, G. & ACKERMANN, P. G. 1975. *Practical Clinical Chemistry,* Boston, Little Brown and Company.

TRAVERSO, N., RICCIARELLI, R., NITTI, M., MARENGO, B., FURFARO, A. L., PRONZATO, M. A., MARINARI, U. M. & DOMENICOTTI, C. 2013.

Role of glutathione in cancer progression and chemoresistance. *Oxid Med Cell Longev,* 972913**,** 20.

TREADWAY, S. 1998. An Ayurvedic herbal approach to a healthy liver. *Clinical Nutrition Insights,* 6**,** 1-3.

TRIVEDI, N., RAWAL U. M. 1998. Effect of aqueous extract of *Andrographis paniculata* on liver tumour. *Indian Journal of Pharmacology,* 30**,** 318-322.

TROMBINO, A. F., NEAR, R. I., MATULKA, R. A., YANG, S., HAFER, L. J., TOSELLI, P. A., KIM, D. W., ROGERS, A. E., SONENSHEIN, G. E. & SHERR, D. H. 2000. Expression of the aryl hydrocarbon receptor/transcription factor (AhR) and AhR-regulated CYP1 gene transcripts in a rat model of mammary tumorigenesis. *Breast Cancer Res Treat,* 63**,** 117-31.

TSE, B. W., SCOTT, K. F. & RUSSELL, P. J. 2012. Paradoxical roles of tumour necrosis factor-alpha in prostate cancer biology. *Prostate Cancer,* 128965**,** 27.

TSENG, M. 2009. Diet, cancer and public health nutrition. *Public Health Nutrition,* 12**,** 737-738.

TUNG, M. H., DUC, H. V., HUONG, T. T., DUONG, N. T., PHUONG DO, T., THAO DO, T., TAI, B. H., KIM, Y. H., BACH, T. T. & CUONG, N. M. 2012. Cytotoxic Compounds from Brucea mollis. *Sci Pharm,* 81**,** 819-31.

TUNG, N. H., UTO, T., HAI, N. T., LI, G. & SHOYAMA, Y. 2017. Quassinoids from the Root of Eurycoma longifolia and Their Antiproliferative Activity on Human Cancer Cell Lines. *Pharmacogn Mag,* 13**,** 459-462.

VALDES, A. F., MARTINEZ, J. M., LIZAMA, R. S., VERMEERSCH, M., COS, P. & MAES, L. 2008. In vitro anti-microbial activity of the Cuban medicinal plants Simarouba glauca DC, Melaleuca leucadendron L and Artemisia absinthium L. *Mem Inst Oswaldo Cruz,* 103**,** 615-8.

VAN DUYN, M. A. S. & PIVONKA, E. 2000. Overview of the Health Benefits of Fruit and Vegetable Consumption for the Dietetics Professional: Selected Literature. *Journal of the Academy of Nutrition and Dietetics,* 100**,** 1511-1521.

VAN TRI, M., POLONSKY, J., MERIENNE, C. & SEVENET, T. 1981. Soularubinone, a new antileukemic quassionoid from Soulamea tomentosa. *J Nat Prod,* 44**,** 279-84.

VAUGHAN, J. G. 1970. *The structure and utilization of oil seeds,* London, Chapman & Hall.

VENKATARAMAN, S., WAGNER, B. A., JIANG, X., WANG, H. P., SCHAFER, F. Q., RITCHIE, J. M., PATRICK, B. C., OBERLEY, L. W. & BUETTNER, G. R. 2004. Overexpression of manganese superoxide dismutase promotes the survival of prostate cancer cells exposed to hyperthermia. *Free Radic Res,* 38**,** 1119-32.

VIEIRA TORQUATO, H. F., RIBEIRO-FILHO, A. C., BURI, M. V., ARAUJO JUNIOR, R. T., PIMENTA, R., DE OLIVEIRA, J. S., FILHO, V. C., MACHO, A., PAREDES-GAMERO, E. J. & DE OLIVEIRA MARTINS, D. T. 2017. Canthin-6-one induces cell death, cell cycle arrest and differentiation in human myeloid leukemia cells. *Biochim Biophys Acta Gen Subj,* 4**,** 958-967.

VIJAYALAKSHMI, A., KUMAR, P. R., SAKTHI PRIYADARSINI, S. & MEENAXSHI, C. 2013. In Vitro Antioxidant and Anticancer Activity of Flavonoid Fraction from the Aerial Parts of Cissus quadrangularis Linn. against Human Breast Carcinoma Cell Lines. *Journal of Chemistry,* 2013**,** 9.

VIKAS, B., AKHIL, B. S., SUJA, S. R. & SUJATHAN, K. 2017. *An Exploration of Phytochemicals from Simaroubaceae*, Asian Pac J Cancer Prev. 2017 Jul 27;18(7):1765-1767. doi: 10.22034/APJCP.2017.18.7.1765.

VOSKOGLOU-NOMIKOS, T., PATER, J. L. & SEYMOUR, L. 2003. Clinical Predictive Value of the in Vitro Cell Line, Human Xenograft, and Mouse Allograft Preclinical Cancer Models. *Clinical Cancer Research,* 9**,** 4227-4239.

WALTERS, M. I. & GERARDE, H. W. 1970. An ultramicromethod for the determination of conjugated and total bilirubin in serum or plasma. *Microchemical Journal,* 15**,** 231-243.

WANG, J., FANG, X., GE, L., CAO, F., ZHAO, L., WANG, Z. & XIAO, W. 2018. Antitumor, antioxidant and anti-inflammatory activities of kaempferol and its corresponding glycosides and the enzymatic preparation of kaempferol. *PLoS One,* 13.

WANG, J., TONG, X., LI, P., CAO, H. & SU, W. 2012. Immuno-enhancement effects of Shenqi Fuzheng Injection on cyclophosphamide-induced immunosuppression in Balb/c mice. *J Ethnopharmacol,* 139**,** 788-95.

WANG, K., FENG, X., CHAI, L., CAO, S. & QIU, F. 2017. The metabolism of berberine and its contribution to the pharmacological effects. *Drug Metab Rev,* 49**,** 139-157.

WANG, L., LI, Z., LI, L., LI, Y., YU, M., ZHOU, Y., LV, X., ARAI, H. & XU, Y. 2014. Acute and sub-chronic oral toxicity profiles of the aqueous extract of Cortex Dictamni in mice and rats. *J Ethnopharmacol,* 2**,** 207-15.

WANG, S., ZHANG, C., YANG, G. & YANG, Y. 2014. Biological properties of 6-gingerol: a brief review. *Nat Prod Commun,* 9**,** 1027-30.

WANG, X., SON, Y.-O., CHANG, Q., SUN, L., HITRON, J. A., BUDHRAJA, A., ZHANG, Z., KE, Z., CHEN, F., LUO, J. & SHI, X. 2011. NADPH Oxidase Activation Is Required in Reactive Oxygen Species Generation and Cell Transformation Induced by Hexavalent Chromium. *Toxicological Sciences,* 123**,** 399-410.

WANG, Y., WANG, W. J., SU, C., ZHANG, D. M., XU, L. P., HE, R. R., WANG, L., ZHANG, J., ZHANG, X. Q. & YE, W. C. 2013. Cytotoxic quassinoids from Ailanthus altissima. *Bioorg Med Chem Lett,* 23**,** 654-7.

WIN, N. N., ITO, T., ISMAIL, KODAMA, T., WIN, Y. Y., TANAKA, M., NGWE, H., ASAKAWA, Y., ABE, I. & MORITA, H. 2015. Picrajavanicins A-G, Quassinoids from Picrasma javanica Collected in Myanmar. *J Nat Prod,* 78**,** 3024-30.

WIN, N. N., ITO, T., WIN, Y. Y., NGWE, H., KODAMA, T., ABE, I. & MORITA, H. 2016. Quassinoids: Viral protein R inhibitors from Picrasma javanica bark collected in Myanmar for HIV infection. *Bioorg Med Chem Lett,* 26**,** 4620-4624.

WINTER, C. A., RISLEY, E. A. & NUSS, G. W. 1962. Carrageenin-induced edema in hind paw of the rat as an assay for antiiflammatory drugs. *Proc Soc Exp Biol Med,* 111**,** 544-7.

WINTROBE, M. M. & GREER, J. P. 2009. *Wintrobe's clinical hematology,* Philadelphia, Wolters Kluwer Health/Lippincott Williams and Wilkins.

WOLF, P. L., WILLIAMS, D., TSUDAKA, T. & ASCOSTA, L. 1972. *Methods and Techniques in Clinical Chemistry,* USA, John Wiley & Sons.

WOYTALA, P. J., MORGIEL, E., LUCZAK, A., CZESAK-WOYTALA, K. & WILAND, P. 2016. The Safety of Intravenous Cyclophosphamide in the Treatment of Rheumatic Diseases. *Adv Clin Exp Med,* 25**,** 479-84.

WRIGHT, C. W., O'NEILL, M. J., PHILLIPSON, J. D. & WARHURST, D. C. 1988. Use of microdilution to assess in vitro antiamoebic activities of Brucea javanica fruits, Simarouba amara stem, and a number of quassinoids. *Antimicrob Agents Chemother,* 32**,** 1725-9.

WU, S., ZHU, W., THOMPSON, P. & HANNUN, Y. A. 2018. Evaluating intrinsic and non-intrinsic cancer risk factors. *Nat Commun,* 9**,** 018-05467.

WU, X., HAWSE, J. R., SUBRAMANIAM, M., GOETZ, M. P., INGLE, J. N. & SPELSBERG, T. C. 2009. The tamoxifen metabolite, endoxifen, is a potent antiestrogen that targets estrogen receptor alpha for degradation in breast cancer cells. *Cancer Res,* 69**,** 1722-7.

XIAO, Y., YANG, Z., WU, Q. Q., JIANG, X. H., YUAN, Y., CHANG, W., BIAN, Z. Y., ZHU, J. X. & TANG, Q. Z. 2017. Cucurbitacin B Protects Against Pressure Overload Induced Cardiac Hypertrophy. *J Cell Biochem,* 118**,** 3899-3910.

XU, D. P., LI, Y., MENG, X., ZHOU, T., ZHOU, Y., ZHENG, J., ZHANG, J. J. & LI, H. B. 2017. Natural Antioxidants in Foods and Medicinal Plants: Extraction, Assessment and Resources. *Int J Mol Sci,* 18.

XU, J., XIAO, D., LIN, Q. H., HE, J. F., LIU, W. Y., XIE, N., FENG, F. & QU, W. 2016. Cytotoxic Tirucallane and Apotirucallane Triterpenoids from the Stems of Picrasma quassioides. *J Nat Prod,* 79**,** 1899-910.

XU, X. H., LI, T., FONG, C. M., CHEN, X., CHEN, X. J., WANG, Y. T., HUANG, M. Q. & LU, J. J. 2016. Saponins from Chinese Medicines as Anticancer Agents. *Molecules,* 21.

XU, Y., GAO, C. C., PAN, Z. G. & ZHOU, C. W. 2018. Irigenin sensitizes TRAIL-induced apoptosis via enhancing pro-apoptotic molecules in gastric cancer cells. *Biochem Biophys Res Commun,* 496**,** 998-1005.

YAMAGATA, K., IZAWA, Y., ONODERA, D. & TAGAMI, M. 2018. Chlorogenic acid regulates apoptosis and stem cell marker-related gene expression in A549 human lung cancer cells. *Mol Cell Biochem,* 441**,** 9-19.

YAMAZAKI, S., MIYOSHI, N., KAWABATA, K., YASUDA, M. & SHIMOI, K. 2014. Quercetin-3-O-glucuronide inhibits noradrenaline-promoted invasion of MDA-MB-231 human breast cancer cells by blocking beta(2)-adrenergic signaling. *Arch Biochem Biophys,* 557**,** 18-27.

YAMSHANOV, V. A., KOVAN'KO, E. G. & PUSTOVALOV, Y. I. 2016. Effects of Amygdaline from Apricot Kernel on Transplanted Tumors in Mice. *Bull Exp Biol Med,* 160**,** 712-4.

YANG, X. L., YUAN, Y. L., ZHANG, D. M., LI, F. & YE, W. C. 2014. Shinjulactone O, a new quassinoid from the root bark of Ailanthus altissima. *Nat Prod Res,* 28**,** 1432-7.

YANG, Y., GU, Y., ZHAO, H. & ZHANG, S. 2019. Loganin Attenuates Osteoarthritis in Rats by Inhibiting IL-1beta-Induced Catabolism and Apoptosis in Chondrocytes Via Regulation of Phosphatidylinositol 3-Kinases (PI3K)/Akt. *Med Sci Monit,* 25**,** 4159-4168.

YAO, H., XU, W., SHI, X. & ZHANG, Z. 2011. Dietary flavonoids as cancer prevention agents. *J Environ Sci Health C Environ Carcinog Ecotoxicol Rev,* 29**,** 1-31.

YAO, L., PENG, S. X., XU, Y. D., LIN, S. L., LI, Y. H., LIU, C. J., ZHAO, H. D., WANG, L. F. & SHEN, Y. Q. 2017. Unexpected Neuroprotective Effects of Loganin on 1-Methyl-4-Phenyl-1,2,3,6-Tetrahydropyridine-Induced Neurotoxicity and Cell Death in Zebrafish. *J Cell Biochem,* 118**,** 615-628.

YEO, D., HUYNH, N., BEUTLER, J. A., BALDWIN, G. S., HE, H. & NIKFARJAM, M. 2016. Glaucarubinone Combined with Gemcitabine Improves Pancreatic Cancer Survival in an Immunocompetent Orthotopic Murine Model. *J Invest Surg,* 29**,** 366-372.

YEO, D., HUYNH, N., BEUTLER, J. A., CHRISTOPHI, C., SHULKES, A., BALDWIN, G. S., NIKFARJAM, M. & HE, H. 2014. Glaucarubinone and gemcitabine synergistically reduce pancreatic cancer growth via down-regulation of P21-activated kinases. *Cancer Lett,* 346**,** 264-72.

YOUNG, D. S., PESTANER, L. C. & GIBBERMAN, V. 1975. Effects of drugs on clinical laboratory tests. *Clin Chem,* 21**,** 1D-432D.

YU, D. & AN, G. Y. 2017. Clinical Effects of Xihuang Pill Combined with Chemotherapy in Patients with Advanced Colorectal Cancer. *Evid Based Complement Alternat Med,* 5936086**,** 28.

YU, F., ZHANG, Z., YE, S., HONG, X., JIN, H., HUANG, F., YANG, Z., TANG, Y., CHEN, Y. & DING, G. 2019. Immunoenhancement effects of pentadecapeptide derived from Cyclina sinensis on immune-deficient mice induced by Cyclophosphamide. *Journal of Functional Foods,* 60**,** 103408.

ZAREI, M. & SHIVANANDAPPA, T. 2013. Amelioration of cyclophosphamide-induced hepatotoxicity by the root extract of Decalepis hamiltonii in mice. *Food Chem Toxicol,* 57**,** 179-84.

ZHAI, X., ZHANG, Z., LIU, W., LIU, B., ZHANG, R., WANG, W., ZHENG, W., XU, F., WANG, J. & CHEN, Y. 2018. Protective effect of ALDH2 against cyclophosphamide-induced acute hepatotoxicity via attenuating oxidative stress and reactive aldehydes. *Biochem Biophys Res Commun,* 499**,** 93-98.

ZHANG, M., DU, H., HUANG, Z., ZHANG, P., YUE, Y., WANG, W., LIU, W., ZENG, J., MA, J., CHEN, G., WANG, X. & FAN, J. 2018. Thymoquinone induces apoptosis in bladder cancer cell via endoplasmic reticulum stress-dependent mitochondrial pathway. *Chem Biol Interact,* 292**,** 65-75.

ZHANG, Q., LI, N., ZHOU, G., LU, X., XU, Z. & LI, Z. 2003. In vivo antioxidant activity of polysaccharide fraction from Porphyra haitanesis (Rhodephyta) in aging mice. *Pharmacol Res,* 48**,** 151-5.

ZHONG, T., PIAO, L., KIM, H. J., LIU, X., JIANG, S. & LIU, G. 2017. Chlorogenic Acid-Enriched Extract of Ilex kudingcha C.J. Tseng Inhibits Angiogenesis in Zebrafish. *J Med Food,* 20**,** 1160-1167.

ZHOU, H., LIU, Y., WANG, C., LIU, L., WANG, H., ZHANG, Y., LONG, C. & SUN, X. 2018. Triptolide inhibits Epstein-Barr nuclear antigen 1 expression by increasing sensitivity of mitochondria apoptosis of nasopharyngeal carcinoma cells. *Journal of Experimental & Clinical Cancer Research,* 37**,** 192.

ZOHEIR, K. M., HARISA, G. I., ABO-SALEM, O. M. & AHMAD, S. F. 2015. Honey bee is a potential antioxidant against cyclophosphamide-induced genotoxicity in albino male mice. *Pak J Pharm Sci,* 28**,** 973-81.

ZUBAIR, H., AZIM, S., AHMAD, A., KHAN, M. A., PATEL, G. K., SINGH, S. & SINGH, A. P. 2017. Cancer Chemoprevention by Phytochemicals: Nature's Healing Touch. *Molecules,* 22.

ZUBAIR, H., AZIM, S., KHAN, H. Y., ULLAH, M. F., WU, D., SINGH, A. P., HADI, S. M. & AHMAD, A. 2016. Mobilization of Intracellular Copper by Gossypol and Apogossypolone Leads to Reactive Oxygen Species-Mediated Cell Death: Putative Anticancer Mechanism. *Int J Mol Sci,* 17.

List of publications

1. **Shaji E. Mathew**, Smitha K. Ramavarma, Thekkekara Devassy Babu, Balu T. Kuzhivelil and Achuthan C. Raghavamenon (2019). Preliminary assessment on phytochemical composition, cytotoxic and antitumor efficacy of *Simarouba glauca* DC. leaf methanonic extract. Annals of Phytomedicine 8(2): 121-126.

2. **Edappilly M Shaji**, Silpa Prabha, Indu M. Suseels, Thekkekara D Babu, Balu T. Kuzhivelil and Achuthan C. Raghavamenon (2017). Hot water extract of *Simarouba glauca* DC (Laxmitaru) curtails cisplatin induced renal damage in mice. Amala Research Bulletin, 37:21-29.

3. **Edappilly Mathew Shaji,** Indu M Suseela, Silpa Prabha, Meera Nair, Thekkekara D Babu, Balu T. Kuzhivelil and Achuthan C. Raghavamenon (2016). *Simarouba glauca* DC (Laxmitaru) prevents inflammation and tumor development in mice. Amala Research Bulletin, 36:93-107.

4. **Edappilly Mathew Shaji,** Smitha K. Ramavarma, Arunaksharan Narayanankutty, Ramya M. Kuttappan, Thekkekara Devassy Babu, Balu T. Kuzhivelil and Achuthan C. Raghavamenon (2015). Preliminary phytochemical screening, cytotoxic, antitumor studies of *Simarouba glauca* DC (Laxmitaru). Amala Research Bulletin, 35:15-23.